

Development of process to remove oligomers and suppress their formation in aging fuels by adsorbing the precursors of their aging procedure using adsorbents

**Jerome Desire Aliebakaa Kpan
2021**

Acknowledgments

My profound and sincere thanks go to Prof. Dr. Jürgen Krahl for accepting me into his research group, Technology Automotive Transfer Centre (TAC) of the Coburg University of Applied Sciences, and supervising me throughout these years to enable me to produce this dissertation. Despite my inadequacies, you patiently guided me to this point. To have worked under one of the best brains in fuel research is but itself an achievement. I am indeed very grateful to you, Prof. Krahl.

I want to express my sincere appreciation to my supervisors, Prof. Dr. Wolfgang Ruck, Prof. Dr. Oliver Opel and Prof. Dr. Brigitte Urban. They allowed me to submit my dissertation to the Faculty of Sustainability of the University of Lüneburg for this doctorate. Big thanks to Dr. Olaf Schröder for helping me find my feet in the laboratory, especially using pieces of equipment. Always at my side in the laboratory anytime I called upon him. Prof. Dr. Markus Jakob, I register my sincere appreciation for your guidance and support in my work in these last years. Words alone cannot express my gratitude to you.

Life in Germany would have been a night mere without you, Anja Singer, and the family. Only God can bless you for all you did for me. My entire family expresses our appreciation to you.

I must mention here the family Kortschack; you made your house my home; God bless you. I am grateful to Mr. Martin Kortschack for your ideas and for staying with me in the laboratory even over weekends and public holidays to enable me to work.

I am grateful to Mr. Martin Unglert for supporting me in carrying out my NMR measurements at TUM.

To all members of the TAC research group, you have all helped in one way or the other by making my stay in Germany hugely enjoyable. I just want to say thank you and the very best of luck wherever we end up.

My heartfelt, sincere gratitude and thanks to my family, the Omegas and especially my wife, Euphemia, and my children, Deborah, Darlington, and Daisy, for their understanding, love, care, and support. God bless you all.

Author's Declaration

I confirm that the material presented within this dissertation is my work, published and unpublished, and produced without any unauthorized assistance. I have not used any aids or material other than that specified. I have referenced all sources used in this dissertation.

PUBLICATIONS

1. **J.D.A. Kpan** and J. Krahl, (2021) Using adsorbents to sustain the oxidation stability of biodiesel and its blends, Presentation at 2021 AOCs Annual Meeting & Expo, <https://doi.org/10.21748/am21.573>
2. **Jerome D.A. Kpan**, Markus Jakob, & Jürgen Krahl, Using Adsorbents to Impact Oxidative Stability of Biodiesel and its Influence on Engine Oil Deterioration, 2020 AOCs Annual Meeting & Expo, <https://doi.org/10.21748/am20.184>
3. **Jerome D.A Kpan** and Jürgen Krahl. Using adsorbents to mitigate biodiesel influence on the deterioration of engine oil, SAE International Journal of Fuels and Lubricants, SAE Int. J. Fuels Lubr. 13(2):177-186, 2020. ISSN: 1946-3952, e-ISSN: 1946-3960
4. **Jerome D.A Kpan** and Jürgen Krahl, Mitigating the influence of biodiesel on the deterioration of engine oil using adsorbents, (Biodiesel/Analytical) AOCs Inform magazine. DOI: 10.21748/inform.05.2020.12
5. **Jerome Kpan** & Jürgen Krahl, Sustaining the oxidation stability of biodiesel and its blends in plug-in hybrid vehicles using adsorbents, <https://doi.org/10.1021/acs.energyfuels.9b02828>
6. **Kpan Jerome** & Jürgen Krahl. Impact of Adsorbents on Oxidative Stability of Biodiesel and the Deterioration of Engine Oil. Proceedings of the 22nd International Colloquium Tribology Industrial and Automotive Lubrication Technische Akademie Esslingen (TAE), Stuttgart, Germany **ISBN 978-3-943563-11-5 Pg 45-46**
7. **Jerome Kpan** & Jürgen Krahl. The impact of adsorbents on the oxidative stability of biodiesel and its influence on the deterioration of engine oil, *Elv Fuel* 256 (2019) 115984
8. **Kpan, J.D.A.**; Jakob, M. & Krahl, J. The influence of adsorbents on the oxidative stability of biodiesel and the deterioration of engine oil. Proceedings of the 10th Biokraftstoff symposium; "Forschung für zukünftige Mobilität". TAC Academy, Coburg, Germany, Coburg 25th-26th July, 2019. https://www.tac-coburg.de/images/The_influence_of_adsorbents_on_the_oxidative_stability_of_biodiesel_and_the_deterioration_of_engine_oil_Kpanj.pdf
9. **Jerome Kpan**, Anja Singer, & Juergen Krahl; Development of an adsorption process to selectively remove oligomers in an aging engine oil resulting from biodiesel or its blends. *Energy&Fuels* DOI: 10.1021/acs.energyfuels.8b02146
10. **Kpan Jerome** & Jürgen Krahl. Development of process to remove oligomers and impact their formation in aging engine oil using adsorbents. Proceedings of the 12th International Colloquium. Fuels: Conventional and Future Energy for Automobiles; Technische Akademie Esslingen (TAE), Stuttgart, Germany, June 25–26, 2019; pp 99–107. **ISBN 978-3-943563-09-2**
11. **Kpan J.**, & Krahl J., separation of oligomers in aging oil mixed with biodiesel using the process of adsorption. Proceedings of the 9th Biokraftstoff symposium; "Forschung für zukünftige Mobilität". **TAC Academy**, Coburg, Germany, Coburg 26th-27th July, 2018 Fuels Joint Research Group Band 26, Cuvillier Verlag Göttingen, **ISBN 978-3-7369-7022-9** Herausgeber: Jürgen Krahl, Axel Munack, Peter Eilts, Jürgen Bünger, 57-71 (2018).

12. Anja Singer, Markus Knorr, **Jerome Kpan** & Jürgen Krahl. Einfluss biogener Kraftstoffe auf das Alterungsverhalten von Grundöl. Proceedings of the 5th tribology and efficiency conference of Győr 5. Győrer tribologie- und effizienztagung 19th-20th June, 2018 Herausgeber: Jan Knaup, Péter Gál and Kay Schintzel **ISBN: 978-615-5776-16-8** UNIVERSITAS-Győr Nonprofit Kft. Győr, pages 21-40.
13. **Kpan Jerome**; Mitigating the deteriorating effect of biofuel in engine oil, Proceedings of the 17th AOCS Latin American Congress and Exhibition on Fats, Oils, and Lipids, Cancun, Mexico, September 11–13, 2017
14. **Kpan J.**, & Krahl J., Development of a process to selective removal of Oligomers formed in motor oil. Proceedings of the 8th Biokraftstoff symposium; "Forschung für zukünftige Mobilität". **TAC Academy**, Coburg, Germany, Coburg 27th-28th July, 2016 Fuels Joint Research Group Band 22, Cuvillier Verlag Göttingen, **ISBN 978-3-7369-9811-7** Herausgeber: Jürgen Krahl, Axel Munack, Peter Eilts, Jürgen Bünger, 68-84 (2016).
15. **Kpan J.**, Mogalle & Krahl J., Development of a process to selectively exclude MMT from Gasoline. Proceedings of the 7th Biokraftstoff symposium; "Forschung für zukünftige Mobilität". **TAC Academy**, Coburg, Germany, Coburg 26th-27th February, 2015 Fuels Joint Research Group Band 14, Cuvillier Verlag Göttingen, **ISBN 978-3-7369-9143-9** Herausgeber: Jürgen Krahl, Axel Munack, Peter Eilts, Jürgen Bünger, 133-142 (2015).
16. **Kpan J.**, Fan Z., Eskiner M. & Krahl J., Sensors for detecting biofuels and their aging status. Proceedings of KORANET-Promofuel Conference. Towards the Future of Biodiesel, Graz 09.2014

PRESENTATIONS AT CONFERENCES

1. **J.D.A. Kpan** and J. Krahl, (2021) Using adsorbents to sustain the oxidation stability of biodiesel and its blends, **Presentation at 2021 AOCS Annual Meeting & Expo**, <https://doi.org/10.21748/am21.573>
2. Using adsorbents to mitigate biodiesel influence on the deterioration of engine oil presented at the 22nd International Colloquium Tribology Industrial and Automotive Lubrication **Technische Akademie Esslingen (TAE)**, Stuttgart, Germany January 28-30, 2020
3. Using Adsorbents to Impact Oxidative Stability of Biodiesel and its Influence on Engine Oil Deterioration, presented at the 2020 **AOCS Annual Meeting & Expo**
4. The influence of adsorbents on the oxidative stability of biodiesel and the deterioration of engine oil. Presented at the 10th Biokraftstoff symposium; "Forschung für zukünftige Mobilität". **TAC Academy**, Coburg, Germany, Coburg 25th-26th July 2019.
5. Development of process to remove oligomers and impact their formation in aging engine oil using adsorbents presented at the 12th International Colloquium. Fuels: Conventional and Future Energy for Automobiles; **Technische Akademie Esslingen (TAE)**, Stuttgart, Germany, June 25–26, 2019
6. Separation of oligomers in aging oil mixed with biodiesel using the process of adsorption. Presented at the 9th Biokraftstoff symposium; "Forschung für zukünftige Mobilität". **TAC Academy**, Coburg, Germany, Coburg 26th-27th July, 2018

7. Mitigating the deteriorating effect of biofuel in engine oil presented at the 17th **AOCS Latin American Congress and Exhibition** on Fats, Oils, and Lipids, Cancun, Mexico, September 11–13, 2017
8. Development of a process to selective removal of Oligomers formed in motor oil presentation at the 8th Biokraftstoff symposium; "Forschung für zukünftige Mobilität." **TAC Academy**, Coburg, Germany, Coburg 27th-28th July 2016
9. Development of a process to selectively exclude MMT from Gasoline presentation at the 7th Biokraftstoff symposium; "Forschung für zukünftige Mobilität". **TAC Academy**, Coburg, Germany, Coburg 26th-27th February, 2015
10. Sensors for detecting biofuels and their aging status presentation at **KORANET-Promofuel Conference**. Towards the Future of Biodiesel, Graz 09.2014

Table of Content

Acknowledgments	2
Author's Declaration	3
PUBLICATIONS	4
Table of Content	7
List of Figures	15
List of Tables	29
1 Introduction	30
1.1 Objectives.....	34
1.2 Thesis Outline.....	35
2 Literature Review	37
2.1 Previous Work	37
2.2 Summary	41
3 Technical Background.....	42
3.1 Vegetable Oils	42
3.2 Biodiesel.....	43
3.3 Fuel stability	49
3.4 Oxidation	50
3.5 Engine oil.....	58
3.5.1 Oxidation of lubricant base oil.....	60
3.5.2 Dominant mechanisms of degradation.....	63
3.6 Oxidative stability of biodiesel and its effect on performance	64
3.7 Entry of fuel into the engine oil	65
3.8 Effect of biodiesel on engine oil.....	65
4 Basic Experimental Techniques for Evaluation	68
4.1 Techniques for evaluating the suppression of oligomers formation.....	68
4.1.1 Size Exclusion Chromatography (SEC)	69
4.1.2 Gas Chromatograph-Mass Spectroscopy (GCMS)	70
4.1.3 Total Acid Number or Value (TAN)	70
4.1.4 Viscosity and Density.....	71

Table of Content

4.1.5	Fourier Transform Infrared Spectroscopy (FTIR)	73
4.1.6	Inductively Coupled Plasma-Mass-Spectrometry (ICP-MS).....	75
4.1.7	Gas Chromatography-Flame Ionization Detector (GC-FID)	76
4.1.8	Induction Period	76
4.1.9	Dielectric property measurement	78
4.1.10	NMR measurement.....	81
5	The focus of the Thesis	83
6	Selection of Adsorbents	89
6.1	Suppression of oligomers formation	89
6.2	The capacity of adsorbents in suppressing Oligomers formation	99
7	Materials and Methods	105
7.1	Chemicals.....	105
7.2	Investigated Fuels and Oil	105
7.3	Neat additives.....	109
7.4	Simulated Aging Procedure	110
7.4.1	Laboratory setup apparatus	110
7.4.2	The Metrohm 873 biodiesel Rancimat	112
7.5	Investigation of suppression of oligomer formation.....	112
7.5.1	Linoleic acid methyl ester (C18_2 ME)	113
7.5.2	Rapeseed oil methyl ester (RME)	114
7.5.3	Investigating the effect of the combined adsorbents of magnesium- aluminum hydrotalcite and 1,3,5-trimethyl-2,4,6-tris(3,5-di-tert-butyl-4- hydroxybenzyl) benzene in a ratio of 1:2 respectively on the oil additives	115
7.6	Stabilization of biodiesel and its blends using combined adsorbents of magnesium-aluminum hydrotalcite and 1,3,5-trimethyl-2,4,6-tris(3,5-di-tert-butyl-4- hydroxybenzyl) benzene in a ratio of 1:2, respectively	117
7.6.1	Investigating the effect of the combined adsorbents of magnesium- aluminum hydrotalcite and 1,3,5-trimethyl-2,4,6-tris(3,5-di-tert-butyl-4- hydroxybenzyl) benzene in a ratio of 1:2 respectively on oxidative stability of biodiesel and its blends at 170 °C.....	118
7.6.2	Investigating the effect of the combined adsorbents of magnesium- aluminum hydrotalcite and 1,3,5-trimethyl-2,4,6-tris(3,5-di-tert-butyl-4- hydroxybenzyl) benzene in a ratio of 1:2 respectively on oxidative stability of biodiesel and its blends at 110 °C.....	119

7.6.3	Investigating the effect of the combined adsorbents of magnesium-aluminum hydrotalcite and 1,3,5-trimethyl-2,4,6-tris(3,5-di-tert-butyl-4-hydroxybenzyl) benzene in a ratio of 1:2 respectively on the storage stability of biodiesel and its blends at 40 °C.....	120
7.7	Measurement techniques	122
7.7.1	Induction period	123
7.7.2	Size Exclusion Chromatography (SEC)	124
7.7.3	Gas Chromatograph-Mass Spectroscopy (GCMS)	125
7.7.4	Total Acid Number (TAN) or Acid value	125
7.7.5	Viscosity and Density	126
7.7.6	Fourier Transform Infrared Spectroscopy (FTIR)	126
7.7.7	Inductively Coupled Plasma-Mass-Spectrometry (ICP-MS).....	127
7.7.8	Gas Chromatography-Flame Ionization Detector (GC-FID)	129
7.7.9	Dielectric properties measurement	129
7.7.10	NMR measurement.....	130
8	Results and Discussion.....	131
8.1	Investigating the effect of the combined adsorbents of magnesium-aluminum hydrotalcite and 1,3,5-trimethyl-2,4,6-tris(3,5-di-tert-butyl-4-hydroxybenzyl) benzene in a ratio of 1:2 respectively in suppressing oxidation in base oil blended with linoleic acid methyl ester (C18_2 ME)	131
8.1.1	Gas Chromatography.....	132
8.1.2	Size Exclusion Chromatography (SEC)	134
8.1.3	FTIR analysis	137
8.1.4	Acid value	144
8.2	Investigating the effect of temperature on the combined adsorbents of magnesium-aluminum hydrotalcite and 1,3,5-trimethyl-2,4,6-tris(3,5-di-tert-butyl-4-hydroxybenzyl) benzene in a ratio of 1:2 respectively in suppressing oxidation in a blend of 80 % base oil and 20 % rapeseed oil methyl ester	148
8.2.1	Size Exclusion Chromatography (SEC)	148
8.2.2	The acid value of 80 % base oil blended with 20 % RME and treated with and without combined adsorbents of magnesium-aluminum hydrotalcite and 1,3,5-trimethyl-2,4,6-tris(3,5-di-tert-butyl-4-hydroxybenzyl) benzene in a ratio of 1:2 respectively and aged at temperatures of 70 °C, 110 °C, 140 °C and 170 °C with airflow of 10 L/h for 8 h per day for a total of 80 h with Rancimat and compared with the neat unaged blend	153

8.2.3	Effect of adsorbents on the viscosity of 80 % base oil blended with 20 % RME and treated with and without combined adsorbents of magnesium-aluminum hydrotalcite and 1,3,5-trimethyl-2,4,6-tris(3,5-di-tert-butyl-4-hydroxybenzyl) benzene in a ratio of 1:2 respectively and aged at temperatures of 70 °C, 110 °C, 140 °C and 170 °C with airflow of 10 L/h for 8 h per day for a total of 80 h with Rancimat and compared with the neat unaged blend	155
8.2.4	Impact of combined adsorbents of magnesium-aluminum hydrotalcite and 1,3,5-trimethyl-2,4,6-tris(3,5-di-tert-butyl-4-hydroxybenzyl) benzene in a ratio of 1:2 respectively on the density of 80 % base oil blended with 20 % RME and treated with and without the adsorbents and aged at temperatures of 70 °C, 110 °C, 140 °C and 170 °C with airflow of 10 L/h for 8 h per day for a total of 80 h with Rancimat and compared with the neat unaged blend	158
8.2.5	FTIR evaluation of neat and aged 80 % base oil blended with 20 % RME and treated with and without combined adsorbents of magnesium-aluminum hydrotalcite and 1,3,5-trimethyl-2,4,6-tris(3,5-di-tert-butyl-4-hydroxybenzyl) benzene in a ratio of 1:2 respectively and aged at temperatures of 70 °C, 110 °C, 140 °C and 170 °C with airflow of 10 L/h at 8 h per day for 80 h with Rancimat	161
8.3	Investigating the effect of the amount of combined adsorbents magnesium-aluminum hydrotalcite and 1,3,5-trimethyl-2,4,6-tris(3,5-di-tert-butyl-4-hydroxybenzyl) benzene in a ratio of 1:2 respectively in suppressing oxidation in rapeseed oil methyl ester and base oil blend	171
8.3.1	GCMS analysis of 80 %base oil blended with 20 % RME biodiesel treated with and without combined adsorbents magnesium-aluminum hydrotalcite and 1,3,5-trimethyl-2,4,6-tris(3,5-di-tert-butyl-4-hydroxybenzyl) benzene in a ratio of 1:2 respectively and aged at 170 °C with airflow of 10 L/h at 8 h per day for a total of 80 h using the Rancimat	171
8.3.2	Size exclusion chromatography (SEC) analysis of 80 %base oil blended with 20 % RME biodiesel treated with and without combined adsorbents magnesium-aluminum hydrotalcite and 1,3,5-trimethyl-2,4,6-tris(3,5-di-tert-butyl-4-hydroxybenzyl) benzene in a ratio of 1:2 respectively and aged at 170 °C with airflow of 10 L/h for 80 h using the Rancimat	175
8.3.3	Acid value	180
8.3.4	Viscosity	182
8.3.5	Density	186
8.3.6	FTIR evaluation of 30 mL 80 %base oil blended with 20 % RME biodiesel treated with and without various amounts of combined adsorbents magnesium-aluminum hydrotalcite and 1,3,5-trimethyl-2,4,6-tris(3,5-di-tert-butyl-4-hydroxybenzyl) benzene in a ratio of 1:2 respectively and aged at 170 °C with airflow of 10 L/h for 80 h using a Rancimat	187

8.3.7	Impact of adsorbents on metallic oil additives	194
8.3.8	Impact of adsorbent on organic additives in the oil	200
8.4	Using combined adsorbents of magnesium-aluminum hydrotalcite and 1, 3,5-trimethyl-2,4,6-tris(3,5-di-tert-butyl-4-hydroxybenzyl) benzene in a ratio of 1:2 respectively to cause stabilization of biodiesel and its blends at 170 °C	209
8.4.1	SEC analysis of biodiesel blends (20 %RME mixed with 80 %diesel fuel) treated with and without 1 g combined adsorbents of magnesium-aluminum hydrotalcite and 1,3,5-trimethyl-2,4,6-tris(3,5-di-tert-butyl-4-hydroxybenzyl) benzene in a ratio of 1:2 respectively and aged at 170 °C with airflow of 10 L/h using a Rancimat.....	209
8.4.2	GCMS analysis of 80 %diesel fuel mixed with 20 %RME treated with and without combined 1 g adsorbents of magnesium-aluminum hydrotalcite and 1,3,5-trimethyl-2,4,6-tris(3,5-di-tert-butyl-4-hydroxybenzyl) benzene in a ratio of 1:2 respectively and aged at 170 °C with airflow of 10 L/h for 48 h at 8 h per day using a Rancimat.....	213
8.4.3	The total acid value of 80 %diesel fuel mixed with 20 %RME treated with and without combined 1 g adsorbents of magnesium-aluminum hydrotalcite and 1,3,5-trimethyl-2,4,6-tris(3,5-di-tert-butyl-4-hydroxybenzyl) benzene in a ratio of 1:2 respectively and aged at 170 °C with airflow of 10 L/h for 48 h at 8 h per day using a Rancimat.....	215
8.4.4	Results of viscosity of 80 %diesel fuel mixed with 20 %RME treated with and without combined 1 g adsorbents of magnesium-aluminum hydrotalcite and 1,3,5-trimethyl-2,4,6-tris(3,5-di-tert-butyl-4-hydroxybenzyl) benzene in a ratio of 1:2 respectively and aged at 170 °C with airflow of 10 L/h for 48 h at 8 h per day using a Rancimat.....	217
8.4.5	Effect of combined adsorbents of magnesium-aluminum hydrotalcite and 1,3,5-trimethyl-2,4,6-tris(3,5-di-tert-butyl-4-hydroxybenzyl) benzene in a ratio of 1:2 respectively on the density of 80 %diesel fuel mixed with 20 %RME and aged at 170 °C with airflow of 10 L/h for 48 h at 8 h per day using a Rancimat.....	221
8.4.6	Interrelationships between acid value, viscosity, and density of 80 %diesel fuel mixed with 20 %RME treated with and without combined 1 g adsorbents of magnesium-aluminum hydrotalcite and 1,3,5-trimethyl-2,4,6-tris(3,5-di-tert-butyl-4-hydroxybenzyl) benzene in a ratio of 1:2 respectively and aged at 170 °C with airflow of 10 L/h for 48 h at 8 h per day using a Rancimat	223
8.4.7	FTIR analysis of 80 %diesel fuel mixed with 20 %RME treated with and without combined 1 g adsorbents of magnesium-aluminum hydrotalcite and 1,3,5-trimethyl-2,4,6-tris(3,5-di-tert-butyl-4-hydroxybenzyl) benzene in a ratio of 1:2 respectively and aged at 170 °C with airflow of 10 L/h for 48 h at 8 h per day using a Rancimat.....	226

8.5	Stabilization of biodiesel and its blends at 110 °C using 0.225 g combined adsorbents of magnesium-aluminum hydrotalcite and 1,3,5-trimethyl-2,4,6-tris(3,5-di-tert-butyl-4-hydroxybenzyl) benzene in a ratio of 1:2, respectively.....	232
8.5.1	Induction period measurements.....	233
8.5.2	SEC analysis of 30 mL 20 % RME mixed with 80 % diesel fuel treated with and without 0.225 g combined adsorbents of magnesium-aluminum hydrotalcite and 1,3,5-trimethyl-2,4,6-tris(3,5-di-tert-butyl-4-hydroxybenzyl) benzene in a ratio of 1:2 respectively using a Rancimat at 110 °C with airflow of 10 L/h at 8 h per day	234
8.5.3	Effect of combined adsorbents of magnesium-aluminum hydrotalcite and 1,3,5-trimethyl-2,4,6-tris(3,5-di-tert-butyl-4-hydroxybenzyl) benzene in a ratio of 1:2 respectively on the acid value of 20 %RME and 80 % diesel fuel blend during the oxidation process	236
8.5.4	Impact of combined adsorbents of magnesium-aluminum hydrotalcite and 1,3,5-trimethyl-2,4,6-tris(3,5-di-tert-butyl-4-hydroxybenzyl) benzene in a ratio of 1:2 respectively on the viscosity of biodiesel blend during aging at 110 °C	238
8.5.5	Analysis of the impact of combined adsorbents of magnesium-aluminum hydrotalcite and 1,3,5-trimethyl-2,4,6-tris(3,5-di-tert-butyl-4-hydroxybenzyl) benzene in a ratio of 1:2 respectively on the density of biodiesel blend during aging at 110 °C	241
8.5.6	Relationship between viscosity and an acid value of 20 % RME mixed with 80 % diesel fuel and treated with and without combined 0.225 g adsorbents of magnesium-aluminum hydrotalcite and 1,3,5-trimethyl-2,4,6-tris(3,5-di-tert-butyl-4-hydroxybenzyl) benzene in a ratio of 1:2 respectively and aged at 110 °C with airflow of 10 L/h for durations of 20 h, 40 h, 60 h, and 80 h at 8 h per day using a Rancimat.....	243
8.5.7	FTIR analysis of 30 mL 20 % RME mixed with 80 % diesel fuel and treated with 0.225 g combined adsorbents of magnesium-aluminum hydrotalcite and 1,3,5-trimethyl-2,4,6-tris(3,5-di-tert-butyl-4-hydroxybenzyl) benzene in a ratio of 1:2 respectively and aged at 110 °C with airflow of 10 L/h at 8 h per day for durations of 20 h, 40 h, 60 h and 80 h using a Rancimat.....	245
8.6	Investigating the effect of the combined adsorbents of magnesium-aluminum hydrotalcite and 1,3,5-trimethyl-2,4,6-tris(3,5-di-tert-butyl-4-hydroxybenzyl) benzene in a ratio of 1:2 respectively in stabilizing rapeseed oil methyl ester and its blends during long term storage conditions	253
8.6.1	Evaluation of induction period of neat biodiesel	253
8.6.2	The induction period of biodiesel blends	254
8.6.3	SEC analysis of aged 40 mL of 80 %diesel fuel blended with 20 %RME treated with and without 0.675 g of combined adsorbents of magnesium-aluminum	

hydrotalcite and 1,3,5-trimethyl-2,4,6-tris(3,5-di-tert-butyl-4-hydroxybenzyl) benzene in a ratio of 1:2 respectively and stored at 40 °C in an oven from 0 up to 120 days	256
8.6.4 Assessment of total acid values of 40 mL of biodiesel treated with and without 0.675 g of combined adsorbents of magnesium-aluminum hydrotalcite and 1,3,5-trimethyl-2,4,6-tris(3,5-di-tert-butyl-4-hydroxybenzyl) benzene in a ratio of 1:2 respectively stored at 40 °C from 0 up to 120 days.....	257
8.6.5 Evaluation of total acid values of 80 %diesel fuel blended with 20 %RME treated with and without 0.675 g of combined adsorbents of magnesium-aluminum hydrotalcite and 1,3,5-trimethyl-2,4,6-tris(3,5-di-tert-butyl-4-hydroxybenzyl) benzene in a ratio of 1:2 respectively and stored at 40 °C from 0 up to 120 days	259
8.6.6 Impact assessment of combined adsorbents of magnesium-aluminum hydrotalcite and 1,3,5-trimethyl-2,4,6-tris(3,5-di-tert-butyl-4-hydroxybenzyl) benzene in a ratio of 1:2 respectively on the viscosity of 80 % diesel fuel blended with 20 %RME	261
8.6.7 Investigation of the effect of the combined adsorbents of 0.675 g magnesium-aluminum hydrotalcite and 1,3,5-trimethyl-2,4,6-tris(3,5-di-tert-butyl-4-hydroxybenzyl) benzene in a ratio of 1:2 respectively on the density of 40 mL 80 % diesel fuel blended with 20 %RME stored in an oven at 40 °C for 120 days.....	264
8.6.8 FTIR analysis of neat biodiesel treated with and without combined 0.675 g adsorbents of magnesium-aluminum hydrotalcite and 1,3,5-trimethyl-2,4,6-tris(3,5-di-tert-butyl-4-hydroxybenzyl) benzene in a ratio of 1:2 respectively and stored at 40 °C in the oven for up to 120 days	267
8.6.9 FTIR analysis of biodiesel blends, 80 %diesel fuel mixed with 20 %RME treated with and without combined 0.675 g adsorbents of magnesium-aluminum hydrotalcite and 1,3,5-trimethyl-2,4,6-tris(3,5-di-tert-butyl-4-hydroxybenzyl) benzene in a ratio of 1:2 respectively and stored at 40 °C in an oven for up to 120 days....	269
8.7 Confirmation of suppression of oligomers formation.....	273
8.7.1 Effect of 0.675 g combined adsorbents of magnesium-aluminum hydrotalcite and 1,3,5-trimethyl-2,4,6-tris(3,5-di-tert-butyl-4-hydroxybenzyl) benzene in a ratio of 1:2 respectively on relative permittivity of 80 % base oil blended with 20 % RME and aged at 170°C	273
8.7.2 The dissipation factor	276
8.7.3 Acid value	277
8.7.4 NMR.....	279
9 Conclusion, outlook, and recommendation	290
9.1 Conclusion.....	290

Table of Content

9.2 Outlook and Recommendation 294

Bibliography..... 296

10 Appendix..... 323

11 Glossary..... 332

List of Figures

Figure 1: Transesterification process for biodiesel production (Abdullah, 2007)..... 44

Figure 2: Autoxidative formation of hydroperoxides as primary oxidation products of oleic acid (Schumacher, 2013)..... 46

Figure 3 Autoxidative formation of hydroperoxides as primary oxidation products of linoleic acid (Schumacher, 2013). 47

Figure 4 Autoxidation formation of hydroperoxides as primary oxidation products of linolenic acid (Schumacher, 2013) 48

Figure 5 Oxidative degradation of hydrocarbon (Ancho, 2006) 57

Figure 6 Oxidation of base oil (Adhvaryu et al. 1998)..... 61

Figure 7: Flow chart of lubricant degradation process under oxidative conduction (Rasberger, 1992)..... 62

Figure 8 Short-chain acid formation (Adapted with permission from Brühl, 2014) 64

Figure 9: Distillation temperature characteristics of biodiesel and diesel fuel (Krahl et al., 2012)..... 66

Figure 10: Typical FTIR spectra showing the spectral differences between neat or original (green line) sample of 20 % biodiesel mixed with 80 % base oil and the aged (red line) sample at 170 °C airflows of 10L/h for 80 h showing the O-H and C=O bands 75

Figure 11: Molecular structure of Ethanox 330, the suppressing agent (Van Lierop et al., 1998)..... 90

Figure 12 The mechanism of the hydrotalcite compound (Endres et al., 1991)..... 92

Figure 13: FTIR spectra of 20 % RME mixed with 80 % base oil treated with and without separate and combined (adsorbent in a ratio of 1:2) the hydrotalcite compound and radical trapping agent (1, 3, 5-trimethyl-2, 4, 6-tris (3, 5-di-tert-butyl-4-hydroxybenzyl) benzene) and aged at 170 °C with an airflow of 10 L/h for 80 h using a Rancimat..... 94

Figure 14: Zoom in on the area of carbonyl vibrations of Figure 13, FTIR spectra of 20 % RME mixed with 80 % base oil treated with and without separate and combined (adsorbent in a ratio of 1:2) the hydrotalcite compound and radical trapping agent (1, 3, 5-trimethyl-2, 4, 6-tris (3, 5-di-tert-butyl-4-hydroxybenzyl) benzene) and aged at 170 °C with an airflow of 10 L/h for 80 h using a Rancimat..... 95

Figure 15: Zoom in on an area of hydroxyl vibrations of Figure 13, FTIR spectra of 20 % RME mixed with 80 % base oil treated with and without separate and combined (adsorbent in a ratio of 1:2) the hydrotalcite compound and radical trapping agent (1, 3, 5-trimethyl-2, 4, 6-tris (3, 5-di-tert-butyl-4-hydroxybenzyl) benzene) and aged at 170 °C with an airflow of 10 L/h for 80 h using a Rancimat..... 96

Figure 16 The acid value of 30 mL 20 % RME mixed with 80 % Base oil and treated with combined 0,675 g adsorbents of magnesium-aluminum hydrotalcite and 1,3,5-trimethyl-2,4,6-tris(3,5-di-tert-butyl-4-hydroxybenzyl) benzene in a ratio of 1:2

respectively and aged at 170°C with airflow of 10 L/h at 8 h per day in a Rancimat for about 300 h.....	102
Figure 17: Evaluation of peak area under C=O bands (1600-1900 cm ⁻¹) of the FTIR spectrum of 30 mL 20 % RME mixed with 80 % Base oil and treated with and without combined 0,675 g adsorbents of magnesium-aluminum hydrotalcite and 1,3,5-trimethyl-2,4,6-tris(3,5-di-tert-butyl-4-hydroxybenzyl) benzene in a ratio of 1:2 respectively and aged at 170°C with airflow of 10 L/h at 8 h per day in a Rancimat for about 300 h.....	104
Figure 18 Laboratory assembled aging apparatus	111
Figure 19 Investigations on the suppression of oligomers formation	113
Figure 20 Experimental investigations on stabilization of biodiesel and its blends	118
Figure 21: Evaluation of GC-chromatogram of 98.4 % base oil blended with 1.6 % C18_2 ME treated with and without combined 0.675 g adsorbents of magnesium-aluminum hydrotalcite and 1,3,5-trimethyl-2,4,6-tris(3,5-di-tert-butyl-4-hydroxybenzyl) benzene in a ratio of 1:2 respectively and aged at 170 °C with airflow of 10L/h for 8 h per day for a total of 80 h with Rancimat compared with the neat blend	134
Figure 22: Evaluation of SEC of 98.4 % base oil blended with 1.6 % C18_2 ME treated with and without combined 0.675 g adsorbents of magnesium-aluminum hydrotalcite and 1,3,5-trimethyl-2,4,6-tris(3,5-di-tert-butyl-4-hydroxybenzyl) benzene in a ratio of 1:2 respectively and aged at 170 °C with airflow of 10 L/h for 8 h per day for a total of 80 h with Rancimat compared with the neat blend.....	136
Figure 23: Zoom in on the higher molecular mass area of SEC of 98.4 % base oil blended with 1.6 % C18_2 ME treated with and without combined 0.675 g adsorbents of magnesium-aluminum hydrotalcite and 1,3,5-trimethyl-2,4,6-tris(3,5-di-tert-butyl-4-hydroxybenzyl) benzene in a ratio of 1:2 respectively and aged at 170 °C with airflow of 10 L/h for 8 h per day for a total of 80 h with Rancimat compared with the neat blend	137
Figure 24: Evaluation of FTIR spectra in absorbance mode (range 1500-4000 cm ⁻¹) of 98.4 % base oil blended with 1.6 % C18_2 ME treated with and without 0.675 g combined adsorbents of magnesium-aluminum hydrotalcite and 1,3,5-trimethyl-2,4,6-tris(3,5-di-tert-butyl-4-hydroxybenzyl) benzene in a ratio of 1:2 respectively and aged at 170 °C with airflow of 10 L/h for 8 h per day for a total of 80 h with Rancimat compared with the neat blend	139
Figure 25: Evaluation of FTIR spectra in absorbance mode (range 1500-1900 cm ⁻¹) of 98.4 % base oil mixed with 1.6 % C18_2 ME treated with and without combined 0.675 g adsorbents of magnesium-aluminum hydrotalcite and 1,3,5-trimethyl-2,4,6-tris(3,5-di-tert-butyl-4-hydroxybenzyl) benzene in a ratio of 1:2 respectively and aged at 170 °C with airflow of 10 L/h for 8 h per day for a total of 80 h with Rancimat compared with the neat blend	141
Figure 26: Evaluation of FTIR spectra in absorbance mode (range 3000-3600 cm ⁻¹) of 98.4 % base oil mixed with 1.6 % C18_2 ME treated with and without combined	

0.675 g adsorbents of magnesium-aluminum hydrotalcite and 1,3,5-trimethyl-2,4,6-tris(3,5-di-tert-butyl-4-hydroxybenzyl) benzene in a ratio of 1:2 respectively and aged at 170 °C with airflow of 10 L/h for 8 h per day for a total of 80 h with Rancimat compared with the neat blend	142
Figure 27: Evaluation of peak area under C=O bands (1600-1900 cm ⁻¹) of the FTIR spectrum of 98.4 % base oil mixed with 1.6 % C18_2 ME treated with and without combined 0.675 g adsorbents of magnesium-aluminum hydrotalcite and 1,3,5-trimethyl-2,4,6-tris(3,5-di-tert-butyl-4-hydroxybenzyl)benzene in a ratio of 1:2 respectively and aged at 170 °C with airflow of 10 L/h for 8 h per day for a total of 80 h with Rancimat compared with the neat blend.....	143
Figure 28: Evaluation of acid values of 98.4 % base oil blended with 1.6 % C18_2 ME treated with and without combined 0.675 g adsorbents of magnesium-aluminum hydrotalcite and 1,3,5-trimethyl-2,4,6-tris(3,5-di-tert-butyl-4-hydroxybenzyl) benzene in a ratio of 1:2 respectively and aged at 170 °C with airflow of 10 L/h for 8 h per day for a total of 80 h with Rancimat compared with the neat blend.....	145
Figure 29: Evaluation of SEC of 30 mL 80 % base oil blended with 20 % RME and treated with and without combined 0.675 g adsorbents of magnesium-aluminum hydrotalcite and 1,3,5-trimethyl-2,4,6-tris(3,5-di-tert-butyl-4-hydroxybenzyl) benzene in a ratio of 1:2 respectively and aged at temperatures of 70 °C, 110 °C, 140 °C and 170 °C with airflow of 10 L/h for 8 h per day for a total of 80 h with Rancimat and compared with the neat unaged blend	150
Figure 30: Zoom in on the area of higher molar mass substances of SEC of 30 mL 80 % base oil blended with 20 % RME and treated with and without combined 0.675 g adsorbents of magnesium-aluminum hydrotalcite and 1,3,5-trimethyl-2,4,6-tris(3,5-di-tert-butyl-4-hydroxybenzyl) benzene in a ratio of 1:2 respectively and aged at temperatures of 70 °C, 110 °C, 140 °C and 170 °C with airflow of 10 L/h for 8 h per day for a total of 80 h with Rancimat and compared with the neat unaged blend .	151
Figure 31 Calculated area of higher molecular mass substances buildup of SEC of 30 mL 80 % base oil blended with 20 % RME and treated with and without combined 0.675 g adsorbents of magnesium-aluminum hydrotalcite and 1,3,5-trimethyl-2,4,6-tris(3,5-di-tert-butyl-4-hydroxybenzyl) benzene in a ratio of 1:2 respectively and aged at temperatures of 70 °C, 110 °C, 140 °C and 170 °C with airflow of 10 L/h for 8 h per day for a total of 80 h with Rancimat and compared with the neat unaged blend	152
Figure 32: Evaluation of acid values of 30 mL 80 % base oil blended with 20 % RME and treated with and without combined 0.675 g adsorbents of magnesium-aluminum hydrotalcite and 1,3,5-trimethyl-2,4,6-tris(3,5-di-tert-butyl-4-hydroxybenzyl) benzene in a ratio of 1:2 respectively and aged at temperatures of 70 °C, 110 °C, 140 °C and 170 °C with airflow of 10 L/h for 8 h per day for a total of 80 h with Rancimat and compared with the neat unaged blend	154
Figure 33: Evaluation of kinetic viscosity at 40°C of 30 mL 80 % base oil blended with 20 % RME and treated with and without combined 0.675 g adsorbents of	

magnesium-aluminum hydrotalcite and 1,3,5-trimethyl-2,4,6-tris(3,5-di-tert-butyl-4-hydroxybenzyl) benzene in a ratio of 1:2 respectively and aged at temperatures of 70 °C, 110 °C, 140 °C and 170 °C with airflow of 10 L/h for 8 h per day for a total of 80 h with Rancimat and compared with the neat unaged blend 157

Figure 34: Evaluation of kinetic viscosity at 100 °C of 30 mL 80 % base oil blended with 20 % RME and treated with and without combined 0.675 g adsorbents of magnesium-aluminum hydrotalcite and 1,3,5-trimethyl-2,4,6-tris(3,5-di-tert-butyl-4-hydroxybenzyl) benzene in a ratio of 1:2 respectively and aged at temperatures of 70 °C, 110 °C, 140 °C and 170 °C with airflow of 10 L/h for 8 h per day for a total of 80 h with Rancimat and compared with the neat unaged blend 158

Figure 35: Evaluation of density at 40 °C of 30 mL 80 % base oil blended with 20 % RME and treated with and without combined 0.675 g adsorbents of magnesium-aluminum hydrotalcite and 1,3,5-trimethyl-2,4,6-tris(3,5-di-tert-butyl-4-hydroxybenzyl) benzene in a ratio of 1:2 respectively and aged at temperatures of 70 °C, 110 °C, 140 °C and 170 °C with airflow of 10 L/h for 8 h per day for a total of 80 h with Rancimat and compared with the neat unaged blend 160

Figure 36: Evaluation of density at 100°C of 30 mL 80 % base oil blended with 20 % RME and treated with and without combined 0.675 g adsorbents of magnesium-aluminum hydrotalcite and 1,3,5-trimethyl-2,4,6-tris(3,5-di-tert-butyl-4-hydroxybenzyl) benzene in a ratio of 1:2 respectively and aged at temperatures of 70 °C, 110 °C, 140 °C and 170 °C with airflow of 10 L/h for 8 h per day for a total of 80 h with Rancimat and compared with the neat unaged blend 161

Figure 37: Evaluation of FTIR spectra in absorbance mode (range 600-4000cm⁻¹) of 30 mL 80 % base oil blended with 20 % RME and treated with and without combined 0.675 g adsorbents of magnesium-aluminum hydrotalcite and 1,3,5-trimethyl-2,4,6-tris(3,5-di-tert-butyl-4-hydroxybenzyl) benzene in a ratio of 1:2 respectively and aged at temperatures of 70 °C, 110 °C, 140 °C and 170 °C with airflow of 10 L/h for 8 h per day for a total of 80 h with Rancimat and compared with the neat unaged blend 164

Figure 38: FTIR spectra in absorbance mode (range 1500-1900cm⁻¹) of 30 mL 80 % base oil blended with 20 % RME and treated with and without combined 0.675 g adsorbents of magnesium-aluminum hydrotalcite and 1,3,5-trimethyl-2,4,6-tris(3,5-di-tert-butyl-4-hydroxybenzyl) benzene in a ratio of 1:2 respectively and aged at temperatures of 70 °C, 110 °C, 140 °C and 170 °C with airflow of 10 L/h for 8 h per day for a total of 80 h with Rancimat and compared with the neat unaged blend . 165

Figure 39: FTIR spectra in absorbance mode (range 3000-3600cm⁻¹) of 30 mL 80 % base oil blended with 20 % RME and treated with and without combined 0.675 g adsorbents of magnesium-aluminum hydrotalcite and 1,3,5-trimethyl-2,4,6-tris(3,5-di-tert-butyl-4-hydroxybenzyl) benzene in a ratio of 1:2 respectively and aged at temperatures of 70 °C, 110 °C, 140 °C and 170 °C with airflow of 10 L/h for 8 h per day for a total of 80 h with Rancimat and compared with the neat unaged blend . 166

Figure 40: Evaluation of peak area under C=O bands ($1600-1900\text{ cm}^{-1}$) of the FTIR spectra of 30 mL 80 % base oil blended with 20 % RME and treated with and without combined 0.675 g adsorbents of magnesium-aluminum hydrotalcite and 1,3,5-trimethyl-2,4,6-tris(3,5-di-tert-butyl-4-hydroxybenzyl) benzene in a ratio of 1:2 respectively and aged at temperatures of 70 °C, 110 °C, 140 °C and 170 °C with airflow of 10 L/h for 8 h per day for a total of 80 h with Rancimat and compared with the neat unaged blend 168

Figure 41: GC-chromatogram evaluation of 30 mL 80 % base oil mixed with 20 % RME treated with and without combined adsorbents of magnesium-aluminum hydrotalcite and 1,3,5-trimethyl-2,4,6-tris(3,5-di-tert-butyl-4-hydroxybenzyl) benzene in a ratio of 1:2 respectively and aged at 170°C with airflow of 10 L/h for 80 h with Rancimat and compared with the neat unaged blend 173

Figure 42: Zoom in on figure 40 GC-chromatogram evaluation of 30 mL 80 % base oil mixed with 20 % RME treated with and without combined adsorbents of magnesium-aluminum hydrotalcite and 1,3,5-trimethyl-2,4,6-tris(3,5-di-tert-butyl-4-hydroxybenzyl) benzene in a ratio of 1:2 respectively and aged at 170°C with airflow of 10 L/h for 80 h with Rancimat and compared with the neat unaged blend 174

Figure 43: SEC evaluation of 30 mL 80 % base oil mixed with 20 % RME treated with and without combined adsorbents of magnesium-aluminum hydrotalcite and 1,3,5-trimethyl-2,4,6-tris(3,5-di-tert-butyl-4-hydroxybenzyl) benzene in a ratio of 1:2 respectively and aged at 170 °C with airflow of 10 L/h for 80 h with Rancimat and compared with the neat unaged blend 177

Figure 44: SEC evaluation (range: 680-1280 g/mol) of 30 mL 80 % base oil blended with 20 % RME treated with and without combined adsorbents of magnesium-aluminum hydrotalcite and 1,3,5-trimethyl-2,4,6-tris(3,5-di-tert-butyl-4-hydroxybenzyl) benzene in a ratio of 1:2 respectively and aged at 170 °C with airflow of 10 L/h for 80 h with Rancimat and compared with the neat unaged blend 178

Figure 45: Calculated area of SEC of 30 mL 80 % base oil mixed with 20 % RME treated with and without combined adsorbents of magnesium-aluminum hydrotalcite and 1,3,5-trimethyl-2,4,6-tris(3,5-di-tert-butyl-4-hydroxybenzyl) benzene in a ratio of 1:2 respectively and aged at 170°C with airflow of 10 L/h for 80 h with Rancimat compared with the neat unaged blend 179

Figure 46: Evaluation of acid values of 30 mL 80 % base oil mixed with 20 % RME treated with and without combined adsorbents of magnesium-aluminum hydrotalcite and 1,3,5-trimethyl-2,4,6-tris(3,5-di-tert-butyl-4-hydroxybenzyl) benzene in a ratio of 1:2 respectively and aged at 170°C with airflow of 10 L/h for 80 h with Rancimat and compared with the neat unaged blend 182

Figure 47: Evaluation of viscosity gradient of 40 mL 80 % base oil mixed with 20 % RME treated with and without combined adsorbents of magnesium-aluminum hydrotalcite and 1,3,5-trimethyl-2,4,6-tris(3,5-di-tert-butyl-4-hydroxybenzyl) benzene in a ratio of 1:2 respectively and aged at 170°C with airflow of 10 L/h for 80 h with Rancimat 184

Figure 48: Evaluation of viscosity index of 30 mL 80 % base oil mixed with 20 % RME treated with and without combined adsorbents of magnesium-aluminum hydrotalcite and 1,3,5-trimethyl-2,4,6-tris(3,5-di-tert-butyl-4-hydroxybenzyl) benzene in a ratio of 1:2 respectively and aged at 170°C with airflow of 10 L/h for 80 h with Rancimat compared with the neat unaged blend 185

Figure 49: Evaluation of density at 40°C of 30 mL 80 % base oil mixed with 20 % RME treated with and without combined adsorbents of magnesium-aluminum hydrotalcite and 1,3,5-trimethyl-2,4,6-tris(3,5-di-tert-butyl-4-hydroxybenzyl) benzene in a ratio of 1:2 respectively and aged at 170°C with airflow of 10 L/h for 80 h with Rancimat 187

Figure 50: FTIR spectra in absorbance mode (range 600-4000cm⁻¹) of 30 mL 80 % base oil mixed with 20 % RME treated with and without combined adsorbents of magnesium-aluminum hydrotalcite and 1,3,5-trimethyl-2,4,6-tris(3,5-di-tert-butyl-4-hydroxybenzyl) benzene in a ratio of 1:2 respectively in various amounts and aged at 170 °C with airflow of 10 L/h for 80 h using Rancimat..... 189

Figure 51: FTIR spectra in absorbance mode (range 1500-1900cm⁻¹) of 30 mL 80 % base oil mixed with 20 % RME treated with and without combined adsorbents of magnesium-aluminum hydrotalcite and 1,3,5-trimethyl-2,4,6-tris(3,5-di-tert-butyl-4-hydroxybenzyl) benzene in a ratio of 1:2 respectively in various amounts and aged at 170 °C with airflow of 10 L/h for 80 h using Rancimat..... 190

Figure 52: Evaluation of peak area under C=O bands (1600-1900 cm⁻¹) of the FTIR spectra of 30 mL 80 % base oil mixed with 20 % RME treated with and without various amounts of combined adsorbents of magnesium-aluminum hydrotalcite and 1,3,5-trimethyl-2,4,6-tris(3,5-di-tert-butyl-4-hydroxybenzyl) benzene in a ratio of 1:2 respectively in various amount and aged at 170 °C with airflow of 10 L/h for 80 h using Rancimat 191

Figure 53: FTIR spectra in absorbance mode (range 3000-3600cm⁻¹) of 30 mL 80 % base oil mixed with 20 % RME treated with and without combined adsorbents of magnesium-aluminum hydrotalcite and 1,3,5-trimethyl-2,4,6-tris(3,5-di-tert-butyl-4-hydroxybenzyl) benzene in a ratio of 1:2 respectively in various amounts and aged at 170 °C with airflow of 10 L/h for 80 h using Rancimat..... 193

Figure 54: Evaluation of peak area under O-H bands (3000-3600 cm⁻¹) of the FTIR spectra of 30 mL 80 % base oil mixed with 20 % RME treated with and without various amounts of combined adsorbents of magnesium-aluminum hydrotalcite and 1,3,5-trimethyl-2,4,6-tris(3,5-di-tert-butyl-4-hydroxybenzyl) benzene in a ratio of 1:2 respectively in various amount and aged at 170 °C with airflow of 10 L/h for 80 h using a Rancimat 194

Figure 55: Evaluation of concentration of selected elements in 30 mL Mannol engine oil treated with and without combined 0.675 g adsorbents of magnesium-aluminum hydrotalcite and 1,3,5-trimethyl-2,4,6-tris(3,5-di-tert-butyl-4-hydroxybenzyl) benzene in a ratio of 1:2 respectively and aged at 170 °C with airflow of 10 L/h for 48 h using a Rancimat..... 196

Figure 56: Concentration of selected elements in 30 mL of B20 mixed with VanlubeBHC additive treated with and without combined 0.675 g adsorbents of magnesium-aluminum hydrotalcite and 1,3,5-trimethyl-2,4,6-tris(3,5-di-tert-butyl-4-hydroxybenzyl) benzene in a ratio of 1:2 respectively and aged at 170 °C with airflow of 10 L/h for 60 h using a Rancimat 197

Figure 57: Concentration of selected elements in 30 mL base oil blended with BHT additive treated with and without combined 0.675 g adsorbents of magnesium-aluminum hydrotalcite and 1,3,5-trimethyl-2,4,6-tris(3,5-di-tert-butyl-4-hydroxybenzyl) benzene in a ratio of 1:2 respectively and aged at 170 °C with airflow of 10 L/h for 50 h using a Rancimat 198

Figure 58: Concentration of selected elements in 30 mL base oil blended with detergent and treated with and without the combined 0.675 g adsorbents of magnesium-aluminum hydrotalcite and 1,3,5-trimethyl-2,4,6-tris(3,5-di-tert-butyl-4-hydroxybenzyl) benzene in a ratio of 1:2 respectively and aged at 170 °C with airflow of 10 L/h for 50 h using a Rncimat 199

Figure 59: Concentration of selected elements in 30 mL base oil blended with corrosion inhibitor additive treated with and without combined 0.675 g adsorbents of magnesium-aluminum hydrotalcite and 1,3,5-trimethyl-2,4,6-tris(3,5-di-tert-butyl-4-hydroxybenzyl) benzene in a ratio of 1:2 respectively and aged at 170 °C with airflow of 10 L/h for 50 h using a Rancimat 200

Figure 60: GC-FID chromatogram of 30 mL of 80 % base oil blended with 20 %RME and mixed with VanlubeBHC neat additive treated with and without combined 0.675 g adsorbents of magnesium-aluminum hydrotalcite and 1,3,5-trimethyl-2,4,6-tris(3,5-di-tert-butyl-4-hydroxybenzyl) benzene in a ratio of 1:2 respectively and aged at 170 °C with airflow of 10 L/h at 8 h per day for 80 h using a Rancimat..... 202

Figure 61: GC-FID chromatogram of 30 mL of 80 % base oil blended with 20 %RME and mixed with VanlubeBHC neat additive treated with and without combined 0.675 g adsorbents of magnesium-aluminum hydrotalcite and 1,3,5-trimethyl-2,4,6-tris(3,5-di-tert-butyl-4-hydroxybenzyl) benzene in a ratio of 1:2 respectively and aged at 170 °C with airflow of 10 L/h at 8 h per day for 80 h using a Rancimat 203

Figure 62: GCFID chromatogram of 30 mL of base oil blended with Vanlube961 additive treated with combined adsorbents of magnesium-aluminum hydrotalcite and 1,3,5-trimethyl-2,4,6-tris(3,5-di-tert-butyl-4-hydroxybenzyl) benzene in a ratio of 1:2 respectively and aged at 170°C with airflow of 10 L/h at 8 h per day for 40 h using a Rancimat..... 204

Figure 63: GCFID chromatogram of 30 mL of base oil blended with Vanlube961 and treated with and without the combined 0.675 g adsorbents of magnesium-aluminum hydrotalcite and 1,3,5-trimethyl-2,4,6-tris(3,5-di-tert-butyl-4-hydroxybenzyl) benzene in a ratio of 1:2 respectively and aged at 170 °C with airflow of 10 L/h at 8 h per day for 40 h using a Rancimat 205

Figure 64: GCFID chromatogram of 30 mL of lubricity additive mixed with a base oil and treated with and without combined 0.675 g adsorbents of magnesium-aluminum

hydrotalcite and 1,3,5-trimethyl-2,4,6-tris(3,5-di-tert-butyl-4-hydroxybenzyl) benzene in a ratio of 1:2 respectively and aged at 170 °C with airflow of 10 L/h at 8 h per day for 50 h using a Rancimat 206

Figure 65: SEC chromatogram of 30 mL 20 %RME mixed with 80 %diesel fuel and treated with and without combined 1 g adsorbents of magnesium-aluminum hydrotalcite and 1,3,5-trimethyl-2,4,6-tris(3,5-di-tert-butyl-4-hydroxybenzyl) benzene in a ratio of 1:2 respectively and aged at 170°C at 8 h per day with airflow of 10 L/h using a Rancimat 210

Figure 66: Zoom in on the region of higher molecular masses of 30 mL 20 %RME mixed with 80 %diesel fuel and treated with and without combined 1 g adsorbents of magnesium-aluminum hydrotalcite and 1,3,5-trimethyl-2,4,6-tris(3,5-di-tert-butyl-4-hydroxybenzyl) benzene in a ratio of 1:2 respectively and aged at 170°C with airflow of 10 L/h at 8 h per day using a Rancimat..... 211

Figure 67: Effective area under the curves of a molecular mass buildup of oligomers of 30 mL 20 %RME mixed with 80 %diesel fuel and treated with and without combined 1 g adsorbents of magnesium-aluminum hydrotalcite and 1,3,5-trimethyl-2,4,6-tris(3,5-di-tert-butyl-4-hydroxybenzyl) benzene in a ratio of 1:2 respectively and aged at 170°C with airflow of 10 L/h at 8 h per day using a Rancimat 212

Figure 68: GCMS chromatogram of 30 mL 80 %diesel fuel mixed with 20 %RME treated with and without combined 1 g adsorbents of magnesium-aluminum hydrotalcite and 1,3,5-trimethyl-2,4,6-tris(3,5-di-tert-butyl-4-hydroxybenzyl) benzene in a ratio of 1:2 respectively and aged at 170 °C with airflow of 10 L/h for 48 h using a Rancimat 214

Figure 69: GCMS chromatogram of 30 mL 80 %diesel fuel blended with 20 %RME (retention time range:33-37 min) treated with and without combined 1 g adsorbents of magnesium-aluminum hydrotalcite and 1,3,5-trimethyl-2,4,6-tris(3,5-di-tert-butyl-4-hydroxybenzyl) benzene in a ratio of 1:2 respectively and aged at 170 °C with airflow of 10 L/h for 48 h at 8 h per day using a Rancimat compared with the neat unaged blend 215

Figure 70: Acid value of 30 mL 20 % RME mixed with 80 % diesel fuel and treated with and without combined 1 g adsorbents of magnesium-aluminum hydrotalcite and 1,3,5-trimethyl-2,4,6-tris(3,5-di-tert-butyl-4-hydroxybenzyl) benzene in a ratio of 1:2 respectively and aged at 170°C with airflow of 10 L/h at 8 h per day in a Rancimat 217

Figure 71: Viscosity at 40 °C of 30 mL 80 % diesel fuel blended with 20 % RME and treated with and without combined 1 g adsorbents of magnesium-aluminum hydrotalcite and 1,3,5-trimethyl-2,4,6-tris(3,5-di-tert-butyl-4-hydroxybenzyl) benzene in a ratio of 1:2 respectively and aged at 170 °C with airflow of 10 L/h at 8 h per day for durations of 12 h, 24 h, 36 h and 48 h using a Rancimat..... 219

Figure 72: Viscosity at 100 °C of 30 mL 80 % diesel fuel blended with 20 % RME and treated with and without combined 1 g adsorbents of magnesium-aluminum hydrotalcite and 1,3,5-trimethyl-2,4,6-tris(3,5-di-tert-butyl-4-hydroxybenzyl) benzene

in a ratio of 1:2 respectively and aged at 170 °C with airflow of 10 L/h at 8 h per day for durations of 12 h, 24 h, 36 h and 48 h using a Rancimat..... 220

Figure 73: Density at 40 °C of 30 mL 80 % diesel fuel blended with 20 % RME and treated with and without combined 1 g adsorbents of magnesium-aluminum hydrotalcite and 1,3,5-trimethyl-2,4,6-tris(3,5-di-tert-butyl-4-hydroxybenzyl) benzene in a ratio of 1:2 respectively and aged at 170 °C with airflow of 10 L/h at 8 h per day for durations of 12 h, 24 h, 36 h and 48 h using a Rancimat compared with a neat unaged blend 222

Figure 74: Density at 100 °C of 30 mL 80 % diesel fuel blended with 20 % RME treated with and without combined 1 g adsorbents of magnesium-aluminum hydrotalcite and 1,3,5-trimethyl-2,4,6-tris(3,5-di-tert-butyl-4-hydroxybenzyl) benzene in a ratio of 1:2 respectively and aged at 170°C with airflow of 10 L/h at 8 h per day for durations of 12 h, 24 h, 36 h and 48 h using a Rancimat compared with the neat unaged blend 223

Figure 75: Viscosity at 40 °C versus the acid value of 30 mL 20 % RME mixed with 80 % diesel fuel treated with and without combined 1 g adsorbents of magnesium-aluminum hydrotalcite and 1,3,5-trimethyl-2,4,6-tris(3,5-di-tert-butyl-4-hydroxybenzyl)benzene in a ratio of 1:2 respectively and aged at 170 °C with airflow of 10 L/h at 8 h per day for durations of 12 h, 24 h, 36 h and 48 h using a Rancimat 224

Figure 76: Viscosity at 40°C versus Density of 30 mL 20 % RME mixed with 80 % diesel fuel and treated with and without combined 1 g adsorbents of magnesium-aluminum hydrotalcite and 1,3,5-trimethyl-2,4,6-tris(3,5-di-tert-butyl-4-hydroxybenzyl)benzene in a ratio of 1:2 respectively and aged at 170 °C with airflow of 10 L/h at 8 h per day for durations of 12 h, 24 h, 36 h and 48 h using a Rancimat..... 225

Figure 77: Evaluation of comparative analysis of FTIR absorbance spectra of 30 mL 20 % RME mixed with 80 % diesel fuel and treated with and without the combined 1 g adsorbents of magnesium-aluminum hydrotalcite and 1,3,5-trimethyl-2,4,6-tris(3,5-di-tert-butyl-4-hydroxybenzyl) benzene in a ratio of 1:2 respectively and aged at 170 °C with airflow of 10 L/h at 8 h per day for durations of 12 h, 24 h, 36 h and 48 h using a Rancimat 227

Figure 78: FTIR spectra in absorbance mode (range 1500-1900cm⁻¹) of 30 mL 20 % RME mixed with 80 % diesel fuel and treated with and without the combined 1 g adsorbents of magnesium-aluminum hydrotalcite and 1,3,5-trimethyl-2,4,6-tris(3,5-di-tert-butyl-4-hydroxybenzyl) benzene in a ratio of 1:2 respectively and aged at 170 °C with airflow of 10 L/h at 8 h per day for durations of 12 h, 24 h, 36 h and 48 h using a Rancimat 228

Figure 79: FTIR spectra in absorbance mode (range 3000-3600cm⁻¹) of 30 mL 20 % RME mixed with 80 % diesel fuel and treated with and without the combined 1 g adsorbents of magnesium-aluminum hydrotalcite and 1,3,5-trimethyl-2,4,6-tris(3,5-di-tert-butyl-4-hydroxybenzyl) benzene in a ratio of 1:2 respectively and aged at

170 °C with airflow of 10 L/h at 8 h per day for durations of 12 h, 24 h, 36 h and 48 h using a Rancimat	229
Figure 80: Evaluation of peak area under C=O bands (1600-1900 cm ⁻¹) of the FTIR spectra of 30 mL 20 % RME mixed with 80 % diesel fuel and treated with and without combined 1 g adsorbents of magnesium-aluminum hydrotalcite and 1,3,5-trimethyl-2,4,6-tris(3,5-di-tert-butyl-4-hydroxybenzyl) benzene in a ratio of 1:2 respectively and age at 170°C with airflow of 10 L/h at 8 h per day for durations of 12 h, 24 h, 36 h and 48 h using a Rancimat.....	230
Figure 81: Evaluation of induction period of 7.5 g of 20 % RME mixed with 80 % diesel fuel treated with and without 0.225 g combined adsorbents of magnesium-aluminum hydrotalcite and 1,3,5-trimethyl-2,4,6-tris(3,5-di-tert-butyl-4-hydroxybenzyl) benzene in a ratio of 1:2 respectively using a Rancimat at 110 °C with airflow of 10 L/h	234
Figure 82: SEC chromatogram evaluation of 30 mL 20 %RME mixed with 80 % diesel fuel and treated with and without combined 0.225 g adsorbents of magnesium-aluminum hydrotalcite and 1,3,5-trimethyl-2,4,6-tris(3,5-di-tert-butyl-4-hydroxybenzyl) benzene in a ratio of 1:2 respectively and aged at 110 °C with airflow of 10 L/h at 8 h per day for durations of 20 h, 40 h, 60 h and 80 h using a Rancimat compared with the neat unaged blends	235
Figure 83: SEC chromatogram (rang 500-800 g/mol) evaluation of 30 mL 20 %RME mixed with 80 % diesel fuel and treated with and without combined 0.225 g adsorbents of magnesium-aluminum hydrotalcite and 1,3,5-trimethyl-2,4,6-tris(3,5-di-tert-butyl-4-hydroxybenzyl) benzene in a ratio of 1:2 respectively and aged at 110 °C with airflow of 10 L/h at 8 h per day for durations of 20 h, 40 h, 60 h and 80 h using Rancimat compared with a neat unaged blend.....	236
Figure 84; Evaluation of the acid value of 30 mL 20 % RME mixed with 80 % diesel fuel and treated with and without combined 0.225 g adsorbents of magnesium-aluminum hydrotalcite and 1,3,5-trimethyl-2,4,6-tris(3,5-di-tert-butyl-4-hydroxybenzyl) benzene in a ratio of 1:2 respectively and aged at 110 °C with airflow of 10 L/h at 8 h per day for durations of 20 h, 40 h, 60 h and 80 h at 8 h per day using Rancimat.....	238
Figure 85: Evaluation of viscosity at 40 °C of 30 mL 20 % RME mixed with 80 % diesel fuel and treated with and without combined 0.225 g adsorbents of magnesium-aluminum hydrotalcite and 1,3,5-trimethyl-2,4,6-tris(3,5-di-tert-butyl-4-hydroxybenzyl) benzene in a ratio of 1:2 respectively and aged at 110 °C with airflow of 10 L/h at 8 h per day for durations of 20 h, 40 h, 60 h and 80 h using a Rancimat.....	240
Figure 86: Evaluation of viscosity at 100 °C of 30 mL 20 % RME mixed with 80 % diesel fuel and treated with and without combined 0.225 g adsorbents of magnesium-aluminum hydrotalcite and 1,3,5-trimethyl-2,4,6-tris(3,5-di-tert-butyl-4-hydroxybenzyl) benzene in a ratio of 1:2 respectively and aged at 110 °C with airflow of 10 L/h for durations of 20 h, 40 h, 60 h, and 80 h at 8 h per day using a Rancimat.....	241

- Figure 87: Evaluation of density at 40 °C of 30 mL 20 % RME mixed with 80 % diesel fuel and treated with and without combined 0.225 g adsorbents of magnesium-aluminum hydrotalcite and 1,3,5-trimethyl-2,4,6-tris(3,5-di-tert-butyl-4-hydroxybenzyl) benzene in a ratio of 1:2 respectively and aged at 110 °C with airflow of 10 L/h for durations of 20 h, 40 h, 60 h, and 80 h at 8 h per day using a Rancimat..... 242
- Figure 88: Evaluation of density at 100 °C of 30 mL 20 % RME mixed with 80 % diesel fuel and treated with combined 0.225 g adsorbents of magnesium-aluminum hydrotalcite and 1,3,5-trimethyl-2,4,6-tris(3,5-di-tert-butyl-4-hydroxybenzyl) benzene in a ratio of 1:2 respectively and aged at 110 °C with airflow of 10 L/h for durations of 20 h, 40 h, 60 h, and 80 h at 8 h per day using a Rancimat..... 243
- Figure 89: Comparative analysis of acid value versus viscosity of 30 mL 20 % RME mixed with 80 % diesel fuel and treated with and without combined 0.225 g adsorbents of magnesium-aluminum hydrotalcite and 1,3,5-trimethyl-2,4,6-tris(3,5-di-tert-butyl-4-hydroxybenzyl) benzene in a ratio of 1:2 respectively and aged at 110 °C with airflow of 10 L/h for durations of 20 h, 40 h, 60 h, and 80 h at 8 h per day using a Rancimat..... 245
- Figure 90: Evaluation of comparative analysis of FTIR spectra in absorbance mode of 30 mL 20 % RME mixed with 80 % diesel fuel and treated with 0.225 g combined adsorbents of magnesium-aluminum hydrotalcite and 1,3,5-trimethyl-2,4,6-tris(3,5-di-tert-butyl-4-hydroxybenzyl) benzene in a ratio of 1:2 respectively and aged at 110 °C with airflow of 10 L/h at 8 h per day for durations of 20 h, 40 h, 60 h and 80 h using a Rancimat 247
- Figure 91: Evaluation of comparative analysis of FTIR spectra in absorbance mode (range 1500-1900 cm^{-1}) of 40 mL 20 % RME mixed with 80 % diesel fuel and treated with 0.225 g combined adsorbents of magnesium-aluminum hydrotalcite and 1,3,5-trimethyl-2,4,6-tris(3,5-di-tert-butyl-4-hydroxybenzyl) benzene in a ratio of 1:2 respectively and aged at 110 °C with airflow of 10 L/h for durations of 20 h, 40 h, 60 h and 80 h using a Rancimat compared with the neat unaged blend..... 248
- Figure 92: Evaluation of comparative analysis of FTIR spectra in absorbance mode (range 3000-3600 cm^{-1}) of 30 mL 20 % RME mixed with 80 % diesel fuel and treated with 0.225 g combined adsorbents of magnesium-aluminum hydrotalcite and 1,3,5-trimethyl-2,4,6-tris(3,5-di-tert-butyl-4-hydroxybenzyl) benzene in a ratio of 1:2 respectively and aged at 110 °C with airflow of 10 L/h for durations of 20 h, 40 h, 60 h, and 80 h at 8 h per day using a Rancimat compared with a neat unaged blend 249
- Figure 93: Evaluation of peak area under C=O bands (1600-1900 cm^{-1}) of the FTIR spectra of 30 mL 20 % RME mixed with 80 % diesel fuel and treated with and without combined 0.225 g adsorbents of magnesium-aluminum hydrotalcite and 1,3,5-trimethyl-2,4,6-tris(3,5-di-tert-butyl-4-hydroxybenzyl)benzene in a ratio of 1:2 respectively and aged at 110 °C with airflow of 10 L/h for durations of 20 h, 40 h,

60 h, and 80 h at 8 h per day using a Rancimat compared with the neat unaged blend 250

Figure 94: PetroOxy induction period of 40 mL RME treated with and without 0.675 g of combined adsorbents of magnesium-aluminum hydrotalcite and 1,3,5-trimethyl-2,4,6-tris(3,5-di-tert-butyl-4-hydroxybenzyl) benzene in a ratio of 1:2 respectively and stored at 40 °C in an oven for 120 days with samples taken every 15 days .. 254

Figure 95: Evaluation of induction period of 40 mL of 20 % RME mixed with 80 % diesel fuel and treated with and without 0.675 g of combined adsorbents of magnesium-aluminum hydrotalcite and 1,3,5-trimethyl-2,4,6-tris(3,5-di-tert-butyl-4-hydroxybenzyl) benzene in a ratio of 1:2 respectively and stored at 40 °C for 120 days with samples taken every 15 days compared with the neat blend 256

Figure 96: Evaluation of SEC chromatogram of 40 mL of 20 % RME mixed with 80 % diesel fuel treated with and without 0.675 g combined adsorbents of magnesium-aluminum hydrotalcite and 1,3,5-trimethyl-2,4,6-tris(3,5-di-tert-butyl-4-hydroxybenzyl) benzene in a ratio of 1:2 respectively and stored at 40 °C in an oven for 120 days with samples taken every 15 days..... 257

Figure 97: Acid value of 40 mL of RME treated with and without 0.675 g of combined adsorbents of magnesium-aluminum hydrotalcite and 1,3,5-trimethyl-2,4,6-tris(3,5-di-tert-butyl-4-hydroxybenzyl) benzene in a ratio of 1:2 respectively and stored at 40 °C in an oven for 120 days with samples taken every 15 days 259

Figure 98: Acid value of 40 mL 20 % RME mixed with 80 % diesel fuel and treated with and without combined 0.675 g adsorbents of magnesium-aluminum hydrotalcite and 1,3,5-trimethyl-2,4,6-tris(3,5-di-tert-butyl-4-hydroxybenzyl) benzene in a ratio of 1:2 respectively and stored at 40 °C for 120 days and samples taken every 15 days 261

Figure 99: Viscosity measured at 40 °C of 40 mL of 20 % RME mixed with 80 % diesel fuel and treated with and without 0.675 g combined adsorbents of magnesium-aluminum hydrotalcite and 1,3,5-trimethyl-2,4,6-tris(3,5-di-tert-butyl-4-hydroxybenzyl) benzene in a ratio of 1:2 respectively and stored at 40 °C in an oven for 120 days and samples were taken every 15 days 263

Figure 100: Viscosity measured at 100 °C of 40 mL neat RME and 40 mL of 20 %RME mixed with 80 %diesel fuel treated with and without 0.675 g combined adsorbents of magnesium-aluminum hydrotalcite and 1,3,5-trimethyl-2,4,6-tris(3,5-di-tert-butyl-4-hydroxybenzyl) benzene in a ratio of 1:2 respectively and stored at 40 °C in an oven for 120 days and samples were taken every 15 days 264

Figure 101: Density measured at 40 °C of 40 mL neat RME and 40 mL of 20 % RME mixed with 80 % diesel fuel and treated with and without 0.675 g combined adsorbents of magnesium-aluminum hydrotalcite and 1,3,5-trimethyl-2,4,6-tris(3,5-di-tert-butyl-4-hydroxybenzyl) benzene in a ratio of 1:2 respectively and stored at 40 °C in the oven for 120 days and samples were taken every 15 days 266

Figure 102: Density measured at 100 °C of 40 mL neat RME and 40 mL of 20 % mixed with 80 % diesel fuel and treated with and without 0.675 g combined adsorbents of magnesium-aluminum hydrotalcite and 1,3,5-trimethyl-2,4,6-tris(3,5-di-tert-butyl-4-

hydroxybenzyl) benzene in a ratio of 1:2 respectively and stored at 40 °C in the oven for 120 days and samples were taken every 15 days.....	267
Figure 103: FTIR spectrum of 40 mL RME treated with and without 0.675 g combined adsorbents of magnesium-aluminum hydrotalcite and 1,3,5-trimethyl-2,4,6-tris(3,5-di-tert-butyl-4-hydroxybenzyl) benzene in a ratio of 1:2 respectively and stored at 40 °C in the oven for 120 days with samples taken every 15 days	268
Figure 104: Evaluation of peak area under C=O band of FTIR spectrum of 40 mL RME treated with and without 0.675 g combined adsorbents of magnesium-aluminum hydrotalcite and 1,3,5-trimethyl-2,4,6-tris(3,5-di-tert-butyl-4-hydroxybenzyl) benzene in a ratio of 1:2 respectively and stored at 40 °C in the oven for 120 days with samples taken every 15 days.....	269
Figure 105: FTIR spectra of 40 mL of 20 % RME mixed with 80 % diesel fuel and treated with and without 0.675 g combined adsorbents of magnesium-aluminum hydrotalcite and 1,3,5-trimethyl-2,4,6-tris(3,5-di-tert-butyl-4-hydroxybenzyl) benzene in a ratio of 1:2 respectively and stored at 40 °C in the oven for 120 days with samples taken every 15 days.....	270
Figure 106: Evaluation of peak area under C=O band of FTIR spectrum of 40 mL of 20 % RME blended with 80 % diesel fuel and treated with and without 0.675 g combined adsorbents of magnesium-aluminum hydrotalcite and 1,3,5-trimethyl-2,4,6-tris(3,5-di-tert-butyl-4-hydroxybenzyl) benzene in a ratio of 1:2 respectively and stored at 40 °C in the oven for 120 days and samples were taken every 15 days	271
Figure 107: The relative permittivity of 30 mL 20 % RME and 80 % base oil treated with and without 0.675 g combined adsorbents of magnesium-aluminum hydrotalcite and 1,3,5-trimethyl-2,4,6-tris(3,5-di-tert-butyl-4-hydroxybenzyl) benzene in a ratio of 1:2 respectively aged for 10 h duration at 170 °C with airflow of 10L/h in a Rancimat	274
Figure 108: The relative permittivity versus duration of aging of 30 mL 20 % RME and 80 % base oil treated with and without 0.675 g combined adsorbents of magnesium-aluminum hydrotalcite and 1,3,5-trimethyl-2,4,6-tris(3,5-di-tert-butyl-4-hydroxybenzyl) benzene in a ratio of 1:2 respectively and aged at 170 °C airflows of 10L/h for 10 h duration in a Rancimat	275
Figure 109: The dissipation factor versus duration of aging of 30 mL 20 % RME and 80 % base oil mixture treated with and without the combined 0.675 g adsorbents of magnesium-aluminum hydrotalcite and 1,3,5-trimethyl-2,4,6-tris(3,5-di-tert-butyl-4-hydroxybenzyl) benzene in a ratio of 1:2 respectively and aged for 10 h at 170 °C with airflow of 10L/h in a Rancimat.....	277
Figure 110: The total acid value versus duration of aging of 30 mL 20 % RME and 80 % base oil mixture treated with and without combined 0.675 g adsorbents of magnesium-aluminum hydrotalcite and 1,3,5-trimethyl-2,4,6-tris(3,5-di-tert-butyl-4-hydroxybenzyl) benzene in a ratio of 1:2 respectively and aged 170 °C with airflow of 10L/h for 10 h duration in a Rancimat	278

Figure 111 Molecular structure of methyl linolenic acid with the ¹ H-NMR assignment to Table 19	282
Figure 112: ¹ H-NMR spectra of 30 mL 20 % RME and 80 % base oil mixture treated with and without combined adsorbents of magnesium-aluminum hydrotalcite and 1,3,5-trimethyl-2,4,6-tris(3,5-di-tert-butyl-4-hydroxybenzyl) benzene in a ratio of 1:2 respectively and aged at 170 °C airflows of 10L/h for 80 h and their extracts.....	285
Figure 113: Zoom in on Figure 112	286
Figure 114: ¹ H-NMR spectrum of neat RME.....	287

List of Tables

Table 1: Bond dissociation energies of hydrogens	52
Table 2: Typical concentration of additive elements of a standard lubricant (Fujita, 2006; Yuegang, 2016; Hilligoss, 2012; Perkinelmer, 2011)	59
Table 3: Physical properties of base oil and Mannol engine oil used in this research .	106
Table 4: Physical properties of the fuels used in this research	107
Table 5: Composition of the samples used in this research.....	109
Table 6: Properties of the biodiesel blend used in this research.....	109
Table 7 Pure additives tested with the adsorbents	110
Table 8 Parameters under which C18_2 ME mixture was investigated	114
Table 9 Parameters used for the RME mixture investigation.....	114
Table 10 Parameters used for investigating RME with adsorbents	115
Table 11 Parameters used for investigating the adsorbents with engine oil	116
Table 12: Neat additives tested in this work	117
Table 13 30 mL blend of biodiesel and diesel fuel treated with 1 g adsorbents to determine the effect of the adsorbents on their oxidative stability at 170 °C	119
Table 14 30 mL blend of biodiesel and diesel fuel treated with 0.225 g of adsorbents to determine the effect of the adsorbents on their oxidative stability at 110 °C	120
Table 15 40 mL blend of biodiesel and diesel fuel treated with 0.675 g of adsorbents to determine the effect of the adsorbents on their storage stability at 40 °C	122
Table 16: ICP-MS parameters	128
Table 17: Viscosity aging index of B20 treated with and without 1 g of combined adsorbent and aged at 170 °C at 8 h per day with an airflow of 10 L/h for various durations using a Rancimat.....	221
Table 18 Evaluation of parameters of aging of 30 mL of 20 % RME mixed with 80 % diesel fuel and treated with and without combined adsorbents of magnesium-aluminum hydrotalcite and 1,3,5-trimethyl-2,4,6-tris(3,5-di-tert-butyl-4-hydroxybenzyl)benzene in a ratio of 1:2 respectively at 110 °C and 170 °C for durations of 48 h and 80 h	252
Table 19: 1H-NMR (400 MHz, CDCL3) chemical shift. The assignment of the signals is shown in Figure 111.....	283

1 Introduction

The research described in this dissertation focuses on developing a process to remove oligomers and suppress their formation by intercepting the aging procedure's precursors using adsorbents when biodiesel and its blends are used as fuel. There has been the search for various energy sources due to the increasing awareness of the depletion of fossil fuel resources, environmental issues, and more urgently is the need to mitigate climate change. Biodiesel has become more attractive in recent times (Daming et al. 2012, Abdullah et al., 2007) as an alternative fuel. Biodiesel, a methyl ester of vegetable oil, is a renewable, low environmental impact, green alternative fuel for diesel engines (EU Regulation, 2012, Ghosh and Dutta, 2012). In addition to its renewable status, biodiesel, compared to fossil fuel, has advantages such as its biodegradability, reduced exhaust emissions, higher cetane number, lubricity, and safer distribution and storage due to its higher flash point (Pereira et al. 2015, Monyem and Van Gerpen, 2001). Biodiesel fuel is chemically fatty acid methyl ester (FAME) derived from different plant oils. It varies slightly in molecular structures due to the degree of unsaturation of the fatty acids in the different sources compared to conventional diesel fuel (Pereira et al. 2015, 2013, Sharma and Singh, 2009). Biodiesel fuels contain significant amounts of esters of oleic, linoleic, or linolenic acids, which influence their oxidative stability. A small percentage of more highly unsaturated fatty compounds have a disproportionately strong effect in reducing oxidation stability and promoting oligomers formation. The oxidation products of the biodiesel in the engine sump influence the degradation of the lubrication oil.

Irrespective of biodiesel's advantages, it is clear from the above that biodiesel comes with attendant problems, especially its oxidation stability. One of the main hindrances of biodiesel is its degradability during storage and usage. This oxidative degradability essentially alters biodiesel's desirable properties and diminishes its applicability as fuel for long-term use.

Biodiesel as fuel introduces challenges into engine oil functions as biodiesel affects engine lubrication through fuel dilution (Zdrodowski et al., 2010). The fuel in oil reduces the oil's life expectancy and hence its effectiveness. But when the motor oil is manufactured, the main goal is to achieve maximum durability of the motor and preserve

all motor properties as long as possible (Sejkorová and Glos, 2017). The lubricant used in an internal combustion engine operates under extremely aggressive conditions and must perform its roles efficiently over the prescribed length of time. Degradation changes the lubricating oil's physical and chemical properties during service, resulting in deterioration of performance. One important factor affecting lubricating oil in recent times is the dilution of the oil by unburnt fuel, especially ester-based like biodiesel and its blends. Because fuel is a natural solvent, fuel dilution in motor oil causes a decrease in viscosity, increasing engine wear. When fuel contaminates the oil in the crankcase, the consequences include reduced oil film strength, increased volatility, reduced oil viscosity, increased engine wear, weakened lubricant detergency, accelerated lubricant oxidation, sludge, and acid formation (TOTAL, 2017; Syntheticoils, 2009; AMSOIL, 2009). Biodiesel accumulates in the engine sump oil, especially in vehicles fitted with a diesel particulate filter (DPF) system (Zdrodowski et al., 2010). Unlike diesel fuel which will evaporate from the lubricating oil under average operating temperatures, biodiesel with long-chain fatty acid esters will not evaporate because of its higher boiling temperature range, 160 °C to 375 °C compared with petroleum diesel fuel, about 175 °C (Tschöke et al., 2009) but rather oxidizes leading to a significant increase in the viscosity. Since the chemical and physical properties of biodiesel are pretty different from fossil diesel fuel, the biogenic components turn to remain in the engine oil leading to problems in the engine lubricant (Rodríguez-Fernández et al., 2016; Tschöke et al., 2009; He et al., 2011; Goodrum, 2002). In addition to the low evaporative rate, biodiesel tends to have higher fuel dilution rates of the lubrication oil than diesel fuel (Bannister et al., 2011). Hence the level of unburnt fuel in the engine oil can build up (Beercheck, 2008). There is always a certain amount of unburnt fuel (Shanta, 2011; Yüksesek et al., 2009). The fuel in the oil reduces the oil's viscosity, degrades its oxidation resistance, and shortens its useful service life (Schneider et al., 2013).

Therefore, a proportion of fuel in vehicles always finds its way into the lubricating oil leading to dilution. This fuel dilution is increasingly significant in vehicles equipped with diesel particulate filters. Diesel vehicles fitted with diesel particulate filters (DPFs) require active regeneration via late injection of fresh fuel. This regeneration brings about an increase in the amount of biodiesel in the sump oil. In these engines, fuel is post-injected

during the expansion stroke into the cylinder to increase the exhaust gas temperature and stoichiometry in a diesel particulate filter. The regeneration is done to help burn carbon-based deposits. During the post-injection for after-treatment system regeneration, some of the fuel is sprayed on cylinder walls and then is scraped by the piston's oil ring into the engine's crankcase. The fuel carried into the engine oil evaporates in the crankcase, particularly the lighter molecular weight fuel. The heavier molecular weight fuel remains in the oil and accumulates. Biodiesel accumulates in the lubricating oil, and unlike mineral diesel fuel, the biodiesel does not evaporate at the average operating temperature of the oil and will instead accumulate. Therefore, when biodiesel degrades within the oil, the degradation products eventually form, leading to a significant increase in the oil viscosity, potentially impacting lubrication oil durability (Bannister et al., 2010). Therefore, the presence of biodiesel in engine oil leads to dilution of the oil, increasing viscosity, oxidation of lubricating oil, and finally, the premature formation of sludge and deposits in the crankcase resulting in a short period of oil drain interval (Knorr et al., 2016; Karavalakis et al., 2011; Bannister et al., 2010; Thornton et al., 2009; Yükses et al., 2009; Beercheck, 2008; Fang et al., 2007; Andrae et al., 2007). The lubricant performance, service intervals, and engine oil durability are impacted by biodiesel and engine oil interaction.

In Europe and according to EN 590, diesel fuel can contain up to 7 % biodiesel (FAME), but in other places such as America, higher percentages of up to 20 % biodiesel can be found. Biodiesel, derived from rapeseed, soybean, waste oils, etc., comprises a range of saturated and polyunsaturated esters. Therefore, it has a typical fatty acid pattern that differs in chain length and double bond content depending on the vegetable oil product used. The fatty acid pattern has an apparent influence on the physical and chemical properties of the fuel. A high proportion of double bonds can improve cold stability, but such fuels are more susceptible to oxidation. The susceptibility of the different fatty acid esters to oxidation differs according to the number of double bonds in the sample. Polyunsaturated compounds are more prone to oxidation than monounsaturated esters, which are more reactive than saturated esters. On exposure to air, these esters are prone to oxidative degradation. Additionally, the esters in FAME are hydrolyzed, resulting in high concentrations of weak acids in lubricants.

As biodiesel is relatively unstable compared to mineral diesel fuel, it readily degrades and aids the lubricating oil's oxidative degradation (Daming et al., 2012; EU Regulation 2012; Abdullah et al., 2007). Biodiesel, therefore, accelerates the degradation of crankcase oil (Pereira et al., 2015, 2013; Ghosh and Dutta, 2012; Shanta, 2011; Yüksek et al., 2009; Sharma and Singh, 2009; Andreae et al., 2007; Monyem and Van Gerpen, 2001).

The share of renewables in Germany's transport is relatively low at around 5 % since most biofuels are currently consumed as blends, typically 10 % or less by volume with mineral fuels. However, biodiesel consumption has increased by 8.6 % (Le Seigneur, 2019; Germany 2020 Energy Policy Review). Its consumption is further projected to be 21,770 ktoe in 2020 (NREAP, 2019).

Various standards cover the use of biodiesel. In Europe, low-level biodiesel/diesel fuel blends, B5, B7 blends, are covered by EN 590, while EN 14214 focuses on biodiesel specifications for diesel engines. EN14214, introduced in 2012, expanded the scope to cover blends up to B10. With EN 16709 introduced in 2015, B20 and B30 blends for use by captive fleets are covered. The FAME component in EN 16709 must satisfy EN 14214, while the diesel component complies with EN 590 (Dieselnet std.php).

The Renewable Energy Directive (RED) requires the EU to achieve a binding target whereby 20 percent of its overall energy use would be powered from renewable sources by 2020. The RED also requires that the transport sector reach a renewable energy-use target of 10 percent. However, in RED II, the overall EU target for renewable energy source consumption by 2030 is raised to 32 %, with a minimum of 14 % target on road and rail transport by 2030. With this, the use of biodiesel is gradually increasing in proportion, and for biodiesel to be fully integrated into the fuel mix, the problem of its impact on lubrication oil changing interval must be overcome. While there have been significant research studies highlighting the effects of biodiesel on engine oil performance (Zdrodowski et al., 2010; Devlin et al., 2008; Andreae et al., 2007; Waynick, 2005; Blackburn et al., 1983; Thornton et al., 2009; Gulzar et al., 2016), understanding the autoxidative mechanisms of biodiesel (Christensen and McCormick, 2014; Flitsch et al., 2014; Ogawa et al., 2009; Fang et al., 2006), there is much to be done in combating the

formation and removal of oligomers. The suppression of oligomer formation shall be the focus of this project.

1.1 Objectives

So far, there has been no attempt to cause the stabilization of biodiesel and its blends using adsorbents from open literature. This investigation is one of the first studies on the use of adsorbents to mitigate biodiesel and diesel fuel's stability behavior—biodiesel blends and the removal of oligomers or suppressing the formation of high molecular mass species in aging oil.

This study's primary aim has been achieved by several experimental measurements that provided results on adsorbents' effect on fuel oxidative stability, especially ester-based fuel like biodiesel and its blends. The chemical composition and some critical rheological analyses of the samples have been measured to understand their role in the oxidation of the sample by comparing the presence and absence of the adsorbents during the aging process.

Furthermore, it aims to use adsorbents to suppress oligomers' formation and remove them in aging oil due to the influence of biodiesel and its blends.

The research project also seeks to stabilize fuel, especially ester-based fuel like biodiesel, and its blends using the adsorbents. The adsorbents' application will enhance biodiesel's oxidative stability and its blends during long-term storage or application, focusing on its use in plug-in hybrid vehicles, emergency power plants, and generators. The combustion engine only starts in plug-in hybrid vehicles if the battery cannot supply energy on longer journeys. As a result, the fuel remains longer in plug-in hybrid vehicles. Fuels that are exposed to heat and oxygen over an extended period can form aging products. These aging products lead to the formation of deposits, especially in the case of diesel fuels mixed with biodiesel content, and can, therefore, endanger the operational safety of the vehicle in critical components such as injectors or filter units (Schroder et al., 2017; Christensen and McCormick, 2014; Flitsch et al., 2014; Ogawa et al., 2009; Fang et al., 2006).

This work's primary focus is adsorbents' use to suppress oligomers formation in aging oil and biodiesel fuel and its blends. A combined adsorbent of hydrotalcite compound and radical trapping agent are applied to interfere with sludge precursors' production and, therefore, suppress oligomers' formation. Other deactivated adsorbents would be applied to remove oligomers when it gets formed in aging oil. The use of adsorbents to remove the oligomers and other potential unstable components of the oil aging procedure resulting from the influence of biodiesel and its blends in the engine sump would promote and prolong the changing interval of lubricating oil in an engine fueled by biodiesel or its blends. The use of adsorbents in this process also makes it possible to increase the proportion of biodiesel or blends used as fuel in the transport sector or emergency power plants. The adsorbents' application in this process will enhance biodiesel's storage stability for a more extended period of duration.

1.2 Thesis Outline

This dissertation consists of 12 chapters, the introductory Chapter 1, where the motivation, problem statement, and objectives for this research work are outlined. Chapter 2 discusses relevant publications on lubricants, biodiesel, oxidation, and the techniques of preventing or delaying oxidation. The different methods for measuring the level of degradation of biodiesel are looked at here. The effect of biodiesel on lubrication oil and previous work carried out within the research group have been summarized. The theoretical framework, essential functions of lubricants, and the lubrication chemistry are highlighted, followed by a summarized description of the production, composition, and means by which the fuel finds its way into the sump are covered in Chapter 3. The underlying mechanism by which the samples or fuel and oil mixture degrade is covered in this chapter. Chapter 4 builds on the basic experimental techniques applied to study the effect and impact of the adsorbents on the degradation of the fuel and oil mixtures. Chapter 5 outlines the focus of this work. The various degradation processes of the oil and fuel mixtures are carried out at relevant temperatures and durations of aging to establish the impact or effectiveness of the adsorbents in suppressing oxidation. While chapter 6 covers the selection of the adsorbents. This chapter provides the theoretical groundwork on which the adsorbents act to achieve the desired goals. The materials and methods applied in this work are covered in chapter 7. This chapter also looks at the

measurement and instrumental techniques employed in this study. In chapter 8, the discussion of the trends in the results, while chapter 9 concludes the dissertation with a focus on the significant findings and perspectives for further work. The relevant publications reviewed and referenced in this dissertation are in chapter 10. The appendix, chapter 11, covers the results of experiments that are not discussed in this dissertation. In chapter 12, the glossary is covered.

2 Literature Review

Introduction

In this chapter, background information on biodiesel and its related oxidation and stability issues is discussed. This elucidates biodiesel's effect on engine lubricating oil and the different approaches for retarding its oxidation. Therefore, this literature review highlights various techniques presently used to subdue oxidation and hence allow the importance of this current study to be put into perspective.

2.1 Previous Work

The oxidative stability of biodiesel, especially the ester base, is associated with its application as fuel. Oxidation stability is the tendency of a fuel to react with oxygen at temperatures near ambient, and it describes the relative susceptibility of the fuel to degradation by oxidation (Christensen and McCormick, 2014). Biodiesel is susceptible to oxidation due to its high proportion of double bonds than diesel fuel during application and long-term storage. The oxidation stability of biodiesel is lower than that of petroleum-based diesel fuel (Botella et al., 2014; Dantas et al., 2011; Jain and Sharma, 2011; Karavalakis et al., 2011; Kivevele et al., 2011), and this hinders its application and long-term storage. It tends to deteriorate via hydrolytic and oxidative reactions because of its high degree of unsaturation (Singer et al., 2014; Abdullah et al., 2007; Fang et al., 2006; Duffield et al., 1998). In long-term storage or application, most biodiesel begins to oxidize immediately during storage. Biodiesel will very likely go out of specification regarding stability within four months. The oxidation stability of biodiesel has been evaluated through many experimental techniques. The Rancimat method is the standardized accelerated oxidation test, EN14112 and ASTM D6751 (Botella et al., 2014). The PetroOXY method is another way biodiesel's oxidation stability is determined and is described in the prEN16091 standard. The European standard for biodiesel (EN 14112) sets a limit of 6 h as the minimum induction period determined by using the Rancimat method (Karavalakis et al., 2010). The Rancimat test method indicates the length of time the fuel can be stored before producing acids, indicating that the fuel is becoming unstable or degrading (Karavalakis et al., 2010). The time that passes until the appearance of these secondary reaction products is called induction time or induction period, which is an

indicator for oxidation stability and characterizes the fuel's resistance to oxidation. At only four months, biodiesel with induction times more extended than seven hours is reported out of specification for oxidation stability (McCormick and Westbrook, 2010). Biodiesel oxidation leads to increased acid value and oligomers' formation (Bannister et al., 2010). Many recent studies have focused on the problem of oxidation stability of biodiesel and its blends and their polymerization effects (TOTAL, 2017; Moser et al., 2013; Bannister et al., 2010; AMSOIL, 2009; Yüksek et al., 2009; Beercheck, 2008)

As stated in the introduction (section 1.0), biodiesel accumulates in the engine sump oil, severely impacting engine lubrication oils. The use of biodiesel leads to substantial lubrication oil dilution, which is not desirable since it affects various tribosystems of the engine (Molina et al., 2014; Gili et al., 2011) and lowers viscosity initially while increasing oil oxidation and causing biodiesel fuel itself and the lubricating oil to oxidize, leading to increased viscosity, premature formation of sludge and deposits in the crankcase resulting in a short period of oil drain interval (Ljubas et al., 2010; Karavalakis et al., 2010; Yüksek et al., 2009; Devlin et al., 2008; McTavish, 2008; Larsson, 2007; Sappok and Wong, 2007; Fang et al., 2006; Devlin et al., 2008; Knothe and Dunn, 2003). Sufficient work has been done for the understanding of the extent of biodiesel dilution in lubricants and its impact on oxidative stability of lubricating oils and sludge formation (Ljubas et al., 2010; Cowart et al., 2008; McTavish, 2008; Devlin et al., 2008; Marsh and Corradi, 2007; Fang et al., 2007; Andrae et al., 2007; Burgeoning, 2007; Infineum, 2007; Fetterman, 2007; Sappok and Wong, 2007; Larsson, 2007; Fang et al., 2006; Agarwal, 2005; Sharp et al., 2000). Shortening of the recommended oil drains between 30 % and 60 % due to biodiesel dilution with a corresponding increase in deposit formation has been reported (Gili et al., 2011). Through the dilution of biodiesel, acidity and viscosity are increased, thereby degrading lubricating oil performance. This oil dilution shortens oil drain intervals (Watson and Wong, 2008; Devlin et al., 2008) though oil with FAME content exceeding 6 % has been recommended for an oil change (Gili et al., 2011). There is an increase in sludge build-up resulting from oxidation due to a significant increase in engine oil dilution by biodiesel fuel (Shanta et al., 2011; Watson and Wong, 2008; Devlin et al., 2008; Avinash, 2003). However, there are varied results from studies on fuel dilution. Rapeseed methyl ester, 50 %, was used in heavy trucks and light vehicles and did not result in increased

deposits (Dairene Uy et al., 2011). Therefore, fuel dilution is attributed to the biodiesel type used. Using soybean methyl ester (SME) recorded a significant increase in oxidation and deposits in fuel-diluted engine oil (Devlin et al., 2008), while Thornton et al. (2009) had no noticeable lubricant aging effects attributable to biodiesel. Sappok and Wong (2008) accelerated oil aging and reported an increased degradation of biodiesel.

The adverse effects of fuel dilution on properties and performance of lubrication engine oils have been extensively researched in recent times (Wakiru et al., 2018; Shanta, 2011; Bannister et al., 2010; Yöksek et al., 2009; Thornton et al., 2009; Beercheck, 2008; Watson and Wong, 2008; Sappok and Wong, 2008). While there has been much research on lubricant dilution, few researchers focused on biodiesel's influence on lubricating oil degradation. Knorr et al. (2016), Singer et al. (2014), and Schumacher (2013) went beyond the concept of dilution and simulated with model substances to trace the influence of biodiesel on the accelerated aging of lubricating oil.

Early work on the oxidation stability of biodiesel took a critical approach to suppress oxidation of biodiesel (Kumar, 2017; Zuleta et al., 2012; Rhet de Guzman et al., 2009; Fang et al., 2006; Duffield et al., 1998). It focused on using ester and polyglycol based formulations (Sharma and Singh, 2009; Woydt et al., 2008), thin-film coatings that may offer wear robustness between FAME and lubricant oil, and ring metallurgies and coatings that may offer wear robustness (Woydt et al., 2009). Sem (2004), in his study, concluded that increased deposits resulting from biodiesel dilution could be reduced with higher amounts of additives in the engine lubricating oils.

Researchers have proposed biodiesel mixtures (Sierra-Cantor and Guerrero-Fajardob, 2017; Serrano et al., 2014; Zuleta et al., 2012), structural modification, antioxidant usage, and blending with diesel fuel. Some researchers (Kumar, 2017; Zuleta et al., 2012; Karavalakis et al., 2011) have reported altering the fatty acid profile with an enhanced saturated fatty acid leading to improved oxidative stability. Here, oil with high saturated fatty acid content for biodiesel production is used compared to the unsaturated portion. Also, a combination of elevated oleic acid with increased stearic acid but critically, such biodiesel exhibits poor cold flow properties due to the level of saturates in the fuel (Sierra-Cantor and Guerrero-Fajardob, 2017). Singh et al. (2019) critiqued this concept and

introduced winterization, where some saturated fatty acid esters are removed. This approach will impact biodiesel's oxidative stability considering the increasing degree of the unsaturated fatty acids in such a winterized fuel. Also, the cloud point is affected (Singh et al., 2019; Sierra-Cantor and Guerrero-Fajardob, 2017; Elias et al., 2016). One of the setbacks of biodiesel is the trade-off between its oxidation tendency and its cold flow properties. Higher saturated molecules are less prone to oxidation than unsaturated ones, but they crystallize at high temperatures. On the contrary, unsaturated biodiesel has good cold flow properties but is very prone to oxidation.

Over 80 years, work had begun on one practical approach to maintaining fuel quality of biodiesel against autoxidation with the use of oxidation inhibitors, antioxidants (Siddharth and Sharma, 2010; Araujo Susana et al., 2009; Aluyor et al., 2009; Jiayu et al., 2009; Sharma et al., 2009). Antioxidants come in many forms, such as natural or synthetic (Kumar, 2017; Singer et al., 2014; Yaakob et al., 2014; Moser et al., 2013; Silitonga et al., 2013; Woydt et al., 2009; Fang et al., 2006). However, it is worthy to note that these antioxidants may suppress acid formation, but other oxidative products such as alcohol and aldehydes still get formed (Waynick, 2005). Therefore, using antioxidants to control lubricant oil degradation focuses on alkyl, peroxy radicals, and hydroperoxides. These primary alkoxy and hydroxy radicals rapidly abstract hydrogen from the lubricating oil and are unlikely to be deactivated by the antioxidants. Olathe Kans (2011) demonstrated an engine oil additive that relieves crankcase oil dilution concerning biodiesel and its blends. Kans traces how the engine oil additive, a combination of specific detergents and antioxidants, counteract the effect of organic acids that develop in the crankcase. The additive prevents oxidation and formation of deposits. This additive is the most innovative measure to counter crankcase oil dilution by biodiesel and its blends. It ideally can retard oxidation but not prevent it since, with time, the additives get depleted (Kans, 2011).

Blending diesel fuel with biodiesel can enhance some characteristic properties of biodiesel (Kumar, 2017). Biodiesel blending modifies its viscosity to conventional diesel fuel values to reach better combustion and avoid engine deposits, high black smoke emissions atomization inside injectors, damaged pumps, and engine corrosion. Biodiesel cold flow properties, i.e., cloud point, pour point, and cold filter plugging point, as well as stability and other fuel properties, are also modified through the blending (Sierra-Cantora and

Guerrero-Fajardob, 2017; Kumar and Saravanan, 2016; Pullen and Saeed, 2012; Karavalakis et al., 2010). Also, blending different biodiesel with varying levels of unsaturation has been carried out, and the results show enhanced oxidative stability of the blend.

2.2 Summary

The reviewed literature suggests that biodiesel dilution of lubricating oil leads to a short oil drain interval. Due to the high degree of unsaturation of ester base biodiesel, it is very susceptible to oxidation, and the conditions of high temperature in the engine facilitate its degradation process (Knothe, 2007). The above review demonstrates a general dependency on antioxidants as the main alternative to prevent or retard biodiesel degradation (Kumar, 2017; Zuleta et al., 2012; Elaine et al., 2011; Rhet de Guzman et al., 2009; Fang et al., 2006; Waynick, 2005; Monyem et al., 2000; Duffield et al., 1998). The current work will highlight mitigating the oxidative stability of biodiesel and its blends using adsorbents. While there has been much research on the dilution of lubricating oil by biodiesel, few or no researchers have removed oligomers using adsorbents to enhance the stability of lubricating oils during their aging process. The use of adsorbents in sustaining lubricant stability shall be the focus of this dissertation. An adsorbent with hydroxyl groups in its molecule, like an antioxidant, can capture any free radical(s) in an oil aging procedure. Such adsorbent is a candidate for suppressing oxidation in biodiesel and its blends.

3 Technical Background

Introduction

This chapter looks at the theoretical framework on vegetable oil and its conversion into biodiesel. The mechanism of oxidation of biodiesel and its impact on lubricant degradation is explained. How the fuel finds its way into the sump is summarized as well. It ends with a summary of the major theories.

3.1 Vegetable Oils

Rudolph Diesel is the first to use vegetable oils as fuel (Monyem, 1998). Since then, several research pieces have been done into vegetable oil-based fuels (Geyer et al., 2013; Pischinger, 1982; Ziejewski and Kaufman, 1983; Pinzi et al., 2009; Graboski and McCormic, 1998). It has been generally concluded that vegetable oils can be used safely in short periods in diesel fuel engines (Monyem, 1998).

Most vegetable oil properties are similar to that of diesel fuel. Vegetable oil has a higher viscosity than diesel fuel due to the triglyceride molecules' high molecular weight. Triglyceride is a mixture of fatty acid triesters of glycerol. These molecules typically consist of three 18-carbon chains attached to a single glycerin backbone. The vegetable oil level of saturation has a significant impact on its use as fuel in the engine. Due to higher molecular weights, vegetable oils have low volatility and are inherently more reactive than diesel fuels. That explains why they are more susceptible to oxidation and thermal polymerization reactions (Kapilan and Reddy, 2008; Jamieson, 1943). Generally, oils with higher levels of saturation are more desirable for fuels. Vegetable oils have lower saturation levels compared with petroleum-based diesel fuels. The double bonds, typically of unsaturated molecules, are susceptible to oxidation (Knothe and Razon, 2017). Petroleum-based diesel fuel can contain both saturated and unsaturated hydrocarbons in aromatics. However, the level of unsaturation is minimal and hence not a threat to oxidation (Geyer, 2013).

Vegetable oils are fatty esters of glycerol and become transformed into biodiesel when subjected to the chemical process of transesterification. This product can then be used in

the diesel fuel engine (Sadeghinezhad et al., 2013; Balat and Balat, 2008; Muniyappa et al., 1996).

3.2 Biodiesel

Biodiesel is a renewable, clean-burning diesel fuel that is very environmentally friendly. It is believed to provide a feasible solution to the crises of petroleum-based fuel depletion and environmental degradation. Biodiesel consists mainly of fatty acid methyl esters (FAMES) and is made from vegetable oils, animal fats, and waste oils (used cooking oil). The production process of FAME is well-established in the public domain (Flitsch et al., 2014; Sharma and Singh, 2009). Unlike fossil diesel fuel which consists of paraffinic and aromatic hydrocarbons, biodiesel has sites of unsaturation. The level of unsaturation, that is, the number of double bonds in biodiesel, depends on its fatty acid composition derived from the feedstock used for its production. Biodiesel is primarily produced from soybean, rapeseed, or palm oils, although it can be synthesized from a wide range of oils (Bannister et al., 2011). According to the UFOP report on global market supply 2019/2020, biodiesel production among the EU-28 states, rapeseed oil accounted for 41 %. However, palm oil imported from Southeast Asia has a 29 % share in EU biodiesel production. Used cooking oil accounted for 18 %, while animal fats 4 %, Soybean oil 5 %, and sunflower oil 3 %.

FAME is produced by the transesterification of oils and fats with alcohol, mostly methanol, in the presence of suitable catalysts such as sodium hydroxide or sodium methylate. This production process yields glycerol. Stoichiometrically, the reaction needs 3 moles of alcohol and 1 mole of triglyceride to produce 3 moles of fatty acid methyl ester and 1 mole of glycerol Figure 1 (Abdullah, 2007). The methyl ester phase is then subjected to a purification process to be used as biodiesel fuel.

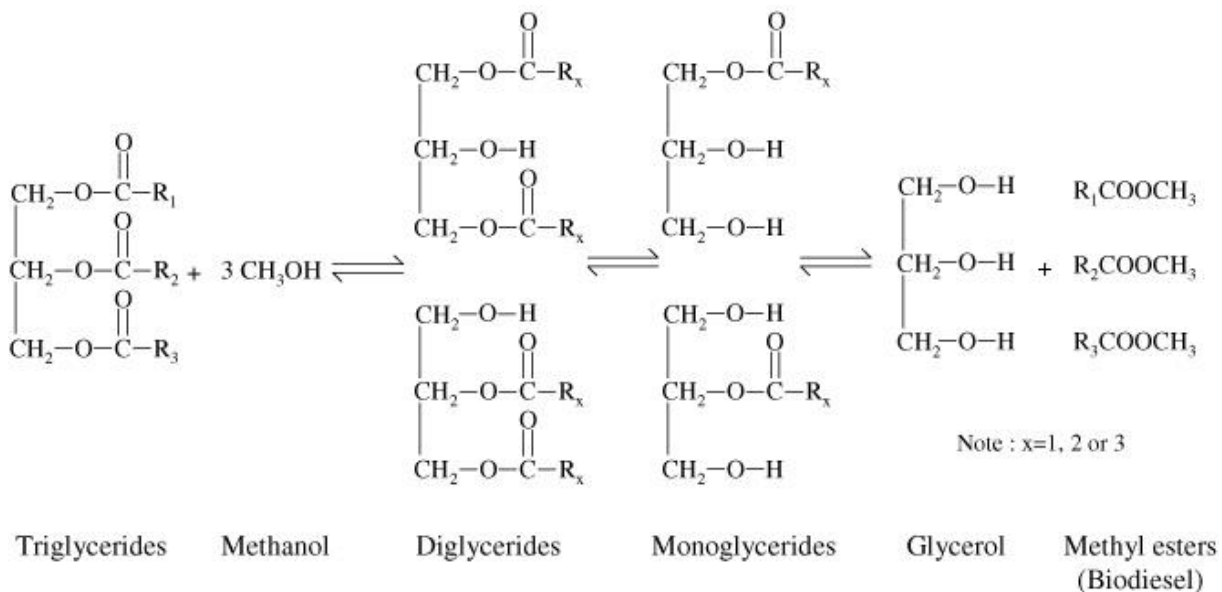


Figure 1: Transesterification process for biodiesel production (Abdullah, 2007)

The bulk of biodiesel produced is a mixture of methyl esters of long-chain fatty acids like palmitic acid (C16:0), stearic acid (C18:0), oleic acid (C18:1), linoleic acid (C18:2), and linolenic acid (C18:3) methyl esters, palmitoleic acid (C16:1) methyl ester is also present in small quantities. As stated earlier, the fatty acid profile varies depending on the feedstock. Generally, palm oil mainly consists of saturated fatty acids; rapeseed oils are high in monounsaturated fatty acids, while soybean, sunflower, and corn oils consist mainly of polyunsaturated fatty acids (Bannister et al., 2011). The double bonds in the monounsaturated fatty acids are the chemically active groups that make the biodiesel fuel chemically and kinetically unstable (Andreae et al., 2007). Unsaturated hydrocarbons generally undergo autoxidation leading to alkyl and peroxy radical formation. These radicals can react with oxygen to form peroxide or hydroperoxides. The peroxides then lead to cyclic products forming acids, aldehydes, ketones, alcohols. They can also react with other alkyl and peroxy radicals to form dimers and oligomers. The reactivity increases from monounsaturated FAME to polyunsaturated FAME. This increase in reactivity is because, in the monounsaturated FAME, allylic hydrogen atoms and the possible hydroperoxides occur at similar ratios. While in the polyunsaturated FAME, bisallylic hydrogen atoms are found. The relative rates of oleic oxidation, linoleic, and linolenic acid are reported to be 1:41:98.3 (Flitsch et al., 2014). The relative oxidation rate gives rise to the oxidation process proportional to the number of bis-allylic sites and not double bonds

in the molecule (Flitsch et al., 2014). The hydroperoxides formed are unstable and hence very reactive. They can, therefore, undergo several secondary reactions simultaneously, leading to a wide range of aging products. These secondary reactions lead to the formation of aldehydes and radicals. The radicals can be further oxidized to acids giving rise to acid values with increasing degradation. This process is illustrated in the next section on the degradation of biodiesel. Other possible reactions of hydroperoxides are epoxidations, dehydrations, and oligomerizations. Epoxides, ketones and dimers, and higher molecular species, oligomers, are formed from these reactions, respectively.

Neat biodiesel is referred to as B100 when it is 100 % pure. The blends are referred to as BXX. The XX indicates biodiesel component in the blend, i.e., a B20 blend is 20 % biodiesel and 80 % mineral diesel fuel.

Degradation of biodiesel

Polyunsaturated fatty acid chains commonly found in many plant-derived oils contain allylic and bis-allylic sites, methylene-interrupted chains. These are crucial to understanding the instability of biodiesel.

Fatty acid methyl esters degrade per autoxidation mechanism (see Figure 2), where various degradation products are formed. In Figure 2, a peroxy radical is formed but relatively inert. It thus selectively abstracts the weakest bound H atom from another fatty acid molecule. This reaction is quite fast. The hydrogen's abstraction from the fatty acid molecule is significantly lower than the hydrogen binding energy. From the binding energies in Table 1, it can be seen that it is easier for the peroxy radical to abstract the H atom from a methylene group of a 1,4-pentadiene system than from a mono-allyl group. This binding energy forms the basis of the differences in the rates at which unsaturated fatty acids autoxidize. It could also be why the peroxy radicals selectively attack the unsaturated fatty acids at room temperature or lower. In oleic acid, H abstraction occurs at methylene groups 8 and 11 (see Figure 2) to give four hydroperoxides isomers (Schumacher, 2013; Jankowski and Baczewski, 2010). Knothe and Dunn, 2003 report similar works; Fang and McCormick, 2006 stipulate that hydroperoxides are the primary initial products of biodiesel degradation.

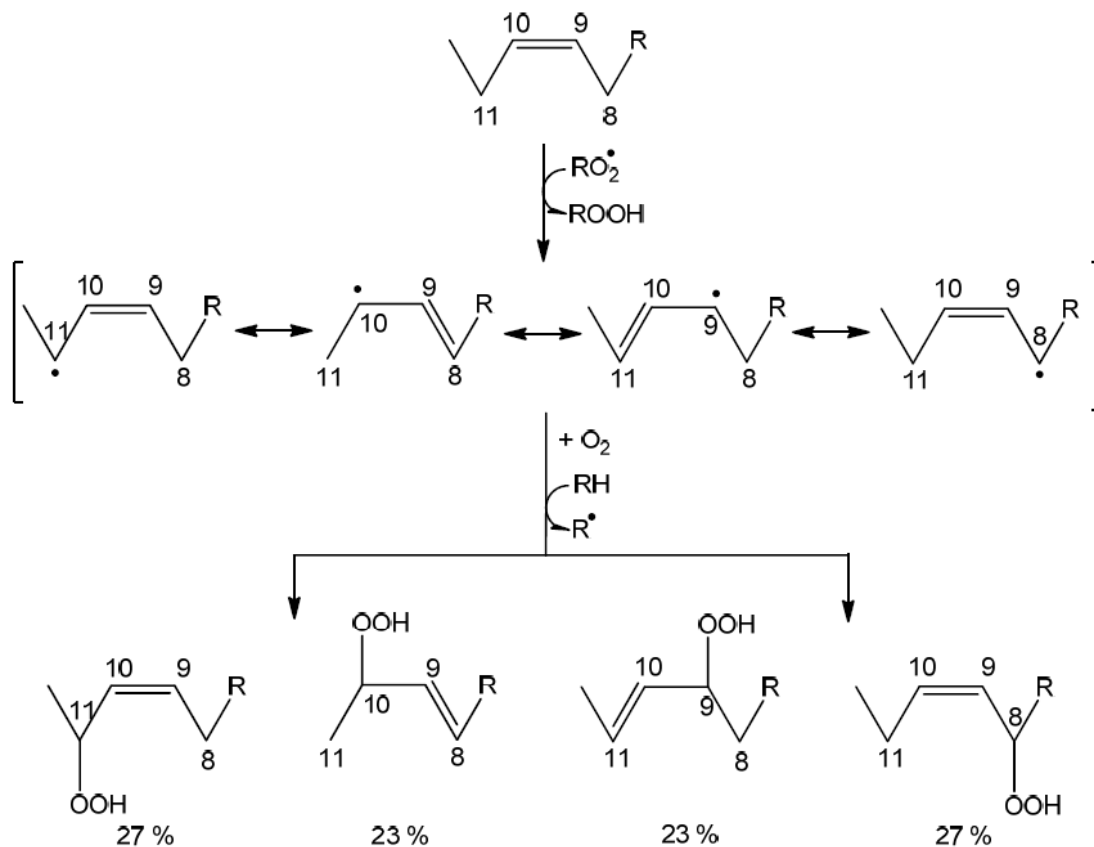


Figure 2: Autoxidative formation of hydroperoxides as primary oxidation products of oleic acid (Schumacher, 2013).

In linoleic acid, the methylene group is in position 11, sandwiching the two adjacent double bonds at positions 9 and 12, making the H-abstraction much more accessible (see illustration Figure 3). The resulting pentadienyl radical stabilizes to form two hydroperoxides in the ratio of 1: 1 (Schumacher, 2013; Jankowski and Baczewski, 2010).

In the autoxidation reaction of linoleic acid, bis-allylic methyl group, and mono-allylic methylene groups (positions 8 and 14 in Figure 3), four hydroperoxides (8, 10, 12, and 14-OOH), each with two isolated double bonds are produced.

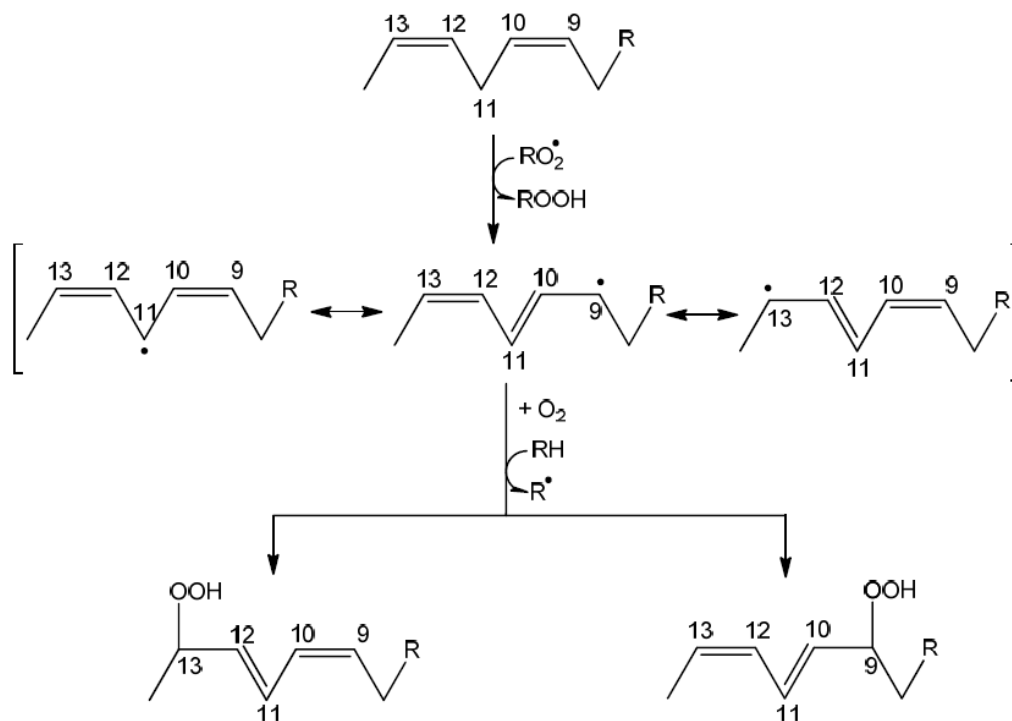


Figure 3 Autoxidative formation of hydroperoxides as primary oxidation products of linoleic acid (Schumacher, 2013).

In most naturally occurring triacylglycerides, multiple fatty acid chain unsaturation occurs in methylene interrupted configuration shown in Figure 4 for linolenic acid. When the double bonds are located in positions 9, 12, and 15 on the carbon chain, two bis-allylic sites thus exist, and the methylene (CH_2) groups interrupting the double bonds are shown at positions 11 and 14.

Four mono hydroperoxides are produced from the autoxidation of linolenic acid, Figure 4. Their formation is assumed to arise from H-abstractions of the methylene groups from positions 11 and 14. The resulting pentadienyl radical stabilizes analogously to the autoxidation of linoleic acid of two hydroperoxides. The result is not equal to the four hydroperoxides formed because the 9 and 16 isomers predominate (Schumacher, 2013; Jankowski and Baczewski, 2010).

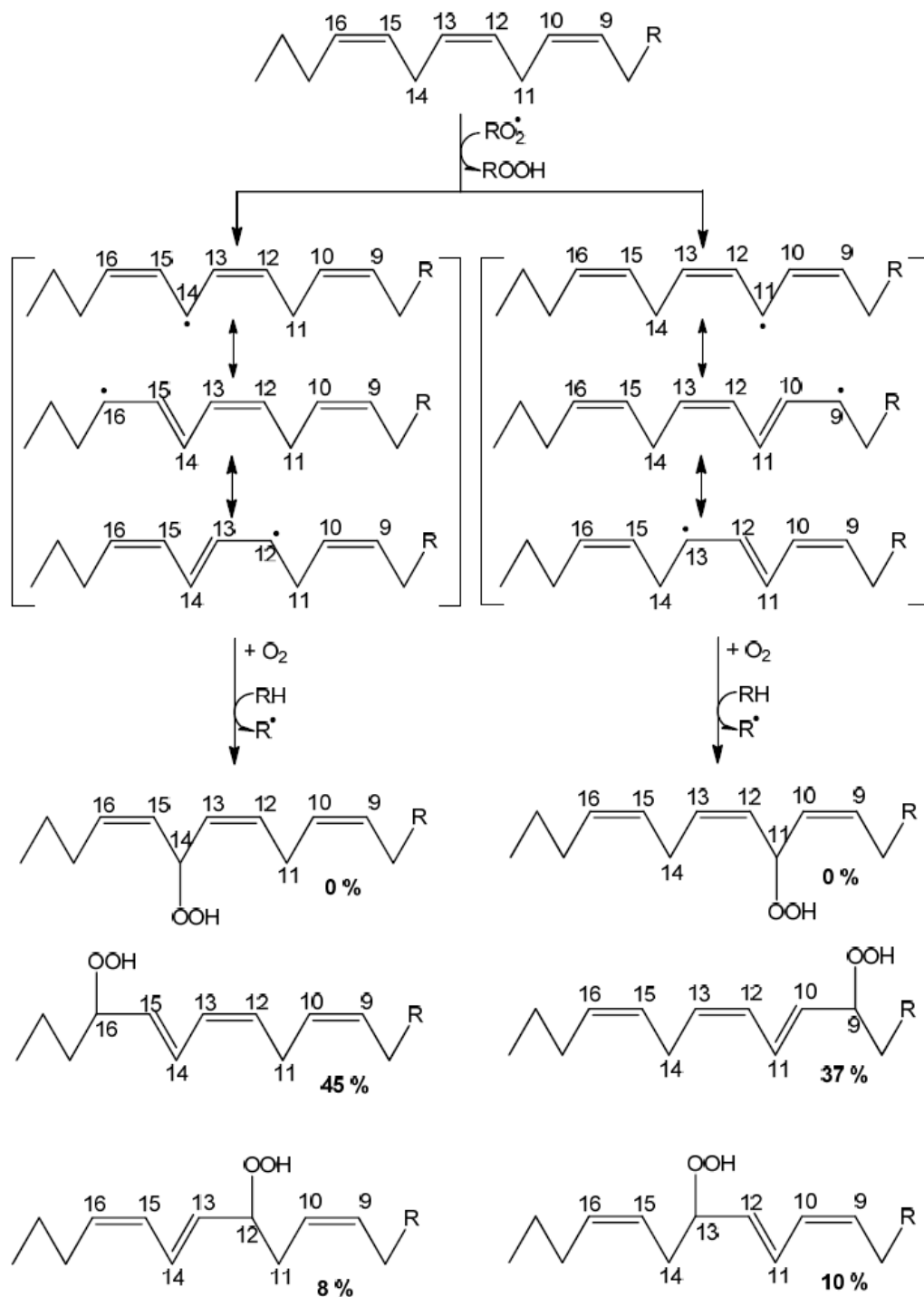


Figure 4 Autoxidation formation of hydroperoxides as primary oxidation products of linolenic acid (Schumacher, 2013)

From the above, it can be concluded that significant aging emanates from only the double bonds in the biodiesel, which is consistent with Fang and McCormick's work, 2006. The number and position of the double bonds determine the rate of the autoxidation process.

According to Knothe et al., 2007, a biodiesel's oxidation temperature is inversely proportional to the amount of bis-allylic hydrogens; in other words, the higher the amount of linoleic acid, the more easily biodiesel is oxidized. The allylic sites are most especially susceptible to oxidation, with the bis-allylic sites been more because of the low binding energy of the methylene hydrogen (see Table 1). Since most biodiesel fuels contain significant amounts of oleic, linoleic, or linolenic acids, it points to the fact that the esters greatly influence the fuel's oxidation stability. Section 2.1 states that a small percent of highly unsaturated fatty compounds have a disproportionately strong effect in lowering the oxidation stability (Schumacher, 2013; Jankowski and Baczewski, 2010).

As shown in section 3.4, the autoxidation mechanism proceeds with forming a radical hydrocarbon species on the bisallylic carbon. The double bonds isomerize into a conjugated structure. The radical reaction with oxygen results in peroxide species, the propagation reaction (Knothe, 2007). The peroxides disintegrate into oxygenated intermediates, which further degrade into short-chain acids, ketones, alkenes, and aldehydes (Monyem, 2000; Morita and Tokita, 2006; Schneider et al., 2008). The peroxide could also form dimers and oligomers via the ether, peroxy, or carbon-carbon bonds (Knothe, 2007; Monyem, 2000).

During biodiesel decomposition, several degradation paths and saturated and unsaturated aldehyde can be formed on the chain with more than one peroxide group (Jankowski and Baczewski, 2010; Schneider et al., 2008; Fang and McCormick, 2006).

In summary, biodiesel's degradation leads to a complex mixture of final products, alkyl hydroperoxides, ROOH, dialkyl peroxides, ROOR, alcohols, ROH, aldehydes, RCHO, and ketones, $RR_1C=O$ (Brühl, 2014).

3.3 Fuel stability

Fuel stability can be considered from three perspectives, storage stability, thermal stability, and oxidative stability.

Storage stability is concerned with any fuel changes that may occur while the fuel is in storage for an extended time. On the other hand, thermal stability is associated with changes in fuel properties while the fuel is subjected to heat. In both storage and thermal

stabilities, the fuel could be exposed to air. Oxidative stability is all about fuel changes in fuel properties through the oxidation process when oxygen from the air is in contact with the fuel.

It is, therefore, evident that biodiesel fuel will oxidize when in contact with oxygen. As explained earlier, when the oxygen comes into contact with biodiesel, the double bond reacts with the oxygen resulting in various chemical products that could alter the fuel's properties.

When this process occurs, the initial products are hydroperoxides. The hydroperoxides may cleave and form aldehydes, ketones, and short-chain acids as the oxidation process continues. Also, sludge and oligomers are formed through polymerization. The level of these changes in the fuel's chemical properties can be quantified.

The induction period or the termed oil stability index may characterize the oxidation stability of a fuel. This method measures the time required for fuel to pass through its induction period. The length of the induction period depends significantly on the fatty acid composition of the fuel. In this method, a stream of purified air is passed through a fuel sample held at a constant temperature. The effluent air from the sample is bubbled through deionized water. The conductivity of the water is then monitored continually with an electrode. The effluent air transports the volatile organic acids from an oxidized sample into the deionized water. The induction period is the point where the rate of change of oxidation is a maximum.

3.4 Oxidation

The mechanism of autoxidation of biodiesel

Biodiesel is oxidized through contact with molecular oxygen in the air. The process of autoxidation is a series of free radical reactions initiated and propagated by free radicals reacting with methylene $-CH_2-$ groups adjacent to double bonds. The radical is oxygen-based, and hence the oxidation rate is strongly affected by the level of saturation of the oil. The hydrogen abstraction leads to a double allylic radical (Meher et al., 2004). When the hydrogen radical is extracted, one of the double bonds moves the radical site to an outer carbon. Dissolved oxygen gets added to this site generating a peroxy radical which

abstracts hydrogen from another methylene group making a hydroperoxide. The hydroperoxides then split to generate two free radicals, a hydroxyl and an alkoxy radical. This reaction is catalyzed by traces of metal ions such as Co, Fe, Cu, or Mn (Rasberger, 1992). Each free radical in the reaction can initiate another chain of reactions. The radicals involved in autoxidation can also participate in polymerization reactions to produce high molecular weight insoluble substances or oligomers.

From the above, molecular oxygen reaction with unsaturated fatty acids is the genesis of biodiesel oxidation. The schemes of these reactions with their rate constants for oxidation of unsaturated fatty acids and fats are well documented (Frankel, 1985, 2005; Cheng and Li, 2007; Kamal-Eldin and Min, 2010; Laguerre et al., 2007; Schaich, 2005; Schaich et al., 2013). The oxidation of biodiesel is generally considered a free radical chain reaction and is illustrated in Figure 5.

The radical reactions consist of four distinct stages: initiation, propagation, chain branching, and termination (Frauscher et al., 2017).

Initiation stage of the radical chain reaction: Creating unstable, reactive radical species sets the reaction into motion. This process usually occurs via homolytic bond cleaving in a radical-controlled reaction to generate two other radical species. In the natural process of oxidation of organic molecules, the initiating step is via oxygen. The breaking of a C-H bond gives rise to a carbon-centered radical and a hydroperoxy radical, termed hydrogen abstraction. The strength of the C-H bond determines the position of attack by oxygen. The bond dissociation energy (BDE) of the various C-H bonds is shown in Table 1. The abstraction H atom in the fatty acid chain is shown in red in Table 1 (Zuletal et al., 2012; Dugmore, 2011; Berton-Carabin et al., 2014; Mortier et al., 2010).

Table 1: Bond dissociation energies of hydrogens

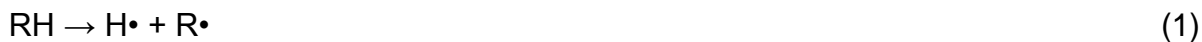
Abstraction hydrogen position	Bond dissociation energy / kJ/mol
H-CH=CH ₂	431
H-CH ₂ -CH ₂ -CH ₃	410
H-CH ₂ -CH=CH ₂	356
R-HCH-CH=CH-CH ₂ -CH ₃	322
R-CH=CH-HCH-CH=CH-	272

The reactivity for hydrogen abstraction increases in the order:



There is no preferentially abstracted hydrogen atom for a uniform molecule, but most have electronic properties that weaken the R-H bond. Therefore, the strength of the R-H bond is directly related to the stability of the resulting R-radical. Though in the oxidation process, homolytic cleaving of bonds is less common, it can naturally occur when the peroxides are formed per the cleavage of the O-O bond to give two alkoxy radicals or a hydroperoxide if one of the R-groups is hydrogen. The abundance of oxygen in the atmosphere is often a relatively small reaction as peroxides are typically the product of radical reactions themselves (Fang and McCormick, 2006; Schumacher, 2013). For initiation of the oxidation, a spontaneous, direct reaction between an acyl chain (RH) and triplet oxygen ($3O_2$) must occur. It is noteworthy that this reaction does not occur naturally because of the opposite direction of the spin of lipid in the ground state compared to that of $3O_2$ (Dugmore, 2011; Christensen and McCormick, 2014). The molecular orbital of oxygen gives rise to a total bond order of 2, consistent with oxygen forming two bonds in stable molecules. The radical nature of oxygen reactions contributes significantly to oxidation chemistry with particular reference to autoxidation. The initiation mechanism, therefore, occurs through different pathways. The first step of autoxidation occurs in the presence of initiators, where an unsaturated fatty acid (RH) loses a hydrogen atom (H) in

an allylic position relative to a fatty acid double bond leading to the formation of an alkyl free radical (R•), according to reaction 1:

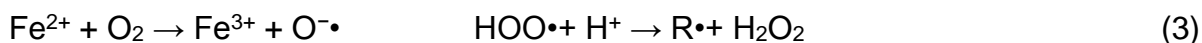


This reaction (1) can be seen in the top left of Figure 5 but it is important to state that it can occur through different pathways:

a. reaction between RH and transition metal ions (M):



b. reaction between RH and oxygen radicals arising from metal autoxidation



c. thermal decomposition of hydroperoxides:



In the work of Berton-Carabin et al. (2014), the high activation energy for this reaction has been reported. Hence the use of other reaction mechanisms which are still in tune with some kinetic observations. One of such reactions involves the use of 2 molecules of hydroperoxides:

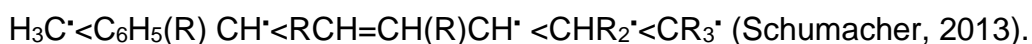


Propagation: This is illustrated in the bottom left of Figure 5. At the propagation stage, alkyl radicals formed during the initiation stage react with oxygen forming peroxy radicals that subsequently abstract hydrogen from another hydrocarbon resulting in a hydroperoxide and another radical, as shown in Figure 5 (Soleimania et al., 2014; Ancho, 2006). Propagation reactions, therefore, ensures the radical cycle continues by continually providing new species of radicals to react. The oxygen-based peroxy, alkoxy, hydroxy,

and hydroperoxyl radicals are key participants in the propagation cycle in oxidation chemistry. The first types of propagation reaction usually involve radicals generated during the initiation reaction stages. One of the most common oxidation reactions involves the carbon-centered radical reacting with the abundant and reactive oxygen in the atmosphere to generate peroxy radicals. These peroxy radicals stabilize themselves by undergoing hydrogen abstraction to form a hydroperoxide and another carbon-centered radical. These two reactions could be the most significant propagation reactions as the products are the other's reagents. Hence, they permit the cycle to be formed and continued as long as oxygen and hydrocarbon are present (Schumacher, 2013). Once an alkyl radical has been formed, it reacts irreversibly with oxygen to form an alkyl peroxy radical:



The reaction rate of carbon-centred radicals with oxygen is dependent on the type of substituents attached to the C atom and, therefore, increases in the order:



The next step in the chain propagation scheme is the hydrogen abstraction by a previously formed peroxy radical from another hydrocarbon:



This reaction leads to a hydroperoxide and an alkyl radical, which can again react with oxygen as in reaction 9. Therefore, peroxy radicals have low reactivity and are therefore present in relatively high concentrations than other radicals. Due to their low energy status, peroxy radicals react selectively. They abstract tertiary hydrogen atoms in preference to secondary and primary hydrogen atoms. Their relative reaction rates are 1:30:300 for C-H primary, C-H secondary, and C-H tertiary (Schumacher, 2013; Rasberger, 1992).

Another type of radicals that could be generated is the alkoxy radicals. These generated radicals can also abstract hydrogen, creating a carbon-centred radical ending up in an appropriate alcohol formation. The alkyl radicals ($R\cdot$) produced is very unstable and, therefore, react very quickly with the triplet oxygen to generate peroxy radicals ($ROO\cdot$)



As the peroxy radicals are unstable, they quickly abstract hydrogen atoms from other unsaturated fatty acids to form hydroperoxides and other alkyl radical products:



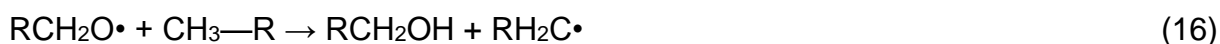
The newly formed alkyl radicals may then react with the triplet oxygen and continue with the process. Therefore, the radical chain reaction perpetuates at a higher rate increasing exponentially the number of hydroperoxides formed.

Chain branching stage: Rasberger (1992) described a stage termed the chain branching stage. The initial stages of autoxidation saw the generation of many kinds of hydroperoxides. As stated in the initiation stage of oxidation, these hydrocarbons may homolytically cleave at low concentrations to yield alkoxy and hydroxy radicals,



This reaction is, however, not favored due to its high activation energy.

As seen already during the propagation stage of oxidation, hydroxy and alkoxy radicals are very reactive, and so they abstract hydrogen atoms in non-selective sites,



From the above study of Rasberger (1992), secondary and tertiary alkoxy radicals form aldehydes and ketones prudentially,

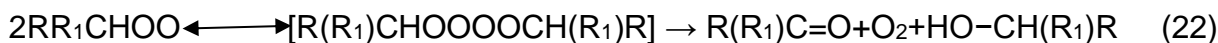


Termination: This is shown on the right side of Figure 5. As hydroperoxides are produced, an increase in autoretardation sets in, leading to the oxidation process's termination. Accumulation of the degradation products formed during this termination stage causes an

increase in viscosity (Soleimania et al., 2014). During this stage, the radicals react together to form stable nonradical compounds, as illustrated on the right side of Figure 5.



The nonradical compounds formed cannot thus participate in the reaction cycle anymore and, therefore, bring the radical chain reaction to an end. As the decomposition pathways are varied, the different radicals are produced with many possible combinations (Berton-Carabin et al., 2014). Thus, when two radicals combine to give a stable molecule, no other radical species are left. Hence autoxidation reaction is followed by what is termed the autoretardation stage. The autoretardation brings a standstill just before the hydrocarbon is completely consumed, which is the termination reaction. It dominates in this final phase of the oxidation process, bringing degradation to a stop. Termination reactions may be caused by the combination of radicals such as peroxy radicals to yield ketones and alcohols:



A carbon-centered radical can combine with a hydroperoxyl radical, resulting in a hydroperoxide. The formed hydroxyl radicals can also combine with a carbon-centered radical to give a more stable alcohol molecule (Ross et al., 1949; Moritani and Nozawa, 2004).

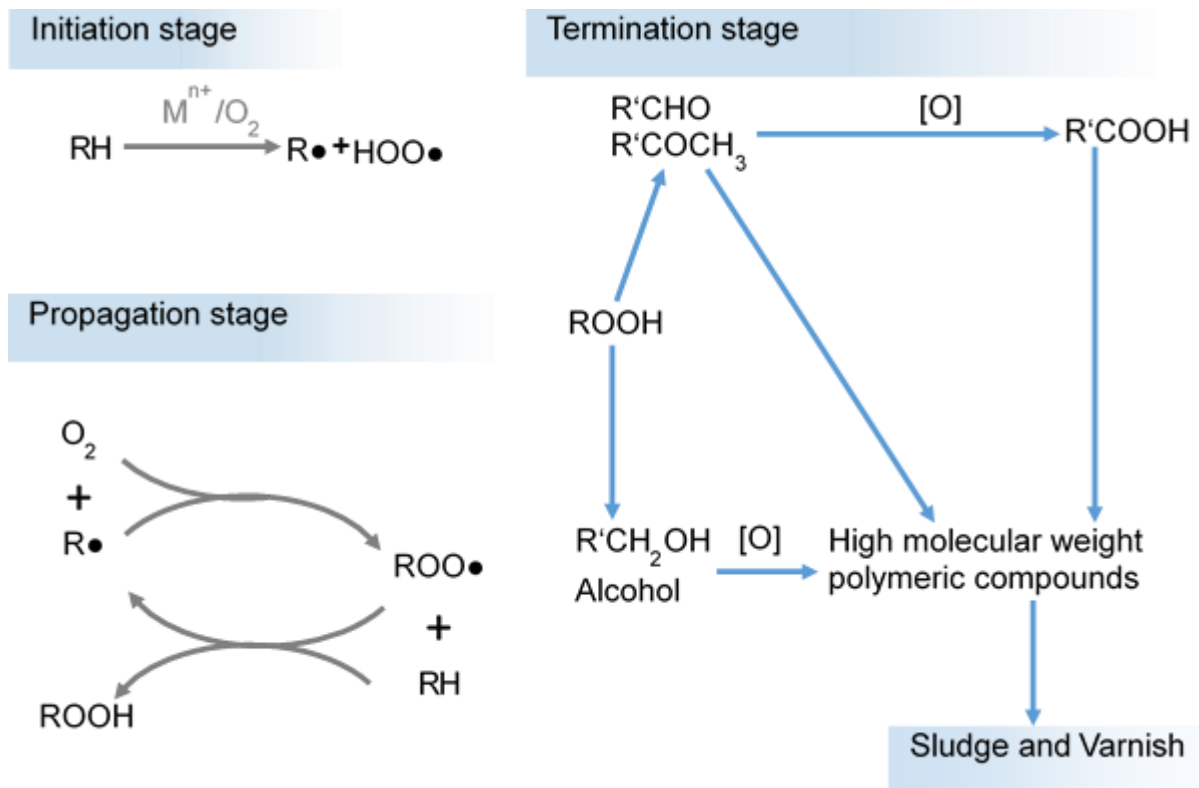


Figure 5 Oxidative degradation of hydrocarbon (Ancho, 2006)

It should be stated that in light, volatile hydrocarbons manifest in the form of combustion. This process requires an initial energy input to get started. This issue is peculiar to heavier hydrocarbons at room temperature. But as the fuel combusts, energy is released to drive the motor. The energy waste from the combustion is released as heat. Therefore, inside the engine, there is a vast increase in temperature. An average temperature of over 250 °C inside the combustion chamber on the cylinder walls can be recorded (Dugmore, 2011).

As stated in the autoxidation process with FAME biodiesel, the unsaturated sites typically have singly or doubly allylic C-H bonds, which are weaker than saturated sites. The process gives rise to their capability to react rapidly with oxygen centred radicals in the autoxidation process to form oxidative products such as ketones and epoxides (Hamberg & Gotthammar, 1973). It occurs primarily during harsh temperatures typically found in combustion engines via the radical cycle. Linoleic acid is a commonly occurring fatty acid and a significant biodiesel component (Dugmore, 2011; Blanksby et al., 2003). As

polyunsaturated compounds are more reactive than monounsaturated and saturated ones, it can be said that methyl linoleate is one of the primary chemicals responsible for the enhanced formation of engine deposits and accelerated rate of lubricant oxidation. During the formation of hydroperoxides, the migration of double bonds on the chain, as shown in Figure 2, Figure 3, and Figure 4, supports the fact that it is the leading cause of fat and lipid degradation (Dugmore, 2011; Ross et al., 1949).

3.5 Engine oil

Engine oil is a lubricating oil that reduces friction, heat and wear between mechanical or moving components in contact. Therefore, lubricants are substances introduced in between two surfaces that are in relative motion. In this work, motor oil, engine oil, lubricants, or lubricating oil are used interchangeably, but all refer to the same thing. Lubrication is used to reduce friction and prevent rust, and, to some extent, seal against water particles, dust, and dirt. In essence, lubricants fulfill very vital functions in the operation of engines and equipment. So, when the motor oil is manufactured, the main goal is to achieve the motor's maximum durability and preserve all motor properties as long as possible (Sejkorová, 2017).

Lubricants are composed of base oil and about 0.1-30 % additive package of the oil volume depending on its application (Fujita, 2006). Base oils are highly complex mixtures of many hydrocarbons with wide variations in their chemical structure and composition due to the differences like their crude sources and even production methods (Adhvaryu et al., 1998). The additive package is expected to perform for a longer duration to meet longer drain intervals. However, upon introducing lubricating oil into an engine, its functionality will be impacted by its operation, environment, and oil degradation. One other major factor that influences lubricating oil durability is degradation. It comes about as a result of a decrease in antioxidant and detergent additives efficiency. The additives get depleted either by decomposition, adsorption onto metal and other surfaces, or separation because of settling or filtration (Yuegang, 2016; Hilligoss, 2012). Additives vary in composition and often come in packages that may be combined to produce a well-balanced additive package to meet specific performance criteria. Additives come in both organic and inorganic forms. Polar additives are more problematic when considering the

use of adsorbents because they contain heteroatoms within the molecule. They possess a polar head and a non-polar or hydrocarbon tail.

Also, the additives contain both metals or metallic salts and non-metallic components in them. Typical additive elements include sodium (Na), Barium (Ba), Copper (Cu), Boron, (B), Magnesium (Mg), Calcium (Ca), Molybdenum (M), Phosphorus (P), Silicon (Si), Potassium (K) and Zinc (Zn) which represent the inorganic components. The elemental content of a typical standard lubricant is shown in Table 2 (Fujita, 2006; Yuegang, 2016; Hilligoss, 2012; Perkinelmer, 2011). The elements of additives in the lubricant do not increase or decrease (Song and Choi, 2008). A lubricant should be oxidatively stable due to high temperatures and air in the engine. High oxidation stability is required to prevent lubricant oxidation; else, it will increase oil viscosity due to sludge formation. Due to long periods of lubricating oil exposure to high temperatures during its usage in the engine, the lubrication oil must have high thermal stability. The lubrication oil's viscosity must be sufficiently stable to form a thick oil film to avoid metal-to-metal contact.

Table 2: Typical concentration of additive elements of a standard lubricant (Fujita, 2006; Yuegang, 2016; Hilligoss, 2012; Perkinelmer, 2011)

Elements	Motor Oil	Possible Range of Concentrations	
		PPM	PPM
Ca	0.18%	0	5000
Mg	0.08%	0	5000
Zn	0.08%	0	3000
P	0.07%	0	5000
Si	0.19%	0	900
Ba	0.06%	0	5000

3.5.1 Oxidation of lubricant base oil

As stated in the introduction, section 3.5, lubricating oil is made of base oil and additives, and as such, oxidation thus plays a role in the degradation of the lubricating oil. The base oil could be mineral oils, synthetic oils, or mixtures (synthetic oils and mineral oils). The base oil quality, such as viscosity, low and high-temperature evaporation behavior, contributes to the engine oil quality. When a lubricating oil is applied in a machine, it gets oxidized with time, depending on the type of oil. The operational environment and conditions also contribute to its oxidation. Therefore, oxidation is a common problem in the engine and can negatively affect lubrication with resultant consequences for its performance (Ancho, 2006). Oxidation is a complex chemical degradation process that occurs a chemical breakdown of base oil molecules with oxygen.

The base oil consists of many different hydrocarbons, and the oxidation process occurs when there is a reaction between the hydrocarbons and oxygen. As seen in biodiesel's oxidation, this process, too, is a self-propagating process occurring through free radicals.

Temperature plays an essential role in oxidation. The oxidation of oil proceeds through the three stages of initiation, propagation, and termination, as shown in Figure 5 in section 3.3 (Ancho, 2006; Adhvaryu et al., 1998).

Hydrocarbons react with oxygen during the initiation stage to form the hydrocarbon free radicals; see top left of Figure 5. The presence of traces of transition metal ions, copper, cobalt, iron, chromium, etc., could catalyze the reaction (Ancho, 2006).

At the propagation stage, bottom left of Figure 5, the free hydrocarbon radicals react with oxygen to form very reactive peroxide radicals. Therefore, they react further with other hydrocarbons from the oil. It results in hydroperoxides and hydrocarbon free radicals reacting with oxygen (Ancho, 2006).

During the termination stage (right side of Figure 5), hydroperoxides formed cleave homolytically to form oxygenated compounds, aldehydes, ketones, alcohols, and water. It can be seen in the schematic illustration in Figure 6. The aldehydes and ketones are formed during the primary oxidation phase. When formed, they combine through Aldol

condensation (Adhvaryu et al. 1998; Naidu et al. 1984) to form high molecular weight substances, sludge precursors.

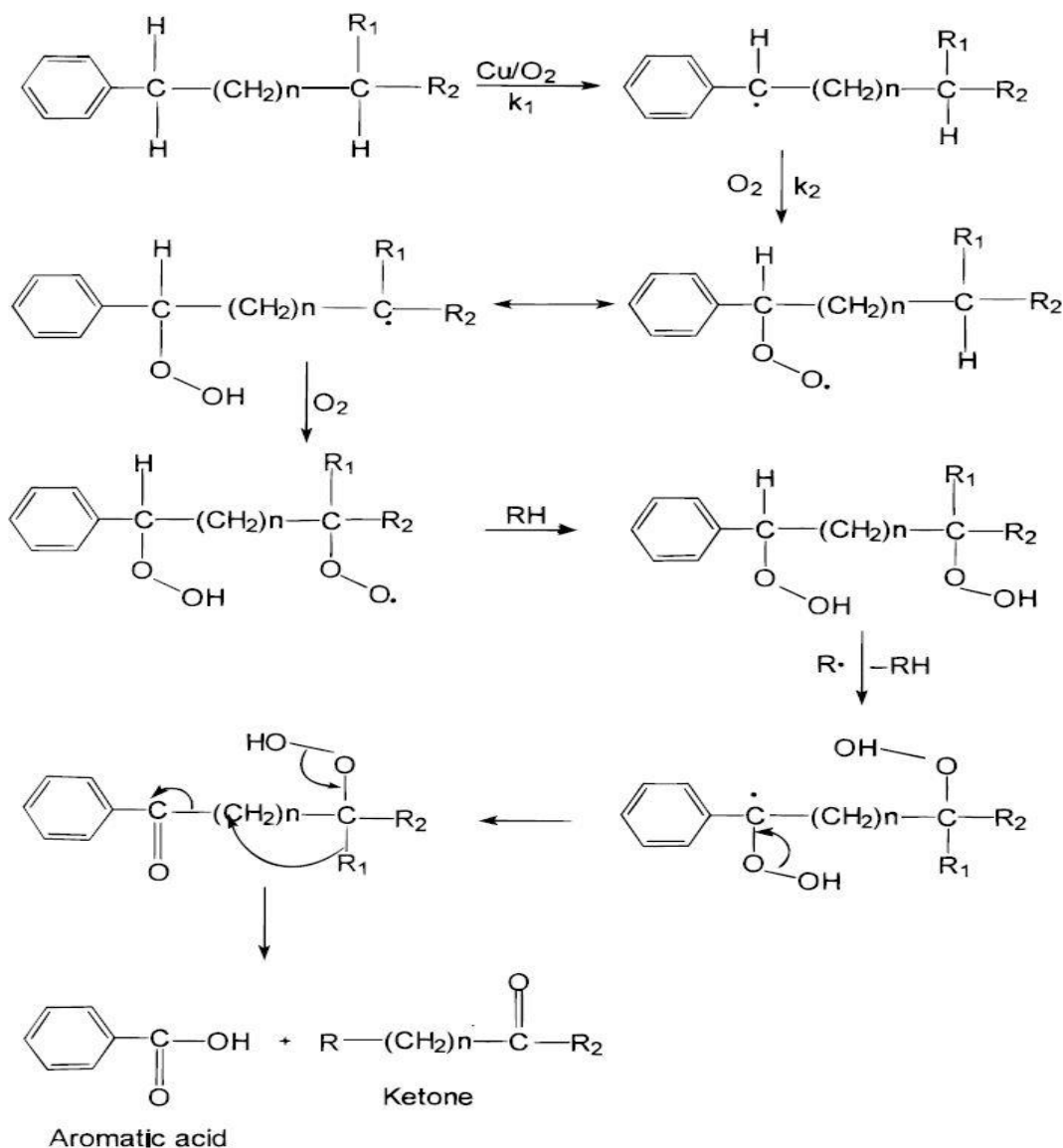


Figure 6 Oxidation of base oil (Adhvaryu et al. 1998)

The formation of insoluble products, sludge, or varnish leads to increases in oil viscosity. Further polycondensation and polymerization reactions of these formed high molecular weight intermediates result in sludge, Figure 7. The alkoxy radicals can initiate polycondensation products, resulting in additional high molecular weight products, contributing to viscosity (Rasberger, 1992). The further reaction of oxygenated

compounds of aldehydes, ketones, alcohols, and water also increases acidity (Ancho, 2006).

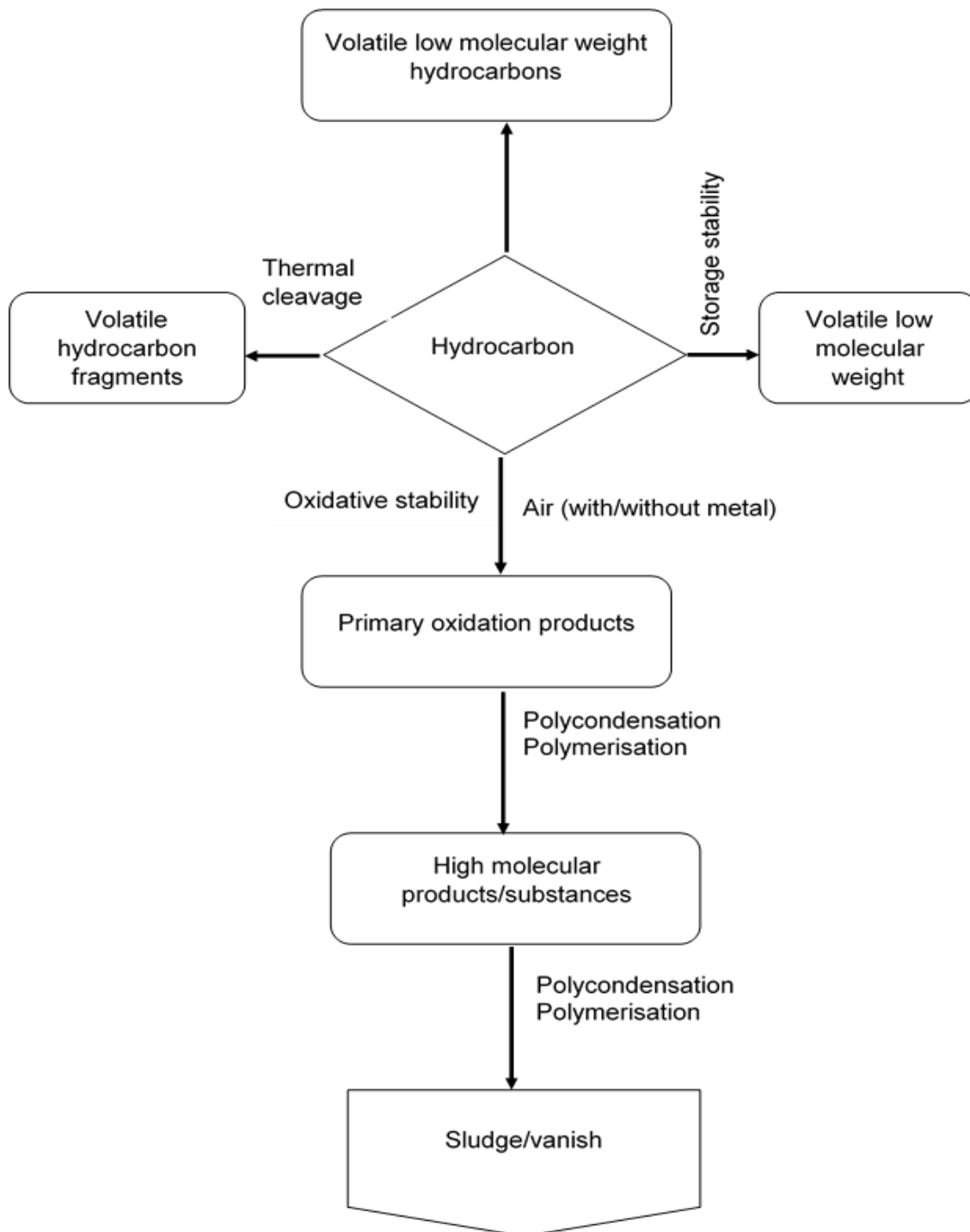


Figure 7: Flow chart of lubricant degradation process under oxidative conductions (Rasberger, 1992)

3.5.2 Dominant mechanisms of degradation

Various products from methyl linoleate and methyl oleate degradation all come from just two main pathways. The scission products, alcohols, and ketones are formed by the initial hydrogen abstraction reaction from an allylic, or doubly allylic C-H bond, whereas epoxides are formed over the C=C bonds (Dugmore, 2011; Brühl, 2014). Confirming the above products' formation also points to the detrimental effects of biodiesel on engines. It is because it can dimerize and also most likely the ability to polymerize further. It is noteworthy that the viscosity of molecules increases exponentially with chain length. Therefore, the polymerization of unburnt fuel can thicken and potentially lead to deposit formation. Since hydrogen abstraction is a necessary step for this process, this could explain why oligomers or sludge formation appears to be aggravated by the use of unsaturated biodiesel. Because the molecule can undergo more accessible hydrogen abstraction due to the weaker doubly allylic C-H bond, it should polymerize more easily theoretically. Therefore, the major products from the autoxidation of methyl oleate and methyl linoleate can be said to be responsible for the mechanisms of autoxidation (Dugmore, 2011).

Short-chain fatty acids are formed during the oxidative degradation of fatty acid methyl esters (Brühl, 2014; Dugmore, 2011). The first step of forming short-chain acids is the connection of oxygen to an unsaturated fatty acid. When the oxygen-linked carbon is split off and a proton is added to the remaining fatty acid chain, the short-chain fatty acid is attached to the glycerol backbone. This reaction leads to the formation of hydroperoxides which decompose rapidly and produces an alkoxy radical. This alkoxy radical can be split by homolytic β -scission at each side of the oxygen-linked carbon. The short-chain fatty acids formed are non-volatile stable products from the fatty acid hydroperoxides' thermal decomposition (Kim et al., 2018; Brühl, 2014). Several short-chain fatty acids are produced during this degradation phase, including aldehydic acid, hydroxyl fatty acid, diacid, furanoid acid, ketoacid, to mention but a few, Figure 8 (Brühl, 2014; Dugmore, 2011). It explains the high level of acidity with increasing aging or degradation of the fatty acid methyl esters.

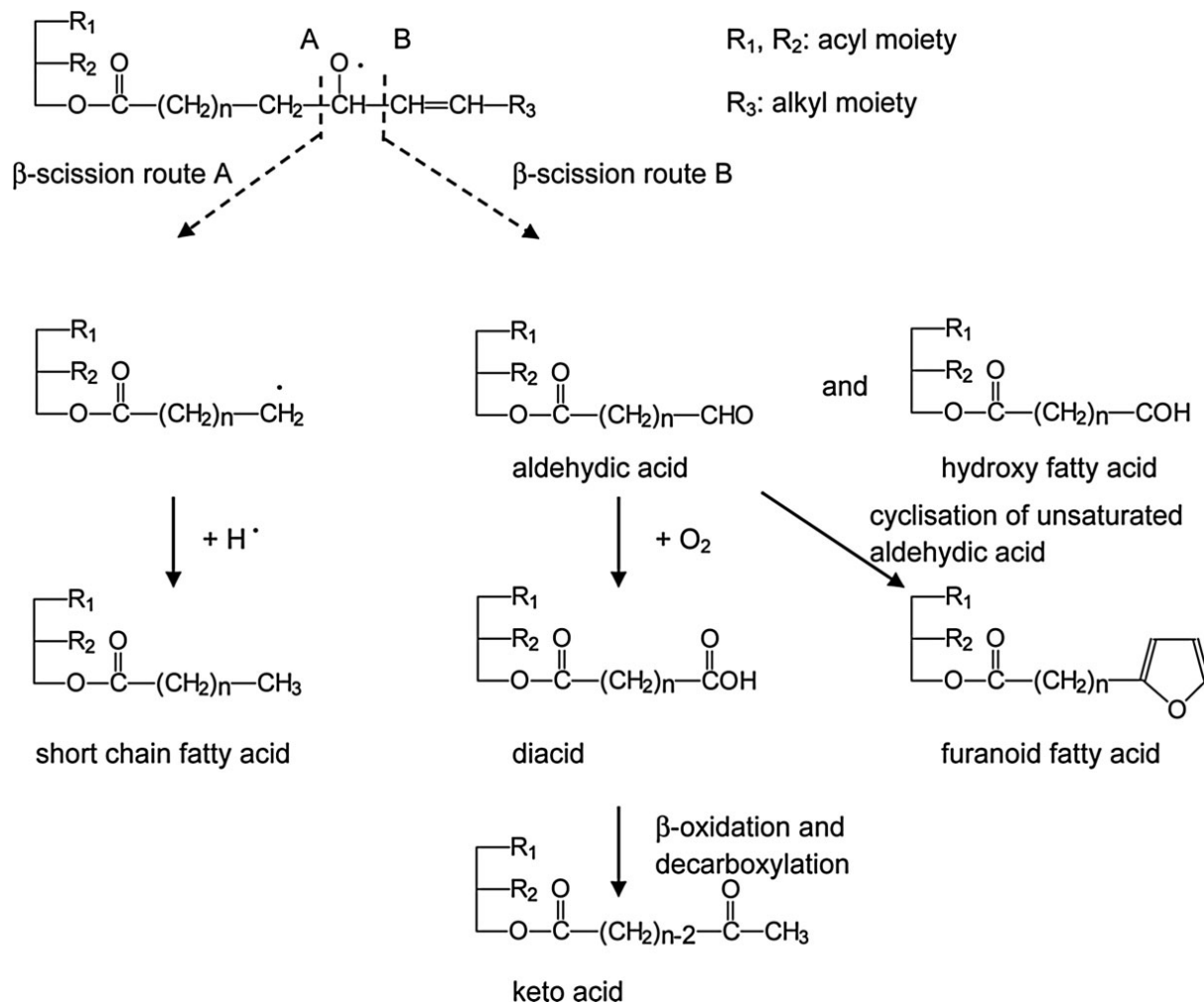


Figure 8 Short-chain acid formation (Adapted with permission from Brühl, 2014)

3.6 Oxidative stability of biodiesel and its effect on performance

One main criterion for the quality of biodiesel is its stability in application or storage. The level of unsaturation makes vegetable oil derivatives susceptible to thermal and oxidative degradation. It usually led to the production of insoluble products, which causes problems. Biodiesel produced from feedstocks with a more significant proportion of saturated fatty acids is more stable than the one with a more significant proportion of unsaturated fatty acids. The degradation of biodiesel is accelerated when oxygen, water, and heat are present. From the above, unsaturates are susceptible to oxidation (Perez, 2000). However, biodiesel's oxidation stability depends not on the total number of double bonds but the total number of bis-allylic sites as stated in section 3.2. The fatty acid methyl esters form radicals during the oxidation process (see Figure 5). A new radical from FAME is

also created by the peroxide radical. The radical then binds with oxygen in the air and promotes the rapid production of many new radicals from a single radical. The result is the formation of a series of many by-products of oxidation. It gets the fuel quality deteriorated.

3.7 Entry of fuel into the engine oil

Fuel dilution seriously reduces oil viscosity and accelerates the engine's wear process due to low lubricity (Wakiru et al., 2017). Fuel dilution could result from over-fueling, defective fuel injectors, leaking high-pressure fuel lines, leaking fuel heat exchangers, etc. Fuel leaks in diesel engines cause a decrease in oil viscosity, which leads to damage of load-bearing components. Other fuel entry sources into engine oil could be due to fuel condensation during the engine warm-up period. The low viscosity due to the oil dilution negatively influences keeping the strength of oil film and the metal parts separated. Therefore, it increases wear within the bearing components (Wakiru et al., 2017; Song and Choi, 2008; Asseff, 1968).

Fuel could also leak into the lubrication oil through the stuffing box or leakages in the fuel pump. Other fuel entry sources include piston movement and the regeneration of diesel particulate filter (DPF) (He et al., 2011). It is a central problem with cars, especially those fitted with DPF. That is the underlying reason why biodiesel blend is limited to 7 %. This impact could be worse with higher percentages of biodiesel blends.

The sump is where the unburnt fuel, which migrates down the cylinder walls, accumulates. The sump also experiences low temperatures far away from the engine's combustion chamber and other moving parts. Accumulated oil is then pumped out from the sump to re-lubricate the piston assembly and the other moving parts of the engine. Lubricant oil dilution reduces the effectiveness of the additives within the oil (Song and Choi, 2008), increases the volatility of the oil, reducing flashpoint, thereby increasing the rate of oxidation, which eventually leads to more frequent oil changes.

3.8 Effect of biodiesel on engine oil

The use of biodiesel, in general, harms oxidative stability of the lubricant and deposit formation (Knothe and Dunn, 2003; Karavalakis et al., 2010; Agarwal, 2005; Hu et al.,

2015). First, there is lubrication oil dilution by the fuel. This biodiesel dilution is not desirable from the lubrication point of view since it affects the engine (Gili et al., 2011). The contamination by fuel causes loss of working capacity and worsens its basic performance properties (Song and Choi, 2008). Heavy molecular mass fuels that distill at temperatures above 340 °C are the most harmful culprit (Koch, 2009). Because of the internal combustion engine's operating temperature, the light molecular mass fuel components evaporate while the heavy molecular mass fuel components accumulate in the motor oil. The distillation range of biodiesel is narrow with high-boiling characteristics of 350 °C to 375 °C as compared with petroleum diesel fuel, about 175 °C, Figure 9 (Wakiru, 2018; Niculescu et al., 2019; iea-amf.org, 2014-band-04-10) and therefore, accumulates in the engine sump leading to engine oil dilution. The changes occurring in the lubrication oil quality enhance the oil's intensive aging (Fang et al., 2007). The oxidation of biogenic fuels in crankcase oils creates increased deposits and enhances corrosion (Gili et al., 2011).

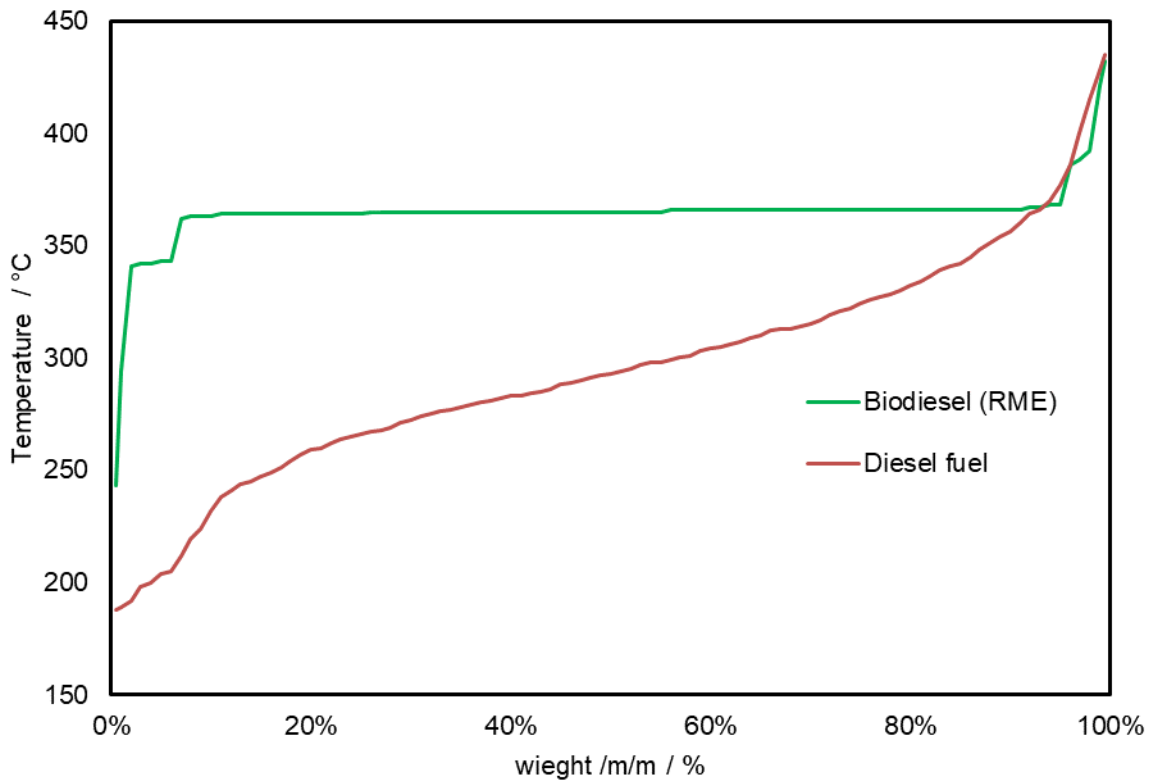


Figure 9: Distillation temperature characteristics of biodiesel and diesel fuel (Krahl et al., 2012)

Applying alternative fuels that are incompatible with lubricants can significantly extract some additives (Koch, 2009). Therefore, fuel in the sump of an engine adversely affects the properties and performance of lubrication engine oils and the engine itself. The use of biodiesel has seen an increase in the formation of higher molecular substances because biodiesel and its blends increase oil dilution in engine sump (Watson and Wong, 2008). The lubrication oil dilution can lead to complex chemical formation between the oxidized biodiesel and some oil additives (Fang et al., 2007). Oxidation promoted through the dilution of lubricating oil by biodiesel increases the lubricant's acidity. Biodiesel degrades engine oil performance resulting in shortening oil drain intervals (Khuong et al., 2016). An increase in engine oil dilution by biodiesel fuel results in a corresponding increase in sludge buildup due to increased oxidation (Devlin et al., 2011; Watson and Wong, 2008).

It is shown in other studies that even a low percentage of fuel dilution can degrade the physicochemical properties of the lubricant such as viscosity, total base number, total acid number, and oxidation stability, as well as the concentration of the additives in the engine oil (Shanta et al., 2011; Song and Choi, 2008). The fuel dilution of engine oil results in reduced viscosity, depletion of additives, and sludge formation, leading to an increase in the lubricating oil's viscosity. Furthermore, fuel in the oil decreases its viscosity and degrades its resistance to oxidation (Watson and Wong, 2008). The lubricating engine oil dilution by biodiesel increases wear and shortens the recommended oil drains between 30 % and 60 %, as reported by Gili et al. (2011).

4 Basic Experimental Techniques for Evaluation

4.1 Techniques for evaluating the suppression of oligomers formation

As discussed in sections 3.4 and 3.5.1, FAME and lubricant base oil oxidation is a complex process. The aging of oil causes a deterioration in oil or biodiesel quality. A growing trend towards the build-up of deposits leads to changes in viscosity, density, acid number, and other physiochemical properties. There are often limits for acceptable viscosity, density, acid value, and induction time to indicate the degree of oxidation in practice. According to literature (Knothe, 2006; Dunn, 1995, 2002, Mittelbach and Gangl, 2001; Bondioli et al. 2002), the quantity of peroxide produced during the oxidation process, as seen in section 3.4, may not be a suitable measurement parameter (Bong-Ha and Yun-Ho, 2008). After an initial increase at the onset of oxidation, it decreases due to the formation of secondary oxidation products, resulting in extensive oxidation of fuel but with an acceptable peroxide value. Suppression of oligomers formation is associated with biodiesel's stability, whose degradation impacts the lubricating oil's stability. It is, therefore, paramount to relate the chemical and physical changes associated with biodiesel oxidation to the conditions of the presence or absence of the adsorbents applied in these experiments.

Several methods have been developed to determine biodiesel's degree of oxidation in an application and long-term storage or determine its susceptibility to oxidation. Acid value and kinematic viscosity are two facile methods for assessing biodiesel fuel quality because they continuously increase with deteriorating fuel quality (Knothe, 2006; Canakci et al., 1995). These methods include acid values (Bouaid et al., 2007; McCormick and Westbrook, 2010; McCormick et al., 2007), the oxidation stability index (Mittelbach and Gangl, 2001), the content of methyl ester (Leung et al., 2006), infrared spectroscopy (Conceição et al., 2007), nuclear magnetic resonance spectroscopy (NMR) (Conceição et al., 2007), size exclusion chromatography (Van Gerpen et al., 2011; Kittirattanapiboon and Krisnangkura, 2008). For the qualitative evaluation of biodiesel degradation in this work, a wide range of techniques is utilized, including Fourier Transform Infrared spectrometry (FTIR), Gas Chromatography with Mass spectrometry (GCMS), and Flame Ionization Detector (GC-FID). High molecular mass substances or polymerization is studied by Size Exclusion Chromatography (SEC).

4.1.1 Size Exclusion Chromatography (SEC)

Size exclusion chromatography (SEC) physically separates a sample into its components based on molecular size. Size exclusion chromatography is also known as gel permeation chromatography (GPC). As illustrated in Figure 7 in section 3.5.1, primary oxidative products' polycondensation eventually results in higher molecular mass substances. These oligomers increase the viscosity and density of the sample. The oxidized biodiesel samples may not be amenable to GC-based analyses due to the formation of higher-molecular-weight species, and therefore the SEC method is perfectly applied here (Knothe, 2006). The impact of the adsorbent in inhibiting the formation of higher molecular mass substances can then be monitored. Peroxyl radicals are predominant free radicals encountered in oil oxidation (Fereidoon and Ying, 2015). The formation of higher molecular mass substances can be monitored with the SEC's measurement, where the area under the curves is constructed with the absence or presence of the adsorbents. The net integrated area under the curves represents the gain due to adsorbents' presence compared to the absence of the adsorbents. It is calculated as an indicator of the adsorbent's scavenging capacity.

SEC separates the molecules according to their adequate size in solution using a stationary phase in the form of either cross-linked polymers that swell on contact with a solvent or a microporous polymer of rigid structure. SEC uses hydrophobic column packing materials like silica gel or styrene-divinylbenzene copolymers and a non-aqueous mobile phase to measure polymers' molecular weight distribution. It is mainly utilized for the determination of molecular weight distribution. In this separation process, the column used is filled with material containing many pores. Therefore, when dissolved molecules of different sizes flow into the column, smaller dissolved molecules flow more slowly due to their deep penetration into the pores.

On the other hand, the larger dissolved molecules will flow quickly through the column since they do not enter the pores and, therefore, elute from the column's void volume. Consequently, larger molecules elute from the column sooner and smaller molecules later, which effectively sorts the molecules by size leading to the average molecular weight values. It is the separation principle of size exclusion chromatography. Therefore,

synthetic polymers having the same average molecular weight could differ in their weight distribution, resulting in their properties. Therefore, the size exclusion chromatography will give information on how much different molecular weights are of a polymer.

4.1.2 Gas Chromatograph-Mass Spectroscopy (GCMS)

The gas chromatography (GC) coupled with a mass-sensitive sensor (MS) separates and analyses volatile organic fuel components in the gaseous phase. Aging products and fuel components, which are not volatile or destroyed during evaporation, cannot be analyzed using the GC-MS system. The basic principle of molecule separation and analysis is the interaction between the mobile gas phase (evaporated sample) and the column's inner surface stationary phase. The GCMS is used in this research to analyze biodiesel and base oil mixtures but not the biodiesel-diesel fuel mixtures because the wide range of carbon compounds in the diesel fuel could generate complex spectra with overlapping signals, resulting in difficulty in identifying.

With this column, the substances such as fatty acid methyl esters, motor oil, and oxidative products, e.g., alcohols, aldehydes, ketones, carboxylic acids, etc., in this work can be separated and detected by their different mass numbers.

The GCMS method takes advantage of retaining the more polar compounds of the sample aged without using the adsorbents than the less polar compounds in the sample aged with the adsorbents. Due to the adsorbents' use, the mixture is less affected by the oxidation process and has fewer oxidative products. The polar column maximizes the separation that can be achieved for identification. However, the GCMS is not an efficient instrument for detecting oligomers due to the high mass of the oligomers formed and their inability to vaporize.

4.1.3 Total Acid Number or Value (TAN)

The total acid number or simply acid number or acid value is the equivalent to the amount of potassium hydroxide in mg required to neutralize acids contained in one g of sample. The standard unit of measure is mg KOH/g. The final component in an oxidation reaction is acid. The acid number test will show value in determining the results of an oxidation or degradation reaction. The total acid number does not represent the absolute acid

concentration of the sample. However, the acid number or acid value measurement detects weak organic acids and inorganic acids (Practicing Oil Analysis, 2007). Carboxylic acids formed during hydrocarbon-based oil or fuel oxidation contribute to the high acidity of the oil or fuel on aging. Therefore, prolonged oxidation's net effect is that the oil becomes acidic chemically while increasing viscosity (Macian et al., 2012). Once fatty oil hydroperoxides are formed during oxidation, they decompose to form aldehydes ultimately. Increased acidity is always a result of the oxidation of fatty oils and biodiesel, resulting in shorter chain fatty acids. It is confirmed by the works of Brühl (2014) illustrated in Figure 8. During the oxidation process of biodiesel, methyl esters of fatty acids form a radical that quickly links with oxygen in the air, forming volatile products such as aldehydes, ketones, and lactones formic, acetic, propionic, and caproic acids (Zuleta et al., 2012). An acid number is a valuable tool in monitoring biodiesel's degradation since the acid number increases with degradation (Jiang et al., 2016). In other words, an increase in acid value indicates the accumulation of acidic decomposition products.

The acid number is thus used to measure the acidic products (fatty acids and other organic acids) generated during oxidation reactions. The relative quantity of acidic products generated during the oxidation process can be determined by titrating KOH's essential solutions in ethanol/water. The acid number (ASTM D-974) is determined by dissolving the sample in a mixture of toluene and isopropyl alcohol containing a small amount of water. The resulting solution is titrated with a standard alcoholic base or alcoholic acid solution to the endpoint (Speight, 2002; ASTM, 2000). The flexion curve determines the neutralization point of the titration in the potentiometric titration. When KOH is the titration base, the sample's acid number is expressed as mg KOH/ g. Therefore, the acid number is a crucial parameter determining the onset of the second stage of the oil degradation process, as illustrated in Figure 5 (Ancho, 2006; Wang, 2002).

4.1.4 Viscosity and Density

Kinematic viscosity is an important physical property for assessing lubricant quality, as mentioned in section 3.5 because it is crucial to retaining oil film thickness. Viscosity is the fuel's resistance to flow and the strength of the oil film between two surfaces (Ashraful et al., 2014). It is also susceptible to various forms of oil degradation. Once oil degradation

impacts a meaningful change in viscosity, other indicators such as insoluble, acidity, density, molecular structure changes, and others may have been affected already. Hence the viscosity test is perfect for monitoring oil degradation (Frauscher et al., 2017). The oxidative decomposition of biodiesel is said to be confirmed by an increase in viscosities. Viscosities of lubricating oils and biodiesel increase due to the formation of carbonyl compounds. These compounds interact with hydrogen bonds during thermal stress (Dantas et al., 2011; Elaine et al., 2011; Knothe, 2005). Therefore, changes in the viscosity could result from oil deterioration and contamination with other fluids (Tič and Lovrec, 2011). One of the apparent results of polymer formation is an increase in oil viscosity. As hydroperoxides decompose, oxidative linking of fatty acid chains can form species with higher molecular weights, i.e., oxidative polymerization. The increase in viscosity is an obvious result of significant levels of higher molecular weight substances. Vinyl polymerization has also been proposed as a mechanism whereby higher molecular weight oligomers of fatty oils or esters can be formed. An increase in viscosity is an indication that the oil is at the third stage of degradation, as seen in Figure 5 (Ancho, 2006; Wang, 2002). An aging index measurement is a popular procedure used to determine aging susceptibility and helps in ranking. The viscosity aging index (VAI) is the viscosity ratio after aging to the viscosity before aging (Mohamad et al., 2014; Asim et al., 2013). The VAI registers the impression of the rate of change in viscosity of the sample due to the aging impact and is defined by the equation:

$$VAI = \frac{\text{Viscosity of aged sample}}{\text{Viscosity of unaged sample}} \quad (30)$$

(Mohamad et al. 2014; Asim et al., 2013)

The viscosity index (VI) (ASTM D-2270) is also used to measure kinematic viscosity variation due to temperature changes between 40 °C and 100 °C. For oils with similar kinematic viscosity, the higher the viscosity index, the smaller is the effect of temperature on its kinematic viscosity. (Speight, 2002; ASTM, 2000). The VI is a unit less measure of the change of viscosity with temperature, and it is mostly used to characterize the viscosity-temperature behavior of oils. The viscosity index is determined by measuring the kinematic viscosity at 40°C and 100°C and then compare with the results of a reference oil. When the viscosity index is high, the changes are smaller with temperature differences. All oils increase in viscosity when the temperature decreases and decrease

in viscosity when temperatures increase. The higher the VI, the more stable the viscosity across a range of temperatures is more desirable. The lower the VI, the more the drop-in viscosity as the oil temperature increases. Therefore, the higher the viscosity index, the “better” the oil because the oil changes less in viscosity with an increase in temperature.

4.1.5 Fourier Transform Infrared Spectroscopy (FTIR)

Infrared spectroscopy is an excellent analytical tool to study lubricant degradation by monitoring additive depletion, degradation products, and possible fuel contaminants (Adhvaryu et al., 1998). FTIR spectroscopy gives detailed information on chemical composition because chemical bonds within a molecule exhibit characteristic IR absorptions. When hydrocarbon-based oil or lubricant is exposed to oxygen and high temperatures, it gets oxidized into various by-products such as esters, carbonates, ketones, aldehydes, and carboxylic acids. These products exhibit characteristic IR absorptions, and the FTIR utilizes this to discover the oxidation problems (Macian et al., 2012). Therefore, the FTIR analysis is applied to monitor the degradation of the oil mixtures by oxidation to obtain the chemical changes due to the aging process. It is based on the carbonyl and hydroxyl compound formation measured by increased adsorption or peak area increase. Wooton et al. (1984), Coates et al. (1984), and Adhvaryu et al. (1998) reported measurement of total oxidation product by the integral area calculation. The oxidation is measured as the change in composition, which is essential in obtaining information about the chemical processes involved in oxidative degradation and its inhibition by the adsorbents. The absorption wavenumbers of most common chemical bonds such as OH, C=O, and CH mostly encountered in oil and fuel studies lay within the range of 4000-1500 cm^{-1} (Cen et al., 2018). This wavenumber range is applied in this work. The FTIR spectra are recorded in absorbance units because the sample's absorption of the IR energy gives a linear response to the absorbing species' concentration (Gurumurthy et al., 2017; Obiols, 2003; Macian et al., 2012). The FTIR spectra representing the characteristic difference in the fresh (green line) and aged (red line) sample mixture are shown in Figure 10. The areas that assess the impact of oxidation or degradation of the sample are 1600 to 1900 cm^{-1} due to the high absorbance resulting from the C=O stretching vibrations and 3000 to 3600 cm^{-1} due to the high absorbance of the O-H (hydroxyl) stretching vibrations (Zuleta et al., 2012).

The absorption peak at 1685 cm^{-1} wavelength of the FTIR spectra confirms the presence of various carbonyl compounds such as carboxylic acid. Their characteristic absorption bands identify the presence of ketone formed at 1715 and 1673 cm^{-1} in the FTIR spectra. Similar results are reported by Adhvaryu et al. (1998) and Naidu et al. (1984) Fang et al. (2006) on the pathway for base oil oxidation. In Figure 10, it is observed that the initial peak present in the range between 1900 cm^{-1} and 1600 cm^{-1} , or at about 1745 cm^{-1} associated with characteristic ester component of carbonyl bonds in the fresh oil, presents an absorbance value of about 0.06 Abs. This same associated peak gradually increases as aging proceeds as a direct consequence of oil degradation. It presents a maximum oil degradation absorbance value of about 0.123 Abs for aging at $170\text{ }^{\circ}\text{C}$ for a duration of 80 h. Though absorption at the C-H stretching vibrations, $3010\text{-}2800\text{ cm}^{-1}$, is not significant than these other two and has not been considered in this work. Therefore, two regions are considered for quantification of oxidation in this work, between 1900 and 1600 cm^{-1} , where ester and the intermediate and deeply oxidized products, such as aldehydes, carboxylic acids, and ketones, occur due to thermal degradation of the oil and between 3600 and 3000 cm^{-1} , where hydroxyl-containing oxidative products, carboxylic acid occur (Soleimania et al., 2014, Adhvaryu et al., 1998). The characteristic oxidation level of degradation is quantified by measuring the broadened area under the carbonyl (C=O) or the double bond (C=C) and hydroxyl bands to determine the concentration of these compounds using the peak area increase and the peak height methods and reported as $\text{Abs}\cdot\text{cm}^{-1}/\text{mm}$.

The spectroscopy gives qualitative analysis for the identification of chemical bonds present. The spectrum peaks' size directly indicates the number of oxidative products present (Gurumurthy et al., 2017). The spectrum is plotted as the corresponding wavenumber against the absorption values. Based on samples' absorption spectrum frequency ranges, samples' oxidization characteristics are evaluated by referring to the presence or absence of the adsorbents and the amount or intensity of specific molecular groups' peaks due to the oxidation reaction.

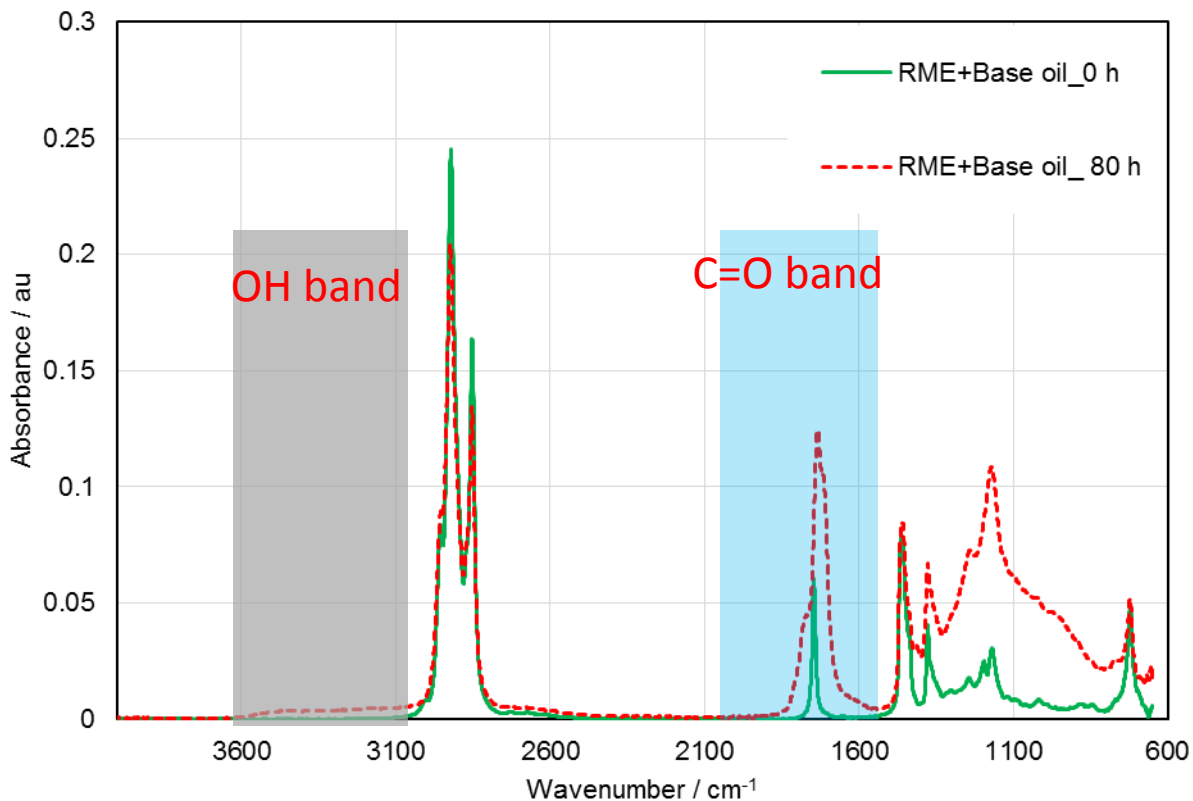


Figure 10: Typical FTIR spectra showing the spectral differences between neat or original (green line) sample of 20 % biodiesel mixed with 80 % base oil and the aged (red line) sample at 170 °C airflows of 10L/h for 80 h showing the O-H and C=O bands

4.1.6 Inductively Coupled Plasma-Mass-Spectrometry (ICP-MS)

ICP-MS is an effective analytical tool for assessing metals' mass concentration and identifying metallic additive elements in a sample. The technique is based upon the spontaneous emission of photons from atoms and ions that have been excited in a radio frequency discharge. The ICP-MS instrument is equipped with a cooled glass baffled cyclonic spray chamber and a type-K glass concentric nebulizer. A small amount of oxygen is added between the spray chamber and the injector base to prevent carbon deposition on the sampler and skimmer cones. With ICP-MS, the ionized sample atoms travel through electrically conductive rods of the quadrupole MS at a rate determined by their mass/charge ratio, allowing selected atoms to reach the detector. ICP-MS has the advantages of low spectral interferences and the possibility of multi-elements analysis. Liquid and gas samples may be injected directly into the instrument, while solid samples require extraction or acid digestion to present the solution's analytes. Therefore, the

samples for ICP-MS are prepared via acid digestions before measurement through microwave-assisted digestion. To evaluate the adsorbents' impact on the additives' inorganic component, accurately measured amounts of 0.2 g of the sample are digested in 6 mL of 99.8 % nitric acid and 2 mL hydrogen peroxide using SPD-Discover microwave from CEM. The microwave digestion is carried out at the pressure of 26 bar and temperature of 200 °C. The microwave is set to first ramp to a temperature of 165 °C in 3 mins with a holding time of 5 mins. A further ramp to 175 °C in 5 mins and held for 10 mins. Finally, it comes to 200 °C in a ramp time of 10 mins and a holding time of 15 mins. The digested sample is then transferred into a 50 mL sample vial. Deionized water is used to top it up to the 50 mL mark. The solutions are then transferred into separate tubes for ICP-MS analysis. The difference in the number of selected ions in the samples treated with and without adsorbents is expected to provide the ions removed from the oil by the sorbent material's surface.

4.1.7 Gas Chromatography-Flame Ionization Detector (GC-FID)

Flame-ionization detection (FID) is a good detector for organic compounds in GC that detect carbon in a sample. An FID typically uses a hydrogen/air flame. The sample is passed to oxidize organic molecules, produce electrically charged particles collected, and produce an electrical signal that is measured. Any hydrocarbons in the sample will produce ions when they are burnt. The adsorbents' impact on an additive's organic components is determined by monitoring their respective abundance under GC-FID. Though additives have a high boiling point making their quantification in an oil matrix by GC difficult, with neat additive and no blending, its determination via GC becomes method dependent (Youk-Meng and Hsiu-Jung, 2001; Farajzadeh, 2006; Khalaf, 2012). Hence the GCFID is applied on neat or pure additives which are not blended.

4.1.8 Induction Period

The oxidation stability, sometimes referred to as the oxidation stability index is applied to measure volatile acids' formation. It measures the oil's resistance to oxidation under prescribed conditions. In conducting this test, the change in distilled water's electrical conductivity in a container is monitored as the biodiesel's oxidation products pass through it. The oxidative stability index is defined as the point of maximum change in the oxidation

rate due to increased conductivity. This test is required for evaluating biodiesel's oxidation (Lin and Chiu, 2010; Wang et al., 2010; McCormick et al., 2007; ASTM D 5554, 2006; Dunn, 2005; Mittelbach, 2003).

The Rancimat method is used for the determination of biodiesel quality per the European standard (EN 14214) for the measurement of the oxidation stability (Lin and Chiu, 2010; Wang et al., 2010; McCormick et al., 2007; ASTM D 5554, 2006; Dunn, 2005; Mittelbach and Schober, 2003). In this method, the biodiesel oxidation is accelerated at a standard temperature of 110 °C and an airflow of 10 L/h passing over the biodiesel. The air supply provides oxygen which oxidizes the biodiesel sample and at the same time transports the volatile compounds and leads them into a water trap with a conductometer in it which measures the changes in the electrical conductivity. The variation in conductivity with time is recorded. A sharp increase in conductivity indicates an accelerated degradation process. The time it takes the test from the beginning to the sudden increase in conductivity is called the induction period. Therefore, the induction time is the maximum point of inflection of the electric conductivity versus the time curve generated in software and determined by the second derivative (Zuletal et al., 2012; Jain and Sharma, 2012; Dunn, 2005).

Rancimat

Per the European standard (EN 14214), the Rancimat is used to determine the induction period. Volatile secondary oxidation products are released and passed over the air stream into a flask containing distilled water and an electrode that measures the water's conductivity during the oxidation process. A rapid increase in conductivity induced by the increase of volatile carboxylic acids in the water generates an induction period (IP), expressed in hours, indicating the sample's oxidation resistance. The oxidation stability is determined from the second derivative of conductivity versus time plot with the volatile acids trapped in deionized water and quantified through conductivity. In evaluating the induction time from the time-conductivity curve obtained, tangents are drawn to the conductivity course. The intersection of the tangents represents oxidation stability (Manual 873 Biodiesel Rancimat, 2009). The oxidation stability, referred to as induction time (period), is the time elapsed from the start of the test until the secondary oxidation

products' appearance, which increases the water's conductivity in the cell. The increase in conductivity after the induction period is caused by the dissociation of short-chain volatile carboxylic acids produced during the oxidation (Gaurav and Sharma, 2014).

The thermal oxidative stability measurements are carried out using the model 873 Rancimat (Metrohm AG, Herisau, Switzerland). The temperature correction factor DT is set to 1.57 °C as recommended by Metrohm. Variability of the determinations has been 61 %. The stabilization factor expresses the effectiveness of all adsorbents,

$$F = IP_x/IP_0 \quad (31)$$

IP_x is the induction period in the presence of the adsorbents, and IP_0 is the induction period in the adsorbents' absence.

PetroOxy

Due to oxidation stability enhancing additives in the diesel fuel used in this work, the PetroOxy determines the biodiesel induction periods blended with diesel fuel and the time elapsed from the start to the time that a 10 % drop in the pressure determines the induction time and is a measure of the sample's oxidation stability. Unlike the Rancimat, with PetroOxy, all the volatile secondary oxidation products are contained until the drop in pressure during the oxidation process.

4.1.9 Dielectric property measurement

Permittivity measures a material's ability to store an electric field in a medium's polarization. Permittivity is usually given as relative permittivity or dielectric constant. Dielectric spectroscopy has been used to monitor the quality of fuels and oils by observing the electric permittivity change at a high frequency of alternating currents (Eskiner et al., 2015, 2020; Biernat et al., 2019; de Souza et al. 2013; Guan et al., 2011; Pérez and Hadfield, 2011). The relative permittivity, ϵ_r , of an oil or a fluid is a measure of its polarity. Polar compounds have a permanent dipole moment, an alternating field that leads to an orientation of the dipoles according to the applied field. Non-polar compounds, on the other hand, show no orientation polarization, so non-polar compounds have small permittivity values, and polar compounds have larger values. Thus, polar and nonpolar

connections can be distinguished by the magnitude of the relative permittivity. The ion polarization describes the shift of negatively and positively charged particles in the electric field. (Köstner et al., 2019). From section 3.5.2, the degradation of hydrocarbon results in an increase in polar oxidative products. Therefore, the presence or absence of the adsorbents in an aged oil will result in polarity changes. Thus, the oil's polarity is a quality factor through which any changes in oil, oil mixtures, neat, and age can be detected (Tič and Lovrec, 2011). It is essential to state that oils change their polarity during the aging process. The measurement of relative permittivity is therefore used to monitor the trend of aging. As the oxidation resistance of the biodiesel decrease with aging, the dependence of capacitance and dielectric suggests the formation of more polar oxidation products leading to an increase in capacitance while the formed products been more viscous lead to an increase in dielectric (Biernat et al., 2019; de Souza et al. 2013; Pérez and Hadfield, 2011). The dielectric constant is high if its molecules are polar or highly polarized (Tič and Lovrec, 2011).

Eskiner et al. (2015, 2020) developed an elaborate method for determining the degree of aging of fuels considering changes in permittivity during aging. This determination correlates with the formation of oligomers. This method is applied to the samples treated with the adsorbents and aged compared to the neat samples for oligomers' formation. The level of the oligomers formed reflect in the permittivity measured.

The measurements of the dielectric parameters in the frequency-domain, relative permittivity, ϵ_r' and dissipation factor $\tan \delta$ is measured by applying an alternating voltage between parallel-plate capacitors of an interdigital sensor at different frequencies. In determining the permittivity, the capacities are first determined. In the first step, the empty capacitance C_0 of the plate capacitor without dielectric is measured. It is followed by measuring the capacitance $C(\omega, T)$ with dielectric material insertion. The insertion of dielectric material between a capacitor's electrodes leads to a decreased primary electric field due to polarization mechanisms, displacement polarization, or orientation polarization (Eskiner et al., 2015, 2020). Interfacial polarization is noticeable in low-frequency regions. When nonpolar molecules or atoms are exposed to an electrical field, there is a positive and negative charge concentrations displacement. An intramolecular electrical field is generated and is opposed to the primary electrical field. However, polar molecules that

act as free charge carriers in the mixture can migrate to the capacitor plates and attenuate the primary electrical field. The polarization decreases the primary electrical field and, therefore, leads to an increase in capacitance. The relative permittivity, ε_r' is defined as the quotient of the capacity with a dielectric $C(\omega, T)$ and the capacity of the empty cell $C_0(\omega, T)$, where ω is the angular frequency and T the temperature (Eskiner et al., 2015, 2020).

$$\varepsilon_r'(\omega, T) = \frac{C(\omega, T)}{C_0(\omega, T)} \quad (32)$$

Commonly, permittivity can be described by a complex-valued function:

$$\varepsilon_r(\omega, T) = \varepsilon_r'(\omega, T) - i\varepsilon_r''(\omega, T) \quad (33)$$

The real part, ε_r' Corresponds to the relative permittivity. It describes the dielectric polarization of induced dipole moments on atoms with permanent polar molecules' dipoles and free charge carriers on the electrodes. On the other hand, the imaginary part designates the polarization and conductivity losses due to the dielectric. The alignment of polar molecules and movement of free charges in dielectrics lead to friction with neighboring molecules and hence losses which are described by the loss or dissipation factor $\tan \delta$:

$$\tan \delta = \frac{\varepsilon_r''(\omega, T)}{\varepsilon_r'(\omega, T)} \quad (34)$$

The physicochemical principles for this method are the determination of the number of oxidation products. The determination of the degree of aging of the biodiesel or fuel, in general, is carried out at the frequency range of 100 Hz to 20 kHz (Eskiner et al., 2015, 2020).

To determine the relative permittivity, the sample mixture of 20 %RME and 80 %base oil treated with and without the adsorbents is aged at 170 °C for 10 h. The 10 h is chosen to cover the induction period, measured as the time required to reach an oxidation endpoint. Samples are taken at the one-hour interval and subjected to the relative permittivity and conductivity losses determination.

4.1.10 NMR measurement

Nuclear magnetic resonance ($^1\text{H-NMR}$) is applied in determining the positions of hydrogen atoms in biodiesel molecules. This instrument is used to assess the molecular deterioration caused by oxidation. The presence of olefinic, allylic, and bis-allylic compounds in biodiesel or its blend sample can be attributed to its degradation process (Mantovani et al., 2020). These allylic compounds are primary oxidation products and unstable and form a variety of secondary oxidation products. The rate of the oxidation process of these unsaturated fatty acids can be related to the number of bis-allylic carbons present in biodiesel. The olefinic compounds are also related to the number of unsaturated esters present in the feedstock (Mantovani et al., 2020).

Mantovani et al. (2020) have shown that NMR signals can provide different information about the functional groups present in fatty acid components. It makes the NMR method suitable for analyzing biodiesel and oil oxidation processes. These same compounds can cause changes in the spectra due to oxidation, thereby modifying some functional groups. Therefore, the concentrations of these functional groups in the base stock, treated with and without the adsorbent before and after aging, will show the adsorbents' impact in suppressing the sample's degradation. In this work, the NMR focuses on analyzing the olefinic, bis-allylic, and allylic protons intensities in the neat and aged samples during the oxidation of biodiesel and its composite samples. The primary characteristic chemical shifts of interest in this work are 5.30-5.43 ppm for the olefinic ($-\text{CH}=\text{CH}-$), 2.74-2.79 ppm for the bis-allylic ($=\text{CH}-\text{CH}_2-\text{CH}=\text{CH}-$) and 1.98-2.04 ppm for the allylic ($-\text{CH}_2-\text{CH}=\text{CH}-$) (Mantovani et al., 2020; Mozammil and Sharma, 2019). Knothe (2001) also reported the peaks of methyl ester (3.6–3.7 ppm) and olefin protons (5.3–5.4 ppm).

NMR Spectra are obtained on a Burkert AV400 (B = 9.4 T; 400 MHz) and Burkert AV400TR (B = 9.4 T; 400 MHz) spectrometer operating at 400 Hz (^1H) and 100 MHz (^{13}C) with tetramethylsilane (TMS) as solvent. The solvent signals are recorded about the signal of TMS as internal standard. In contrast, the signals of the incompletely deuterated contamination of the deuterated solvent are used to reference the chemical shifts of ^1H and ^{13}C spectra. The chemical shift values from literature (Fulmer et al., 2010) are used

to reference the signals. The chemical shifts are expressed in ppm using TMS as an internal standard.

5 The focus of the Thesis

It is known that the oxidation sensitivity of biodiesel is mainly due to the presence of unsaturated fatty acids in the ester (Bannister et al., 2011; McCormick and Westbrook, 2010). As seen in chapter two and described in 3, the auto-oxidation primary mechanism is illustrated in Figure 5, forming a radical hydrocarbon species on the bisallylic carbon. This mechanism is generally considered a free radical chain reaction consisting of initiation, propagation, and termination stages. Any accumulation of degraded or decomposition products in oil indicates the onset of oxidation (Wang et al., 2008, Wang, 2001). The free fatty acids cause high acid values in biodiesel (Wang et al., 2008). High acid values could be designated as the second stage of degradation (see Figure 5). In contrast, an increase in viscosity can be designated as the third stage of degradation (see Figure 5) (Wang, 2001). Therefore, controlling oxidation is a priority means sustaining the oxidative stability of the fuel. Mainly antioxidants have been used as the main alternative to prevent or retard biodiesel degradation (Nogales-Delgado et al., 2019; Yahagi et al., 2019; Varatharajan and Pushparani, 2017; Osawa et al., 2016; McCormick and Westbrook, 2007; Schober and Mittelbach, 2004; Goodrum, 2002). This problem of oxidation stability of biodiesel can be mitigated using adsorbents.

The adsorbents' effectiveness is measured by stressing a fatty oil or ester molecule treated with the adsorbents and then comparing the physiochemical changes occurring with the same fatty oil without any adsorbent treatment. The adsorbents in this work are applied in the same context supposing the adsorbents inhibit the oxidation initiation stage (see top left of Figure 5) by scavenging the process's precursors. In that case, the amount of hydroperoxides produced is impacted, resulting in no or fewer primary oxidation products, low acid values since carboxylic acids produced during this process increases the acidity (Soleimania et al., 2014; Xin et al., 2009), Figure 5 but on the other hand, if it enhances the termination stage, then there will be a reduction in the length of the propagation stage (see bottom left of Figure 5) resulting in a minor increase in oil viscosity (Soleimania et al., 2014; Xin et al., 2009). Beyond these two stages, oligomers (see right side of Figure 5) or sludge will result (Knothe, 2007), reflecting an increase in viscosity Figure 7 will entail their separation using deactivated adsorbents.

In consequence, the conventional oxidation process results in rheological changes of physical and chemical characteristics. In this work, the effect of adsorbents in suppressing oligomers formation during oxidation of biodiesel and its blends is monitored by assessing the acidity of the degraded sample due to the number of volatile oxidation products. The overall amount of oxidation products increases with higher degradation (Bacha et al., 2015). Oxidation is associated with changes in viscosity, density, acid value, and peroxide value of the biodiesel sample under aging. The acid number is used to measure the acid products generated in oxidation reactions. Fourier transform infrared spectroscopy, and gas chromatography-mass spectrometry is used to further elucidate the mechanism of degradation and examine the formation of the various oxidation products, significantly increasing the peak area of the carbonyl band in an FTIR spectrum.

Due to this background, this experimental research has been carried out mainly on two topics: suppression of oligomers' formation and adsorption. The suppression of oligomers formation is further carried out on two different applications: engine oil and biodiesel.

Rapeseed oil methyl ester (RME), biodiesel from rapeseed oil, is applied to represent biodiesel's role. RME contains around 60 % monounsaturated oleic fatty acids and about 6 % saturated fatty acids. The physical and chemical properties of the RME are provided under section 7.2. It must be pointed out that the RME used in this work contains no additives.

Fang and McCormick (2006) defined a biodiesel admixture of 20 % up to 30 % as a worst-case. They showed that mixtures containing 20 % to 30 % biodiesel have the highest tendency for deposit formation. So, a 20 % oil dilution by biodiesel is simulated in this experiment.

Oil usually experiences different environmental conditions, temperature changes, and various aeration levels within a running engine. The temperature within the bearings increases as the oil passes through, but a coolant is cooling within the heat exchanger. The engine's operating temperature is generally between 90 °C and 140 °C, but higher local temperatures can be experienced. For this work, a temperature of 170 °C has been used. This temperature has been selected because, according to Singer et al. (2014), the results of engine oil used to cover a distance of 30,000 km can be achieved in the

laboratory with a constant temperature of 170 °C for a 40 h duration. Therefore, to achieve results that would cover a longer oil usage distance, the aging duration is doubled to 80 h. The aging process is turned off after every eight hours. It accommodates the rest period, which translates into the engine downtimes at room temperature lasting about 12 h.

Understanding the adsorbents, hydrotalcite compound, and 1,3,5-trimethyl-2,4,6-tris(3,5-di-tert-butyl-4-hydroxybenzyl) benzene mixed in a ratio of 1:2 respectively on oxidation on the properties of biodiesel fuel, the suppression of oligomers formation, seven tests are conducted. These tests determine the level of degradation of the oil-fuel mixture in the absence and presence of the adsorbents during the aging process.

From chapter 3, section 3.3, and Figure 7, fuel stability is considered from storage/thermal stability and oxidative stability perspectives. Four experiments based on the oxidative stability of biodiesel on the degradation of the oil are carried out. The experiments involving linoleic acid methyl ester (C18_2 ME) and biodiesel were all independently mixed with base oil to ascertain the adsorbents' impact in suppressing the formation of higher molecular mass substances. Here, the base oil described above is blended with C18_2 ME, treated with and without adsorbents, and aged at 170 °C for 80 h. The linoleic acid methyl ester is a single component of biodiesel which contributes highly to its instability. This experiment is used to investigate how the adsorbent could suppress its role in the oxidation process initiation. Its dosage in this experiment is at the level of its natural occurrence in diesel fuel blended with 7 % RME, i.e., 1.6 wt % for C18_2 ME (Besser et al. 2017, Munari et al. biodiesel_an10212; AGQM files/2515).

Temperature affects the storage stability and thermo-oxidative degradation of biodiesel and its blends. In understanding the temperature impact on the adsorbents in suppressing oligomers formation, the same sample mixture of 20 % RME and 80 % base oil treated with and without the adsorbents is aged at different temperatures of 70 °C, 110 °C, 140 °C, and 170 °C at eight hours per day for 80 h each. The same sample mixture in the same proportions is aged at the temperature of 170 °C for 80 h, but in this time round mixed with different masses, 0.225 g, 0.45 g, and 0.675 g of the adsorbent in the same ratio as above. It is to enable the calculation of the relative adsorption effect of the adsorbent per volume of sample.

Lubricants, as seen in chapter 3, section 3.5, are composed of base oil and additives. Since these additives get depleted either by decomposition, adsorption onto metal and other surfaces, or separation because of settling or filtration, two experiments are carried out to test if the adsorbents would remove any additives in the lubricating oil. A market-ready lubricating engine oil, Mannol universal oil, and pure additives are tested with the adsorbents. The concentration of the additives in the sample treated with and without the adsorbent and aged are compared. Mannol engine oil and other neat additives, VanlubeBHC, Vanlube961, corrosion inhibitor, antioxidant and friction modifier are treated with the adsorbents in the same ratio and aged at 170 °C for various durations from 40 h to 80 h. It is done to study the effect of the adsorbents on the oil additives.

The oxidation process changes the structure and amount of olefinic, allylic, bisallylic protons in biodiesel and its blends. NMR spectroscopy measurement enables detecting these changes concerning the presence or absence of the adsorbents in the samples aged at 170 °C for 80 h. The oxidative behavior of biodiesel-base oil mixture with and without the adsorbents using ¹H and ¹³C NMR-derived structural parameters is reported. The variation in the carbon skeleton on degradation in the presence or absence of the adsorbents during aging due to structural rearrangements and molecular conversions are monitored. The changes occurring in the mixture's structural parameters with and without the adsorbents and neat base oil-biodiesel mixture are studied.

Long-term biodiesel storage for low-use applications such as plug-in-hybrid vehicles and backup generators requires higher oxidation stability than is necessary for typical use to ensure that the fuel remains stable (Christensen and McCormick, 2014). The formation of deposits caused by oxidation in storage or an engine fuel system is a significant issue because of the fuel pump and injector fouling potential.

The experiments under stabilizing biodiesel and its blends look at the adsorbents' influence on biodiesel's oxidative stability blended with diesel fuel under accelerated aging conditions of 170 °C for various durations of aging up to 48 h. This section's last experiment is carried out to examine the adsorbents' impact on the storage stability or long-term applicability of biodiesel and its blends. The Rancimat method cannot directly measure the overall storage stability of fuels because other storage conditions also

contribute to the deterioration of fuel quality during storage (Xin et al., 2009). The sample is made of 80 Vol % diesel fuel and 20 Vol % biodiesel. It is hereafter referred to as B20 in this work. The B20 is splash blended. The B20 samples in a volume of 40 mL are oven stored at a temperature of 40 °C for 120 days though samples are taken out for analysis every 15 days. According to Alves and Starck (2016), biodiesel or fuel in general aging on-board is equivalent to 4-5 months of storage. The sample under this test is treated with 0.675 g of the adsorbents in the ratio of 1:2 (magnesium-aluminum hydrotalcite:1,3,5-trimethyl-2,4,6-tris(3,5-di-tert-butyl-4-hydroxybenzyl) benzene). The adsorbents used are intended to inhibit oxidation by scavenging the precursors of the process. Therefore, the adsorbents effect's impact is tested by comparing the results of the samples treated with and without the adsorbents. The induction period is one key parameter that can showcase the adsorbents' impact on biodiesel's oxidative stability.

In section 3.4, hydroperoxides (Figure 2, Figure 3 and Figure 4, Figure 5) are the primary biodiesel degradation products (Fang and McCormick, 2006). Therefore, the amount of hydroperoxides produced in the sample treated with the adsorbents is compared with the sample aged without the adsorbents. Dantas et al. (2011) report that viscosities and acid values of mineral lubricant oils increase when subjected to thermal stress due to the formation of carbonyl compounds such as aldehyde or high molecular weight polymers (formed from peroxide radicals, Figure 5)(Siddharth and Sharma, 2010). There are several pathways for the degradation of biodiesel, leading to the formation of oligomers. Peroxides formed in the initial stage of oxidation can decompose to form aldehydes, ketones, and acids. These can react further in condensation to form oligomers. As seen on the right side of Figure 5, in the biodiesel oxidation process's termination stage, the insoluble oligomers of high molecular weight are produced by recombining the oxidation products. The quantity of oxidative products formed has an impact on the dielectric conductivity of biodiesel and its blends. The peroxides can also react with fatty acid chains to form oligomers. Deposits form when the polarity and molecular weight of these oligomers is high enough.

Furthermore, most studies reported that the acid value and viscosity correlate well with each other, indicating that the polymeric compounds responsible for the increased viscosity are related directly to the formation of the acidic products (Pullen and Saeed

2012; Karavalakis et al., 2011; Ahmed, 2009; Lacoste and Lagardere, 2003). The acid value, viscosity, and other properties are subjected to analysis under these sets of experiments.

The number of degradation products formed by the adsorbent's impact in inhibiting the formation of higher molecular mass substances is assessed. The formation of higher molecular mass substances is monitored with SEC. The integrated area under the SEC curves is the area gained due to adsorbents' presence compared to the adsorbents' absence. It is an indicator of the adsorbent's scavenging capacity. A similar result is reported in the literature (Fereidoon and Ying, 2015)

These experiments' collective results are used to identify the impact of adsorbents on biodiesel's oxidative stability and its blends.

6 Selection of Adsorbents

6.1 Suppression of oligomers formation

Oxidation generally in oxygen shows a free radical character shown in Figure 5 and equations 1-8 in section 3.4. The primary carbon-centered free radical species lead to the development of oxygen-centered radicals and hydroperoxides. The carbon-centered radical is regenerated in the propagation stage to keep the chain reaction. It is summarised in equations 9-18 in section 3.4. Any adsorbent with hydroxyl groups in its molecule can scavenge any free radical(s) in an oxidation procedure.

The selected adsorbing compound in this work has methylene groups connecting the phenolic groups to a central benzoic ring. It has three liable hydrogen atoms marked red in Figure 11, which it readily releases to capture the radicals. This donation allows the generation of stable products and thus breaks the oxidation chain reaction mechanism through hydrogen exchange with the methyl groups bond to the central benzene ring (Watson and Wong, 2008; Aluyor and Ori-Jesu, 2008). The adsorbents, therefore, retard the oxidation process by intercepting these oxidation process precursors, which prevents the peroxide radicals from creating another radical by autoxidation mechanism. The oxidation chain reaction is thus interrupted (Van Lierop et al., 1998).

The compound 1, 3, 5-trimethyl-2, 4, 6-tris (3, 5-di-tert-butyl-4-hydroxybenzyl) benzene, commonly known as ethanox 330, is a radical scavenger that contains an easily abstracted hydrogen in its structure. This compound is used as a radical trapping agent. The radical trapping agent is a compound that can trap free radicals that cause radical polymerization. It has been used as a stabilizer to improve polymers, food, and other materials that can undergo oxidative degradation (Mendiara and Coronel, 2006). It has a melting point of about 250 °C.

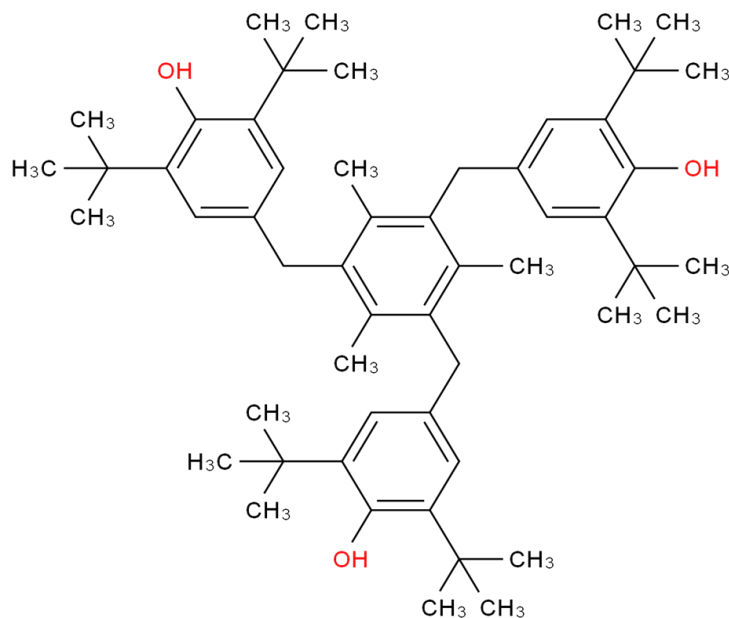
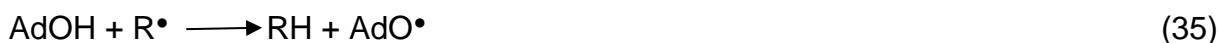


Figure 11: Molecular structure of Ethanox 330, the suppressing agent (Van Lierop et al., 1998).

The primary carbon-centered free radical species, $R\bullet$, could also be stabilized by the compound per its hydrogen donation. Assuming AdOH stands for the trapping compound (suppressing agent), the following illustration demonstrates one of the means it could interrupt the oxidation process:



The trapping compound's adsorbent behavior is well collaborated by the work of Mendiara and Coronel (2006). It is also reported that with sterically hindered compounds like the trapping agent, the first step of its suppression action is hydrogen bonding to the radical species. It is followed by a benzylic hydrogen donation leading to a quinone structure. This oxidation sequence may take place over each phenolic group available (Mendiara and Coronel, 2006).

During the oxidation process of biodiesel, volatile organic products, including formic, acetic, propionic, and caproic acids and many other shorter chain fatty acids, are formed (Zuleta et al., 2012; Brühl, 2014). These acidic products have to be controlled as they can lead to issues of corrosion and others.

The hydrotalcite compound, magnesium-aluminum hydroxycarbonate, ($\text{Mg}_6\text{Al}_2(\text{OH})_{16}(\text{CO}_3)\cdot 4\text{H}_2\text{O}$), is a double-layered hydroxide with many applications, including oil adsorption. The hydrotalcite compound has both positively charged hydroxide layers and interlayers composed of carbonate anions and water molecules. It is a solid powder with a melting point above 250 °C (Endres et al., 1991; Arruda et al., 2013). It is in powder form to adsorb acid components in oil when it comes into contact with the oil. It has a chemical composition of $\text{Mg}_6\text{Al}_2(\text{OH})_{16}(\text{CO}_3)\cdot 4\text{H}_2\text{O}$, roughly 60 mass-% MgO and 40 mass-% Al_2O_3 . Magnesium aluminum hydrotalcite, when in oil, releases ions while adsorbing anions and can thus adsorb acidic substances within the oil, contributing to the suppression of oil deterioration. Although weakly basic, it contains a relatively small amount of hydroxide ions and a relatively large amount of carbonate ions. In its structure, when trivalent ones isomorphically substitute divalent cations, the layers generate a positive residual charge. It is, therefore, able to adsorb the acids formed in the oil (Arruda et al., 2013). Magnesium-aluminum hydrotalcites have aryl-heteroatom bonds, which are readily cleaved by hydrogen at temperatures below 350°C. Hydrotalcite exhibits a Lewis acid catalysis mechanism for this process. By this process, the hydrotalcite is converted to an active hydrogenation catalyst at these temperatures. It can suppress the oxidation process, forming oligomers through any hydrogen donor molecule occurring on the hydrotalcite. Therefore, the hydrotalcite compound functions as an ion exchanger and adsorb acid in oil while releasing anions. Hydrotalcite's acid-scavenging mechanism is presented in Figure 12.



Figure 12 The mechanism of the hydrotalcite compound (Endres et al., 1991)

From the above description, the hydrotalcite compound has an acid and alkali adsorption ability and thus serves to adsorb acidic components to prevent oil deterioration. However, the hydrotalcite compound has a setback which is its elution property. It makes the acid substances adsorbed elute off at some point in time. These acid substances that elute off again have adverse effects on the deterioration of the oil. The hydrotalcite compound is thus used along with the radical trapping agent, which can suppress oxidation and curb sludge precursors' production by the acid substances released by the hydrotalcite compound. Therefore, the combined adsorbents suppress oil deterioration for a prolonged period giving the oil a more extended life period.

The ratio of the hydrotalcite compound added to the radical trapping agent's amount is set by experiment. The adsorbents are individually added to the sample and aged to examine their impact on suppressing higher molecular mass substance formation. The amount ratio of 1:1, 1:2, etc. of the added combined adsorbents in units of g are experimentally selected based on 1 L of oil. The addition ratio is set depending on the size of the oil sample. A mass of 0.675 g of the trapping agent and the hydrotalcite compound are each added to 30 ml of the 20 % RME mixed with 80 % base oil, while their combination in the same ratio is also added to 30 mL of the same sample and aged at 170 °C with an airflow of 10 L/h for 80 h. The aged samples treated with the adsorbents are compared with the neat aged samples without any adsorbent treatment using FTIR analysis.

Figure 13 illustrates FTIR spectra of 20 % RME mixed with 80 % base oil treated with and without the separate and combined radical trapping agent and the hydrotalcite compound and aged at 170 °C for 80 h. Figure 14 is the zoom-in on Figure 13, showing the region in

which the carbonyl-containing degradation products are adsorbed. In the mixture treated with the hydrotalcite compound only, the ester vibration has widened more. However, the production of the degradation products has been significantly reduced by approximately a factor of 7 compared with the sample aged without any adsorbent treatment, which increased by a factor of 10. However, the amount of degraded products is likely to increase with aging since the hydrotalcite has an elution tendency. This tendency can be seen around a wave number of 1600 cm^{-1} , where significant adsorption is registered. Therefore, the amount of it in the application for this process must be minimized and controlled.

The treatment with the radical trapping agent (1, 3, 5-trimethyl-2, 4, 6-tris (3, 5-di-tert-butyl-4-hydroxybenzyl) benzene) has shown much significant reduction by a factor of 3 in the formation of degradation products than the sample treated with the hydrotalcite compound. However, the sample treated with the combination of the two adsorbents, hydrotalcite compound, and the radical trapping agent in a ratio of 1:2, respectively, has suppressed the amount of sludge produced to nearly zero and therefore, giving the oil a much more extended period of useful life.

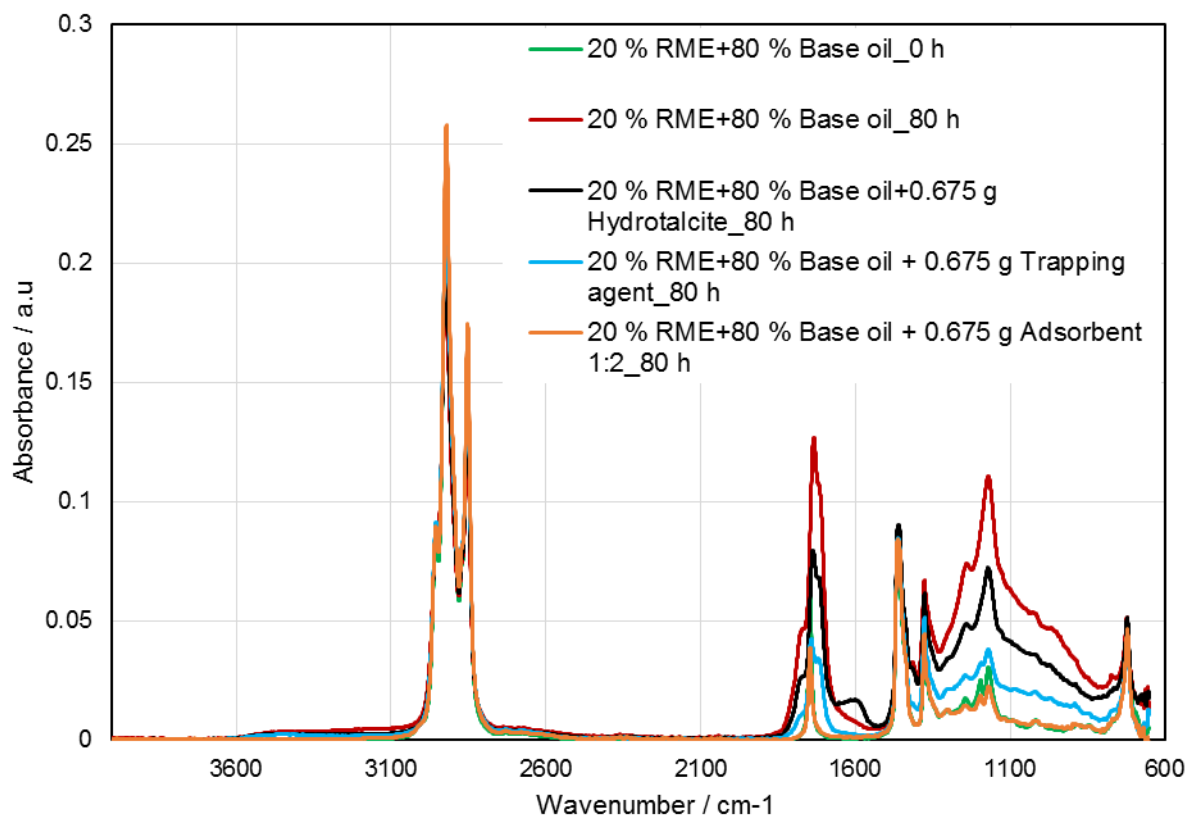


Figure 13: FTIR spectra of 20 % RME mixed with 80 % base oil treated with and without separate and combined (adsorbent in a ratio of 1:2) the hydrotalcite compound and radical trapping agent (1, 3, 5-trimethyl-2, 4, 6-tris (3, 5-di-tert-butyl-4-hydroxybenzyl) benzene) and aged at 170 °C with an airflow of 10 L/h for 80 h using a Rancimat

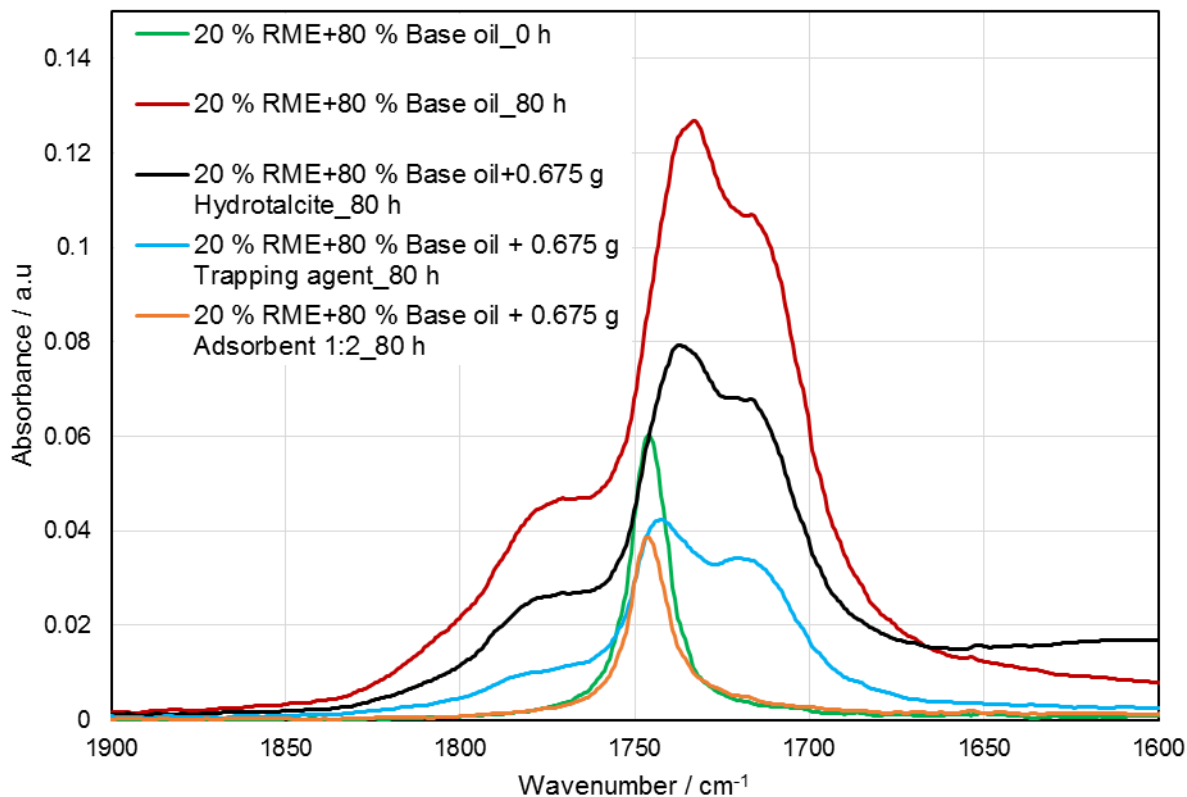


Figure 14: Zoom in on the area of carbonyl vibrations of Figure 13, FTIR spectra of 20 % RME mixed with 80 % base oil treated with and without separate and combined (adsorbent in a ratio of 1:2) the hydrotalcite compound and radical trapping agent (1, 3, 5-trimethyl-2, 4, 6-tris (3, 5-di-tert-butyl-4-hydroxybenzyl) benzene) and aged at 170 °C with an airflow of 10 L/h for 80 h using a Rancimat

Figure 15 illustrates the area of hydroxyl vibrations. The OH peak is attributable to the organic compounds, including water, alcohol, hydroperoxides, and carboxylic acids with the OH functional group. These signals are not significant in the sample aged with the combined adsorbents than those treated with the individual components.

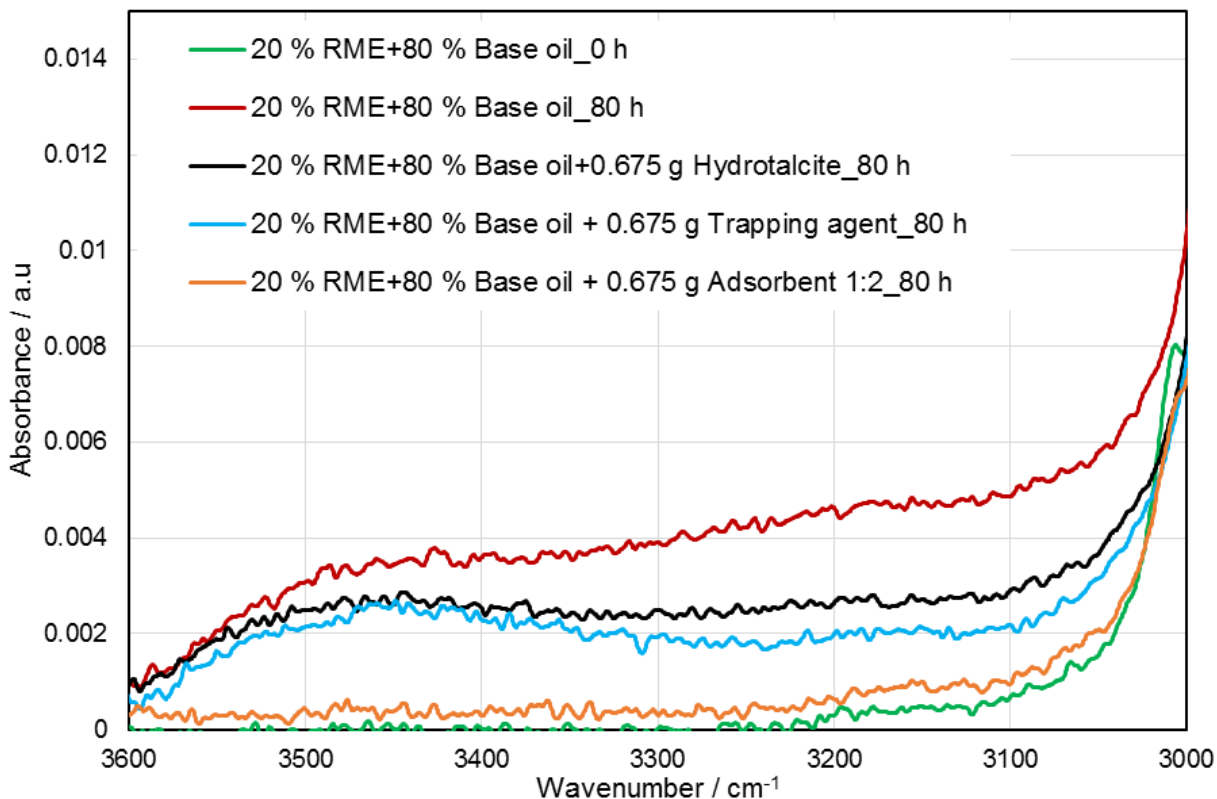


Figure 15: Zoom in on an area of hydroxyl vibrations of Figure 13, FTIR spectra of 20 % RME mixed with 80 % base oil treated with and without separate and combined (adsorbent in a ratio of 1:2) the hydrotalcite compound and radical trapping agent (1, 3, 5-trimethyl-2, 4, 6-tris (3, 5-di-tert-butyl-4-hydroxybenzyl) benzene) and aged at 170 °C with an airflow of 10 L/h for 80 h using a Rancimat

The combination of the hydrotalcite compound and the radical trapping agent on treatment with the oil sample under high temperature curb the oil deterioration for a prolonged period. Therefore, the combination of hydrotalcite compound and the radical trapping agent in a ratio of 1:2 has been applied to suppress oligomers formation in this work. The hydrotalcite compound and the radical trapping agent are added in the least amount of 7.5 g and a maximum amount of 22.5 g in a ratio of 1:2 to 1 L and 4 L, respectively of the sample in this work.

The adsorbent's impact in inhibiting higher molecular mass substances and other oxidation products is monitored. Peroxyl radicals are predominant free radicals encountered in oil and biodiesel oxidation. Therefore, the formation of higher molecular mass substances is monitored by the measurement with GPC, where the area under the

curves is constructed considering the adsorbents' absence or presence. The net integrated area under the curves, which is the area gained due to adsorbents' presence compared to that of the absence of the adsorbents, is then calculated as an indicator of the adsorbents scavenging capacity effect. The level of suppression of the formation of oxidation products by the adsorbents is calculated using the equation (Shahidi and Zhong 2015):

$$\text{Adsorbent suppression activity} = \frac{\text{Abs of control} - \text{Abs sample with adsorbent}}{\text{Abs of control}} \times 100$$

Abs of control is the relative molecular masses of the oil aged without adsorbents and the Abs sample with adsorbents. These are the relative molecular masses of the sample mixed with the adsorbent and aged.

Using the measurements with the GPC, a volume of 30 ml of the sample is applied with 0.225 g, 0.45 g, and 0.675 g of the adsorbents and aged at 170 °C for 80 h.

$$\begin{aligned} \text{Adsorbent suppression activity at 0.225 g} \\ &= (402 \text{ g/mol} - 361 \text{ g/mol}) / (402 \text{ g/mol}) \times 100 \\ &= 10.199 \% \end{aligned}$$

$$\begin{aligned} \text{Adsorbent suppression activity at 0.45 g} \\ &= (402 \text{ g/mol} - 224 \text{ g/mol}) / (402 \text{ g/mol}) \times 100 \\ &= 44.279 \% \end{aligned}$$

$$\begin{aligned} \text{Adsorbent suppression activity at 0.675 g} \\ &= (402 \text{ g/mol} - 157 \text{ g/mol}) / (402 \text{ g/mol}) \times 100 \\ &= 60.945 \% \end{aligned}$$

The adsorbents in the amounts of 0.225 g: 0.45 g: 0.675 g give efficiency in factors of 1:4:6 in suppressing oligomers formation in 30 mL of the sample mixture age at 170 °C. Ideally, using adsorbents in amounts ratio of 1:2:3 should translate into 1:2:3 ratio of efficiency but it is not the case. This observed trend between 0,225 g and 0,45 g of adsorbents could be as result of the elution of the oxidation products after the capacity of

the adsorbents had been exceeded during the duration of the aging procedure due to small amount used. Between 0, 45 g and 0,675 g, the observed trend agrees with the amount of the adsorbents used. An increase by a factor of 1 has been recorded and this means that the 0, 45 g of adsorbent used is in the capacity within which the elution of the oxidation products does not occur.

The level of degradation or oligomerization is also assessed by monitoring the area under the carbonyl bands in the FTIR spectrum in the presence and absence of the adsorbents. Broadband at a wavenumber of about $1,750\text{ cm}^{-1}$ is due to the presence of carbonyl contained degradation products. For the C=O peak area, the efficiency of the adsorbents is calculated as follows:

$$\begin{aligned} \text{Adsorbent suppression activity at } 0.225\text{ g} &= (9.28\text{ abs} - 7.79\text{abs}) / (9.28\text{ abs}) \times 100 \\ &= 16\% \end{aligned}$$

$$\begin{aligned} \text{Adsorbent suppression activity at } 0.45\text{ g} &= (9.28\text{ abs} - 3.61\text{ abs}) / (9.28\text{ abs}) \times 100 \\ &= 61\% \end{aligned}$$

$$\begin{aligned} \text{Adsorbent suppression activity at } 0.675\text{ g} &= (9.28\text{ abs} - 1.11\text{ abs}) / (9.28\text{ abs}) \times 100 \\ &= 88\% \end{aligned}$$

The adsorbents' use in the amounts of 0.225 g: 0.45 g: 0.675 g suppressed carbonyl contained degradation products in factors of 1:3.8:5.5.

The ratio obtained from the SEC's measurement does not differ significantly from that of the FTIR determinations. The differences in the use of 0.675 g of the adsorbents could result from a measurement error. However, the focus is on the efficiency in the suppression of formation of higher molecular mass substances and, therefore, will use the results of the GPC to illustrate the efficiency of the adsorbents. Hence, using a mass of 0.225 g per 30 mL of oil will translate into 7.5 g per 1 L of oil with an efficiency of about 16 %. For a volume of 4 L, which is about the usual volume of oil in the engine, a mass of about 30 g of the adsorbents will be needed. On the other hand, using 0.675 g of adsorbents per 30 mL of oil will rise to 22.5 g per 1 L of oil. In effect, for 4 L of oil for an

efficiency of 88 % in suppressing the formation of higher molecular mass substances, a mass of 90 g of the adsorbents in their usual mass ratio of 1: 2 is required.

6.2 The capacity of adsorbents in suppressing Oligomers formation

Wolak (2018) demonstrated that knowledge of acid number and total base number measurements strongly enhances evaluating the remaining useful life of engine oil. The acid number is a vital oil parameter for monitoring oil conditions.

The pathways of lubricant degradation are oxidation, additive depletion, and contamination. The acid number test is one standard method available for oil analysis to estimate the rate of degradation, oxidation, additive depletion, and contamination. The acid number can be said to determine merely the by-product of oxidation. This is very important in determining the remaining useful life of an oil and how much adsorption or suppression can be carried out by the adsorbents, as stated earlier.

Concurrently, monitoring the underlying components that affect the acid number during lubricant aging, the life span of the adsorbents in impacting the suppression and adsorption of the oligomers, or the general degradation of the lubricants can be determined. It is clear that once the lubricant is in usage, the base oil begins to oxidize once the additives, especially the antioxidants, are depleted. Therefore, by trending the acid number, its increase resulting from the lubricant aging can be detected. Comparing the changes in the acid number with the standard acceptable level of acidity in any lubricant in usage, the breakthrough volume is determined.

The acid number of engine oil determined using ASTM D664 standard method to be equal to its original acid value + 2.5 mgKOH/g (New oil value + 2.5 mgKOH/g) should be drained (MTU Friedrichshafen GmbH handbook; Petro-Canada Lubricants Handbook, 2017)) should be drained. Therefore, an acid value of an engine oil whose original acid number plus an increase of 2.5 mgKOH/g is accepted as the standard acid value for oil drain interval. It should be pointed out that though the acid number is critical for the oil drain interval, it does not depend on only the acid but also the engine oil quality, conditioning, the operating conditions, and the fuel used.

Before starting the aging process, the initial concentration is about 0,09 mgKOH/g, just 0,04 above the maximum initial acceptable limit of 0.05 mgKOH/g. As the oil aging progresses, the impact of the adsorbents in suppressing or adsorption of the acidic products shows until the acid value of the original oil acid value + 2.5 mgKOH/g is reached, and the adsorption or suppression step is discontinued. Beyond this value, the acid concentration will rise rapidly as the adsorbents become saturated. The time required to reach the maximum allowable acid value of new oil value + 2.5 mgKOH/g is considered the breakthrough volume of the adsorbents. The steepness of the breakthrough curve determines the extent to which the capacity of the adsorbent can be utilized. The shape of the curve is critical in determining the quantity of adsorbents and length of usage for suppression or adsorption.

In selecting adsorbent for this process, the separation and suppression of the oligomer's formation, a range of physical and chemical properties of the adsorbent, and the oligomers to be trapped and suppressed must be considered. Tables of breakthrough volumes often guide the selection of adsorbents. This helps in the determination of the trapping efficiency of the analytes on the adsorbents. Most previous publications on breakthrough volumes have only been carried out at room temperature (Raposo et al. 2019; Wolak, 2018; Negrea et al. 2020). This work's breakthrough volume is at an elevated temperature of 170°C and for a maximum duration of about 300 h of aging using the adsorbent in the sample mixtures.

The Figure 16 is a plot of the acid concentration or acid number in the oil mixture as a function of time from the start of the aging process. The S-shaped curve obtained is very typical of breakthrough volume curves. The initial acid value plus 2.5 mgKOH/g acid value of the oil sample used in this work will result in a maximum acid value of 2.59 mgKOH/g, at which the oil drain should occur. With aging at 170°C for 190 h, the acid value is 2.41 mgKOH/g, 0.18 less than the maximum allowable acid number. After 190 h of aging, a steep rise in acid value, 2.41 mgKOH/g to 7,92 mgKOH/g at 200 h, is recorded and further to 16,36 mgKOH/g at 240 h. The acid value after 190 h of aging has exceeded the threshold value of 2.59 mgKOH/g. An average slide increase of 0.27 in acid value from the start of the aging to about 60 h of aging is noteworthy. From 80 h to 150 h of aging, the increase is about 1.54, while from 160 h to 190 h, the increase is about 2.16. The

increased level is within the allowable acid value of 2.59 mgKOH/g, and the oil still has a sustainable remaining useful life. The Figure 16 diagram shows that the acid value at 190 h of aging is within the determined limits, proving that the oil using the adsorbents still meets the criteria of a standard allowable acid value.

From Figure 16 the average increase in acid value from the start of the aging till 190 h of aging has been 1.13. Therefore, an identical average exceeding by 1,13 compared to the value of fresh oil at the onset of the aging process. Considering the average allowable acid value of 2.59, it translates into the same amount of adsorbents, 0,675g, in aging 30 mL of oil at 170°C for 2.29 times for the period of 190 h each. It is worth mentioning that oils treated with the adsorbents after 190 h of aging are not inclined to exceed the critical value of the total acid number. The results obtained can be attributed to the adsorbents used. In short, 0,675 g of the adsorbents can be utilized 2.29 times when applied to 30 mL of the oil sample at a temperature of 170°C. It is worth noting that the adsorbents have been applied to oil sample mixture which have no additives. Therefore, when these adsorbents are applied to an oil sample which has additives, the duration of the impact of the adsorbents on the oxidation process would be much higher than the figure determined in this work. It must be pointed that the engine condition, the operations and load on the engine all contribute to the rate of the oil degradation and could also impact on the adsorbents capacity.

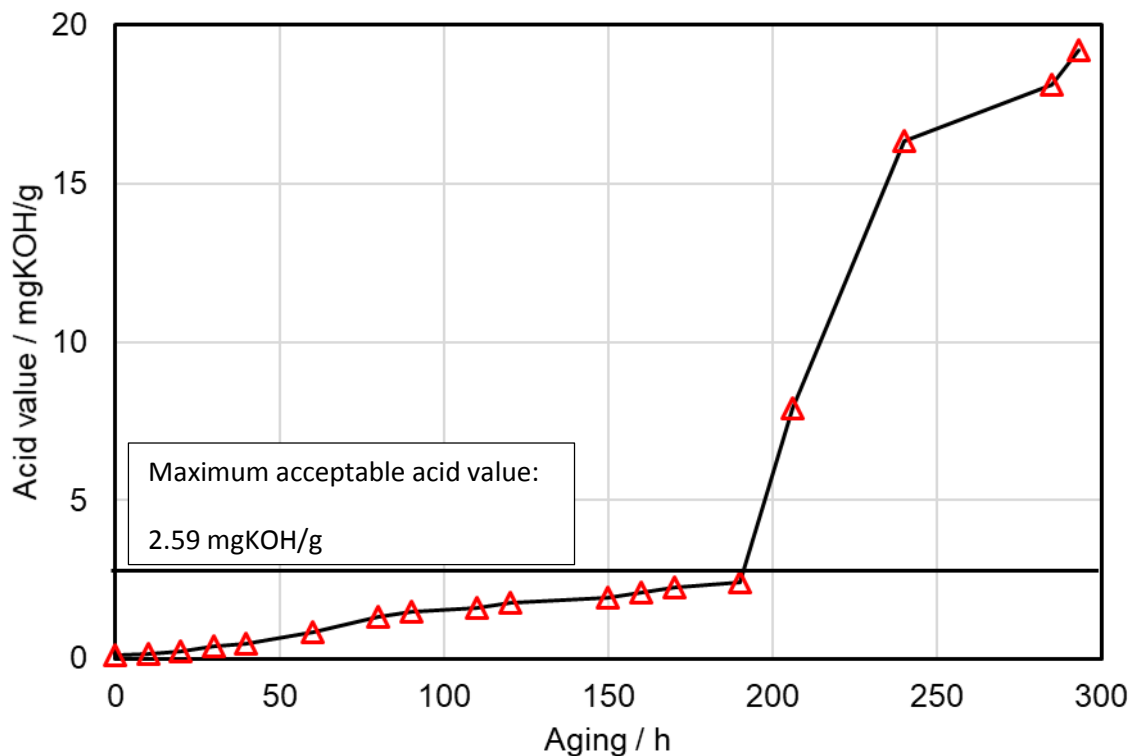


Figure 16 The acid value of 30 mL 20 % RME mixed with 80 % Base oil and treated with combined 0,675 g adsorbents of magnesium-aluminum hydrotalcite and 1,3,5-trimethyl-2,4,6-tris(3,5-di-tert-butyl-4-hydroxybenzyl) benzene in a ratio of 1:2 respectively and aged at 170°C with airflow of 10 L/h at 8 h per day in a Rancimat for about 300 h

There is a correlation between the acid number and the number of oxidation products formed during oil degradation. Fourier transform infrared (FTIR) spectra of the samples are analyzed considering the effect of the oil degradation. The typical wavenumber range between 1800 and 1650 cm^{-1} quantifies oxidation products, such as aldehydes, carboxylic acids, ketones, and esters, which occur due to thermal degradation of the oil and biodiesel dilution has been assessed, Figure 17. These critical portions of the spectra have been integrated. The graph of the integrated area of aged samples treated with the adsorbents against the aging duration produces an S-shaped curve typical of the breakthrough volume curves obtained in Figure 16.

Similarly, after 190 h of aging, there is a steep rise in the number of degraded products as seen in the rise in acid number in Figure 17. It confirms values obtained for the breakthrough volume of the adsorbents as the steepness of the breakthrough curve, which determines the extent to which the capacity of an adsorbent can be utilized. The samples without adsorbent treatment show a consistent, steady rise in the integrated area with increasing aging duration. Contrary to the results of the samples not treated with the adsorbents, the oil mixture treated with the adsorbents sustained very low insignificant values until the breakthrough volume has reached. This demonstrates the impact of the adsorbents in suppressing oligomer formation in this work. Therefore, in actual practice, the steepness of the concentration profiles shown previously can increase or decrease, depending on the presence or absence of the adsorbents.

The rate of change in acid concentration in the samples treated with the adsorbents is very gradual until the breakthrough volume point and then increased faster, and steepens with time until a constant pattern is attained. It can be seen in the both measured acid values and the level of oligomers formed as determined with FTIR, Figure 16 and Figure 17

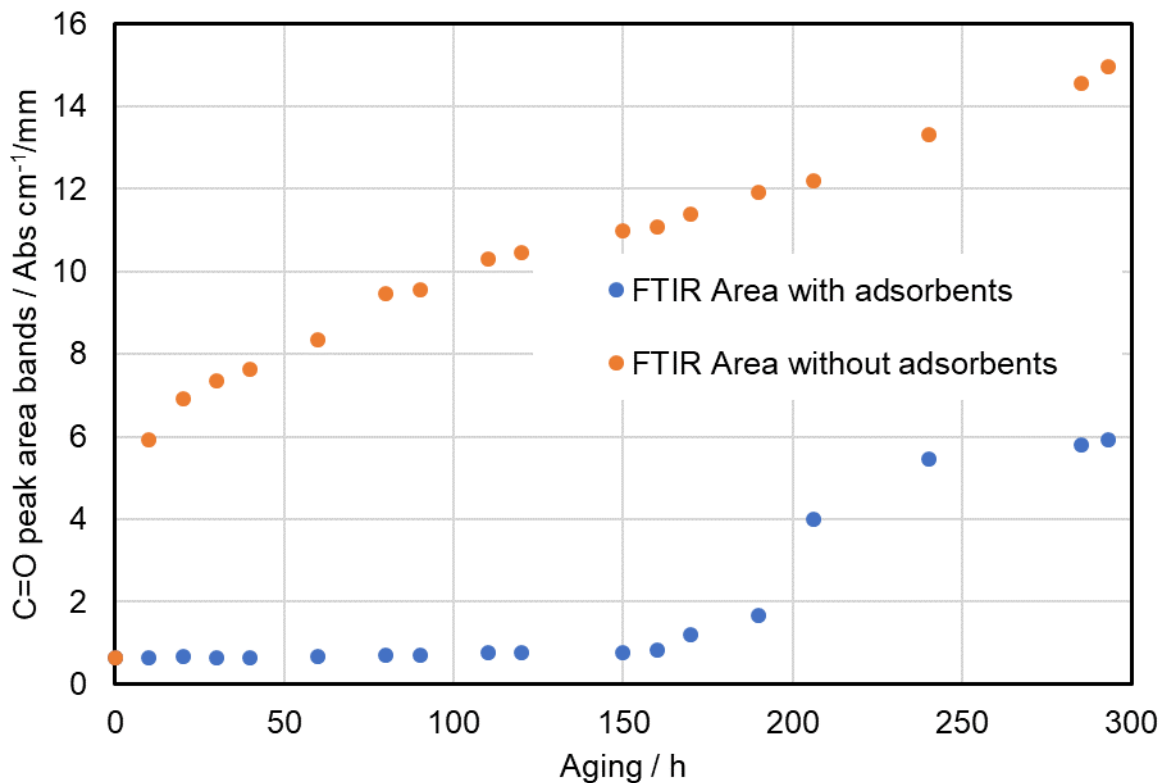


Figure 17: Evaluation of peak area under C=O bands (1600-1900 cm⁻¹) of the FTIR spectrum of 30 mL 20 % RME mixed with 80 % Base oil and treated with and without combined 0,675 g adsorbents of magnesium-aluminum hydrotalcite and 1,3,5-trimethyl-2,4,6-tris(3,5-di-tert-butyl-4-hydroxybenzyl) benzene in a ratio of 1:2 respectively and aged at 170°C with airflow of 10 L/h at 8 h per day in a Rancimat for about 300 h

7 Materials and Methods

Introduction

In this chapter, the materials and methods used to accomplish the study's objectives are discussed. The first section looks at the various materials employed in this study to arrive at the objectives; the chemicals, the different oils, and fuels. A simulated aging setup is constructed to assess the adsorbents' impact on the chemical and physical processes associated with biodiesel oxidation, thus the second section. The third section describes the equipment employed to acquire the data to evaluate the adsorbents' impact on the oxidized fuel and oil.

7.1 Chemicals

Magnesium-aluminum hydrotalcite, 1,3,5-trimethyl-2,4,6-tris(3,5-di-tert-butyl-4-hydroxybenzyl) benzene are obtained from Sigma Aldrich Chemie GmbH, Taufkirchen, Germany. Tetrahydrofuran (99.9 %), toluene (99.8 %) and isopropanol (99.9 %) all ultraviolet (UV) / infrared (IR) grade, and KOH in (0.1 mol/L (0.1 N)) isopropanol volumetric standard solution, nitric acid (supra quality), and hydrogen peroxide (ultra-quality) are supplied by Carl Roth GmbH+Co. KG, Karlsruhe, Germany. Apart from the adsorbents, all the chemicals are used without any modification.

7.2 Investigated Fuels and Oil

Some representative fuels and oils are investigated in assessing the adsorbents' impact on the composition, physical and chemical properties of the fuel and oil. The representative fuels, oils, and blends are presented in Table 3 to Table 6 below. Their most critical physicochemical properties are provided in the tables.

This investigation's base oil does not contain additives obtained from a project partner, Volkswagen AG. This base oil composition of 53 % mineral oil of API-group III and 47 % synthetic oil of API-group IV. As stated in section 3.5, lubricating oil is made up of base oil and additives. The base oil used is without additives to avoid the additives' influence on the oil's oxidation.

The RME, a biodiesel representative, is without additives and obtained from ADM, Hamburg, Germany.

Ultra-low sulfur diesel fuel is obtained from a fuel station pump in Coburg, Germany, while the lubricating oil, Mannol universal engine oil, is procured from the open market. The diesel fuel and market-ready Mannol lubricating oil contain additives.

Table 3: Physical properties of base oil and Mannol engine oil used in this research

Sample	Base oil	Mannol Oil	Unit
Kinematic viscosity, -20 °C		9500	mm ² /s
Kinematic viscosity, 40 °C	30.97	170.7	mm ² /s
Kinematic viscosity, 100 °C	5.91	18.3	mm ² /s
Viscosity index		119	
Density at 15 °C	870	894	kg/m ³
Flashpoint		225	°C
Pour point		-25	°C
TBN		5.4	g KOH/kg

Table 4: Physical properties of the fuels used in this research

Sample	Diesel Fuel	RME	C18-2 ME
Kinematic viscosity, 40 °C	2.76 mm ² /s	4.52 mm ² /s	4.06 mm ² /s
Kinematic viscosity, 100 °C	1.15 mm ² /s	1.77 mm ² /s	1.65mm ² /s
Density, 15 °C	0.83 kg/m ³	0.88 kg/m ³	0.89 kg/m ³
Flashpoint	92 °C	182 °C	
CFPP	-20 °C	-17 °C	-35 °C
Cetane number	53.6 % (m/m)	55 %(m/m)	
Induction time		6.8 h	
Calorific value	43.1 MJ/Kg	37.1 MJ/Kg	
Acid value	0.02 mg KOH/g	0.11 mg KOH/g	
Water		86 mg/Kg	
Iodine number		112 g lod/100 g	
HFRR (60 °C)	191 µm		
Distillation			
Begin	170 °C	340.9 °C	
3 % (V/V)	190 °C		
10 % (V/V)		342 °C	
20 % (V/V)		344 °C	
40 % (V/V)		351.6 °C	

Materials and Methods

59 % (V/V)	240 °C	
60 % (V/V)		355.4 °C
80 % (V/V)		362.8 °C
95 % (V/V)		368.8 °C
97 % (V/V)	290 °C	
End	350 °C	375.3 °C
C16:0 Palmitic acid		4.7 %
C16:1 Palmitolein		0.3 %
C18:0, Stearic acid		1.4 %
C18:1, Oleic acid		60.8 %
C18:2, Linoleic acid		20.0 %
		99.9 %
C18:3, Linolenic acid		9.7 %
C20:0, Arachidic acid		0.5 %
C20:1, Eicosenoic acid		1.4 %
C22:0, Belienic acid		0.3 %
C22:1, Erucic acid		0.4 %

The blends for the aging experiments had a composition of 20 % RME and 80 % of the other components; base oil or diesel fuel but all by percent volume. The sample matrix is given in Table 5. The representation of a simulation of 20 % lubricating oil dilution is thus investigated. Though Bai et al. (2016) recommended 20–50 % blending of biodiesel to provide environmental and technical advantages, Fang and McCormick (2006) defined this biodiesel admixture as a worst-case, resulting in the highest tendency for deposit formation. For stabilizing biodiesel and its blends using the adsorbents, 20 % biodiesel

and 80 % diesel fuel (B20) and neat RME are also investigated in Table 5. McCormick and Westbrook (2009) showed significant deposits or oxidative product results with biodiesel blends in the range of 20-30 %.

Table 5: Composition of the samples used in this research

Sample	Composition by % volume			
Base oil	98.4	80	-	-
C18:2	1.6	-	-	-
RME	-	20	20	100
Diesel fuel	-	-	80	-

The table below gives the properties of the B20 mixture. This B20 sample mixture is investigated on the stabilization of biodiesel and its blends using the adsorbents.

Table 6: Properties of the biodiesel blend used in this research

Sample	B20
Kinematic viscosity, 40 °C	3.04 mm ² /s
Kinematic viscosity, 100 °C	1.26 mm ² /s
Density, 15 °C	0.85 kg/m ³

7.3 Neat additives

The neat oil additives used in this investigation to determine the adsorbents' impact are obtained from a project partner and listed in Table 7.

Table 7 Pure additives tested with the adsorbents

Additive applied
VanlubeBHC
Vanlube961
Corrosion inhibitor
BHT
Friction modifier
Detergent
Lubricity improver

7.4 Simulated Aging Procedure

7.4.1 Laboratory setup apparatus

The accelerated aging has been carried out using a laboratory setup based on Schumacher (2013) and Singer et al. (2014) to simulate the aging of base oil and fuel mixtures. The aging apparatus is constructed based on the standard DIN EN 14112 (2014) to determine the oxidation stability of FAME. While it is impossible to equate this aging process to that of a vehicle's reality, it is very suitable to simulate the aging phenomena and eventually the oligomers' formation. According to Schumacher (2013), an engine oil change interval of approximately 3,000 km can be simulated within one week at a constant temperature of 170 °C for 40 h duration. Achieving results that cover a longer distance of oil usage, the duration of aging has been doubled to 80 h. In addition to thermal aging, synthetic air is passed at 300 mL/h through the sample mixture. This method promotes a shorter time for the formation of oligomers (Schumacher, 2013). The work of Singer et al. (2014) provided evidence that the aging at a constant temperature of 170 °C with an airflow rate of 300 ml/min is comparable to the results of aging following the temperature profile of Schumacher (2013). According to Schumacher (2013), 170 °C is approximately

the aging temperature profile's average temperature with a minimum variation of approximately 10 %.

Figure 18 Laboratory assembled aging apparatus

Figure 18 illustrates the structure of the aging equipment built. The oxidation study of oil-fuel mixtures in the presence and absence of the adsorbents is performed according to Schumacher (2013) at 170 °C. This apparatus has been used in this project to generate oligomers. The apparatus consists of a heating plate that supplies the heat to age the sample thermally. The aging of the oil is carried out in a borosilicate glass sample tube. The sample tube has a vented head for air and oil introduction. The setup has an oil bath in which the sample containing the tube is immersed. The oil bath is then heated using the heating plate to the desired temperature of 170 °C. The sample has an air inlet pipe through which synthetic air is supplied at about 300 mL/min from a mechanical pump into the mixture. At the same time, a thermometer is used to monitor the temperature during the experiment. The airstream carries the volatile organic compounds (VOC) formed during the aging process into a collecting vessel for subsequent analysis.

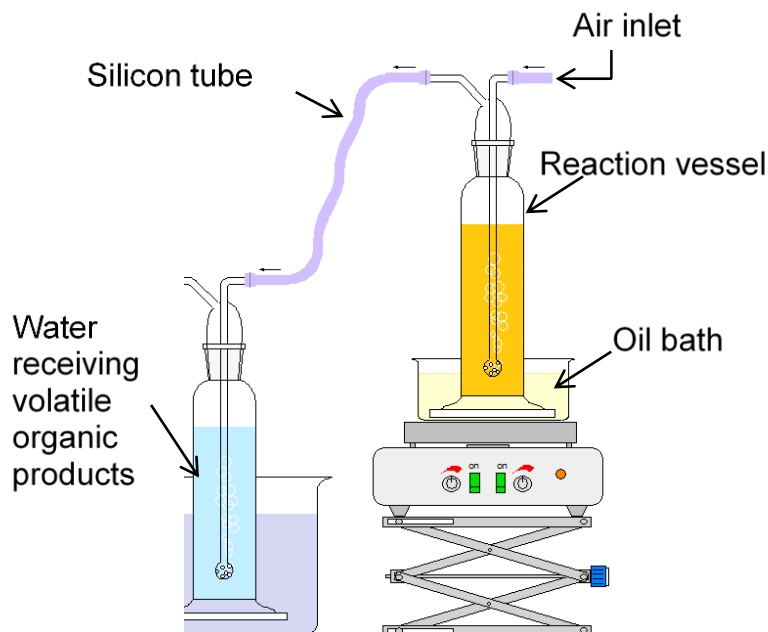


Figure 18 Laboratory assembled aging apparatus

7.4.2 The Metrohm 873 biodiesel Rancimat

The Metrohm 873 biodiesel Rancimat (Herisau, Switzerland) has also been used in this work to age samples. While maintaining the prescribed airflow of 10 L/h at a temperature of 170 °C, a volume of 30 ml of the sample is aged. The Rancimat is used in this work because its parameters are standard and facilitate the reproducibility of the process.

7.5 Investigation of suppression of oligomer formation

As seen in section 3.3, biodiesel oxidizes with time when it comes into contact with oxygen. According to the mechanism described in section 3.4, biodiesel's aging affects fuel chemistry and fuel properties. From sections 3.4 and 3.5.2, oxidation is seen as a complex process resulting in various products, including shorter chain fatty acids, aldehydes, and ultimately higher molecular substances (Kim et al., 2018; Brühl. 2014; Bannister et al., 2010). Therefore, assessing the suppression of formation of higher molecular mass substances, the samples are treated with the adsorbents. The treated and non-treated samples with the adsorbents are aged. The level of degradation or oligomerization is assessed by monitoring the area under the carbonyl and the hydroxyl bands in the FTIR spectrum (see Figure 10) and comparing it to that obtained for the neat non-aged oil. With the peak area method, the absorbance of the neat, treated, and non-treated with adsorbent and aged oil is determined and then compared. Here the absorbance of the oxidized oil is usually much larger than the neat oil, and therefore, the corresponding difference gives the level of degradation. The absorbance peak area of oxidized oil treated with the adsorbents is compared with original oil aged without any treatment with the adsorbents. The area gives the extent to which the adsorbents have quantitatively suppressed the degradation of the oil or suppressed the formation of high molecular mass substances in the oil under investigation. Other physicochemical properties such as acid number, kinematic viscosity, and density which are generally altered due to oxidation (Cen et al., 2018), are monitored to ascertain the adsorbents' impact. Figure 19 illustrates the experimental investigations procedure for suppressing oligomers formation using adsorbents during accelerated aging and the oxidation product analysis methods.

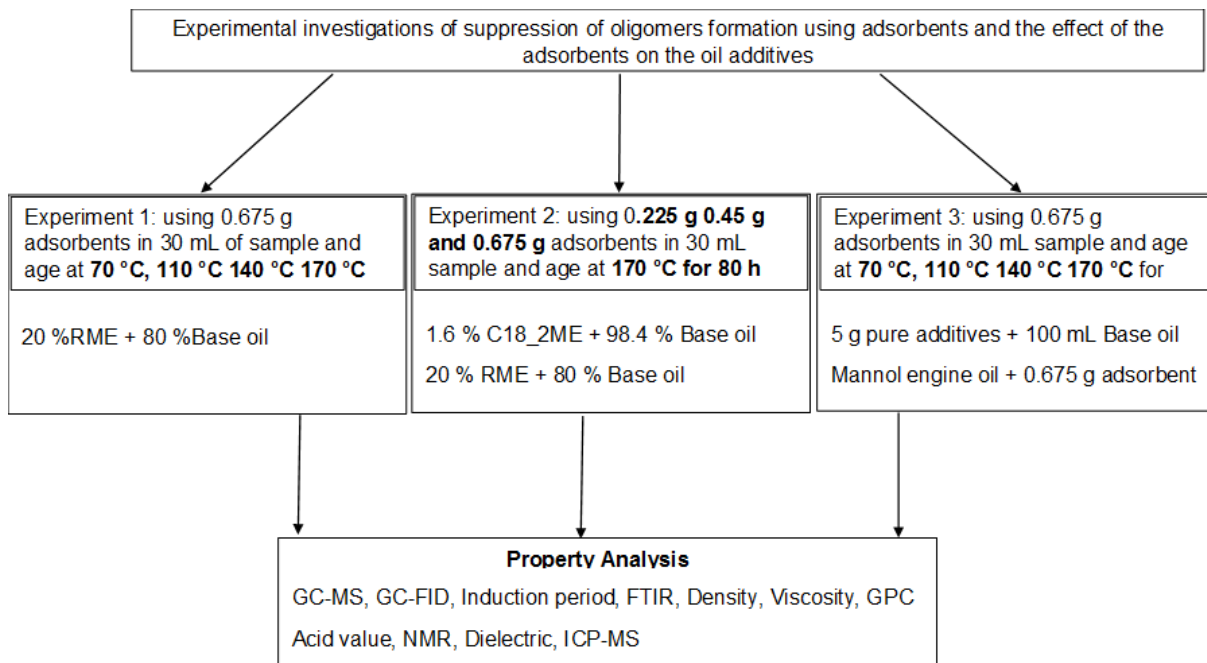


Figure 19 Investigations on the suppression of oligomers formation

7.5.1 Linoleic acid methyl ester (C18_2 ME)

In this work, linoleic acid methyl ester (C18_2 ME), a FAME model substance, is blended with a base oil in its natural proportion of 1.6 % in RME biodiesel (Besser et al. 2017) and investigated to determine their role in the initiation of the oxidation process. C18_2 ME is used because it polymerizes at high temperatures (Kim et al. 2018) and is most unstable due to its level of unsaturation. A volume of 30 ml of the sample, C18_2 ME, and base oil mixture is aged. Different amounts of the adsorbents, 0.225 g, 0.45 g, and 0.675 g in mass ratios of 1:1, 1:2, 1:3, and 1:4 and vice versa of hydrotalcite compound: 1,3,5-trimethyl-2,4,6-tris(3,5-di-tert-butyl-4-hydroxybenzyl) benzene is added manually to the 30 mL of the sample with continuous agitation on a magnetic stirrer. The agitation of the mixture stayed on for about two hours till homogeneity is attained and then aged at 170 °C for the 80 h duration using the Rancimat described in section 7.4.2. The oxidation level is measured with a focus on the changes in physicochemical properties described in the literature (section 2.1), considering the use with and without the adsorbents. The number of oxidation products formed is evaluated using GCMS, FTIR, and GPC. The mass ratio

of 1:2 of the adsorbents is reported because this ratio gave about the best results after several trials with the different ratios.

Table 8 Parameters under which C18_2 ME mixture was investigated

Sample	Temperature / °C	Mass of adsorbent	Duration of aging	Analysis
1.6 %C18_2ME+98.4 %Base oil	170	0.225 g, 0.45 g, 0.675 g	80 h	GCMS, FTIR, SEC

7.5.2 Rapeseed oil methyl ester (RME)

Investigating the effect of temperature on the adsorbents in suppressing oxidation

For the effect of temperature on the adsorbents in suppressing oxidation of base oil and RME mixture, the samples are aged at different temperatures of 70 °C, 110 °C, 140 °C, and 170 °C using the Rancimat, as shown Figure 19. The ratio composition of the sample mixture is as shown in Table 9. A volume of 30 ml of the sample is treated with 0.675 g of the adsorbents in the ratio of 1:2 (hydrotalcite compound: 1,3,5-trimethyl-2,4,6-tris(3,5-di-tert-butyl-4-hydroxybenzyl) benzene). The sample volume without any treatment with the adsorbents is also aged under the same conditions.

Table 9 Parameters used for the RME mixture investigation

Sample	Temperature / °C	Mass of adsorbent	Duration of aging	Analysis
20 %RME+80 % base oil	70,110, 140,170	0.675g	80 h	GCMS, FTIR, SEC

Investigating the effect of the amount of the adsorbent on oxidation

The mixtures of the neat base oil and RME for the aging experiments had 80 % base oil and 20 % RME all by percent volume. Various amounts of the adsorbents, 0.225 g, 0.45 g, and 0.675 g, are added to 30 ml of the sample each and aged using the Rancimat at a temperature of 170 °C. While another set of the same sample mixtures without adding the adsorbents are also aged under the same conditions and compared. The conditions under which this investigation is carried out are listed in Table 10.

Table 10 Parameters used for investigating RME with adsorbents

Sample	Temperature / °C	Mass of adsorbent / g	Duration of aging	Analysis
20 %RME+80 % base oil	170	0.225,0.45, 0.675	80 h	GCMS, FTIR, SEC

The base oil and RME mixture in a volume of 200 mL is also aged, just as done to the mixtures reported above. This mixture is treated the same as all the other experiments on the suppression of oligomers formation, and the same set of parameters are examined. The results from this experiment are presented in Figure_Apx 1 to Figure_Apx 10 in appendix 10. Since the adsorbents' impact follows the same pattern as the lower volume, 30 mL of samples used in this work, these results are not discussed.

7.5.3 Investigating the effect of the combined adsorbents of magnesium-aluminum hydrotalcite and 1,3,5-trimethyl-2,4,6-tris(3,5-di-tert-butyl-4-hydroxybenzyl) benzene in a ratio of 1:2 respectively on the oil additives

To ensure that the adsorbents used to suppress oligomers formation do not affect the additives in the lubricating oil, a market-ready lubricating oil, Mannol universal engine oil, is treated with the adsorbents. Neat oil additives are also treated with adsorbents. It is done to assess the potential impact of the adsorbents on the additives.

Engine oil

Mannol engine oil in a volume of 30 ml is mixed with 0.675 g adsorbents in the mass ratio of 1:2 as stated above, and another set without the adsorbents is also aged at 170 °C for 80 h duration. The inorganic components' concentration, the elements (Table 2), are examined after the aging process in the sample with and without the adsorbent treatment using the ICPMS. The samples are treated as described in section 7.4.2 before determining the concentrations. It is done to examine the impact of the adsorbents on the inorganic additives in engine oil. The organic components of the additives are determined using the GC-FID.

Table 11 Parameters used for investigating the adsorbents with engine oil

Sample	Temperature / °C	Mass of adsorbent	of Duration of aging	of Analysis
Mannol engine oil	170	0.675g	80 h	ICPMS, GCFID

Pure additives

Various neat oil additives, Table 12, are tested. A mass of 5 g of the neat additive is added to a 100 mL mixture of 20 % RME and 80 % base oil. In other cases, the neat additive is added to the only base oil. 30 mL of the prepared mixture is then treated with and without the adsorbents in the same mass ratio of 1:2. These mixtures are aged at 170 °C for 80 h duration using the Rancimat. The samples are treated as described in section 7.4.2 before determining the concentrations of the inorganic elements. It is done to examine the adsorbents' impact on the inorganic additive elements in the engine oil. GC-FID is used for the determination of the organic components of the additives.

Table 12: Neat additives tested in this work

Additives	VanlubeBHC	Vanlube961	Corrosion inhibitor	BHT	Friction modifier	Detergent	Lubricity improver
Mass / g	5	5	5	5	5	5	5
Base oil	80 %	100 %	100 %	100 %	100 %	100 %	100 %
RME	20 %						
Volume of sample / mL	100	100	100	100	100	100	100

7.6 Stabilization of biodiesel and its blends using combined adsorbents of magnesium-aluminum hydrotalcite and 1,3,5-trimethyl-2,4,6-tris(3,5-di-tert-butyl-4-hydroxybenzyl) benzene in a ratio of 1:2, respectively

From section 3.3, biodiesel suffers from stability due to the fatty acid ester composition of the feedstock from which it is made. Implying that biodiesel is unstable and, therefore, loses its quality with time hinders its long-term storage or applicability, as explained in section 3.3. It is well established in the literature (Botella et al., 2014; Dantas et al., 2011; Karavalakis et al., 2011; Kivevele et al., 2015; Jain and Sharma, 201). The more biodiesel and its blend degrade, the higher its acidity (Khalid et al., 2013). Hence the physiochemical properties, acid value, viscosity, density, insoluble substances, or higher molecular substances increase with increasing storage time. (Khalid et al., 2013; Leung et al., 2006; Westbrook, 2005). The changes in these properties are well described in section 2.1.

The adsorbents seen in section 6 are applied to biodiesel and its blend during the aging process. The adsorbents' impact in stabilizing biodiesel and its blends is monitored through the area under the carbonyl and the hydroxyl bands in the FTIR spectrum (see Figure 10 of section 4.1.5) and compared to that obtained for the neat fuel. Other physicochemical properties such as acid number, kinematic viscosity, and density altered by oxidation are monitored to ascertain the adsorbents' impact (Fattah et al., 2014; Ashraful et al., 2014). The different experimental investigations for biodiesel's stabilization and its blends using adsorbents are illustrated in Figure 20.

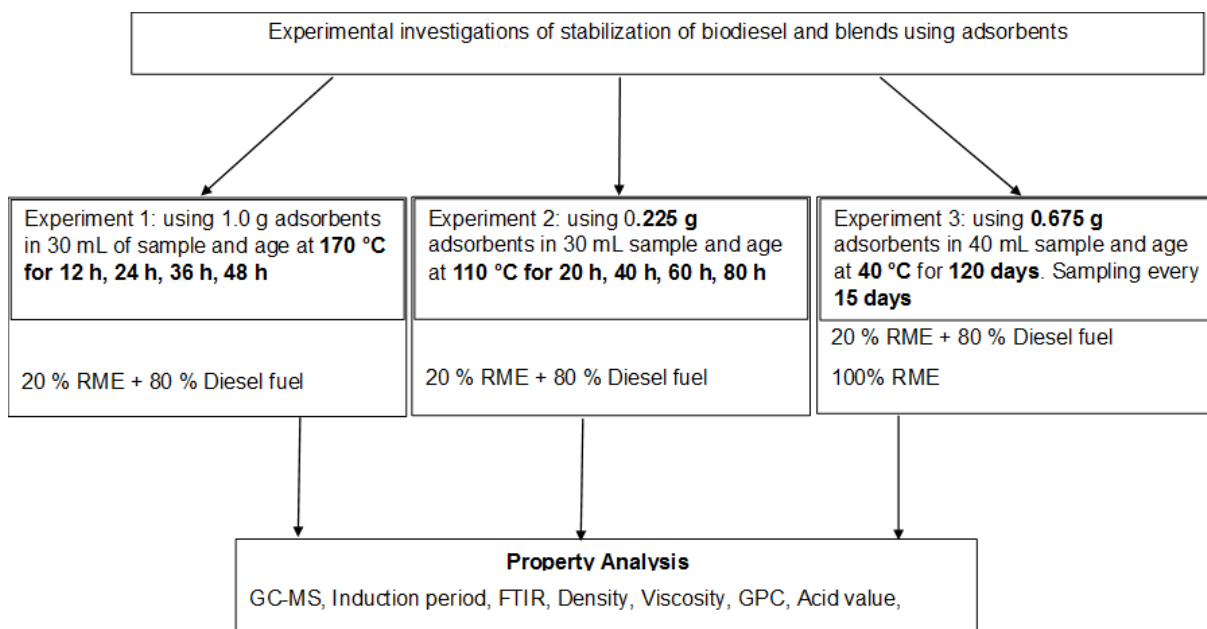


Figure 20 Experimental investigations on stabilization of biodiesel and its blends

7.6.1 Investigating the effect of the combined adsorbents of magnesium-aluminum hydrotalcite and 1,3,5-trimethyl-2,4,6-tris(3,5-di-tert-butyl-4-hydroxybenzyl) benzene in a ratio of 1:2 respectively on oxidative stability of biodiesel and its blends at 170 °C

Table 6 the 80 Vol % diesel fuel and 20 Vol % biodiesel herein referred to as B20 is splash blended. This mixing process of the fuels is done with continuous stirring for uniformity at room temperature and pressure. The samples are treated with a mass of 1 g of the adsorbents in the ratio of 1:2 (magnesium-aluminum hydrotalcite: 1,3,5-trimethyl-2,4,6-

tris(3,5-di-tert-butyl-4-hydroxybenzyl) benzene). The adsorbents are added manually to the entire volume of 30 mL with continuous agitation on a magnetic stirrer. The agitation of the mixture stayed on for about two hours till homogeneity is attained. The B20 treated with and without the adsorbents is aged at 170 °C for various durations of 12 h up to 48 h using the Rancimat. Aging at this temperature of 170 °C is extreme considering the temperature fuel usually experiences in a system. Still, it stimulates the production of oligomers or aid biodiesel to oxidize faster within the experiment's time frame and, therefore, make the adsorbent's impact stand out. The adsorbents' impact on biodiesel's oxidation stability and blends is thus studied by measuring the induction period, viscosity, density, and total acid number. The molecular vibrations of functional groups are detected with FTIR, while size exclusion chromatography detects the molecular weight of high molecular mass substances formed.

Table 13 30 mL blend of biodiesel and diesel fuel treated with 1 g adsorbents to determine the effect of the adsorbents on their oxidative stability at 170 °C

Sample	Temperature / °C	Mass of adsorbent / g	Duration of aging	Analysis
20 %RME+80 % diesel fuel	170	1	48 h	Viscosity, density, acid number, FTIR, GCMS, SEC

7.6.2 Investigating the effect of the combined adsorbents of magnesium-aluminum hydrotalcite and 1,3,5-trimethyl-2,4,6-tris(3,5-di-tert-butyl-4-hydroxybenzyl) benzene in a ratio of 1:2 respectively on oxidative stability of biodiesel and its blends at 110 °C

Aging biodiesel or its blends at a temperature of 170 °C, as seen in section 7.6.1, is at the extreme compared to what fuel experiences in its actual application. Therefore, B20, as treated above, is here again aged at a temperature of 110 °C. It is the standard temperature used in biodiesel oxidative stability studies. The B20, 80 Vol % diesel fuel, and 20 Vol % biodiesel are splash blended. The samples are treated with a mass of

0.225 g of the adsorbents in the ratio of 1:2 (magnesium-aluminum hydrotalcite:1,3,5-trimethyl-2,4,6-tris(3,5-di-tert-butyl-4-hydroxybenzyl) benzene). The adsorbents are added manually to the entire volume of 30 mL with continuous agitation on a magnetic stirrer till homogeneity is attained. The mass ratio of 1:2 of the adsorbents is maintained since that ratio has given the best results so far. The B20 treated with and without the adsorbents is aged at 110 °C for various durations of 20 h up to 80 h using the Rancimat. The changes in biodiesel's physiochemical properties resulting from oxidation are measured and compared between the samples treated with and without the adsorbents.

Table 14 30 mL blend of biodiesel and diesel fuel treated with 0.225 g of adsorbents to determine the effect of the adsorbents on their oxidative stability at 110 °C

Sample	Temperature / °C	Mass of adsorbent / g	Duration of aging	Analysis
20 %RME+80 %diesel fuel	110	0.225	80 h	Induction period, viscosity, density, acid number, FTIR, GCMS, SEC

7.6.3 Investigating the effect of the combined adsorbents of magnesium-aluminum hydrotalcite and 1,3,5-trimethyl-2,4,6-tris(3,5-di-tert-butyl-4-hydroxybenzyl) benzene in a ratio of 1:2 respectively on the storage stability of biodiesel and its blends at 40 °C

This experiment evaluates the adsorbents' impact on fuel stability of diesel/biodiesel blends and biodiesel alone during four months of fuel storage at conditions representative of the fuel's ambient conditions during storage fuel tanks. The results of Starck et al. (2015) revealed significant variations on FAME and their blends depending on their feedstock on storage at 40°C. At four months of storage, as reported by Starck et al. (2015) and Ben Amara et al. (2014), it can lead to higher TAN values than the technical criteria. The fuel samples are stored for 120 days in an oven at 40 °C±5 (Starck et al., 2015; Westbrook, 2005). The duration of 120 days and temperature of 40 °C are chosen,

considering that ambient temperature is an essential factor affecting biodiesel's degradation and blends (Khalid et al., 2013). Leung et al. (2006) temperature affect the degradation rate of biodiesel during storage. Fuel during storage or in tanks of standby generators or plug-in hybrid vehicles experiences ambient conditions of a temperature of 40 °C, as reported in the work of Leung et al. (2006).

In this experimental work, RME mixed with diesel fuel, B20, is studied along with pure biodiesel, RME. The samples in a volume of 40 mL are treated with a mass of 0.675 g of the adsorbents in the ratio of 1:2 (magnesium-aluminum hydrotalcite: 1,3,5-trimethyl-2,4,6-tris(3,5-di-tert-butyl-4-hydroxybenzyl) benzene) in a capped glass bottle. The samples are not exposed to light. The samples are stored for 120 days at 40 °C ambient temperature to simulate extended storage conditions in fuel tanks of plug-in-hydride vehicles and standby generating plants. These aging conditions are less aggressive compared with the thermooxidative aging method described in sections 7.5.1 and 7.5.2. However, these samples provide a very realistic and a bit precise determination of vehicle-like aging conditions. The samples are vented for 15 minutes every two weeks. It is to renew the containers' overhead air following the works of Westbrook (2005), where the sample bottles are capped but vented periodically for 12 weeks. It must be stated that the samples are not shaken during the entire process duration. The samples are monitored every two weeks for 120 days. High molecular mass substances formed, induction period, change in viscosity, density, and acid value are measured to follow the samples' evolution during the storage. This experiment's main objective is to study the impact of the adsorbents on the changes in biodiesel's physio-chemical properties and its blends during the storage period.

Table 15 40 mL blend of biodiesel and diesel fuel treated with 0.675 g of adsorbents to determine the effect of the adsorbents on their storage stability at 40 °C

Sample	Temperature / °C	Mass of adsorbent / g	Duration of aging	Analysis
20 %RME+80 %diesel fuel	40	0.675	120 days	Induction-period, viscosity, density, acid number, FTIR, SEC
RME	40	0.675	120 days	SEC

7.7 Measurement techniques

In this section, the equipment that is used to accomplish the objectives of this thesis is discussed. These measurements are carried out to evaluate the impact of the adsorbents on the oxidized oil and fuel.

The neat sample's induction period and the sample treated with the adsorbent are determined using Rancimat and PetroOxy equipment. The induction period and aging product build-up are essential to determining the adsorbents' impact on the sample mixtures' oxidation or degradation. These oxidation products are detected and analyzed using Fourier transform infrared spectroscopy (FTIR), gas chromatography, size-exclusion chromatography (SEC), and their acid values are treated using Metrohm potentiometric titrator. Kinematic viscosity and density are measured using an automated SVM 3000 Anton Paar rotational Stabinger viscometer densimeter. GC-FID and ICP-MS are used to study the impact of the adsorbents on oil/fuel additives. All the measurements carried out are based on changes in the physical and chemical effects due to aging. The fundamentals of the physical and chemical effects have been described in section 4.3. Therefore, the measurement techniques and applications used in this work are outlined in this chapter.

7.7.1 Induction period

Oxidation stability is one of the most critical properties describing fuel or oil stability because FAME from literature, section 2.1 oxidizes easily compared with petroleum diesel fuel and produces reaction products that can degrade its quality (Bacha et al., 2015; Biodiesel Guidelines, 2009).

Rancimat

The oxidation stability of biodiesel is measured by accelerated oxidation using the Rancimat. The Metrohm 873 biodiesel Rancimat (Deutsche METROHM GmbH & Co. KG) is employed to measure the induction period or to quantify the oxidation stability as specified in EN15751. The accelerated oxidation test is carried out by heating a 7.50 g mass of sample at 110 °C in a sealed test tube while passing purified air at a flow rate of 10 L/h through it (Manual 873 Biodiesel Rancimat, 2009). The 7.50 g sample mixture is weighed using an electronic balance Sartorius Mechatronics AG with an accuracy of 0.01 g for the experiments to determine the mixtures' stability. In avoiding contamination of the pipettes, the graduated pipettes used for the samples during weighing are cleaned with an appropriate solvent. During the oxidation process, volatile secondary oxidation products are released and passed over the air stream into a flask containing distilled water and an electrode that measures the water's conductivity. A rapid increase in conductivity induced by the increase of volatile carboxylic acids in the water generates an induction period (IP), expressed in an hour, indicating the sample's oxidation resistance. The oxidation stability is determined from the second derivative of conductivity versus time plot with the volatile acids trapped in deionized water and quantified through conductivity. In evaluating the time-conductivity curve obtained, tangents are drawn to the time course of the conductivity. The intersection of the tangents represents oxidation stability (Manual 873 Biodiesel Rancimat 2009). The oxidation stability referred to as induction time (period) is, therefore, the time that elapsed from the start of the test until the secondary oxidation products' appearance, which increases the water's conductivity in the cell. The increase in conductivity after the induction period is caused by the dissociation of short-chain volatile carboxylic acids produced during the oxidation (Gaurav and Sharma, 2014).

PetroOxy

Due to oxidation stability enhancing additives in the diesel fuel used in this research, the PetroOxy determines the biodiesel induction periods blended with diesel fuel. With the PetroOxy method, a hermetically sealed test chamber with 5 mL of sample is pressurized with oxygen at 700 kPa and then heated to 140 °C. This method requires the consumption of oxygen for the oxidation of the fuel or the fuel deterioration. Because of the heating, there is an increase in pressure to a maximum. As the oxygen is consumed during the aging process, a drop in the pressure is recorded every second. The test ends when a pressure drop of 10 % from the maximum pressure to a predetermined level is reached. The time elapsed from the start to a 10 % drop in the pressure determines the induction time and measures the sample's oxidation stability.

7.7.2 Size Exclusion Chromatography (SEC)

Size-exclusion chromatogram (SEC) is measured using an Agilent GPC system (Agilent 1260 Infinity Quaternary LC system) in this research. The Agilent G1362A 1260RID refractive index detector and the Agilent G1365D 1260 MWDVL ultraviolet (UV) detector are used. With these detectors, the peak area increases proportionally with concentration which enables quantitative analysis of analytes. For the separation and determination of large aging products, three columns in a row are used. All of them are packed with styrene-divinylbenzene copolymers (3 x 30 cm PSS SDV) with particle sizes of 3 µm. The porosities of the used columns are 50 nm, 100 nm, and 1000 nm, respectively. The three columns are used in series with a 0.5 mL/min flow rate at 45 °C. The column length is 30 cm with a pore size of 5 microns and a porosity of 100 nm. Tetrahydrofuran (THF) is used as a solvent. Before the measurement, the SEC device is calibrated with standard substances to determine their molar masses. The calibration is done with polyethylene glycol standards (Agilent PEG calibration kit Part No.: PL2070-0100) with different molecular masses between 106 and 4040 Da. Using PEG for calibration, the molar mass of methyl oleate is about 335 Da though the actual molar mass of methyl oleate is 296.45 Da. Since the molecular size of the calibration standards and the analytes are not identical, it has become difficult to make quantitative statements. Hence all measured molecular weights are computed relative to the standard (PEG) molecular weights.

Therefore, relative molar masses are reported in this work. The SEC measurements are performed using 10 mg of the sample mixed with 1000 μ L THF as solvent.

7.7.3 Gas Chromatograph-Mass Spectroscopy (GCMS)

The gas chromatography (GC) with a coupled mass-sensitive sensor (MS) is used to determine volatile organic fuel components in the gas phase. The studied samples' chemical composition is performed using an Agilent GC7890A gas chromatography coupled with Agilent 5973 quadrupole mass spectrometer (Agilent Technologies, Germany). A Phenomenex Zebron ZB5-HT (USA) column with a length of 60 m, an inner diameter of 0.25 mm, and a film thickness of 0.25 μ m are used for GCMS separation. The coating consists of 5 % phenyl 95 % dimethylpolysiloxane. With this column, the substances such as fatty acid methyl esters, motor oil, and oxidative products, e.g., alcohols, aldehydes, ketones, carboxylic acids, etc., in this work could be separated and detected by their different mass numbers. Helium is used as carrier gas with a flow rate of 13.3 mL/min. The oven's heating profile has a temperature ramp from 110 $^{\circ}$ C for 5 minutes and then increases by 5 $^{\circ}$ C/min to 280 $^{\circ}$ C for 15 minutes. The total run time for this method is 50 min. The differences in components are identified by comparison of the retention times and mass spectra of 20 % RME mixed with 80 % base oil without the adsorbent before and after aging with those of the mixture of 20 % RME and 80 % base oil with adsorbent after aging at 170 $^{\circ}$ C for 80 h. A sample of mass 10 mg is mixed with 1 mL Cyclohexane and used for the analysis. The GCMS method takes advantage of retaining the more polar compounds of the sample aged without using the adsorbents than the less polar compounds in the sample aged with the adsorbents. Due to the adsorbents' use, the mixture is less affected by the oxidation process and fewer oxidative products. The polar column maximizes the separation that can be achieved for identification.

7.7.4 Total Acid Number (TAN) or Acid value

An acid number is a valuable tool in monitoring biodiesel's degradation since the acid number increases with degradation (Jiang et al., 2016). The acid number is measured according to ASTM D664 using a fully automated measurement system developed by Metrohm (Titrando 888) (Herisau, Switzerland). 0.1 N volumetric standard solution of KOH

in isopropanol is the titrant, while the solvent is made of 50 % toluene, 49.5 % isopropanol, and 0.5 % CO₂-free water. 50 mL of the solvent is added to about 0.2 g of the sample and titrated against the standard KOH in isopropanol for the acid value. The total acid number (TAN) is the amount of potassium hydroxide in mg required to neutralize the acids in one g of sample.

7.7.5 Viscosity and Density

Kinematic viscosity is an essential measurement for assessing lubricant quality, as mentioned in section 4. The measured parameters are viscosity, kinematic viscosity, and density. Kinematic viscosity is measured at 40 °C and 100 °C. Measurements of viscosity and density in this research are performed using an automated SVM 3000 Anton Paar rotational Stabinger viscometer (Graz, Austria). The SVM 3000 uses Peltier elements for fast and efficient thermostability. The temperature uncertainty is 0.02 °C. The absolute uncertainty of the density is 0.005 kg/m³, and the relative uncertainty of the kinematic viscosity is less than 0.5 %. The SVM 3000 viscosimeter has a density measuring cell that employs the well-known oscillating U-tube principle. Both density and viscosity cells are filled in one cycle, and the measurements are carried out simultaneously. The density value measured at 15 °C and the kinematic viscosity measured at 40 °C are used to compare further and evaluate the changes in quality of the fuel mixtures for the presence and absence of the adsorbents. The kinematic viscosity and density measurements' reproducibility are 0.35 % and better than 0.005 kg/m³, respectively.

7.7.6 Fourier Transform Infrared Spectroscopy (FTIR)

In this work, FTIR measurements are carried out according to EN 14078 to determine the adsorbents' impact on the aging mixtures. The FTIR spectra are obtained employing a Nicolet 6700 FTIR from Thermo Scientific Company (Thermo Fisher Scientific, Germany). The Thermo Scientific Omnic software is used for the evaluation of the measurements. This instrument is equipped with an ATR crystal for ATR spectroscopy and uses a DTGS detector and an XT-KBr beam splitter. The crystal needs just a drop of the sample, which is sufficient for analysis. Therefore, the adsorbents' impact on the aging of the samples will show in the spectra's difference before and after aging and with and without the use of the adsorbents. The C=O stretch of esters absorbs light at $1745 \pm 5 \text{ cm}^{-1}$, utilized in the

analysis. The broad absorption band around 3000-3600 cm^{-1} emerging in the spectrum is attributable to intermolecular O-H stretching bands. These bands show a significant impact due to the oxidation of biodiesel (Westberg, 2012). The samples are scanned in the range of 4000 to 500 cm^{-1} . The test disc is cleaned with isopropanol between the scans, and a background scan is performed with nothing attached to the disc to obtain a clear baseline. The background and sample are each scanned 16 times.

7.7.7 Inductively Coupled Plasma-Mass-Spectrometry (ICP-MS)

Inductively Coupled Plasma-Mass-Spectrometry (ICP-MS) is used for the detection of elemental content. ICP-MS has the advantages of low spectral interferences and multi-elements analysis. The ICP-MS used in this work is model iCAP Q from Thermo Fisher Scientific. ICP-MS technique enables the determination of low and ultra-low elemental concentrations. The elements are led through a plasma source, where they become ionized and are sorted out according to their masses. The ICP-MS parameters are listed in the table below:

Table 16: ICP-MS parameters

Standard mode	
<hr/>	
Sensitivity (kcps/ppb)	
$^7\text{Li}^b$	80
$^{59}\text{Co}^b$	200
$^{115}\text{In}^b$	400
$^{238}\text{U}^b$	500
Detection Limits (ppt)	
^9Be	<0.5
^{115}In	<0.1
^{209}Bi	<0.1
Oxides (%)	
CeO/Ce ^b	<2
Double Charged (%)	
Ba ⁺⁺ /Ba ^{+b}	<3
Background (cps)	
m/z 4.5 ^b	<1
Stability (% RSD)	
Short Term ^b	<2(10 min)
Long Term	<3(2 h)
Isotope Ratio Precision (%RSD)	
$^{107}\text{Ag}/^{109}\text{Ag}$	<0.1

7.7.8 Gas Chromatography-Flame Ionization Detector (GC-FID)

An Agilent 7820A gas chromatograph (Santa Clara, USA) equipped with a flame ionization detector (FID) is used. An injection port system is a splitless injector. The GC-FID has a column length of 30 m; internal diameter of column 0.25 mm; thickness of stationary phase, 0.5 μm (Machery Nagel, Germany). The flow rate of helium as a carrier gas is 0.2 mL min^{-1} , and nitrogen as makeup gas is 12.5 mL min^{-1} . Air and hydrogen for FID flame had flow rates of 50 and 15 mL min^{-1} , respectively, and the injection port and detector temperature is 220 $^{\circ}\text{C}$. The temperature programming is 150 $^{\circ}\text{C}$ for 3 min and then ramped to 250 $^{\circ}\text{C}$ and 320 $^{\circ}\text{C}$ respectively at 30 $^{\circ}\text{C min}^{-1}$ and held for 5 and 30 min respectively. 10 μL of 1-Decanol as internal standard is added to 20 μL of the sample and then mixed with 1 mL Cyclohexane for the GC-FID analysis.

7.7.9 Dielectric properties measurement

Eskiner et al. (2015, 2020) developed an elaborate method for determining the degree of aging of fuels considering changes in dielectric properties during aging. This determination correlates with the formation of oligomers. The sensor measures dielectric parameters in low-frequency ranges where polar oxidation products like alcohols, acids, and oligomers can be detected. Polar and high molecular compounds show at higher frequencies less mobility because of inertia. Therefore, the polar molecules acting as free charge carriers in the mixture can migrate to the capacitor plates and attenuate the primary electrical field, leading to a change in the capacitance in a parallel plate capacitor. This method is applied to the samples treated with the adsorbents and aged compared to the samples without the adsorbents and aged for the number of oligomers formed. The level of the oligomers formed reflect in the permittivity measured. The developed sensor is a parallel-plate capacitor that is used to determine the dielectric parameters ϵ'_r and $\tan \delta$. The sensor consists of two electrodes. Each electrode consists of 18 plates. Furthermore, the electrodes are parallel and fixated on a Teflon plate to ensure a constant distance between them and maintain a constant capacity. The parallel arrangement ensures a high capacity is achieved and is necessary to perform measurements in the low-frequency range.

7.7.10 NMR measurement

NMR Spectra measurements are acquired directly from samples on a Burker AV400 (B = 9.4 T; 400 MHz) and Burker AV400TR (B = 9.4 T; 400 MHz) spectrometer operating at 400 Hz (^1H) and 100 MHz (^{13}C) with tetramethylsilane (TMS) as solvent. The solvent signals are recorded regarding the signal of TMS as an internal standard. In contrast, the signals of the incompletely deuterated contamination of the deuterated solvent are used to reference the chemical shifts of ^1H and ^{13}C spectra. The temperature is kept constant at $37.00\pm 0.01^\circ\text{C}$. Before NMR analysis, the samples are placed in a thermal box at about $37.0\pm 0.5^\circ\text{C}$ for at least 30 min to bring it to the thermal equilibrium with the NMR spectrometer. Then, 3.0 ml of the sample is transferred into an 18 mm NMR tube and then submitted to the NMR analysis. Measurements are performed averagely three times to improve accuracy. The chemical shift values from literature (Fulmer et al., 2010) are used to reference the signals.

8 Results and Discussion

The adsorbents, magnesium-aluminum hydrotalcite, and 1,3,5-trimethyl-2,4,6-tris(3,5-di-tert-butyl-4-hydroxybenzyl) benzene in a ratio of 1:2 respectively used to suppress the formation of oligomers is covered in the first section of this chapter. The combined adsorbents' influence on the oxidation stability is reported concerning the sample mixtures' degree of degradation. A comparison is made between the presence and absence of the adsorbents in the aged sample. Three different fuel and oil matrices are treated with the combined adsorbents to investigate their impact on oxidation. The acid value, viscosity, density, molecular masses of oligomers formed, changes in molecular structures, permittivity, and NMR analysis are all reported here. The impact of the combined magnesium-aluminum hydrotalcite and 1,3,5-trimethyl-2,4,6-tris(3,5-di-tert-butyl-4-hydroxybenzyl) benzene in a ratio of 1:2 respectively on oil additives during the suppression process of oligomers is also reported in this section.

The second section of this chapter presents the effects of the adsorbents on biodiesel's stability and blends. The neat biodiesel and its blends treated with the combined adsorbents are investigated for their oxidative and storage stability. For oxidative stability, two experiments are carried out to examine the effect of the amount of the adsorbents used and the impact of temperature on the adsorbents in augmenting the samples' oxidative stability. The neat biodiesel and its blends treated with the combined adsorbents are stored in an oven at 40 °C for 120 days on storage stability. Samples are examined every 15 days for induction period changes, acid number, viscosity, induction period, and density.

8.1 Investigating the effect of the combined adsorbents of magnesium-aluminum hydrotalcite and 1,3,5-trimethyl-2,4,6-tris(3,5-di-tert-butyl-4-hydroxybenzyl) benzene in a ratio of 1:2 respectively in suppressing oxidation in base oil blended with linoleic acid methyl ester (C18_2 ME)

This second section of the chapter considers the impact of adsorbents on biodiesel's oxidation in the base oil. In achieving this, a biodiesel model, linoleic acid methyl ester (C18_2 ME) as a single component, is investigated to determine how the adsorbent can suppress its role in initiating the oxidation process. According to Kim et al. (2018), the

content of unsaturated fatty acids in biodiesel is directly related to the extent of oxidation stability. The oxidation rate increases with double bonds in fatty acid chains (Kim et al., 2018). The linoleic acid methyl ester dosage in this blend is at the level of its natural occurrence in biodiesel blended with diesel fuel at 7 %, i.e., 1.6 wt % for C18_2 ME (Dunn, 2005). Linoleic acid methyl ester (C18_2 ME) is chosen because it is a commonly occurring fatty acid in many biodiesel production crops (Dugmore, 2011, Balat and Balat, 2008). It is, therefore, a significant component of biodiesel, especially in rapeseed oil methyl ester (RME) (Dugmore, 2011). The polyunsaturated compounds are more reactive than monounsaturated and saturated ones and have been seen in section 3.4; therefore, the hypothesis is that linoleic acid methyl ester is one of the primary chemicals responsible for the enhanced formation of oligomers. The accelerated rate of lubricant oxidation can thus be investigated (Dugmore, 2011). Therefore, base oil and linoleic acid methyl ester represent biodiesel's oxidative degradation in lubricant engine oil. The base oil blended with linoleic acid methyl ester is treated with 0.225 g, 0.45 g, and 0.675 g combined adsorbents of magnesium-aluminum hydrotalcite and 1,3,5-trimethyl-2,4,6-tris(3,5-di-tert-butyl-4-hydroxybenzyl) benzene in a ratio of 1:2 respectively and aged at 170 °C for 80 h. This 170 °C temperature represents the average temperature found in different diesel engine areas, from the sump (the lowest) to the piston ring assembly, which has the highest temperature (Dugmore, 2011). The same mixture without any adsorbent treatment is also aged compared to the sample treated with the adsorbents.

8.1.1 Gas Chromatography

Figure 21 shows the change in the content of C18_2 ME traces using the GCMS for base oil blended with linoleic acid methyl ester and treated with and without adsorbents and oxidized in the static oxidation reaction at 170 °C for durations of 40 h and 80 h. The abscissa represents the retention times in min for which the respective components are eluted from the column. The ordinates represent the amount or the concentration of the various components present in the sample. In Figure 21, there are significant eluted C18_2 ME component peaks of the neat sample at approximately 36.12 min. However, this same peak is virtually completely degraded, significantly reduced, or gradually disappeared in the aged blend that has not been treated with the adsorbents at even 40 h duration of aging. The content of C18_2 ME, therefore, gradually disappears as the

oxidation time increased. The C18_2 ME undergoes oxidation or polymerization under the influence of temperature and oxidative aging duration (Kim et al., 2018). The degradation of the signal for the C18_2 ME molecule aged without the adsorbent confirms its oxidative instability or susceptibility to oxidation due to the low bond dissociation energies (see Table 1 on section 3.4) resulting from the degree of unsaturation. The rapid decrease in C18_2 ME content translates into increased acid number, density, and kinematic viscosity by oxidation and biodiesel polymerization (Kim et al., 2018). The C18_2 ME signals in the mixture treated with the adsorbents and aged are still very prominent at about 40 % and 60 % for the 40 h and 80 h duration of aging. Considering the presence of allylic hydrogen atoms in C18_2 ME, which are susceptible to the radical attack leading to hydroperoxides' formation, the adsorbent's use has entrapped these radicals preventing the formation of the peroxides.

The suppression of the adsorbents' degradation can be explained as due to the donation of hydrogen (see section 6), which permits the generation of stable products and hence breakdown the chain reaction mechanism of oxidation. This result agrees with the works of Christensen and McCormick (2014) and Dunn (2005). It is worthy to note that during the oxidation of the base oil and C18_2 ME mixture, the unaged C18_2 ME peak intensity had about 2,104,387 counts, but as the oxidation progressed, the counts reduced by 62.2 % at 40 h duration to about 1,309,083 and further to about 848,701 counts at 80 h duration representing about 40 % of the original. However, between the 40 h and 80 h duration of aging, the reduction is about 20 %, signifying that the adsorbents' impact in suppressing the mixtures' degradation is not linearly dependent on aging but on the amount of the adsorbent applied. Also, the aging of C18_2 ME at 170 °C for only 40 h sees it thoroughly degraded. The methyl ester signals decreased, coinciding with an increase in acid value. Therefore, 40 % of C18_2 ME after aging for 80 h demonstrates the adsorbents' significant impact in suppressing the oxidation process. It also reflects the low change in acid values. The model component, C18_2 ME, showed less stability in the mixture aged without adsorbents than the corresponding mixture aged with the adsorbent from the GCMS results. These results confirm that the model component, C18_2 ME, degrades primarily from the start of the aging process and, therefore, confirms its role in initiating the oxidation process (Besser et al., 2017). Similar results reported by Bacha et

al. (2015) confirmed that the low stability of C18_2 ME is attributable to their level of unsaturation and, subsequently, their number of bisallylic sites. The C18_2 ME is wholly lost in the model mixture, while a residual amount of 40 % is found in the mixture aged with the adsorbents after 80 h of aging. The above results are obtained due to the adsorbent behavior of hydrogen bonding to the radical species. Once the radical species are trapped on the adsorbent's surface, the oxidation process is interrupted and delayed.

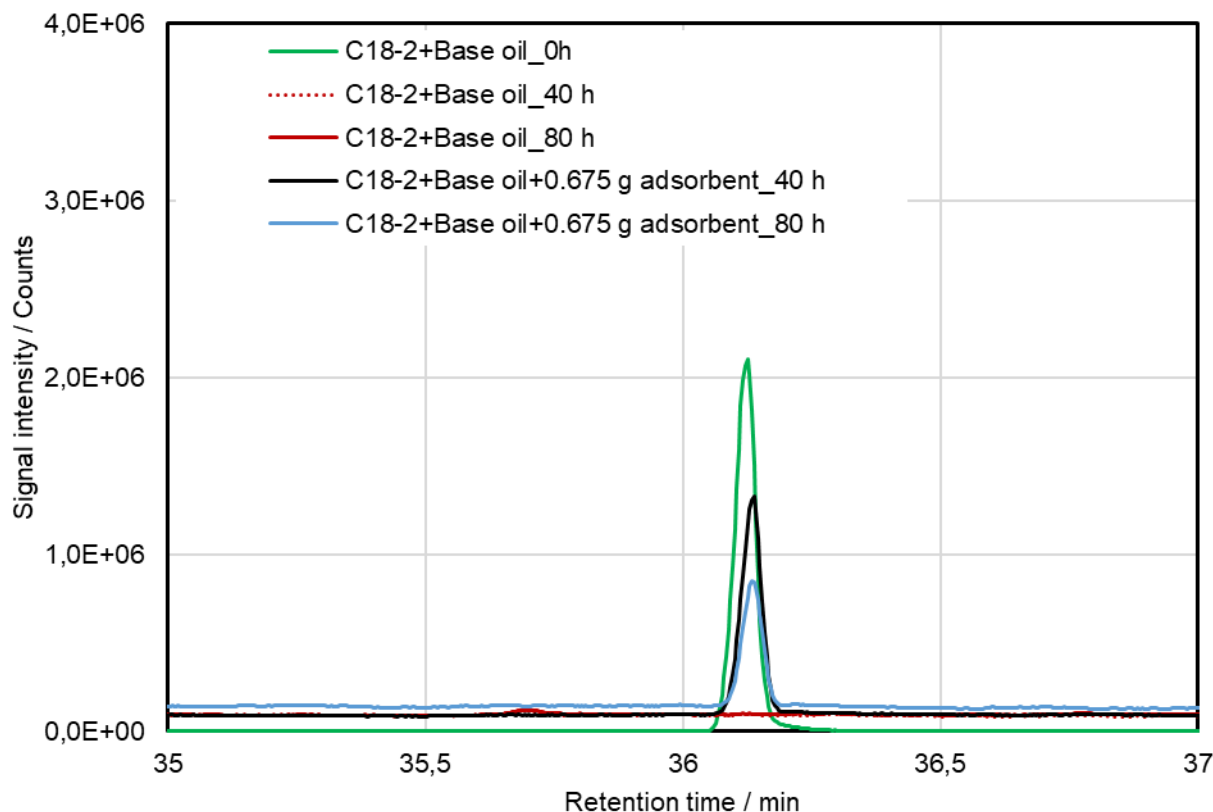


Figure 21: Evaluation of GC-chromatogram of 98.4 % base oil blended with 1.6 % C18_2 ME treated with and without combined 0.675 g adsorbents of magnesium-aluminum hydroxalcite and 1,3,5-trimethyl-2,4,6-tris(3,5-di-tert-butyl-4-hydroxybenzyl) benzene in a ratio of 1:2 respectively and aged at 170 °C with airflow of 10L/h for 8 h per day for a total of 80 h with Rancimat compared with the neat blend

8.1.2 Size Exclusion Chromatography (SEC)

Figure 22 shows the molar mass distribution and molecular weight fractions of the higher molecular mass substances in Figure 23. The analysis with SEC in Figure 22 presents the different molar masses of the 98.4 % base oil blended with 1.6 % C18_2 ME with and

without treatment with 0.225 g, 0.45 g, and 0.675 g adsorbents and aged at 170 °C with an airflow of 10 L/h for 8 h per day for 80 h compared with the neat base oil and C18_2 mixture. The molar mass distribution shows that the distribution of the masses of the oligomers formed differs depending on the presence or absence of the adsorbents in the sample. The samples aged without the treatment with the adsorbent increased in molar masses by a factor of about 30 to molar masses of about 1100 g/mol. Compared with the samples treated with the adsorbents and aged at the same temperature and duration, molar masses recorded are under 800 g/mol, just as the neat sample indicates a negligible increase. However, a component in the mixture that appears around 420 g/mol in the neat sample is degraded to about 90 % in proportion in the sample treated with the adsorbents than the sample without any adsorbent treatment and aged. The SEC's results can be explained by suppressing the higher molecular mass substances formation by the adsorbents applied in this experiment. According to Kim et al. (2018), C18_2 ME undergoes polymerization under the influence of temperature and time of aging (Kim et al., 2018). Since C18_2 ME polymerizes at higher temperatures (Kim et al., 2018), its oxidation causes more degradation compounds that polymerize into higher molecular weights substances during the accelerated oxidation process, leading to an increase in molecular masses (Kim et al., 2018; Brühl, 2014). This buildup of oligomers observed from section 3.4 is attributed to the migration of double bonds on the chain during the formation of hydroperoxides on the oxidation of methyl linoleate. As seen in section 3.2, during the oxidation process, radicals react with oxygen to form peroxide or hydroperoxides. The peroxides then react, leading to cyclic products forming acids, aldehydes, ketones, alcohols. These radicals react further with other alkyl and peroxy radicals to form dimers and oligomers, resulting in higher molecular mass substances. Therefore, the higher molecular masses registered by the blends aged without using the adsorbents are very expected. Similar results are reported in the literature, Refaat (2009); Christensen and McCormick (2014). The mixtures treated with the adsorbents and aged have shown a less significant buildup of higher molecular mass. It is expected based on the suppressive action of the adsorbents duly described in section 6. This is because the radical trapping agent's surface predominantly exhibits proton donor properties due to liable hydrogen groups in its structural matrix and intercepts the oxidation precursors, inhibiting their ability to polymerize into higher molecular mass substances.

On the other hand, the hydrotalcite compound releases ions while adsorbing anions and, therefore, adsorb the acidic products in an ionic exchange fashion. Their presence retarded the oxidation process, and hence the low molecular mass substances resulted, Figure 22 and Figure 23. It agrees with the work of Mendiara and Coronel (2006).

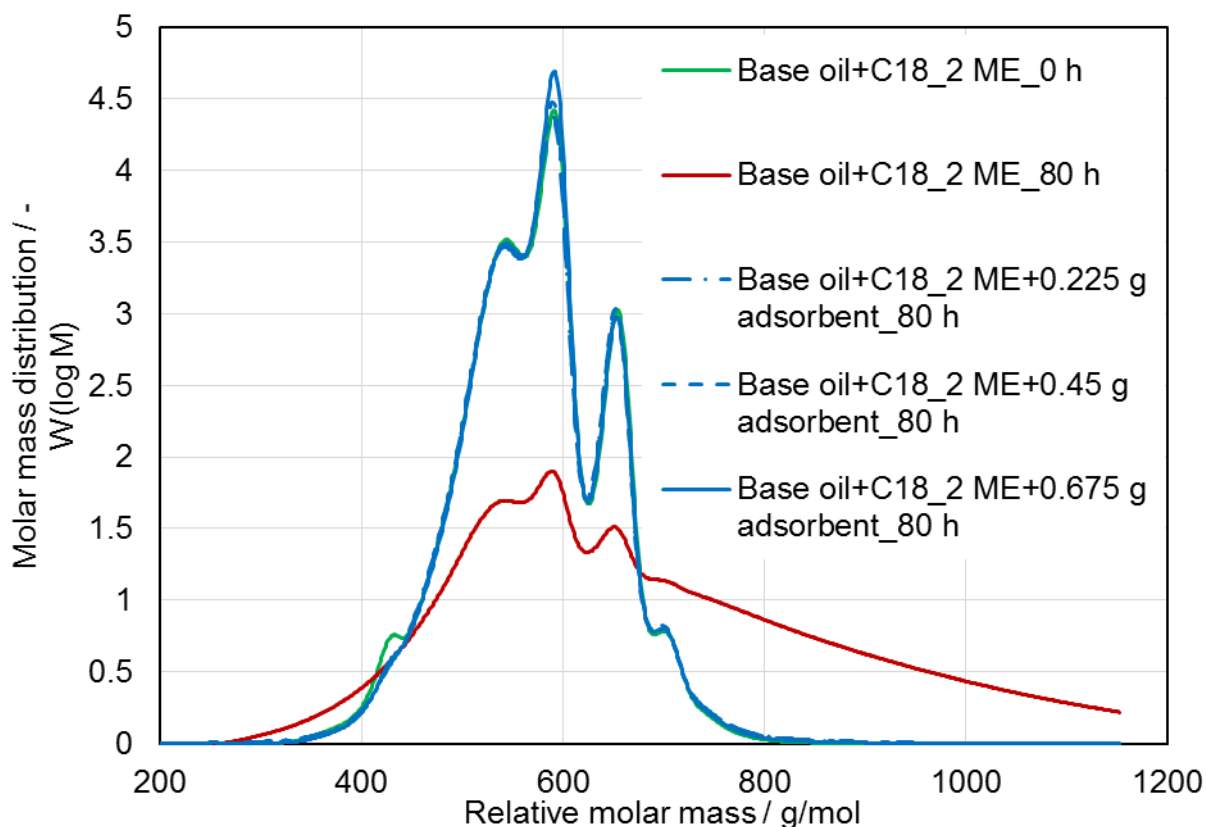


Figure 22: Evaluation of SEC of 98.4 % base oil blended with 1.6 % C18_2 ME treated with and without combined 0.675 g adsorbents of magnesium-aluminum hydrotalcite and 1,3,5-trimethyl-2,4,6-tris(3,5-di-tert-butyl-4-hydroxybenzyl) benzene in a ratio of 1:2 respectively and aged at 170 °C with airflow of 10 L/h for 8 h per day for a total of 80 h with Rancimat compared with the neat blend

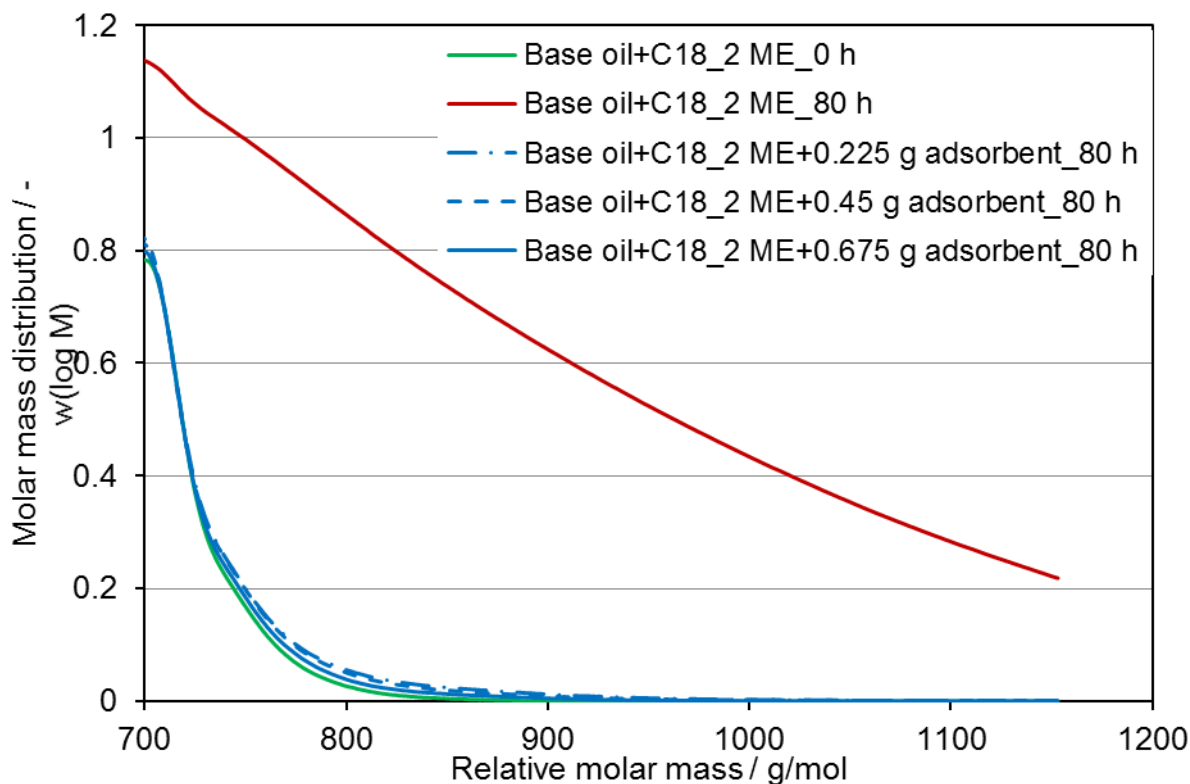


Figure 23: Zoom in on the higher molecular mass area of SEC of 98.4 % base oil blended with 1.6 % C18_2 ME treated with and without combined 0.675 g adsorbents of magnesium-aluminum hydrotalcite and 1,3,5-trimethyl-2,4,6-tris(3,5-di-tert-butyl-4-hydroxybenzyl) benzene in a ratio of 1:2 respectively and aged at 170 °C with airflow of 10 L/h for 8 h per day for a total of 80 h with Rancimat compared with the neat blend

8.1.3 FTIR analysis

From section 4.1.5, the adsorbents' impact on the aging of the mixtures shows in the differences in the blends' spectra before and after aging and with and without the presence of the adsorbents. Figure 24 is the spectra of the 98.4 % base oil blended with 1.6 % C18_2 ME with and without treatment with 0.225 g, 0.45 g, and 0.675 g adsorbents and aged at 170 °C with an airflow of 10 L/h per day for 80 h compared with the neat base oil and C18_2 ME mixture. The infrared range, from 1500 to 4000 cm^{-1} , is considered for analysis in this work. The 400 to 1500 cm^{-1} range, the fingerprint region, has not been considered for analysis. In Figure 24, a significant peak is observed at about 1740 cm^{-1} for the aged sample mixture without adsorbents. This peak corresponds to the carbonyl group absorption, typical of ester and degradation product compounds. This peak is basically due to the degradation of the C18_2 ME component in the mixture due to its high

oxidation susceptibility and polymerization at high temperatures (Kim et al., 2018). This band is characteristic of carbonyl bonds' axial deformations, present in most oxidation products (Fang and McCormick, 2006). The adsorbents' impact on the oxidation of the mixture is quantified by integrating the spectral band around 1740 cm^{-1} measured from 1600 to 1900 cm^{-1} . The carbonyl band area at 1740 cm^{-1} used to evaluate the samples' oxidation level is presented in Figure 27. Several studies about biodiesel's oxidative degradation have been analyzed utilizing FTIR spectra in which this area of the carbonyl band is used for purposes of comparison studies (Fang and McCormick, 2006; Lira et al., 2010; Conceição, 2007). Therefore, comparing the aged mixture treated with adsorbents is made with the aged mixture with no treatment. The carbonyl and hydroxyl areas are shown in Figure 25 and Figure 26, respectively, for clarity. The mixtures aged without using the adsorbents generated spectra strong enough for evaluation and comparison with the spectra of the mixtures aged with the adsorbent. There are distinct differences in both mixtures' absorbance bands attributed to the adsorbents' use.

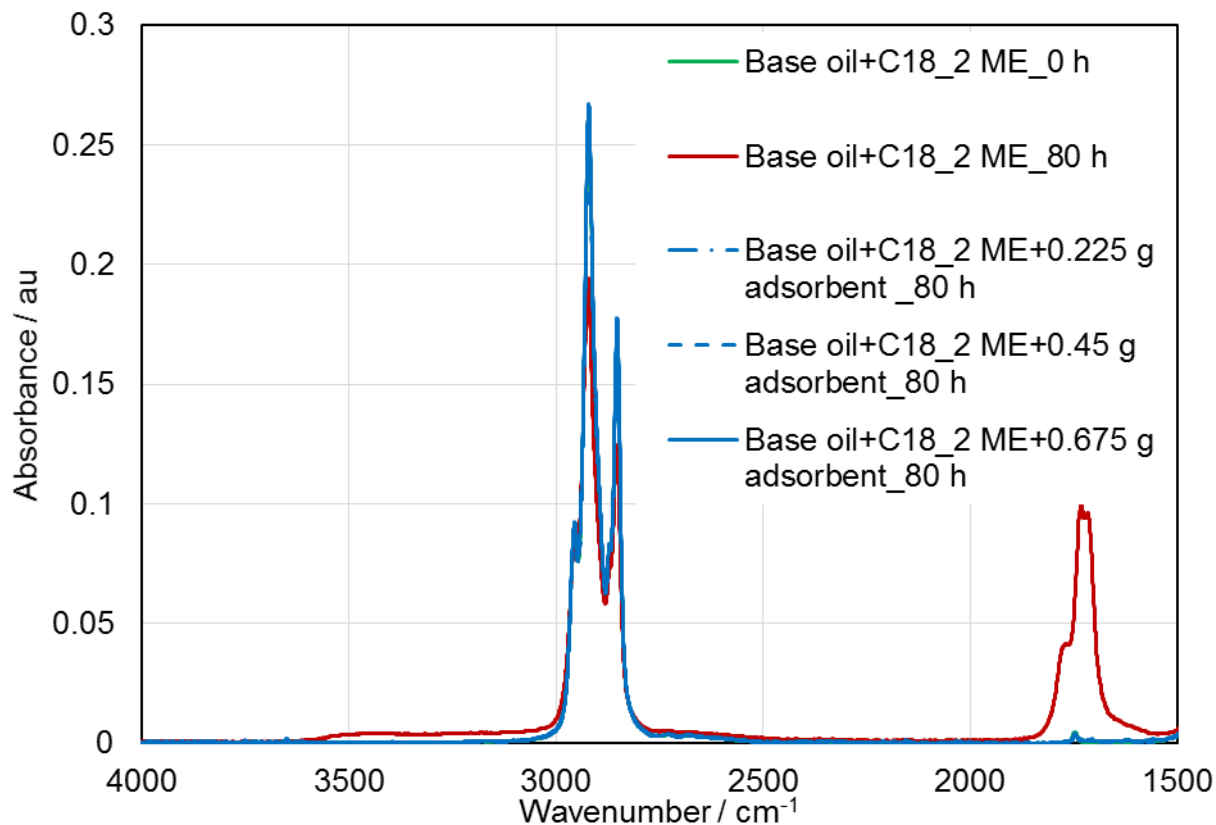


Figure 24: Evaluation of FTIR spectra in absorbance mode (range 1500-4000 cm^{-1}) of 98.4 % base oil blended with 1.6 % C18_2 ME treated with and without 0.675 g combined adsorbents of magnesium-aluminum hydrotalcite and 1,3,5-trimethyl-2,4,6-tris(3,5-di-tert-butyl-4-hydroxybenzyl) benzene in a ratio of 1:2 respectively and aged at 170 °C with airflow of 10 L/h for 8 h per day for a total of 80 h with Rancimat compared with the neat blend

The broadening of the band at about 1740 cm^{-1} , as seen in Figure 25 for the sample aged without the adsorbents, is due to polymerization of C18_2 ME at high temperatures resulting in an absorption of about 0.1 au from an initial absorption of about 0.001 au. With increasing oxidation, the mixture without the adsorbents shows a strong absorption resulting in two maxima. These results largely coincide with literature results (Kim et al., 2018; Knothe, 2006). It is due to carbonyl-containing degradation species such as ketones and aldehydes from the oxidation process (Westberg, 2012). The increase or broadening of the carbonyl-containing signal coincides with an increase in the presence of higher molecular mass species detected by the SEC results reported in 8.1.2. According to

Knothe (2007) and Bannister et al. (2011), this result, during the oxidation of biodiesel, proceeds with forming a hydrocarbon radical species on the bisallylic carbon by which the double bonds isomerizes into a conjugated structure. This radical reacting with oxygen forms a peroxide species, which propagates the reaction. The peroxides break down into oxygenated intermediates. These oxygenated intermediates further degrade into small chain acids, ketones, alkenes, and aldehydes, resulting in dimers, oligomers, and high molecular mass species. Hence three different shoulders can be seen in the spectrum of the sample aged without using the adsorbents, indicating at least three different oxidation products as seen in Figure 25.

However, the broadened band described above is absent in the mixture treated with the adsorbents and aged. The adsorbents' presence contributed through the liable hydrogens in its structure to stabilize the oxidation process's precursors, resulting in less to insignificant oxidation products, as shown in Figure 25. This suppression of oxidation largely coincides with literature results on oxidation inhibiting technologies (Saifuddin and Refal, 2014; Caramit et al., 2013; Moser, 2012; Kivevele and Mbarawa, 2011).

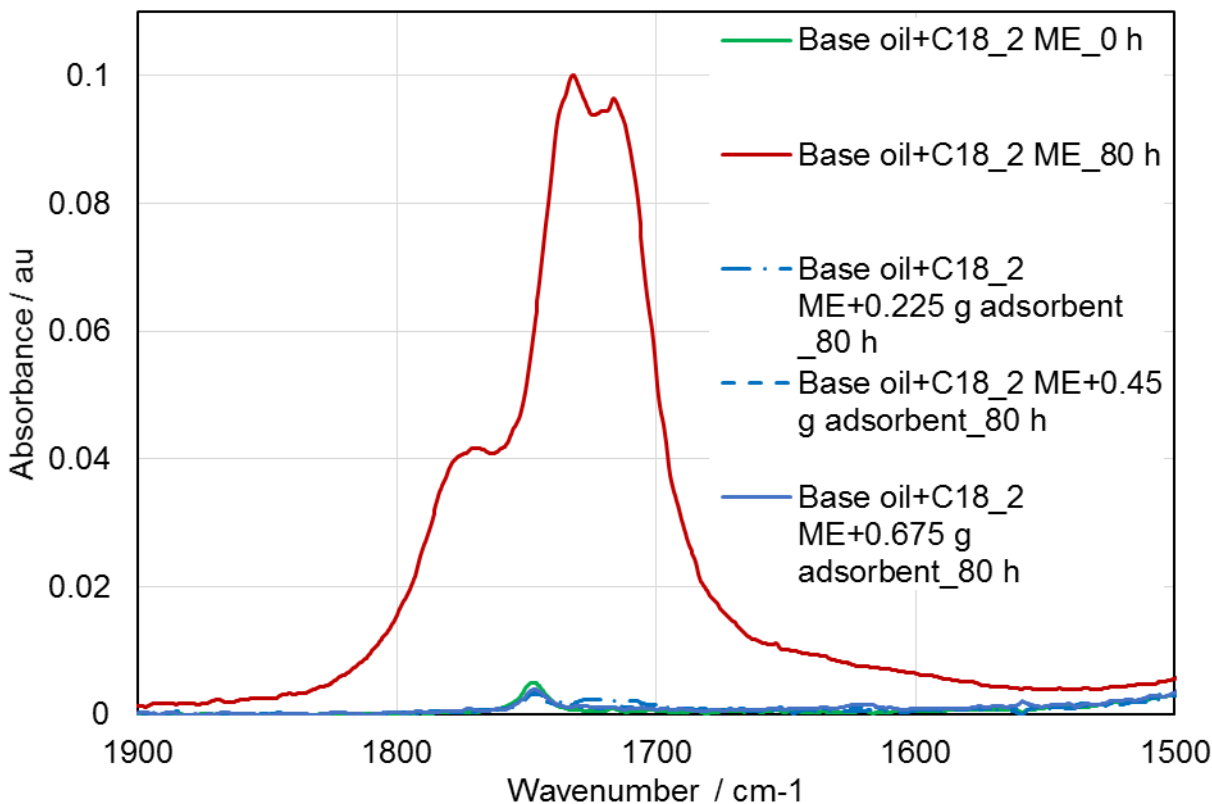


Figure 25: Evaluation of FTIR spectra in absorbance mode (range 1500-1900 cm^{-1}) of 98.4 % base oil mixed with 1.6 % C18_2 ME treated with and without combined 0.675 g adsorbents of magnesium-aluminum hydrotalcite and 1,3,5-trimethyl-2,4,6-tris(3,5-di-tert-butyl-4-hydroxybenzyl) benzene in a ratio of 1:2 respectively and aged at 170 °C with airflow of 10 L/h for 8 h per day for a total of 80 h with Rancimat compared with the neat blend

The broad O-H stretch around 3400 cm^{-1} , as shown in Figure 26, is more pronounced in the blend aged without treatment with the adsorbents relative to the mixture treated with the adsorbents confirming the impact of suppression of oxidation by the adsorbents. The high peak of the OH band seen in the sample aged without the adsorbent is attributable to the organic compounds, including alcohol, hydroperoxides, and carboxylic acids with the OH functional group (Besser et al., 2017). These signals are negligible in the samples treated with the adsorbents and aged. The adsorbents impacted the production of the primary oxidation products, the hydroperoxides (see section 3.4) lead to low oxidation activity (Kim et al., 2018; Besser et al., 2017). This result agrees with the GCMS results

(8.1.1) and size exclusion chromatography determination (8.1.2), where the C18_2 ME component is least affected by the oxidation process in the blends treated with the adsorbents.

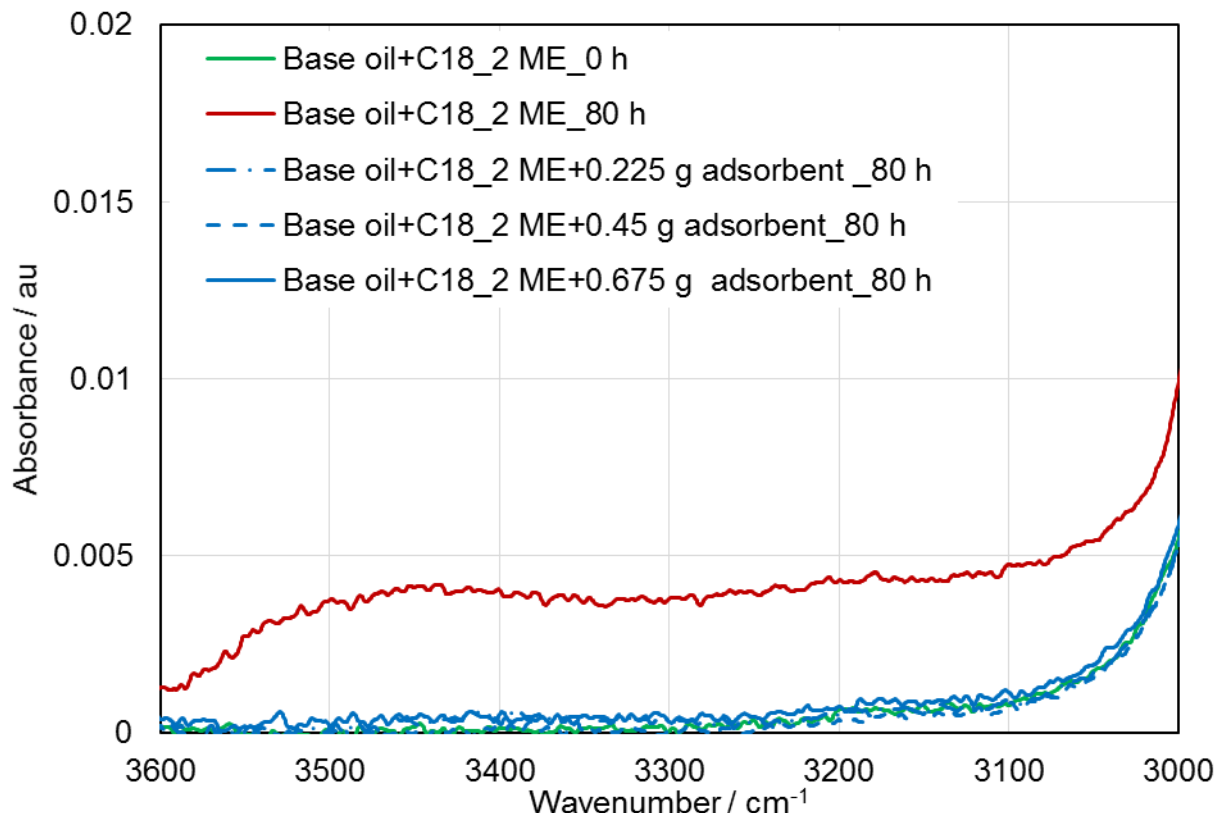


Figure 26: Evaluation of FTIR spectra in absorbance mode (range 3000-3600 cm^{-1}) of 98.4 % base oil mixed with 1.6 % C18_2 ME treated with and without combined 0.675 g adsorbents of magnesium-aluminum hydrotalcite and 1,3,5-trimethyl-2,4,6-tris(3,5-di-tert-butyl-4-hydroxybenzyl) benzene in a ratio of 1:2 respectively and aged at 170 °C with airflow of 10 L/h for 8 h per day for a total of 80 h with Rancimat compared with the neat blend

The differences in the C=O-bonds between 1600 and 1900 cm^{-1} due to the adsorbents' use have been integrated to show the absorption level or the number of degradation products formed in Figure 27. Comparing the aged base oil and the C18_2 ME, mixtures without treatment with adsorbents showed higher carbonyl vibrations (7.89 au absorption). In contrast, the mixtures treated with the different amounts of adsorbents showed insignificant carbonyl vibrations, 0.18, 0.18, and 0.2 au, according to the amount of the adsorbents applied, respectively. Comparing the sample treated with the adsorbents with

an average absorption of 0.2 a.u to the samples aged without any adsorbent treatment, absorption of 7.89 au, the latter underwent more severe accelerated aging. The samples treated with the adsorbents only aged to about 2.4 % of the original value. This result can be explained based on the scavenging of the oxidation process's precursors by the combined adsorbents leading to less sample degradation. Hence, little carbonyl contained degradation products are recorded. The presence of the hydrogen atoms on the surface of the adsorbents does cause the stability of the radicals. It is also evident from its FTIR analysis that the ester component in the sample treated with the adsorbent has been insignificantly affected by the oxidation process. The adsorbents' use has significantly decreased carbonyl vibration bonds than the mixtures aged without the adsorbent.

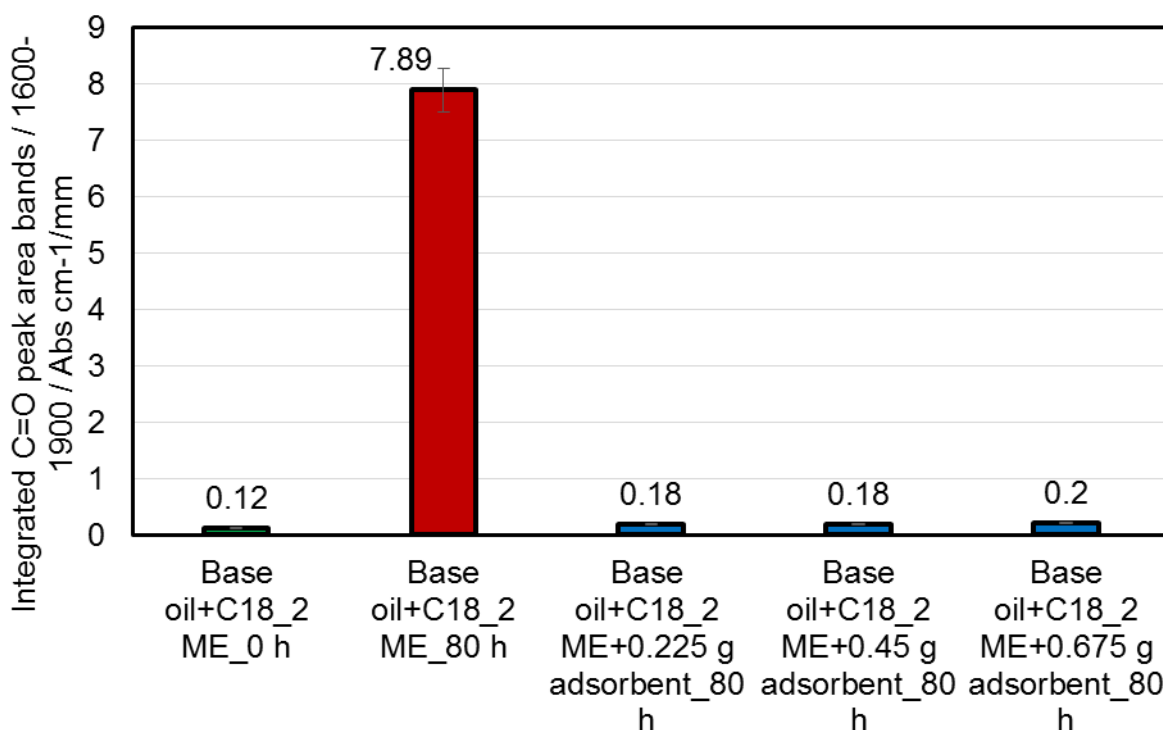


Figure 27: Evaluation of peak area under C=O bands (1600-1900 cm⁻¹) of the FTIR spectrum of 98.4 % base oil mixed with 1.6 % C18_2 ME treated with and without combined 0.675 g adsorbents of magnesium-aluminum hydrotalcite and 1,3,5-trimethyl-2,4,6-tris(3,5-di-tert-butyl-4-hydroxybenzyl)benzene in a ratio of 1:2 respectively and aged at 170 °C with airflow of 10 L/h for 8 h per day for a total of 80 h with Rancimat compared with the neat blend

8.1.4 Acid value

From section 4.1.3, the acid value is a valuable measure for monitoring hydrocarbons' degradation, biodiesel. The acid number increases with increasing oxidation, and this is used as a general indicator of fuel degradation (Saltas et al., 2017). The linoleic acid methyl ester is fully decomposed after 24 h of aging at 110 °C (Flitsch et al., 2014). The composition shows a strong correlation with the formation of aging products at the end of the induction period (Flitsch et al., 2014).

Figure 28 is an illustration of the acid values of the 98.4 % base oil blended with 1.6 % C18_2 ME and treated with and without 0.225 g, 0.45 g, and 0.675 g adsorbents and aged at 170 °C with an airflow of 10 L/h at 8 h per day for a total of 80 h duration using a Rancimat. The blend of aged samples without the treatment with the adsorbents shows an increase in acid value from 0.07 mg KOH/g at the initial stage to about 32 mg KOH/g at the end of the aging, increasing in acid value, increasing oxidation duration. The oxidation of the C18_2 ME explains the increase in acid values.

During this oxidation process, free radicals are formed, as explained in section 3.4. These radicals, on further reaction with oxygen, are converted to hydroperoxides. Monyem, 2000; Morita and Tokita, 2006; and Schneider et al., 2008 indicated that these hydroperoxides and their reactive products cause an increase in acidity during aging, supporting these results. This observed trend of higher acid value agrees with the results of the integrated areas of the FTIR spectra in Figure 27 and that of the SEC in Figure 22. Since C18_2 ME polymerizes at higher temperatures (Kim et al., 2018) and is an initiator of oxidation of biodiesel, its degradation leads to the production of compounds with higher molecular weights during the accelerated oxidation process, which also brings about an increase in acid value (Kim et al., 2018; Brühl, 2014). However, the blend treated with the adsorbents shows a lower acid value because the adsorbents inhibited hydroxyl compounds' production during the oxidation process by intercepting the radicals, which are the precursors of the oxidation process through its liable hydrogen atoms on its molecular structure. The acid values of the samples treated with the adsorbents are 2.23 mg KOH/g, 1.53 mg KOH/g, and 1.5 mg KOH/g according to the various amounts of the adsorbents used 0.225 g, 0.45 g, and 0.675 g, respectively. The low values are

indicative of a less harsh oxidation process. Hydroperoxides are significant products of the initiation and propagation stages of the oxidation process. This interference occurs during the initiation stage, leading to little or no production of the primary oxidation products. The hydroperoxides, which would have broken down further into other products such as acids (see section 3.2), are adsorbed by the adsorbents. This result agrees with the low to negligible absorption peak observed at wavenumbers of 3000 to 3600 cm^{-1} in Figure 26. The low acid values of the blends treated with the adsorbents and aged prove the insignificant production of degraded oxidation products reflected in the SEC and FTIR analysis results in sections 8.1.2 and 8.1.3, respectively. It confirms that the adsorbents' suppression activity is limited to the first stage of the oxidation process, illustrated in the top left side of Figure 5 in section 3.4.

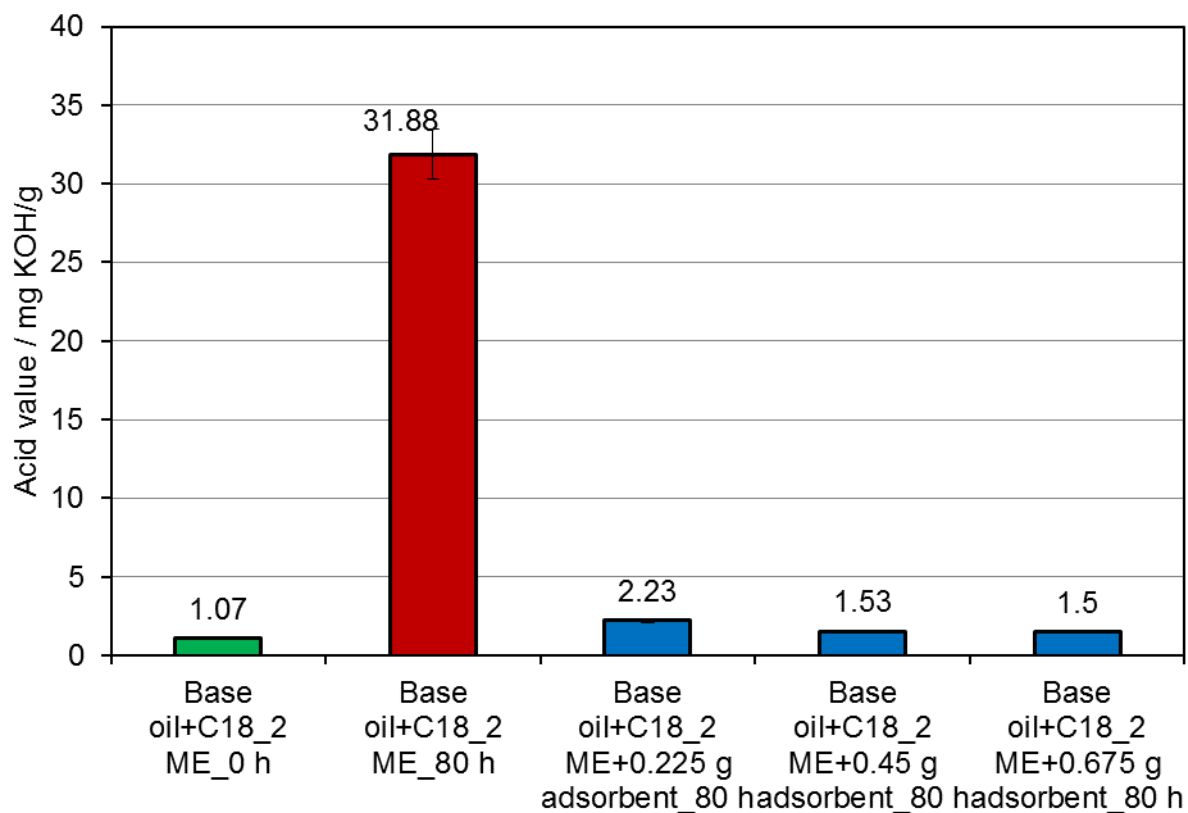


Figure 28: Evaluation of acid values of 98.4 % base oil blended with 1.6 % C18_2 ME treated with and without combined 0.675 g adsorbents of magnesium-aluminum hydroxide and 1,3,5-trimethyl-2,4,6-tris(3,5-di-tert-butyl-4-hydroxybenzyl) benzene in a ratio of 1:2 respectively and aged at 170 °C with airflow of 10 L/h for 8 h per day for a total of 80 h with Rancimat compared with the neat blend

Summary

This experiment has been carried out to investigate the level of degradation of 98.4 % base oil blended with 1.6 % C18_2 ME due to the presence or absence of combined magnesium-aluminum hydrotalcite and 1,3,5-trimethyl-2,4,6-tris(3,5-di-tert-butyl-4-hydroxybenzyl) benzene in a ratio of 1:2 respectively. The differences in peak area increase between the neat blend, the blend treated with 0.225 g, 0.45 g, and 0.675 g of adsorbents and the blend not treated with adsorbents and oxidized at 170 °C with an airflow of 10 L/h at approximately 8 h per day for a total of 80 h using a Rancimat and analyzed with SEC, GCMS, FTIR, and the acid value is compared. The rapid decrease in the content of C18_2 ME with the attendant increase in acid value, viscosity, density, higher molecular mass substances due to oxidation and polymerization confirms the impact of unsaturation level of fatty acids in the oxidative instability of biodiesel. The neat blend oxidized increased in molar masses by a factor of about 30 compared with the samples treated with the adsorbents and aged. The blend treated with the adsorbents and oxidized hardly showed any increased molar masses with the SEC analysis. However, a typical C18_2 ME component which appears around 420 g/mol in the neat blend, is about 90 % degraded in the sample treated with the adsorbents though it is absent in the neat blend aged without any adsorbent treatment.

The suppression action of 1, 3, 5-trimethyl-2, 4, 6-tris (3, 5-di-tert-butyl-4-hydroxybenzyl) benzene is due to the interaction between the radicals and its surface, mainly as a result of hydrogen bonding. The hydrogen bonds are established between the ester carbonyl and the trapping agent's hydroxyl groups (Tischinger-Wagner et al., 1987). During the initiation stage of hydrocarbon oxidation, a free radical attack abstracts an allyl hydrogen atom. It then generates an allylic radical (see section 3.4). The degradation of hydroperoxides in oil generally produces the free radical initiator. The free radical propagation is interrupted with the interaction of a hydrogen atom from the surface of the hydroxyl group of the adsorbent with the immediate peroxy radicals leading to retardation of the oxidation process.

With the GCMS analysis, a significant elution of C18_2 ME component peaks in the neat blend is observed at approximately 36.12 min. This same peak is completely degraded in

the mixture aged without any adsorbent treatment. About 40 % content of C18_2 ME is still present in the sample treated with the adsorbent at the end of the 80 h aging duration.

The differences were calculated between the unoxidized base oil blended with C18_2 ME and the oxidized neat base oil mixed with C18_2 ME in the peak area increase for carbonyl compounds (C=O) using the FTIR are 0.12 and 7.89 Abs cm⁻¹/mm, respectively. However, compared with the base oil mixed with C18_2 ME and treated with the adsorbents, the peak area increase is averagely 0.2 Abs cm⁻¹/mm. The neat oxidized blend increased in peak area by 66 times while the blend treated with the adsorbents and aged has a factor of 2 in terms of peak area increase.

The acidity of the blend aged without any treatment with adsorbents shows an increase of about a factor of 30. On the other hand, the blend treated with the adsorbent before aging only showed an increase in its acid value by approximately a factor of 2, signifying a more significant suppression of degradation of the blend during the aging process. The low acid values for the samples treated with the adsorbents and aged correlate well with the SEC analysis results shown in Figure 27, where no or very negligible amount of oxidation products are recorded. Indeed, the higher the oxidation level, the higher the oxidation products formed and the higher the acid values.

It is, therefore, evidenced that the presence of the adsorbents has caused much significant difference in oxidation between the neat, plain, and adsorbent treated oxidized samples. The above results show that the adsorbents have markedly reduced the intensity of oxidation due to liable hydrogen groups in its structural matrix, which entraps the oxidation process's precursors. The hydrotalcite compound with its ion exchange potential adsorbs acidic products, enabling the recorded low acid values.

8.2 Investigating the effect of temperature on the combined adsorbents of magnesium-aluminum hydrotalcite and 1,3,5-trimethyl-2,4,6-tris(3,5-di-tert-butyl-4-hydroxybenzyl) benzene in a ratio of 1:2 respectively in suppressing oxidation in a blend of 80 % base oil and 20 % rapeseed oil methyl ester

The main goal of this experiment is to evaluate the impact of temperature on the adsorbent's effect on suppression of formation of oligomers using size exclusion chromatography, acid value, and viscosity, density, and FTIR spectra, among others. These are the commonly used parameters for monitoring the condition of oils or lubricants in many applications.

8.2.1 Size Exclusion Chromatography (SEC)

SEC is employed to gain information on the formation of higher molecular mass species of the blends of 30 mL of 80 % base oil and 20 % rapeseed oil methyl ester on aging using the Rancimat with airflow of 10 L/h for 80 h at the different temperatures. Using polyethylene glycol standards as explained in section 4.1.1, it is possible to classify monomers' chromatographic signals, oxidized monomers, dimers, trimers, and oligomers. However, there is no exact correlation due to differing hydrodynamic volumes of polyethylene glycol standard and biodiesel. Hence, the relative molar mass is reported here (see the x-axis of Figure 29 and Figure 30). Therefore, the SEC analysis detects the changes in molecular mass of the species formed during the aging procedure. In Figure 29, neat 80 % base oil blended with 20 % RME and treated with and without 0.675 g combined adsorbents of magnesium-aluminum hydrotalcite and 1,3,5-trimethyl-2,4,6-tris(3,5-di-tert-butyl-4-hydroxybenzyl)benzene in a ratio of 1:2 respectively, aged at temperatures of 70 °C, 110 °C, 140 °C and 170 °C for 80 h duration using a Rancimat is shown. This experiment demonstrates the effect of temperature on the adsorbent impact in suppressing biodiesel degradation. In this Figure 29, the neat blend aged developed more considerable molecular mass substances with relative molar masses between 942 and 1200 g/mol at the end of the aging period compared with the neat unaged blend with about 800 g/mol. The blends treated with the radical scavenger adsorbents hardly developed any significant amount of higher molecular substances. It must be pointed out that the amount of the highest molecular mass substances formed during the aging at the

different temperatures in the blends treated with the adsorbents is essentially the same. For clarity, the region of higher built molecular mass substances is zoomed-in Figure 30, illustrating the level of the oligomers built up. Figure 31 is an illustration of the quantitative increase in the level of degradation with increasing temperature and the extent to which the 0.675 g combined adsorbents of magnesium-aluminum hydrotalcite and 1,3,5-trimethyl-2,4,6-tris(3,5-di-tert-butyl-4-hydroxybenzyl) benzene in a ratio of 1:2 respectively applied has reduced the degree of oxidation evaluated in terms of peak area changes.

The peak area values calculated for the neat oxidized blends are found to be 28, 50, 196, 317 g/mol at temperatures 70 °C, 110 °C, 140 °C, and 170 °C, respectively. It means that the level of degradation increased by 4 %, 9 %, 35 %, and 52 % according to aging temperature, respectively, Figure 31. The observed oxidation trend can be explained because oil oxidation begins slowly during the induction period until the adsorption of oxygen is at its maximum, then increases autocatalytically. At higher temperatures, the induction period is reduced (Amat et al., 2013). So, one could say that with temperatures of 70 °C and 110 °C, the aging taking place is still within the sample mixture's induction period. Beyond 140 °C and finally 170 °C, the induction period had reduced, causing the rapid increase in the rate of oxidation of the sample mixture resulting in high amounts of oxidation products formation.

The calculated increase in peak area values for the oxidized blends treated with the adsorbent at the same temperatures are compared with the above values. The results signify the adsorbents' effect in suppressing the oxidation process by influencing the blends' level of degradation. The calculated increase in peak area values for the oxidized blends treated with the adsorbents are found to be 28, 28, 30, 38 g/mol at the respective increasing temperatures, Figure 31. The aging was carried out at temperatures 140 °C and 170 °C which showed an increase in peak area value of about 5 % and 7 %, respectively. The results indicate the practical impact of combined adsorbents in suppressing the base oil's thermal-oxidative degradation blended with RME. These results agree with Amat et al. (2013). Even the 7 % increase in oxidation is still within the induction period of the sample mixture. It can, therefore, guarantee a more prolonged use period of the oil mixture upon the application of the adsorbents.

Also, C18₂ ME, a principal component of RME, polymerizes at high temperatures, according to Kim et al. (2018). The adsorbents' use hindered the oxidation's propagation, thereby inhibiting its thermooxidative degradation, and this confirms the results reported in section 8.1. This result comes about because the radical trapping agent is a compound that entraps free radicals due to liable hydrogens' presence on its structure. The higher amounts of ester components remaining in the mixture under these conditions (see Figure 29 at a relative molar mass of about 400 g/mol) is significant evidence that the adsorbent effectively suppresses the ester's deterioration components. When matched with FTIR, viscosity and acid value measurements thus support the adsorbents' attributes in suppressing biodiesel degradation during the aging process.

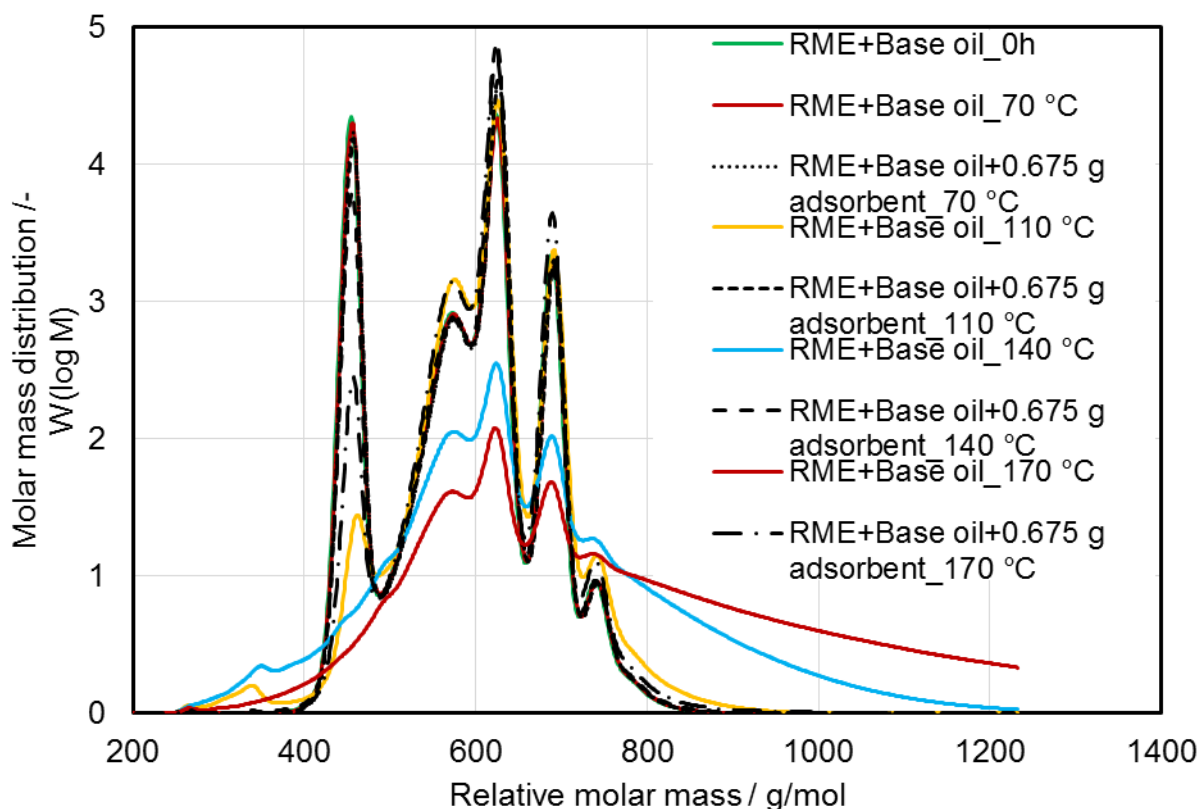


Figure 29: Evaluation of SEC of 30 mL 80 % base oil blended with 20 % RME and treated with and without combined 0.675 g adsorbents of magnesium-aluminum hydrotalcite and 1,3,5-trimethyl-2,4,6-tris(3,5-di-tert-butyl-4-hydroxybenzyl) benzene in a ratio of 1:2 respectively and aged at temperatures of 70 °C, 110 °C, 140 °C and 170 °C with airflow of 10 L/h for 8 h per day for a total of 80 h with Rancimat and compared with the neat unaged blend

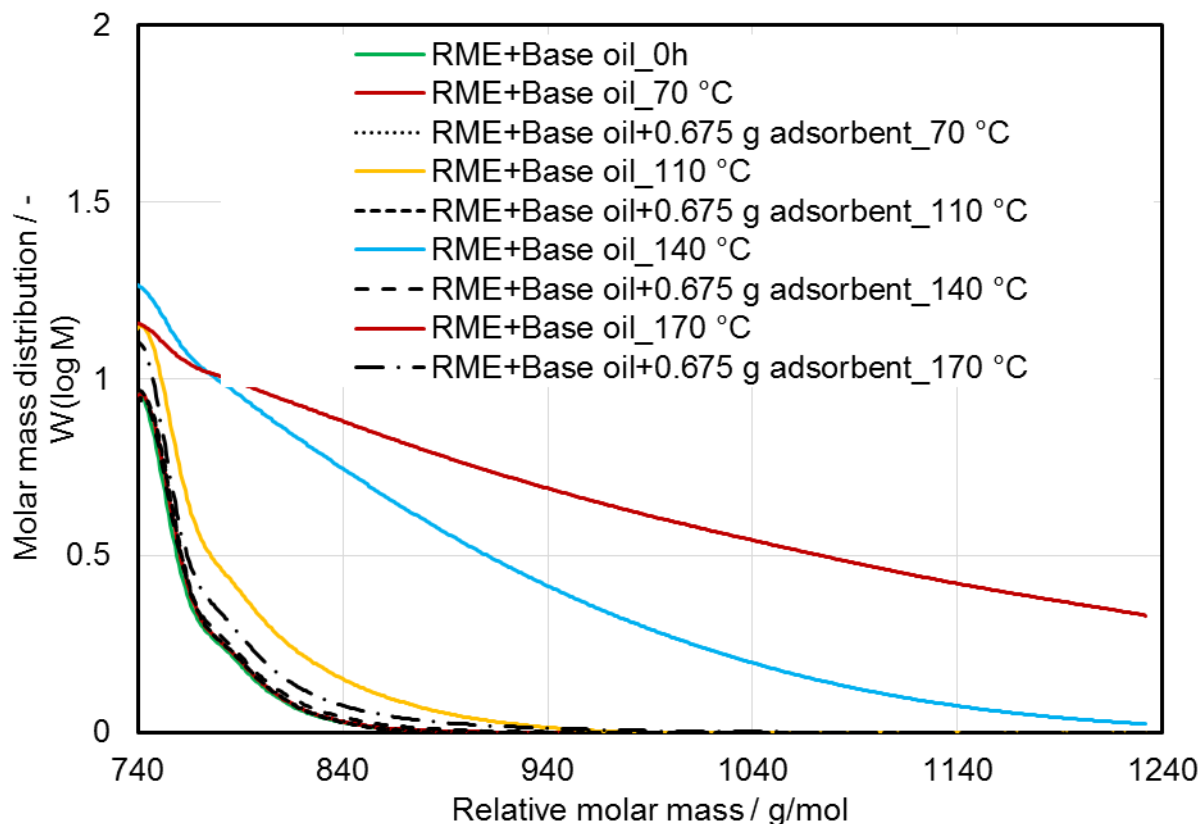


Figure 30: Zoom in on the area of higher molar mass substances of SEC of 30 mL 80 % base oil blended with 20 % RME and treated with and without combined 0.675 g adsorbents of magnesium-aluminum hydrotalcite and 1,3,5-trimethyl-2,4,6-tris(3,5-di-tert-butyl-4-hydroxybenzyl) benzene in a ratio of 1:2 respectively and aged at temperatures of 70 °C, 110 °C, 140 °C and 170 °C with airflow of 10 L/h for 8 h per day for a total of 80 h with Rancimat and compared with the neat unaged blend

The relative oxidation rate of the mixture without adsorbents treatment increased with an increase in temperature from 70 °C to 170 °C in factors of 1: 2:8:12, respectively. However, with the adsorbents' application, the oxidation rate is essentially stable at factors of about 1:1:1:2, respectively. This trend can be seen in Figure 31. It depicts that the adsorbents' effectiveness decreases with increased temperature, though on a tiny scale.

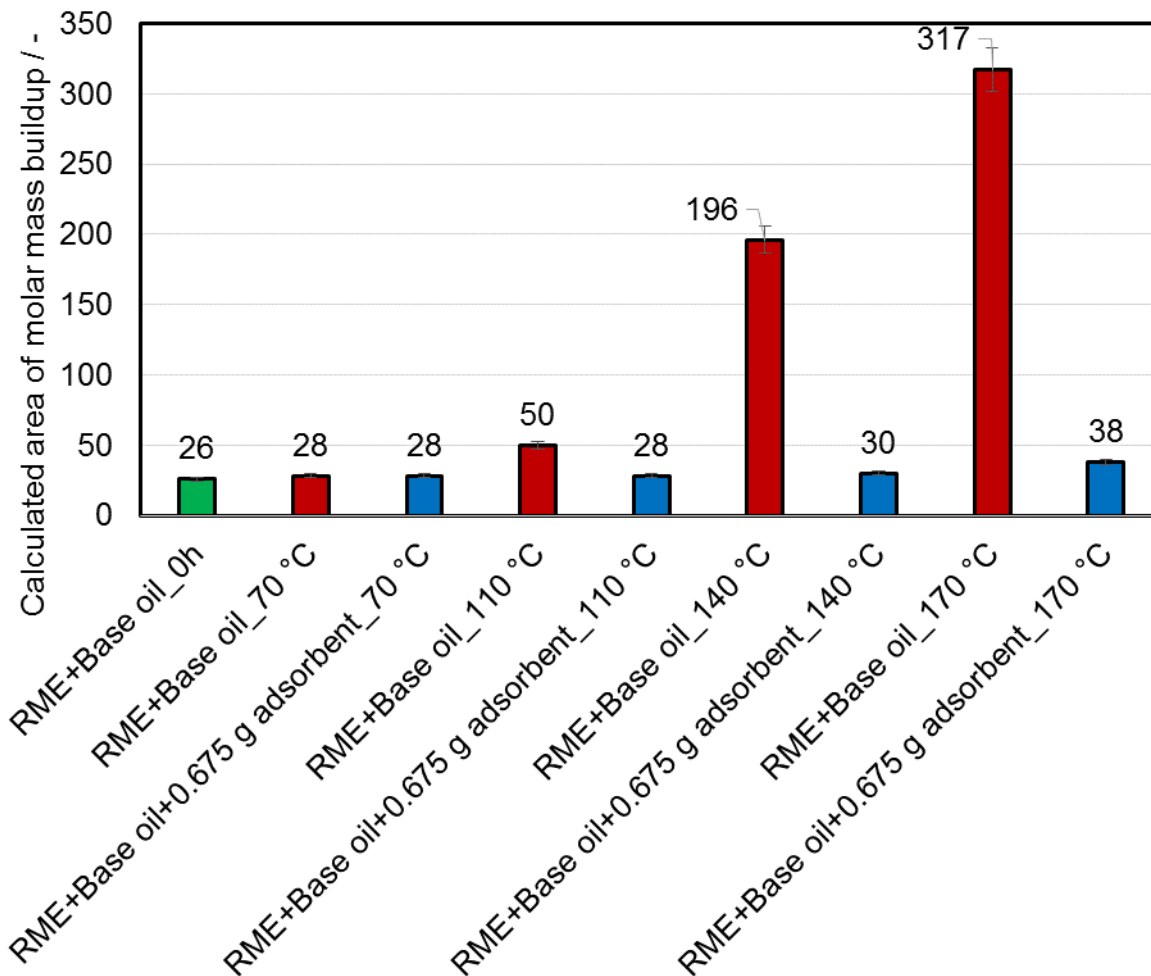


Figure 31 Calculated area of higher molecular mass substances buildup of SEC of 30 mL 80 % base oil blended with 20 % RME and treated with and without combined 0.675 g adsorbents of magnesium-aluminum hydrotalcite and 1,3,5-trimethyl-2,4,6-tris(3,5-di-tert-butyl-4-hydroxybenzyl) benzene in a ratio of 1:2 respectively and aged at temperatures of 70 °C, 110 °C, 140 °C and 170 °C with airflow of 10 L/h for 8 h per day for a total of 80 h with Rancimat and compared with the neat unaged blend

8.2.2 The acid value of 80 % base oil blended with 20 % RME and treated with and without combined adsorbents of magnesium-aluminum hydrotalcite and 1,3,5-trimethyl-2,4,6-tris(3,5-di-tert-butyl-4-hydroxybenzyl) benzene in a ratio of 1:2 respectively and aged at temperatures of 70 °C, 110 °C, 140 °C and 170 °C with airflow of 10 L/h for 8 h per day for a total of 80 h with Rancimat and compared with the neat unaged blend

The changes in acid values as oxidation progresses at different temperatures are shown in Figure 32. The acid value of the neat unaged blend is 0.1 mg KOH/g. While the neat blend aged at 70 °C had 5.59 mg KOH/g acid value, it increased to 19.31 mg KOH/g at 110 °C and further to 33.12 mg KOH/g at 140 °C and finally to 40.1 mg KOH/g at 170 °C. The blends treated with an adsorbent, on the other hand, and aged had acid values of 0.16, 0.17, 0.57, and 1.29 mg KOH/g, respectively. It is a clear indication that there are no significant changes in acid values upon aging of the blends treated with the adsorbents. According to the temperature applied, the adsorbents suppressed the buildup in acid values in a range of 97 % and 90 %. However, the acid values increased with aging time for the neat blends aged, as shown in Figure 32. Since ester is proved in literature to degrade quickly (Cen et al., 2018) and the results of the aging of C18_2ME in section 8.1 support, the use of the adsorbents must have interfered in its degradation process resulting in a low level of degradation products and hence low acid values recorded. This result collaborates with the SEC results reported in section 8.2.1, where low amounts of high molecular mass species are formed.

The rate of change in acid value is more rapid for the mixtures aged without the adsorbent treatment at the low temperatures till about 140 °C, where it slowed down. The acid values increase can be explained by the fatty acid methyl esters (see section 3.4). During the oxidation of FAME, free radicals are formed through the abstraction of hydrogen from the methylene groups in the unsaturated FAME's allylic positions. This radical reaction process leading to a build-up of acidic products is well captured in section 3.4. The alkoxy radical product split homolytically, resulting in short-chain fatty acids (Brühl, 2014). From section 3.5.2, short-chain fatty acids are formed during oxidative degradation of fatty acid methyl esters (Brühl, 2014; Dugmore, 2011; Bannister et al., 2010). It explains the high level of acidity with increasing aging or degradation of the fatty acid methyl esters.

Therefore, the rapid increase in acid value indicates that hydroperoxide formation is accelerated during the neat blends' accelerated oxidation. The degradation process slows down when most of the oxygen adsorbing surfaces are filled up. The higher the degree of degradation, the higher the acidity (see section 3.2). The use of adsorbents interrupted the oxidation process and subdued the complex secondary oxidation reactions, which should have led to more reactive products (see section 4.1.3). Hence, the low acid values were recorded.

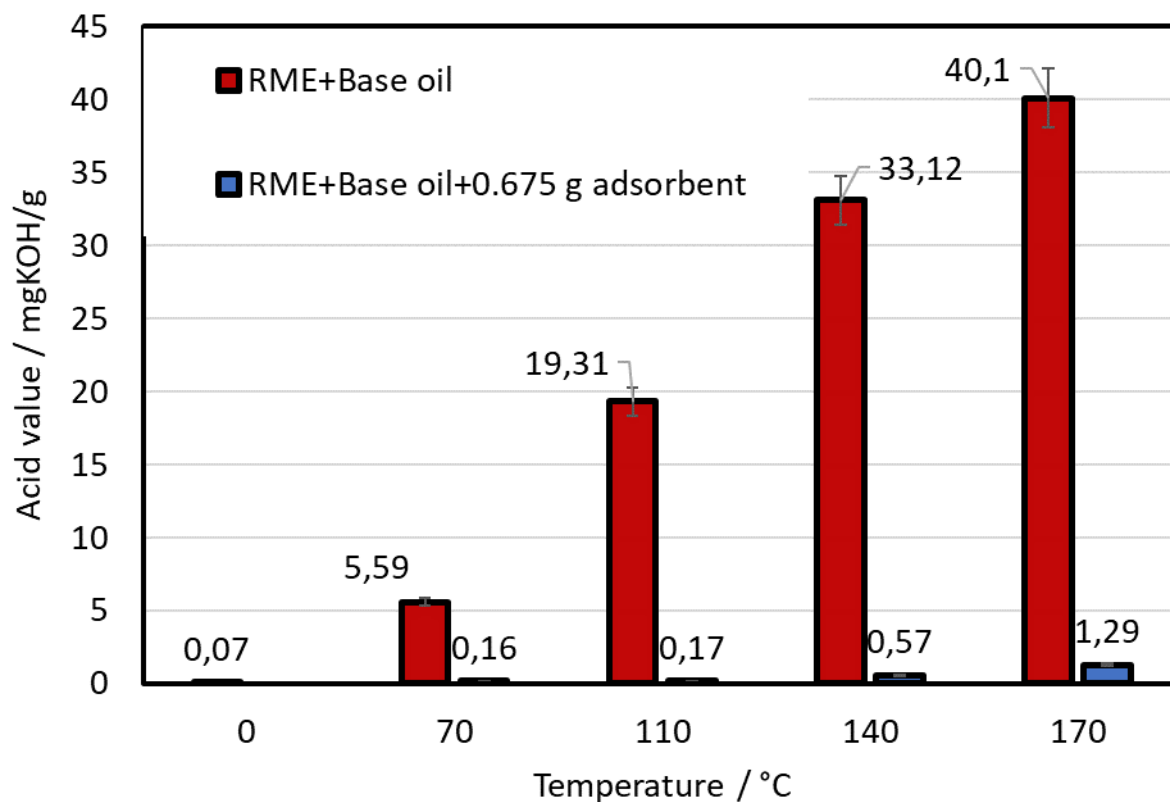


Figure 32: Evaluation of acid values of 30 mL 80 % base oil blended with 20 % RME and treated with and without combined 0.675 g adsorbents of magnesium-aluminum hydrotalcite and 1,3,5-trimethyl-2,4,6-tris(3,5-di-tert-butyl-4-hydroxybenzyl) benzene in a ratio of 1:2 respectively and aged at temperatures of 70 °C, 110 °C, 140 °C and 170 °C with airflow of 10 L/h for 8 h per day for a total of 80 h with Rancimat and compared with the neat unaged blend

8.2.3 Effect of adsorbents on the viscosity of 80 % base oil blended with 20 % RME and treated with and without combined adsorbents of magnesium-aluminum hydrotalcite and 1,3,5-trimethyl-2,4,6-tris(3,5-di-tert-butyl-4-hydroxybenzyl) benzene in a ratio of 1:2 respectively and aged at temperatures of 70 °C, 110 °C, 140 °C and 170 °C with airflow of 10 L/h for 8 h per day for a total of 80 h with Rancimat and compared with the neat unaged blend

Figure 33 and Figure 34 illustrates the changes in viscosity as a result of the degradation of the blends treated with and without the combined adsorbents of magnesium-aluminum hydrotalcite and 1,3,5-trimethyl-2,4,6-tris(3,5-di-tert-butyl-4-hydroxybenzyl) benzene in a ratio of 1:2 respectively and aged at temperatures of 70 °C, 110 °C, 140 °C and 170 °C using a Rancimat with an airflow of 10 L/h for 80 h. There is an exponential increase in the viscosity measured at temperatures 40 °C and 100 °C for the mixtures aged without using the adsorbents as degradation proceeds. It suggests the formation of high molecular weight, condensed oxygenated compounds, which are essentially sludge precursors. On the other hand, the blends treated with the adsorbents have insignificant or minimal viscosity changes. High viscosity recorded by blends aged without adsorbents is due to oxidation resulting in more insoluble materials. It results from the greater tendency of biodiesel to form polymeric deposits, which increases the viscosity. Since hydroperoxides' formation is a prerequisite for oligomers production, the above result implies a more remarkable ability of the adsorbents to suppress hydroperoxide formation. The use of the adsorbents retarded the formation of higher molecular weight substances leading to low viscosities registered. The suppression action of the adsorbents is well covered in section 6. The kinematic viscosity values also showed a trend similar to the acid values and density during the accelerated oxidation test. It means there is a close relationship between the increase in viscosity and density and acid values changes during oxidation. The viscosity of biodiesel increases with increasing thermal degradation due to the trans-isomers formation on double bonds (Ayhan, 2007). Oxidation of the neat blends led to the production of oxygenates, acids, alcohols, aldehydes, and peroxides, causing the accumulation of deposits and gum and increased viscosity, density, and molecular

masses (Dunn, 2005). Figure 31 and Figure 32 show that increasing the temperature of aging from 70 °C through to 170 °C sees accelerated oxidation resulting in higher viscosity. There is similar result in literature (Pereira et al., 2015). Typical engine oil viscosity limits are set at $\pm 10\%$ for warning and $\pm 20\%$ for critical (Bong-Ha and Yun-Ho, 2008). Using a 20 % change in the engine oil's viscosity measured at 40 °C as the critical stage of the oil, the samples treated with the adsorbents and aged at 170 °C for 80 h are just 10 % above the critical point. The neat samples aged without adsorbent treatment at 170°C is about several thousand (3038 %) above the critical mark. The allylic hydroperoxides are the primary oxidation products of esters. As seen already, these hydroperoxides are unstable and, therefore, react quickly to form several secondary oxidation products, aldehydes, and acids resulting in higher molecular weight substances (Knothe, 2007; Refaat, 2009). The liable hydrogen on the surface of the adsorbents entraps the degradation products' radicals and, therefore, interrupts the oxidation process resulting in little or no biodiesel degradation. Hence low values of viscosity were recorded.

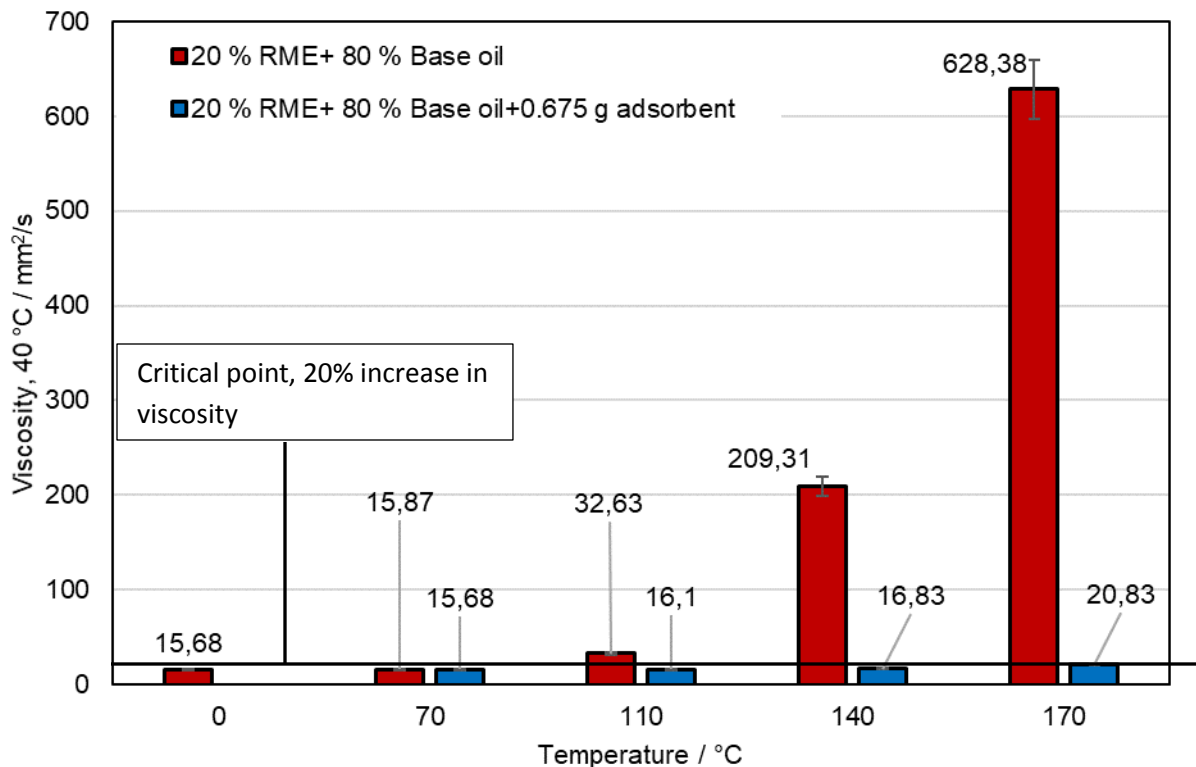


Figure 33: Evaluation of kinetic viscosity at 40°C of 30 mL 80 % base oil blended with 20 % RME and treated with and without combined 0.675 g adsorbents of magnesium-aluminum hydrotalcite and 1,3,5-trimethyl-2,4,6-tris(3,5-di-tert-butyl-4-hydroxybenzyl) benzene in a ratio of 1:2 respectively and aged at temperatures of 70 °C, 110 °C, 140 °C and 170 °C with airflow of 10 L/h for 8 h per day for a total of 80 h with Rancimat and compared with the neat unaged blend

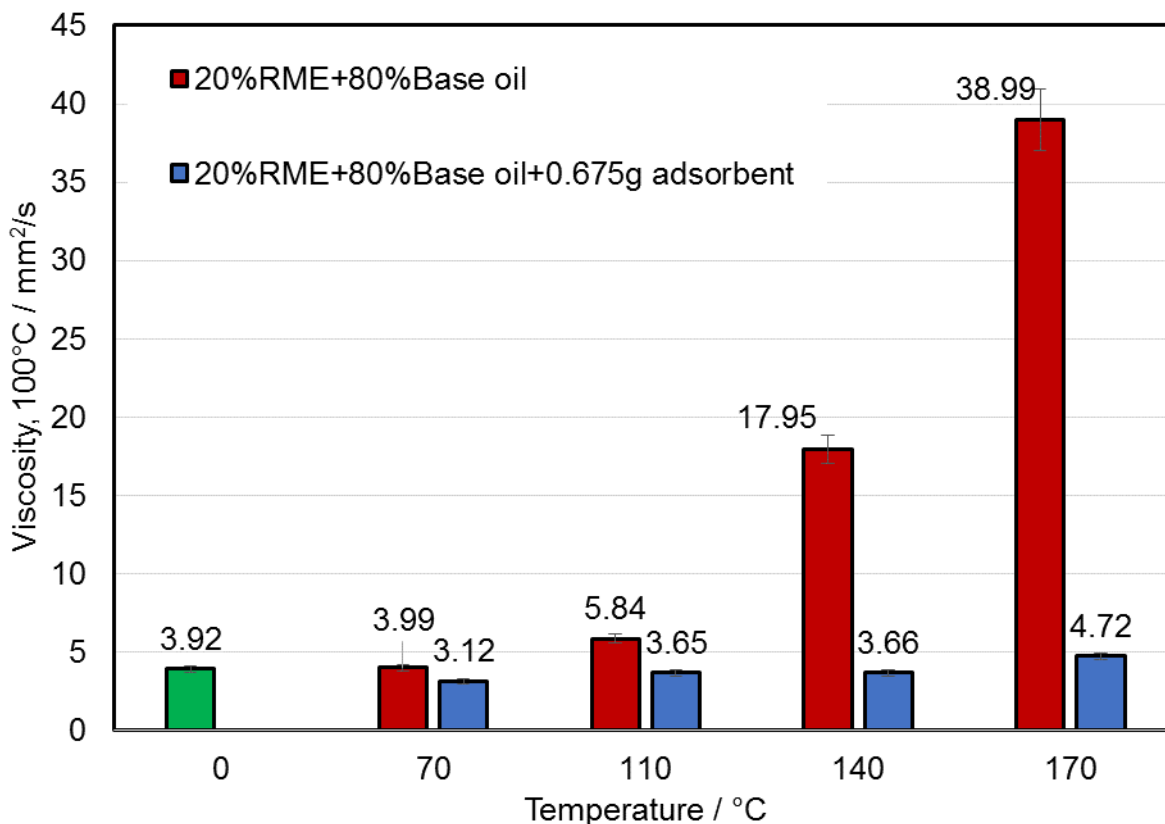


Figure 34: Evaluation of kinetic viscosity at 100 °C of 30 mL 80 % base oil blended with 20 % RME and treated with and without combined 0.675 g adsorbents of magnesium-aluminum hydrotalcite and 1,3,5-trimethyl-2,4,6-tris(3,5-di-tert-butyl-4-hydroxybenzyl) benzene in a ratio of 1:2 respectively and aged at temperatures of 70 °C, 110 °C, 140 °C and 170 °C with airflow of 10 L/h for 8 h per day for a total of 80 h with Rancimat and compared with the neat unaged blend

8.2.4 Impact of combined adsorbents of magnesium-aluminum hydrotalcite and 1,3,5-trimethyl-2,4,6-tris(3,5-di-tert-butyl-4-hydroxybenzyl) benzene in a ratio of 1:2 respectively on the density of 80 % base oil blended with 20 % RME and treated with and without the adsorbents and aged at temperatures of 70 °C, 110 °C, 140 °C and 170 °C with airflow of 10 L/h for 8 h per day for a total of 80 h with Rancimat and compared with the neat unaged blend

The measurement of the changes in density at 40 °C and 100 °C of the blends treated with and without the adsorbents and aged for 80 h at different temperatures are illustrated in

Figure 35 and Figure 36, respectively. The density values for the neat aged blends increase with increasing aging temperature. The increase in the density is exponentially at temperatures 40 °C and 100 °C for the blends aged without using the adsorbents. However, after the aging at 110 °C, the increase rate seems more intense than at the lower temperatures. For the blends treated with the adsorbents and aged, the density values remained similar to that of the unaged sample. According to Schumacher (2013), unsaturated FAME brings about biodiesel polymerization, leading to compounds with higher molecular weights, increasing the density of the aged blends (Schumacher, 2013). Therefore, the presence of the adsorbents has retarded the polymerization process and hence low-density values. During the degradation of biodiesel from literature (Saltas et al., 2017; Jain and Sharma, 2011; Chacon et al., 2000), the decomposition of hydroperoxides leads to secondary acidic formation oxidation products leads to an increase of density. The trend of increased density agrees with the trends with viscosity, acid value, and especially the SEC results in section 8.2.1, indicating the low to no formation of high molecular mass substances upon aging for 80 h duration.

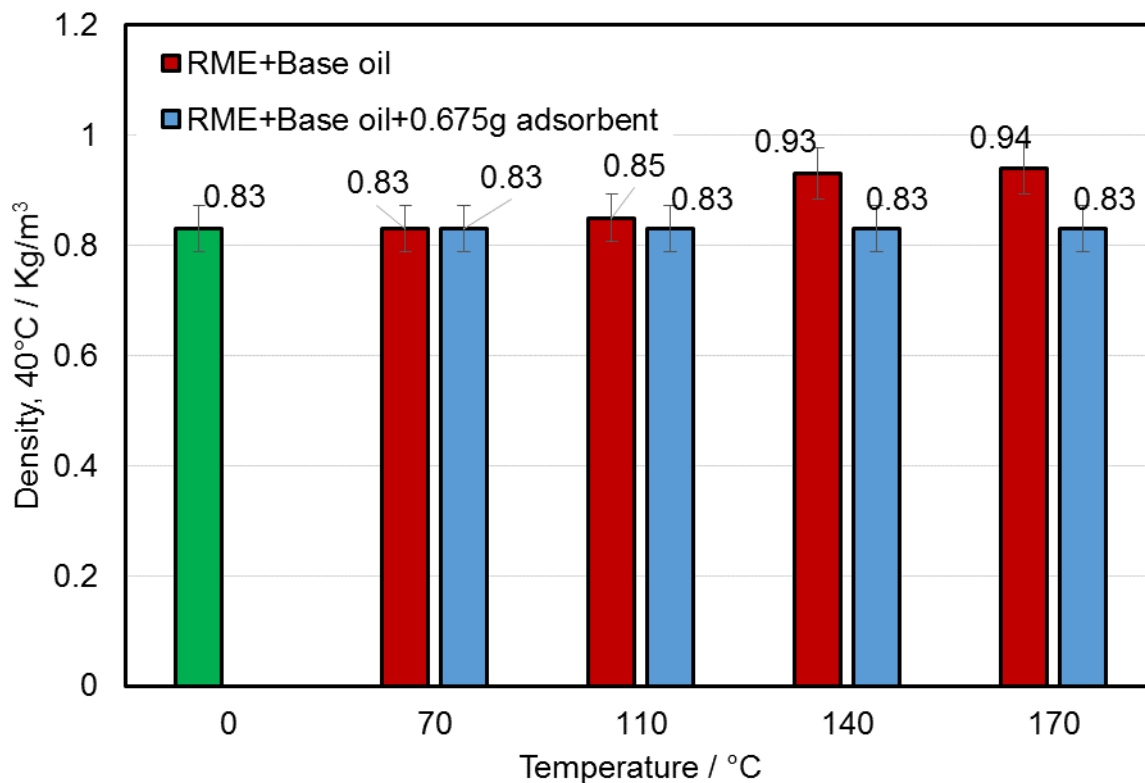


Figure 35: Evaluation of density at 40 °C of 30 mL 80 % base oil blended with 20 % RME and treated with and without combined 0.675 g adsorbents of magnesium-aluminum hydrotalcite and 1,3,5-trimethyl-2,4,6-tris(3,5-di-tert-butyl-4-hydroxybenzyl) benzene in a ratio of 1:2 respectively and aged at temperatures of 70 °C, 110 °C, 140 °C and 170 °C with airflow of 10 L/h for 8 h per day for a total of 80 h with Rancimat and compared with the neat unaged blend

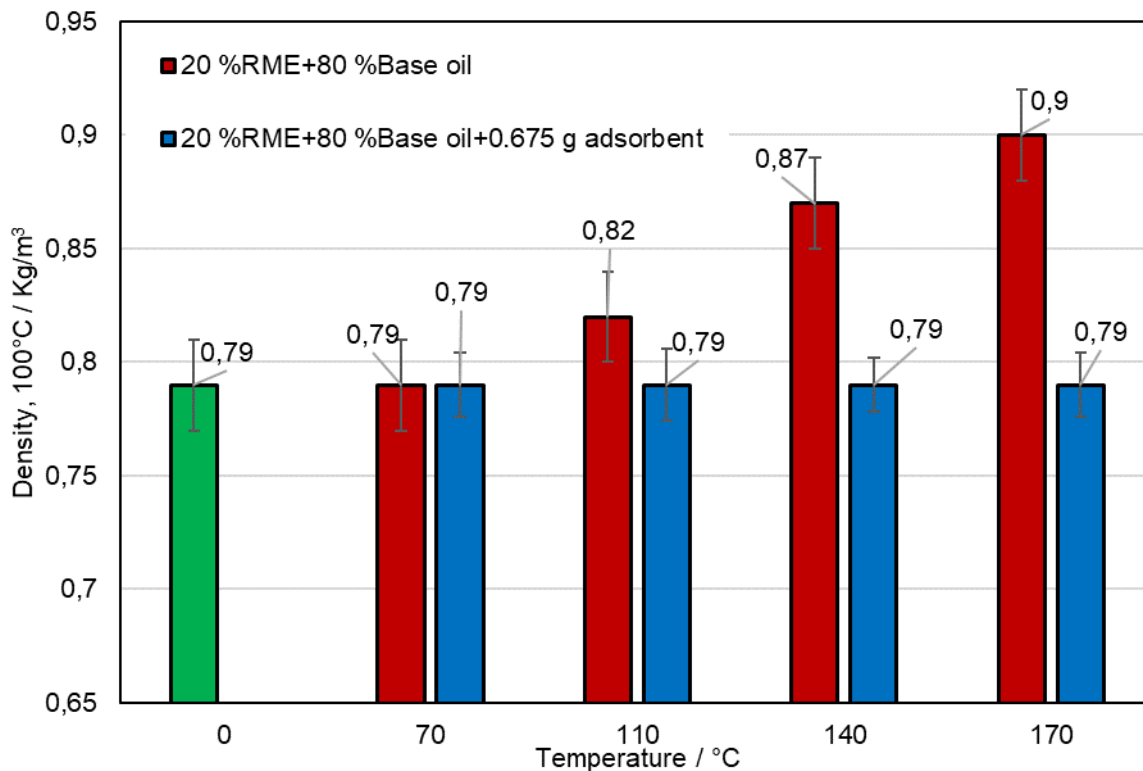


Figure 36: Evaluation of density at 100°C of 30 mL 80 % base oil blended with 20 % RME and treated with and without combined 0.675 g adsorbents of magnesium-aluminum hydrotalcite and 1,3,5-trimethyl-2,4,6-tris(3,5-di-tert-butyl-4-hydroxybenzyl) benzene in a ratio of 1:2 respectively and aged at temperatures of 70 °C, 110 °C, 140 °C and 170 °C with airflow of 10 L/h for 8 h per day for a total of 80 h with Rancimat and compared with the neat unaged blend

8.2.5 FTIR evaluation of neat and aged 80 % base oil blended with 20 % RME and treated with and without combined adsorbents of magnesium-aluminum hydrotalcite and 1,3,5-trimethyl-2,4,6-tris(3,5-di-tert-butyl-4-hydroxybenzyl) benzene in a ratio of 1:2 respectively and aged at temperatures of 70 °C, 110 °C, 140 °C and 170 °C with airflow of 10 L/h at 8 h per day for 80 h with Rancimat

FTIR spectrometry has been extensively used to track relative oxidative changes in functional groups in biodiesel and its blends. The fresh blend's spectra, the blend treated with the adsorbents, and the neat blend without any adsorbent treatment and aged at 8 h per day for a total of 80 h at varying temperatures are compared. In this way, the molecular

changes occurring due to the oxidation process can be spectrally visualized. Figure 37 shows the IR-spectra of the blend 80 %base oil and 20 %RME treated with and without the adsorbents before and after the aging process in this study. The mixture of 20 % RME and 80 % base oil treated with 0.675 g adsorbents magnesium-aluminum hydrotalcite and 1,3,5-trimethyl-2,4,6-tris(3,5-di-tert-butyl-4-hydroxybenzyl) benzene in a ratio of 1:2 respectively and aged at 70 °C, 110 °C, 140 °C and 170 °C for 80 h duration is represented on the graph for comparison with the same sample mixture aged without any treatment with the adsorbents and the neat blend. The plot illustrates the amount of absorption and the wave number at which the absorption occurred. The spectra' key portions have been integrated, and the corresponding peak area calculated is illustrated in Figure 40. In Figure 37, the complete spectra of all the aged blends, both treated and none-treated with any adsorbents, including the neat/fresh blend, can be observed; this is depicted in green color in the illustration. The blends are scanned in the range of 4000 to 600 cm^{-1} . The fingerprint region (1500-400 cm^{-1}) is challenging to assess due to interfering peaks of functional groups' varieties. As depicted in Figure 37, all the mixtures aged at different temperatures reveal very similar spectra, indicating that the degradation process is the same and comparable to those reported in the literature for FAME oxidation (Saltas et al., 2017). The region between 1600 and 1900 cm^{-1} registered an enhanced absorption, Figure 37, Figure 40. The measurement of the oxidation levels is evaluated per peak area increase.

The neat blend of 80 %base oil and 20 %RME before aging showed an ester vibration (C=O) at approximately 1750 cm^{-1} with an absorbance value of about 0.059 au. With aging proceeding, this mixture of base oil and RME without the adsorbent showed enhanced and more comprehensive carbonyl bands than a mere ester vibration with an absorbance value of about 0.064 au at aging temperature 70 °C. Beyond this temperature, it developed a double maximum with absorbance, 0.046 au and 0.035 au at aging temperature 110 °C, 0.124 au, and 0.11 au at temperature 140 °C. At temperature 170 °C, the absorbance went up to 0.123 au and 0.121 au. Broadband centered around 1750 cm^{-1} is due to the presence of carbonyl-containing degradation products, Figure 38. The broadness of the peak is due to the presence of a wide variety of oxidation products. As seen in section 4.1.5, the sample's absorption level linearly represents the absorbing

species' concentration. This means the increase in absorbance of the sample aged without any treatment with the adsorbents has undergone significant degradation resulting in more oxidative products. This increase in absorbance is, however, significantly absent in the blend treated with the adsorbent. The absorbance of the sample treated with the adsorbents and aged is 0.063 au at both 70 °C and 110 °C temperature of aging. At 140 °C, it reduced to 0.058 and finally to 0.037 au at 170 °C of aging. These low absorbance values can be mainly caused by the adsorbents' use and reveal the reduction in the extent of degradation (Amat et al., 2013). Also, a decrease of CH, CH₂, and CH₃ vibrations in the blend of aged without adsorbent treatment is detected within the range of 2800 cm⁻¹ to 3000 cm⁻¹. However, the same decrease in signals is absent in the blend treated with the same band's adsorbent. The high peak of the OH band seen in the sample aged without adsorbent treatment, Figure 39, is attributable to the organic compounds including alcohol, hydroperoxides, and carboxylic acids with the OH functional group. These signals are virtually absent in the blend treated with the adsorbents. With this absence of the OH functional group signals due to the adsorbents' application, it can be concluded that the adsorbents thus interrupt the production of hydroperoxides. Hence, the adsorbent suppression's impact is at the initiation stage of the oxidation process, as illustrated in Figure 5. It is, therefore, not surprising to see the insignificant changes in acid values of the samples after the entire aging duration (see section 8.2.2).

Considering Figure 38 and using the enhanced absorbance observed in the region between 1600 and 1900 cm⁻¹, it is evident that temperature impacted the adsorbents' suppression ability. The absorption of the mixture without any treatment with the adsorbents at the start of the aging process increased by about 13 % during the 70 °C aging. At 110 °C, there is a further increase of about 55 %, while the aging at 140 °C, it is 87 %. At 170 °C, the increase has not changed from that of the aging at 140 °C. On the other hand, the blend treated with the adsorbents at the start of the aging process increased absorption by 9 %, way below the mixture without recorded adsorbent treatment. This absorbance increased by 12 % at 110 °C and reduced to an average of about 6.5 % for the aging at temperatures 140 °C and 170 °C. Significantly, the adsorbents' use has drastically reduced the impact of oxidation on the blend, hence reducing oxidative degradation products (Cristina et al., 2011). The adsorbents' impact in

suppressing the formation of high molecular substances is not entirely independent of the temperature at which it is applied.

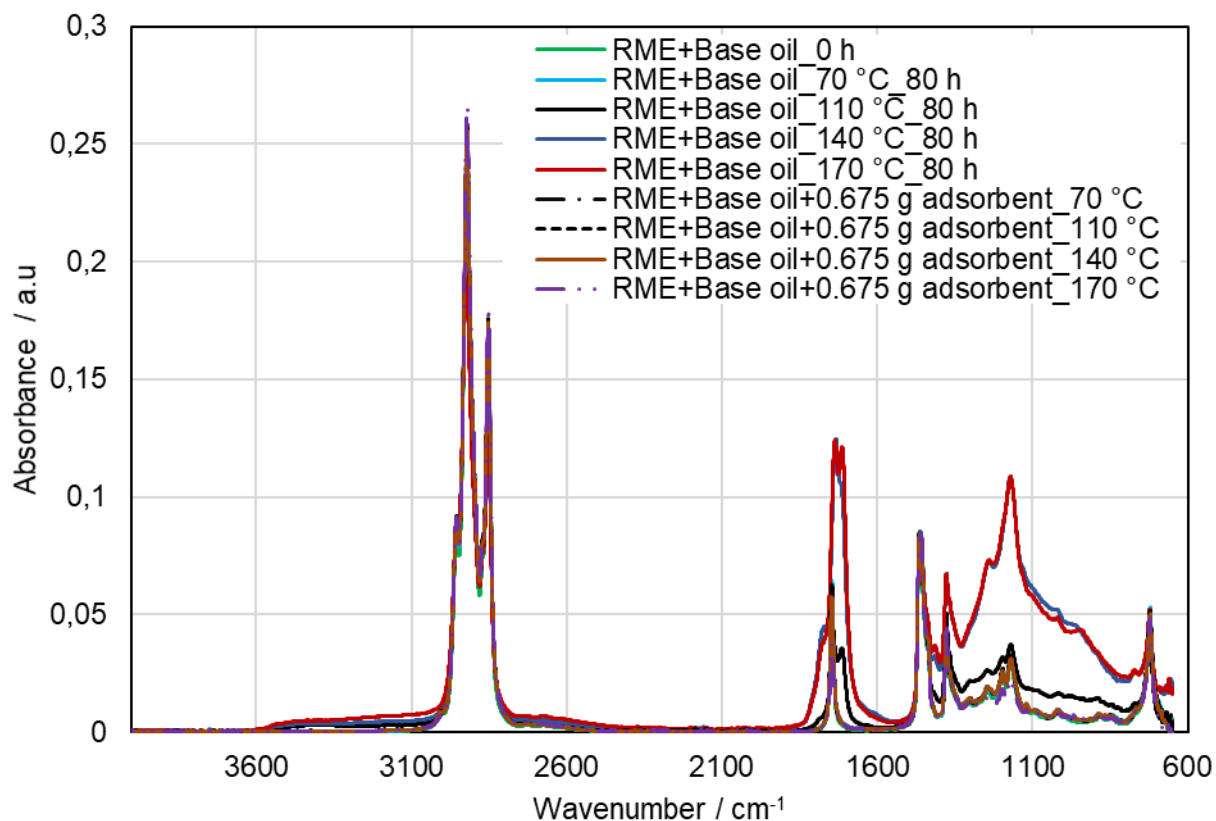


Figure 37: Evaluation of FTIR spectra in absorbance mode (range 600-4000 cm^{-1}) of 30 mL 80 % base oil blended with 20 % RME and treated with and without combined 0.675 g adsorbents of magnesium-aluminum hydrotalcite and 1,3,5-trimethyl-2,4,6-tris(3,5-di-tert-butyl-4-hydroxybenzyl) benzene in a ratio of 1:2 respectively and aged at temperatures of 70 °C, 110 °C, 140 °C and 170 °C with airflow of 10 L/h for 8 h per day for a total of 80 h with Rancimat and compared with the neat unaged blend

As stated earlier, in section 3.4, hydroperoxides formed in the initial stages of oxidation are very unstable and, therefore, form hydroxyl and alkoxy radicals which can decompose to alkyl aldehydes and alkyl radicals and produce acids as oxidation advances or undergo polymerization by reacting with other alkenes (Pereira et al., 2015; Kim et al., 2018). These secondary products, aldehydes, alcohols, and hydrocarbons (Knothe, 2007), are observed in the region 1600 and 1900 cm^{-1} , Figure 38. Around 1745 cm^{-1} in Figure 38 is the characteristic ester C=O stretch. However, in the spectra of the blend aged without using the adsorbent, this band has broadened and shifted more near 1735 cm^{-1} which,

according to Westberg (2012), is typical for deteriorated FAME. The blend aged without the adsorbents registered a significant absorbance compared to the blend treated with the adsorbents.

On the other hand, the presence of adsorbents in the blend has increased its stability by interfering in the rate of free radical production and hence insignificant or no production of hydroperoxides. It is worthy to note that the ester peak in the sample treated with the adsorbents and aged at 170 °C for 80 h is much smaller than the peak area for the unaged sample. It signifies that the adsorbents can adsorb the biodiesel at high temperatures hence the low absorption peak registered.

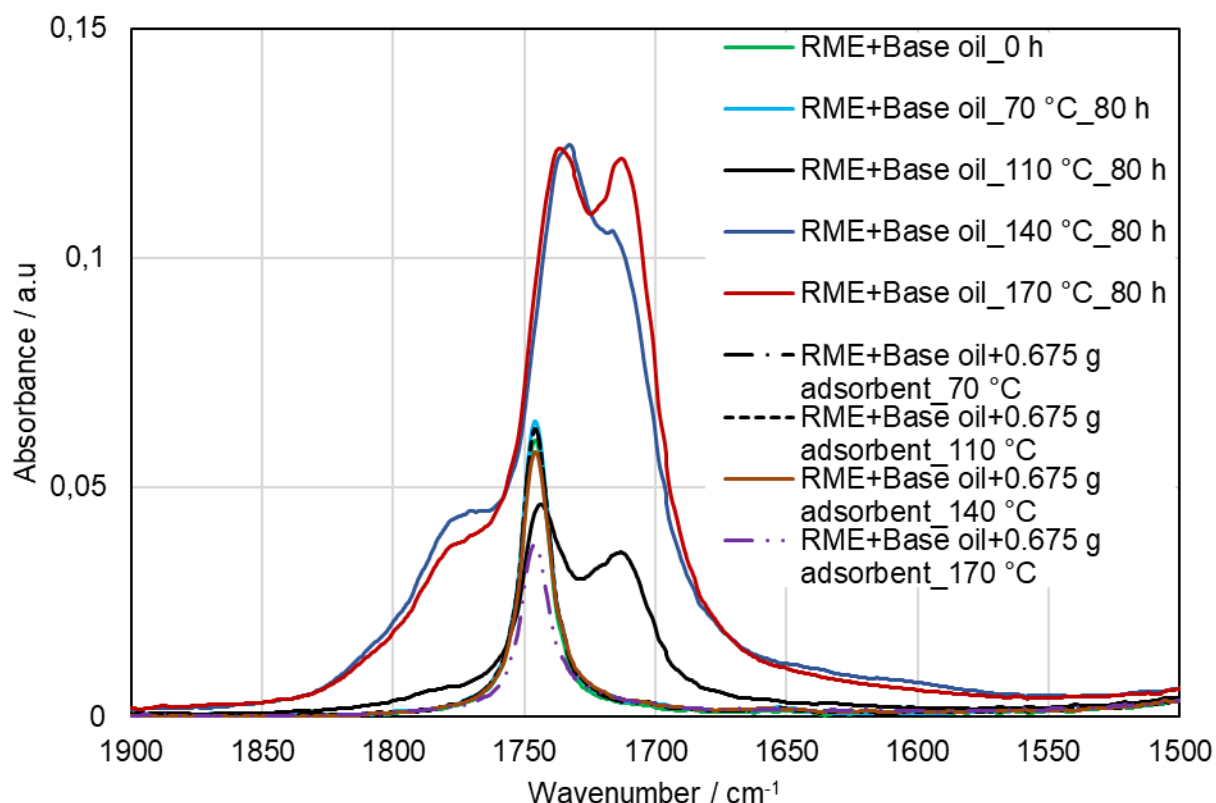


Figure 38: FTIR spectra in absorbance mode (range 1500-1900cm⁻¹) of 30 mL 80 % base oil blended with 20 % RME and treated with and without combined 0.675 g adsorbents of magnesium-aluminum hydrotalcite and 1,3,5-trimethyl-2,4,6-tris(3,5-di-tert-butyl-4-hydroxybenzyl) benzene in a ratio of 1:2 respectively and aged at temperatures of 70 °C, 110 °C, 140 °C and 170 °C with airflow of 10 L/h for 8 h per day for a total of 80 h with Rancimat and compared with the neat unaged blend

The broad absorption band around 3000 to 3600 ± 5 cm^{-1} emerging in the spectrum is assigned to the intermolecular O-H stretching band (Westberg, 2012), Figure 39. The combination of these absorption bands' shifts indicates oxidation reactions, leading to hydrogen bonds to double-bonded fatty acids as indicated in the oxidation process in section 3.4. In general, the rate of a chemical reaction approximately doubles for every 10 $^{\circ}\text{C}$ increase (Pereiraa et al., 2015). Increasing temperature accelerated the formation of oxidation products. Therefore, the elevated temperatures increased exponentially the rate of degradation of the mixture aged without the adsorbents, Figure 40. This trend is collaborated by the work of Pereiraa et al. (2015). However, there is virtually no change or subtle changes in the absorbance of the blends treated with the adsorbents. The adsorbents, irrespective of the application temperature, depressed the blend's degradation and hence the insignificant impact of oxidation. This result agrees with the acid values and viscosity of the same sample seen in 8.2.2 and 8.2.3, confirming less or no build-up of degradation products.

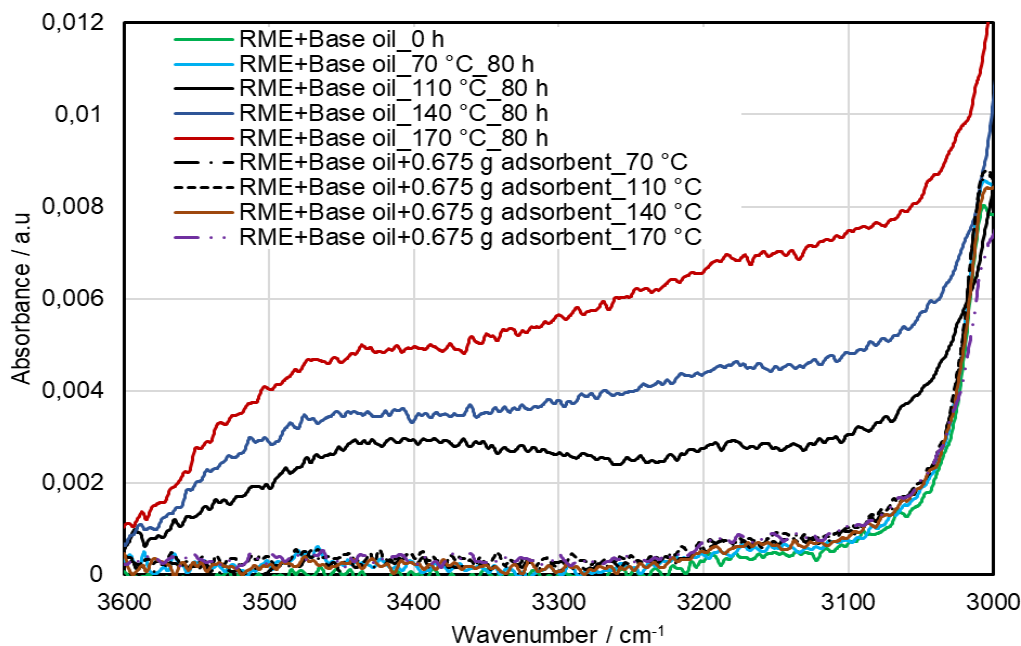


Figure 39: FTIR spectra in absorbance mode (range 3000-3600 cm^{-1}) of 30 mL 80 % base oil blended with 20 % RME and treated with and without combined 0.675 g adsorbents of magnesium-aluminum hydrotalcite and 1,3,5-trimethyl-2,4,6-tris(3,5-di-tert-butyl-4-hydroxybenzyl) benzene in a ratio of 1:2 respectively and aged at temperatures of 70 $^{\circ}\text{C}$, 110 $^{\circ}\text{C}$, 140 $^{\circ}\text{C}$ and 170 $^{\circ}\text{C}$ with airflow of 10 L/h for 8 h per day for a total of 80 h with Rancimat and compared with the neat unaged blend

The oxidation impact is evaluated per peak area increase around 1745 cm^{-1} characteristic of ester, C=O stretch. Figure 40 present the results of oxidation quantification using peak area increase. At the same time, the neat blend not treated with adsorbents represent maximum oil degradation with increasing area values of $1.4\text{ Abs}\cdot\text{cm}^{-1}/\text{mm}$, $2.73\text{ Abs}\cdot\text{cm}^{-1}/\text{mm}$, $9.28\text{ Abs}\cdot\text{cm}^{-1}/\text{mm}$ and $9.56\text{ Abs}\cdot\text{cm}^{-1}/\text{mm}$ concerning the temperature of aging. The samples treated with adsorbents and aged, on the other hand, maintained an average increase in the area of about $1.3\text{ Abs}\cdot\text{cm}^{-1}/\text{mm}$. There is, therefore, a good correlation between an increase in peak area and the acid value of oxidized oils. Here, it is seen that the acidity is directly related to the carbonyl compounds formed during the oxidation of the oil. The higher the level of oxidation or degradation of the blend, the higher the carbonyl products' production and the higher the acidity and the viscosity. However, the sudden jump in the peak area increase from $2.73\text{ Abs}\cdot\text{cm}^{-1}/\text{mm}$ to $9.28\text{ Abs}\cdot\text{cm}^{-1}/\text{mm}$ can be explained that until $2.73\text{ Abs}\cdot\text{cm}^{-1}/\text{mm}$, the aging is still within the induction period of the sample. The oxidation becomes rapid beyond the induction period but slows down between $9.28\text{ Abs}\cdot\text{cm}^{-1}/\text{mm}$ to $9.56\text{ Abs}\cdot\text{cm}^{-1}/\text{mm}$. At this stage, the hydroperoxides' breakdown rate is less than the oxidative products' formation and, hence, the low increase in the peak area. This band area measurement gives complementary information to the acid number on the blend's degradation by oxidation (Obiols, 2003).

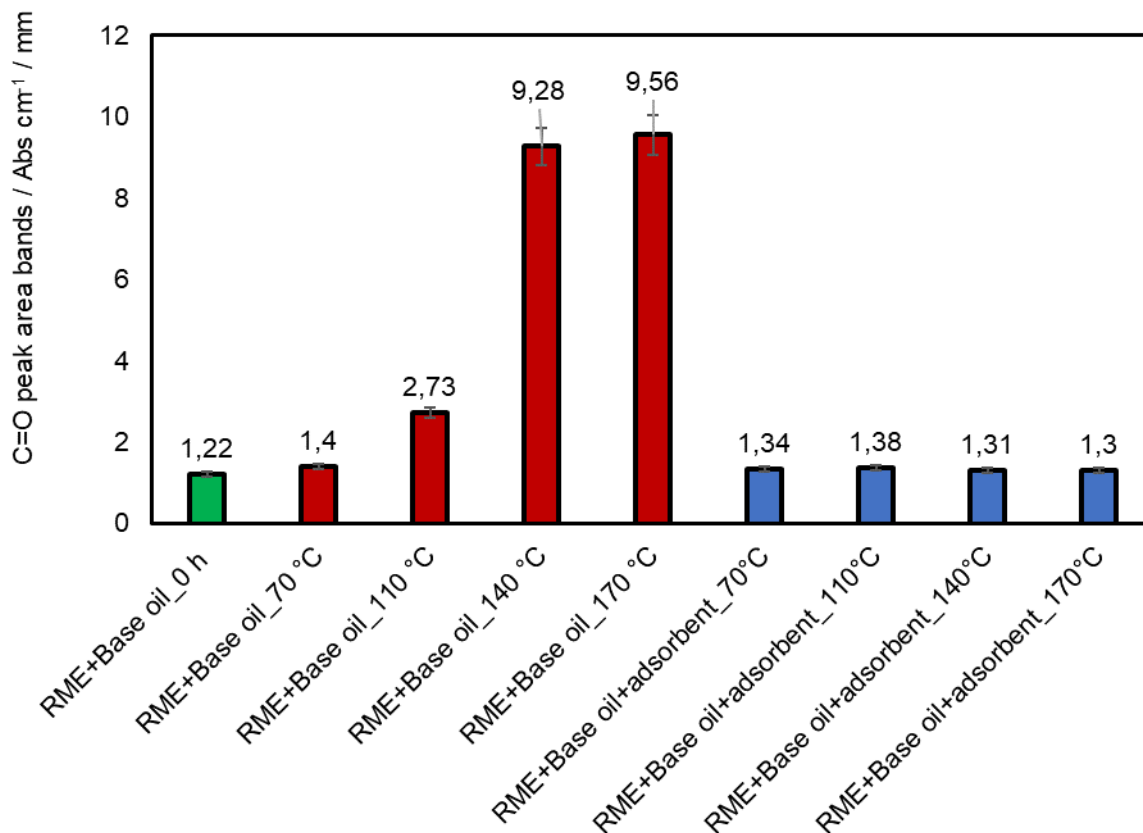


Figure 40: Evaluation of peak area under C=O bands ($1600-1900\text{ cm}^{-1}$) of the FTIR spectra of 30 mL 80 % base oil blended with 20 % RME and treated with and without combined 0.675 g adsorbents of magnesium-aluminum hydrotalcite and 1,3,5-trimethyl-2,4,6-tris(3,5-di-tert-butyl-4-hydroxybenzyl) benzene in a ratio of 1:2 respectively and aged at temperatures of 70 °C, 110 °C, 140 °C and 170 °C with airflow of 10 L/h for 8 h per day for a total of 80 h with Rancimat and compared with the neat unaged blend

Summary

In summarizing the data on the 80 % base oil blended with 20 % RME treated with and without the combined 0.675 g adsorbents of magnesium-aluminum hydrotalcite and 1,3,5-trimethyl-2,4,6-tris(3,5-di-tert-butyl-4-hydroxybenzyl) benzene in a ratio of 1:2 respectively before and after accelerated aging, it is noted that as the aging proceeds at different temperatures the compounds containing ester groups or hydrocarbons in general in the mixture not treated with the adsorbents are decomposed. In contrast, the blend treated with the adsorbents remained practically unchanged or experienced very slight decomposition. Its suppression action is from the structure of the 1, 3, 5-trimethyl-2, 4, 6-tris (3, 5-di-tert-butyl-4-hydroxybenzyl) benzene due to the interaction between the radical

and its surface, mainly as a result of hydrogen bonding. The hydrogen bonds are established between the ester carbonyl and the hydroxyl groups of the trapping agent. Recall that from the three stages involved in oxidation (Figure 5), it is during the initiation stage that free radical attacks the hydrocarbon abstracting an allyl hydrogen atom (see section 3.4). The degradation of hydroperoxides in oil generally produces the free radical initiator. This free radical propagation is interrupted by the interaction of a hydrogen atom from the surface of the hydroxyl group of the trapping agent with the immediate peroxy radicals. It explains the suppression of oxidation by the adsorbents during the first stage of the oxidation process leading to low levels of oxidation products such as alcohols, ketones, organic acids, aldehydes oligomers resulting in low values viscosity, acid number, density, and high molecular mass substances.

This experiment has illustrated the impact of temperature on the adsorbents' efficiency in suppressing biodiesel's degradation and blends. An amount of 0.675 g of the combined adsorbents of magnesium-aluminum hydrotalcite and 1,3,5-trimethyl-2,4,6-tris(3,5-di-tert-butyl-4-hydroxybenzyl) benzene in a ratio of 1:2 respectively has been applied to a volume of 30 ml of the sample and aged at the different temperatures of 70 °C, 110 °C, 140 °C, and 170 °C at 8 h per day for a total of 80 h each. Considering that an adsorbent's effectiveness in suppressing oligomers' formation depends mainly on the amount used and the temperature at which it is applied, a constant amount of 0.675 g of the adsorbents is used for all the samples. The results show that temperature has an invariably insignificant impact on the adsorbents' suppression effect effectiveness.

For the buildup of higher molecular mass substances, the sample aged without any adsorbent treatment increased by approximately a factor of 1:2:8:12 according to the increasing temperature of aging, respectively. The samples treated with the adsorbents remained virtually stable, with an insignificant amount of higher molecular mass substances formed in the ratio of 1:1:1.2:1.5 according to the aging temperature. At the highest temperature of 170 °C, the sample aged without any adsorbent treatment had about 1200 % growth in higher molecular masses. The sample treated with the adsorbent had 150 % growth in higher molecular mass substances.

From the area under the region's curve for the absorption of carbonyl contained compounds, 1600-1900 / cm^{-1} , the samples aged without any adsorbent treatment increased in the number of carbonyl products by about factors 1:2:8:8 according to the temperatures of the aging respectively. The samples treated with the adsorbents remained pretty the same with the number of carbonyl compounds produced during the aging with an average factor of 1.1 in respective of the temperature.

The viscosity measurement at 40 °C of these samples treated with the adsorbents and aged at the various temperatures does not differ from the amount of carbonyl compounds formed. The samples aged without any adsorbent treatment increased their viscosity in the factor range of about 1:2:13:40 according to the increasing aging temperatures.

The acid value of the neat sample treated with 0.675 g adsorbent, 0.07 mg KOH/g increased by approximate factors of 2.3:2.4:31:54 according to the aging at 70 °C, 110 °C, 140 °, and C170 °C, respectively. The acid values of the neat samples aged without any adsorbent treatment increased by factors of 79:276:473:573 according to the increasing temperature of aging, respectively.

In effect from this experiment, the temperature at which aging occurs does not impact the adsorbents' efficiency in suppressing the formation of higher molecular mass substances.

It is also clear from the experiments that the viscosity, density, and acid value increase linearly as the reaction temperature increases. The possible explanation for this behavior trend could be the Diels Alder reaction, which essentially is thermal degradation. This reaction leads to the formation of polymers at higher temperatures.

8.3 Investigating the effect of the amount of combined adsorbents magnesium-aluminum hydrotalcite and 1,3,5-trimethyl-2,4,6-tris(3,5-di-tert-butyl-4-hydroxybenzyl) benzene in a ratio of 1:2 respectively in suppressing oxidation in rapeseed oil methyl ester and base oil blend

8.3.1 GCMS analysis of 80 %base oil blended with 20 % RME biodiesel treated with and without combined adsorbents magnesium-aluminum hydrotalcite and 1,3,5-trimethyl-2,4,6-tris(3,5-di-tert-butyl-4-hydroxybenzyl) benzene in a ratio of 1:2 respectively and aged at 170 °C with airflow of 10 L/h at 8 h per day for a total of 80 h using the Rancimat

The GCMS analysis of base oil and RME mixture treated with and without the adsorbents and aged at 170 °C for 80 h are shown in

Figure 41. The abscissa represents the retention times in min for which the respective components are eluted from the column. The ordinates cater to the amount or the counts of the various components present in the sample. The RME component peaks are very prominent, as shown by the unaged blend of 80 %base oil and 20 %RME. These peaks get degraded as aging progresses. The degradation of these peaks relates to FTIR analysis, where a decrease in the CH, CH₂, and CH₃ vibrations has been recorded within wave numbers 2800 cm⁻¹ to 3000 cm⁻¹. The signals of the unaged RME in the blend are very prominent and conspicuous, as shown in

Figure 41. After the aging for 80 h at 170 °C, the signal for the RME in the mixture without the adsorbent treatment is virtually completely degraded, a confirmation of its oxidative instability, hence more prone to oxidation due to its higher degree of unsaturation.

The signals of the RME in the mixture treated with the adsorbent and aged are still very prominent. The neat mixture peaks at a retention time of 33.53 min had 491,921, which got drastically degraded to about 78,575 counts representing almost 84 % reduction on aging for 80 h. The mixtures treated with the different adsorbents were equally degraded by 82 %, 67 %, and 60 % according to the amount of the adsorbents, which were 0.225 g, 0.45 g, and 0.675 g. The peaks were observed at a retention time of 37.34 min. The count

of the unaged mixture is 1,533,934, but on aging for 80 h, this peak got thoroughly degraded, and so are the samples treated with the adsorbents at masses of 0.225 g and 0.45 g. However, the mixture treated with 0.675 g of the adsorbents recorded a peak reduction by about 63 % to 567,614 counts. At a retention time of 37.47 min, the mixtures treated with the adsorbent masses of 0.675 g and 0.45 g had peak reductions of 34 % and 89 %, respectively. The mixture treated with 0.225 g adsorbent got degraded entirely, just as the mixture without adsorbent treatment. Because RME is rich in allylic hydrogen atoms that are susceptible to radical attack leading to the formation of peroxides, the adsorbent intercepted these radicals, preventing the peroxides' formation. Hence the reduction in the degradation of the peaks of the RME in the mixture treated with the adsorbent.

Figure 42 is a zoom-in on the peaks within the retention times of 37.2 min to 37.6 min for clarity to show how the different adsorbents impact the blend's degradation of the RME molecules.

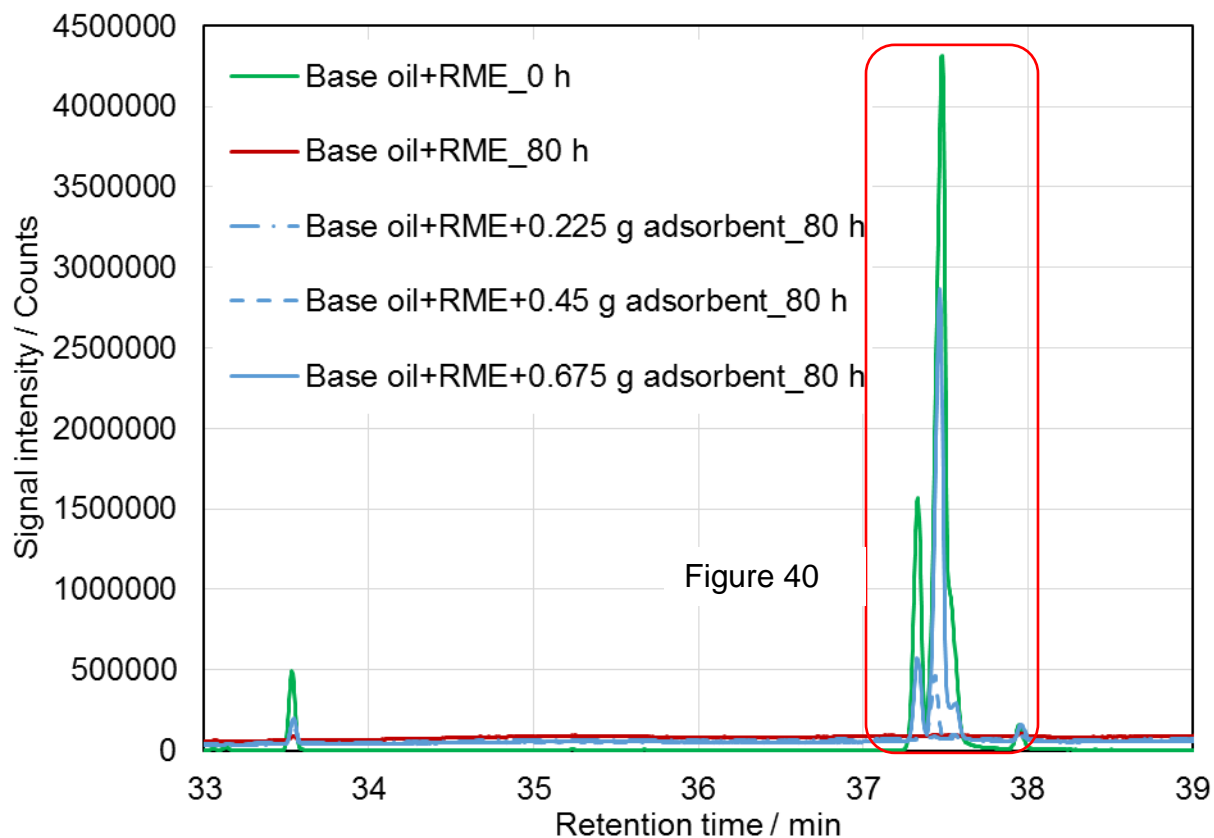


Figure 41: GC-chromatogram evaluation of 30 mL 80 % base oil mixed with 20 % RME treated with and without combined adsorbents of magnesium-aluminum hydrotalcite and 1,3,5-trimethyl-2,4,6-tris(3,5-di-tert-butyl-4-hydroxybenzyl) benzene in a ratio of 1:2 respectively and aged at 170°C with airflow of 10 L/h for 80 h with Rancimat and compared with the neat unaged blend

Figure 42 shows the GC traces for RME mixed with base oil. In Figure 42, there is an elution component peak at approximately 37.33 min, attributed to the C18_2 ME component in the RME molecule, as seen in section 8.1.1 (Kim et al., 2018). However, this same peak is virtually degraded in the blend treated with the combined adsorbents of magnesium-aluminum hydrotalcite and 1,3,5-trimethyl-2,4,6-tris(3,5-di-tert-butyl-4-hydroxybenzyl) benzene in a ratio of 1:2 respectively at amounts of 0.225 g. However, it can still be seen clearly in the 0.45 g amount of the adsorbent treated sample. The degradation of this signal for the C18_2 ME molecule in the RME treated with 0.675 g of

the combined adsorbent and aged is still conspicuous. It confirms that the adsorbent acts differently on the biodiesel molecule's different components, especially the C18_2 ME, which polymerizes at high temperatures (Kim et al., 2018). The adsorbents used to play a critical role in the suppression process. It also shows that the linoleic acid methyl ester (C18_2 ME) is most reactive to oxidation because it is an unsaturated acid (Berrios et al., 2012). The peaks at a retention time of 37.96 min remain virtually unaffected by the oxidation process. It is worthy to note that the adsorbents' impact in suppressing the blends' degradation is not linearly dependent on the amount of the adsorbent but the reaction of the biodiesel's different components.

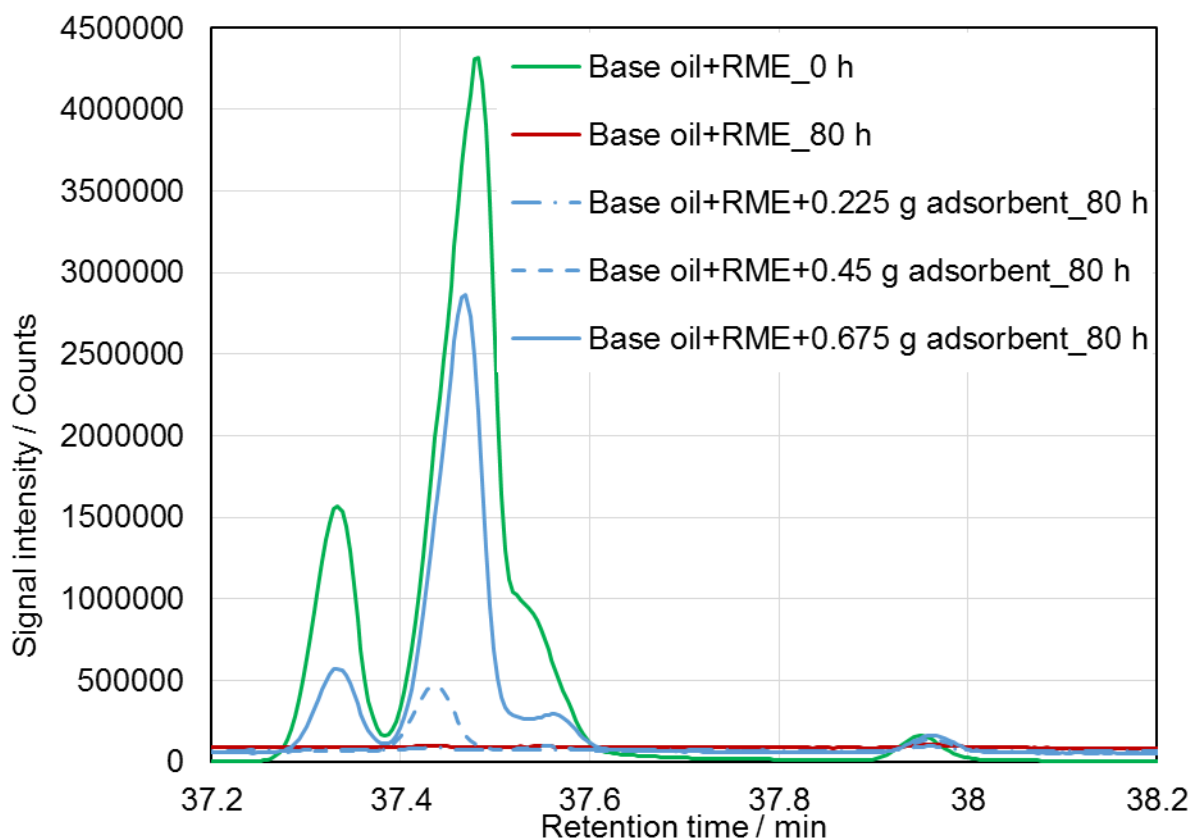


Figure 42: Zoom in on figure 40 GC-chromatogram evaluation of 30 mL 80 % base oil mixed with 20 % RME treated with and without combined adsorbents of magnesium-aluminum hydrotalcite and 1,3,5-trimethyl-2,4,6-tris(3,5-di-tert-butyl-4-hydroxybenzyl) benzene in a ratio of 1:2 respectively and aged at 170°C with airflow of 10 L/h for 80 h with Rancimat and compared with the neat unaged blend

8.3.2 Size exclusion chromatography (SEC) analysis of 80 %base oil blended with 20 % RME biodiesel treated with and without combined adsorbents magnesium-aluminum hydrotalcite and 1,3,5-trimethyl-2,4,6-tris(3,5-di-tert-butyl-4-hydroxybenzyl) benzene in a ratio of 1:2 respectively and aged at 170 °C with airflow of 10 L/h for 80 h using the Rancimat

It is clear from previous analysis that the oxidized biodiesel sample is not amenable to GC-based analysis due to the formation of higher molecular weight substances. FTIR applications cannot detect more giant molecules or higher molecular mass substances formed during an aging process. It is, however, imperative to show evidence of their formation using size exclusion chromatography (SEC) to elucidate the impact of the adsorbents in suppressing the formation of higher molecular mass substances. The SEC analysis detects the change in the molar mass of the molecules formed during the aging procedure. In Figure 43, neat 80 %base oil blended with 20 %RME treated with and without the adsorbents and aged at 170 °C at 8 h per day for a total of 80 h are shown. In this figure, more giant molecules with relative molar masses of about 1200 g/mol at the end of the aging period for the mixtures aged without adsorbent treatment have counterparts with adsorbent treatment registering masses of about 800 g/mol. The most critical area of the SEC chromatogram of the aged substances showing higher molecular mass substances is shown in Figure 42 and integrated into Figure 43, illustrating the number of oligomers formed. From Figure 44, the highest amount of the adsorbent used, 0.675 g, resulted in about a 60 % reduction in the formation of oligomers. The trend of suppressing oligomers formation follows relatively with the amount of the applied adsorbents giving a fairly relationship between the amount of the added adsorbents and the suppression of oligomers formation. This same trend is also seen in the aging of 200 mL of the same sample mixture treated with 1.5 g of the combined adsorbents and aged at 170 °C for 80 h with an airflow of 300 mL/h; the laboratory assembled aging apparatus. These results are shown in the appendix, Figure_Apx 1 and Figure_Apx 2 but not discussed in this report since the trends do not differ.

In Figure 43, a peak occurring at approximately 400 mg/mol is attributable to the RME molecule. The peak is conspicuously degraded in the mixture aged without adsorbents treatment. However, with the blends treated with adsorbents, the peak reduction depends

on the adsorbents' amount. Its total disappearance in a neat blend aged without any adsorbent treatment confirms the high biodiesel degradation rate due to the level of unsaturation or susceptibility to oxidative attack. It also confirms that biodiesel thus facilitates lubricating oil degradation when present or diluted in it. These results largely coincide with literature results on oxidation inhibition (Abdul-Munaim et al., 2019; Fattah et al., 2014; Obadiah et al., 2012). The absence or low level of oligomers formed in the blends treated with the adsorbents testifies the adsorbents' impact in suppressing the oxidation process (Cristina et al., 2011). The degradation of fatty acid methyl ester usually results in hydroperoxides and other low molecular weight carboxylic acids, aldehydes, and ketones. These very reactive primary oxidation products polymerize into higher molecular weight products, according to Obadiah et al. (2012). These compounds are precursors to oligomers. Therefore, their nonappearance or low quantity indicates the adsorbents' impact in suppressing their formation during the first stage of the oxidation process (see the top left side of Figure 5).

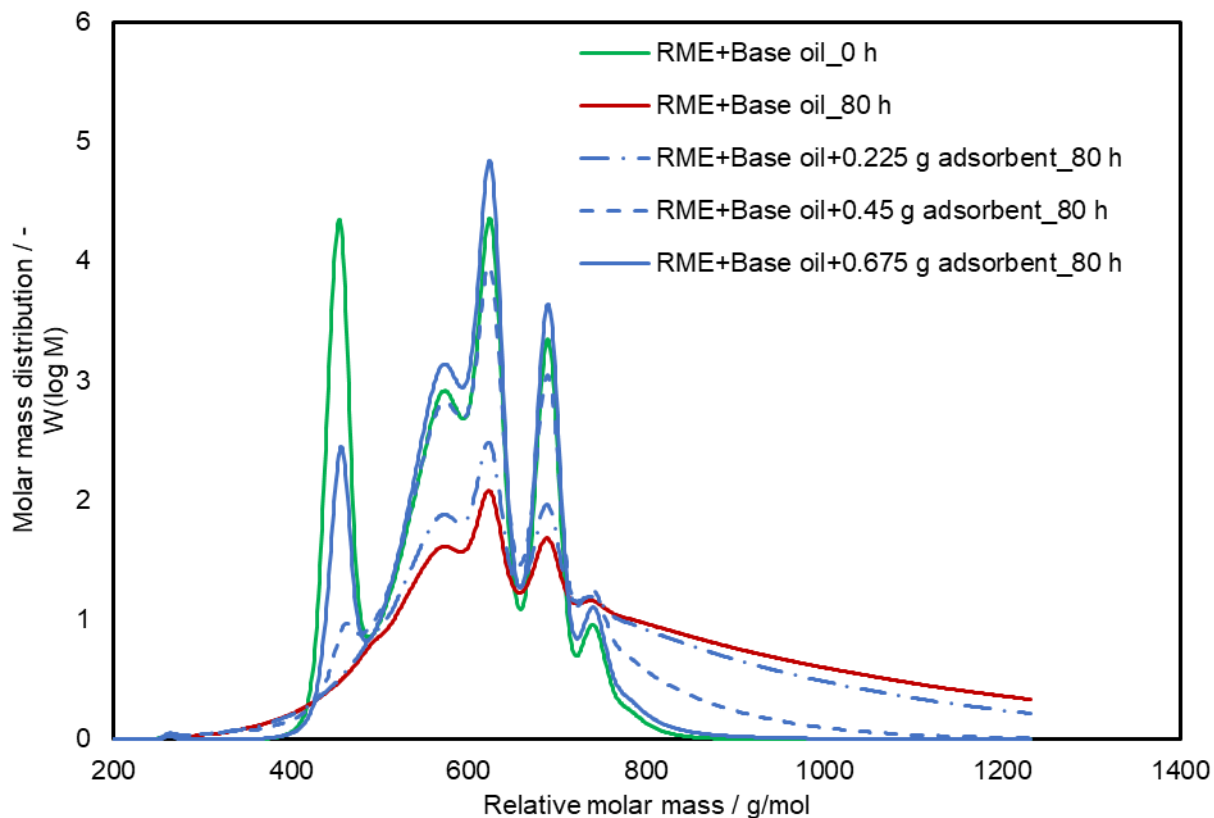


Figure 43: SEC evaluation of 30 mL 80 % base oil mixed with 20 % RME treated with and without combined adsorbents of magnesium-aluminum hydrotalcite and 1,3,5-trimethyl-2,4,6-tris(3,5-di-tert-butyl-4-hydroxybenzyl) benzene in a ratio of 1:2 respectively and aged at 170 °C with airflow of 10 L/h for 80 h with Rancimat and compared with the neat unaged blend

The zoom-in on the SEC chromatogram of the aged substances showing the region of higher molecular mass substances is shown in Figure 44. Considering that at least two dimers with a molar mass of about 340 mg/mol each come together to form an oligomer, the x-axis is plotted from at least 680 mg/mol. The y-axis represents the distribution of the molar masses. The suppression of molecules' formation with higher molar masses seems directly dependent on the mass of the adsorbent applied. It is expected since the amount of the liable hydrogens involved in the suppression process is more in concentration in a higher amount of the adsorbents in use.

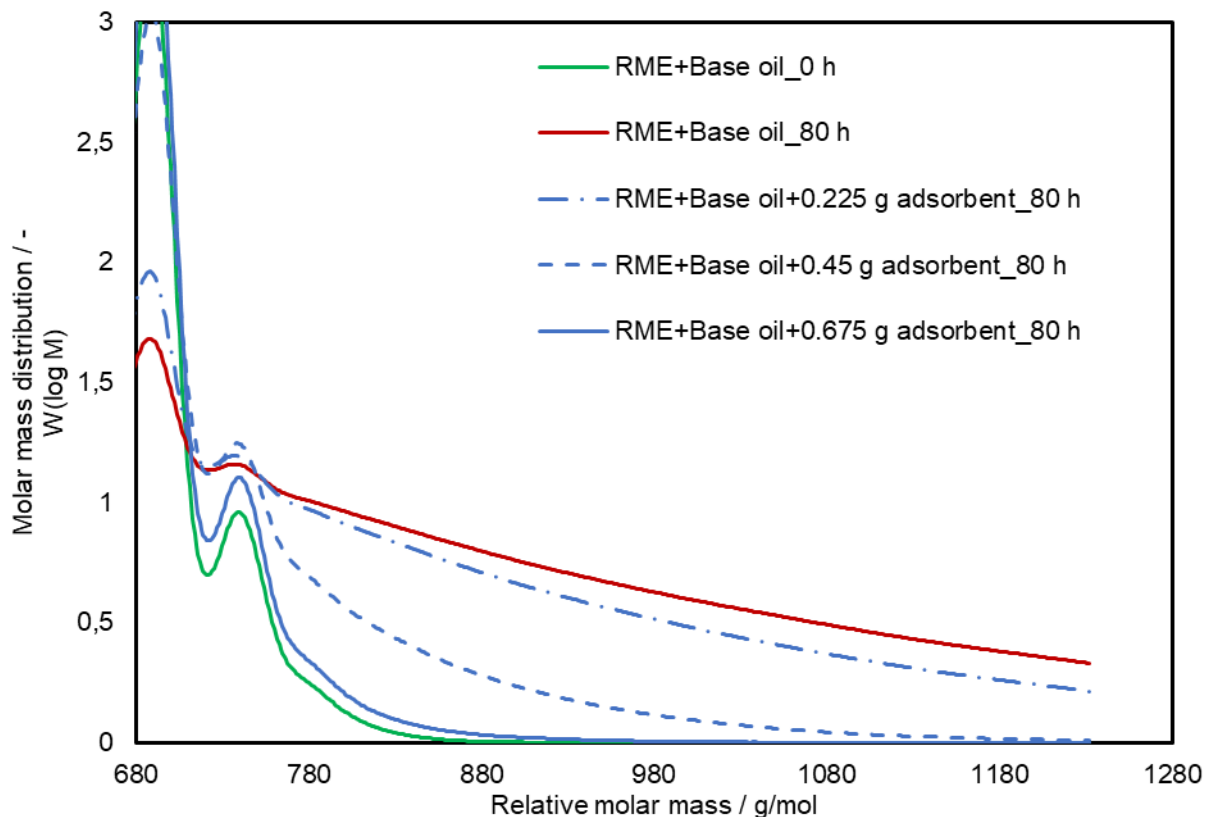


Figure 44: SEC evaluation (range: 680-1280 g/mol) of 30 mL 80 % base oil blended with 20 % RME treated with and without combined adsorbents of magnesium-aluminum hydrotalcite and 1,3,5-trimethyl-2,4,6-tris(3,5-di-tert-butyl-4-hydroxybenzyl) benzene in a ratio of 1:2 respectively and aged at 170 °C with airflow of 10 L/h for 80 h with Rancimat and compared with the neat unaged blend

The region of the more significant molecular masses buildup in the SEC chromatogram of the aged substances is integrated and shown in Figure 45, indicating the number of oligomers formed. Comparing with the blend aged without adsorbent treatment, the mixtures treated with the adsorbents depressed the formation of oligomers. Considering that the oil change interval of 30,000 km can be simulated at a constant temperature of 170 °C for 40 h duration (as seen in section 7.4), the SEC test results reveal that without the use of the adsorbents, the oil under this aging condition should cover a distance of about 10,000 km before been changed. However, the use of the adsorbents, on the other hand, would enable a distance coverage of 11,000 km, 18,000 km, and 25,000 km, respectively, according to the mass of 0.225 g, 0.45 g, and 0.675 g of the combined adsorbents of magnesium-aluminum hydrotalcite and 1,3,5-trimethyl-2,4,6-tris(3,5-di-tert-

butyl-4-hydroxybenzyl) benzene in a ratio of 1:2 respectively applied. It is with the assumption that no other processes interfere with the action of the adsorbents. The amounts of the adsorbents applied depressed the formation of oligomers in the percentages of 10 %, 44 %, and 60 %, respectively. Therefore, an average amount of 0.31 g of the combined adsorbents in the ratio of 1:2 applied to a volume of 30 mL of biodiesel will result in about 38 % suppression of oligomers formation. The same suppression trend is recorded for the aging of 200 mL of the same sample mixture and reported in the appendix, Figure_Apx 3. It is, however, not conclusive since other factors are also considered in determining the oil changing interval.

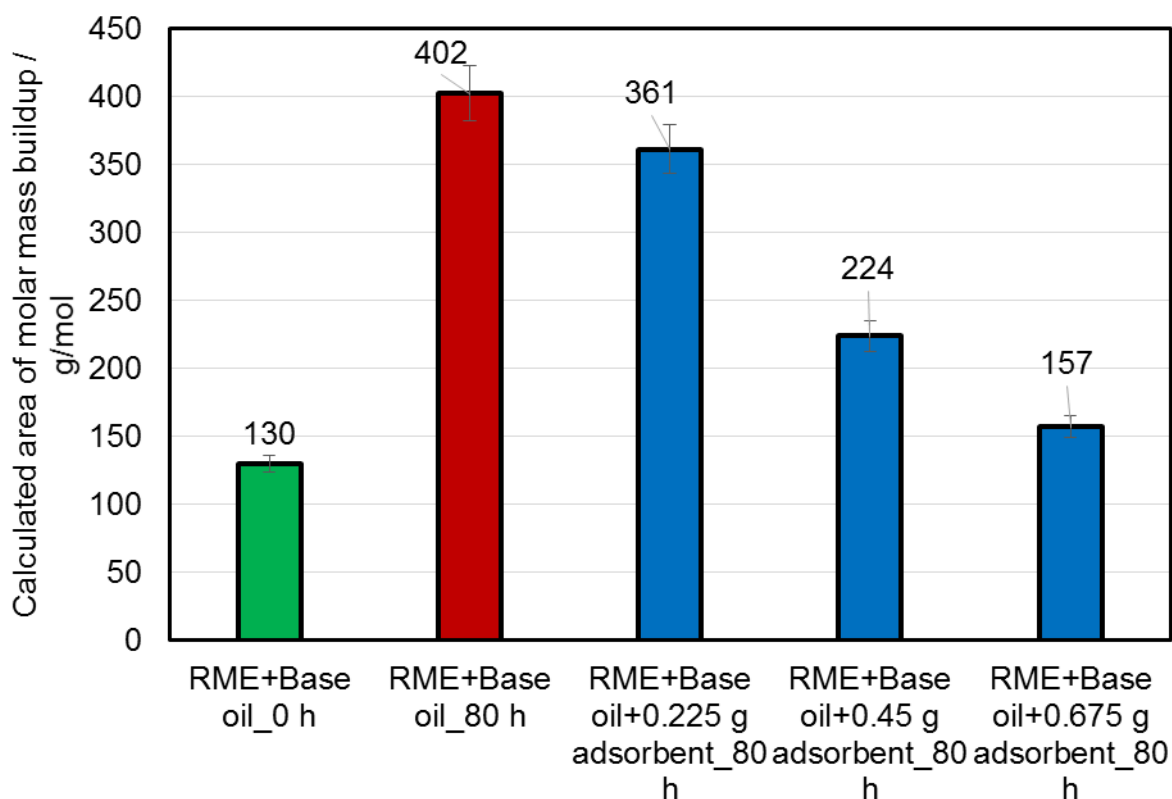


Figure 45: Calculated area of SEC of 30 mL 80 % base oil mixed with 20 % RME treated with and without combined adsorbents of magnesium-aluminum hydrotalcite and 1,3,5-trimethyl-2,4,6-tris(3,5-di-tert-butyl-4-hydroxybenzyl) benzene in a ratio of 1:2 respectively and aged at 170°C with airflow of 10 L/h for 80 h with Rancimat compared with the neat unaged blend

8.3.3 Acid value

The acid value indicates how oxidized oil or fuel has become. Acid values increase with oil oxidizing (Song and Choi, 2008). Low acid values due to the application of the adsorbents are observed, as shown in

Figure 46. While the blend aged without adsorbent treatment has 41.3 mg KOH/g acid value, the samples treated with the adsorbents and aged have 29.6, 1.9, and 1.3 mg KOH/g the adsorbents applied. It translates into a 28 %, 95 %, and 97 % reduction in the buildup of acid values of the 0.225 g, 0.45 g, and 0.675 g of adsorbents applied. This result depicts that the suppression in the buildup of acid values is adsorbent concentration driven. It gives rise to the non-linear trend observed.

However, between the application of the 0.45 g and 0.675 g of adsorbents, a difference of 0.62 mg KOH/g acid value is registered. The difference is an indication that the 0.45 g adsorbent is a sufficient amount with an excellent capacity to cause the retardation of the mixture's oxidation. The increase in acid value in the blend aged without any adsorbent treatment is because when fatty acid methyl ester degrades, they produce hydroperoxides, other low molecular weight carboxylic acids, aldehydes, and ketones (Obadiah et al. (2012). These primary oxidation products are very reactive and can polymerize into higher molecular weight products (Figure 5 and Figure 7), leading to increased acidity (Knothe, 2010; Obadiah et al., 2012). Also, biodiesel-free fatty acids due to the incomplete transesterification process can contribute to the high acid values (Kenreck, 2007). The higher the degree of degradation, the higher the acidity. Figure_Apx 9 in the appendix shows that the same trend is seen with the aging of 200 mL of the same sample mixture with 1.5 g of the combined adsorbents treatment though not discussed here. Literature indicates that fuel aging is better reflected by the acid number representing secondary oxidation products (Saltas et al., 2017; Davannendran et al., 2016). The active hydroxyl group of the adsorbents interrupt the complex secondary oxidation reactions by providing protons that inhibit the formation of free radicals and interrupt the propagation of the free radicals and thus delay the rate of oxidation which would have led to the formation of more reactive products, hence the low acid values recorded. The acid value results collaborate with the SEC results illustrated in section

8.3.2, where very low to no high molecular mass species are formed in the samples treated with the adsorbents. The observation exhibited in SEC by the samples aged without the adsorbents indicating an increasing trend of higher molecular mass substances. A similar observation is seen with an increasing trend in acid value. The relation of deposits or high molecular mass substances formed with samples aged without using the adsorbents is verified by a direct increase of high molecular mass substances formed with a corresponding increasing higher acid value. The results agree with the GCMS results in section 8.3.1, where about 40 % of the methyl ester signal is recorded after aging the blend treated with the adsorbents for 80 h duration at 170°C. As the methyl ester signal decreases in the sample mixture's GCMS determination, it coincides with an increase in acid value without the adsorbent treatment. The oxidation of methyl ester results in high degradation products, which translates into high acid values. On the other hand, the adsorbents' use suppressed oxidation in the blend by interrupting the oxidation reactions through the liable hydrogen on its surface, reducing the sample's oxidation rate, and curbing the production of the secondary oxidation products to low acid values.

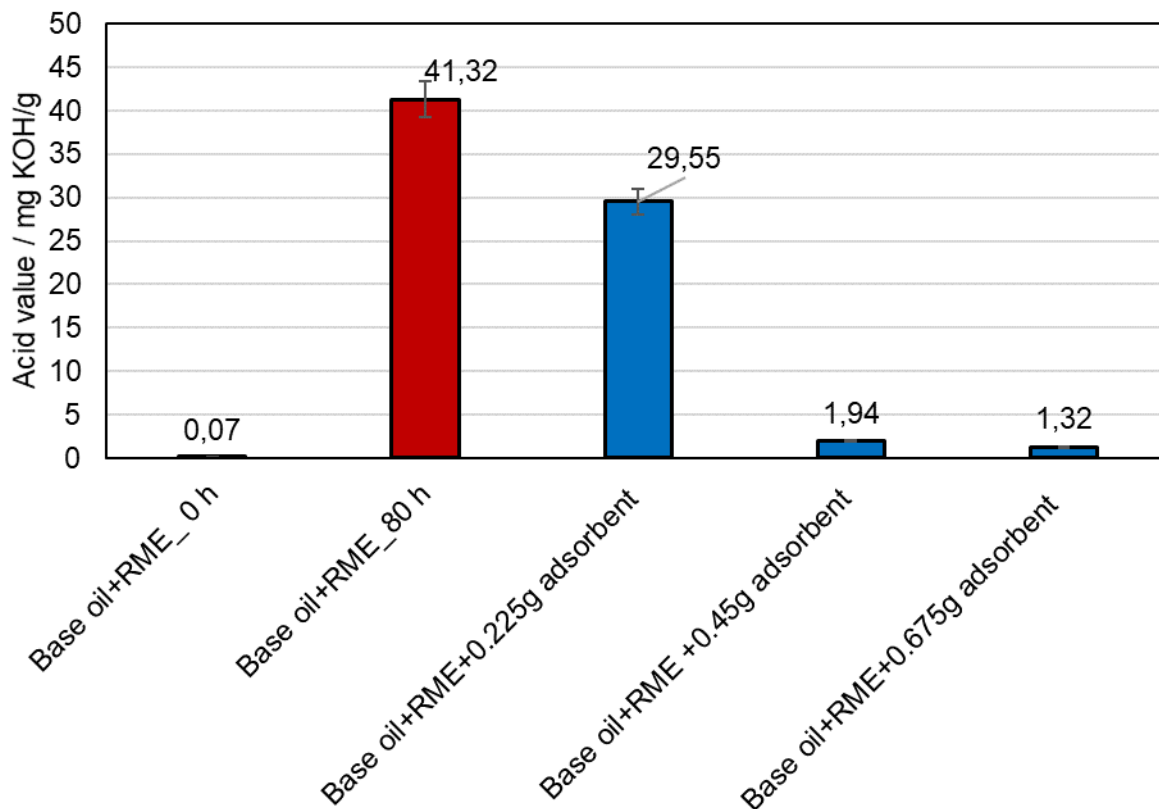


Figure 46: Evaluation of acid values of 30 mL 80 % base oil mixed with 20 % RME treated with and without combined adsorbents of magnesium-aluminum hydrotalcite and 1,3,5-trimethyl-2,4,6-tris(3,5-di-tert-butyl-4-hydroxybenzyl) benzene in a ratio of 1:2 respectively and aged at 170°C with airflow of 10 L/h for 80 h with Rancimat and compared with the neat unaged blend

8.3.4 Viscosity

The adsorbents' impact on the blends' aging has been determined using viscosity gradient as defined in the standard ASTM D2270. The blends' viscosity is assessed at two temperatures, 40 °C, and 100 °C, and the viscosity index is calculated. That is the only way that conclusions can be drawn on viscosity changes with sufficient accuracy. The gradient of the mixture aged without any adsorbent treatment is very steep, 84 ° as compared to the blends treated with the various amounts of the adsorbents, 75 °, 33 °, and 15 ° according to 0.225 g, 0.45 g, and 0.675 g of adsorbents applied respectively, Figure 47. It is worth noting that the gradient of the neat and unaged sample mixture is 11 °. High viscosity recorded by the blend aged without any adsorbent treatment, 84 ° from an initial 11 ° giving rise to 89 % increase, is due to oxidation resulting in more insoluble materials

formation. When fatty acid methyl ester degrades, they produce hydroperoxides and other low molecular weight carboxylic acids, aldehydes, and ketones. These primary oxidation products are very reactive and polymerize into higher molecular weight products (Figure 5 and Figure 7), leading to increased viscosity (Kim et al., 2018; Knothe, 2010). The greater tendency of biodiesel to form polymeric deposits can also increase viscosity. The formation of higher molecular weight components of the sample aged without using the adsorbents recorded by the SEC results in section 8.3.2 thus correlates well with the high viscosity seen here. As reported in the literature (Moraes and Bahia, 2015), the oxidation products of biodiesel degradation increase viscosity.

The use of the adsorbents, on the other hand, retarded the formation of higher molecular weight substances leading to a reduction in the number of sludge precursors formed and, finally, the low viscosities observed. The use of the adsorbents suppressed the formation of higher molecular species by 24 %, 74 %, and 95 % in respect of the 0.225 g, 0.45 g, and 0.675 g of adsorbents applied, leading to only an increase of 76 %, 26 %, and 5 % compared with 89 % increase in the sample aged without the use of the adsorbents. The adsorbents' suppression action led to the low gradients of 75 °, 33 °, and 15 °. It gives rise to the more significant usage of oil in its application. The viscosity results also confirm that the adsorbents' application in the ratio of 1:2:3 does not impact linearly per this ratio. The trend of the adsorbents' impact on the viscosity is consistent with that of the 200 mL of the same sample mixture aged using the laboratory aging set reported in Figure_Apx 8 and tallies with that of the acid value as seen above, section 8.3.3. Such observed increment, as explained earlier, is due to the formation of peroxides and hydroperoxides, which oxidized into acids and eventually resulted in higher molecular mass species, leading to the rise in viscosity. There is, therefore, a linear relation between acid value and viscosity.

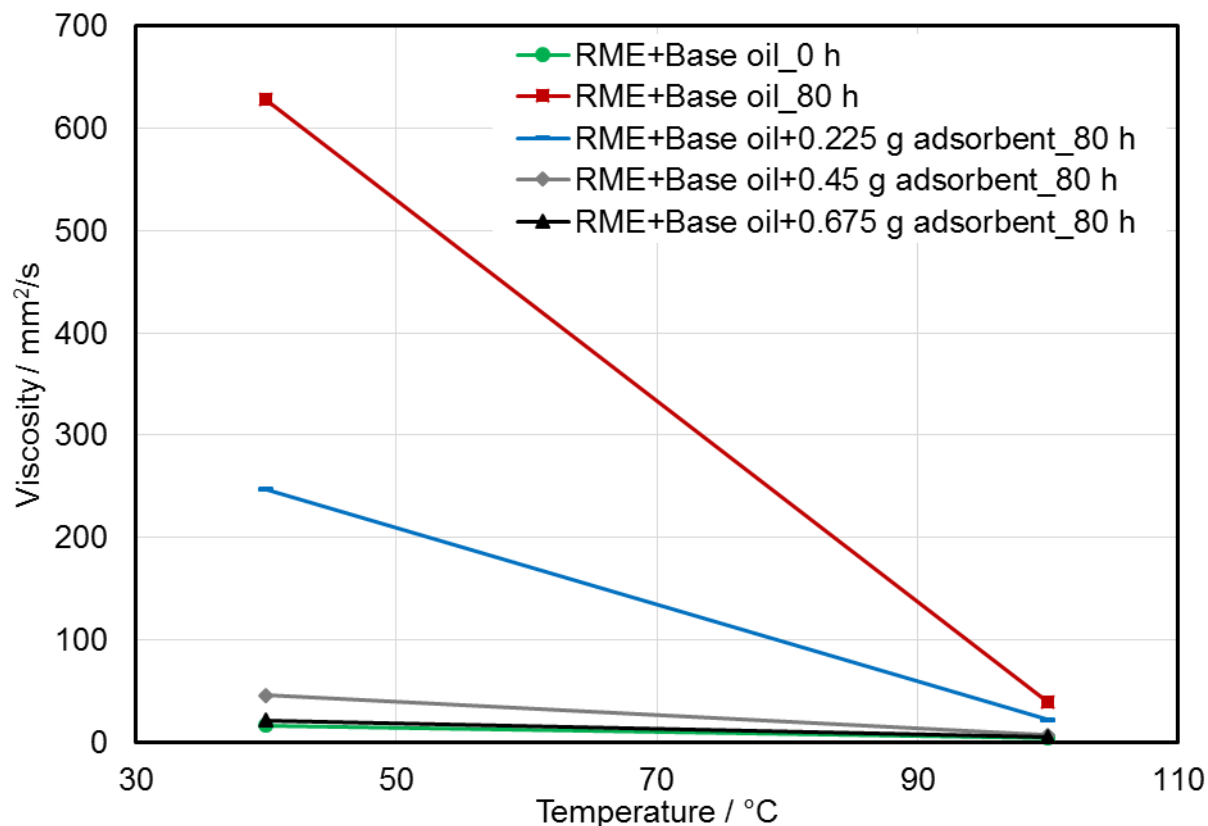


Figure 47: Evaluation of viscosity gradient of 40 mL 80 % base oil mixed with 20 % RME treated with and without combined adsorbents of magnesium-aluminum hydrotalcite and 1,3,5-trimethyl-2,4,6-tris(3,5-di-tert-butyl-4-hydroxybenzyl) benzene in a ratio of 1:2 respectively and aged at 170°C with airflow of 10 L/h for 80 h with Rancimat

Viscosity index is an arbitrary number used to characterize kinematic viscosity variation due to changes in a petroleum product's temperature between 40 and 100°C. (ASTM D2270). In the viscosity index, Figure 48, the blend aged without the treatment with the adsorbents had the lowest value of the viscosity index. In contrast, the samples treated with the adsorbents and aged had the highest values, as seen in Figure 48. Figure 48 illustrates the viscosity index over the aging period. It is seen that the viscosity index of the blends treated with the adsorbents and aged show positive values above that of the sample aged without any treatment with the adsorbents. The higher the viscosity index, the “better” the oil because it changes less viscosity with temperature (Oelcheck summer, 2012). Hence a higher viscosity index is indicative of a smaller decrease in viscosity with increasing temperature. On the other hand, a lower viscosity index indicates that there are higher viscosity changes with temperature. Therefore, the samples treated with the

adsorbents are expected to undergo little or insignificant changes in viscosity with extreme temperatures and are considered viscosity stable (Ashraful et al., 2014). The viscosity index is inversely proportional to the number of degradation products formed resulting from the oxidation process. This observation is explainable as the adsorbents' use interfered with the oxidation process resulting in low or no degradation products. The viscosity index results correlate the SEC's results, which indicated the no to very insignificant production of higher molecular mass substances due to the use of the adsorbents and agreed perfectly with the low acid values.

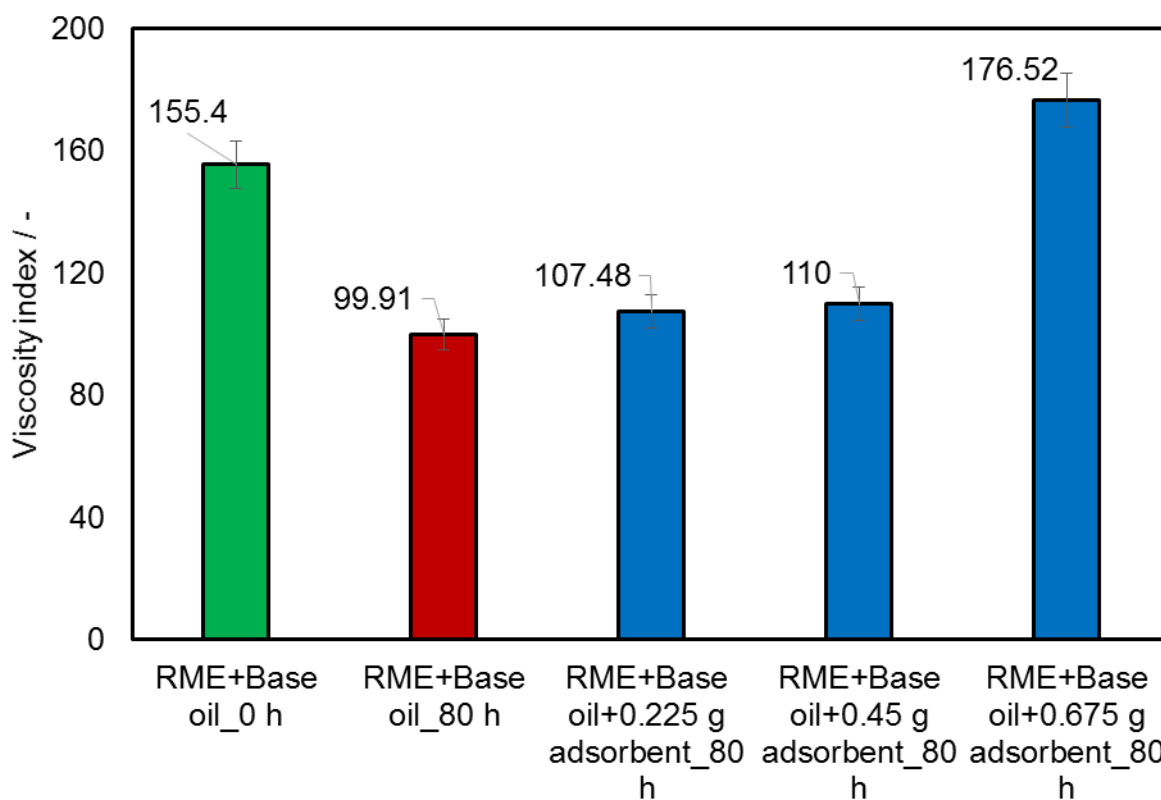


Figure 48: Evaluation of viscosity index of 30 mL 80 % base oil mixed with 20 % RME treated with and without combined adsorbents of magnesium-aluminum hydrotalcite and 1,3,5-trimethyl-2,4,6-tris(3,5-di-tert-butyl-4-hydroxybenzyl) benzene in a ratio of 1:2 respectively and aged at 170°C with airflow of 10 L/h for 80 h with Rancimat compared with the neat unaged blend

8.3.5 Density

Figure 49 shows the changes in density measured at 40 °C of 80 %base oil blended with 20 %RME treated with and without adsorbents and aged at 170 °C with an airflow of 10 L/h for 80 h duration using a Rancimat. In Figure 49, the density of biodiesel in the blend aged without treatment with adsorbents increased. Due to the formation of insoluble substances resulting from degradation with a consequence increase in molecular interaction of the degraded biodiesel as peroxides are formed (Pattamaprom and Ngamjaroen, 2012; Ayhan, 2007). With the application of 0.675 g of adsorbent for the duration of 80 h of aging at 170 °C, an increase of 0.0001 Kg/m³ is reported, and this is very negligible or very insignificant as compared to the growth of 0.107 Kg/m³. It translates into about a 13 % increase in density of the blend aged without applying the adsorbents. For the various amounts of adsorbents, 0.225 g, 0.45 g, and 0.675 g, the increase in density at the end of 80 h duration of aging are 10 %, 4 %, and 0.01 %, respectively. From the results, the relationship between the amount of the adsorbent applied and the increase in the density of the mixture correlates well with that of the mixtures' viscosity, as seen in section 8.3.4 above. The formation of the degradation products leads to an increase in density and essentially viscosity. Still, since the liable hydrogens on the adsorbents' surface entrapped and stabilized the radicals, there is a very insignificant production of degradation products.

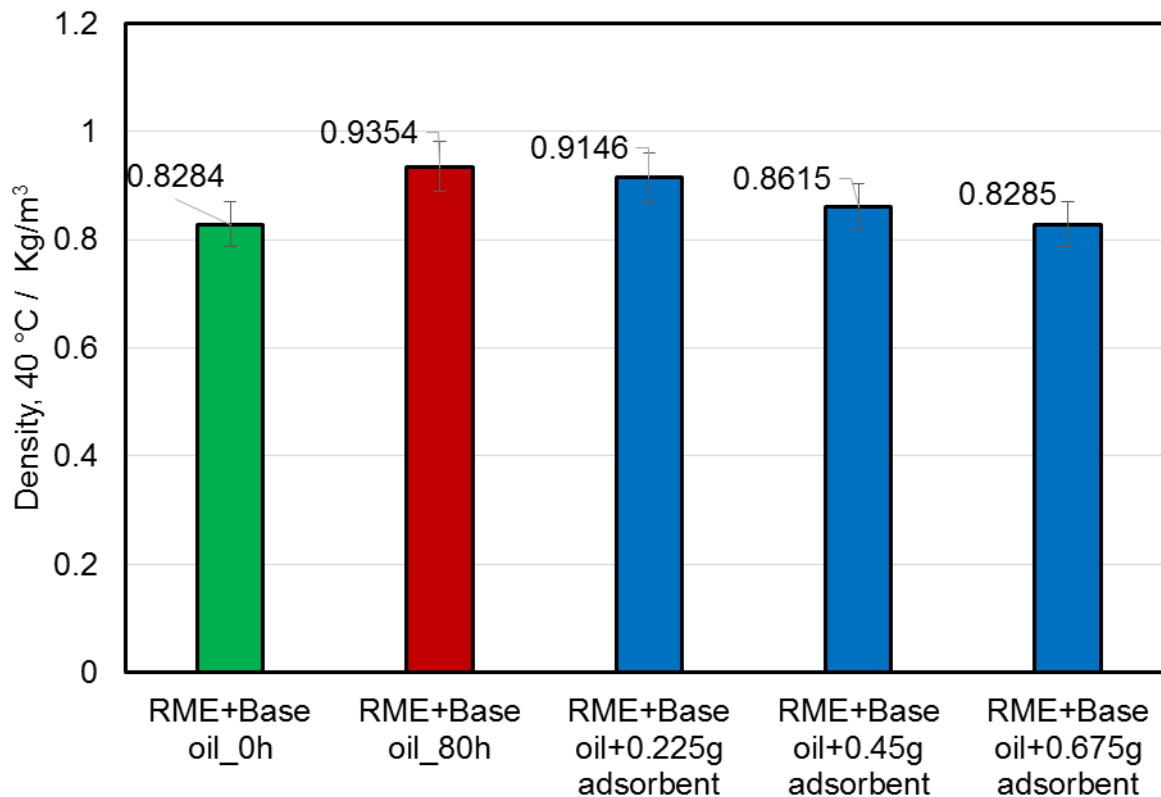


Figure 49: Evaluation of density at 40°C of 30 mL 80 % base oil mixed with 20 % RME treated with and without combined adsorbents of magnesium-aluminum hydrotalcite and 1,3,5-trimethyl-2,4,6-tris(3,5-di-tert-butyl-4-hydroxybenzyl) benzene in a ratio of 1:2 respectively and aged at 170°C with airflow of 10 L/h for 80 h with Rancimat

8.3.6 FTIR evaluation of 30 mL 80 %base oil blended with 20 % RME biodiesel treated with and without various amounts of combined adsorbents magnesium-aluminum hydrotalcite and 1,3,5-trimethyl-2,4,6-tris(3,5-di-tert-butyl-4-hydroxybenzyl) benzene in a ratio of 1:2 respectively and aged at 170 °C with airflow of 10 L/h for 80 h using a Rancimat

Figure 50 shows the IR-spectra of the blend during the aging process of 80 %base oil blended with 20 %RME treated with and without various amounts of adsorbents, 0.225 g, 0.45 g, and 0.675 g used in this study. The relationship between peak areas and oxidation level is more easily seen when the spectra' regions for the sample mixture in which the carbonyl and hydroxyl compounds are absorbed, Figure 51 and Figure 53, are considered. Similar results are seen in the report of Naidu et al. (1984). The critical portions of the spectra have been integrated into Figure 52 and Figure 54. Also, the decrease of CH,

CH₂, and CH₃ vibrations in the aged blend without the adsorbents is detected within the range of 2800 cm⁻¹ to 3000 cm⁻¹. However, the same decrease in signals is absent in the blend treated with the same band's adsorbents. These test results mean that the adsorbents' use leads to a small or insignificant amount of sludge precursor production.

The adsorbents' impact on the mixtures' oxidation follows the substantially same pattern as other FTIR analyses on the suppression of oligomers formation. Even with a high sample volume of 200 mL, the trend remains the same though not discussed here, Figure_Apx 4. The results obtained using the FTIR technique agree with the gas chromatography technique and the size exclusion chromatography (see sections 8.3.1 and 8.3.2). It also correlates very well with the results of the acid value. The main components of concern in this work are the OH group centered on 3400 cm⁻¹. It, therefore, reveals the formation of oxidation products and the absorbance at around 1740 cm⁻¹ which is characteristic of the C=O (carbonyl) group, as seen in section 4.1.5. This band reflects the formation of ketones, aldehydes, and free carboxylic acids in the deposit formed in the mixture aged without using the adsorbents. It supports the formation of higher molecular mass substances, as seen in the SEC results reported in section 8.3.2. Similar results are reported in the literature by Karavalakis et al. (2011). However, these peaks are absent in the mixture treated with the adsorbents and aged, as seen in Figure 50.

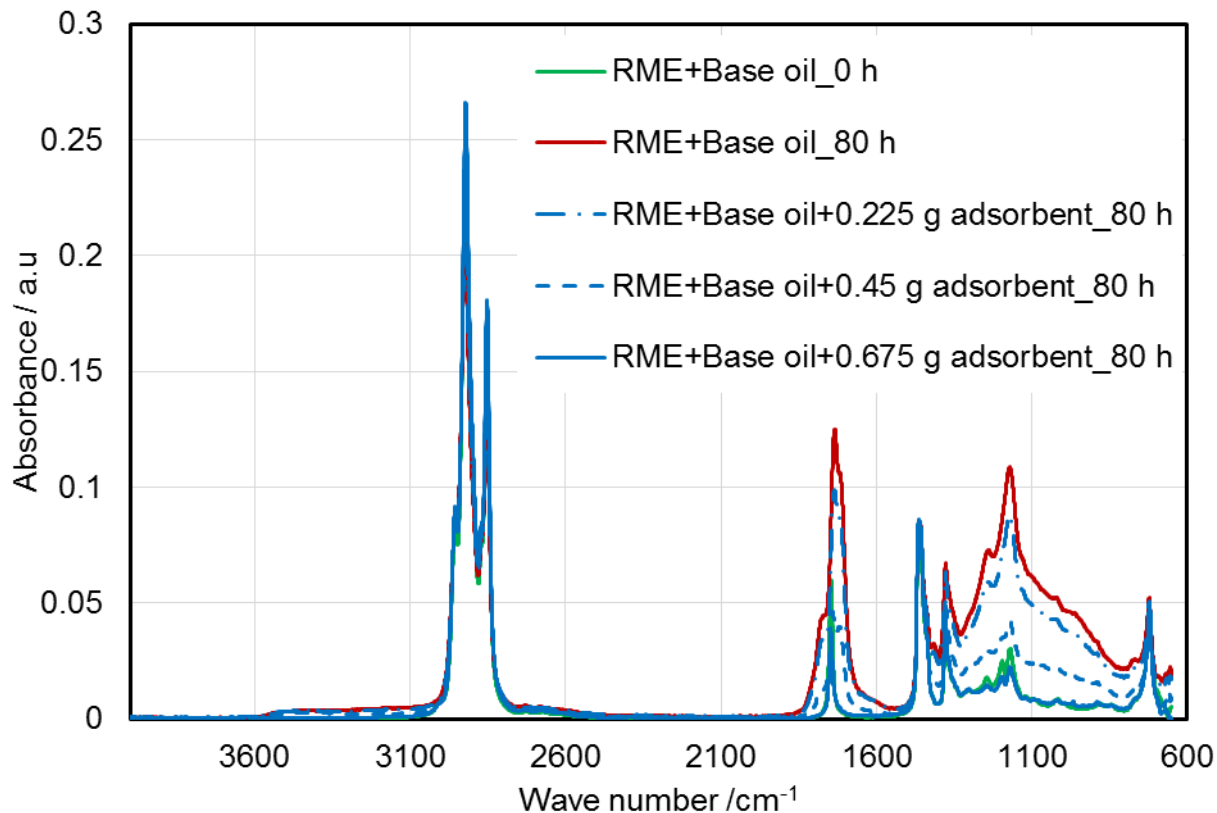


Figure 50: FTIR spectra in absorbance mode (range 600-4000 cm^{-1}) of 30 mL 80 % base oil mixed with 20 % RME treated with and without combined adsorbents of magnesium-aluminum hydrotalcite and 1,3,5-trimethyl-2,4,6-tris(3,5-di-tert-butyl-4-hydroxybenzyl) benzene in a ratio of 1:2 respectively in various amounts and aged at 170 °C with airflow of 10 L/h for 80 h using Rancimat

Figure 51 is a zoom-in on the carbonyl region, 1600 to 1900 cm^{-1} of Figure 50. Within this region, as aging proceeded, the mixture of base oil and RME without adsorbent treatment showed an enhanced absorbance around 1750 cm^{-1} due to the presence of carbonyl-containing degradation products. An overlay of the FTIR spectra of the oxidized mixture with and without the adsorbents and the neat unoxidized mixture (Figure 49) shows three significant peaks at 1715, 1740, 1775 cm^{-1} . As oxidation progressed, it is observed that the absorption of the 1715 and 1775 cm^{-1} peaks significantly increased. The 1740 cm^{-1} band from Adhvaryu et al. (1998) arises mainly from ester-type compounds. The band at 1715 cm^{-1} is attributed to ketones. The 1775 cm^{-1} band is expected mainly from peroxy ester-type compounds. These degraded products, polar compounds undergo condensation polymerization reactions, leading to an increase in the oil's viscosity, as

seen in section 8.3.4. A similar result is reported by Adhvaryu et al. (1998). As seen in section 3.4, during the propagation phase of biodiesel's degradation, the peroxides disintegrate into oxygenated intermediates, which further degrade into short-chain acids, ketones, alkenes, and aldehydes (Knothe, 2007, Brühl, 2014). The presence of this wide variety of oxidation products contributes to the broadness of the peak. The increase in this signal's broadness is significantly absent in the base oil and RME mixture treated with the adsorbents and aged. The hydroxyl ions in the adsorbent subdue a hydrogen ion's abstraction from the hydrocarbon backbone in the ester and, therefore, retard the biodiesel's degradation.

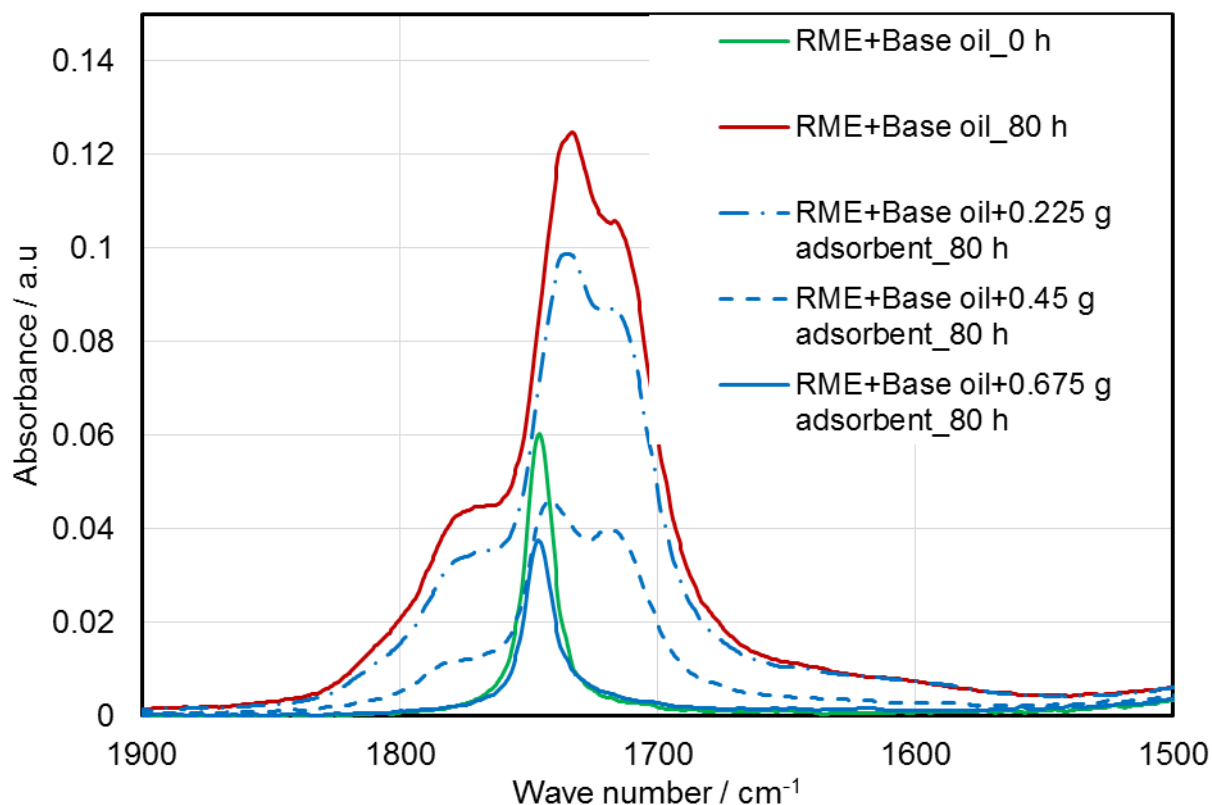


Figure 51: FTIR spectra in absorbance mode (range 1500-1900cm⁻¹) of 30 mL 80 % base oil mixed with 20 % RME treated with and without combined adsorbents of magnesium-aluminum hydrotalcite and 1,3,5-trimethyl-2,4,6-tris(3,5-di-tert-butyl-4-hydroxybenzyl) benzene in a ratio of 1:2 respectively in various amounts and aged at 170 °C with airflow of 10 L/h for 80 h using Rancimat

Figure 52 shows the change in the carbonyl's calculated spectral peak area, C=O bands absorption (1650-1815 cm⁻¹) in the IR spectra due to the formation of certain oxygenated

compounds during oxidative degradation. Adhvaryu et al. (1998) reported similar observations. Therefore, by comparing the aged base oil and RME mixtures at the carbonyl vibrations (1600-1900 cm^{-1}), higher C=O vibrations (0.124 au) in the mixture aged without the application of the adsorbents. It can be recognized that the mixtures treated with the adsorbents showed slightly increased carbonyl vibration bonds (0.097, 0.045, and 0.036 au), representing 81 %, 35 %, and 14 %, according to the amount of the adsorbents used respectively compared to the aged mixture without adsorbents treatment. The amount of absorption obtained for carbonyl compounds upon aging with the mass of 0.675 g of the adsorbents at a temperature of 170 °C is consistent with that shown in Figure 27 in section 8.1.3.

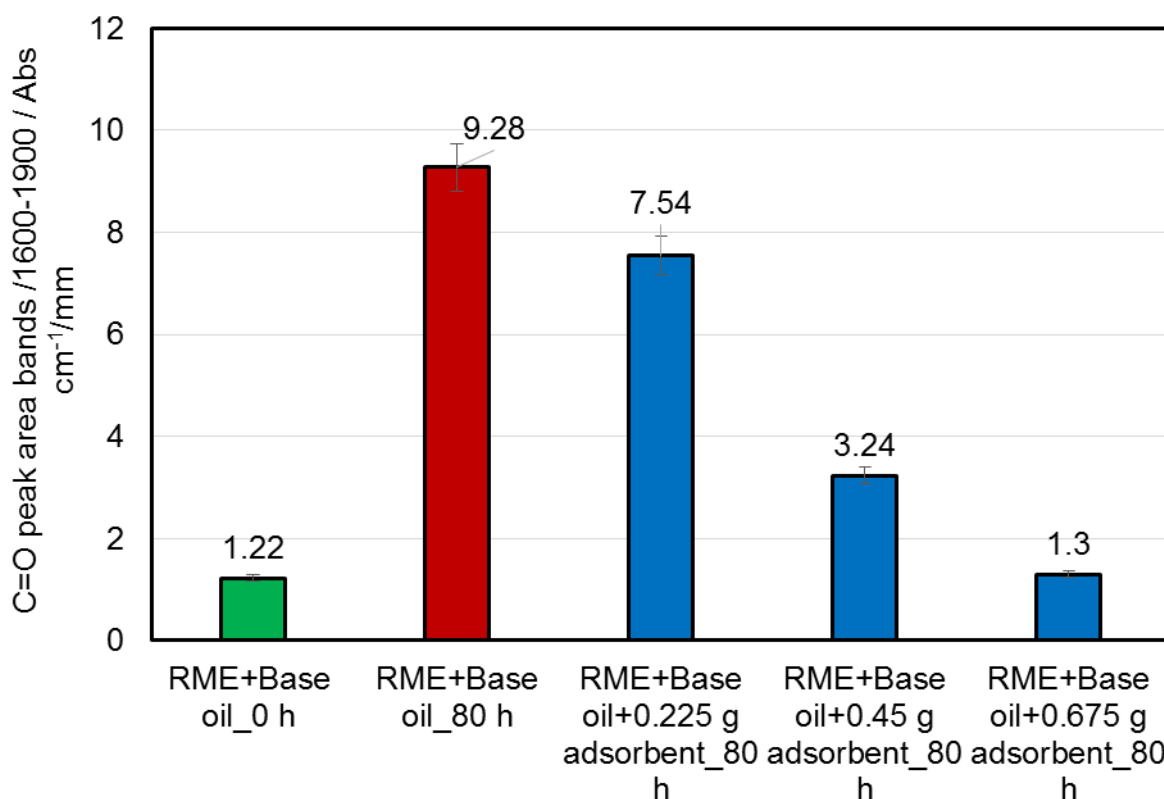


Figure 52: Evaluation of peak area under C=O bands (1600-1900 cm^{-1}) of the FTIR spectra of 30 mL 80 % base oil mixed with 20 % RME treated with and without various amounts of combined adsorbents of magnesium-aluminum hydrotalcite and 1,3,5-trimethyl-2,4,6-tris(3,5-di-tert-butyl-4-hydroxybenzyl) benzene in a ratio of 1:2 respectively in various amount and aged at 170 °C with airflow of 10 L/h for 80 h using Rancimat

Figure 53 is an illustration of the hydroxyl vibrations region of Figure 50. The high peak of the OH band seen in the sample aged without the adsorbent treatment is attributable to

the organic compounds, including water, alcohol, hydroperoxides, and carboxylic acids with the OH functional group. These signals are not significant in the sample treated with the adsorbents and aged. The level of increase of the OH vibrations varies according to the amount of the adsorbents applied. Infrared spectroscopy measures the infrared light absorbed by bonds in molecules when the infrared light's frequency and vibration frequency are the same. Therefore, it identifies the chemical functionalities that correspond to the different functional groups to the wavenumber. Invariably, the peak intensity is a function of the functional groups' concentration present (Cavallia et al., 2018). Considering the absorbance of the OH functional groups, 0.003 au, it can be concluded that there has been very little or insignificant production of hydroperoxides which are the precursors for the propagation stage of the oxidation process. Hence, the adsorbents thus act on the initiation stage of the sample mixture's degradation, thereby interrupting the oxidation process, retarding it, and leading to low or no oxidation product formation.

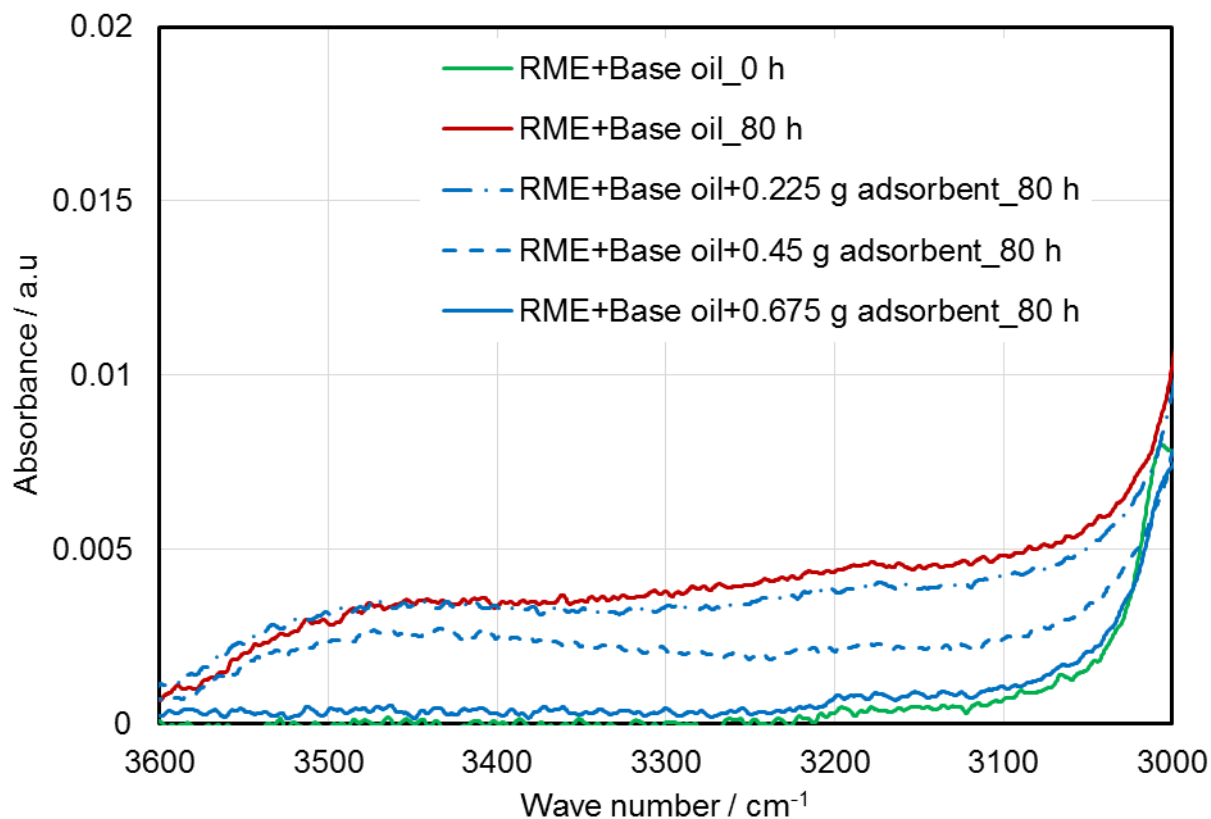


Figure 53: FTIR spectra in absorbance mode (range 3000-3600 cm^{-1}) of 30 mL 80 % base oil mixed with 20 % RME treated with and without combined adsorbents of magnesium-aluminum hydrotalcite and 1,3,5-trimethyl-2,4,6-tris(3,5-di-tert-butyl-4-hydroxybenzyl) benzene in a ratio of 1:2 respectively in various amounts and aged at 170 °C with airflow of 10 L/h for 80 h using Rancimat

The calculated variations in hydroxyl vibrations are presented in Figure 54. Mixtures treated with the adsorbents show a smaller formation of long-chain acids or alcohols after aging than those without adsorbents treatment. After the aging process, the differences in the built-up of OH-bonds between the mixtures treated with and without the adsorbents, especially the mixture with the highest amount of adsorbents, are negligible. The FTIR analysis results correlate with the number of acid values and the higher molecular mass substance formed in the sample treated with the adsorbents and aged.

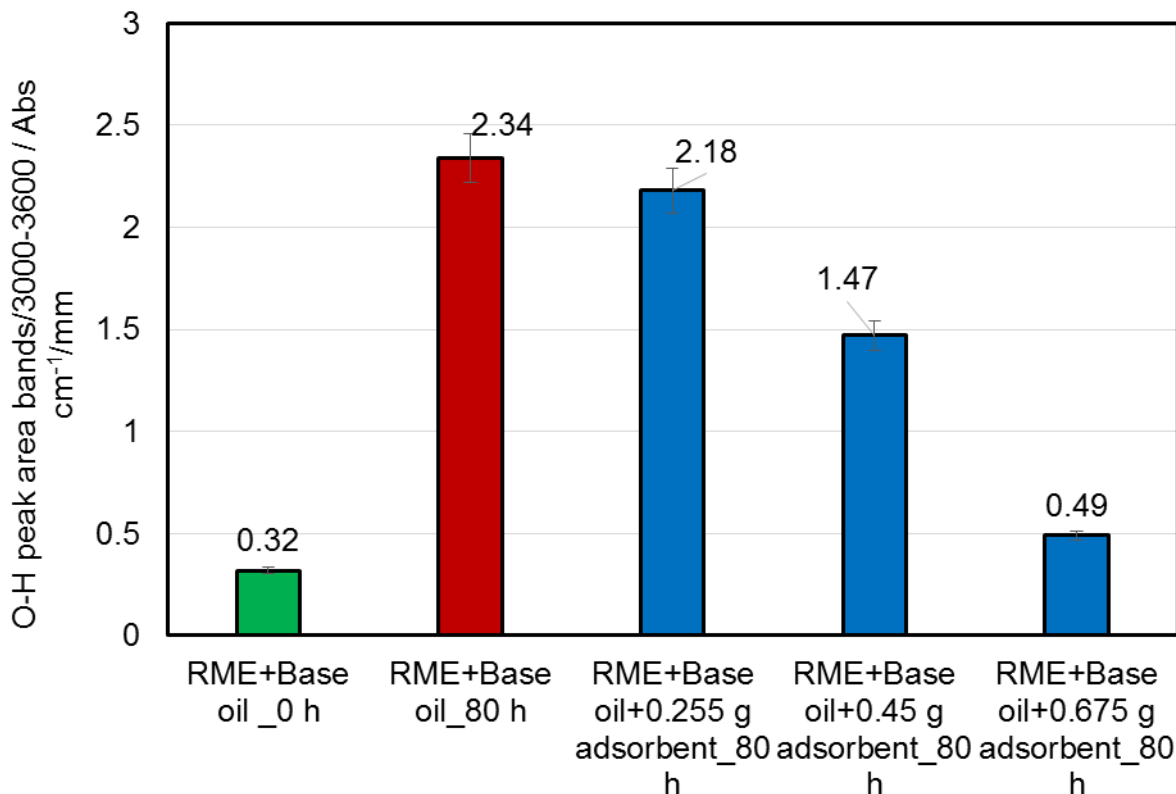


Figure 54: Evaluation of peak area under O-H bands ($3000\text{-}3600\text{ cm}^{-1}$) of the FTIR spectra of 30 mL 80 % base oil mixed with 20 % RME treated with and without various amounts of combined adsorbents of magnesium-aluminum hydrotalcite and 1,3,5-trimethyl-2,4,6-tris(3,5-di-tert-butyl-4-hydroxybenzyl) benzene in a ratio of 1:2 respectively in various amount and aged at $170\text{ }^{\circ}\text{C}$ with airflow of 10 L/h for 80 h using a Rancimat

8.3.7 Impact of adsorbents on metallic oil additives

From section 3.5, it is observed that oil additives get depleted either by decomposition, adsorption onto metal and other surfaces, or separation because of settling and filtration. Since oil additives vary in composition and come in organic and inorganic forms, it is imperative to ensure that the adsorbents' use does not significantly affect their composition. The polarity of oil additives must be considered in adsorbents because they contain heteroatoms within their molecules. The impact of adsorbents on the oil additives cannot be generalized since some oil additives contain polar and nonpolar parts. Therefore, the additives must be treated differently for metals or metallic salts and non-metallic components.

The concentrations of Boron, Calcium, Sodium, Phosphorus, silicon, and Zinc (see Table 2) representing the metallic content are determined using the ICP-MS. Mannol engine oil and different neat oil additives are tested. The samples are treated with 0.675 g of the combined adsorbents of magnesium-aluminum hydrotalcite and 1,3,5-trimethyl-2,4,6-tris(3,5-di-tert-butyl-4-hydroxybenzyl) benzene in a ratio of 1:2 respectively and aged at 170 °C with an airflow of 10 L/h for different durations to see the impact of the adsorbents on the additives using a Rancimat.

The results in Figure 55 show the concentration of the selected elements in Mannol engine oil treated with and without the adsorbents and aged at 170 °C for 48 h. The concentration is reported in percentage as the measurement is normalized. There is essentially no significant negative impact of the adsorbents on the additives. The mixture treated with the adsorbents showed a relatively enhanced concentration of the additives' elements after aging for 48 h. The enhanced concentration of the elements could result from the adsorbents' use since the adsorbents contributed to the suppression of the oxidation process with its liable hydrogens and the impact of the additives. Since the adsorbents' action is not physical sorption, one can state that there seems to be no observable interaction between the adsorbents and the blend's additives. Hence, fewer additives, especially the antioxidants, might have been used in synergy with the adsorbents. The concentration of silicon element, however, shows less concentration in the mixture treated with the adsorbents. It could be a measurement mistake.

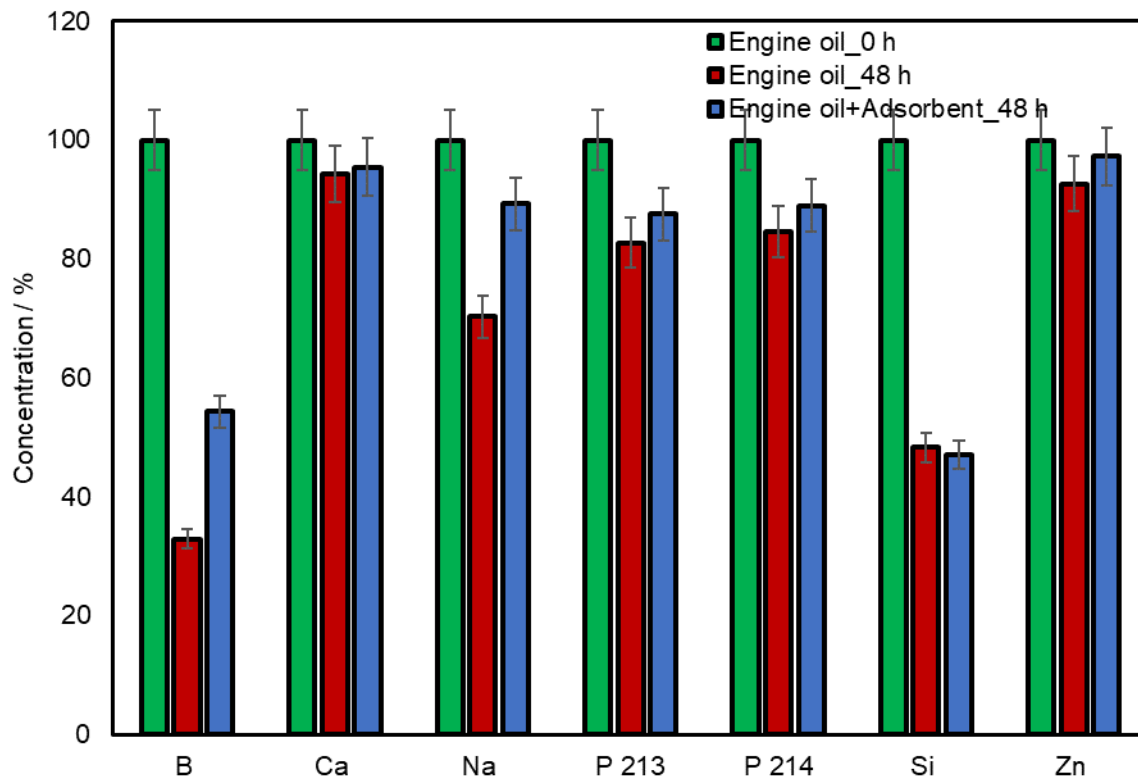


Figure 55: Evaluation of concentration of selected elements in 30 mL Mannol engine oil treated with and without combined 0.675 g adsorbents of magnesium-aluminum hydrotalcite and 1,3,5-trimethyl-2,4,6-tris(3,5-di-tert-butyl-4-hydroxybenzyl) benzene in a ratio of 1:2 respectively and aged at 170 °C with airflow of 10 L/h for 48 h using a Rancimat

Figure 56 illustrates the normalized concentration of selected elements in VanlubeBHC additive treated with and without the 0.675 g combined adsorbents and aged at 170 °C for 60 h using a Rancimat. While the concentration of the elements in the mixture not treated with the adsorbents and aged decreased substantially, the mixture's concentration in the mixture treated with the adsorbents and aged remains relatively close to the neat mixture's concentration. The explanation for this observed trend does not differ from the non-physical interaction between the adsorbents and the additive in the blend, just as the experiment with Mannol engine oil.

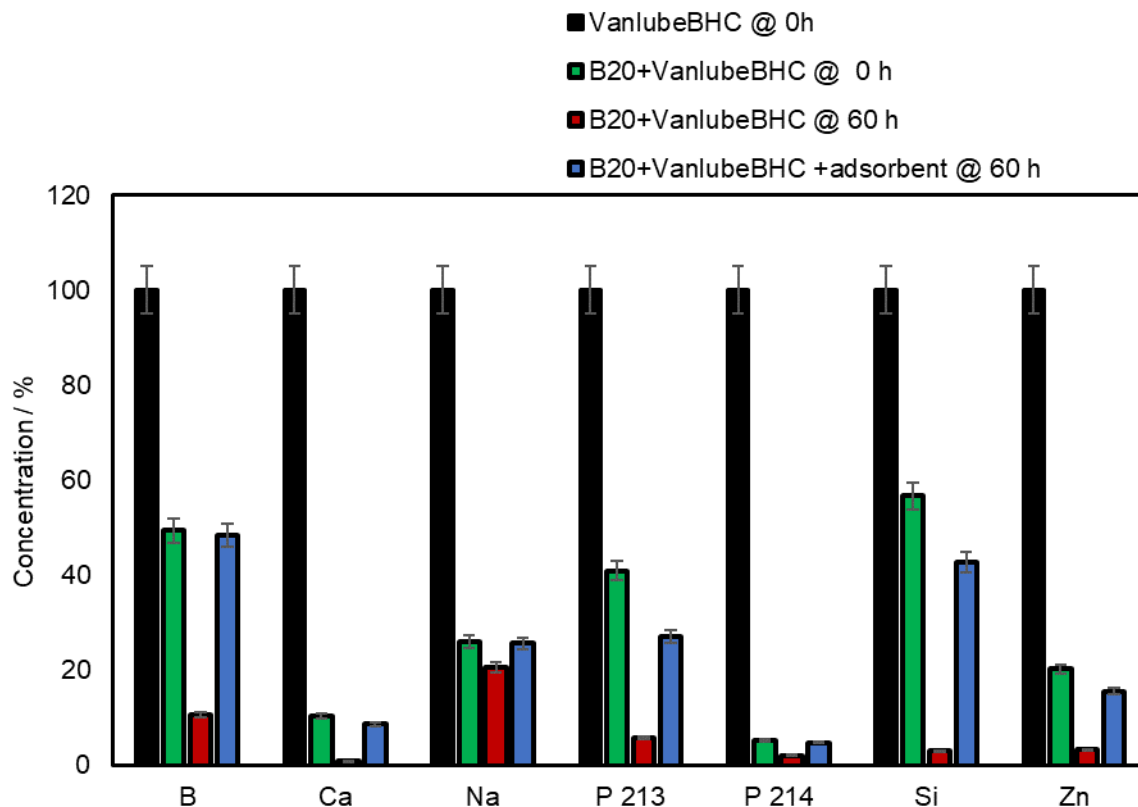


Figure 56: Concentration of selected elements in 30 mL of B20 mixed with VanlubeBHC additive treated with and without combined 0.675 g adsorbents of magnesium-aluminum hydrotalcite and 1,3,5-trimethyl-2,4,6-tris(3,5-di-tert-butyl-4-hydroxybenzyl) benzene in a ratio of 1:2 respectively and aged at 170 °C with airflow of 10 L/h for 60 h using a Rancimat

Figure 57 shows the normalized concentration of the selected elements in butylated hydroxytoluene (BHT) additive mixed with a base oil and treated with and without combined adsorbents and aged at 170 °C for 50 h duration. The results show that there is essentially no net negative impact on the additives by the adsorbents. Since BHT is an antioxidant, it is expected to resist oxidation during this aging duration and reduce its concentration. However, in the mixtures treated with the adsorbents, BHT concentration is relatively affected by the aging process. It could result from the synergic effects of the BHT and the adsorbents in suppressing the oxidation process. The net effect, however, is not linear between the different selected elements under consideration.

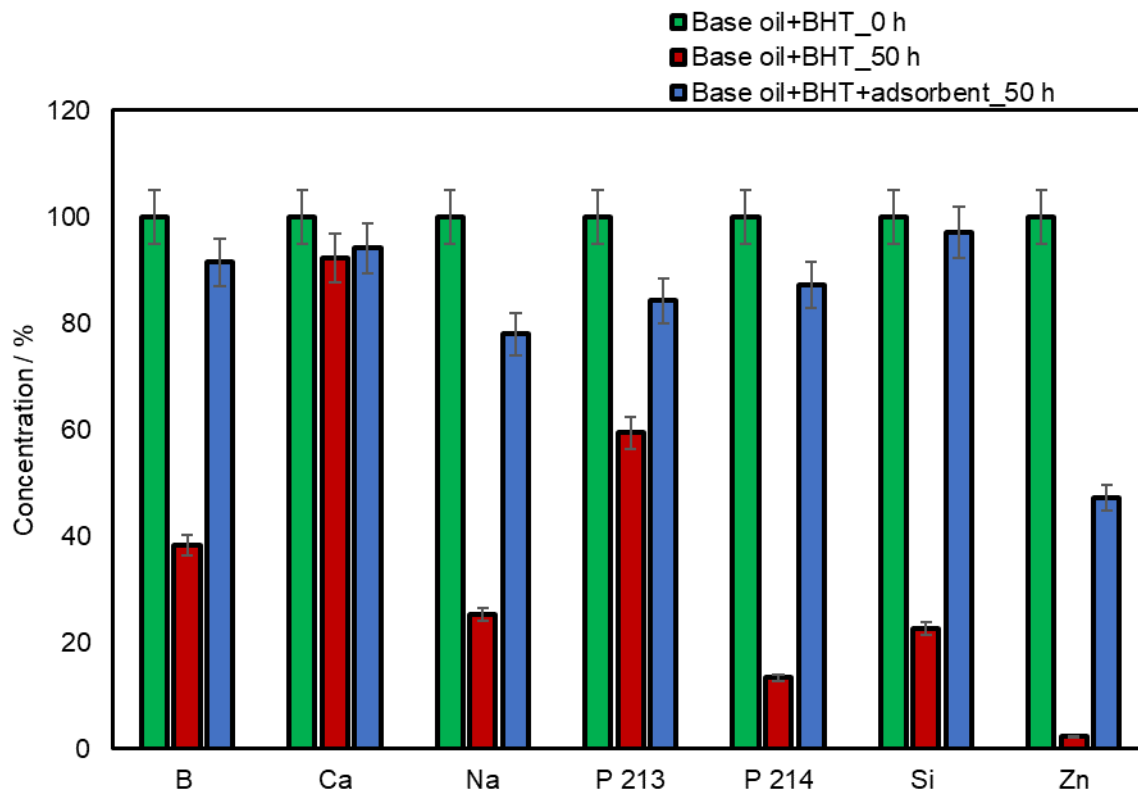


Figure 57: Concentration of selected elements in 30 mL base oil blended with BHT additive treated with and without combined 0.675 g adsorbents of magnesium-aluminum hydrotalcite and 1,3,5-trimethyl-2,4,6-tris(3,5-di-tert-butyl-4-hydroxybenzyl) benzene in a ratio of 1:2 respectively and aged at 170 °C with airflow of 10 L/h for 50 h using a Rancimat

Figure 58 illustrates the selected elements' concentration in a detergent additive mixed with a base oil, treated with and without adsorbents, and aged at 170 °C for 50 h. Atoms are neither created nor destroyed, but the comparison of values of the elements in mixtures treated with adsorbents and the neat aged mixtures indicates possible additive depletion or mixing. The results essentially do not differ from that of the other measurements. The mixtures treated with the adsorbents have pretty higher amounts of additives after aging for 80 h. The adsorbents have no or negligible impact on the additives.

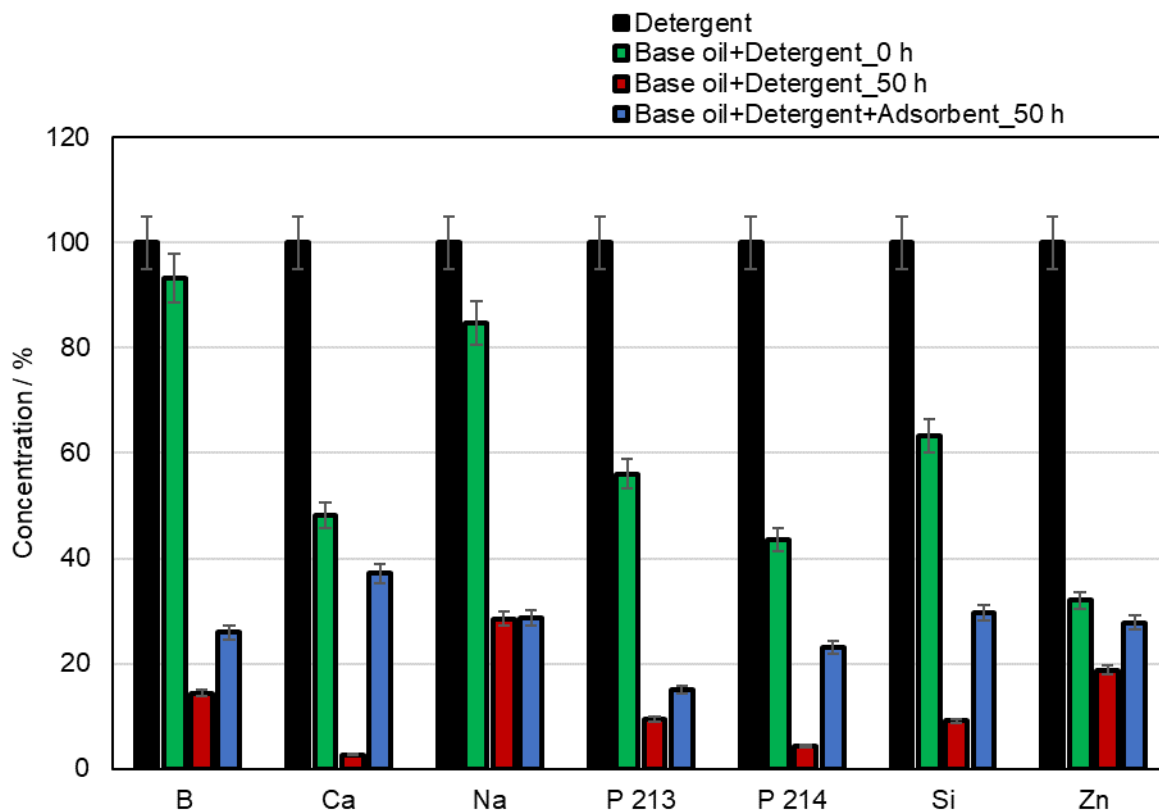


Figure 58: Concentration of selected elements in 30 mL base oil blended with detergent and treated with and without the combined 0.675 g adsorbents of magnesium-aluminum hydrotalcite and 1,3,5-trimethyl-2,4,6-tris(3,5-di-tert-butyl-4-hydroxybenzyl) benzene in a ratio of 1:2 respectively and aged at 170 °C with airflow of 10 L/h for 50 h using a Rnacimat

The concentration of the selected elements in a corrosion inhibiting additive treated with and without the adsorbents and aged is shown in Figure 59. The mixtures are aged at 170 °C for 50 h. While there is a drastic reduction in the concentration of elements in mixtures aged without adsorbents treatment like in all other measurements on the additives before, the concentration in the mixtures treated with the adsorbents and aged are much higher. These results confirm that the adsorbents' suppression action is through the donation of liable hydrogen and not physical adsorption. As such, it does contribute synergistically to curb the degradation of the oil.

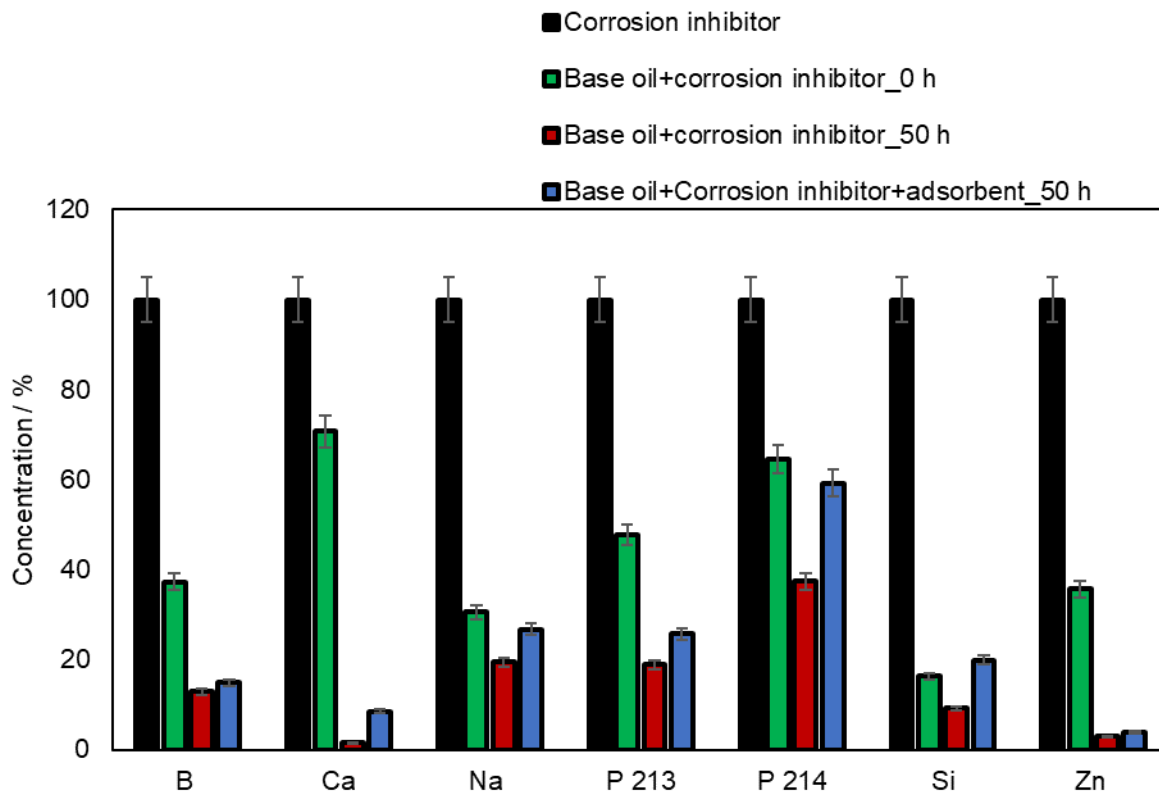


Figure 59: Concentration of selected elements in 30 mL base oil blended with corrosion inhibitor additive treated with and without combined 0.675 g adsorbents of magnesium-aluminum hydrotalcite and 1,3,5-trimethyl-2,4,6-tris(3,5-di-tert-butyl-4-hydroxybenzyl) benzene in a ratio of 1:2 respectively and aged at 170 °C with airflow of 10 L/h for 50 h using a Rancimat

8.3.8 Impact of adsorbent on organic additives in the oil

Consider the impact of the adsorbents on the additives' non-metallic components (see section 3.5). The additive concentrations are determined using gas chromatography with flame ionization detection (GC-FID), and the results are illustrated. In the chromatogram, blends without the additive are compared with the same blend with the additive included. It is observed that the peaks are the additive contribution since the same peaks are absent in the blend without the additive. In all the illustrations below, Figure 60, Figure 62, and Figure 64, the additive peak in the sample treated with the adsorbents can be seen to degrade about 50 % less than in the sample aged without using the adsorbents. This pattern of the adsorbents' effect on the additives in all the pure additives assessed showed

very similar results. The results indicate no observable apparent negative interactive impact of the adsorbents with the additives' organic components.

Figure 60 and more clearly in Figure 61 is shown the GC-FID chromatogram of VanlubeBHC additive treated with and without the adsorbents and aged at 170 °C with an airflow of 10 L/h for 80 h duration using the Rancimat. The VanlubeBHC additive peaks begin to appear after about 18.5 min until about 21 min. These peaks are absent from the neat base oil and RME mixture signifying the peaks are the additives' contribution only. The highest peak occurred at about 19.5 min. The additive peaks in the mixture treated with the adsorbents after 80 h of aging reduce by about 50 % of the unaged mixture compared with those without the adsorbents' treatment. Because the additive is an antioxidant that should have depleted at the same rate as the mixture aged without the adsorbents treatment, it can only be said that the adsorbents contributed in synergy to the suppression of the oxidation process resulting in less amount of the additive been used.

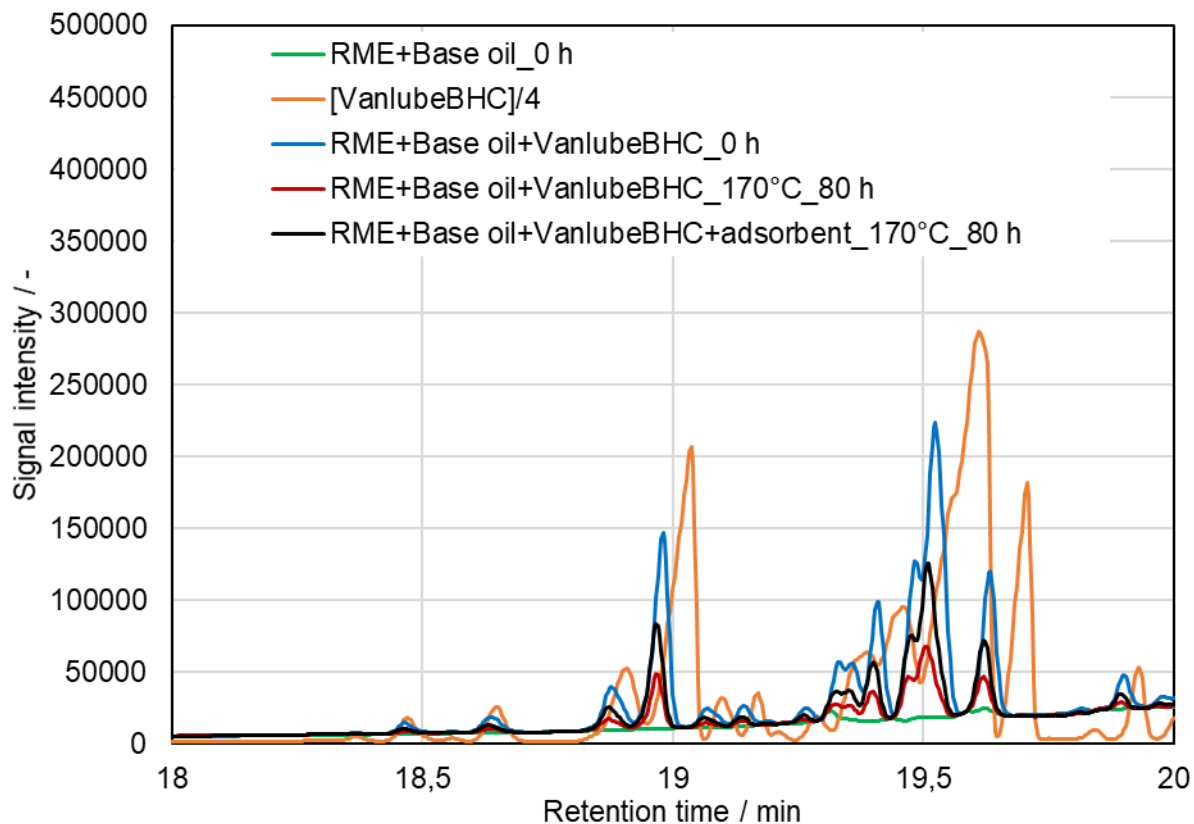


Figure 60: GC-FID chromatogram of 30 mL of 80 % base oil blended with 20 %RME and mixed with VanlubeBHC neat additive treated with and without combined 0.675 g adsorbents of magnesium-aluminum hydrotalcite and 1,3,5-trimethyl-2,4,6-tris(3,5-di-tert-butyl-4-hydroxybenzyl) benzene in a ratio of 1:2 respectively and aged at 170 °C with airflow of 10 L/h at 8 h per day for 80 h using a Rancimat

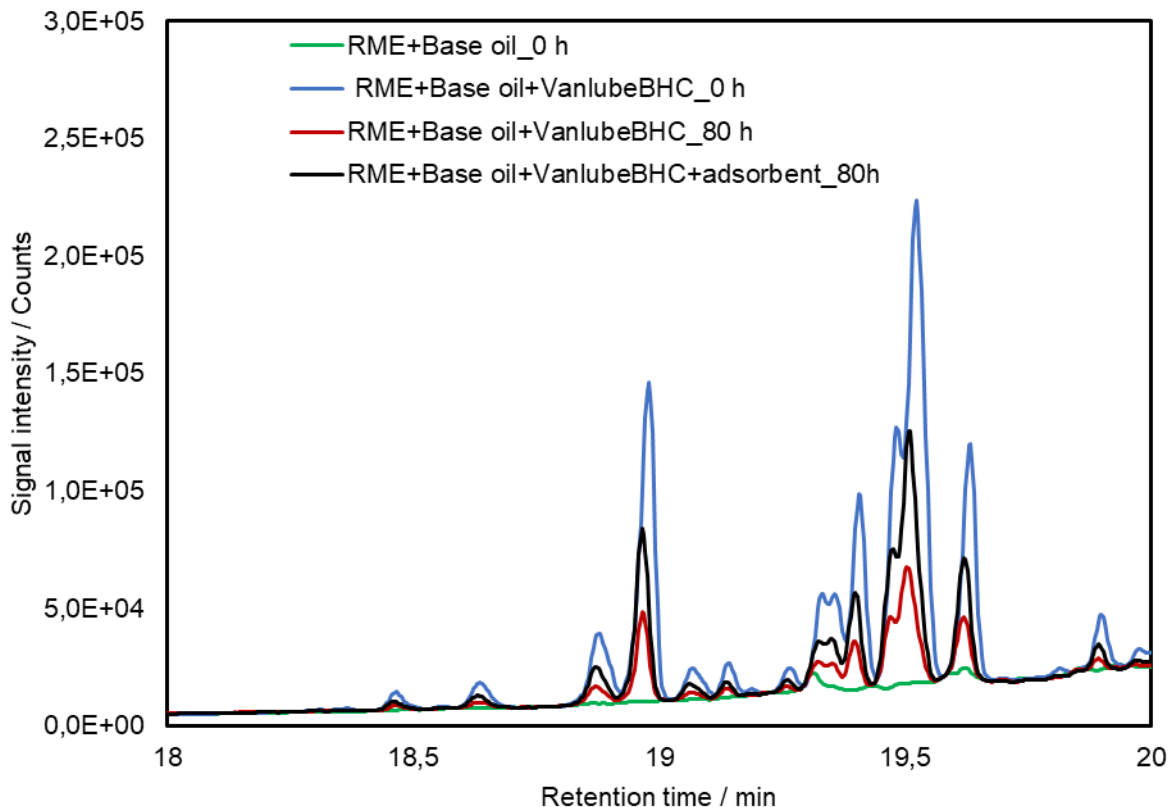


Figure 61: GC-FID chromatogram of 30 mL of 80 % base oil blended with 20 %RME and mixed with VanlubeBHC neat additive treated with and without combined 0.675 g adsorbents of magnesium-aluminum hydrotalcite and 1,3,5-trimethyl-2,4,6-tris(3,5-di-tert-butyl-4-hydroxybenzyl) benzene in a ratio of 1:2 respectively and aged at 170 °C with airflow of 10 L/h at 8 h per day for 80 h using a Rancimat

Changes occurring on the concentration of additive Vanlube961 mixed with a base oil and treated with and without the adsorbents and aged at 170 °C for 40 h are shown in Figure 62. The additive peaks in the mixture treated with the adsorbents show less degradation of about 48 % better than those aged without the adsorbent treatment. A peak occurring at about 21.5 min presents an interesting observation. The peak is absent on the graph for the neat aged additive and base oil mixture, and it is also absent from the graph on the neat and unaged additive and base oil mixture treated with the adsorbents. Imperatively, the peak is a product of oxidation.

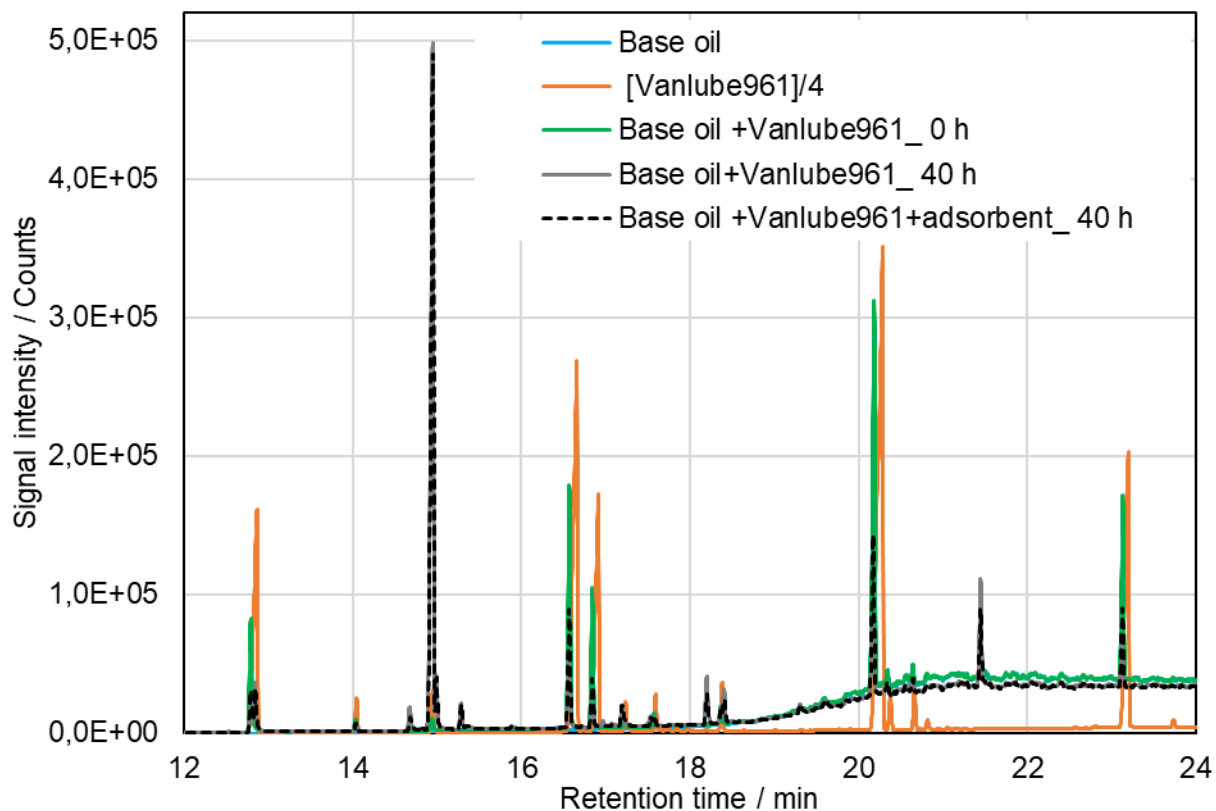


Figure 62: GCFID chromatogram of 30 mL of base oil blended with Vanlube961 additive treated with combined adsorbents of magnesium-aluminum hydrotalcite and 1,3,5-trimethyl-2,4,6-tris(3,5-di-tert-butyl-4-hydroxybenzyl) benzene in a ratio of 1:2 respectively and aged at 170°C with airflow of 10 L/h at 8 h per day for 40 h using a Rancimat

Notably, the oxidation product's peak is less intense in the mixture treated with the adsorbents than the mixture aged without the treatment with the adsorbents. From about 16 to 18 min retention time, one can observe that the adsorbents' use impacted the additive's aging degradation. Hence, the mixture treated with the adsorbents degraded less. At about 16.56 min, the peak shows considerable registered degradation in the mixture without applying the adsorbents. From an initial signal count of about 179,282, the mixture aged without the adsorbents treated degraded by about 70 %.

In comparison, the same mixture was treated with the adsorbents and aged degraded by about 53 %. Another peak that appeared at 16.84 min also degraded by about 79 % in the mixture aged without applying the adsorbents, while the mixture with the adsorbent application degraded by about 65 %. The degradation at 16.56 min occurs in a ratio of

1:1.6 while that of the 16.84 min, the ratio is 1:1.7. Essentially, the degradation ratio shows that the adsorbents' impact on these two different peaks is the same. Conclusively, it can be said that the adsorbents play a role in retarding the oxidation process through their liable hydrogen atom on their surfaces and not physical adsorption and hence less on the concentration of the vanlube961 additive as seen in the graph.

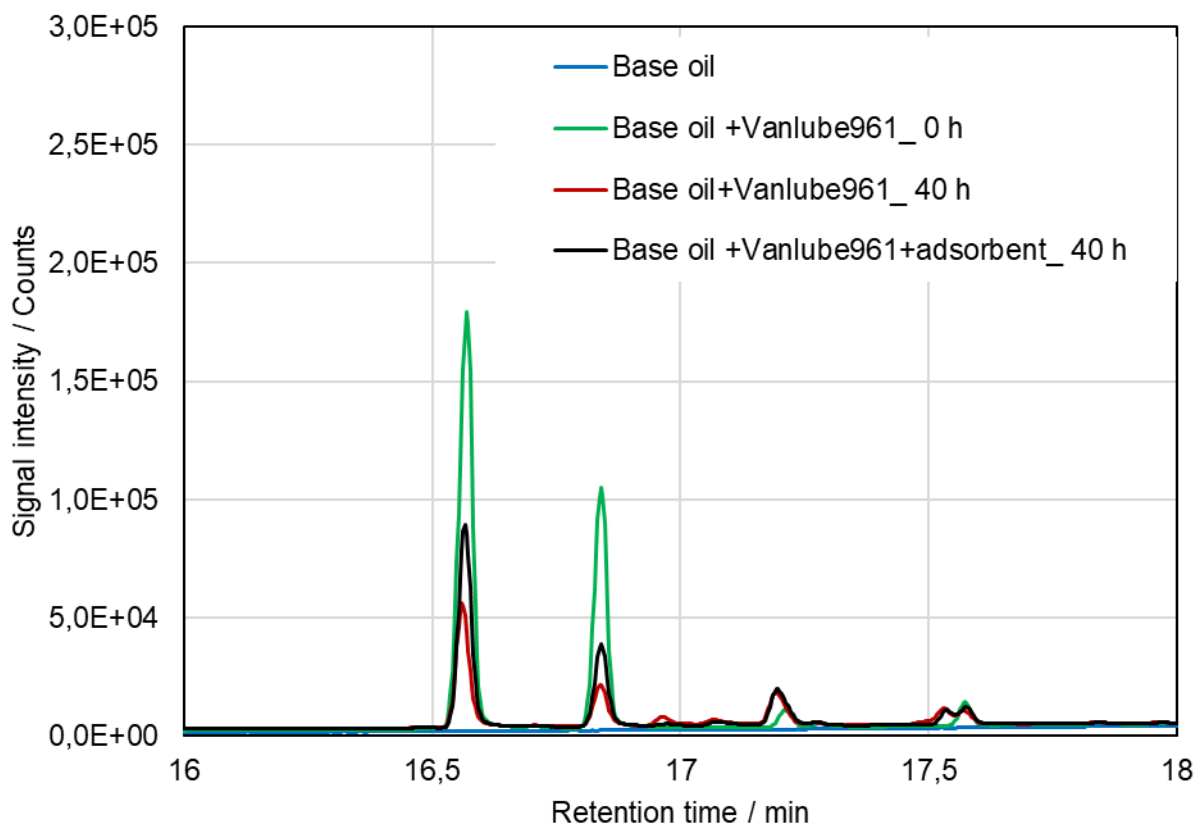


Figure 63: GCFID chromatogram of 30 mL of base oil blended with Vanlube961 and treated with and without the combined 0.675 g adsorbents of magnesium-aluminum hydroxide and 1,3,5-trimethyl-2,4,6-tris(3,5-di-tert-butyl-4-hydroxybenzyl) benzene in a ratio of 1:2 respectively and aged at 170 °C with airflow of 10 L/h at 8 h per day for 40 h using a Rancimat

A rather strange trend is observed for a lubricity additive mixed with a base oil and treated with and without the adsorbents and aged at 170 °C for 50 h duration (Figure 64). A lubricity additive is an additive that is added to lubricating oil to perform one or more specific tasks. These tasks include reducing wear, lowering torque through reduced friction, preventing metal-metal welding, or controlling friction within a specific range (Yuegang, 2016). Since none of those, as mentioned earlier, tasks occur during this

laboratory aging process, one would expect the additive concentration to remain unchanged, but this has not been the case. The additive peak is completely degraded in both the mixtures treated with and without the adsorbents and aged at 170 °C for 50 h.

Further analysis needs to be pursued on this effect. However, it has been shown that additive aging is independent of the presence or absence of the adsorbents. Hence the adsorbents have no impact on the additive, and this is the goal of this experiment.

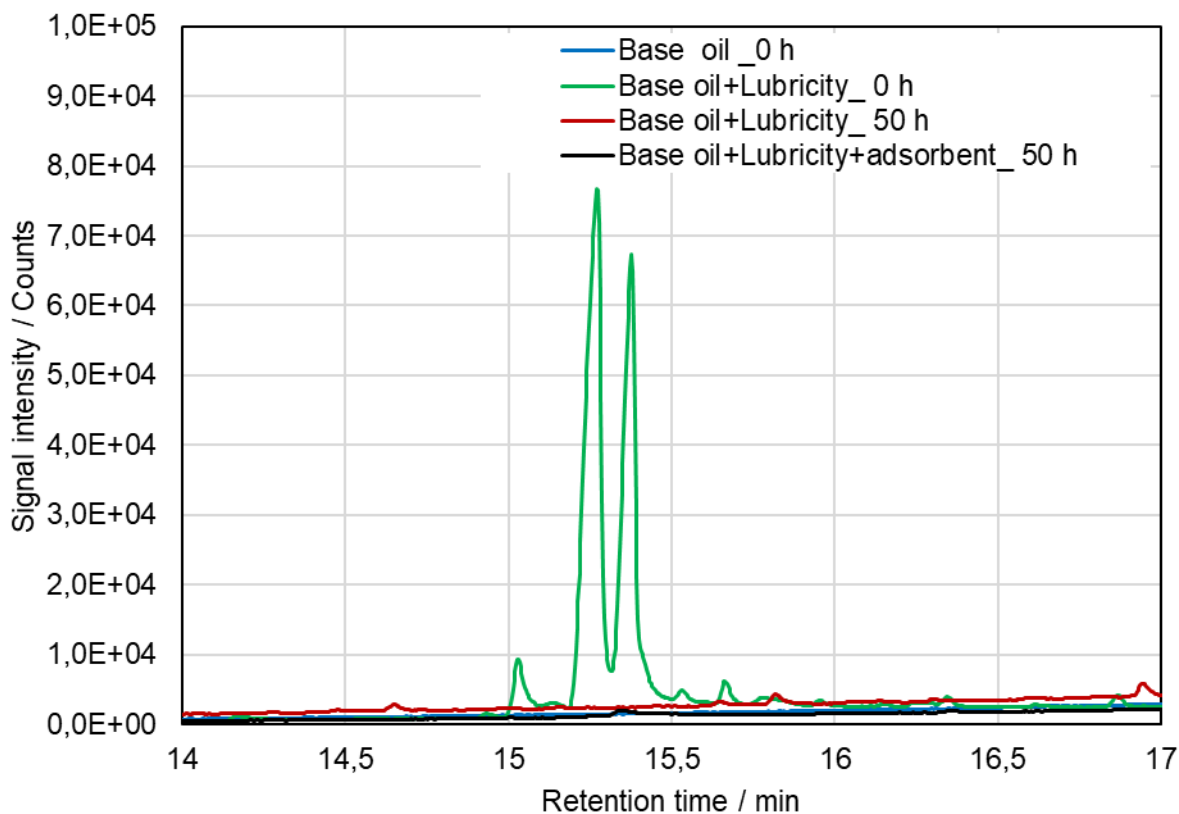


Figure 64: GCFID chromatogram of 30 mL of lubricity additive mixed with a base oil and treated with and without combined 0.675 g adsorbents of magnesium-aluminum hydrotalcite and 1,3,5-trimethyl-2,4,6-tris(3,5-di-tert-butyl-4-hydroxybenzyl) benzene in a ratio of 1:2 respectively and aged at 170 °C with airflow of 10 L/h at 8 h per day for 50 h using a Rancimat

Summary

The experiment has been carried out to test the impact of the combined adsorbents magnesium-aluminum hydrotalcite and 1,3,5-trimethyl-2,4,6-tris(3,5-di-tert-butyl-4-hydroxybenzyl) benzene in a ratio of 1:2 respectively in masses of 0.225 g, 0.45 g, and 0.675 g and aged at 170 °C using a Rancimat running with airflow of 10 L/h at 8 h per day for a total of 80 h in suppressing the degradation of 30 mL of 80 %base oil blended with 20 % biodiesel. The adsorbents are applied to the blend and aged at 170 °C, and their impact on the degradation process is evaluated by tracking the physio-chemical changes occurring during oxidation. The use of different amounts of adsorbents showed that the suppression beyond a specific duration of aging is independent of the amount of the adsorbent applied. It is because the adsorbents have a capacity for their adsorption efficiency. Its structure explains the efficiency of the adsorbents. The 1, 3, 5-trimethyl-2, 4, 6-tris (3, 5-di-tert-butyl-4-hydroxybenzyl) benzene has three hydroxyl groups (OH) in its aromatic rings, and the hydrogen atom abstracted from the OH is donated to the free radical to interrupt the chain propagation with the interaction of hydrogen atom from the surface of the hydroxyl group of the trapping agent with the immediate peroxy radicals and inhibit the rate of oxidation in the biodiesel.

Linoleic acid methyl ester (C18:2 ME) is chosen because it is one of the primary components responsible for the enhanced formation of oligomers (Dugmore, 2011). It is worthy to note that during the oxidation of the base oil and C18_2ME mixture treated with the adsorbents for 80 h, the C18_2ME peak intensity is reduced by about 40 % of the original mixture not treated with the adsorbents had degraded completely. The adsorbents' use led to about 60 % reduction in oligomer formation, a total acid value reduction of about 90 %, and more than 50 % reduction in viscosity increment. The adsorbents increase the oil resistance towards the formation of secondary oxidation products, leading to an increase in acid number, viscosity, density, and others. It falls in agreement with the work of Dinkov et al. (2009).

Oil additives are depleted either by decomposition, adsorption onto metal, or other surfaces or separation because of settling and filtration. The impact of adsorbents on oil additives has been tested. The concentration of the selected elements, Boron, Calcium,

Sodium, Phosphorus, silicon, and Zinc, show no observable negative interaction of the adsorbents with the inorganic components of the additives. On the other hand, the results from GC-FID determination indicate no apparent negative interactive impact of the adsorbents with the additives' organic components. The selected elements in their stable state have no direct interaction with the adsorbents chemically. The adsorbent's impact on the biodiesel's oxidation is due to its donation of hydroxyl ion on its surface structure, making it unable to react with the additives and cause their reduction in quantity.

According to Gili et al. (2011), the shortening of the recommended oil drains due to biodiesel dilution is between 30 % and 60 %, with a corresponding increase in deposit formation. Suppose emissions, soot, and other products do not impact the adsorbents' capacity during the engine run. In that case, it suffices to say that using the adsorbents at 90 g per 4 L of the engine oil would eliminate the above percentage dilution factor and promote the typically required length of the engine oil's useful life despite the presence of the biodiesel. It is considered that no other internal combustion processes, such as soot production, etc., will impact the adsorbents. Adding the adsorbents seems to be an easy path to delaying the rate of oxidation. It must be stated that the optimum impact of the adsorbents in suppressing the oxidation process depends on the concentration or the amount of the adsorbents applied to the process. The use of adsorbents, therefore, results in a good yield of oxidation suppression.

Usually, engine oil needs to be replaced every 5000 miles. With biodiesel dilution resulting in a 60 % reduction in the recommended oil drain interval, according to Gili et al. (2011), the oil will have to be changed after 3000 miles coverage if the above percentage is actual. Imperatively, the use of 90 g of the adsorbents at its 60 % efficiency will eliminate this effect and enable the standard 5000 miles to be covered if there are no other interferences.

Estimating approximately 726,000 passenger cars in Germany, equipped with diesel particulate filters and average annual mileage of approximately 18,500 kilometers on a volume of four liters of oil per vehicle. It translates into an annual total of 2,904,000 liters of oil. Applying these adsorbents at an efficiency of 60 % would translate into a saving of about 1,742,400 liters of engine oil annually and save the environment from oil waste.

8.4 Using combined adsorbents of magnesium-aluminum hydrotalcite and 1,3,5-trimethyl-2,4,6-tris(3,5-di-tert-butyl-4-hydroxybenzyl) benzene in a ratio of 1:2 respectively to cause stabilization of biodiesel and its blends at 170 °C

The evaluation of biodiesel's oxidative stability and blends is based on changes in viscosity, total acid number, and absorption changes at 1710cm^{-1} using FTIR spectroscopy and the buildup of higher molecular mass substances.

8.4.1 SEC analysis of biodiesel blends (20 %RME mixed with 80 %diesel fuel) treated with and without 1 g combined adsorbents of magnesium-aluminum hydrotalcite and 1,3,5-trimethyl-2,4,6-tris(3,5-di-tert-butyl-4-hydroxybenzyl) benzene in a ratio of 1:2 respectively and aged at 170 °C with airflow of 10 L/h using a Rancimat

The size exclusion chromatography (SEC) analysis detects the changes in the built molecules' molar mass during the aging process. In Figure 65 and Figure 66, the chromatograms of neat B20 and 30 mL B20 treated with 1 g combined adsorbents of magnesium-aluminum hydrotalcite and 1,3,5-trimethyl-2,4,6-tris(3,5-di-tert-butyl-4-hydroxybenzyl) benzene in a ratio of 1:2 respectively after an aging duration of up to 48 h are shown. While the unaged mixture had a relative molar mass of about 500 g/mol, the blends treated with the adsorbent and aged had a relative molar mass of about 550 g/mol, and the mixture aged without any adsorbent treatment recorded a relative molar mass of about 1100 mg/mol. This SEC analysis presents a higher molar mass species indicating more giant molecules' building during the mixtures' aging process without any adsorbent treatment. The lower curves in Figure 65 illustrate the effect of adding adsorbents at the indicated concentrations. As expected, the oxidation is almost wholly inhibited, resulting in a very marginal buildup of oxidation products. The results observed in Figure 67 confirm the adsorbents' significant impact in reducing the initial oxidation rate by about 75 %.

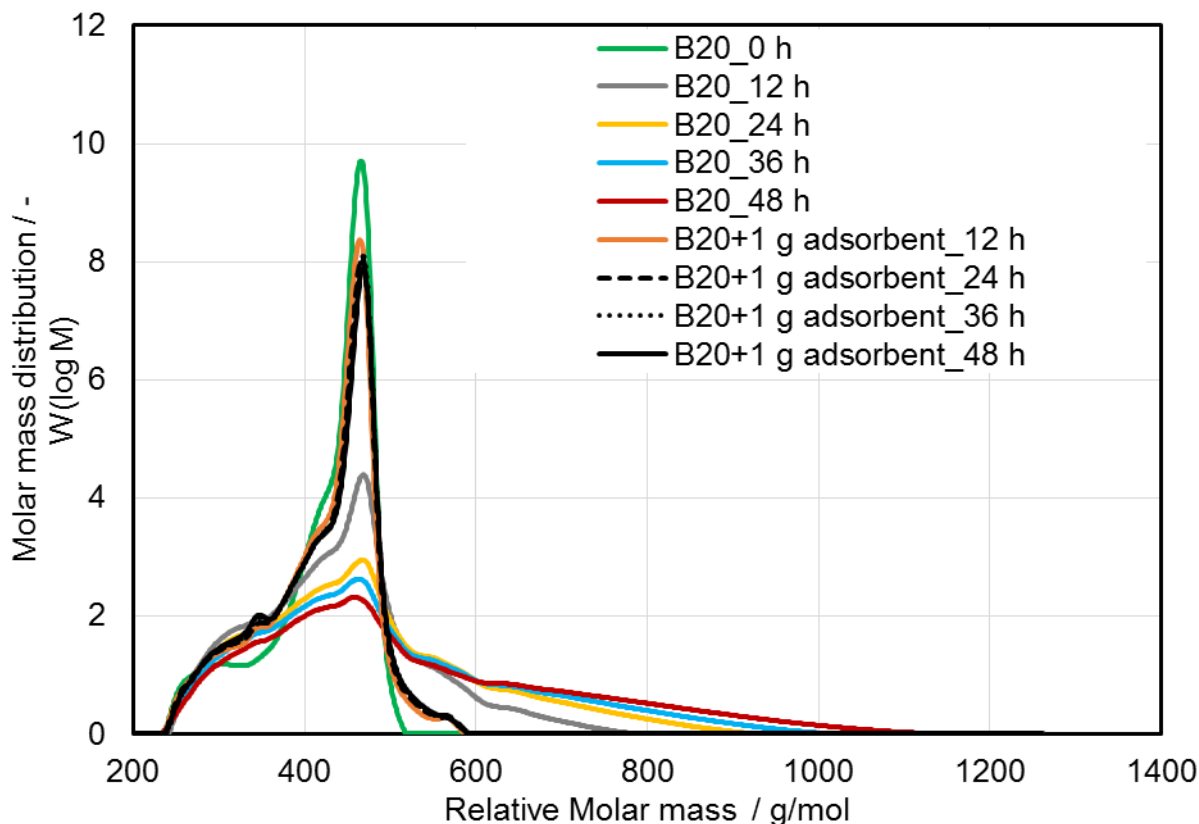


Figure 65: SEC chromatogram of 30 mL 20 %RME mixed with 80 %diesel fuel and treated with and without combined 1 g adsorbents of magnesium-aluminum hydrotalcite and 1,3,5-trimethyl-2,4,6-tris(3,5-di-tert-butyl-4-hydroxybenzyl) benzene in a ratio of 1:2 respectively and aged at 170°C at 8 h per day with airflow of 10 L/h using a Rancimat

The analysis results with SEC collaborate with the FTIR and confirm the low molar mass built up for the B20 treated with adsorbents, Figure 66. It indicates the adsorbents' ability to suppress the formation of higher molecular masses substances during the aging process. The amounts of formed high molecular mass species increased consistently with aging time in the blend aged without any adsorbent treatment. Since the formation of oligomers depends on hydroperoxides presence and a similar pattern of development is not observed in the samples treated with the adsorbents, it can be said that the adsorbents impacted the production of hydroperoxides, that is, during the initiation stage of the oxidation process. As explained in section 6.2, the complex secondary reactions are suppressed with the interception of the adsorbents' oxidative precursors, which results in low molecular mass products. The adsorbents' application resulted in a marginal increase

in higher molecular species by 21 %, 16 %, 14 %, and 13 %, with increasing aging duration for 12, 24, 36, and 48 h, respectively.

On the other hand, the mixture aged without the adsorbent treatment resulted in high molecular species growth in the ranges of 73 %, 84 %, 85 %, and 86 %, respectively. It is, therefore, clear from Figure 67 that with the increasing duration of aging, the formation of oligomers increases. It signifies a linear relationship between the number of oligomers formed and the duration of aging.

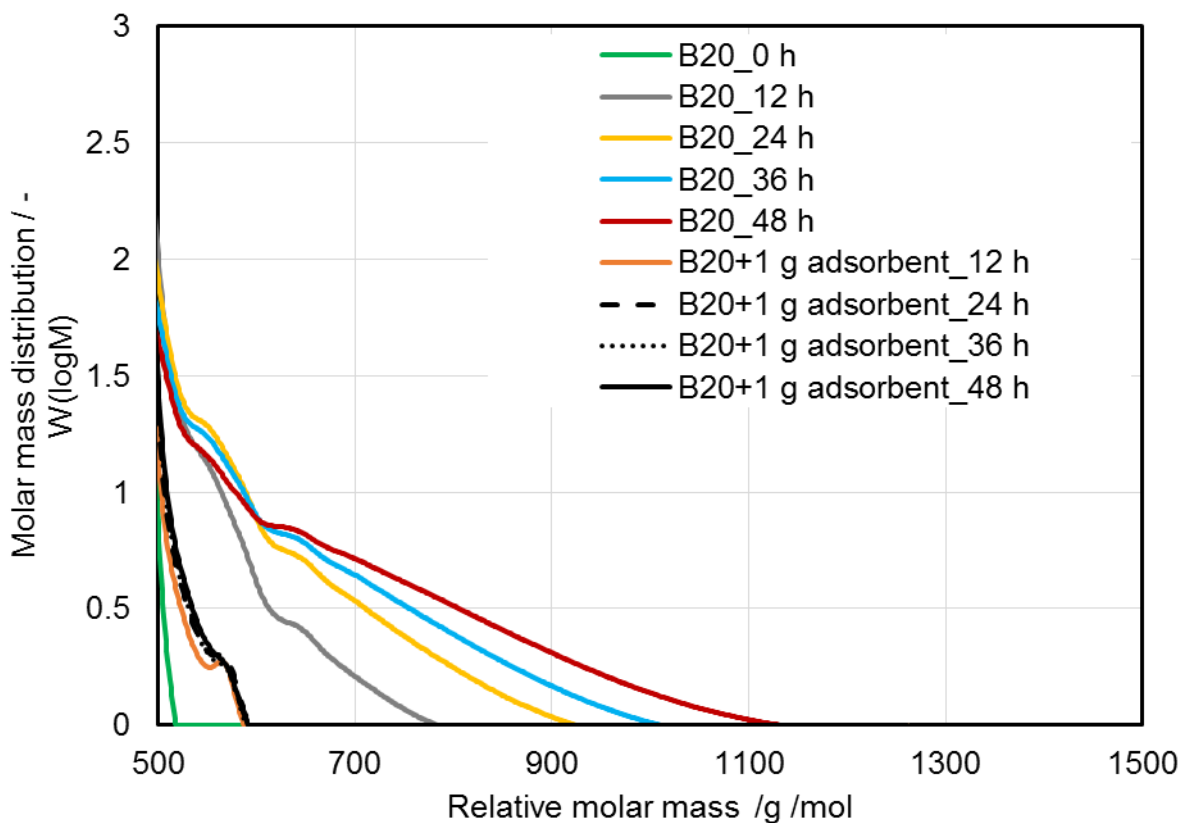


Figure 66: Zoom in on the region of higher molecular masses of 30 mL 20 %RME mixed with 80 %diesel fuel and treated with and without combined 1 g adsorbents of magnesium-aluminum hydrotalcite and 1,3,5-trimethyl-2,4,6-tris(3,5-di-tert-butyl-4-hydroxybenzyl) benzene in a ratio of 1:2 respectively and aged at 170°C with airflow of 10 L/h at 8 h per day using a Rancimat

The adsorbent's efficiency in retarding the oxidation process is represented by the amount of molar mass build-up. The more efficient the adsorbents, the less the amount of higher molecular mass substances formed. For aging 48 h, an efficiency of about 87 % in

oxidation suppression is registered. The results, however, show that the mixture of diesel fuel and RME at the onset of the aging had already undergone some form of degradation. In Figure 67, while B20 aged without the adsorbent treatment had a higher molecular mass substance built up by a factor of 7, the same B20 treated with the adsorbents had a factor of 0.13 of higher molecular mass substances formed. Thus, demonstrating the impact of the adsorbents in the suppression of the oxidation process. With the treatment with the adsorbents, the average build-up of higher molecular substances is about 16 %. The result is very insignificant as compared with the blends aged without any adsorbent treatment.

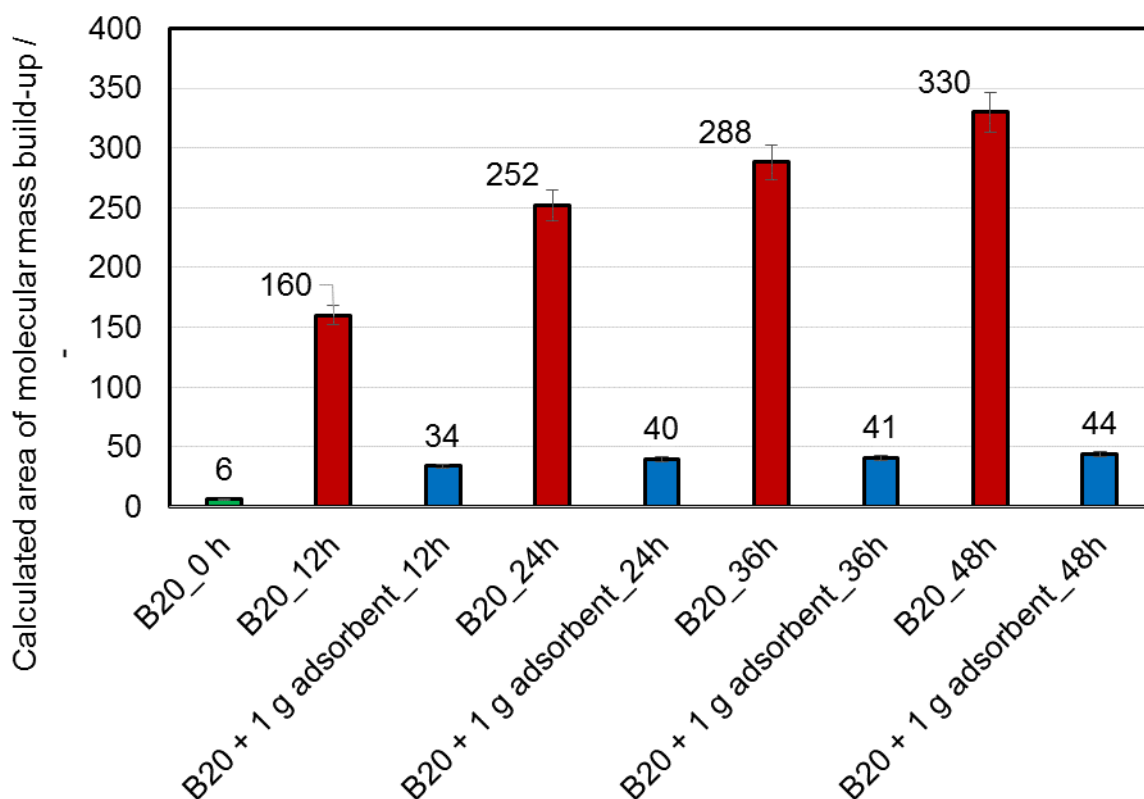


Figure 67: Effective area under the curves of a molecular mass buildup of oligomers of 30 mL 20 %RME mixed with 80 %diesel fuel and treated with and without combined 1 g adsorbents of magnesium-aluminum hydrotalcite and 1,3,5-trimethyl-2,4,6-tris(3,5-di-tert-butyl-4-hydroxybenzyl) benzene in a ratio of 1:2 respectively and aged at 170°C with airflow of 10 L/h at 8 h per day using a Rancimat

8.4.2 GCMS analysis of 80 %diesel fuel mixed with 20 %RME treated with and without combined 1 g adsorbents of magnesium-aluminum hydrotalcite and 1,3,5-trimethyl-2,4,6-tris(3,5-di-tert-butyl-4-hydroxybenzyl) benzene in a ratio of 1:2 respectively and aged at 170 °C with airflow of 10 L/h for 48 h at 8 h per day using a Rancimat

The GCMS analysis of 80 %diesel fuel blended with 20 %RME treated with and without the adsorbents and aged at 170 °C for 48 h is shown in Figure 68. The abscissa represents the retention times in min for which the respective components are eluted from the column. The ordinate caters for the amount or the counts of the various components present in the sample. The significant RME component peaks are as shown by the unaged mixture of diesel fuel and RME. The focus is more on the peaks at times, 36.1 and 36.3 min, respectively. These peaks, as aging progresses, get degraded. The degradation of these peaks is in the range of 16 % and 14 % at 36.1 and 36.3 min, respectively, for the mixture treated with the adsorbents. After the aging for 48 h at 170 °C, the signal for the RME in the mixture without the adsorbent treatment is degraded by about 89 %. This degradation correlates with the results of C18_2 ME in section 8.1.1, which polymerizes more at high temperatures (Kim et al., 2018). The signals of the unaged RME in the mixture are very prominent, as shown in Figure 68. The signals of the RME in the mixture treated with the adsorbent and aged are also very prominent. Because RME is rich in allylic hydrogen atoms that are susceptible to radical attack leading to the formation of peroxides, the adsorbents, through the interaction of its liable hydrogen atoms on its surface, intercepted these radicals, preventing the peroxides' formation. Hence, the low reduction in the degradation of the peaks of the RME in the blend treated with the adsorbents. The difference in the degradation of 16 % and 14 % is due to the different degrees of polymerization of the C18_2 ME component of the RME, as earlier explained in 8.1.1.

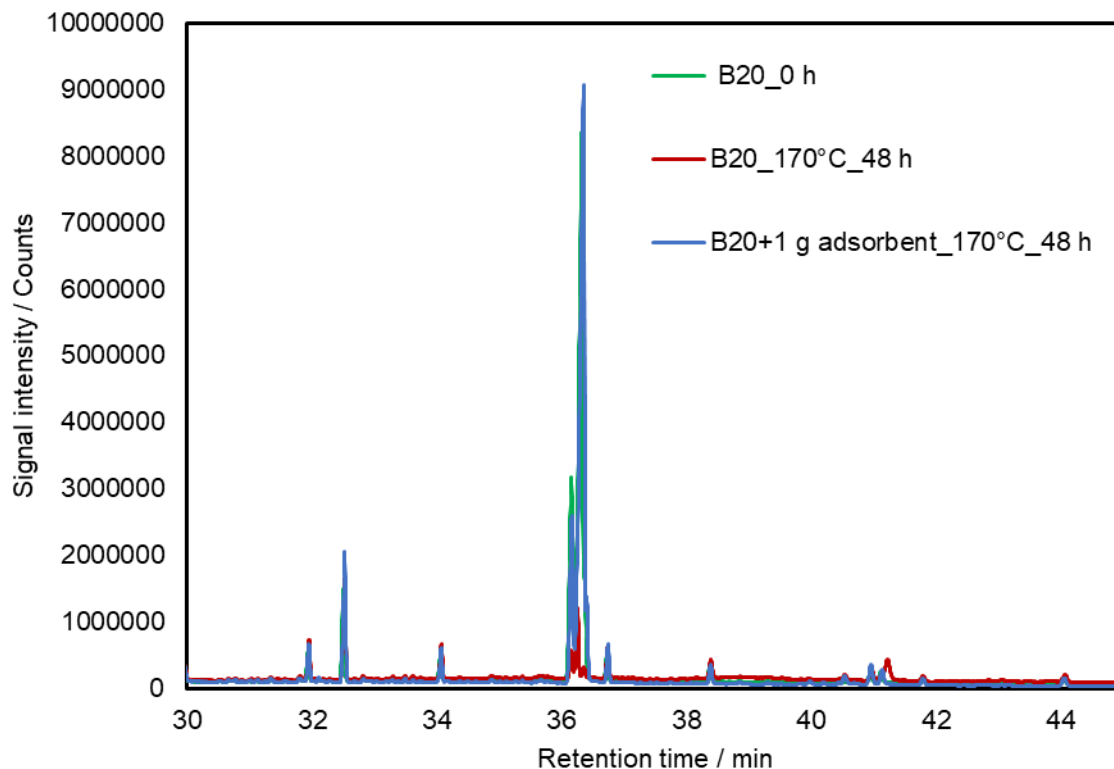


Figure 68: GCMS chromatogram of 30 mL 80 %diesel fuel mixed with 20 %RME treated with and without combined 1 g adsorbents of magnesium-aluminum hydrotalcite and 1,3,5-trimethyl-2,4,6-tris(3,5-di-tert-butyl-4-hydroxybenzyl) benzene in a ratio of 1:2 respectively and aged at 170 °C with airflow of 10 L/h for 48 h using a Rancimat

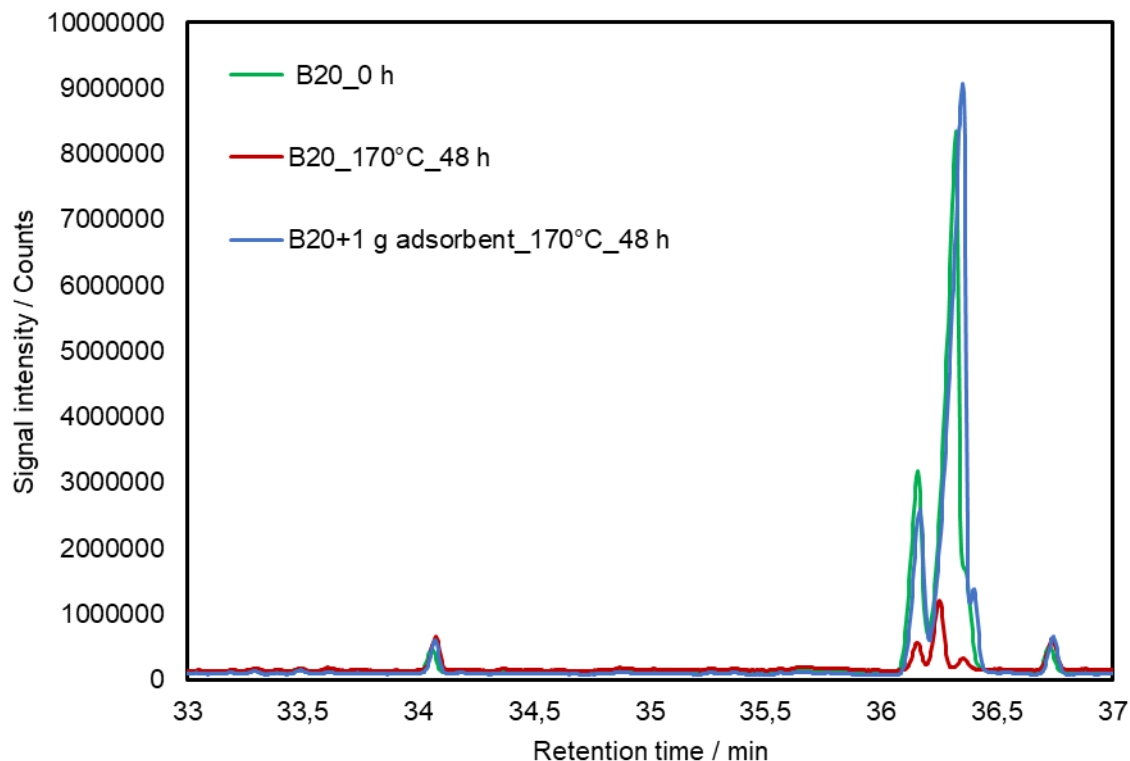


Figure 69: GCMS chromatogram of 30 mL 80 %diesel fuel blended with 20 %RME (retention time range:33-37 min) treated with and without combined 1 g adsorbents of magnesium-aluminum hydrotalcite and 1,3,5-trimethyl-2,4,6-tris(3,5-di-tert-butyl-4-hydroxybenzyl) benzene in a ratio of 1:2 respectively and aged at 170 °C with airflow of 10 L/h for 48 h at 8 h per day using a Rancimat compared with the neat unaged blend

8.4.3 The total acid value of 80 %diesel fuel mixed with 20 %RME treated with and without combined 1 g adsorbents of magnesium-aluminum hydrotalcite and 1,3,5-trimethyl-2,4,6-tris(3,5-di-tert-butyl-4-hydroxybenzyl) benzene in a ratio of 1:2 respectively and aged at 170 °C with airflow of 10 L/h for 48 h at 8 h per day using a Rancimat

Figure 70 illustrates the relationship between the acid value and the duration of aging at a constant temperature. From Figure 70, it is evident that generally, higher acid values result from a longer duration of aging. Hydroperoxides are produced during the oxidative degradation of the biodiesel or its blends, and they undergo complex secondary reactions, further oxidizing into acids. This increases in acid value (Knothe et al., 2010). As seen in

section 3.5.2, acidity increases with increasing aging. The hydroperoxides produced from the oxidation after the complex secondary reactions could also split into more reactive aldehydes, further oxidizing into acids and increasing acid value. The adsorbents' use has given stability to the sample by the interception of the oxidation process's precursors. 1,3,5-trimethyl-2,4,6-tris(3,5-di-tert-butyl-4-hydroxybenzyl) benzene possesses reduction potentials considerably lower than those of the free radicals generated during thermo-oxidation, can thus scavenge them (Aladedunye, 2011). The adsorbents react with peroxy radicals by hydrogen donation from the phenolic OH group on its structure. Therefore, the rate of change of acid value in the aged blends treated with the adsorbents is slower than the neat blends aged without using the adsorbents.

The fuel has a much longer usage or storage time with such a significantly low total acid value. A reduction of about 90 % in acid value is recorded for the aged blend treated with the adsorbents. The aged blends treated with the adsorbents had about a 2 % increase in the acid value. This is crucial since the rate at which the acid number changes is essential in fuel management compared to the acid value.

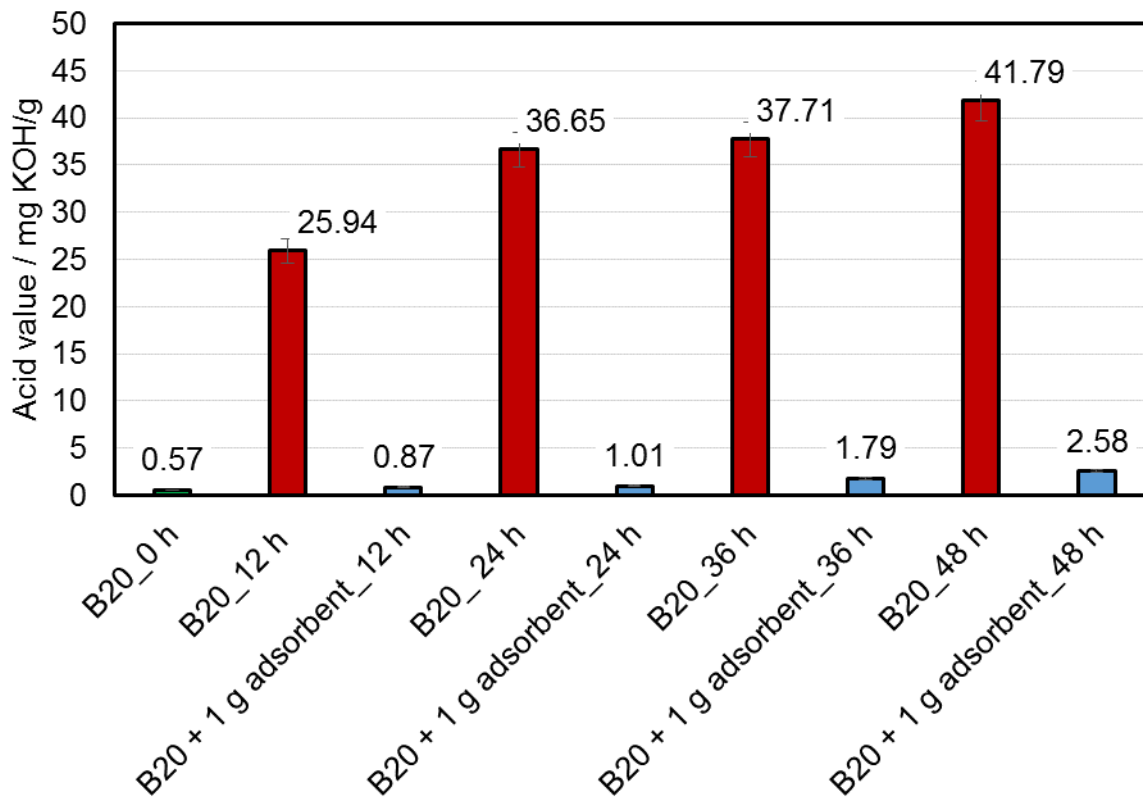


Figure 70: Acid value of 30 mL 20 % RME mixed with 80 % diesel fuel and treated with and without combined 1 g adsorbents of magnesium-aluminum hydrotalcite and 1,3,5-trimethyl-2,4,6-tris(3,5-di-tert-butyl-4-hydroxybenzyl) benzene in a ratio of 1:2 respectively and aged at 170°C with airflow of 10 L/h at 8 h per day in a Rancimat

8.4.4 Results of viscosity of 80 %diesel fuel mixed with 20 %RME treated with and without combined 1 g adsorbents of magnesium-aluminum hydrotalcite and 1,3,5-trimethyl-2,4,6-tris(3,5-di-tert-butyl-4-hydroxybenzyl) benzene in a ratio of 1:2 respectively and aged at 170 °C with airflow of 10 L/h for 48 h at 8 h per day using a Rancimat

According to the standard, the kinematic viscosity of aged B20 treated with and without the adsorbents and the neat unaged blend has been measured at 40 °C and 100 °C. The results of the measurement taken are illustrated in Figure 71 and Figure 72. With aging comes the buildup of higher molecular masses resulting from the fuel's degradation, increasing viscosity (Obadiah et al., 2012). From Figure 71, it is shown that all the B20 samples aged without the use of the adsorbents have a significant increase in viscosity

with increasing aging duration. The increase in viscosity with aging is attributable to the oxidation with subsequent polymeric compounds resulting from the reaction between the oxidation products formed during the aging process. As hydroperoxides decompose, oxidative linking of fatty acid chains occurs, leading to higher molecular weights. An obvious result of the formation of higher molecular weight materials is the increase in oil viscosity. Similar results are reported in the literature (Siddharth and Sharma, 2010). However, the blends treated with the adsorbents and aged showed more minor viscosity increase tendencies. The adsorbents' presence has increased the intramolecular binding forces resulting in a much higher energy requirement for the fuel to reach its bond dissociation energy. This results in a low oxidation effect with insignificant degradation product build-up (Mannekote and Kailas, 2012). At 48 h of aging, the B20 without the adsorbent treatment had increased in viscosity by factor 7, while the B20 treated with the adsorbents increased by a factor of 2.

The marginal increase in viscosity can be attributed to the use of the adsorbents. This then gives rise to a more extended period of the useful life of the fuel. Figure 71 also illustrates the relationship between the viscosity and the duration of aging. From the graph, there is a linear relationship between the viscosity and the level of aging. The high viscosity recorded for the blend aged without using the adsorbents is oxidation, resulting in more insoluble materials. The viscosity trend at 40 °C does not differ from the trend measured at 100 °C, Figure 72. This confirms the greater tendency of biodiesel to form polymeric deposits with increasing aging duration, as seen in section 8.2.1 and in agreement with the work of Kim et al. (2018). It then increases viscosity. The adsorbents' use has resulted in decreased formation of higher molecular weight substances of about 91 %, leading to low viscosities registered compared with the blend aged without the treatment with adsorbent giving rise to a viscosity of about 21 mm²/s.

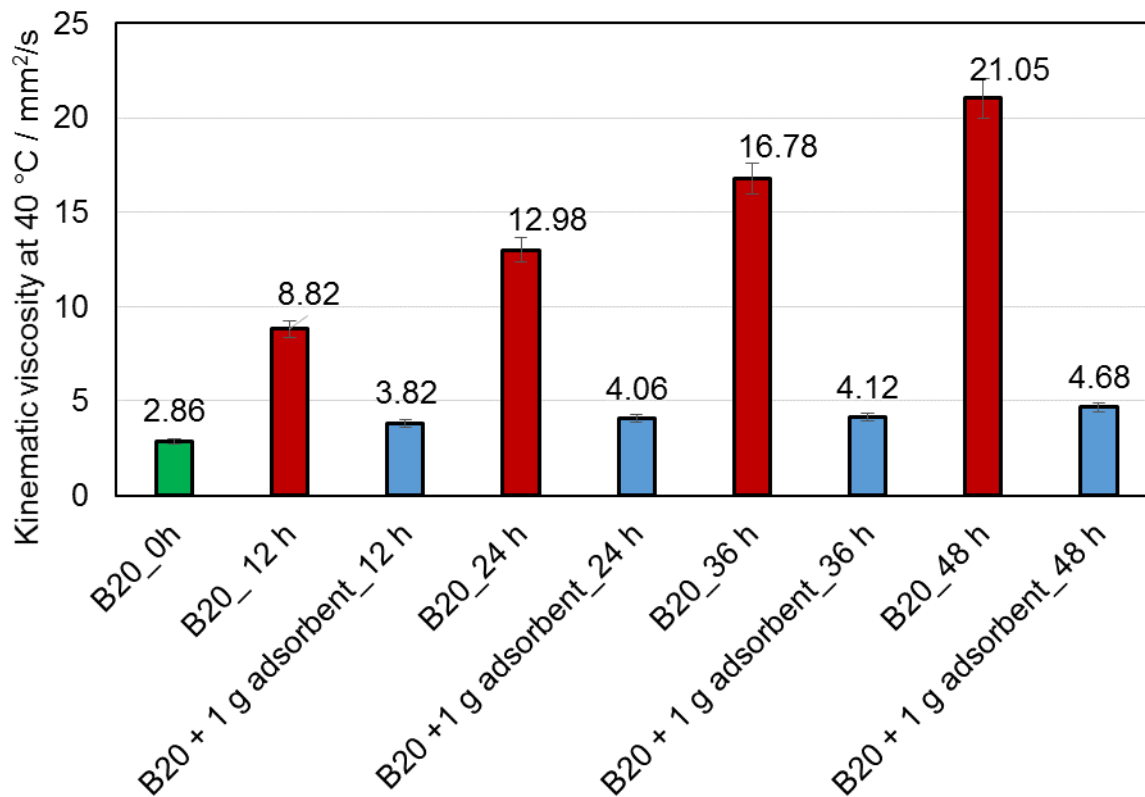


Figure 71: Viscosity at 40 °C of 30 mL 80 % diesel fuel blended with 20 % RME and treated with and without combined 1 g adsorbents of magnesium-aluminum hydrotalcite and 1,3,5-trimethyl-2,4,6-tris(3,5-di-tert-butyl-4-hydroxybenzyl) benzene in a ratio of 1:2 respectively and aged at 170 °C with airflow of 10 L/h at 8 h per day for durations of 12 h, 24 h, 36 h and 48 h using a Rancimat

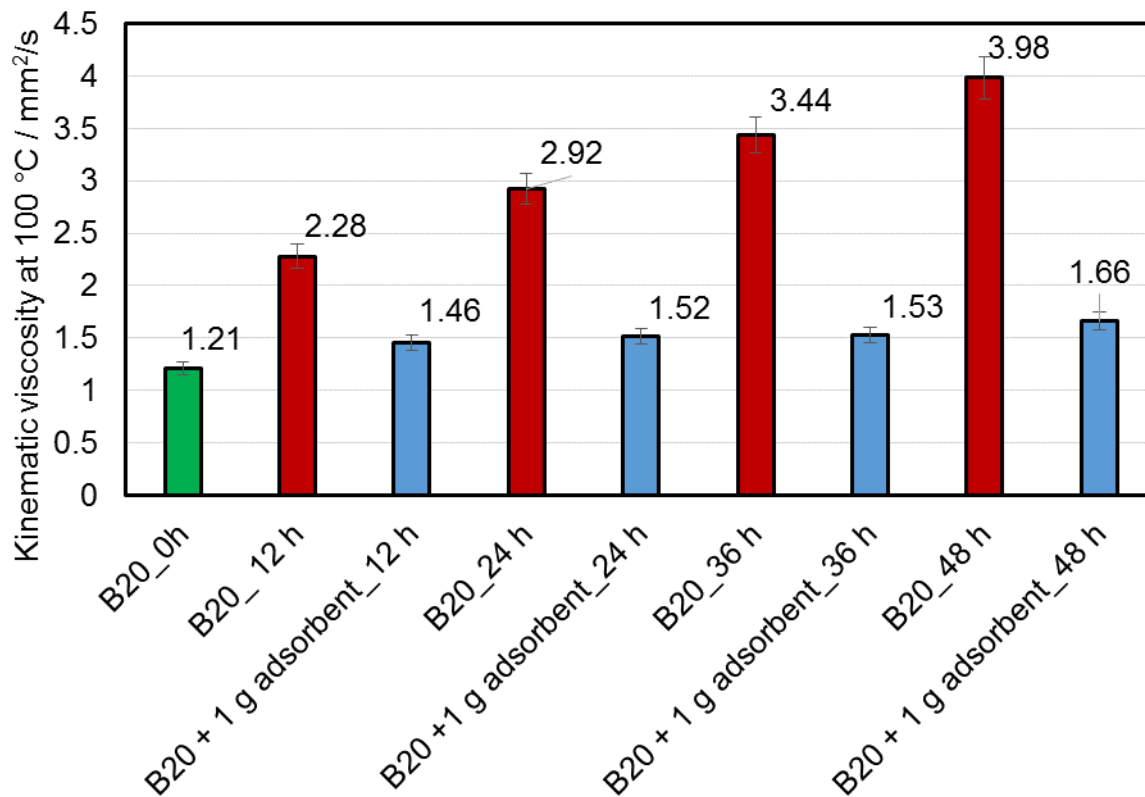


Figure 72: Viscosity at 100 °C of 30 mL 80 % diesel fuel blended with 20 % RME and treated with and without combined 1 g adsorbents of magnesium-aluminum hydrotalcite and 1,3,5-trimethyl-2,4,6-tris(3,5-di-tert-butyl-4-hydroxybenzyl) benzene in a ratio of 1:2 respectively and aged at 170 °C with airflow of 10 L/h at 8 h per day for durations of 12 h, 24 h, 36 h and 48 h using a Rancimat

Table 17 shows the viscosity aging index (VAI) of the blends measured in this experiment. It can be seen in Table 17 that the blends aged without any adsorbent treatment have exhibited higher viscosity aging index compared to the blends treated with the adsorbents. This high VAI results from insoluble materials' build-up due to the oxidation caused by the aging process. However, the VAI of the blends treated with the adsorbents barely registered any significant increase, and it remained relatively constant throughout the aging process. This has to do with the adsorbents' presence, which increased the binding effect on the fuel molecules and, consequently, low aging index values.

Table 17: Viscosity aging index of B20 treated with and without 1 g of combined adsorbent and aged at 170 °C at 8 h per day with an airflow of 10 L/h for various durations using a Rancimat

Aging / h	Viscosity aging Index	
	B20	B20+adsorbent
0	0	0
12	1.07	1.02
24	1.09	1.02
36	1.1	1.02
48	1.11	1.02

8.4.5 Effect of combined adsorbents of magnesium-aluminum hydrotalcite and 1,3,5-trimethyl-2,4,6-tris(3,5-di-tert-butyl-4-hydroxybenzyl) benzene in a ratio of 1:2 respectively on the density of 80 %diesel fuel mixed with 20 %RME and aged at 170 °C with airflow of 10 L/h for 48 h at 8 h per day using a Rancimat

Density is mass per unit volume, usually expressed in kilogram per cubic meter (kg/m³). It is reported that fuel density generally increases with the increasing molecular weight (Prajapati and Nandlal, 2015). Figure 73 illustrates the trend of changes in the blends' density at different durations measured at 40 °C. The density of biodiesel increases with aging duration due to an increase in molecular interaction of degraded products. Since the degraded biodiesel now contains shorter chain hydrocarbon and more saturated fatty acid, there is a high tendency of crystallization, leading to a reduction of its volume and consequently an increase in its density. Also, the mass of the fuel is increased as a consequence of oxidation products. However, the increasing density value for the blends treated with the adsorbents and aged is not as significant as the blend aged without using the adsorbents. From Figure 73, the use of the adsorbents resulted in a less significant increase in the density. This observed trend is also seen in the same blends' density at

100 °C, Figure 74. This is because the radicals which would have polymerized into oligomers, as seen in section 3.2, have been intercepted and stabilized by the adsorbents. 1,3,5-trimethyl-2,4,6-tris(3,5-di-tert-butyl-4-hydroxybenzyl) benzene has a hydrogen band donor count of 3 and a hydrogen band acceptor count of 3. It can suppress the thermo-oxidative degradation of biodiesel and its blends by donating hydrogen atoms on its surface structure to the peroxy radicals, thereby interfering with the oxidation process (PubChem Database). Hence the process of oxidation is thus delayed resulting in marginal oxidative products. It has given rise to low densities recorded, unlike the blends aged without using the adsorbents.

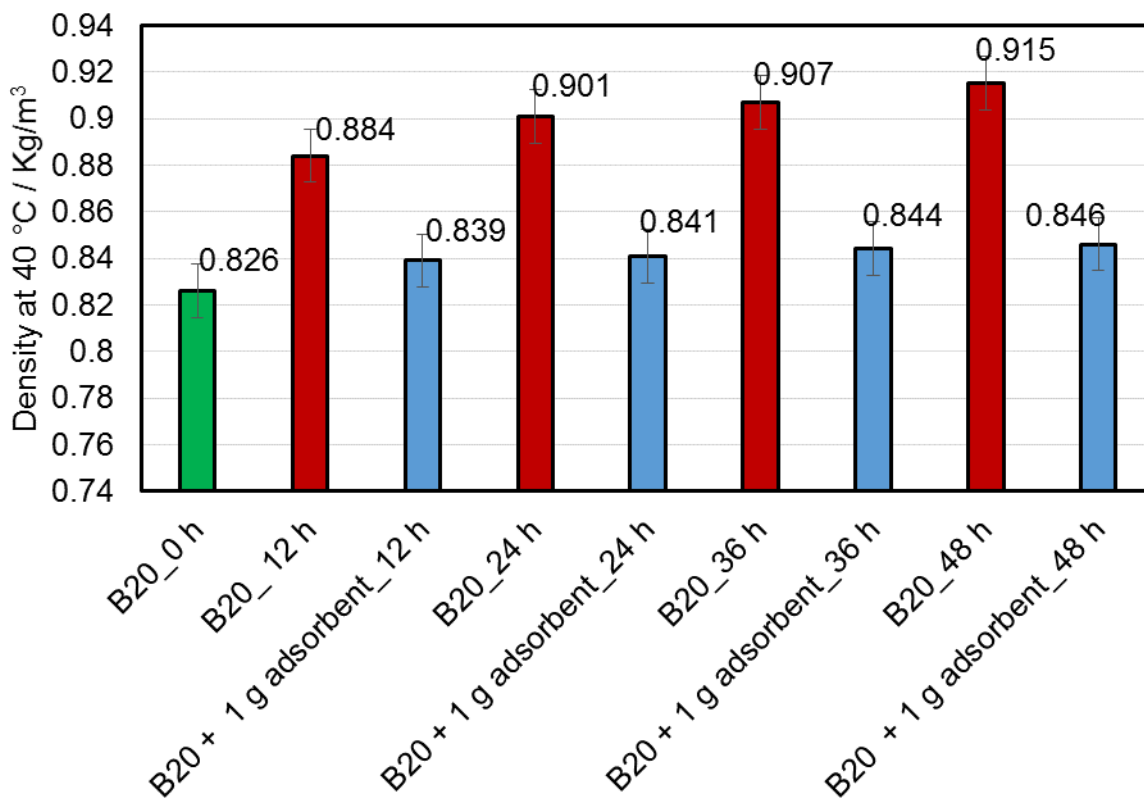


Figure 73: Density at 40 °C of 30 mL 80 % diesel fuel blended with 20 % RME and treated with and without combined 1 g adsorbents of magnesium-aluminum hydrotalcite and 1,3,5-trimethyl-2,4,6-tris(3,5-di-tert-butyl-4-hydroxybenzyl) benzene in a ratio of 1:2 respectively and aged at 170 °C with airflow of 10 L/h at 8 h per day for durations of 12 h, 24 h, 36 h and 48 h using a Rancimat compared with a neat unaged blend

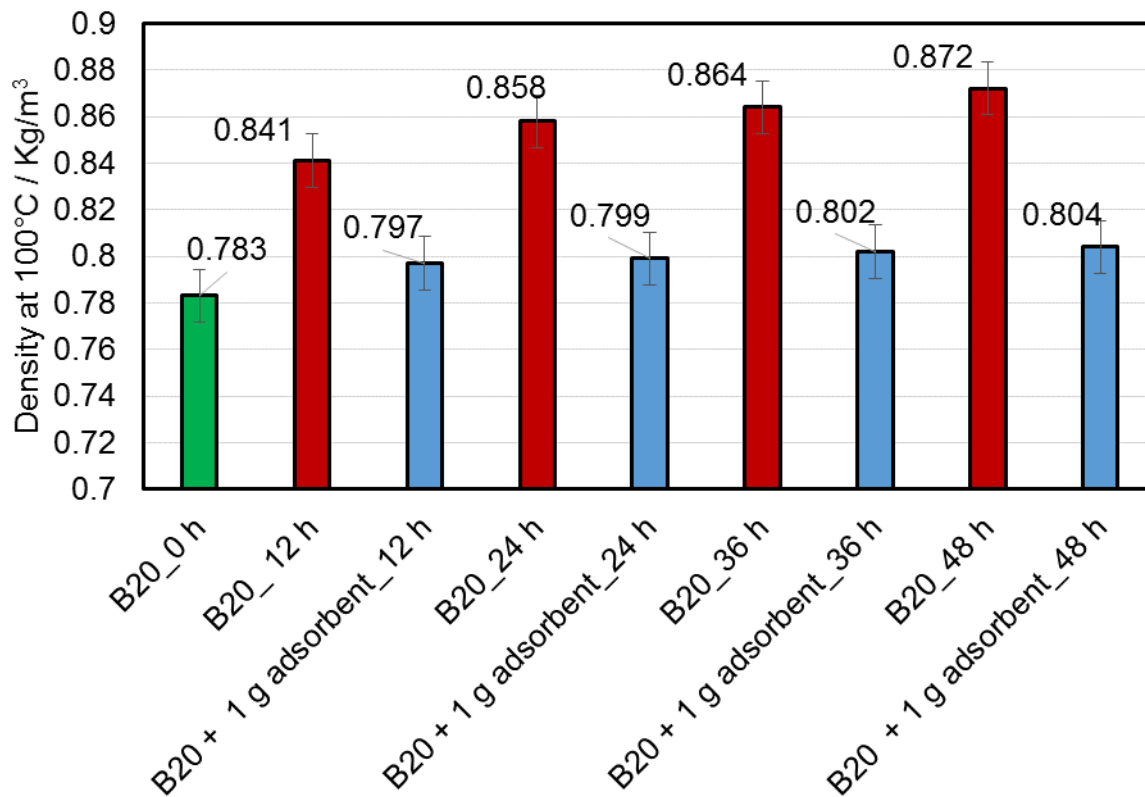


Figure 74: Density at 100 °C of 30 mL 80 % diesel fuel blended with 20 % RME treated with and without combined 1 g adsorbents of magnesium-aluminum hydrotalcite and 1,3,5-trimethyl-2,4,6-tris(3,5-di-tert-butyl-4-hydroxybenzyl) benzene in a ratio of 1:2 respectively and aged at 170°C with airflow of 10 L/h at 8 h per day for durations of 12 h, 24 h, 36 h and 48 h using a Rancimat compared with the neat unaged blend

8.4.6 Interrelationships between acid value, viscosity, and density of 80 %diesel fuel mixed with 20 %RME treated with and without combined 1 g adsorbents of magnesium-aluminum hydrotalcite and 1,3,5-trimethyl-2,4,6-tris(3,5-di-tert-butyl-4-hydroxybenzyl) benzene in a ratio of 1:2 respectively and aged at 170 °C with airflow of 10 L/h for 48 h at 8 h per day using a Rancimat

Figure 75 shows the relationship between viscosity and acid value. The graph plots the viscosity measured at 40 °C versus the acid value measured over the entire duration of aging at 170 °C. A linear relationship is seen between the viscosity and the acid value. For all neat blends aged without any adsorbent treatment, their viscosity increased as the

acid value increased with the increasing duration of aging. The viscosity against acid value curves falls in the graph's lower value region for the blends treated with the adsorbents and aged. As the acid value has not increased with increasing aging duration, the value for viscosity remained nearly constant. Therefore, the more the sample degrades, the higher the acid value and viscosity (Obadiah et al., 2012). Figure 75 shows that the biodiesel blend's viscosity increases with aging due to high molecular weight species formation. Hence, the higher the viscosity, the higher the degree of deterioration, the higher the acid values. This agrees with the findings of Jain and Sharma (2011). Therefore, both acid value and viscosity support evidence of the adsorbents' impact on suppressing biodiesel degradation. Thus, the adsorbents impact substantially equal terms on the acid value and the viscosity, resulting in an insignificant increase.

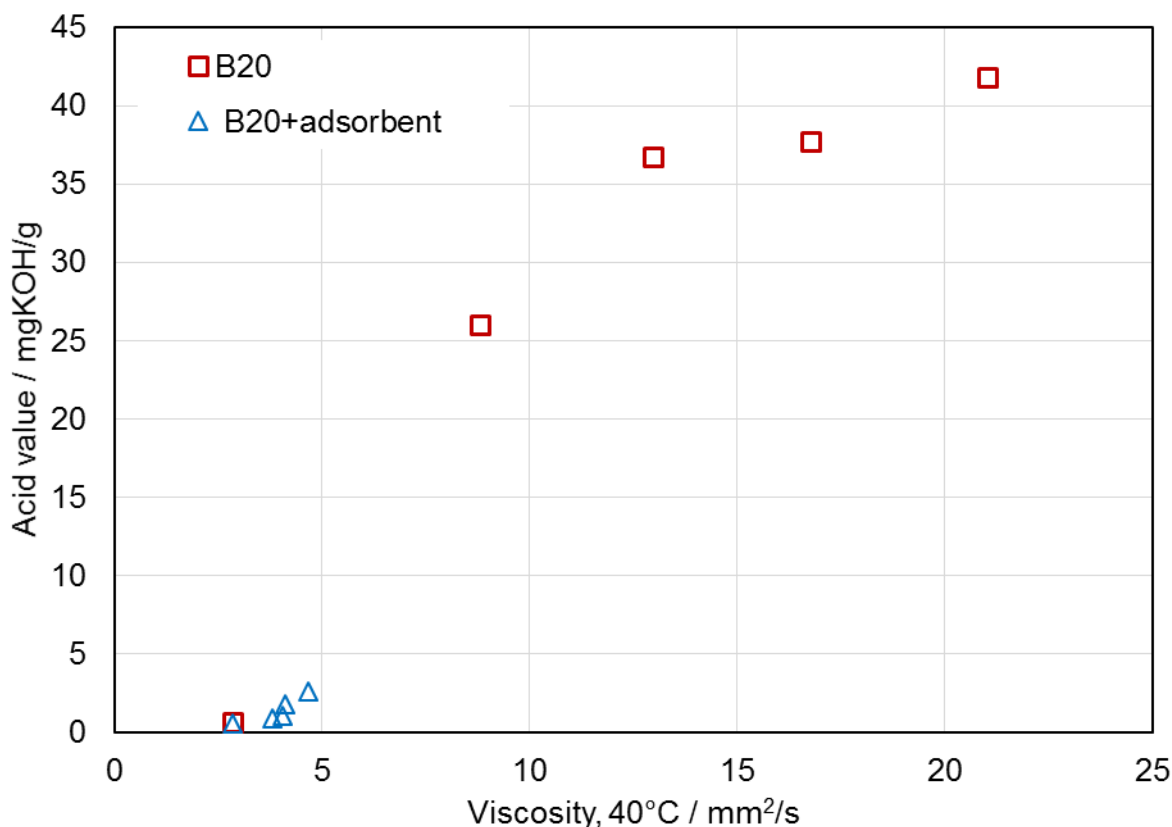


Figure 75: Viscosity at 40 °C versus the acid value of 30 mL 20 % RME mixed with 80 % diesel fuel treated with and without combined 1 g adsorbents of magnesium-aluminum hydroxalcite and 1,3,5-trimethyl-2,4,6-tris(3,5-di-tert-butyl-4-hydroxybenzyl)benzene in a ratio of 1:2 respectively and aged at 170 °C with airflow of 10 L/h at 8 h per day for durations of 12 h, 24 h, 36 h and 48 h using a Rancimat

Figure 76 illustrates the relationship between viscosity and density. The graph plots the viscosity against density measured at 40 °C over the entire duration of aging at 170 °C. A linear relationship is seen between the viscosity and the density. For the neat blends aged without any adsorbent treatment throughout aging at 170 °C, the viscosity and density increased as the aging progressed. For the blends treated with the adsorbents and aged, on the other hand, the viscosity and density values fall in the lower value region of the graph. The density's values-centered on 0.838 to 0.847 kg/m³ while 5mm²/s viscosity value for the blends treated with adsorbents. The aged blends without adsorbents treatment resulted in high values for both density and viscosity. This could have come about due to the presence of the oxidation products resulting from the aging. As aging progresses, the oxidative products seen in section 3.4 result in higher molecular mass substances, which increase the values as seen in Figure 76.

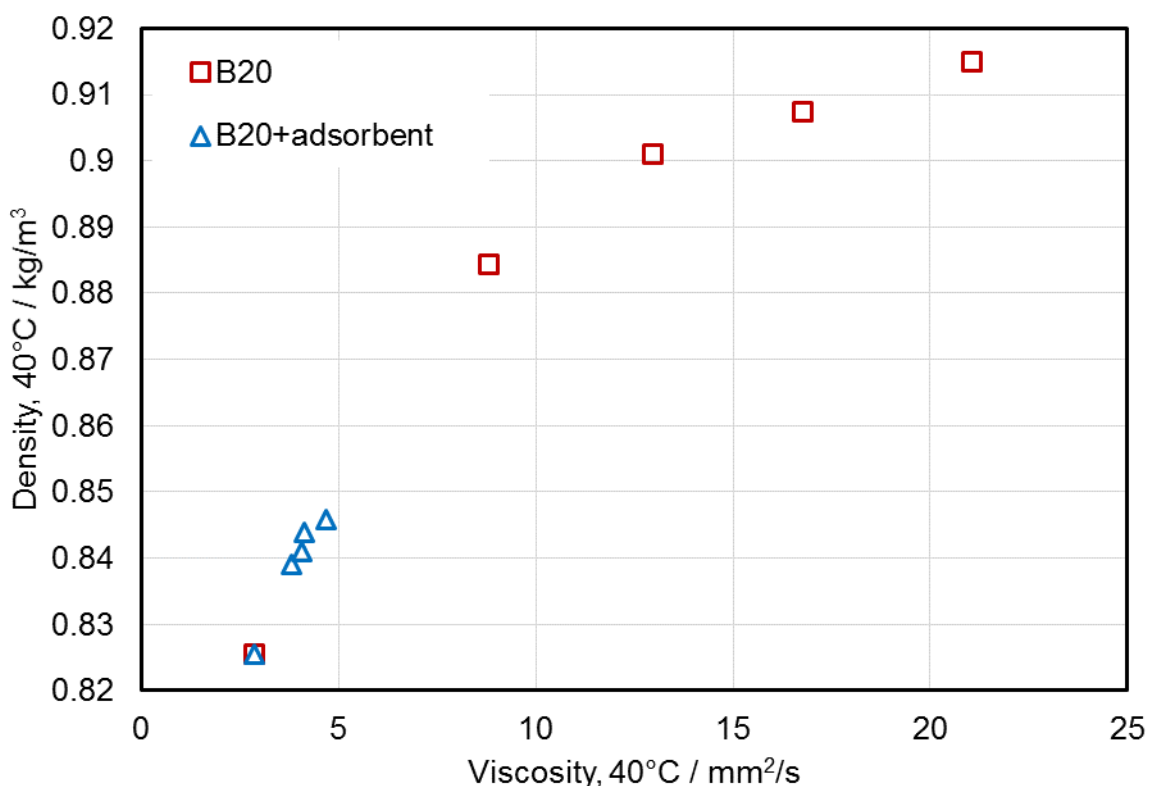


Figure 76: Viscosity at 40°C versus Density of 30 mL 20 % RME mixed with 80 % diesel fuel and treated with and without combined 1 g adsorbents of magnesium-aluminum hydrotalcite and 1,3,5-trimethyl-2,4,6-tris(3,5-di-tert-butyl-4-hydroxybenzyl)benzene in a ratio of 1:2 respectively and aged at 170 °C with airflow of 10 L/h at 8 h per day for durations of 12 h, 24 h, 36 h and 48 h using a Rancimat

8.4.7 FTIR analysis of 80 %diesel fuel mixed with 20 %RME treated with and without combined 1 g adsorbents of magnesium-aluminum hydrotalcite and 1,3,5-trimethyl-2,4,6-tris(3,5-di-tert-butyl-4-hydroxybenzyl) benzene in a ratio of 1:2 respectively and aged at 170 °C with airflow of 10 L/h for 48 h at 8 h per day using a Rancimat

FTIR application determines the changes occurring in the functional groups in the aged sample, be it treated with or without the adsorbents. The FTIR measurements focus on the level of oxidation by a general response in absorption in the carbonyl (C=O) region between 1900 to 1600 cm^{-1} , C-H region (2600-3000 cm^{-1}), and the hydroxyl region, 3000-3600 cm^{-1} , Figure 77, Figure 78 and Figure 79. In the carbonyl (C=O) region, the IR energy is absorbed due to the carbon-oxygen bonds in the oxidized fuel mixture. With neat fuel or unaged fuel, few compounds are found with significant absorbencies in this area. Therefore, monitoring this region is thus a direct measurement of the fuel mixture's level of degradation. As stated earlier, oxidation impacts the carbonyl vibrations at 1740 cm^{-1} but widely in the range of 1600-1900 cm^{-1} . Comparing the vibrations of B20, B20 treated with the adsorbents and aged, and unaged B20 at 0 h, the carbonyl vibrations illustrate many differences. It can be recognized that the B20 treated with the adsorbents have recorded only minor changes in vibrations during the aging process. This resulted from the adsorbents intercepting the oxidation precursors and, therefore, inhibiting polymerization into oligomers. In the FTIR spectrum of neat unaged biodiesel blend (B20), Figure 77, the most substantial characteristic ester peak is found at 1750 cm^{-1} . Upon degradation, the bands at approximately 3000 cm^{-1} decrease slightly in intensity. This is an indication of a decrease in the level of unsaturation. As oxidation proceeds, hydroperoxides' concentration increases and can be reflected by increased band intensity at 3470 cm^{-1} (range of 3000-3600 cm^{-1}) (Saifuddin and Refal, 2014; Guillen and Ruiz, 2005). An increase of the peak area around 1700-1750 cm^{-1} . These are the oxidation decomposition products such as ketone and aldehyde. Compared with the FTIR spectrum of biodiesel blends treated with the adsorbents, variation in the peak area is not significant. It shows a similar pattern of FTIR spectrum of the neat unaged biodiesel blend. It can be noted that there is only a slight and negligible deterioration compared with biodiesel blend aged without the adsorbents treatment as depicted in Figure 77.

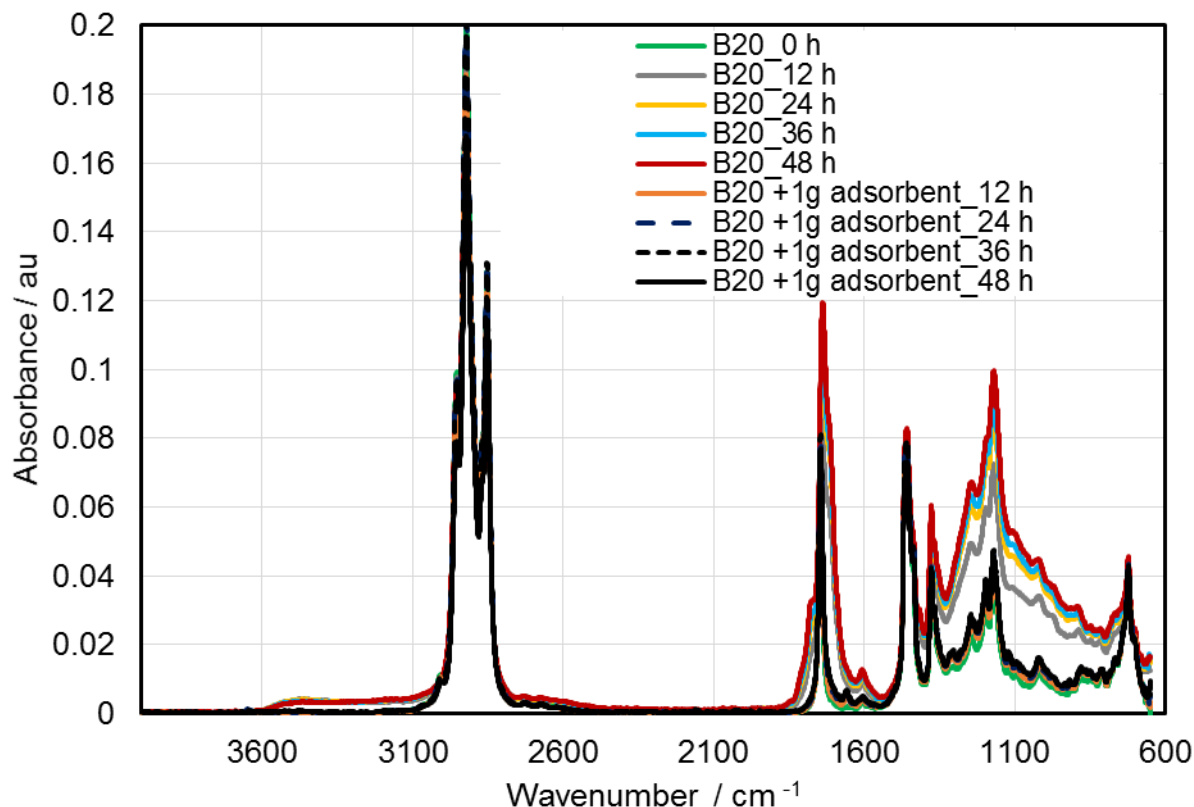


Figure 77: Evaluation of comparative analysis of FTIR absorbance spectra of 30 mL 20 % RME mixed with 80 % diesel fuel and treated with and without the combined 1 g adsorbents of magnesium-aluminum hydrotalcite and 1,3,5-trimethyl-2,4,6-tris(3,5-di-tert-butyl-4-hydroxybenzyl) benzene in a ratio of 1:2 respectively and aged at 170 °C with airflow of 10 L/h at 8 h per day for durations of 12 h, 24 h, 36 h and 48 h using a Rancimat

From Figure 78, a closer look at the region of carbonyl groups at about 1715 cm⁻¹ shows an enhanced absorption. Oxidation products, Ketones, and aldehydes are said to be formed. A further absorption band emerges at about 1695 cm⁻¹. This is also attributable to the carbonyl groups (Kerkering and Andersson, 2015). It is, therefore, observed that the amount of carbonyl-containing degradation products increases with the increasing duration of aging. However, these increases are absent or insignificant in the samples' blends treated with the adsorbents before the aging process. This result can only be explained by the adsorbents' suppression action by stabilizing the radical precursors, thereby interrupting the oxidation process, as seen in section 6.

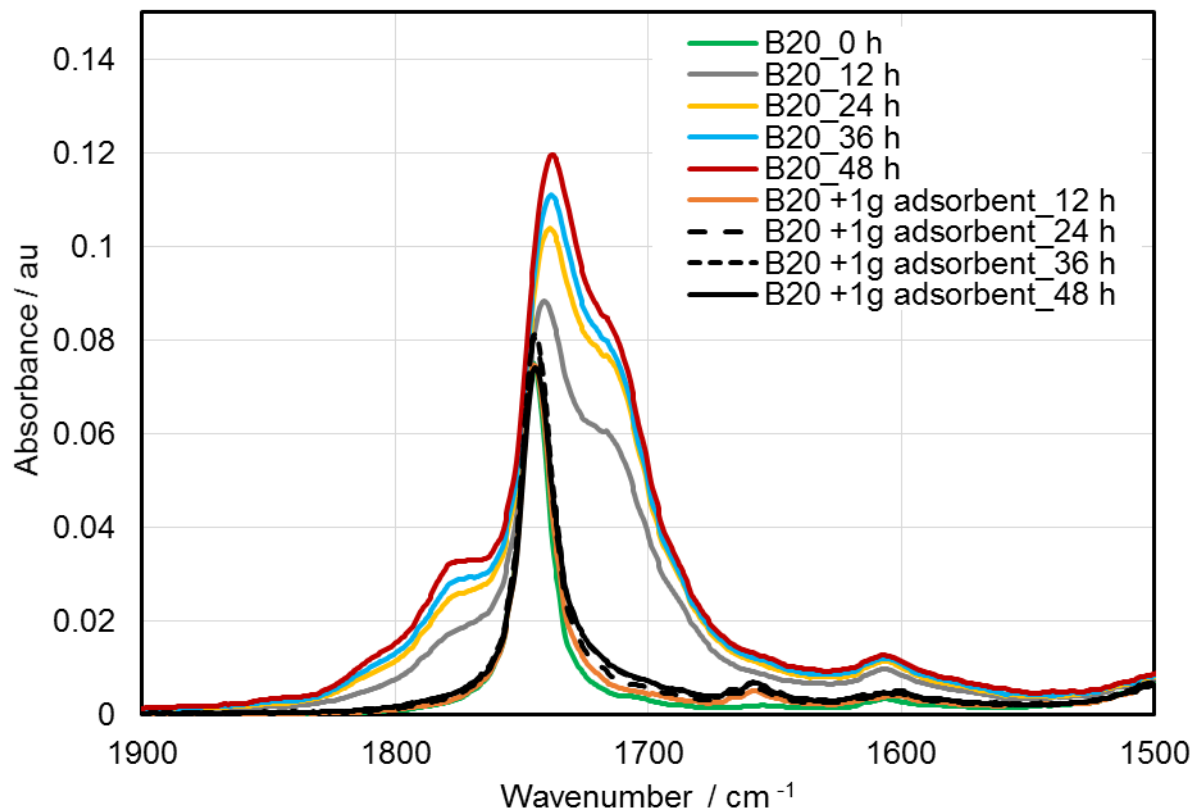


Figure 78: FTIR spectra in absorbance mode (range 1500-1900cm⁻¹) of 30 mL 20 % RME mixed with 80 % diesel fuel and treated with and without the combined 1 g adsorbents of magnesium-aluminum hydrotalcite and 1,3,5-trimethyl-2,4,6-tris(3,5-di-tert-butyl-4-hydroxybenzyl) benzene in a ratio of 1:2 respectively and aged at 170 °C with airflow of 10 L/h at 8 h per day for durations of 12 h, 24 h, 36 h and 48 h using a Rancimat

The hydroxyl components observed within 3000-3600 cm⁻¹ in Figure 79 are attributable to the organic compounds, including water, alcohol, hydroperoxides, and carboxylic acids with the OH functional group. The use of the adsorbents interrupted the breaking down of the fatty acid methyl ester molecules. This then subdued the complex secondary oxidation reactions, which would have resulted in more reactive aldehydes. Also, it can be said that the adsorbent's impact is at the initiation stage of the oxidation process as it has shown that hydroperoxides have not been formed, hence the no or very negligible amount of OH functional group absorption. This, therefore, results in very marginal changes in vibrations and decreased peaks registered within these wave members for the mixtures treated with the adsorbents and aged compared with those aged without the adsorbent treatment.

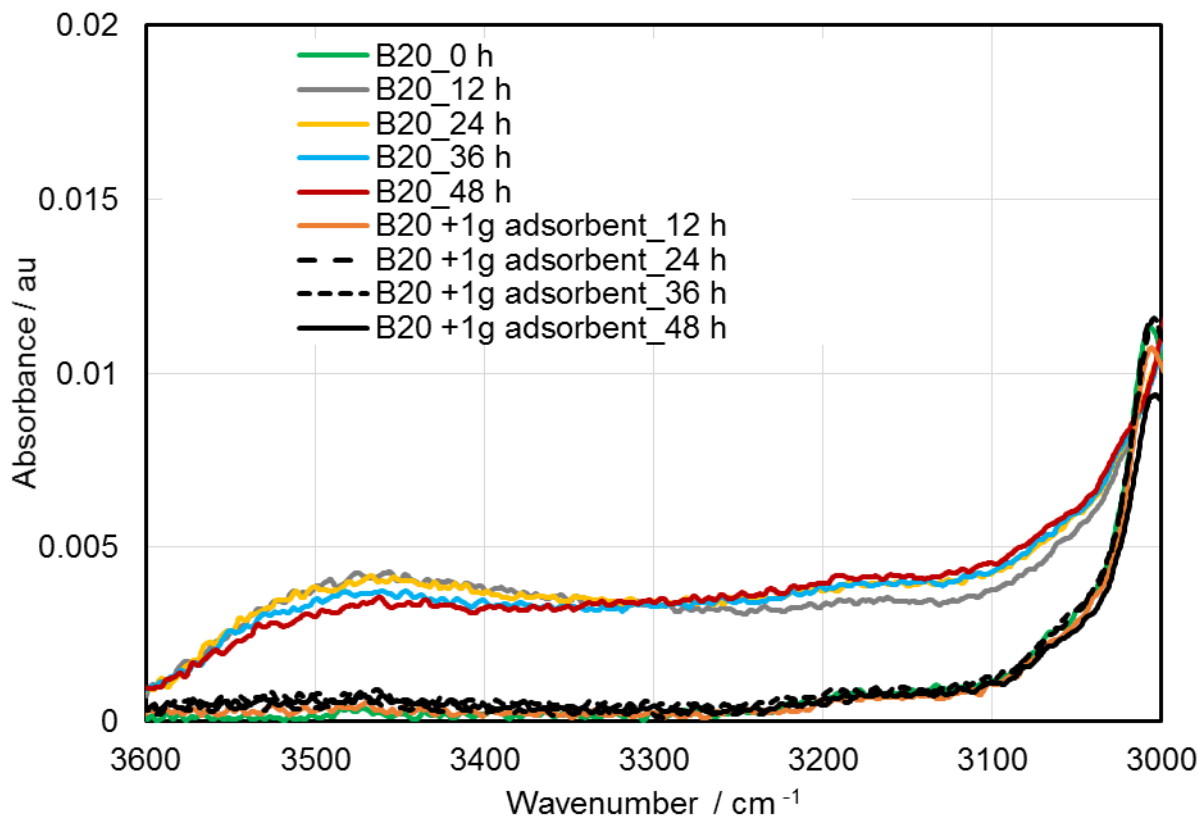


Figure 79: FTIR spectra in absorbance mode (range 3000-3600 cm^{-1}) of 30 mL 20 % RME mixed with 80 % diesel fuel and treated with and without the combined 1 g adsorbents of magnesium-aluminum hydrotalcite and 1,3,5-trimethyl-2,4,6-tris(3,5-di-tert-butyl-4-hydroxybenzyl) benzene in a ratio of 1:2 respectively and aged at 170 °C with airflow of 10 L/h at 8 h per day for durations of 12 h, 24 h, 36 h and 48 h using a Rancimat

The differences in the C=O-bonds shown in Figure 78 above have been integrated, and the increase in peak area is illustrated in Figure 80. By comparing the aged B20 treated with the adsorbents and the blend without any adsorbent treatment, the carbonyl vibrations (1600-1900 cm^{-1}) of the B20 without adsorbent treatment showed higher C=O vibrations. The highest vibrations increased by 70 % at 12 h of age to 76 % at 24 h, 77 % at 36 h, and finally to 80 % at 48 h of aging. The increase in vibrations at 0 h to 12 h of aging has been much repaid to 24 h of aging. Beyond 24 h of aging, the increase reduced to a gradual pace. It can be recognized that the B20 blends treated with the adsorbents showed a slight increase in carbonyl vibration bonds compared to the unaged B20, as well as the blends aged without treatment with the adsorbents. With an increase of 13 % at 12 h, the blends treated with the adsorbents further increased by 23 % at 24 h, 30 % at

36 h, and finally to 26 % after 48 h of aging. The 30 % increase at 36 h, which is relatively more significant than the 26 % increase reported after the 48 h, could be due to experimental errors. Nevertheless, the adsorbents' impact is seen in the insignificant increase in the C=O vibrations in the blends treated with the adsorbents and aged. This means the adsorbents' use results in fewer degradation products, hydroperoxides, and other low molecular weight carboxylic acids, aldehydes, and ketones, as seen in Obadiah's report al. (2012).

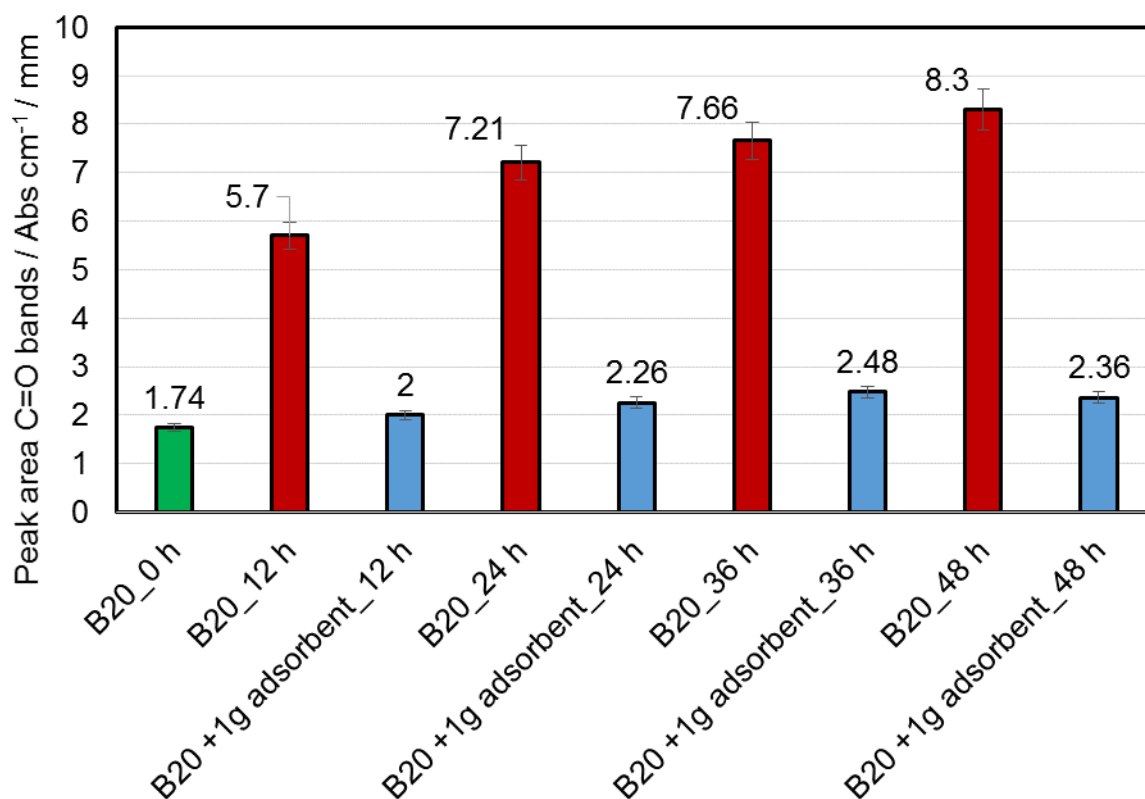


Figure 80: Evaluation of peak area under C=O bands ($1600-1900\text{ cm}^{-1}$) of the FTIR spectra of 30 mL 20 % RME mixed with 80 % diesel fuel and treated with and without combined 1 g adsorbents of magnesium-aluminum hydrotalcite and 1,3,5-trimethyl-2,4,6-tris(3,5-di-tert-butyl-4-hydroxybenzyl) benzene in a ratio of 1:2 respectively and age at 170°C with airflow of 10 L/h at 8 h per day for durations of 12 h, 24 h, 36 h and 48 h using a Rancimat

Summary

A blend of 20 %RME mixed with 80 %diesel fuel is treated with and without 1 g combined adsorbents of magnesium-aluminum hydrotalcite and 1,3,5-trimethyl-2,4,6-tris(3,5-di-tert-butyl-4-hydroxybenzyl) benzene in a ratio of 1:2 respectively and aged at 170 °C using a Rancimat running with an airflow of 10 L/h at 8 h per day.

The degradation of biodiesel and its blend under 170 °C is represented in Figure 65 to Figure 80. The degradation is monitored by the level of oligomers formed with and without the treatment of adsorbents on biodiesel and its blends with increasing residing time of aging. As shown in the figures, there is a consistent increase in biodiesel degradation with increasing temperature. The FTIR detects functional groups and has been used extensively to follow biodiesel and the blends' oxidative changes. It has shown a relationship between the temperature and the amount of distortion in the molecular structure. The carbonyl region in the blend aged 48 h at 170 °C without any adsorbent treatment had enhanced adsorption of about 80 %. The carbonyl groups centered on 1715 cm^{-1} in the blends aged without any adsorbent treatment show enhanced absorption in the spectra. This is due to oxidation products such as ketones and aldehydes formed after chain scission (Kerkering and Andersson, 2015). Also, a clear enhanced signal around $3,495\text{ cm}^{-1}$ in the blends aged without treatment with the adsorbents is seen in the spectra. This is attributable to hydroxyl groups. According to Kerkering and Andersson (2014), the OH band can be derived from water or ascribed to organic compounds containing the OH functional groups such as hydroperoxides, carboxylic acids, and alcohols. The adsorbents' use (1 g of the combined adsorbents in 30 ml of B20) has resulted in about 70 % reduction in the enhanced adsorptions registered at the carboxyl and hydroxyl regions in the FTIR spectra.

For the other parameters, viscosity at 40 °C, acid value, density, etc., there exist a linear relationship between the temperature and the duration of aging. The adsorbents' use suppressed the growth in viscosity measured at 40 °C by 78 % during the aging at 170 °C for 48 h duration. A similar trend is seen in the changes in density measured at 40 °C. A key parameter of fuel quality, the acid value, is also impacted by using the adsorbents. The adsorbents' use suppressed the increase of acidity by 94 % for the aging at 170 °C

for 48 h. These results largely coincide with literature, Zhou et al., 2017; Dunn, 2008, 2005; Liang et al., 2006.

The above results have been obtained due to the adsorbents' suppression action resulting from the interaction between the free radicals and their surface, mainly due to hydrogen bonding. The hydrogen bonds are established between the ester carbonyl and the adsorbents' hydroxyl groups, leading to the free radical propagation's interruption. This is because of the hydrogen atom interaction from the surface of the hydroxyl group of the adsorbents with the immediate peroxy radicals. With the free radical propagation interruption, oxidation is retarded, resulting in less or no significant sample degradation. Hence, the use of the adsorbents can enhance and extend the oxidation stability of biodiesel and its blends.

8.5 Stabilization of biodiesel and its blends at 110 °C using 0.225 g combined adsorbents of magnesium-aluminum hydrotalcite and 1,3,5-trimethyl-2,4,6-tris(3,5-di-tert-butyl-4-hydroxybenzyl) benzene in a ratio of 1:2, respectively

In section 8.4, the experiments have been carried out at a temperature of 170 °C, which is an extreme temperature considering what is experienced by the fuel in an engine. However, it is done to simulate the formation of higher molecular mass substances and, therefore, make the impact of the adsorbents easier to identify. In this section, the experiments of section 8.4 are repeated at a temperature of 110 °C a standard temperature is used to study fuel stability (Mittelbach and Gangl, 2001). According to Dantas et al. (2011), biodiesel's oxidation temperature is inversely proportional to the number of bisallylic hydrogens; in other words, the higher the amount of linoleic acid, the more easily biodiesel is oxidized. The impact of the adsorbents on the oxidation stability of biodiesel and its blends in this section is, therefore, studied by measuring the viscosity, density, FTIR, size exclusion chromatography, and the acid number before and after aging of the sample mixture treated with and without the 0.225 g combined adsorbents of magnesium-aluminum hydrotalcite and 1,3,5-trimethyl-2,4,6-tris(3,5-di-tert-butyl-4-hydroxybenzyl) benzene in a ratio of 1:2 respectively at 110 °C of temperature, 8 h per day for 80 h duration with airflow of 10 L/h using the Rancimat.

8.5.1 Induction period measurements

The adsorbents' impact on the oxidation stability of 80 %diesel fuel blended with 20 %biodiesel is shown in

Figure 81. The induction period is plotted against the blend treated with and without the adsorbents. A measurable positive impact on the stability of biodiesel is seen. Due to the efficiency of the adsorbents' scavenging ability, the induction time has increased by more than a factor of about 4. Here, the induction period of RME without additives determined under the same conditions is 6.3 h indicating that it had met the standard induction period per EN14214 specifications of 6 h. As seen in section 4.1.8, the induction period factor illustrates the adsorbents' stabilization impact in suppressing the formation of higher molecular substances. This improvement could be explained based on the adsorbent's interference with the oxidation process resulting in less oxidation impact on the blend treated with the adsorbents. Oxidation is a significant contributor to biodiesel's instability, which usually increases high molecular insoluble polymers affecting the fuel quality (Kim et al., 2018). It can be stated that the adsorbents suppressed the production of oxygenates such as alcohols, acids, aldehydes, and peroxides, whose presence would have decreased the induction period of the mixture (Kim et al., 2018, Obadiah et al. 2012, Dunn, 2008). With the addition of the adsorbents, there is a provision of protons to inhibit the formation of free radicals, thereby considerably delaying the oxidation rate. The adsorbent's hydroxyl group interrupted the complex secondary oxidation reactions by providing protons that inhibit the formation of free radicals and interrupt the free radicals' propagation, thus retarding the oxidation rate (see section 3.4). This then reinforces the resistance of the biodiesel to oxidation degradation, increasing its induction period. The accumulation of degraded or decomposition products in fuel indicates the onset of oxidation; therefore, it could be designated as the second stage of degradation (see Figure 5) (Wang, 2001). The obtained results show an increase in the biodiesel blend's induction period treated with the adsorbents indicating a protective effect and inhibiting the oxidation initiation step. Therefore, this supports the initial results in this work, which suggested that the adsorbents impacted the initiation stage of the oxidation process.

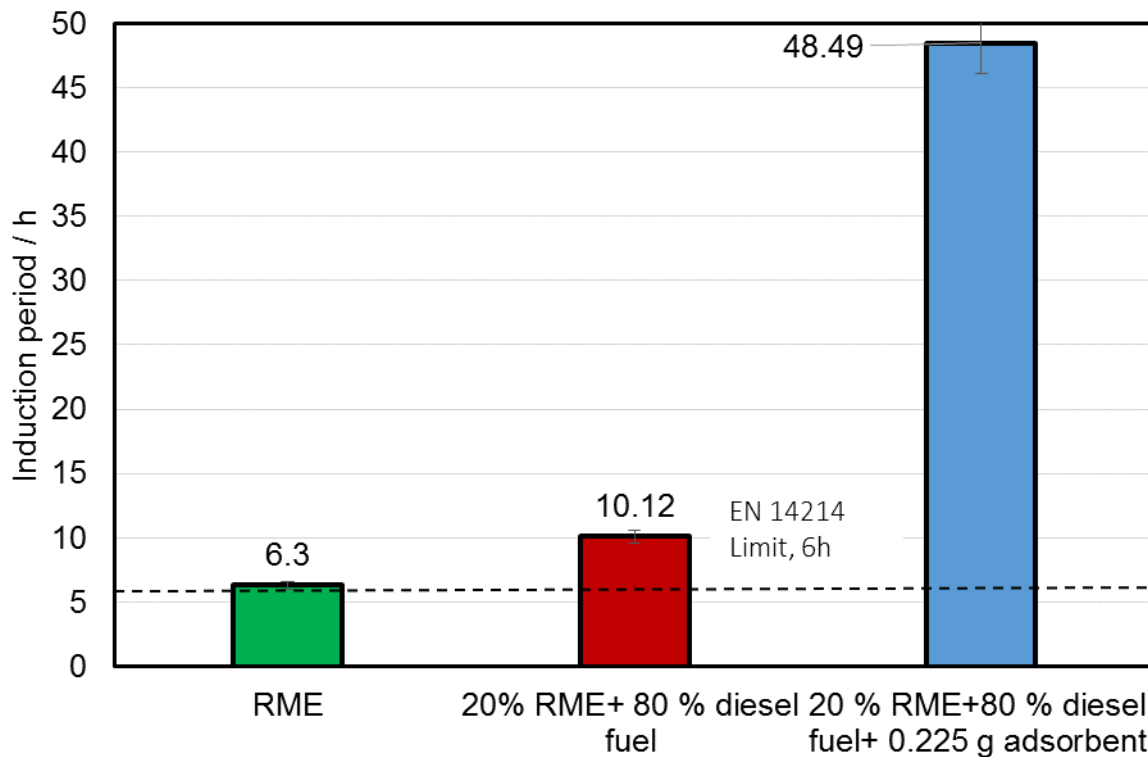


Figure 81: Evaluation of induction period of 7.5 g of 20 % RME mixed with 80 % diesel fuel treated with and without 0.225 g combined adsorbents of magnesium-aluminum hydrotalcite and 1,3,5-trimethyl-2,4,6-tris(3,5-di-tert-butyl-4-hydroxybenzyl) benzene in a ratio of 1:2 respectively using a Rancimat at 110 °C with airflow of 10 L/h

8.5.2 SEC analysis of 30 mL 20 % RME mixed with 80 % diesel fuel treated with and without 0.225 g combined adsorbents of magnesium-aluminum hydrotalcite and 1,3,5-trimethyl-2,4,6-tris(3,5-di-tert-butyl-4-hydroxybenzyl) benzene in a ratio of 1:2 respectively using a Rancimat at 110 °C with airflow of 10 L/h at 8 h per day

The SEC analysis, as earlier stated, detect changes in the molar mass of molecules during the aging process. The separation in the SEC procedure is based on the size and not the sample's molecular weight in solution (Moraes & Bahia, 2015). Figure 80 and Figure 81 indicate that the chromatograms of neat B20 and B20 treated with the adsorbents and aged for 80 h are shown. The formation and accumulation of higher molecular mass substances during the various aging durations of 20 h, 40 h, 60 h, and 80 h increased consistently over the entire aging period, just as seen in section 8.4. While the unaged mixture had a relative molar mass of about 540 g/mol, the blends treated with the

adsorbent and aged had a relative molar mass of about 550 g/mol, indicating a relative increase of about 10 g/mol, while the blends aged without adsorbent treatment had relative molar masses close to 750 mg/mol. This is an increase of about 210 g/mol. As stated in section 3.4, during the oxidation process, once hydroperoxides are formed, they decompose and inter-react to form numerous secondary oxidation products, including aldehydes, alcohols, shorter chain carboxylic acids, and eventually result in higher molecular weight substances. The blends treated with the adsorbents have less high molecular mass substances formed, indicating the suppression of their formation (see section 3.4). This is corroborating evidence of the high induction period recorded for the mixture treated with the adsorbents seen in section 8.5.1.

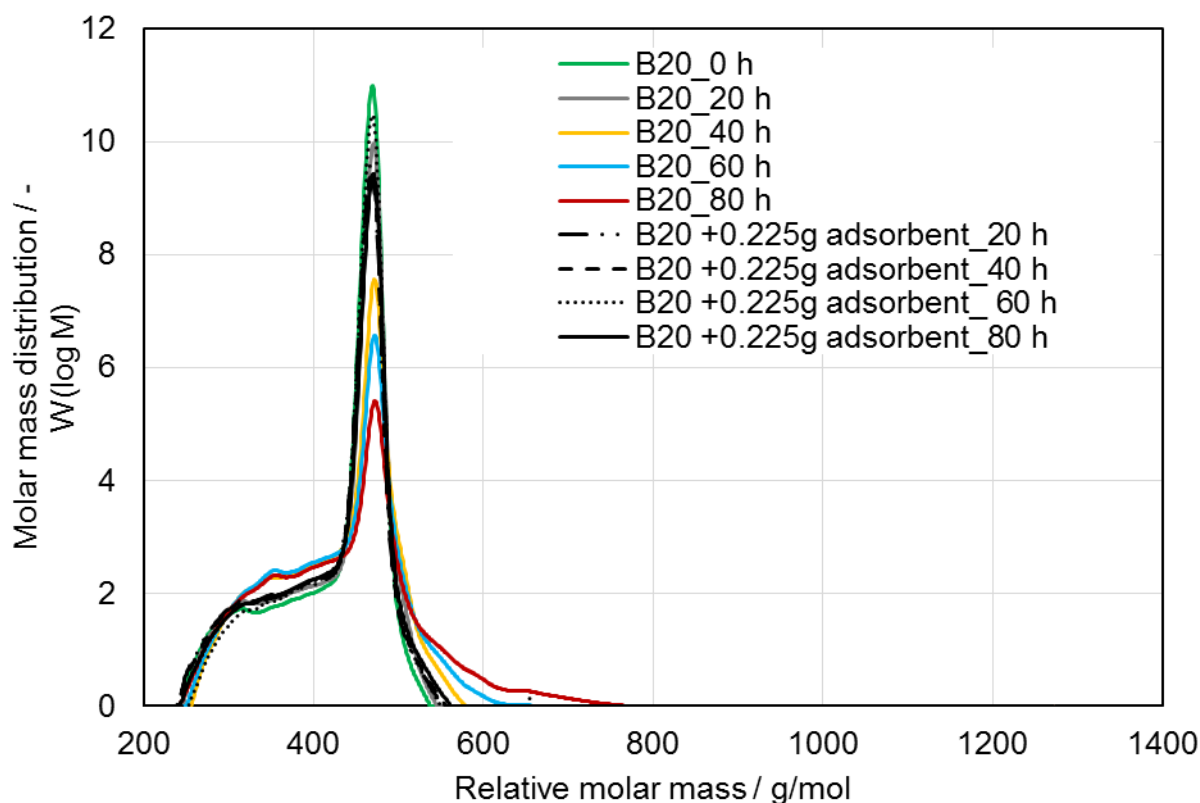


Figure 82: SEC chromatogram evaluation of 30 mL 20 %RME mixed with 80 % diesel fuel and treated with and without combined 0.225 g adsorbents of magnesium-aluminum hydrotalcite and 1,3,5-trimethyl-2,4,6-tris(3,5-di-tert-butyl-4-hydroxybenzyl) benzene in a ratio of 1:2 respectively and aged at 110 °C with airflow of 10 L/h at 8 h per day for durations of 20 h, 40 h, 60 h and 80 h using a Rancimat compared with the neat unaged blends

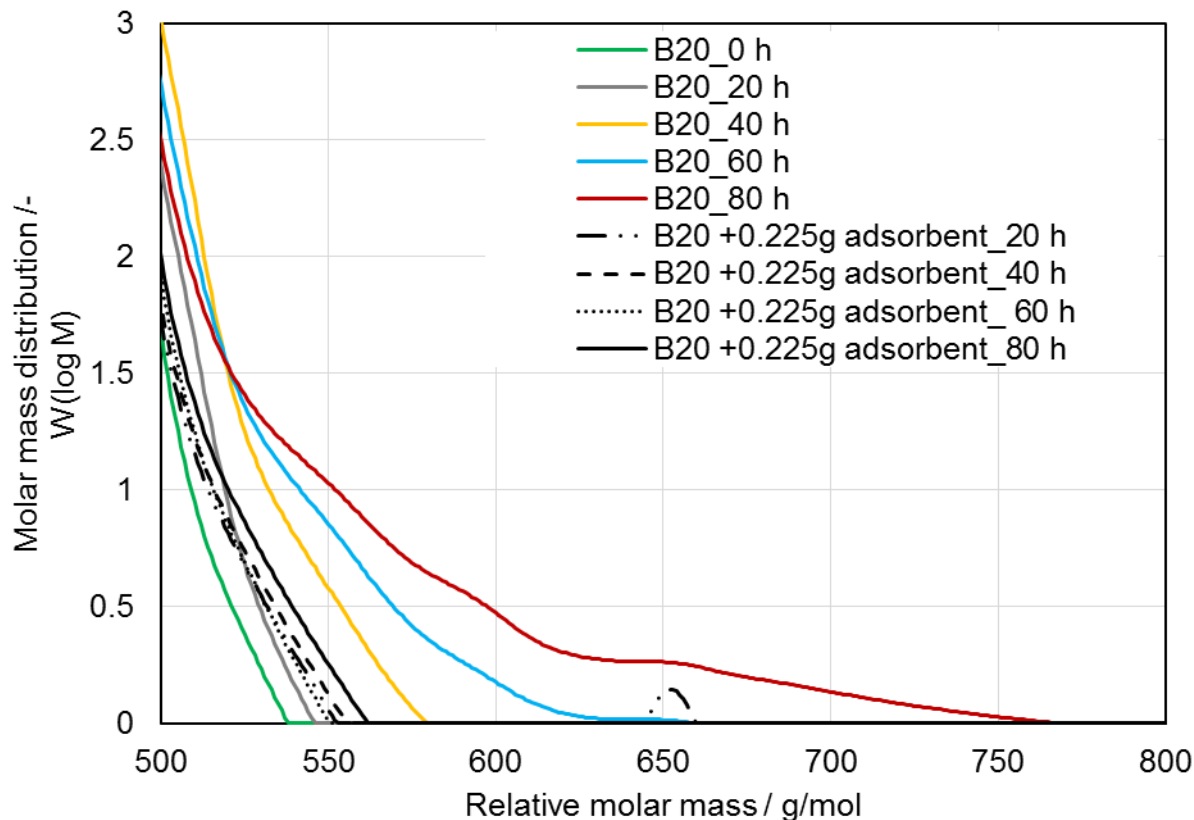


Figure 83: SEC chromatogram (rang 500-800 g/mol) evaluation of 30 mL 20 %RME mixed with 80 % diesel fuel and treated with and without combined 0.225 g adsorbents of magnesium-aluminum hydrotalcite and 1,3,5-trimethyl-2,4,6-tris(3,5-di-tert-butyl-4-hydroxybenzyl) benzene in a ratio of 1:2 respectively and aged at 110 °C with airflow of 10 L/h at 8 h per day for durations of 20 h, 40 h, 60 h and 80 h using Rancimat compared with a neat unaged blend

8.5.3 Effect of combined adsorbents of magnesium-aluminum hydrotalcite and 1,3,5-trimethyl-2,4,6-tris(3,5-di-tert-butyl-4-hydroxybenzyl) benzene in a ratio of 1:2 respectively on the acid value of 20 %RME and 80 % diesel fuel blend during the oxidation process

Figure 84 illustrates the relationship between the acid value and the duration of aging at a temperature of 110 °C. From Figure 84, it is evident that generally, higher acid values result from a longer aging duration. These results correspond with the FTIR measurement, which demonstrates that the absorption bands of carbonyl or hydroxyl groups formed during the oxidation processes increase steadily with time in biodiesel. This has been seen in section 4.1.5. The use of the adsorbents has given stability to the biodiesel blend. Therefore, the rate of change of acid value in the aged blends treated with adsorbents is

negligible, about 0.51 mgKOH/g from 0.08 mgKOH/g compared to the blends aged without any use of the adsorbents, which also increased from 0.08 mgKOH/g to about 10.89 mgKOH/g on the average. A linear relationship can be seen in the acid value with an aging duration, which slightly differs from the aging at 170 °C. The adsorbents interrupt the oxidation reactions and reduce the rate of oxidation of the sample. This observation has been exhibited in SEC in this work by the samples aged without the adsorbents indicating an increasing trend of higher molecular mass substances. It is a similar observation seen here with an increasing trend in acid value. The relation of deposits or high molecular mass substances formed with samples aged without using the adsorbents is verified by a direct increase of high molecular mass substances formed with a corresponding increasing higher acid value. The acid value of the mixture aged without adsorbents treatment increased in the ratio of 1:11:17:24 while the mixture treated with the adsorbent increased by a factor of about 1. Averagely, the adsorbents caused the suppression of the increase in acid value by about 95 %. Literature indicates that fuel aging is better detected by an acid number representing the secondary oxidation products (Saltas et al., 2017; Davannendran et al., 2016). Therefore, the very low acid values results agree with the SEC illustrated in section 8.5.2 and collaborate the induction period results. The trend shown in all samples aged with the adsorbents' use revealed similar aging time and temperature results compared to those reported in section 8.4.

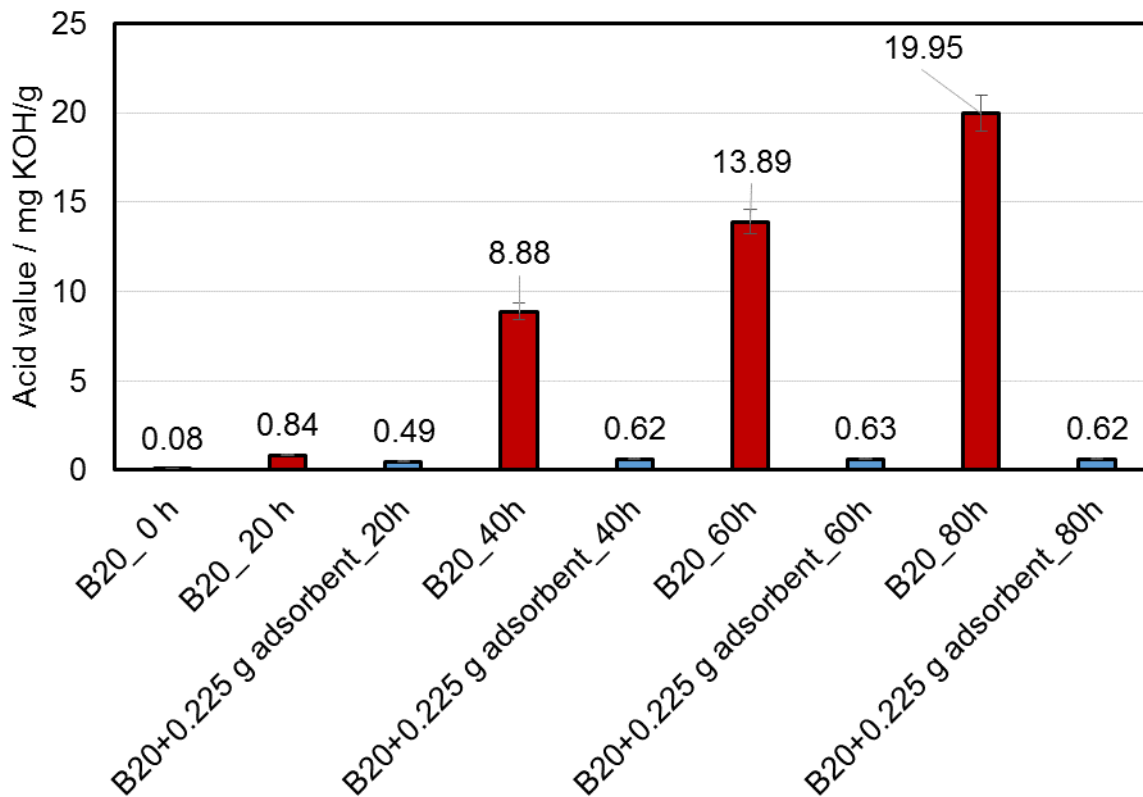


Figure 84; Evaluation of the acid value of 30 mL 20 % RME mixed with 80 % diesel fuel and treated with and without combined 0.225 g adsorbents of magnesium-aluminum hydrotalcite and 1,3,5-trimethyl-2,4,6-tris(3,5-di-tert-butyl-4-hydroxybenzyl) benzene in a ratio of 1:2 respectively and aged at 110 °C with airflow of 10 L/h at 8 h per day for durations of 20 h, 40 h, 60 h and 80 h at 8 h per day using Rancimat

8.5.4 Impact of combined adsorbents of magnesium-aluminum hydrotalcite and 1,3,5-trimethyl-2,4,6-tris(3,5-di-tert-butyl-4-hydroxybenzyl) benzene in a ratio of 1:2 respectively on the viscosity of biodiesel blend during aging at 110 °C

Kinematic viscosity of aged B20 treated with and without adsorbents has been measured at 40 °C and 100 °C per standard procedure. The results of the measurements are illustrated in Figure 85 and Figure 86, respectively. It is seen from both figures that the B20 samples aged without the use of the adsorbents have shown a significant increase in viscosity from 3.044 mm²/s at 0 h to 6.797 mm²/s at 80 h at an average of about 2.239 mm²/s increase with increasing aging duration. The increase in viscosity with aging is attributable to the oxidation with subsequent polymeric compounds resulting from the reaction between the oxidation products formed during the aging process. However, the

samples treated with the adsorbents and aged showed more minor viscosity increase tendencies with an average of 0.531 mm²/s. Hence low oxidation effect with insignificant degradation products build-up (Mannekote and Kailas, 2012). This then gives rise to a more extended period of the useful life of the fuel. The rate of change in the viscosity at 110 °C is less significant than that conducted at 170 °C. The formation of higher molecular weight components of the sample aged without using the adsorbents recorded by the SEC results in section 8.5.2 thus correlates well with the high viscosity seen here. The increase in higher molecular mass species has been consistent with the increase in the mixtures' degradation without adsorbents treatment. The more severe the oxidative degradation, the greater the number of oligomers formed and the higher the viscosity. Hence, the oxidation products of the degradation of biodiesel blends increase viscosity. With the adsorbents' application, the mixtures' viscosity increased at an average of 14 %, while the mixtures aged without adsorbents treatment increased linearly at an average of 39 %. The trend for the samples' viscosity measured at 40 °C does not differ from the viscosity measured at 100 °C. These results are shown in Figure 85 but not discussed in this work.

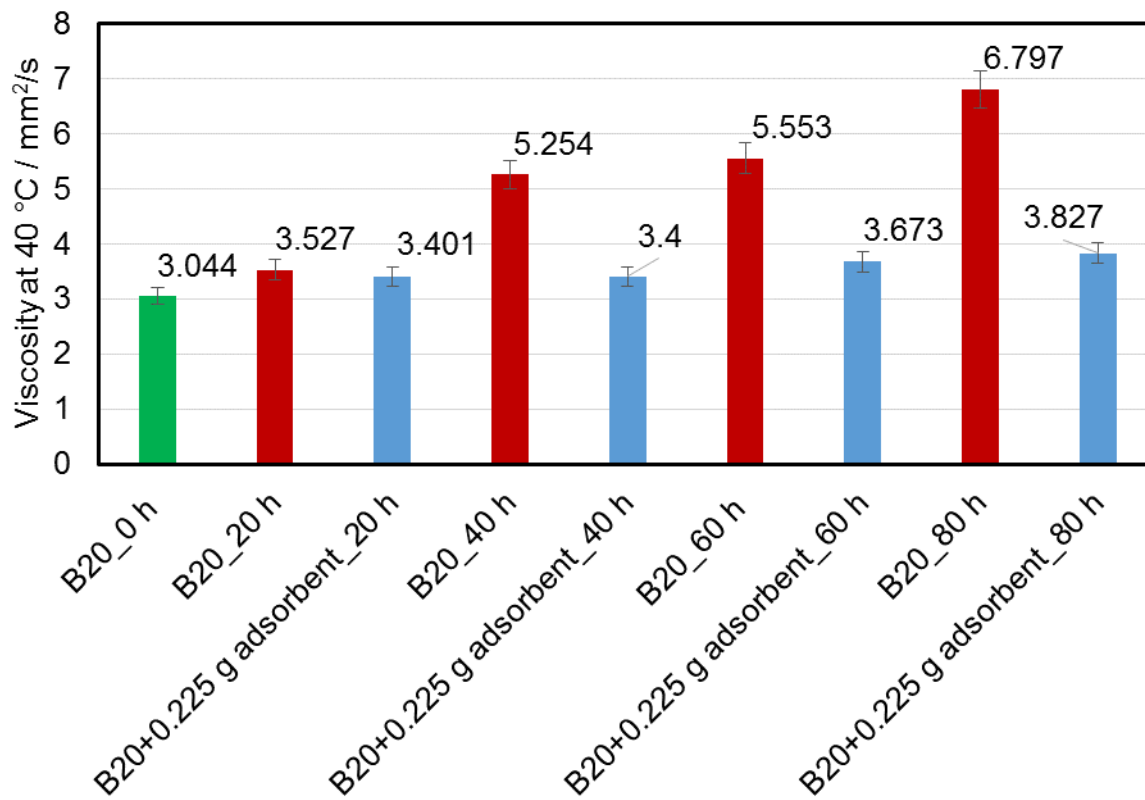


Figure 85: Evaluation of viscosity at 40 °C of 30 mL 20 % RME mixed with 80 % diesel fuel and treated with and without combined 0.225 g adsorbents of magnesium-aluminum hydrotalcite and 1,3,5-trimethyl-2,4,6-tris(3,5-di-tert-butyl-4-hydroxybenzyl) benzene in a ratio of 1:2 respectively and aged at 110 °C with airflow of 10 L/h at 8 h per day for durations of 20 h, 40 h, 60 h and 80 h using a Rancimat

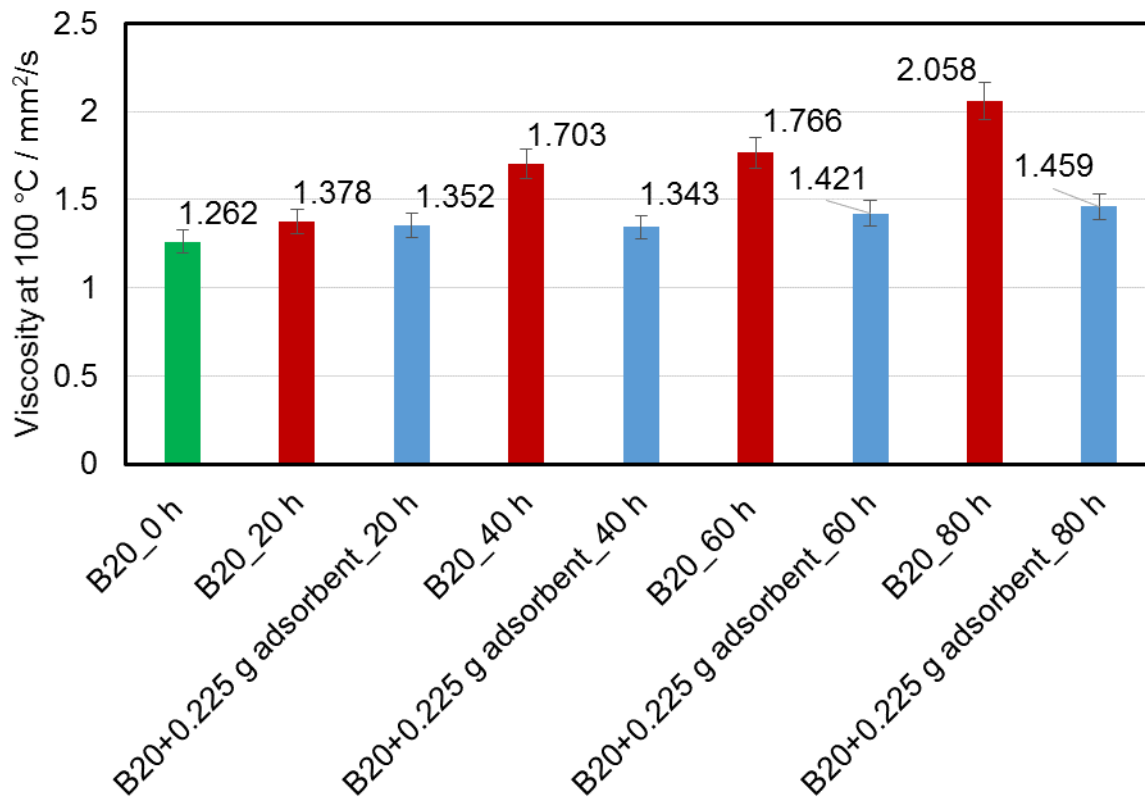


Figure 86: Evaluation of viscosity at 100 °C of 30 mL 20 % RME mixed with 80 % diesel fuel and treated with and without combined 0.225 g adsorbents of magnesium-aluminum hydrotalcite and 1,3,5-trimethyl-2,4,6-tris(3,5-di-tert-butyl-4-hydroxybenzyl) benzene in a ratio of 1:2 respectively and aged at 110 °C with airflow of 10 L/h for durations of 20 h, 40 h, 60 h, and 80 h at 8 h per day using a Rancimat

8.5.5 Analysis of the impact of combined adsorbents of magnesium-aluminum hydrotalcite and 1,3,5-trimethyl-2,4,6-tris(3,5-di-tert-butyl-4-hydroxybenzyl) benzene in a ratio of 1:2 respectively on the density of biodiesel blend during aging at 110 °C

Figure 87 and Figure 88 illustrate the trend of changes in the density of the blends aged for different durations and measured at 40 °C and 100 °C, respectively. As seen in section 4.1.4, biodiesel density increases with aging duration due to increased molecular interaction of degraded products (Pattamaprom and Ngamjaroen, 2012). The increase in density of the blends treated with the adsorbents and aged is less significant (an average increase at 0.87 %) than that of the blend aged without using the adsorbents (an average increase at 3.4 %). The adsorbents have intercepted the radicals that would have

polymerized into oligomers during the mixture's oxidation. Hence, oxidation is thus retarded, resulting in marginal oxidative products and hence the low-density values.

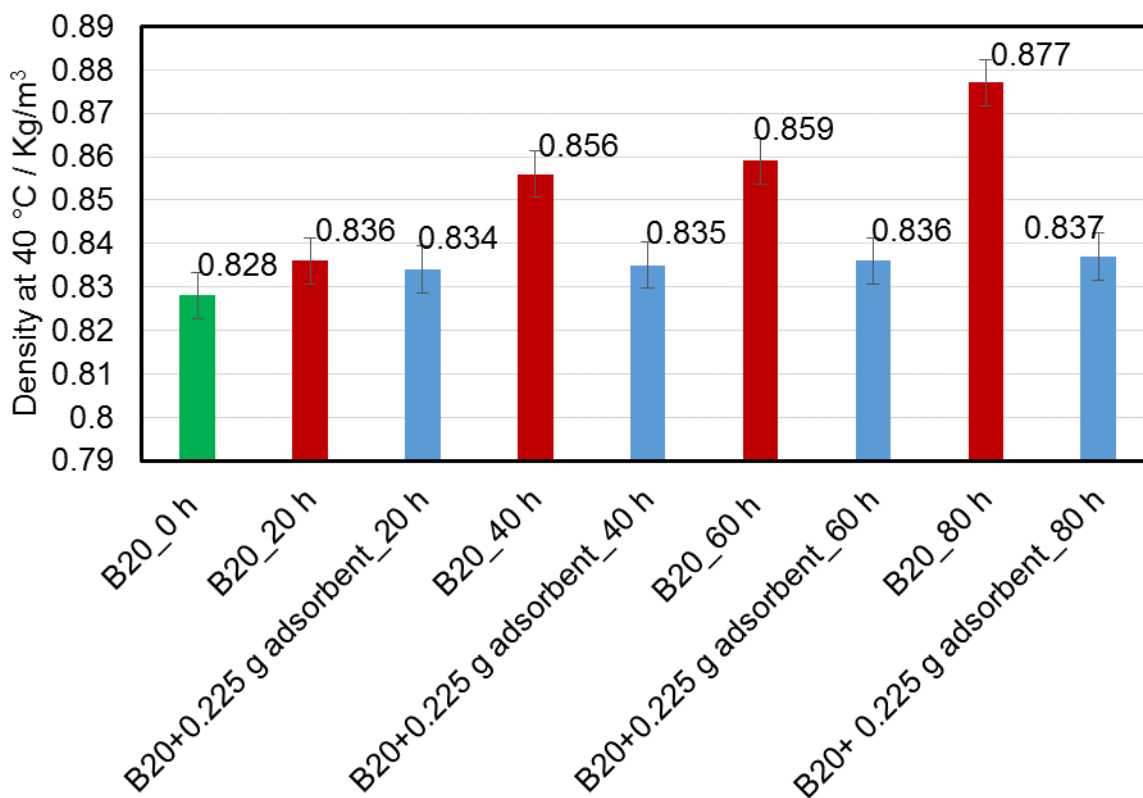


Figure 87: Evaluation of density at 40 °C of 30 mL 20 % RME mixed with 80 % diesel fuel and treated with and without combined 0.225 g adsorbents of magnesium-aluminum hydrotalcite and 1,3,5-trimethyl-2,4,6-tris(3,5-di-tert-butyl-4-hydroxybenzyl) benzene in a ratio of 1:2 respectively and aged at 110 °C with airflow of 10 L/h for durations of 20 h, 40 h, 60 h, and 80 h at 8 h per day using a Rancimat

The change in density of the blends treated with the adsorbents measured at 100 °C is negligible, an average of 0.00725 kg/m³, Figure 88. With increasing aging duration, the average change in density of the mixture treated with the adsorbents is about 0.9 %. However, the blend aged without using the adsorbents recorded an average increase of 3.6 %, which is 0.2 % different from what is observed at the 40 °C measurements. The adsorbents' presence enhanced hydroperoxide formation inhibition, resulting in low-density values compared to the mixtures aged without any adsorbents treatment. Otherwise, as hydroperoxides decompose, oxidative linking of fatty acid chains occurs, leading to higher molecular weights. An obvious result of the formation of higher molecular

weight materials is the increase in oil density. Similar reports are in literature, Siddharth and Sharma (2010).

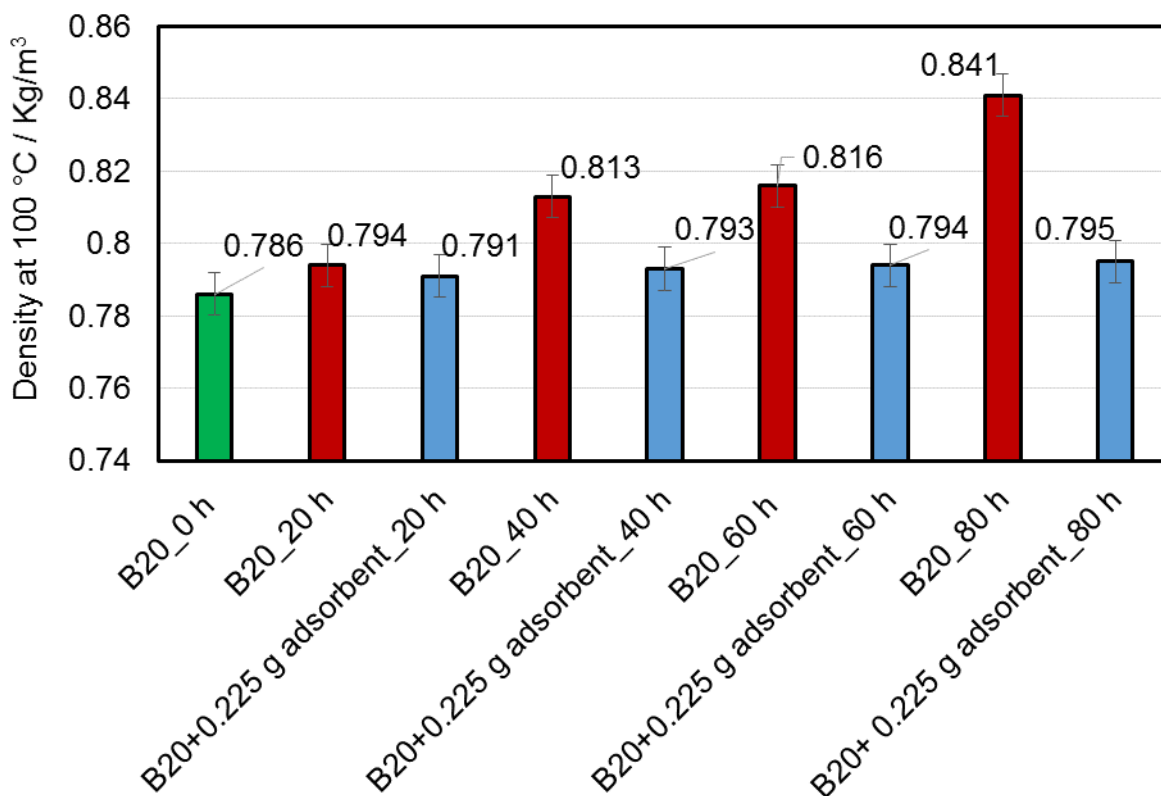


Figure 88: Evaluation of density at 100 °C of 30 mL 20 % RME mixed with 80 % diesel fuel and treated with combined 0.225 g adsorbents of magnesium-aluminum hydrotalcite and 1,3,5-trimethyl-2,4,6-tris(3,5-di-tert-butyl-4-hydroxybenzyl) benzene in a ratio of 1:2 respectively and aged at 110 °C with airflow of 10 L/h for durations of 20 h, 40 h, 60 h, and 80 h at 8 h per day using a Rancimat

8.5.6 Relationship between viscosity and an acid value of 20 % RME mixed with 80 % diesel fuel and treated with and without combined 0.225 g adsorbents of magnesium-aluminum hydrotalcite and 1,3,5-trimethyl-2,4,6-tris(3,5-di-tert-butyl-4-hydroxybenzyl) benzene in a ratio of 1:2 respectively and aged at 110 °C with airflow of 10 L/h for durations of 20 h, 40 h, 60 h, and 80 h at 8 h per day using a Rancimat

Figure 89 illustrates the relationship between the viscosity and the acid value of 20 % RME mixed with 80 % diesel fuel and treated with and without combined adsorbents of magnesium-aluminum hydrotalcite and 1,3,5-trimethyl-2,4,6-tris(3,5-di-tert-butyl-4-hydroxybenzyl) benzene in a ratio of 1:2 respectively and aged at 110 °C with airflow of

10 L/h for durations of 20 h, 40 h, 60 h and 80 h at 8 h per day using a Rancimat. From the graph, there is a linear relationship between the viscosity and the acid value. The high viscosity translates to high acid value, resulting from higher aging or degradation of the blend aged without any adsorbent treatment. A strong correlation was found between acid value and viscosity. With time, the viscosity and acid increased for all biodiesel and diesel fuel blends aged without the adsorbent treatment. The correlation between acid value and viscosity curves coincides. The coincidence supports the hypothesis that there is a coupling between the reactions that form the acid compounds and the polymerization reactions that increase the viscosity. This can be explained as due to oxidation that took place, resulting in more insoluble materials. This confirms the greater tendency of biodiesel to form polymeric deposits with increasing aging, which increases viscosity.

On the other hand, the adsorbents' usage decreased the formation of higher molecular weight species leading to low viscosities and low acid values. It is apparent from the results that the extent of inhibition during the oxidation process depends on the adsorbents' concentration. The higher the amount of the adsorbents, the lower the values of the parameters obtained.

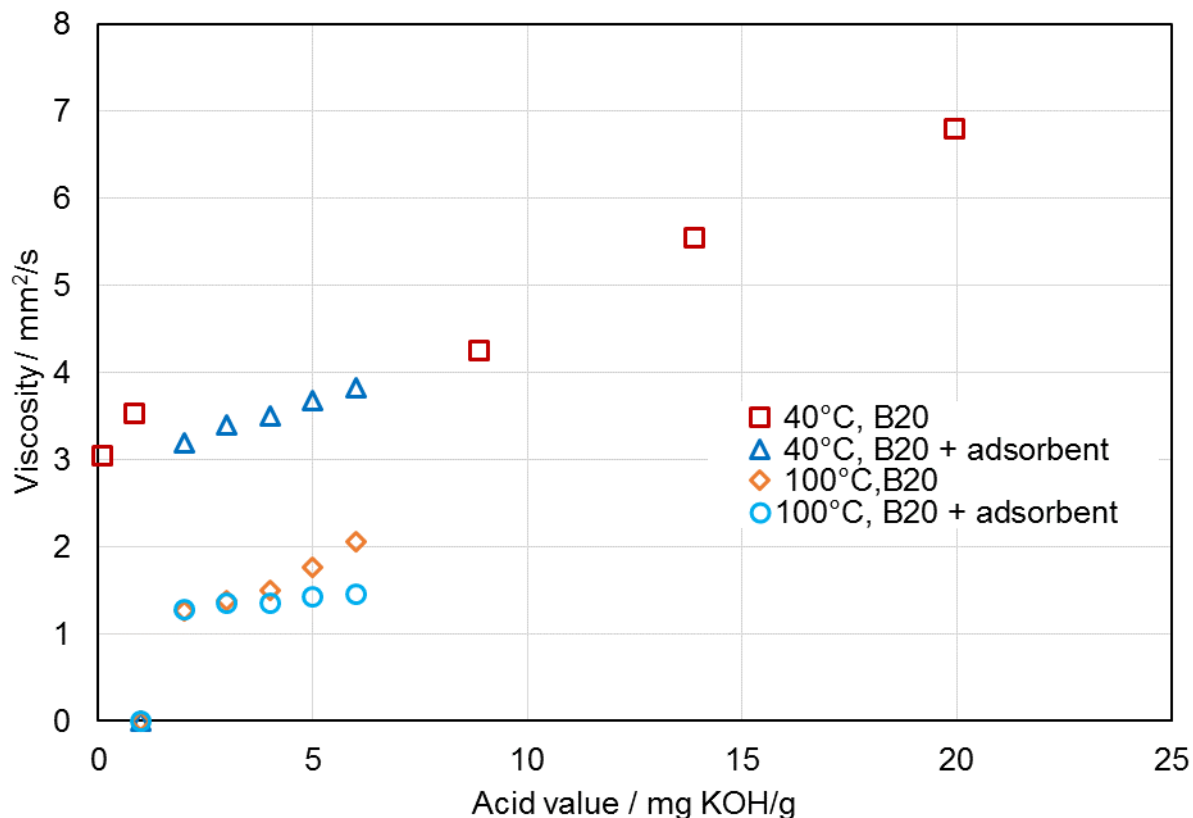


Figure 89: Comparative analysis of acid value versus viscosity of 30 mL 20 % RME mixed with 80 % diesel fuel and treated with and without combined 0.225 g adsorbents of magnesium-aluminum hydrotalcite and 1,3,5-trimethyl-2,4,6-tris(3,5-di-tert-butyl-4-hydroxybenzyl) benzene in a ratio of 1:2 respectively and aged at 110 °C with airflow of 10 L/h for durations of 20 h, 40 h, 60 h, and 80 h at 8 h per day using a Rancimat

8.5.7 FTIR analysis of 30 mL 20 % RME mixed with 80 % diesel fuel and treated with 0.225 g combined adsorbents of magnesium-aluminum hydrotalcite and 1,3,5-trimethyl-2,4,6-tris(3,5-di-tert-butyl-4-hydroxybenzyl) benzene in a ratio of 1:2 respectively and aged at 110 °C with airflow of 10 L/h at 8 h per day for durations of 20 h, 40 h, 60 h and 80 h using a Rancimat

Figure 88 shows the infrared spectra obtained for the samples with the wavenumbers in cm^{-1} plotted against absorbance. The spectra of the blends aged without any adsorbent treatment show large carbonyl and hydroxyl peaks indicating degradation in the blend with increasing duration of aging. These results agree with that their acid values. The intensity of the carbonyl/hydroxyl peaks is insignificant or absent in most of the aged blends treated with the adsorbents indicating the retardation of the oxidation process. In Figure 88, Figure

89, and Figure 90, it can be recognized that the B20 treated with the adsorbents have recorded only minor changes in vibrations during the aging process. This resulted from the adsorbents intercepting the oxidation precursors and, therefore, inhibiting polymerization into oligomers.

Oxidative and thermal instability of fatty oils and esters during chemical reactivity is determined by the amount and configuration of the olefinic unsaturation on the fatty acid chains. Therefore, their molecular structure is key to understanding the impact of oxidation. The FTIR application determines the oxidation level by the response in absorption in the carbonyl (C=O) region between 1900 to 1600 cm^{-1} and the hydroxyl region, 3000-3600 cm^{-1} . The IR energy is absorbed in this region due to the carbon-oxygen bonds in the oxidized fuel mixture. Therefore, monitoring this region is thus a direct measurement of the fuel mixture's level of degradation. As seen earlier in section 4.1.5, oxidation impacts the carbonyl vibrations at 1750 cm^{-1} . Comparing the vibrations of aged B20 treated with and without the adsorbents and the neat unaged blend, the carbonyl vibrations illustrate many differences. The FTIR results for the aging of the blends treated with and without the adsorbents at both temperatures, 170 °C, and 110 °C, follow a similar trend. The difference is that the higher temperature of 170 °C resulted in higher production of oxidative products, which agrees with Abdulkadir et al. (2016). It is expected since higher temperature provides much harsh conditions and promotes a higher degree of oxidation. However, the impact of the adsorbents in suppressing the formation of higher molecular substances remains unaffected. Hence, the adsorbents' impact on the degree of soil degradation can be reasonably inferred from a simple visual analysis of the blends sample spectra presented.

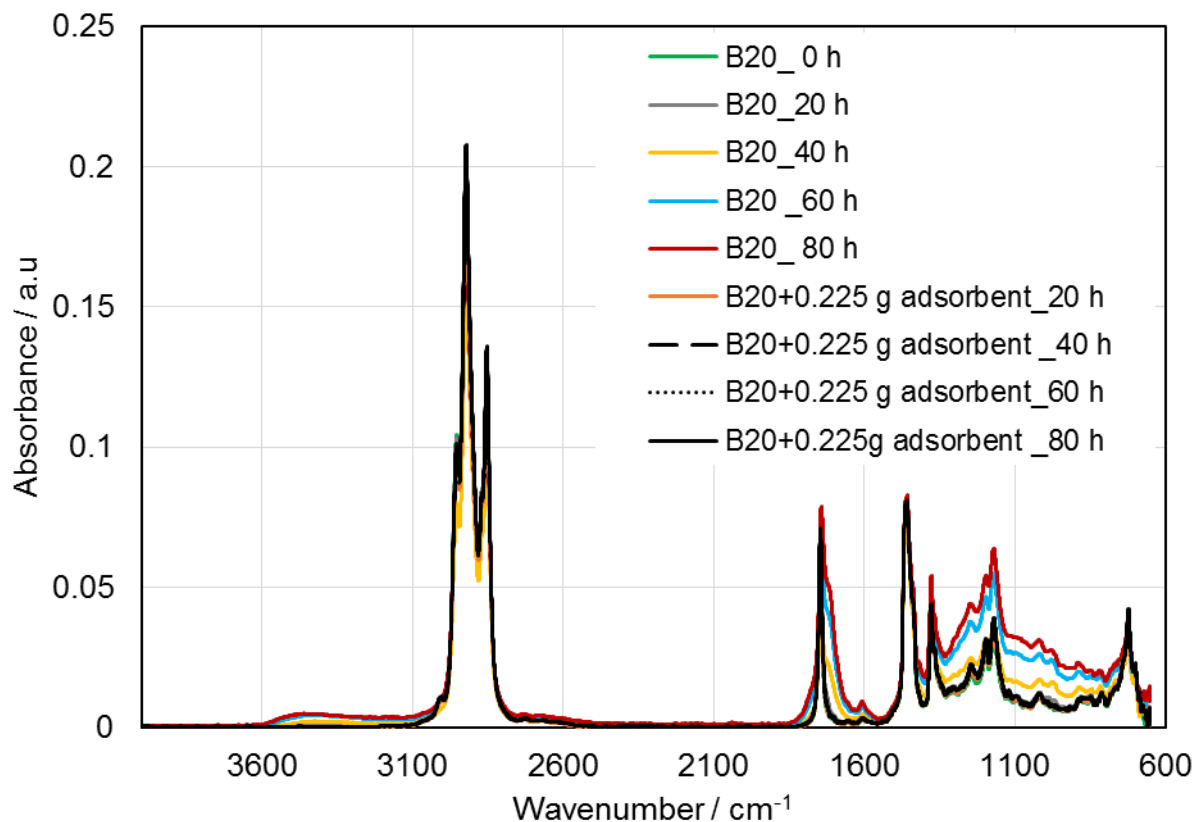


Figure 90: Evaluation of comparative analysis of FTIR spectra in absorbance mode of 30 mL 20 % RME mixed with 80 % diesel fuel and treated with 0.225 g combined adsorbents of magnesium-aluminum hydrotalcite and 1,3,5-trimethyl-2,4,6-tris(3,5-di-tert-butyl-4-hydroxybenzyl) benzene in a ratio of 1:2 respectively and aged at 110 °C with airflow of 10 L/h at 8 h per day for durations of 20 h, 40 h, 60 h and 80 h using a Rancimat

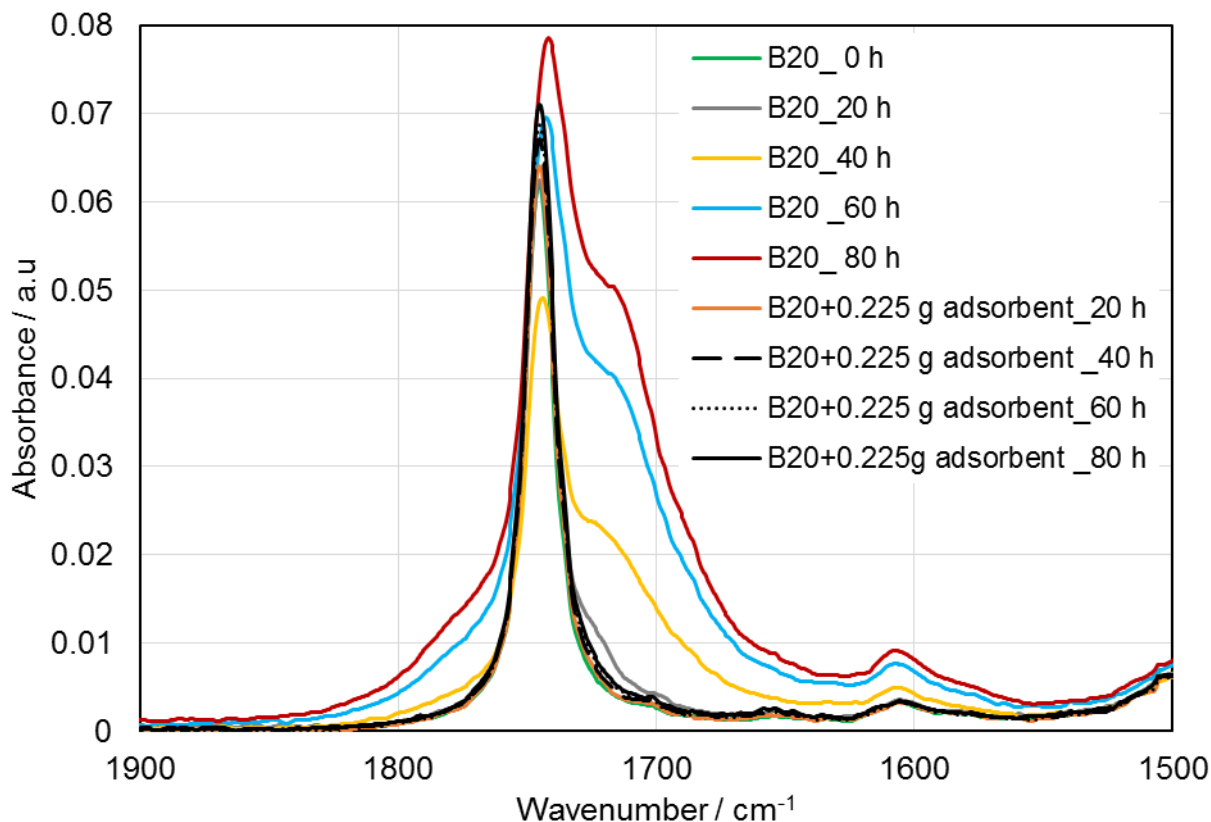


Figure 91: Evaluation of comparative analysis of FTIR spectra in absorbance mode (range 1500-1900 cm^{-1}) of 40 mL 20 % RME mixed with 80 % diesel fuel and treated with 0.225 g combined adsorbents of magnesium-aluminum hydrotalcite and 1,3,5-trimethyl-2,4,6-tris(3,5-di-tert-butyl-4-hydroxybenzyl) benzene in a ratio of 1:2 respectively and aged at 110 °C with airflow of 10 L/h for durations of 20 h, 40 h, 60 h and 80 h using a Rancimat compared with the neat unaged blend

The apparent increases in this region's signals and centering at about 3495 cm^{-1} in

Figure 92 is attributable to the hydroxyl groups. The OH band in this region is ascribed to organic compounds containing the OH functional groups such as alcohols, hydroperoxides, and carboxylic acids (Kerkering and Andersson, 2015). Understandably, viscosity increases with the formation of hydroperoxides resulting in oxidized polymeric compounds. Also, the acid value of blends aged without any treatment with the adsorbents increased with increasing aging duration. Such observed increment, as seen above in the samples aged without adsorbents treatment, is due to the formation of hydroperoxides oxidized into acids and higher molecular mass species. The signals are low and sometimes absent in the blends treated with the adsorbents before the aging point to

suppress the formation of precursors of the oxidation, hydroperoxides. This indicates the adsorbents impacting the initiation phase of the oxidation process, leading to fewer hydroperoxides.

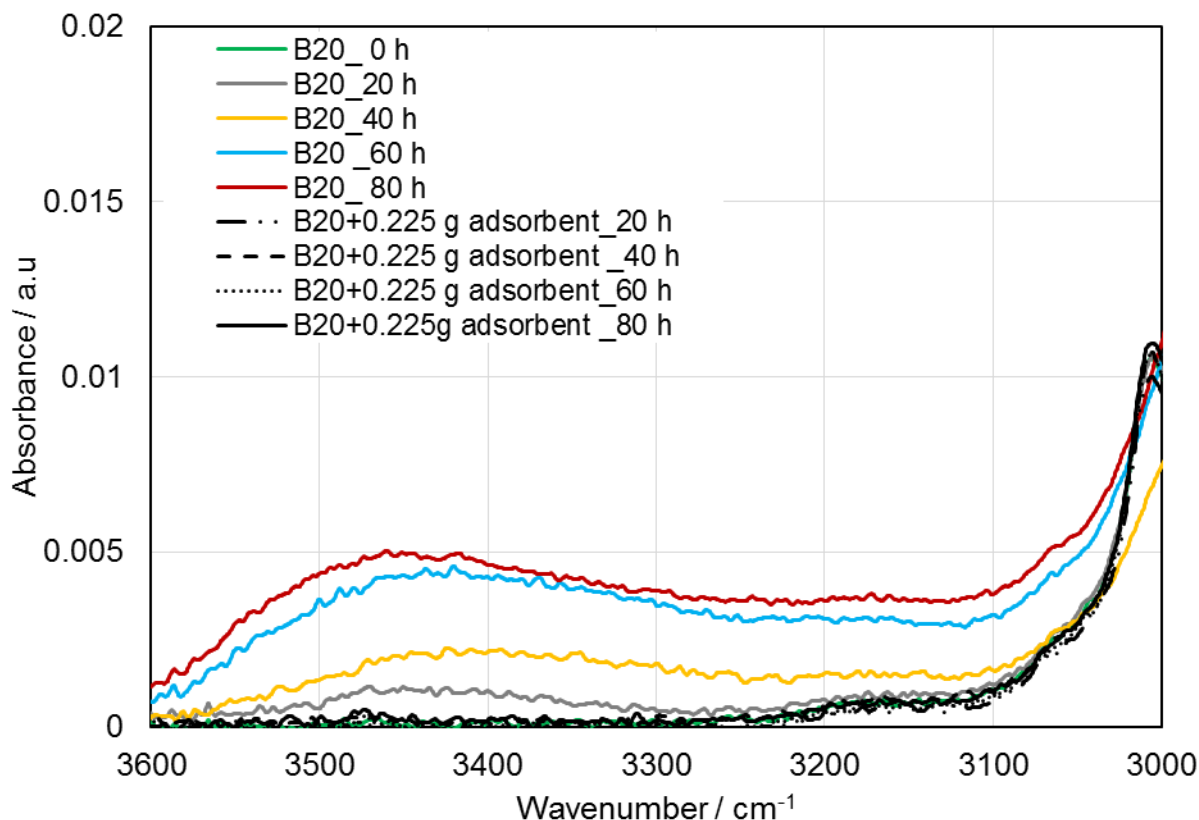


Figure 92: Evaluation of comparative analysis of FTIR spectra in absorbance mode (range 3000-3600 cm^{-1}) of 30 mL 20 % RME mixed with 80 % diesel fuel and treated with 0.225 g combined adsorbents of magnesium-aluminum hydrotalcite and 1,3,5-trimethyl-2,4,6-tris(3,5-di-tert-butyl-4-hydroxybenzyl) benzene in a ratio of 1:2 respectively and aged at 110 °C with airflow of 10 L/h for durations of 20 h, 40 h, 60 h, and 80 h at 8 h per day using a Rancimat compared with a neat unaged blend

The differences in the C=O-bonds, as shown earlier in

Figure 91, have been integrated and illustrated in Figure 93. When the vibrations of B20 treated with the adsorbents and aged are compared with the blend without any adsorbent treatment, the carbonyl vibrations (1600-1900 cm^{-1}) in the B20 without any adsorbent treatment show much higher C=O-vibrations. With an increase of 2 % at 20 h, the blends treated with the adsorbents further increased by 10 % at 40 h, 12 % at 60 h, and 16 % after 80 h of aging. Nevertheless, the adsorbents' impact is seen in the insignificant

increase in the C=O vibrations in the blends treated with the adsorbents and aged. This means the adsorbents' use results in fewer degradation products, hydroperoxides, and other low molecular weight carboxylic acids, aldehydes, and ketones (Obadiah et al., 2012). For the blends not treated with the adsorbents, the increase is by 15 % at 20 h, 39 % at 40 h with a further increase by 65 % at 60 h, and finally to 72 % after 80 h of aging. The trend exhibited here is not different from that seen in section 8.5.7 (see Figure 80). The insignificant increase in the C=O vibrations in the blends treated with the adsorbents and aged results from the adsorbents impacting the aging process per the explanation given in section 6.

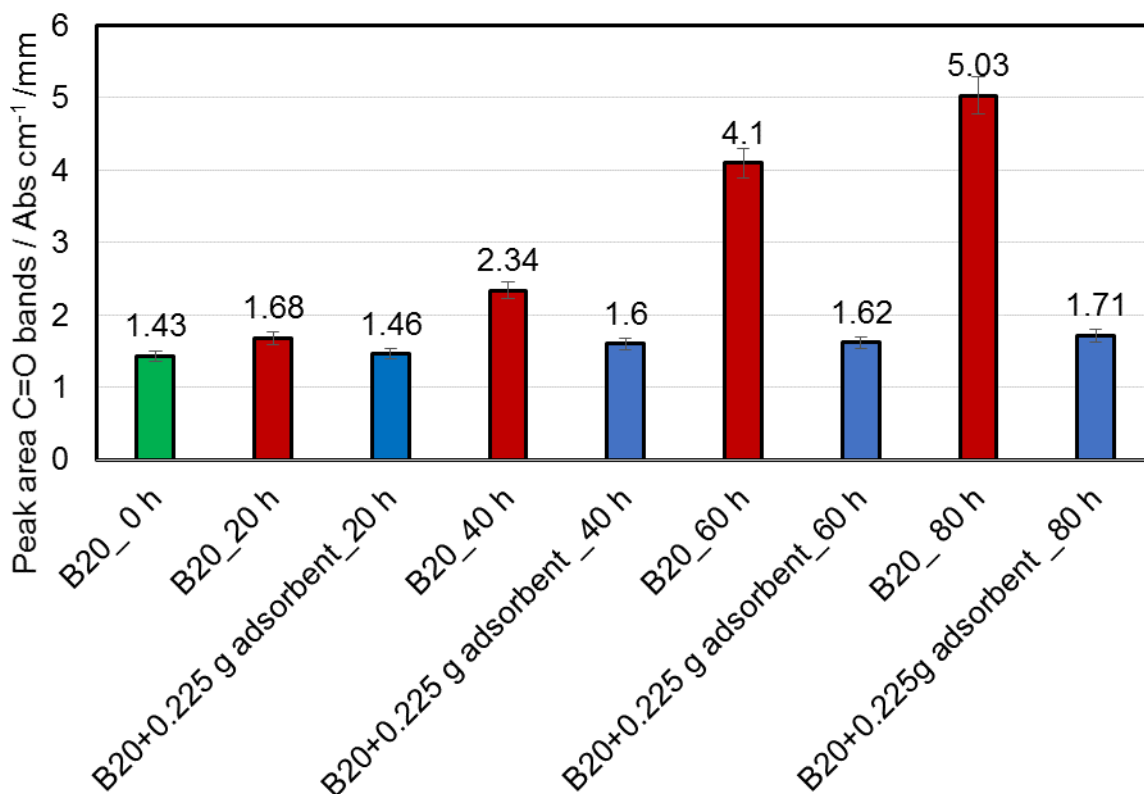


Figure 93: Evaluation of peak area under C=O bands (1600-1900 cm⁻¹) of the FTIR spectra of 30 mL 20 % RME mixed with 80 % diesel fuel and treated with and without combined 0.225 g adsorbents of magnesium-aluminum hydrotalcite and 1,3,5-trimethyl-2,4,6-tris(3,5-di-tert-butyl-4-hydroxybenzyl)benzene in a ratio of 1:2 respectively and aged at 110 °C with airflow of 10 L/h for durations of 20 h, 40 h, 60 h, and 80 h at 8 h per day using a Rancimat compared with the neat unaged blend

Summary

A volume of 30 mL of B20 sample made of 80 Vol % diesel fuel and 20 Vol % biodiesel is treated with a mass of 1 g and 0.225 g of the adsorbents in the ratio of 1:2 (magnesium-aluminum hydrotalcite:1,3,5-trimethyl-2,4,6-tris(3,5-di-tert-butyl-4-hydroxybenzyl)benzene) and aged at 170 °C and 110 °C for durations up to 48 h and 80 h respectively using the Rancimat at 8 h per day. The changes in the physicochemical properties resulting from oxidation are measured and compared between the samples treated with and without the adsorbents.

Figure 65 to Figure 93 shows biodiesel's blend degradation under different temperatures of 110 °C and 170 °C. The degradation is represented by the number of oligomers formed with and without the treatment with biodiesel's adsorbents and its blends with increasing residing time of aging. The carbonyl region of the blend aged 48 h at 170 °C without any adsorbent treatment under the FTIR had enhanced adsorption of about 80 % compared to the same blend aged at 110 °C, for 80 h. The carbonyl groups centered on 1715 cm^{-1} in the blends aged without any adsorbent treatment show enhanced absorption in the spectra. This is due to oxidation products such as ketones and aldehydes formed after chain scission (Kerkering and Andersson, 2015). Also, a clear enhanced signal around $3,495\text{ cm}^{-1}$ in the blends aged without treatment with the adsorbents is seen in the spectra. This is attributable to hydroxyl groups. According to Kerkering and Andersson (2014), the OH band can be derived from water or ascribed to organic compounds containing the OH functional groups such as hydroperoxides, carboxylic acids, and alcohols.

For the other parameters, viscosity at 40 °C, acid value, density, etc., there is a linear relationship between temperature and aging duration Table 18. Using the 1 g and 0.225 g of adsorbents suppressed an increase in viscosity measured at 40 °C by 78 % for the aging at 170 °C for 48 h duration. In contrast, during the aging at 110 °C for 80 h, the depression is about 56 %. A similar trend is seen in density measured. The adsorbents, 1 g, and 0.225 g suppressed the increase of acidity by 94 % for the aging at 170 °C for 48 h while the suppression at 110 °C for 80 h has been 97 %, respectively. These results largely coincide with literature, Zhou et al. 2017; Dunn, 2008, 2005; Liang et al., 2006.

These experiments are not in strict comparison as the mass of the adsorbents used and the duration of aging differs through physical calculations; correlations are established.

Table 18 Evaluation of parameters of aging of 30 mL of 20 % RME mixed with 80 % diesel fuel and treated with and without combined adsorbents of magnesium-aluminum hydrotalcite and 1,3,5-trimethyl-2,4,6-tris(3,5-di-tert-butyl-4-hydroxybenzyl)benzene in a ratio of 1:2 respectively at 110 °C and 170 °C for durations of 48 h and 80 h

Parameters	Samples and conditions of aging			
	B20 at 110 °C for 80 h	B20+0.225 g combined adsorbents at 110 °C for 80 h	B20 at 170 °C for 48 h	B20 + 1 g combined adsorbents at 170 °C for 48 h
Total acid number / mgKOH/g	19.95	0.62	41.79	2.58
FTIR (C=O band area) / Abs cm ⁻¹ /mm	5.03	1.71	8.3	2.36
SEC (area under the curve) / -	244	175	330	44
Viscosity at 40 °C / mm ² /s	6.797	3.827	21.05	4.68
Density / Kg/m ³	0,877	0.837	0.915	0.846

These experiments are obtained due to the adsorbents' suppression action because of the interaction between its surface and the free radical, mainly due to hydrogen bonding. The hydrogen bonds are established between the ester carbonyl and the adsorbents' hydroxyl groups, leading to the free radical propagation's interruption. This is because of the hydrogen atom interaction from the surface of the hydroxyl group of the adsorbents with the immediate peroxy radicals. With the free radical propagation interruption, oxidation is retarded, resulting in less or no significant degradation product formation. The impact of the adsorbents has not been affected by the temperature at which it has been applied. It confirms the results reported in section 8.2.

8.6 Investigating the effect of the combined adsorbents of magnesium-aluminum hydrotalcite and 1,3,5-trimethyl-2,4,6-tris(3,5-di-tert-butyl-4-hydroxybenzyl) benzene in a ratio of 1:2 respectively in stabilizing rapeseed oil methyl ester and its blends during long term storage conditions

One of the main critical quality parameters of biodiesel is its storage stability. Biodiesel tends to deteriorate owing to hydrolytic and oxidative reactions, as seen in section 3.4. Their degree of unsaturation makes them susceptible to thermal and or oxidative polymerization. Biodiesel can oxidize, leading to the formation of sediments during a long period of storage, resulting in high density, high viscosity, and high acidity (section 2.1) (Knothe and Dun, 2003; Fang et al., 2006).

In this test of using adsorbents to stabilize fuel during storage or application, 40 mL of neat biodiesel, RME and its blends, B20 in the ratio of 20 % RME and 80 % EN950 diesel fuel are treated with 0.675 g of the combined and the neat B20 without the adsorbents are stored in a temperature-controlled oven at 40 °C for 120 days. The samples are taken out of the oven every 15 days to analyze the following parameters, stability (induction period), viscosity, density, size exclusion chromatography, and molecular structure changes using FTIR. These parameters are affected during the oxidative degradation of biodiesel.

8.6.1 Evaluation of induction period of neat biodiesel

To gain insight into biodiesel's stability with the adsorbents, the induction times are determined using the PetroOXY method during the 120 days of storage. All the test samples are stored under identical conditions, at 40 °C and only open for air exchange for 10 min every 15 days. Figure 94 shows the evaluation of the oxidation stability with time. While the biodiesel RME without any adsorbent treatment shows initial oxidation stability of 16.53 min, this stability decreased exponentially to 8.28 min after 120 days of storage, giving rise to about 50 % reduction stability. ON THE OTHER HAND, the RME treated with the adsorbents started with an initial induction time of 76.36 min and this induction time decreased gradually to 58.11 min at the 120 days of storage. This represents just about a 24 % decrease in the induction period. At 120 days of storage, the biodiesel treated with the adsorbents has better oxidative stability of about 26 % than the neat biodiesel not treated with the adsorbents. The adsorbents' impact can be explained

by having OH groups that donate a hydrogen ion to stabilize the aging procedure's precursors. This, therefore, offers more room for the formation of complexes between the free radical and adsorbents radical, leading to the stabilization of the ester chain and thus giving it more stability. Hence, the adsorbents increase biodiesel's inherent resistance to oxidation (Freja et al., 2016). It represents the adsorbents' impact on the oxidation stability of the biodiesel in long-term storage or application.

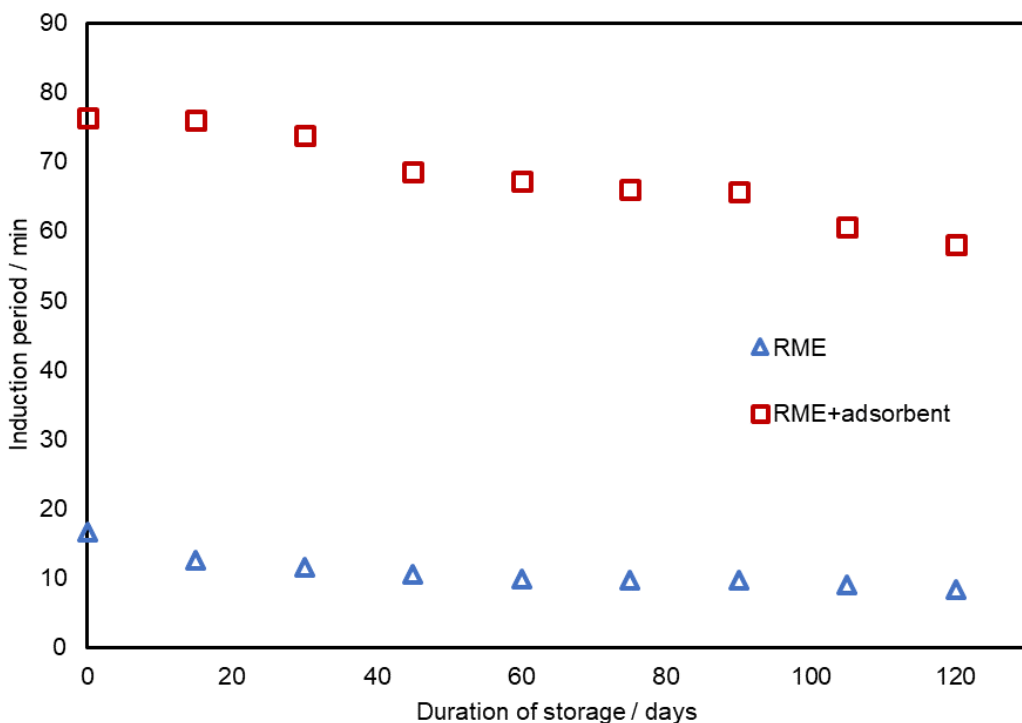


Figure 94: PetroOxy induction period of 40 mL RME treated with and without 0.675 g of combined adsorbents of magnesium-aluminum hydrotalcite and 1,3,5-trimethyl-2,4,6-tris(3,5-di-tert-butyl-4-hydroxybenzyl) benzene in a ratio of 1:2 respectively and stored at 40 °C in an oven for 120 days with samples taken every 15 days

8.6.2 The induction period of biodiesel blends

The stability or induction time of biodiesel is simply the length of time of its oxidation resistance. According to Ashraful et al. (2014), the induction period is a linear function of the test temperature. Therefore, with oxidation taking place over the storage duration, the biodiesel or fuel samples become oxidized and cause a decrease in their resistance to oxidation and hence a low induction time.

Figure 95 illustrates the evaluation of the oxidation stability of 40 mL of 80 %diesel fuel blended with 20 %RME treated with 0.675 g of adsorbents and the neat blend stored at 40 °C for 120 days. The induction times are determined using the PetroOXY method and reported in minutes. While the biodiesel blend without adsorbent treatment shows initial oxidation stability of 31.91 min, this stability decreased exponentially to 10.33 min after 120 days of storage. Ashraful et al. (2014) work indicate a decrease in stability with increasing storage time of biodiesel. The decrease in the induction period is rapid from day 1 to about day 75. After that, it begins to decrease at a slow rate up today 120. The biodiesel blend treated with the adsorbents had an initial induction time of 268.11 min. Instead, this induction time increased to 281.68 min at 75 days of storage before decreasing to 266.75 min. The net change in oxidation stability due to the adsorbents' use is about 5 %, which is negligible and can be considered unchanged. However, the initial increase in the induction period can be explained based on mixing the adsorbents with the blends. As time progresses, more OH groups are released into the mixture, thereby increasing its oxidation resistance. After 75 days of storage, the OH groups diminish in quantity, reduce oxidation resistance, and lower induction times. At 120 days of storage, the blends treated with the adsorbents have better oxidative stability, allowing free radical and adsorbent radical complexes to stabilize the ester chain. Therefore, the adsorbents increase biodiesel's inherent resistance to oxidation (Freja et al., 2016). Also, it is evident from the observation above that there is an inversely proportional relationship between the induction period and the duration of storage. This observation agrees with the findings of Ashraful et al. (2014).

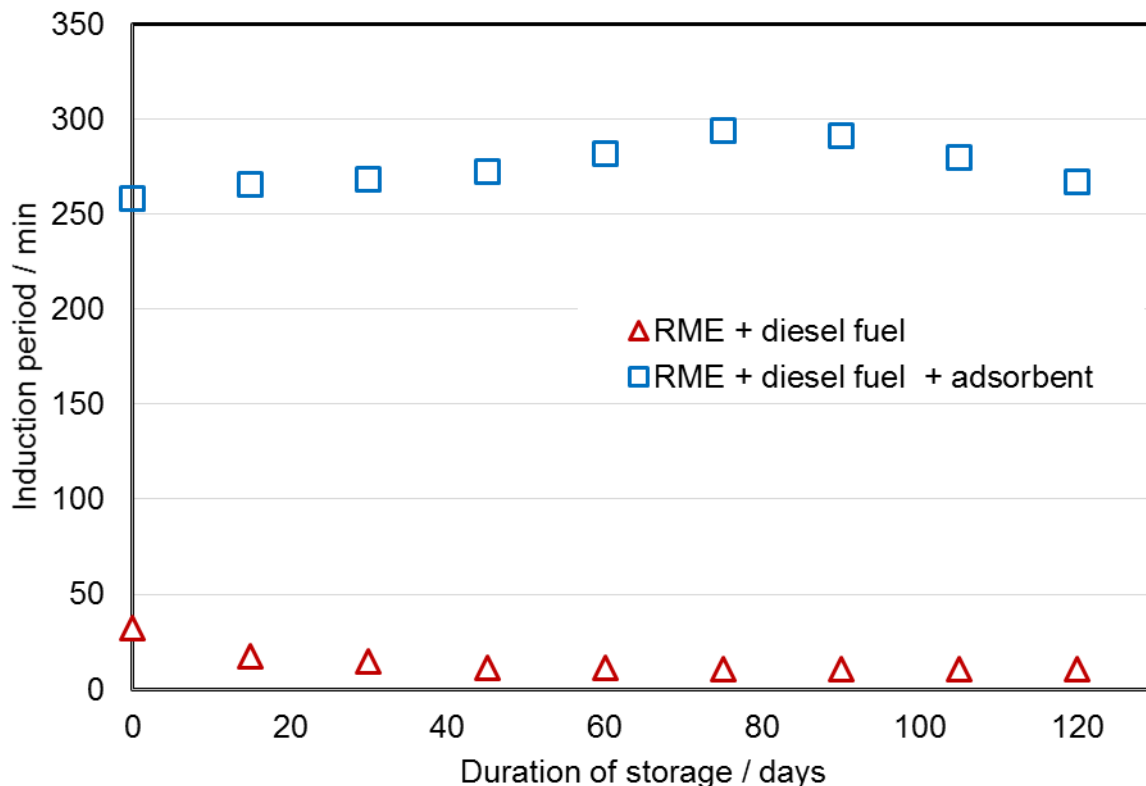


Figure 95: Evaluation of induction period of 40 mL of 20 % RME mixed with 80 % diesel fuel and treated with and without 0.675 g of combined adsorbents of magnesium-aluminum hydrotalcite and 1,3,5-trimethyl-2,4,6-tris(3,5-di-tert-butyl-4-hydroxybenzyl) benzene in a ratio of 1:2 respectively and stored at 40 °C for 120 days with samples taken every 15 days compared with the neat blend

8.6.3 SEC analysis of aged 40 mL of 80 %diesel fuel blended with 20 %RME treated with and without 0.675 g of combined adsorbents of magnesium-aluminum hydrotalcite and 1,3,5-trimethyl-2,4,6-tris(3,5-di-tert-butyl-4-hydroxybenzyl) benzene in a ratio of 1:2 respectively and stored at 40 °C in an oven from 0 up to 120 days

In Figure 96, the SEC shows that the buildup of higher molecular mass substances during the storage process is not significant at the end of 120 days of storage. This is seen in the FTIR analysis, where there is no substantial increase in absorption. Hence, no further SEC analysis of the sample stored in the oven is treated in this work.

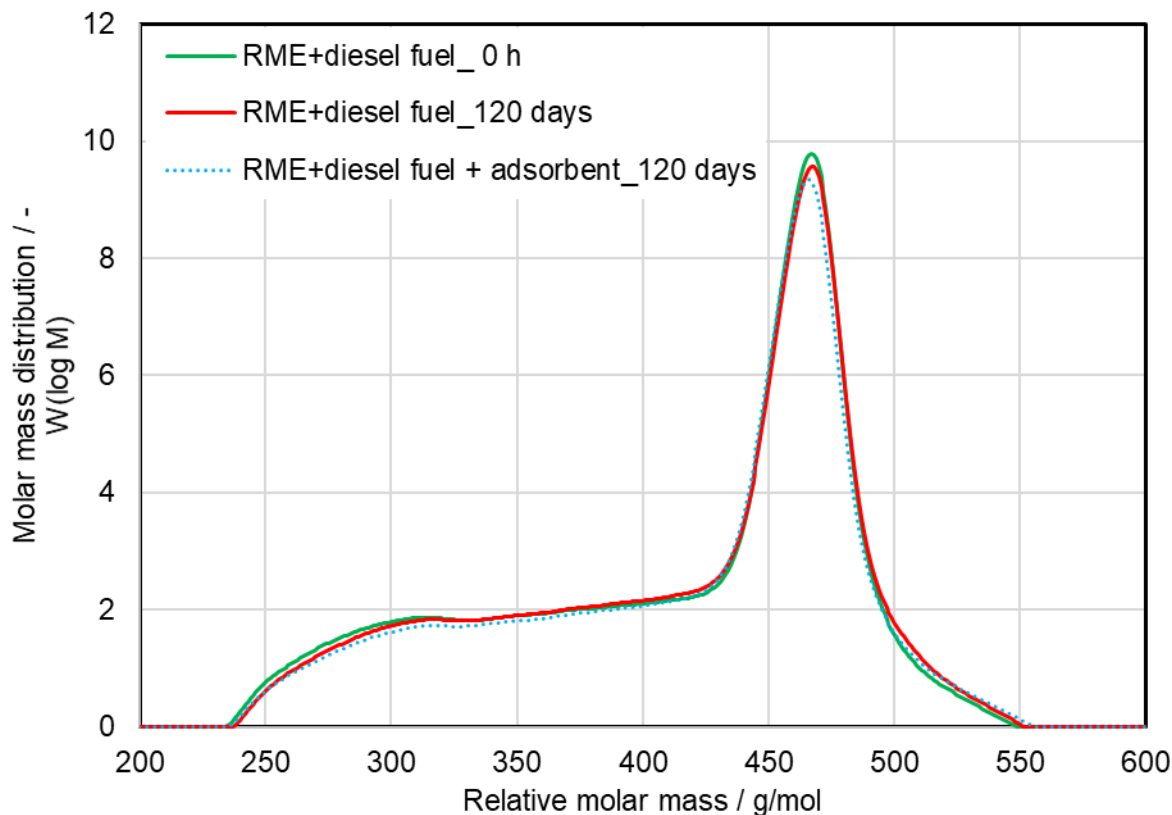


Figure 96: Evaluation of SEC chromatogram of 40 mL of 20 % RME mixed with 80 % diesel fuel treated with and without 0.675 g combined adsorbents of magnesium-aluminum hydrotalcite and 1,3,5-trimethyl-2,4,6-tris(3,5-di-tert-butyl-4-hydroxybenzyl) benzene in a ratio of 1:2 respectively and stored at 40 °C in an oven for 120 days with samples taken every 15 days

8.6.4 Assessment of total acid values of 40 mL of biodiesel treated with and without 0.675 g of combined adsorbents of magnesium-aluminum hydrotalcite and 1,3,5-trimethyl-2,4,6-tris(3,5-di-tert-butyl-4-hydroxybenzyl) benzene in a ratio of 1:2 respectively stored at 40 °C from 0 up to 120 days

The acid value data for each sample over the entire storage period is shown in Figure 97 and. Figure 97 indicates the variation of acid values as a function of the biodiesel's storage duration, 40 mL of RME treated with and without the adsorbents under the same storage conditions of 40 °C for the testing period of 120 days. From Figure 97, the samples treated with the adsorbents are relatively stable and have low acid values. In contrast, those without any adsorbent treatment have high acid values, which indicate a high level of

degradation of the ester. However, it is not sufficient enough to reflect on the FTIR and SEC results seen above. A higher rise in acid value occurs after 90 days of storage for those samples stored without treatment with the adsorbents. Also, the samples stored without adsorbent treatment went out of specification after 90 days of storage (McCormick and Westbrook, 2010). The ASTM fuel specifications for biodiesel allow for a maximum acid value of 0.5 mg of KOH/g for B100 after six months (Freja et al., 2016). It is observed that the biodiesel treated with the adsorbents and stored for the 120 days is about 61 % lower than the standard acid value, while the biodiesel without any adsorbent treatment is above the standard acid value by about 17 %. It means that the adsorbents' use has given a more significant period of useful life for the fuel. The results from this observation also confirm that when biodiesel degrades, its acid value increases (Gunstone et al., 2010; Leung et al., 2006). This comes about due to fatty acid methyl ester molecules breaking down during the degradation process, and the fatty acid chains increase the acid value of the biodiesel (see the right side of Figure 5 during the termination stage of autoxidation mechanism of hydrocarbon degradation) (Starck et al., 2015; Ancho, 2006). As seen in the introduction, increased acid values are influenced by the increase in the content of hydroperoxides, which oxidize into acids (Ashraful et al., 2014). Thus, the more the degradation, the higher its acidity (Shahabuddin et al., 2012). Also, free fatty acids are a significant cause of biodiesel's high acid values (Wang et al., 2008). The accumulation of degraded or decomposition products in the fuel leading to increased acid values indicates the onset of oxidation. Hence, it can be concluded that the second stage of degradation or oxidation has been set in (see the bottom left side of Figure 5) (Wang, 2001).

From the trend or pattern of the graphs for each sample concerning the positive slope obtained, it can be stated that there exists a direct positive proportional relationship between the acid values and the storage time (Ashraful et al., 2014). On the other hand, the adsorbents' use retard the degradation process and suppressed the ester molecules' breaking down, resulting in lower acid values and a nominal rate of change in the acid value. 1, 3, 5-trimethyl-2, 4, 6-tris (3, 5-di-tert-butyl-4-hydroxybenzyl) benzene is a radical scavenger. The presence of liable hydrogen atoms in its structure permits stable products, resulting in the breakdown of the oxidation chain mechanism (section 3.4) (Aluyor and Ori-Jesu, 2008; Christensen and McCormick, 2014). Therefore, the samples treated with

the adsorbents and stored showed a low degradation rate and degradation level during the entire storage duration.

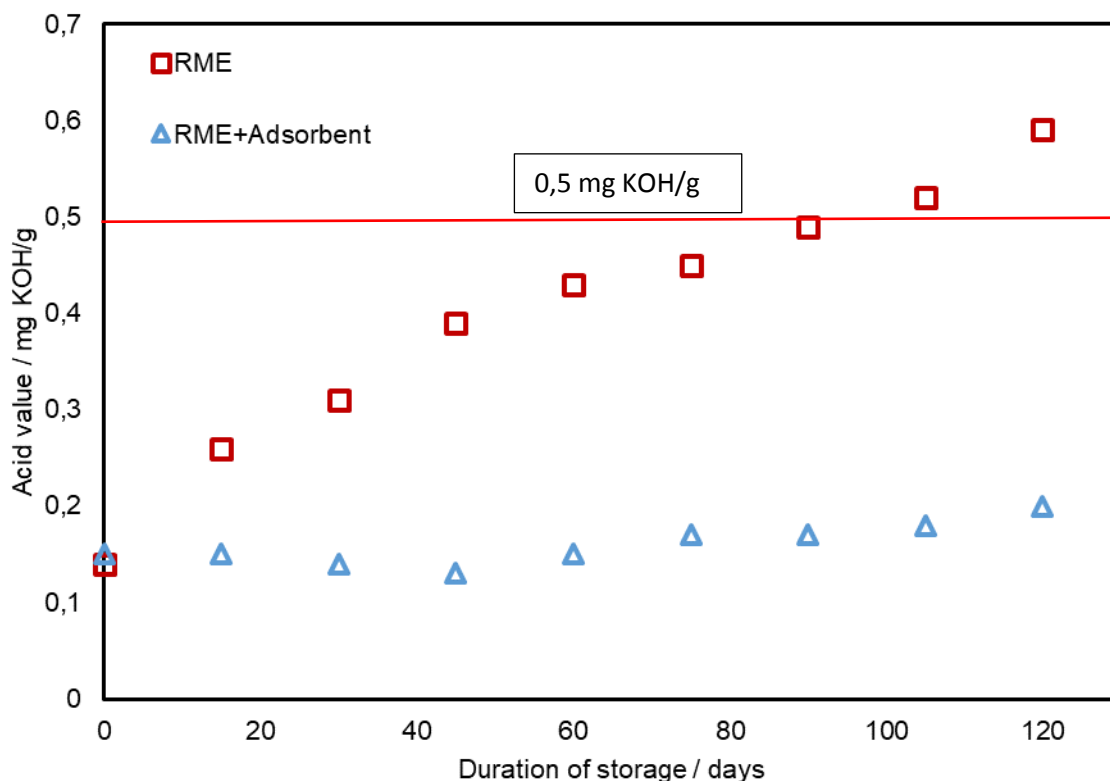


Figure 97: Acid value of 40 mL of RME treated with and without 0.675 g of combined adsorbents of magnesium-aluminum hydrotalcite and 1,3,5-trimethyl-2,4,6-tris(3,5-di-tert-butyl-4-hydroxybenzyl) benzene in a ratio of 1:2 respectively and stored at 40 °C in an oven for 120 days with samples taken every 15 days

8.6.5 Evaluation of total acid values of 80 %diesel fuel blended with 20 %RME treated with and without 0.675 g of combined adsorbents of magnesium-aluminum hydrotalcite and 1,3,5-trimethyl-2,4,6-tris(3,5-di-tert-butyl-4-hydroxybenzyl) benzene in a ratio of 1:2 respectively and stored at 40 °C from 0 up to 120 days

Figure 98 shows the variation of acid values as a function of the biodiesel blend's storage duration, B20 treated with and without the adsorbents under the same storage conditions of 40 °C in an oven for 120 days. Several studies have found that acid value increases after a period of storage. The rate of increase in acidity depends on the period of storage (Ashraful et al., 2014; Pattamaprom and Ngamjaroen, 2012; Berrios et al., 2012; Obadiah

et al., 2012). The increase in acid value depends on the storage temperature (McCormick and Westbrook, 2010; Leung et al., 2006). From Figure 98, the acid values of the biodiesel blend without adsorbent treatment increase from 0.14 to 0.62 mg KOH/g, and the blends treated with the adsorbents increase from 0.1 to 0.17 mg KOH/g. While there is an order of magnitude increase in the acid values for those stored without treatment with the adsorbents, the samples' values remain relatively the same. Also, the initial acidity of 0.1 mg KOH/g of the blend treated with the adsorbents demonstrates the adsorbents' ability to adsorb any residual acids in the ester before the aging process sets in.

Therefore, the lower acid value than the original acid value of 0.14 mg KOH/g. The acid value measures the number of acidic substances in fuel. The high acid values recorded by the mixtures stored without any adsorbent treatment for the experiments' duration can be explained; the mixtures not treated with the adsorbents during the storage period produced hydroperoxides. These hydroperoxides then undergo complex secondary reactions resulting in more reactive aldehydes, which further oxidize into acids. This then leads to an increase in the acid value (Asraful et al., 2014). Hydroperoxides are, therefore, the main contributor to increasing acid value. From the above, the acid value directly correlates with the level of degradation of the sample. Therefore, the longer the sample degrades or ages, the higher its acidity (Bannister et al., 2010) (see section 2.1). The low acid values for the samples treated with the adsorbents demonstrate the adsorbents' ability to impact the fuel's degradation.

ASTM fuel specifications for biodiesel blends allow for a maximum acid value of 0.5 mg of KOH/g for B100 and 0.3 mg of KOH/g for B6–B20 (Freja et al., 2015). From Figure 98, it is observed that the blend treated with the adsorbents and stored for the 120 days is about 44 % lower than the standard acid value, while the mixture not treated with the adsorbents is over and above the standard acid value by 53 %. This means that the adsorbents' use reduces acidity's buildup, giving the fuel a perfect helpful life.

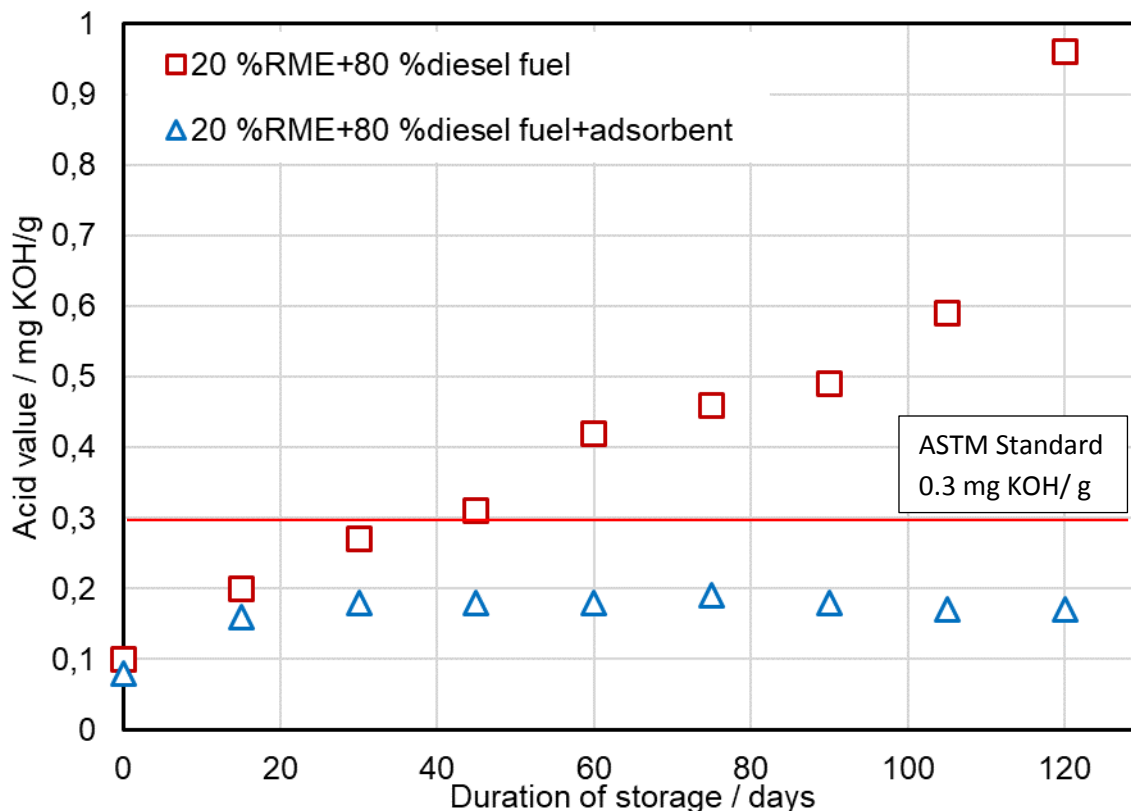


Figure 98: Acid value of 40 mL 20 % RME mixed with 80 % diesel fuel and treated with and without combined 0.675 g adsorbents of magnesium-aluminum hydrotalcite and 1,3,5-trimethyl-2,4,6-tris(3,5-di-tert-butyl-4-hydroxybenzyl) benzene in a ratio of 1:2 respectively and stored at 40 °C for 120 days and samples taken every 15 days

8.6.6 Impact assessment of combined adsorbents of magnesium-aluminum hydrotalcite and 1,3,5-trimethyl-2,4,6-tris(3,5-di-tert-butyl-4-hydroxybenzyl) benzene in a ratio of 1:2 respectively on the viscosity of 80 % diesel fuel blended with 20 %RME

Figure 99 and Figure 100 shows the viscosity changes for all neat 40 mL of biodiesel and its blends treated with and without 0.675 g of combined adsorbents of magnesium-aluminum hydrotalcite and 1,3,5-trimethyl-2,4,6-tris(3,5-di-tert-butyl-4-hydroxybenzyl) benzene in a ratio of 1:2 respectively over the storage period of 120 days at 40 °C in an oven. The adsorbents' addition leads to slight increases in blends' viscosity compared with the samples stored without any treatment with the adsorbents. From initial viscosities of

4.13 and 3.01 mm²/s measured at 40 °C of biodiesel and its blends treated with adsorbents, it ended at the storage period of 120 days 4.31 and 3.12 mm²/s respectively. It translates into an increase of about 4 %, which is negligible. The viscosities' trend at 100 °C does not differ from the viscosities measured at 40 °C. These increases in the viscosity of the blends treated with the adsorbents can be considered marginal. Viscosity increase during storage (Karavalakis et al., 2011; Ashraful et al., 2014; Mittelbach and S. Gangl, 2001) owing to the formation of hydroperoxides which lead to oxidized polymeric compounds resulting in the formation of gums and sediments (Karavalakis et al., 2011; Zuleta et al. (2012); Bouaid et al., 2007).

Under the current storage conditions, no significant amount of degradation products are formed in the biodiesel and its blends treated with the adsorbents. However, for the samples stored without treatment with the adsorbents, there is an increase in the biodiesel's viscosity and the blend. It ended storage from viscosities of 4.17 and 3.07 mm²/s measured at 40 °C of neat biodiesel and its blends without any treatment with adsorbents respectively at the start of an aging period of 120 days with 4.6 and 3.41 mm²/s. This translates to an increase of about 10 %. This increase in the sample's viscosity not treated with the adsorbents supports the hypothesis that oxidation products' formation during storage conditions requires a more extended time, higher temperatures, and atmospheric oxygen (Karavalakis et al., 2011). The change in the fuel samples' mass within this storage period gives insight into the extent and duration of oxygen incorporation during the oxidation process, as outlined in Figure 2, Figure 3, and Figure 4. The change in mass relative to the starting mass could be explained by hydroperoxides formation during storage. The increase in fuel mass occurs as oxygen is incorporated during the formation of hydroperoxides and oxidation of aldehydes to carboxylic acids and the formation of other oxidation products, water, alcohols, ketones, etc. (Ashraful et al., 2015) (see reaction 3.4). Similar trends are observed in a study by Freja et al. (2016). The result is the formation of insoluble oxidative products resulting in increased viscosity. Notably, the neat biodiesel and its blends treated with the adsorbents resulted in lower viscosities than those not treated with the adsorbents. However, the limit value of 5.0 mm²/s at 40 °C for the viscosity was not reached in any cases during the storage period,

Figure 99.

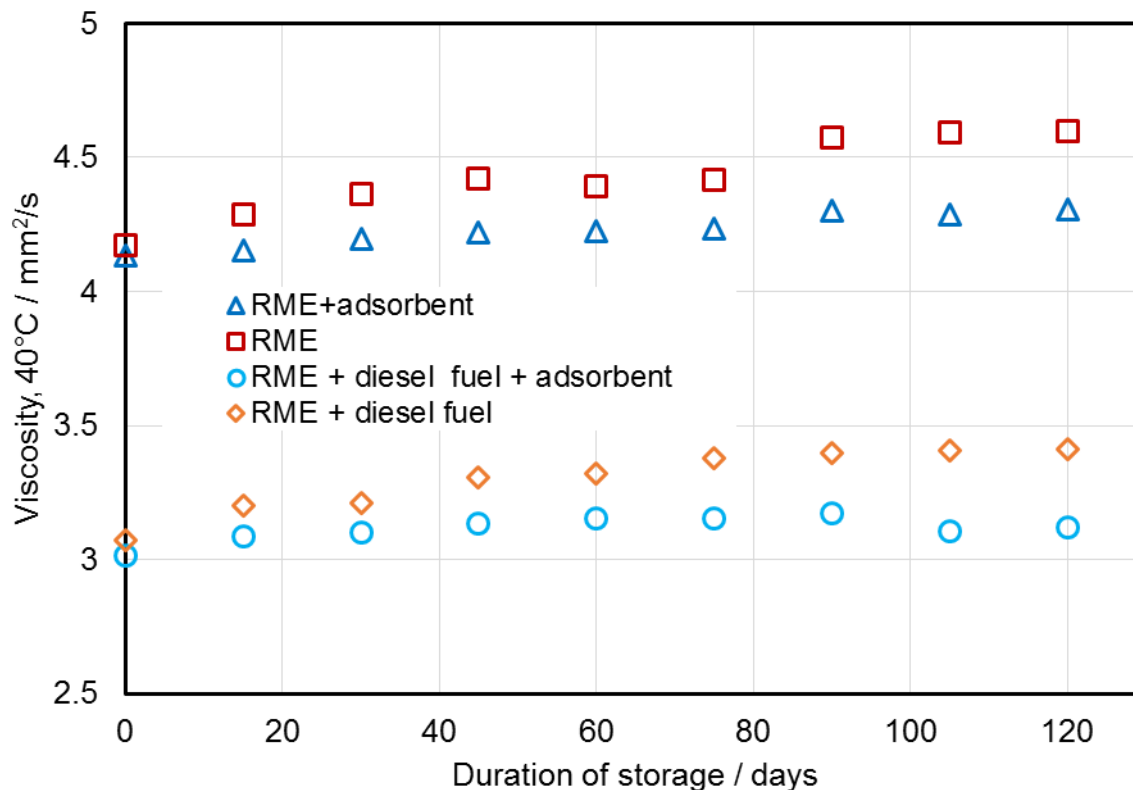


Figure 99: Viscosity measured at 40 °C of 40 mL of 20 % RME mixed with 80 % diesel fuel and treated with and without 0.675 g combined adsorbents of magnesium-aluminum hydroxide and 1,3,5-trimethyl-2,4,6-tris(3,5-di-tert-butyl-4-hydroxybenzyl) benzene in a ratio of 1:2 respectively and stored at 40 °C in an oven for 120 days and samples were taken every 15 days

Fuel age increases the amount of shorter chain hydrocarbon and more saturated fatty acid, resulting in more prone to crystallization (Brühl, 2014) (see section 3.5.2). This could cause the reduction of its volume and consequently increased viscosity. Therefore, the fuel's mass increases due to the oxidation products, increasing viscosity, as seen in Figure 100. This confirms most studies that had found that the kinematic viscosity increases after a certain period of storage (Ashraful et al., 2014; Berrios et al., 2012; Pattamaprom and Ngamjaroen, 2012; Obadiah, 2012). Based on Figure 100, the trend of viscosity of the samples measured at 100 °C throughout storage of 120 days are primarily similar to the previous analysis carried out at 40 °C. However, the samples treated with the adsorbents maintain the kinematic viscosity with minor changes. The adsorbents, therefore, give more stability to biodiesel to maintain its properties by suppressing the formation of oxidized polymeric compounds, which are the main contributor to the increase in viscosity (Ashraful

et al., 2014; Obadiah et al., 2012). Higher molecular weight substances give rise to higher viscosity. There is a negligible increase in the samples treated with the adsorbents in this analysis, and it supports the adsorbents' above claim suppressing the sample's oxidation.

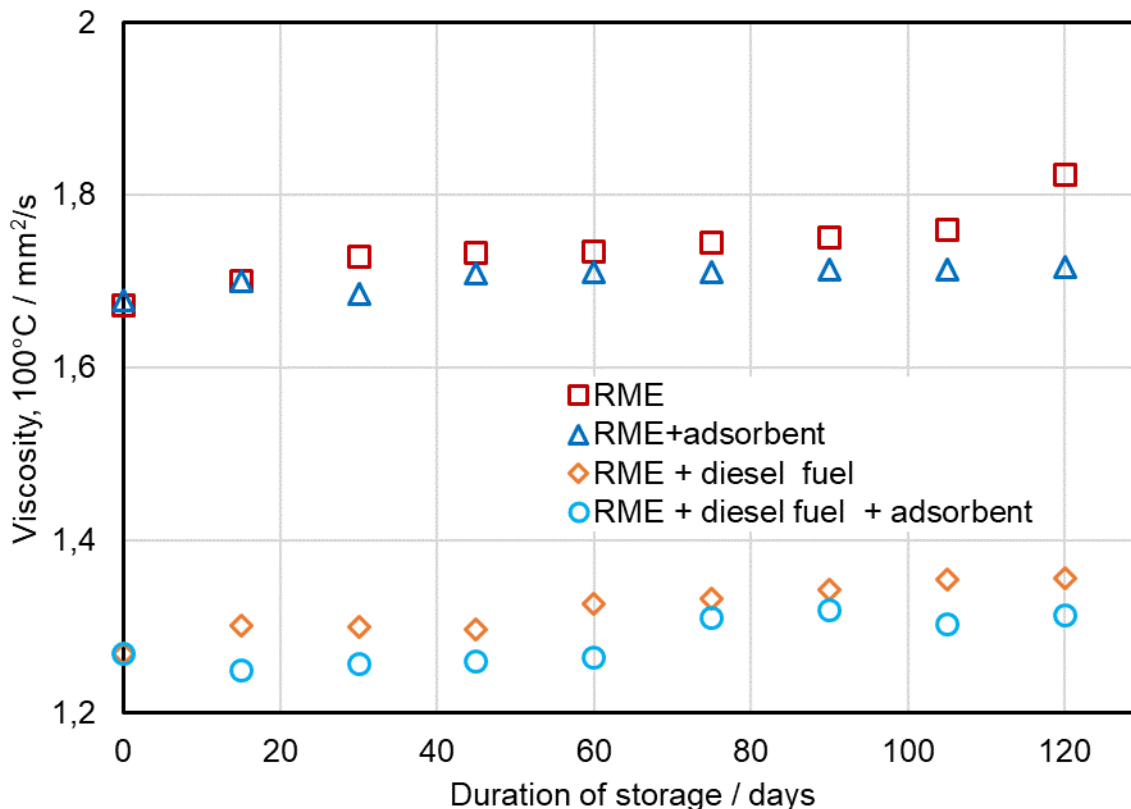


Figure 100: Viscosity measured at 100 °C of 40 mL neat RME and 40 mL of 20 %RME mixed with 80 %diesel fuel treated with and without 0.675 g combined adsorbents of magnesium-aluminum hydrotalcite and 1,3,5-trimethyl-2,4,6-tris(3,5-di-tert-butyl-4-hydroxybenzyl) benzene in a ratio of 1:2 respectively and stored at 40 °C in an oven for 120 days and samples were taken every 15 days

8.6.7 Investigation of the effect of the combined adsorbents of 0.675 g magnesium-aluminum hydrotalcite and 1,3,5-trimethyl-2,4,6-tris(3,5-di-tert-butyl-4-hydroxybenzyl) benzene in a ratio of 1:2 respectively on the density of 40 mL 80 % diesel fuel blended with 20 %RME stored in an oven at 40 °C for 120 days

Density is one of the parameters in ASTM D 6751 or EN 14214 influenced by oxidative degradation. As density is a measure of mass per unit volume, it increases with the fuel molecules' increasing molecular weight (Prajapati and Nandlal, 2015). Figure 101 and

Figure 102 represents the density measured at 40 °C and 100 °C of the neat biodiesel and the blends treated with and without 0.675 g of the combined adsorbents of magnesium-aluminum hydrotalcite and 1,3,5-trimethyl-2,4,6-tris(3,5-di-tert-butyl-4-hydroxybenzyl) benzene in a ratio of 1:2 respectively and stored at 40 °C in an oven for 120 days. The increase in the neat biodiesel density and the blends treated with the adsorbents, Figure 101 and Figure 102, can be considered marginal compared with the samples stored without any treatment with the adsorbents. The density, just like viscosity, increases with the formation of hydroperoxides which lead to oxidized polymeric compounds resulting in the formation of gums and sediments (Karavalakis et al., 2011; Zuleta et al. (2012); Bouaid et al., 2007). As density is directly proportional to mass, therefore, when the biodiesel mass increases with aging, the density also increases. The densities of biodiesel increase with storage time, potentially due to increased molecular interaction of degraded biodiesel as peroxides are formed (Karavalakis et al., 2011; Pattamaprom and Ngamjaroen, 2012). This collaborates with Shahabuddin et al. (2012), who also found an increasing densities pattern with a storage duration though the increase has been in a small range. This density data agrees with Starck et al. (2015), who investigated the density variation during storage. Looking at Figure 101 and Figure 102, the adsorbents' use results in a less significant increase in the density at both temperatures at which the density is measured. This is because the adsorbents have intercepted the radicals, which would have polymerized into oligomers. Hence the process of oxidation is suppressed, resulting in marginal oxidative products. This has given rise to low densities recorded, unlike the mixture stored without the adsorbents' use.

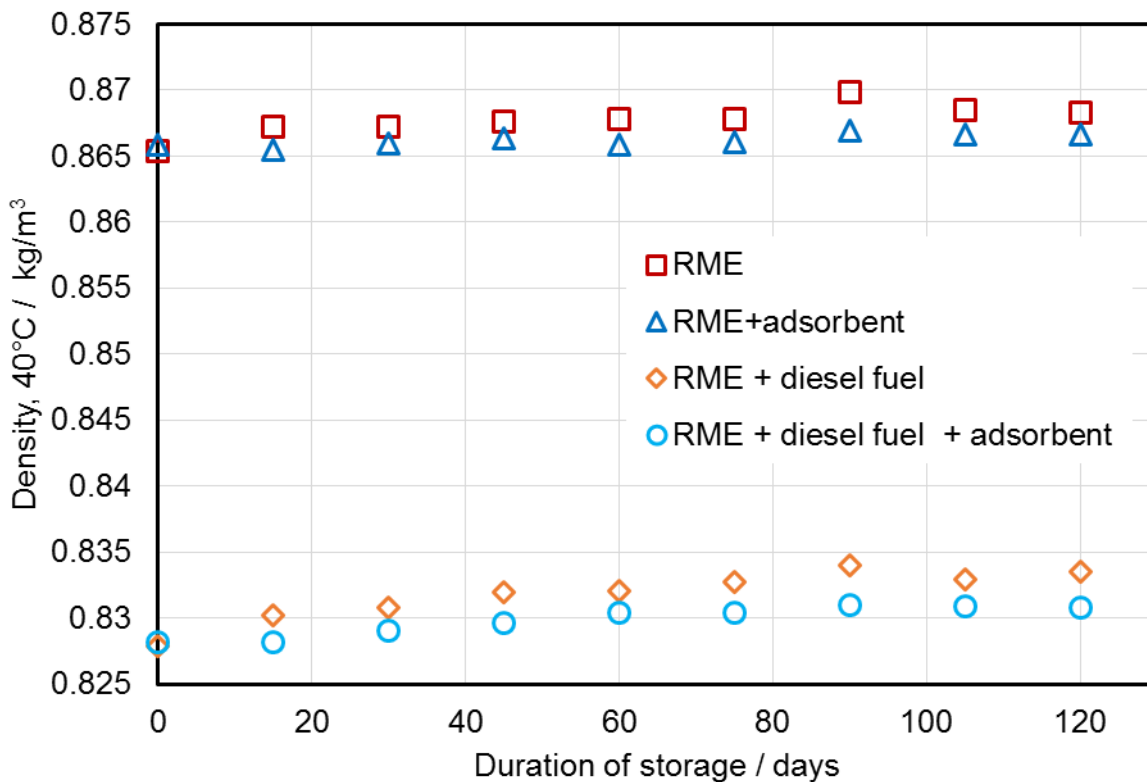


Figure 101: Density measured at 40 °C of 40 mL neat RME and 40 mL of 20 % RME mixed with 80 % diesel fuel and treated with and without 0.675 g combined adsorbents of magnesium-aluminum hydrotalcite and 1,3,5-trimethyl-2,4,6-tris(3,5-di-tert-butyl-4-hydroxybenzyl) benzene in a ratio of 1:2 respectively and stored at 40 °C in the oven for 120 days and samples were taken every 15 days

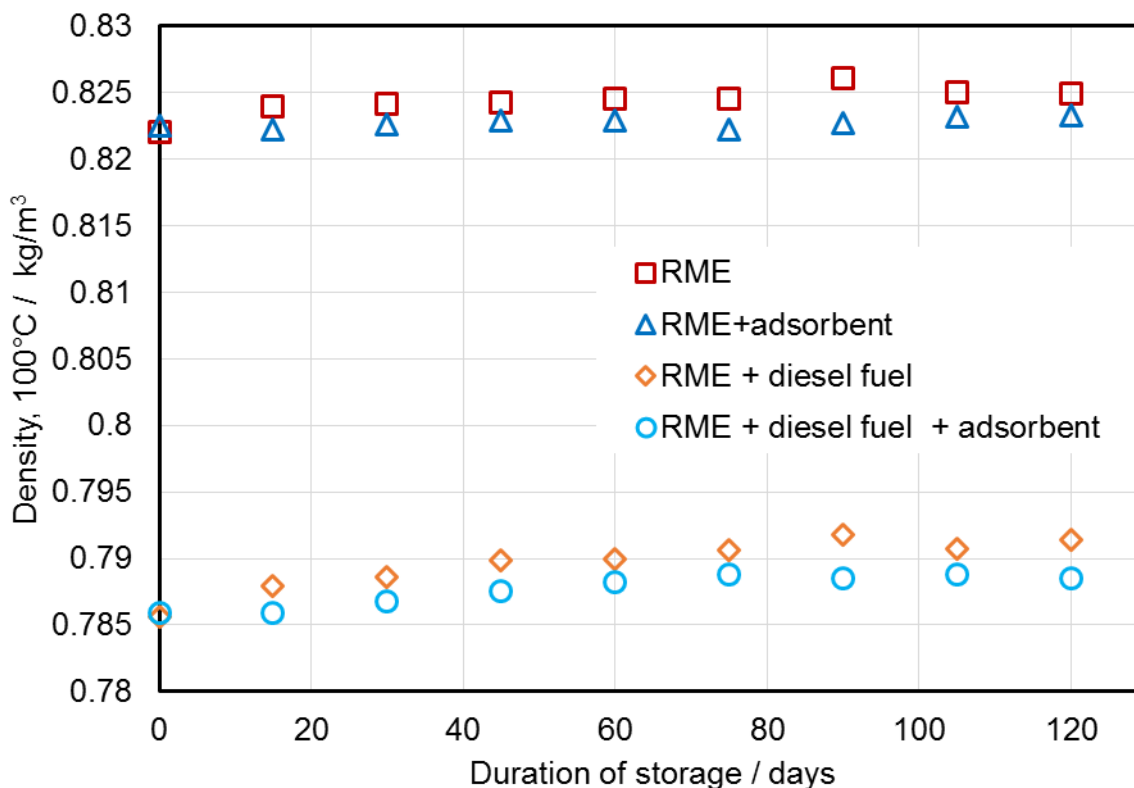


Figure 102: Density measured at 100 °C of 40 mL neat RME and 40 mL of 20 % mixed with 80 % diesel fuel and treated with and without 0.675 g combined adsorbents of magnesium-aluminum hydrotalcite and 1,3,5-trimethyl-2,4,6-tris(3,5-di-tert-butyl-4-hydroxybenzyl) benzene in a ratio of 1:2 respectively and stored at 40 °C in the oven for 120 days and samples were taken every 15 days

8.6.8 FTIR analysis of neat biodiesel treated with and without combined 0.675 g adsorbents of magnesium-aluminum hydrotalcite and 1,3,5-trimethyl-2,4,6-tris(3,5-di-tert-butyl-4-hydroxybenzyl) benzene in a ratio of 1:2 respectively and stored at 40 °C in the oven for up to 120 days

The FTIR application determines the oxidation level by a general response in the carbonyl (C=O) region. As seen in earlier FTIR analysis in section 4.1.5, the IR energy of absorption in this region is due to the carbon-oxygen bonds in the oxidized fuel. The FTIR analysis has not shown any significant change during the storage process, Figure 103 and Figure 104. For oxidation impact on the molecular structure of fuel, aging's temperature and duration thus count a lot according to Kerkering and Andersson (2015). These experiments are carried out slightly above ambient temperature, 40 °C, and no significant

registered molecular change. No further considerable treatment is given to this FTIR analysis in this work.

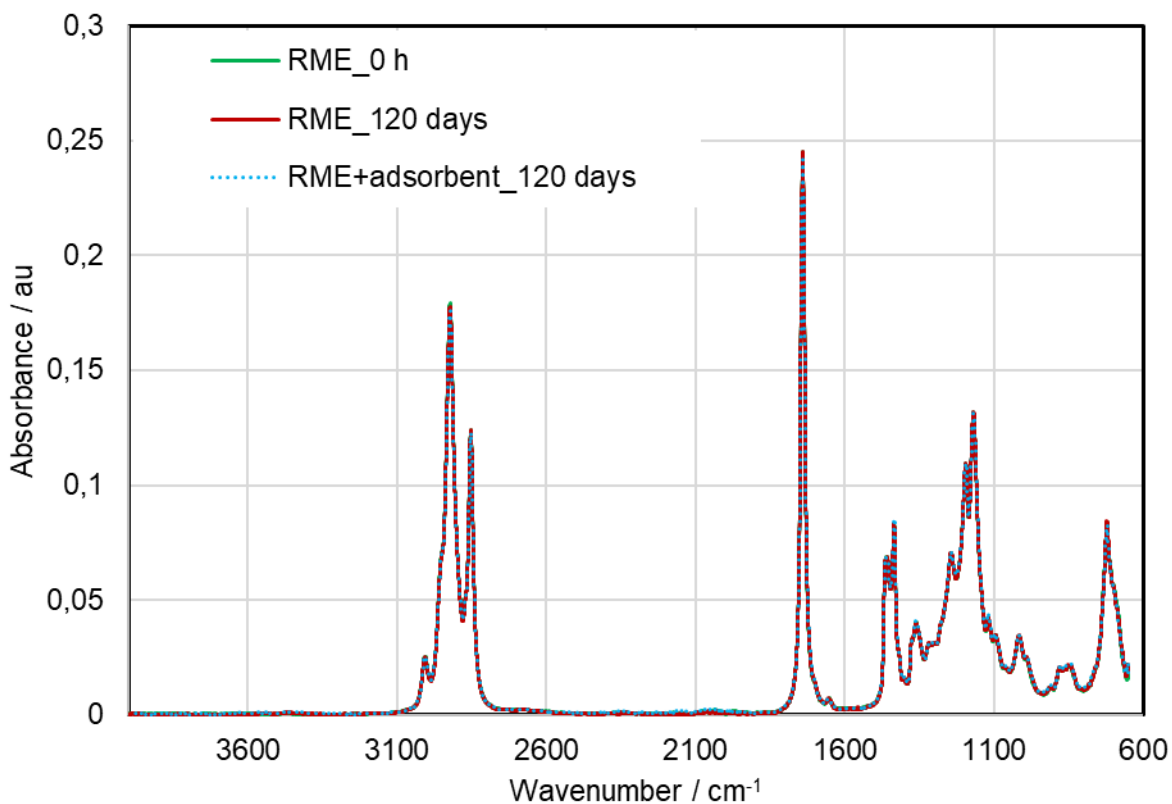


Figure 103: FTIR spectrum of 40 mL RME treated with and without 0.675 g combined adsorbents of magnesium-aluminum hydrotalcite and 1,3,5-trimethyl-2,4,6-tris(3,5-di-tert-butyl-4-hydroxybenzyl) benzene in a ratio of 1:2 respectively and stored at 40 °C in the oven for 120 days with samples taken every 15 days

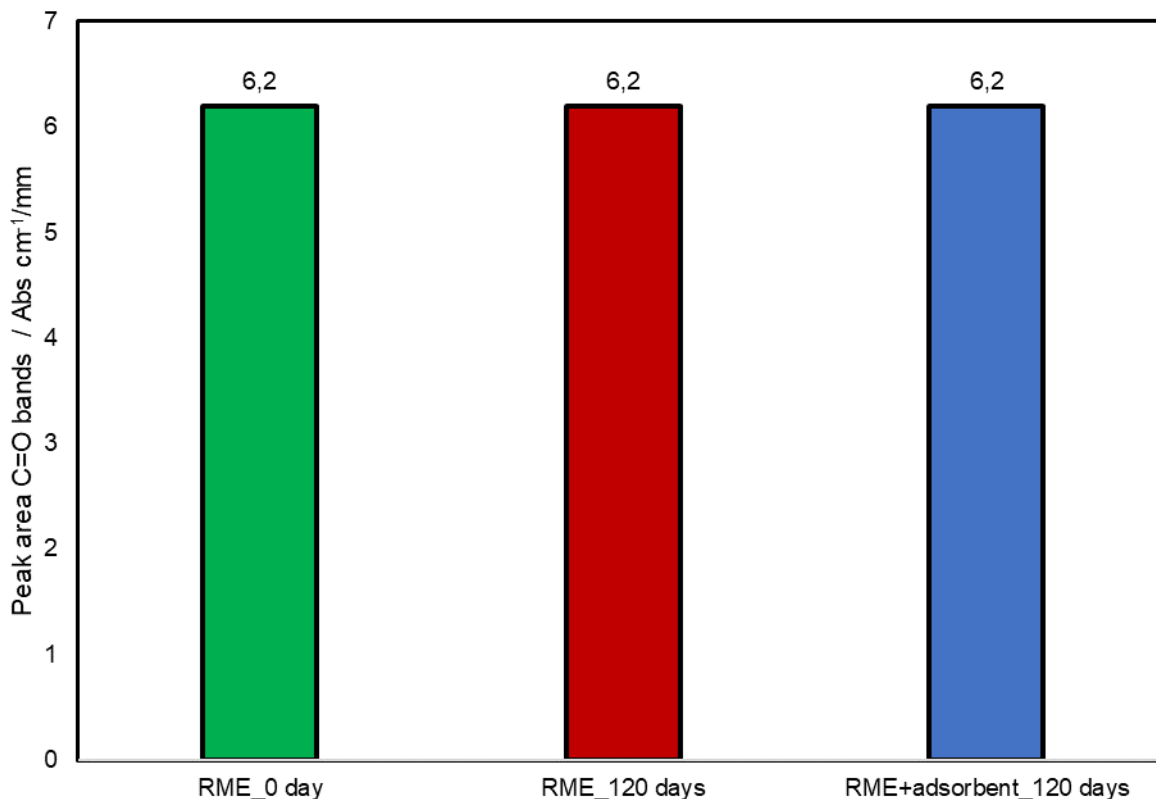


Figure 104: Evaluation of peak area under C=O band of FTIR spectrum of 40 mL RME treated with and without 0.675 g combined adsorbents of magnesium-aluminum hydrotalcite and 1,3,5-trimethyl-2,4,6-tris(3,5-di-tert-butyl-4-hydroxybenzyl) benzene in a ratio of 1:2 respectively and stored at 40 °C in the oven for 120 days with samples taken every 15 days

8.6.9 FTIR analysis of biodiesel blends, 80 %diesel fuel mixed with 20 %RME treated with and without combined 0.675 g adsorbents of magnesium-aluminum hydrotalcite and 1,3,5-trimethyl-2,4,6-tris(3,5-di-tert-butyl-4-hydroxybenzyl) benzene in a ratio of 1:2 respectively and stored at 40 °C in an oven for up to 120 days

The FTIR application determines the oxidation level considering the general response in the carbonyl (C=O) region. The IR energy is absorbed in this region due to the carbon-oxygen bonds in the oxidized fuel mixture. With neat fuel or unaged fuel, few compounds are found with significant absorbencies in this area. Therefore, monitoring this region is thus a direct measurement of the fuel mixture's level of degradation. The FTIR analysis has not shown any significant change during the storage process, as shown in Figure 105

and Figure 106. Therefore, no further treatment is given to any FTIR analysis of these samples stored in the oven.

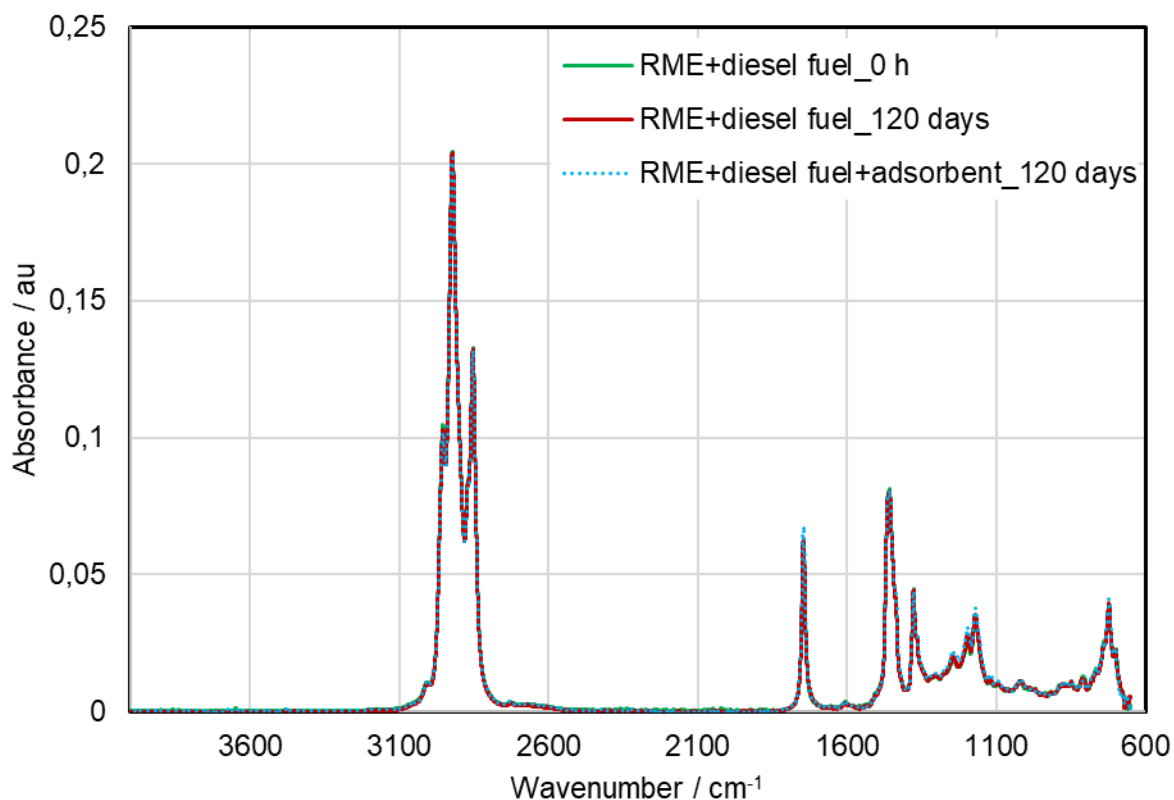


Figure 105: FTIR spectra of 40 mL of 20 % RME mixed with 80 % diesel fuel and treated with and without 0.675 g combined adsorbents of magnesium-aluminum hydrotalcite and 1,3,5-trimethyl-2,4,6-tris(3,5-di-tert-butyl-4-hydroxybenzyl) benzene in a ratio of 1:2 respectively and stored at 40 °C in the oven for 120 days with samples taken every 15 days

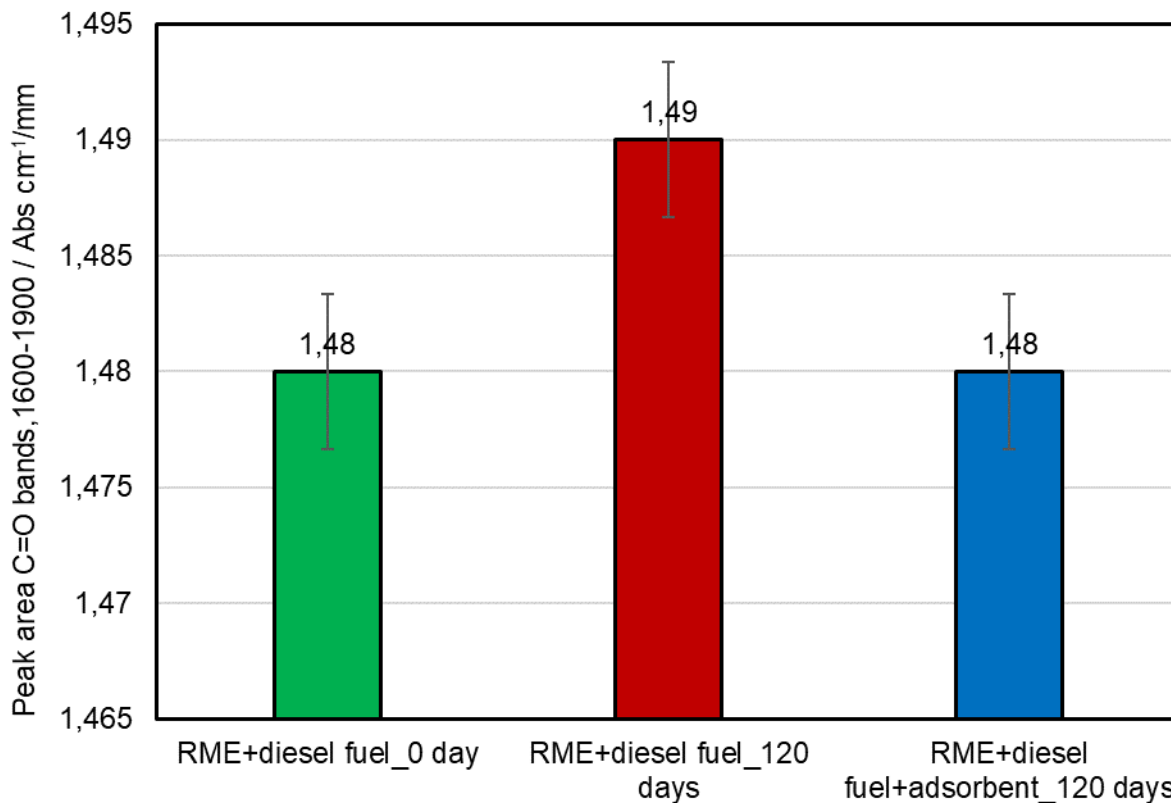


Figure 106: Evaluation of peak area under C=O band of FTIR spectrum of 40 mL of 20 % RME blended with 80 % diesel fuel and treated with and without 0.675 g combined adsorbents of magnesium-aluminum hydrotalcite and 1,3,5-trimethyl-2,4,6-tris(3,5-di-tert-butyl-4-hydroxybenzyl) benzene in a ratio of 1:2 respectively and stored at 40 °C in the oven for 120 days and samples were taken every 15 days

Summary

The stability of biodiesel and its blends during storage and in an application is critical due to oxidation. As explained in the introduction, during the termination stage of biodiesel oxidation, insoluble oligomers of high molecular masses are produced by the recombination of oxidation products (Figure 5). When stored for long periods, Biodiesel and its blends get degraded, increasing acid values, viscosity, and decreased oxidative stability (Zuleta et al., 2012; McCormick and Westbrook, 2009; Bouaid et al., 2007; Leung et al., 2006). The acid value increases with the formation of peroxides. The peroxides are further transformed into aldehydes, which oxidize into organic acids (Zuleta et al., 2012). The biodiesel oxidation leads to high molecular weight substances that increase viscosity and density and reduce oxidative stability.

This section focuses on improving biodiesel's stability, neat and blends with EN590 diesel fuel, concerning oxidation during storage or application. Therefore, 40 mL of neat biodiesel, RME and its blends, B20 in the ratio of 20 % RME and 80 % EN950 diesel fuel are treated with 0.675 g of the combined adsorbents magnesium-aluminum hydrotalcite and 1,3,5-trimethyl-2,4,6-tris(3,5-di-tert-butyl-4-hydroxybenzyl) benzene in a ratio of 1:2 respectively. The neat B20 without the adsorbents were stored in a temperature-controlled oven at 40 °C for 120 days, and samples were taken out every 15 days for analysis.

For the acid value of the stored samples, an increasing acid value of the neat samples with a long duration of storage time has been observed. The results collaborate with Shahabuddin et al., 2012, who reported an increasing amount of acid value with a storage duration in his study. Hydroperoxides are observed as the primary contributor to increasing acid value. There is a good correlation between the acid values during the biodiesel storage and its blend treated with the adsorbents. Thus, the relatively stable acid values suggest that the adsorbents suppress hydroperoxides' formation, resulting in no significant oxidation.

The insoluble substance formation results in high molecular weight molecules leading to an increase in viscosity and density. However, there has not been any significant increase in these physio-chemical parameters during the storage period, which indicates the adsorbents suppressing the oxidation process by intercepting the process's precursors, as explained in section 3.4.

As already stated earlier, biodiesel is more sensitive to oxidation during long-term storage than conventional diesel fuel. Therefore, preventing the degradation of fuel quality has been a significant issue in the advent of biofuel. The adsorbents' use has an average 83 % improvement on all the parameters tested during this experiment during the storage period.

The above results obtained for stabilizing the biodiesel and its blends can be explained based on the adsorbents' suppression action because of the interaction between the free radical and its surface, mainly due to hydrogen bonding. This has been explained in section 6. The hydrogen bonds are established between the ester carbonyl and the adsorbents' hydroxyl groups, leading to the free radical propagation's interruption. This is

because of the hydrogen atom interaction from the surface of the hydroxyl group of the adsorbents with the immediate peroxy radicals. With the free radical propagation interruption, oxidation is retarded, resulting in less or no significant biodiesel degradation and blends during the storage or long-term application.

8.7 Confirmation of suppression of oligomers formation

8.7.1 Effect of 0.675 g combined adsorbents of magnesium-aluminum hydrotalcite and 1,3,5-trimethyl-2,4,6-tris(3,5-di-tert-butyl-4-hydroxybenzyl) benzene in a ratio of 1:2 respectively on relative permittivity of 80 % base oil blended with 20 % RME and aged at 170°C

Figure 107 shows the relative permittivity versus the samples' frequency of 80 %base oil blended with 20 %RME and treated with and without combined 0.675 g adsorbents and aged at 170 °C for 10 h. This duration of 10 h is selected to cover the samples' induction period without any additives in them. The higher molecular mass substances formed during the aging of a blend of RME and base oil without the adsorbent treatment increased the polarity in the dielectric and thus the content of orientation polarization. Hence the higher the number of polar oxidation products, the higher the relative permittivity. Oil oxidation causes modification in oxygen-containing groups, leading to the formation of alkyl and aryl ethers oxygen bridges, resulting in increased polarity (Markova et al., 2007). As seen in section 4.1.9, the relative permittivity of oil is a measure of its polarity (Soleimania et al., 2014). Therefore, with the degradation of hydrocarbon, increasing polar oxidative products will increase relative permittivity. Considering that a charge will yield more electric flux in a medium with low permittivity than in a medium with high permittivity, the level of permittivity measured indicates the oil's level of degradation. The sample aged without the adsorbent treatment increased in relative permittivity from about 2.359 (0 h) to 3.123 (10 h), the relative permittivity of RME and base oil mixture treated with the adsorbents remain pretty the same, 2.359 (0 h) as the neat or unaged RME and base oil mixture for the entire duration of aging. This result could be explained that within the 10 h duration of aging, there are no polar oxidation products formed in the sample treated with the adsorbents. In other words, the adsorbents suppressed the formation of the polar oxidation products by donating its liable hydrogens to stabilize the radicals formed.

Therefore, during the aging process, the formation of polar compounds and high molecular weight species leads to remarkable changes in the dielectric properties, which provides a scheme for monitoring the impact of the adsorbents on the oil-biodiesel blends degradation process.

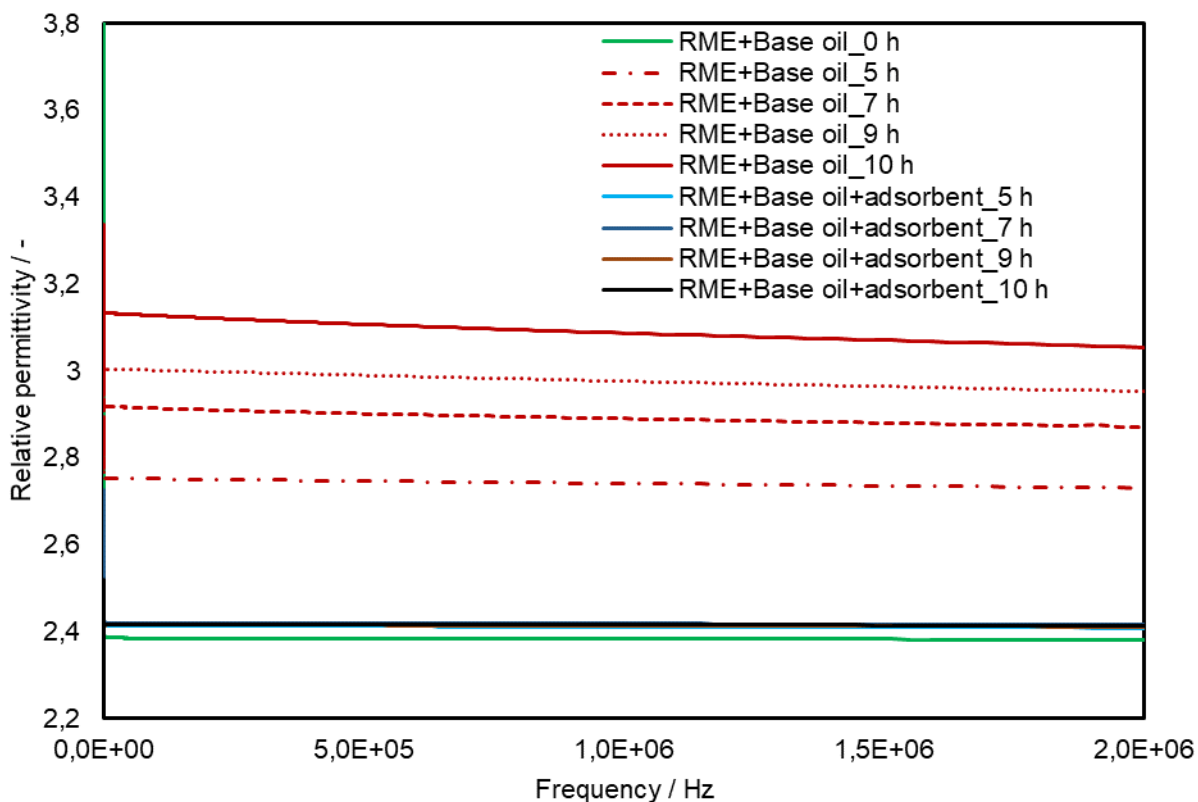


Figure 107: The relative permittivity of 30 mL 20 % RME and 80 % base oil treated with and without 0.675 g combined adsorbents of magnesium-aluminum hydrotalcite and 1,3,5-trimethyl-2,4,6-tris(3,5-di-tert-butyl-4-hydroxybenzyl) benzene in a ratio of 1:2 respectively aged for 10 h duration at 170 °C with airflow of 10L/h in a Rancimat

Figure 108 is the graph of the relative permittivity versus the duration of aging at 170 °C of the samples 40 mL of 20 %RME and 80 %base oil treated with and without 0.675 g of adsorbents at frequencies between 0 Hz and 20 kHz. For the mixture of 20 %RME and 80 %base oil treated with the adsorbents, the relative permittivity is about 2.384 (± 0.002) (0 h), and it remains nearly constant over the entire aging duration of 10 h (± 0.005). In contrast to the above, the relative permittivity of the mixture 20 %RME and 80 %base oil aged without the use of the adsorbents show a reasonably linear increase from 2.384

(± 0.002) at 0 h to 3.06 (± 0.002) at 10 h ($R^2 = 0.99$). It is clear from the results that the higher molecular mass substances formed during the aging of the mixture RME and base oil without using the adsorbents increase the polarity in the dielectric constant and thus the orientation polarization content. This supports the findings of Eskiner et al. 2015, 2020; Tic and Lovrec, 2011. Hence, the polar oxidation products lead to the increase of relative permittivity. Again, it is clear that the constant dielectric increases due to the oil's oxidation and degradation or deterioration (Tic and Lovrec, 2011). The low level of degradation of the blend treated with the adsorbents is due to the adsorbents' action, as explained in section 6. Dielectric spectra correlate better with the FTIR due to the high molecular weight polar oxidation species, with a higher frequency dielectric relaxation.

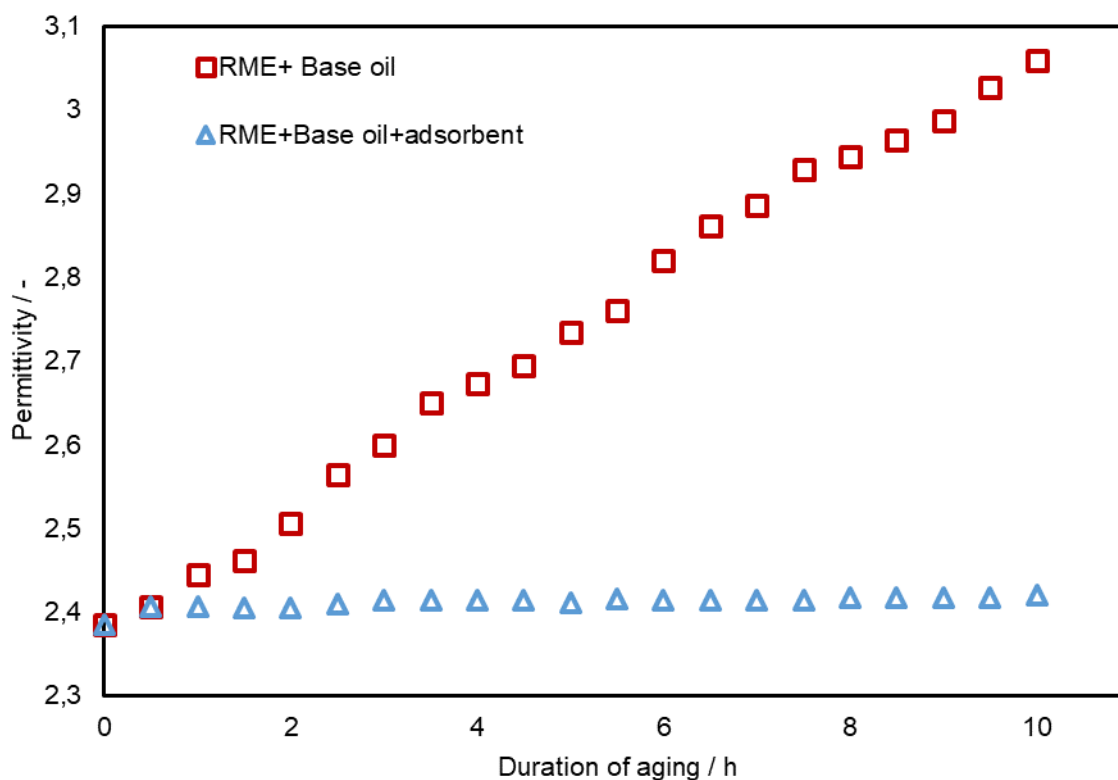


Figure 108: The relative permittivity versus duration of aging of 30 mL 20 % RME and 80 % base oil treated with and without 0.675 g combined adsorbents of magnesium-aluminum hydrotalcite and 1,3,5-trimethyl-2,4,6-tris(3,5-di-tert-butyl-4-hydroxybenzyl) benzene in a ratio of 1:2 respectively and aged at 170 °C airflows of 10L/h for 10 h duration in a Rancimat

8.7.2 The dissipation factor

Figure 109 represents the dissipation factor versus the duration of aging at different frequencies and room temperatures. In the graph, a strong frequency dependence with increasing aging duration is shown. The graph also reveals a relatively linear increase in the dissipation factor with the increasing duration of aging. While the dissipation factor of 20 %RME and 80 %base oil mixture without adsorbents treatment is about 0.001 (± 0.020) at 0 h of the aging, it increased to 0.027 (± 0.020) ($R^2 = 0.98$) after 10 h of aging at 170 °C. In comparison, the dissipation factor of 20 %RME and 80 %base oil mixture treated with adsorbents is about 0.001 (± 0.020) at 0 h and remains relatively constant over the aging duration of 10 h. The dissipation factor's impact can be explained from the formation of oxidation products perspective, as seen in section 3.4. The hydroperoxides formation in the allylic or bis-allylic positions in unsaturated compounds leads to polar products (Obadiah et al., 2012). Their polarity forces these degradation products to align in the alternating electric field, and therefore, the higher the frequency, the lesser the giant molecules align in the alternating field (Soleimania et al., 2014; Eskiner et al., 2015, 2020). Therefore, on conductivity losses, the ions present as oxidation products from dissociated carboxylic acids move between the plates and cause collisions with vicinal atoms or molecules. This produces additional friction leading to an increase of dissipation factor. As seen in Figure 109, with the increasing oxidation, an apparent increase is observed for the dissipation factor at around 2 h of aging till after 10 h of aging. This rapid increase in intensity with increasing degradation is likely due to the relaxation process of highly polar oxidation products. It is essentially absent in the mixture treated with the adsorbents and aged. The adsorbents' presence retarded the oxidation process leading to low production of oxidation products and hence low dissipation factors recorded.

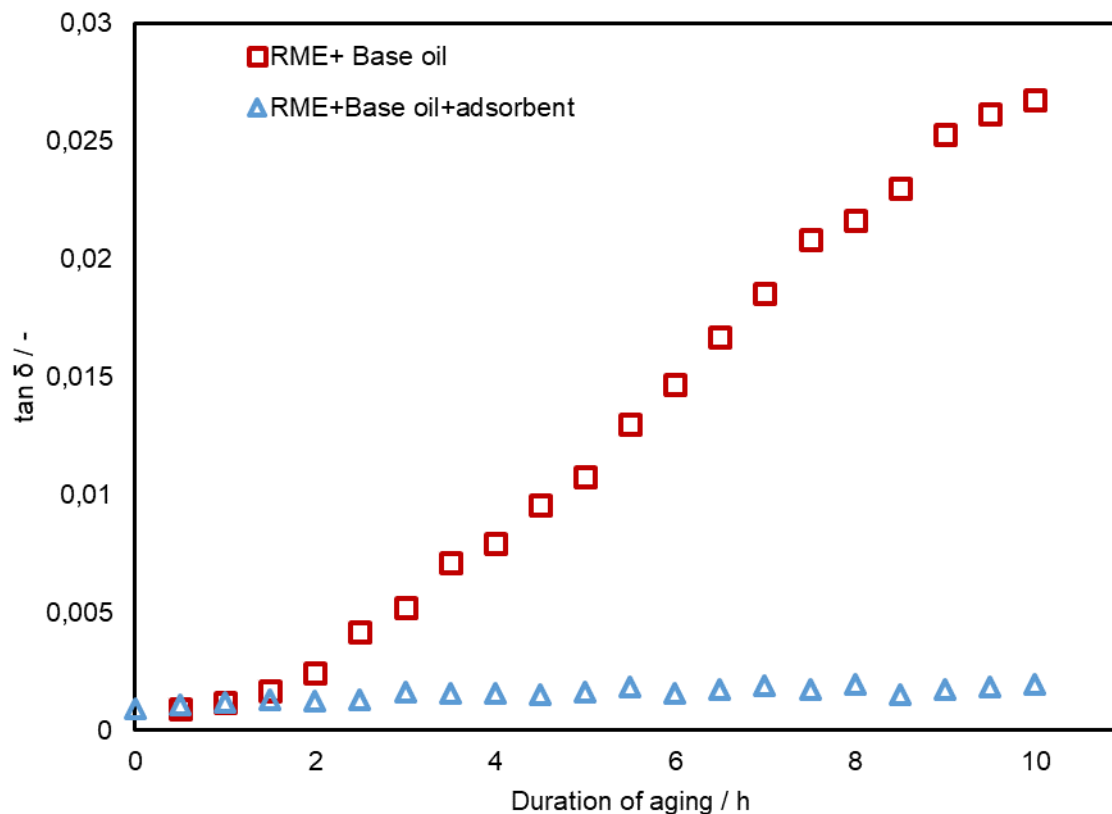


Figure 109: The dissipation factor versus duration of aging of 30 mL 20 % RME and 80 % base oil mixture treated with and without the combined 0.675 g adsorbents of magnesium-aluminum hydrotalcite and 1,3,5-trimethyl-2,4,6-tris(3,5-di-tert-butyl-4-hydroxybenzyl) benzene in a ratio of 1:2 respectively and aged for 10 h at 170 °C with airflow of 10L/h in a Rancimat

8.7.3 Acid value

The acid value is a measure of the number of acidic substances in a fuel or oil sample. The acid number measured is represented in Figure 110. The acid number shows similar behavior in trend as observed with the relative permittivity measurements. As shown in Figure 110, the acid number of 20 % RME and 80 % base oil mixture without treatment with the adsorbents increase linearly over the entire aging duration from 0.09 mg KOH / g at the start to about 10.03 mg KOH / g ($R^2 = 0.99$) at the end of the aging period, 10 h. The acid number of 20 % RME and 80 % base oil mixture treated with 0.675 g combined adsorbents and aged at 170 °C remain nearly constant throughout the entire duration of

the aging period. It is known that during the aging process, hydroperoxides produced from the oxidative degradation (Figure 5) undergo complex secondary reactions, including a split into more reactive aldehydes, which further oxidize into acids, leading to an increase in acid value (Soleimania et al., 2014; Obadiah et al., 2012; Leung et al. 2006). There is a correlation between the acid number and oxidation products formed during the degradation process. Thus, the nearly constant acid value results can be explained based on the adsorbents suppressing the oxidation process. This result collaborates with the dissipation factor above, section 8.7.2, where it is evident that no or insignificant polar products are formed.

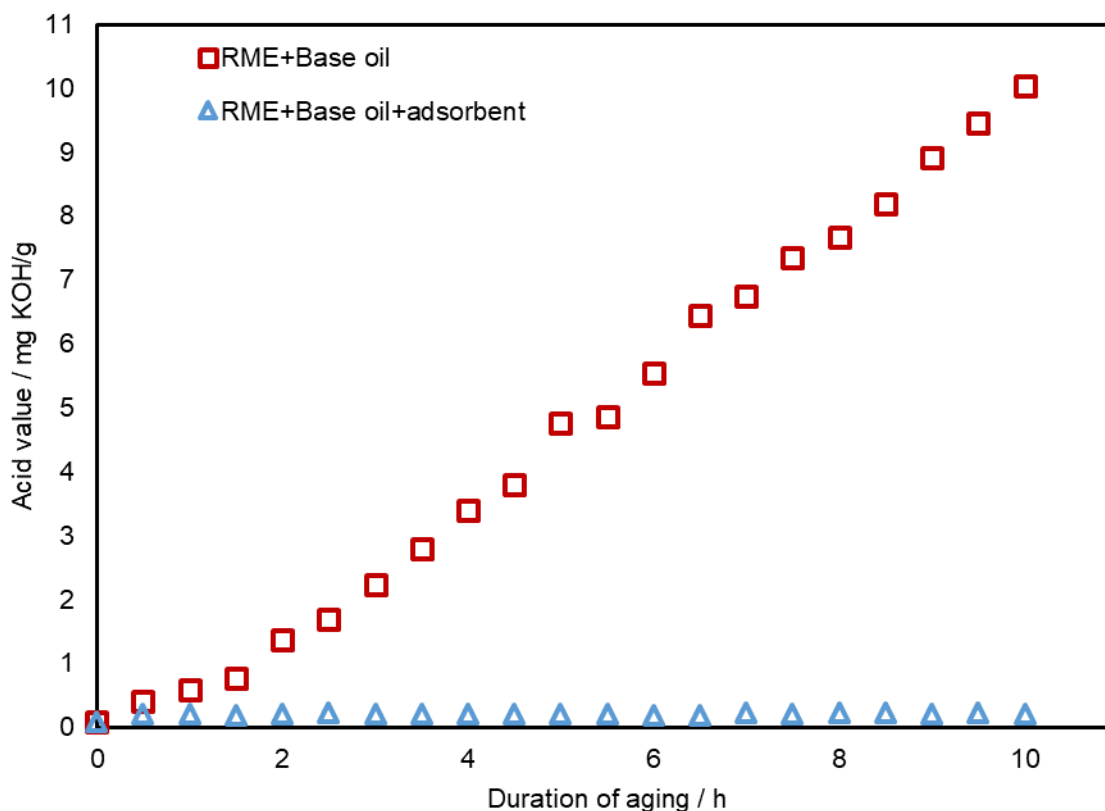


Figure 110: The total acid value versus duration of aging of 30 mL 20 % RME and 80 % base oil mixture treated with and without combined 0.675 g adsorbents of magnesium-aluminum hydrotalcite and 1,3,5-trimethyl-2,4,6-tris(3,5-di-tert-butyl-4-hydroxybenzyl) benzene in a ratio of 1:2 respectively and aged 170 °C with airflow of 10L/h for 10 h duration in a Rancimat

There is a good consistency between the dielectric spectroscopy studies, the change in dielectric property, dissipation factor, and the acid number during the degradation process. The increase of these parameters is significant only after 2 h of aging, which

could signify the end of the induction period. After this period, a sharp rise is observed, indicating the rapid degradation process of the blends. However, the above changes in parameter observations are absent and insignificant in the samples treated with the adsorbents.

The dielectric spectroscopy analysis is consistent with FTIR, SEC, and other results obtained in this work. As seen from all FTIR figures in this work for the samples not treated with the adsorbents, the ester carbonyl peak intensity at about 1746 cm^{-1} changed little before the induction period. There is a noticeably broadened band revealing an increasing degradation of the blends. Hence, the sample blends' degradation level can be clearly distinguished by monitoring the intensity of the characteristic carbonyl band.

The adsorbents' application extended the induction period by stabilizing the oxidation precursors with its liable hydrogen on its surface and, therefore, delay the beginning of the oxidation process. The onset of the oxidation process is accompanied by the formation of primary oxidation products, hydroperoxides. These hydroperoxides are unstable and can further decompose to secondary oxidation products, such as aldehydes, ketones, alcohols, carboxylic acids, and oligomers. Therefore, the absence of these oxidation products in the sample blends treated with the adsorbents confirms the adsorbents' suppression action.

8.7.4 NMR

The samples subjected to the NMR determination include 20 % RME blended with 80 % base oil treated with and without 0.675 g adsorbents and aged at $170\text{ }^{\circ}\text{C}$ for a duration of 80 h. After the aging process of the 20 % RME and 80 % base oil blend treated with the adsorbents, the used adsorbent is separated from the blend. The adsorbate is subjected to soxhlet extraction to remove any analyte on the surface of the adsorbents. The extract is then subjected to the NMR analysis as well.

The ^1H NMR spectra of the 20 % RME and 80 % base oil blend treated with and without the adsorbents and the extract of the adsorbate acquired are illustrated in Figure 112 and Figure 113.

The spectrum of the neat RME is shown in Figure 114. The chemical shifts and coupling constants reported in Hz and their resonance multiplicities, s = singlet, d = doublet, t = triplet, q = quartet, m = multiplet, are reported in Table 19 regarding Figure 111. The signals A and B of RME are superimposed with the CH₃ and CH₃₂ signals of the base oil, and the superimposed signals are indicated together. From section 3.4 and Table 1, position F (Figure 111) is most susceptible to oxidation due to the low bond dissociation energy, and therefore, radicals are formed at this position. Considering the signal shifts in Table 19, signal F has almost completely degraded or changed in shape in the mixture aged without any adsorbent treatment while only barely decreased in intensity in the sample mixture treated with the adsorbents and aged and also in their extracts as well. The signal F's significant presence confirms the adsorbents suppressing the oxidation of the blend by inhibiting radicals' formation since the process of autoxidation is a series of free radical reactions. The F signal's degrading also confirms that the radicals attack the methylene group adjacent to double bonds to set oxidation into motion. The shifts experienced in the F signal in the blend aged without any adsorbent treatment, which eventually affected the J signal, confirm a migration of the double bond during aging or oxidation or the formation of hydroperoxides stated in section 3.4.

According to Meher et al. (2006), the hydrogen abstraction at position F leads to a double allylic radical formation, causing double bond shifts. It moves the radical site to an outer carbon allowing oxygen to get added and generate a peroxy radical. The radical abstracts hydrogen from another methylene group making a hydroperoxide, therefore affecting position J. From Table 19, the signal for position J has disappeared entirely in the mixture aged 80 h without any adsorbent treatment. Since the adsorbents' presence inhibited the formation of the radicals, J's signal is still prominent in the aged blend treated with the adsorbents and in its extracts. The signal J decreases coinciding with the increase in acid value. Through chain cleavage during oxidation, saturated species may arise, leading to shorter-chain acids and high acidity. This is confirmed by Brühl (2014) and Knothe (2006) in literature. The singlet peak or signal G caused by the methyl ester in the sample aged without treatment with the adsorbents decreases during the reaction; the same signal for the sample treated with the adsorbents remains unchanged. The singlet peak increase in

the former can be explained by the formation of acids that have been suppressed in the latter. The high acidity of the mixtures aged without treatment with the adsorbents (

Figure 28,

Figure 46, and Figure 70) corroborates the significant shift in signal G for the same mixture. As the methyl ester signal, G, decreases, there is a considerable increase in acid value. This shift and increase in acid value in the sample aged without any treatment with the adsorbents is relatively insignificant in the blend treated with the adsorbents.

It is remarkable to notice that there is no or little change of the signal for C18_3 fatty acid after 80 h of aging at 170 °C in the blend treated with the adsorbents. The signal $A_{C18:3}$ is still strong with no change in shape.

Though the fatty acids with methylene interrupted double bonds are susceptible to oxidation, the double bond in 18:3 in the blend treated with the adsorbents is largely retained. However, it could indicate that other double bond positions in 18:3 are preferentially affected by the process of oxidation, according to Knothe (2006). The $A_{C18:3}$, however, shows an intense change in shape in the blend aged without any treatment with the adsorbents.

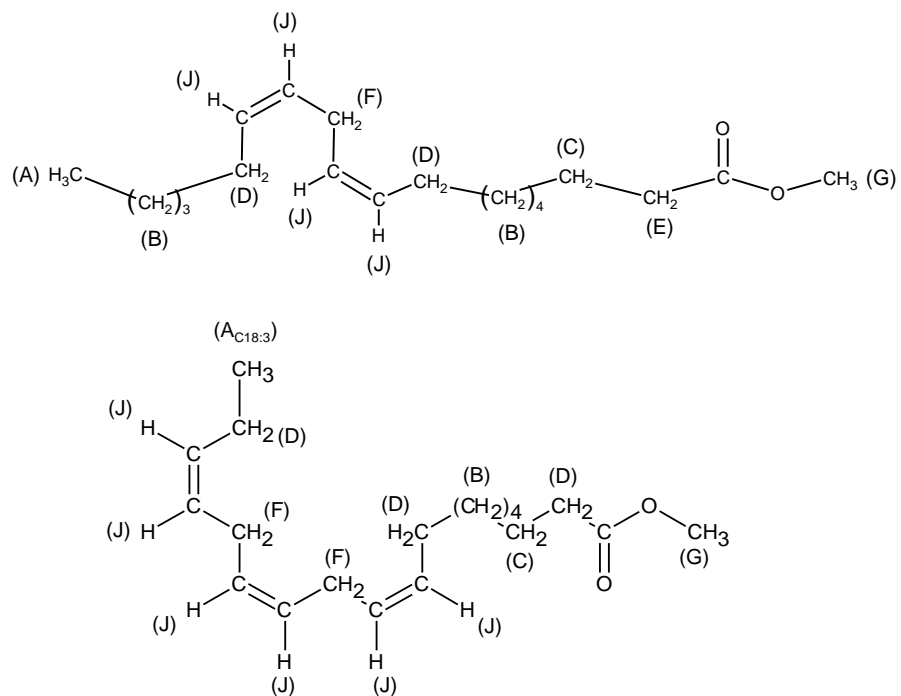


Figure 111 Molecular structure of methyl linolenic acid with the 1H-NMR assignment to Table 19

Table 19: $^1\text{H-NMR}$ (400 MHz, CDCl_3) chemical shift. The assignment of the signals is shown in Figure 111

Sample	Aging time [h]	A	B	C	D	E	F	G	$\text{A}_{\text{C}_{18:3}}$	J
RME	0	0.90–0.73 (m, 3H)	1.35–1.17 (m)	1.59 (dd)	2.10–1.90 (m)	2.27 (t, J = 7.5 Hz, 2H)	2.82–2.71 (m)	3.63 (s)	1.00–0.91 (m)	5.44–5.22 (m)
		<u>RME + Oil overlaid</u>		C	D	E	F	G	$\text{A}_{\text{C}_{18:3}}$	J
<u>Extract RME + Oil + Ad</u>	80	0.94–0.70 (m, 57H)	1.80–0.97 (m, 214H)	1.66–1.57 (m, 5H)	2.01 (dd, J = 12.5 Hz, 6.6 Hz, 2H)	2.30 (t, J = 7.5 Hz, 2H)	2.80–2.62	3.66 (s, 3H)	(---)	5.45–5.26 (m, 1H)
RME + Oil+ Ad	80	0.96 – 0.64 (m, 69H)	1.84 – 0.97 (m, 256H)	1.65 – 1.57 (m, 5H)	2.01 (dd, J = 12.5, 6.7 Hz, 2H)	2.30 (t, J = 7.5 Hz, 2H)	2.80–2.62	3.66 (s, 3H)	(---)	5.39–5.29 (m, 1H)
RME + Oil	0	1.03–0.64 (m, 18H)	1.04–1.63 (m, 62H)	1.74–1.54 (m, 2H)	2.14–1.94 (m, 2H)	2.31 (t, J = 7.5 Hz, 1H)	2.86–2.72 (m, 1H)	3.67 (s, 3H)	1.01–0.96 (m)	5.47–5.25 (m, 1H)
RME + Oil	80	0.97 – 0.65 (m, 27H)	1.75 – 0.99 (m, 100H)		2.12 (s, J = 9.9 Hz, 1H)	2.42 – 2.23 (m, 3H)	2.67–2.65	3.65 (s, 1H)		
Oil	0	0.85 – 0.62 (m, 1H).	1.29 – 0.96 (m, 1H)							

The $^1\text{H-NMR}$ spectra of the base oil and biodiesel mixture were treated with and without the adsorbents and aged at 170 °C for 80 h, and their extracts are illustrated below. The key of colors to the graphs are as follows:

Turquoise: 20 %RME + 80 %base oil aged at 170 °C for 80 h

Green: Extract of 20 %RME + 80 %base oil + adsorbent after aging at 170 °C for 80 h

Blue: 20 %RME + 80 %base oil + adsorbent aged at 170 °C for 80 h

Red: 20 %RME + 80 %base oil 0 h (unaged or neat)

In the ^1H NMR spectrum of degraded base oil blended with biodiesel and aged at 170 °C for 80 h, Figure 112 and Figure 113, the peaks' intensity at 2 ppm, 2.3 ppm, 2.8 ppm, 3.65 ppm, and 5.35 ppm decreased as compared with the neat unaged blend. The peak decrease is attributed to oxidation. The methyl ester singlet peak decreases during the degradation process, and the formation of free fatty acids could explain this. The methyl ester peak's most significant decreases are observed for the oxidized samples aged without using the adsorbents. This coincides with these samples having the highest acid, kinematic viscosity, density, molar mass substances, and IR absorption values. These peak decreases are not significant in the blends treated with the adsorbents, demonstrating the adsorbents' impact in retarding the oxidation process. It also showed a minor increase in acid, kinematic viscosity, and the other above-stated parameter values. The peaks of the extracts of the blends treated with the adsorbents do not differ from that of the blends treated with the adsorbent, bringing to light that the oligomers are not retained on the surface of the adsorbents.

The NMR evaluation has indicated an increasing trend coincides nicely with the increasing kinematic viscosity, density, FTIR absorption, high molecular mass species, acid values, and the other physiochemical parameters of the sample without the adsorbents and aged at 170°C for 80 h as reported in this work. The high acid values, viscosity, and other parameters result from the increasing amount of saturated fatty acid compounds as degrading proceeds. These compounds possess higher viscosity than their unsaturated ones. The formation of shorter-chain acids also gives rise to greater viscosity than the standard methyl esters. The formation of free fatty acids and more saturated species also supports higher-molecular weight species detected by the SEC. These results largely coincide with the literature (Knothe, 2006; Dunn, 2002). With the absence of the above observation in the samples treated with the adsorbents and aged, it can be concluded that the adsorbents impacted the degradation process. Hence, the samples did not get

oxidized. It confirms the surface reaction of the free radical produced during the first stage of the oxidation process with a hydrogen atom from the hydroxyl group of the adsorbent, thereby stabilizing the radical and interfering in the radical propagation.

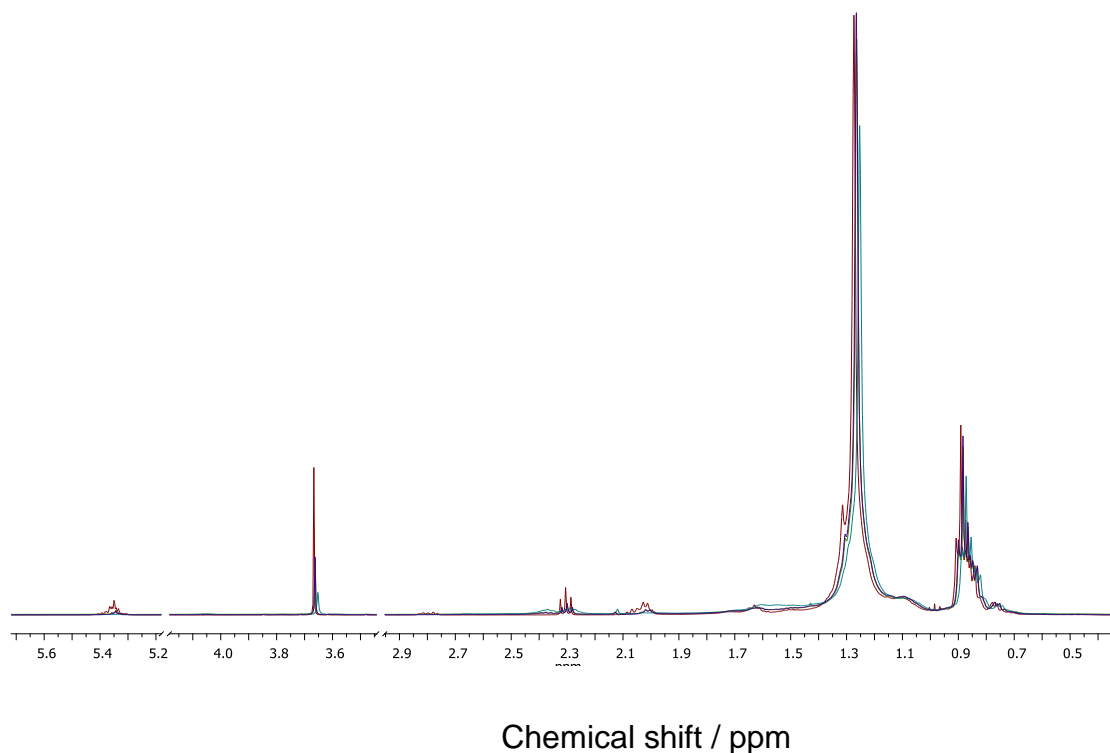


Figure 112: ¹H-NMR spectra of 30 mL 20 % RME and 80 % base oil mixture treated with and without combined adsorbents of magnesium-aluminum hydrotalcite and 1,3,5-trimethyl-2,4,6-tris(3,5-di-tert-butyl-4-hydroxybenzyl) benzene in a ratio of 1:2 respectively and aged at 170 °C airflows of 10L/h for 80 h and their extracts

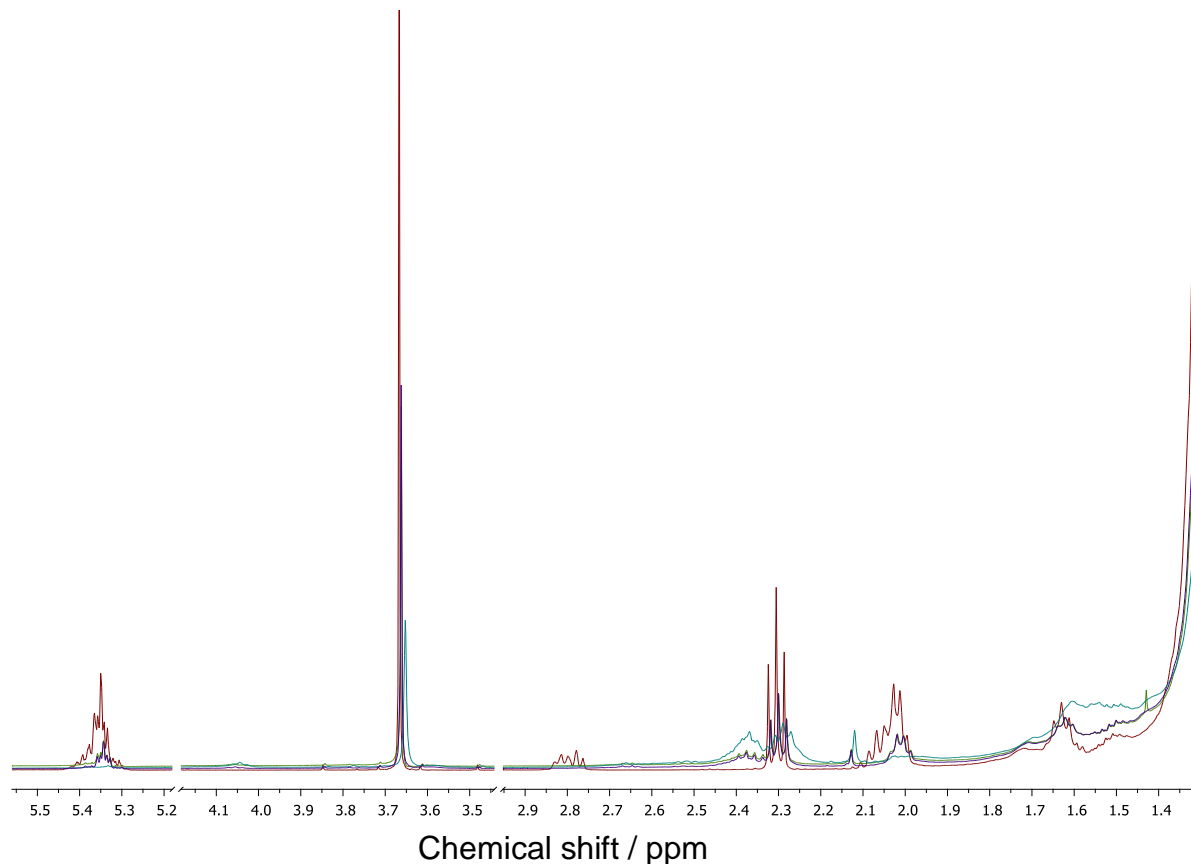


Figure 113: Zoom in on Figure 112

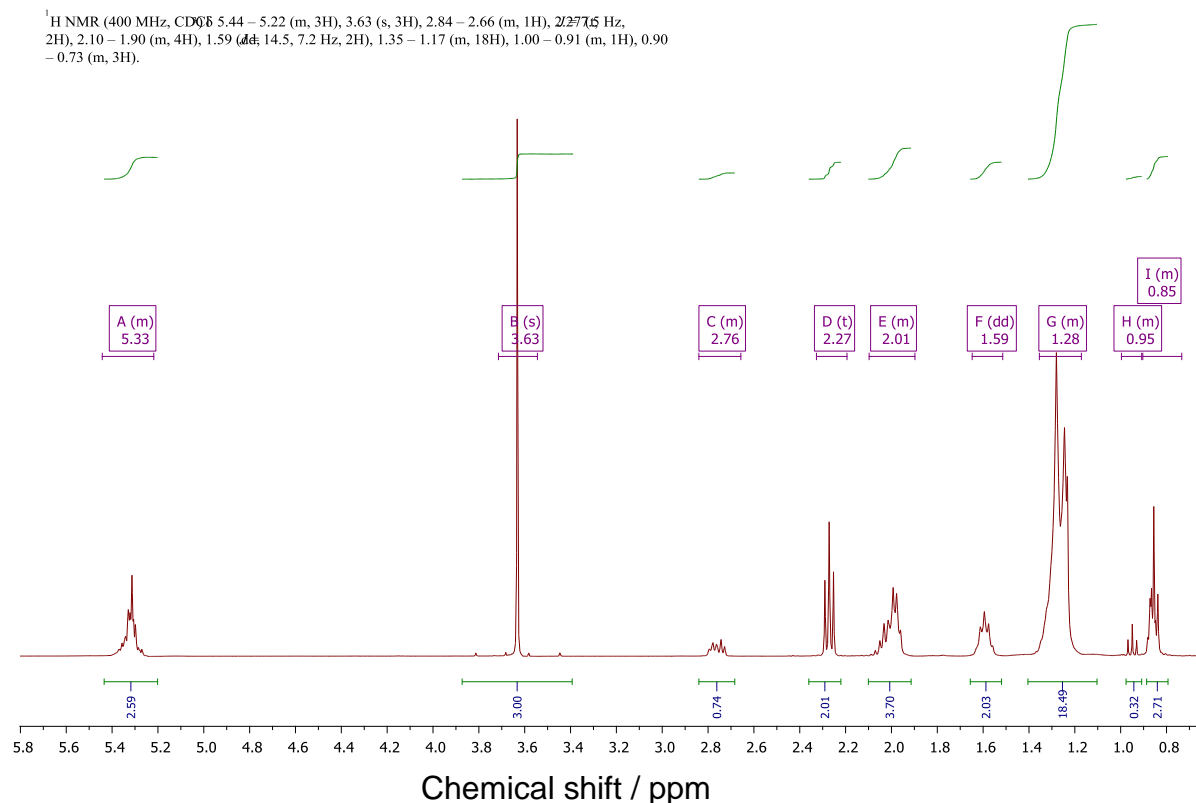


Figure 114: ¹H-NMR spectrum of neat RME

Summary

Permittivity is indicative of a material's ability to store an electric field in the polarization of a medium (Eskiner, 2015; seins, 2020). During the aging of the sample, 40 mL of 20 %RME and 80 %base oil were treated with the 0.675 g combined magnesium-aluminum hydrotalcite and 1,3,5-trimethyl-2,4,6-tris(3,5-di-tert-butyl-4-hydroxybenzyl) benzene in a ratio of 1:2 respectively had relative permittivity of about 2.384 (± 0.002) (0 h). It remained nearly constant over the entire aging duration of 10 h (± 0.005) while that of the mixture 20 %RME and 80 %base oil aged without the use of the adsorbents show a reasonably linear increase from 2.384 (± 0.002) at 0 h to 3.06 (± 0.002) at 10 h ($R^2 = 0.99$). The net change in permittivity of the sample aged without any adsorbent treatment is 0.676.

There is a fairly linear increase in dissipation factor for dissipation factor with the increasing duration of aging. While the dissipation factor of 20 %RME and 80 %base oil mixture without adsorbents treatment has about 0.001 (± 0.020) at 0 h of the aging, it increased to 0.027 (± 0.020) ($R^2 = 0.98$) after 10 h of aging at 170 °C. The dissipation factor of 20 %RME and 80 %base oil mixture was treated with combined, with a combination of 0.675 g magnesium-aluminum hydrotalcite and 1,3,5-trimethyl-2,4,6-tris(3,5-di-tert-butyl-4-hydroxybenzyl) benzene in a ratio of 1:2 respectively is about 0.001 (± 0.020) at 0 h, and this remains relatively constant over the aging duration of 10 h. The formation of oxidation products can explain the dissipation factor results. The hydroperoxides formation in the allylic or bis-allylic positions in unsaturated compounds leads to polar products, aldehydes, ketones, carboxylic acids, and oligomers (Obadiah et al., 2012). Their polarity forces these degradation products to align in the alternating electric field, and therefore, the higher the frequency, the lesser the big molecules align in the alternating field (Eskiner et al., 2014, 2020). While on conductivity losses, the ions present as oxidation products from dissociated carboxylic acids move between the plates and cause collisions with molecules that produce additional friction, leading to increased dissipation.

It is clear from the results that the oligomers' formation during the aging of the mixture RME and base oil without using the adsorbents increases the polarity in the dielectric and thus the orientation polarization. It agrees with the findings of Eskiner et al. 2014, 2020. Hence, the polar oxidation products resulting from degradation or oxidation lead to an increase in relative permittivity.

An increasing rate of acid value with increasing duration of aging has been observed for the acid value. This collaborates Shahabuddin et al. 2012 indicating hydroperoxide production as the main contributor to the increasing acid value. There is a good correlation between the acid value and its aging duration. The mixtures aged without any treatment with the adsorbents showed a steady increase in the acid values with increasing aging duration, from 0.09 mg KOH / g at the start to about 10.03 mg KOH / g at 10 h. On the other hand, the blend treated with 0.675 g combined adsorbents and aged at 170 °C, on the other hand, remained nearly constant throughout the entire aging period. Thus, the relatively stable acid values suggest the adsorbents suppress hydroperoxides' formation, resulting in no significant oxidation products and, hence, low acid values.

The analysis with the NMR shows that the adsorbents suppress the formation of oxidative products. In the ^1H NMR spectrum of degraded base oil blended with biodiesel aged at $170\text{ }^\circ\text{C}$ for 80 h, the peaks' intensity at 2 ppm, 2.3 ppm, 2.8 ppm 3.65 ppm, and 5.35 ppm compared with the neat unaged blend decreased significantly, and this is attributable to oxidation. These peaks in the blends treated with the adsorbents are not significantly affected. The blends' peaks treated with the adsorbents do not differ from those treated with the adsorbent.

9 Conclusion, outlook, and recommendation

9.1 Conclusion

The use of biodiesel as a green alternative fuel for diesel engines is promising. However, biodiesel comes with attendant problems, especially regarding its oxidation stability. One of the main hindrances of biodiesel is its degradability during storage and usage. This oxidative degradability essentially alters the very desirable properties of biodiesel. It diminishes its applicability as fuel for long-term use, especially in the tanks of plug-in hybrid vehicles. One important factor affecting lubricating oil in recent times is its dilution by biodiesel and its blends. This reduces the oil's viscosity, degrades its oxidation resistance, and shortens its useful service life. Engine oil performance is affected by biodiesel as they accumulate in a vehicle's sump and impact the engine oil durability.

This work aimed to explore adsorbents' use in mitigating biodiesel degradation and its adverse effects on lubricants' physicochemical properties to enhance their oxidation stability. For this purpose, laboratory analysis was carried out in which neat biodiesel and base oil blended with biodiesel were treated with various amounts of adsorbents to examine their impact on physicochemical properties. Combined adsorbents of 1, 3, 5-trimethyl-2, 4, 6-tris (3, 5-di-tert-butyl-4-hydroxybenzyl) benzene and magnesium-aluminum hydroxycarbonate in a ratio of 1:2 were applied. This methodology allowed for comparing and quantifying the mass variation of oxidative products built up regarding the physicochemical properties.

For investigating the suppression of oxidation in a simulated 20 % engine oil dilution, 30 mL blend of 80 % base oil and 20 % rapeseed oil methyl ester is treated with amounts of 0.225 g, 0.45 g, and 0.675 g of the combined adsorbents of magnesium-aluminum hydrotalcite and 1,3,5-trimethyl-2,4,6-tris(3,5-di-tert-butyl-4-hydroxybenzyl) benzene in a ratio of 1:2 and aged at a temperature of 170 °C for 80 h duration using a Rancimat with airflow of 10 L/h for 80 h.

For evaluating the impact of temperature on the adsorbent's effect on suppression of formation of oligomers, 30 mL blend of 80 % base oil and 20 % rapeseed oil methyl ester was treated with 0.675 g of the combined adsorbents of magnesium-aluminum

hydrotalcite and 1,3,5-trimethyl-2,4,6-tris(3,5-di-tert-butyl-4-hydroxybenzyl) benzene in a ratio of 1:2 and aged at temperatures of 70 °C, 110 °C, 140 °C and 170 °C for 80 h duration.

The results of these tests showed that the use of the adsorbents, 0.675 g of 1, 3, 5-trimethyl-2, 4, 6-tris (3, 5-di-tert-butyl-4-hydroxybenzyl) benzene and magnesium-aluminum hydroxycarbonate combined in a ratio of 1:2 respectively in 30 mL of 80 % base oil blended with 20 % RME aged at 170 °C for 80 h resulted in more than 60 % reduction in the oligomer formation, about 90 % reduction in total acid number and more than 50 % reduction in viscosity increment. The suppression of oxidation is dependent on the weight of the adsorbents applied. This means with increasing proportions of biodiesel dilutions, higher amounts of adsorbents are required, potentially resulting in other adverse effects. From literature (Fang and McCormick, 2006; Schmidt, 2014), 20 % biodiesel admixture seem to result in the maximum proportion of higher molecular mass species in the aged model fuels. From this work, a maximum of 90 g of the adsorbents is required to salvage 4 L of engine oil or lubricant, which contains about 20 % unsaturated fuel at 60 % suppression of oligomers formation at a temperature of 170 °C. This translates into 22.5 g adsorbents per 1 L of oil with no apparent negative interactive impact on the oil additives. The suppression of oligomers formation results mapped nearly the unaged mixtures' primary data set and confirmed by the permittivity signal combined with the aging duration, acid value, dissipation factor, and the NMR signal. The relative permittivity of 20 % RME and 80 % base oil aged without using the adsorbents recorded an increase of about 22 %, while the sample treated with the adsorbent remained unchanged in relative permittivity. On the other hand, the dissipation factor increased by 27 for 20 % RME and 80 % base oil mixture without adsorbents treatment. Again, that of the sample treated with the adsorbents remained unchanged.

This work has shown that the adsorbents, 1, 3, 5-trimethyl-2, 4, 6-tris (3, 5-di-tert-butyl-4-hydroxybenzyl) benzene and magnesium-aluminum hydroxycarbonate with hydroxyl groups in its molecule can scavenge any free radical(s) in the oxidation procedure and also adsorb acidic products. The results indicate the potential of using adsorbents to suppress the degradation of biodiesel and its blends and, therefore, extend the useful

service life of lubricating oil in engines fueled with biodiesel and its blends. The use of the adsorbents showed enhanced oxidation stability of biodiesel and its blends.

For stabilizing biodiesel blends, the adsorbents have shown a significant enhancement of the oxidation stability from this study. Applying 1 g of the combined adsorbents in stabilizing 30 mL B20 during thermal aging at 170 °C resulted in an average improvement of about 77 % on all the critical fuel quality parameters tested during the experiment. These results, among others, largely coincide with literature, Zhou et al. 2017; Dunn, 2008, 2005 and Liang et al., 2006. From literature (Nogales-Delgado et al., 2019; Yahagi et al., 2019; Varatharajan and Pushparani, 2017; Osawa et al., 2016; McCormick and Westbrook, 2007; Schober and Mittelbach, 2004), oxidation cannot be genuinely prevented, but the use of these adsorbents has significantly slowed the oxidation process of biodiesel and can, therefore, be used to extend the useful service life of lubricants.

The stability of biodiesel and its blends during storage and application is critical due to oxidation. During the storage period under this work, the adsorbents' use resulted in an average of about 83 % improvement on all the parameters tested during this experiment using 0.675 g combined adsorbents in 40 mL of B20 at a temperature of 40 °C. This is corroborating evidence of the suppression of degradation of biodiesel blends. The low values reported for acid number, viscosity, density, and the level of oligomers formed indicate that the adsorbents impacted the oxidation process by retarding the formation of hydroperoxides. As the hydroperoxides are the main contributor to increasing acid value, the low acid values indicate the suppression of hydroperoxides' production. It is, therefore, conclusive to state that the adsorbents suppress the degradation process by interfering at the initiation stage of oxidation. The adsorbents, magnesium-aluminum hydrotalcite, and 1,3,5-trimethyl-2,4,6-tris (3,5-di-tert-butyl-4-hydroxybenzyl) benzene have enhanced the oxidative stability of biodiesel and its blends by suppressing the formation of oligomers through its liable hydroxyl ions. Therefore, treating biodiesel with these adsorbents is a means for increasing its resistance to oxidation and extending its oxidation stability.

These results open up the possibility of increasing the biodiesel proportion that can be blended with diesel fuel and the possible use of B100 fuels in diesel engines without a

noticeable negative impact on the engine oil/lubricant. The adsorbents have an additional advantage in retarding biodiesel's deterioration when added to oxidizing biodiesel through the oxidation products' adsorption. This work has shown the effectiveness of adsorbents in the maintenance of engine oil drain intervals and lubricant performance. It has contributed to creating a robust oil film in the engines fueled by biodiesel and its blends by subduing the impact of fuel dilution.

The above efficiencies estimation of the adsorbents in suppressing biodiesel oxidation is based on the laboratory experiments carried out in this work. Further studies are still required for the improvement of the results and to arrive at a definite conclusion through a field experiment with the adsorbents in a possible cartridge connected in a vehicle's oil loop or a running engine. This will consider other engine effects such as soot because not all oils handle soot equally.

9.2 Outlook and Recommendation

Despite the results of this work demonstrating the potential of adsorbents suppressing the oxidation of biodiesel and its blends, carrying out an electron paramagnetic resonance or electron spin resonance spectroscopy would be a useful tool for determining how the radicals are being adsorbed or scavenged by the adsorbents. This technique is entirely “blind” to molecules without unpaired electrons hence, precise. As free radicals are short-lived or short stable, adding the adsorbent will increase their detection since the adsorbent will react or catch the free radical to form a stable radical product. This will be conclusive on the act of the adsorbents impacting the initiation stage of the oxidation process leading to insignificant production of hydroperoxides. However, the lack of this instrument constrained the carrying out of this measurement.

The adsorbents employed in this work enhance biodiesel fuel quality and its blends during storage and application and, therefore, should not initiate phase separation and other transitions that could lead to degradation as the adsorbents get dissolved at high temperatures but return to solid on cooling down. Further study will be necessary to determine whether overall conclusions obtained from this work apply to reducing the oxidative degradation of biodiesel fuel quality during their application in actual engine conditions. In general, increasing adsorbents concentration increases its suppression activity. The exact activity increment by smaller proportional increments of adsorbents needs to be determined.

The method of using adsorbents to suppress oxidation presented here opens up new opportunities in the biodiesel industry. These adsorbents could be applied during the biodiesel production process, enhancing the biodiesel's oxidation stability, making it more stable during aging. Also, the combustion and emissions behavior of an engine is predetermined by the fuel mixture. Therefore, the adsorbents' impact on fuel degradation offers further optimization potential in reducing engine emissions. This, however, needs further investigations

Testing the adsorbents' impact against different antioxidants to study their efficacy is potentially exciting for the future. This area can introduce competition for the lubricant market as the adsorbents have a more significant potential to extend the induction period

of fuel, especially ester base fuel in general, compared with the traditional antioxidants. More research is required to acquire knowledge about these adsorbents, which may help establish their potential as antioxidants since they exhibit antioxidant tendencies. Also, the possibility of using these adsorbents in the form of additives in formulating lubricating oils can be exploited.

An oil filter-like cartridge containing about 90 g of the adsorbents should be incorporated into a real machine engine and operated over a given distance or time. The oil quality should then be examined before and after the test to determine the actual impact on the adsorbents' degradation or oxidation.

When added to the biodiesel, B100, the adsorbents' efficiency in estimating the storage time by monitoring the oxidation reaction at different temperatures would be another area for future research.

Bibliography

Abdulkadir, I., Uba, S., Salihu A.A., et al. (2016) A Rapid Method of Crude Oil Analysis Using FT-IR Spectroscopy, *Nigerian Journal of Basic and Applied Science*, 24(1): 47-55

Abdullah, N., Razali, H., Mootabadi, et al. (2007) Critical technical areas for future improvement in biodiesel technologies, *Environ. Res. Lett.* 2 (July-September 2007) 034001 doi:10.1088/1748-9326/2/3/034001

Abdul-Munaim, A.M., Holland, T., Sivakumar, P. et al. (2019), Absorption Wavebands for Discriminating Oxidation Time of Engine Oil as Detected by FT-IR Spectroscopy, *Lubricants* 7, 24

Adhvaryu, A., Perez, J.M., Singh, I.D., et al. (1998) Spectroscopic Studies of Oxidative Degradation of Base Oils, *Energy & Fuels* 12, 1369-1374

Agarwal, A.K. (2005), Experimental investigations of the effect of biodiesel utilization on lubricating oil tribology in Diesel engines, *Proc. IMechE, Vol.219, Part D: J. Automobile Eng.*, pp. 703 713. DOI: 10.1243/095440705X11239

Ahmed R. (2009) Correlation between the chemical structure of biodiesel and its physical properties, *International Journal of Environmental Science and Technology* 6(4) DOI: 10.1007/BF03326109

Aladedunye, A. F., (2011) Inhibiting Thermo-oxidative degradation of oils during frying, Ph.D. Thesis Submitted to the School of Graduate Studies of the University of Lethbridge, Canada

Aluyor E. O., Obahiagbon K. O., Ori-jesu M. (2009), Biodegradation of vegetable oils: a review. *Scientific Research and Easy*;4(6):543–8.;

Aluyor, E. O., Ori-Jesu, M. (2008), The use of antioxidants in vegetable oils – A review. *African Journal of Biotechnology*, 7 (25), pp. 4836-4842

Alves F. M. and Starck, L., (2016)"Oxidation Stability of Diesel-Biodiesel Blends: Impact of Physical-Chemical Properties Over Ageing into Fuel Injection Systems (FIS) and Storage," SAE Technical Paper 2016-01-2267

Amat, S., Braham, Z., Le Dre´au, Y., et al. (2013) Simulated aging of lubricant oils by chemometric treatment of infrared spectra: Potential antioxidant properties of sulfur structures. *Talanta* 107, 219–224

Ancho L. C. (2006) The Filter, C.C. JENSEN A/S No4 February 2006
https://www.cjc.dk/fileadmin/root/File_Admin_Filter/doc_Brochures/The_Fiter_No_4_UK_Feb_2006.pdf

Andreae M. M., Fang, H.L., Bhandary, K. (2007) Biodiesel and fuel dilution of engine oil. SAE technical paper series 2007-01-4036.

Andreae, M.M., Fang, H. L., Bhandary, K. (2007), Biodiesel on Fuel Dilution of Engine Oil”, Document Number 2007-01-4036, Powertrains, Fuels and Lubricants Meeting, October 2007, Chicago, IL, USA

Arau´ jo S. V., Luna, F. M.T., Rola Jr., E. M., et al. (2009), A rapid method for evaluation of the oxidation stability of castor oil FAME: influence of antioxidant type and concentration. *Fuel Processing Technology*

Arruda, C.C., Cardoso, P.H.L., Dias I.M.M., et al. (2013), Hydrotalcite (Mg₆Al₂(OH)₁₆(CO₃) · 4H₂O): A Potentially Useful Raw Material for Refractories, 56th International Colloquium on Refractories 2013 September 25th and 26th, 2013, EUROGRESS, Aachen, Germany

Ashraful, A. M., Masjuki, H. H., Kalam, M. A., et al. (2014), Study of the Effect of Storage Time on the Oxidation and Thermal Stability of Various Biodiesels and Their Blends, *Energy Fuels*, 28, 1081–1089

Asim, H. A., Nuha, S. M., Mohamed, R. K., (2013) Investigations of Physical and Rheological Properties of Aged Rubberised Bitumen, *Advances in Materials Science and Engineering* Volume 2013, Article ID 239036, 7 pages
<http://dx.doi.org/10.1155/2013/239036>

Asseff, P.A. (1968) Engine Performance as Influenced by Lubricant Deterioration, in *SAE Int. J. Fuels Lubr.*, Doi:10.4271/680760

ASTM D664: Standard Test Method for Acid Number of Petroleum Products by Potentiometric Titration; ASTM International: West Conshohocken, PA, USA, 2009.

ASTM. 2000. Annual Book of ASTM Standards. American Society for Testing and

Avinash, K. A. (2003) Lubricating Oil Tribology of a Biodiesel-Fuelled Compression Ignition Engine, 2003 Fall Technical Conference, ASME Internal Combustion Engine Division and Rail Transportation Division, Erie, Pennsylvania, USA, September 7-10, 2003

Ayhan, D. (2007) Thermal Degradation of Fatty Acids in Biodiesel Production by Supercritical Methanol, *Energy Exploration & Exploitation*, 25, (1) pp. 63–70

Bacha, K., Benamara, A., Vannier, A., et al. (2015), Kinetics of diesel/biodiesel fuels oxidation and evolution of oxidation products formed at different stages of oxidation. International Congress and Expo on Biofuels & Bioenergy, 7, 2015 Valencia, Spain, *J Fundam Renewable Energy Appl*, 5:5

Bacha, K., Benamara, A., Vannier, A., et al. (2015). Oxidation stability of diesel/biodiesel fuels measured by a PetroOxy device and characterization of oxidation products. *Energy Fuels*, 29:4345–55.

Bai, A., Jobbágy, P., Popp, J., et al. (2016) Technical and environmental effects of biodiesel use in local public transport, 47, 323-335

<https://doi.org/10.1016/j.trd.2016.06.009>

Balat, M. and Balat, H., (2008), A critical review of biodiesel as a vehicular fuel, *Energy Conversion and Management* 49, 2727–2741;

Bannister, C. D., Chuck, C. J., Bounds, M., et al. (2011). Oxidative Stability of Biodiesel Fuel. *Proceedings of the Institution of Mechanical Engineers, Part D: Journal of Automobile Engineering*, 225(1), 99–114. <https://doi.org/10.1243/09544070JAUTO1549>

Bannister, C.D., Chuck, C.J., Hawley, J.G., et al. (2010), Factors affecting the decomposition of biodiesel under simulated engine sump oil conditions. *Proc Inst Mech Eng Part D-J Automob Eng*; 224:927.

Beercheck, D. (2008), Green Fuels give engine oils the blues, L'n'G | Europe – Middle East – Africa May/June 2008

Berrios, M., Martín, M. A., Chica, A. F., et al. (2012), Storage Effect in the quality of Different Methyl Esters and Blends with Diesel, Fuel, vol. 91, no. 1, pp. 119–125

Berton-Carabin, C. C., Ropers, M.H., and Genot, C. (2014), Lipid Oxidation in Oil-in-Water Emulsions: Involvement of the Interfacial Layer; Comprehensive Reviews in Food Science and Food Safety; Vol.13, 2014 Doi: 10.1111/1541-4337.12097;

Besser, C., Pisarova, L., Frauscher, M., et al. (2017) Oxidation products of biodiesel in diesel fuel generated by artificial alteration and identified by mass spectrometry, Fuel 206, 524–533

Biernat, K., Bocian, P., Bukrejewski, P., et al. (2019) Application of the Impedance Spectroscopy as a New Tool for Studying Biodiesel Fuel Aging Processes, Energies 12, 738.

Biodiesel guidelines, (March 2009), Worldwide Fuel Charter Committee

Blackburn, J., Pinchin, R., Nobre, J., et al. (1983) Performance of lubricating oils in vegetable oil ester-fuelled diesel engines. SAE Technical Paper.

Blanksby, S.J., Ellison, G.B. (2003), Bond Dissociation Energies of Organic Molecules, Acc. Chem. Res., 36 (4), pp 255–263 DOI: 10.1021/ar020230d

Bondioli, P., Gasparoli, A., Della B. L., et al. (2002) Evaluation of biodiesel storage stability using reference methods. Eur Lipid Sci Technol. 104, 777–784.

Bong-Ha, S. and Yun-Ho, C. (2008) Investigation of lubricating oil variations diluted by post-injected fuel for the regeneration of CDPF and its effects on engine wear. Journal of Mechanical Science and Technology 22, 2526-2533. DOI 10.1007/s12206-008-0903-x

Botella, L., Bimbela, F., Lorena, M., et al. (2014), Oxidation stability of biodiesel fuels and blends using the Rancimat PetroOXY methods. Effect of 4-allyl-2,6 dimethoxyphenol and catechol as biodiesel additive on oxidation stability; Frontiers in Chemistry | Chemical Engineering, 2014 Volume 2 Article43; DOI: 10.3389/fchem.2014.00043

Bouaid, A., Martinez, M., Aracil, J., (2007) Long storage stability of biodiesel from vegetable and used frying oils, *Fuel*, 86, 16, Pages 2596-2602

Brühl, L. (2014), Fatty acid alterations in oils and fats during heating and frying. *European journal of lipid science and technology*. Heft 6/ (Band: 116) S. 707-715 DOI: 10.1002/ejlt.201300273

Burgeoning Biodiesel, Infineum Insight, June 2007, p.9

Canakci, M., Monyem, A., Van Gerpen, J. (1995): Accelerated oxidation processes in biodiesel. *Trans ASAE.*, 42, 1565–1572.

Caramit, R.P., de Freitas Andrade, A.G., de Souza, J.B.G., et al. (2013). A new voltammetric method for the simultaneous determination of the antioxidants TBHQ and BHA in biodiesel using multi-walled carbon nanotube screen-printed electrodes. *Fuel*, 105: 306-313.

Cavallia, M.C., Zaumanis, M., Mazza, E., et al. (2018) Effect of aging on the mechanical and chemical properties of binder from RAP treated with bio-based rejuvenators, *Composites Part B* 141, 174–181

Cen, H., Morina, A., Neville, A. (2018) Effect of lubricant aging on lubricants' physical and chemical properties and tribological performance; Part I: effect of lubricant chemistry. *Industrial Lubrication and Tribology*, 70 (2). pp. 385-392. ISSN 0036-8792

Chacon, J.N., Gaggini, P., Sinclair, R.S. (2000) Photo- and thermal-oxidation studies on methyl and phenyl linoleate: anti-oxidant behavior and rates of reaction Elsevier *Chem Phys Lipids*, 107 pp. 107-120, 10.1016/S0009-3084(00)00157-2

Cheng, Z., Li, Y. (2007), What is responsible for the initiating chemistry of iron-mediated lipid peroxidation: an update. *Chem Rev* 107:748 66

Christensen, E., and McCormick, R. L. (2014), Long-term storage stability of biodiesel and biodiesel blends. *Fuel Processing Technology* 128, 339–348

Coates, J. P., Setti, L. C., McCaa, B. B. (1984) SAE Paper No. 841373, SP-589, 81.

Conceição, M. M., Candeia, R. A., Silva, F. C., et al. (2007), Thermoanalytical characterization of castor oil biodiesel, *Renewable and Sustainable Energy Reviews*, Elsevier, vol. 11(5), pages 964-975,

Conceição, M.M., Valter, J., Fernandes, V.J. Jr., (2007) Thermal and Oxidative Degradation of Castor Oil Biodiesel, *Energy & Fuels* 2007 21 (3), 1522-1527, DOI: 10.1021/ef0602224

Cowart, J., Hamilton, L., Caton, P., (2008) Performance, Efficiency and Emissions Comparison of Diesel Fuel and a Fischer-Tropsch Synthetic Fuel in a CFR Single Cylinder Diesel Engine”, Document Number: 2008-01-2382, Powertrains, Fuels and Lubricants Meeting, October 2008, Chicago, IL, USA

Dairene Uy, Zdrodowski, R. J., O'Neill, A.E., et al. (2011), Comparison of the Effects of Biodiesel and Mineral Diesel Fuel Dilution on Aged Engine Oil Properties, *Tribology Transactions*, 54:5, 749-763

Daming H., Haining Z., Lin L., (2012) Biodiesel: An Alternative to Conventional Fuel, *Energy Procedia* 16, 1874 – 1885

Dantas, M.B., Albuquerque, A.R., Barros, A.K., et al. (2011), Evaluation of the oxidative stability of corn biodiesel, *Fuel* 90,773–778

Davannendran, C., Hoon, K.N., Harrison, L.N.L. et al. (2016) Deterioration of palm biodiesel fuel under common rail diesel engine operation. *Fuel* 2016. <http://dx.doi.org/10.1016/j.energy.11.136>.

De Souza, J.E., Scherer, M.D., Cáceres, J.A.S., et al. (2013) A close dielectric spectroscopic analysis of diesel/biodiesel blends and potential dielectric approaches for biodiesel content assessment. *Fuel* 105, 705–710.

Devlin, C. C., Passut, C., Campbell, R. (2008), Biodiesel Fuel Effect on Diesel Engine Lubrication, Document Number: 2008-01-2375, Powertrains, Fuels and Lubricants Meeting, October 2008, Chicago, IL, USA

Devlin, C., Passut, C., Campbell, R., et al. (2008), Biodiesel Fuel Effect on Diesel Engine Lubrication," SAE Technical Paper 2008-01-2375, 2008, <https://doi.org/10.4271/2008-01-2375>

Dinkov, R., Hristov, G., Stratiev, D., et al. (2009), Effect of commercially available antioxidants over biodiesel/diesel blends stability, *Fuel* 88, 732–737

Duffield, J., Shapouri, H., Graboski, M., et al. (1998), U.S. Biodiesel Development: New Markets for Conventional and Genetically Modified Agricultural Products. Economic Research Service/USDA;

Dugmore, T. I. J. (2011), The Autoxidation of Biodiesel and its Effects on Engine Lubricants, A thesis submitted for the degree of Doctor of Philosophy, The University of York, Department of Chemistry, September 2011

Dunn, R. O. (1995) Analysis of oxidative stability of methyl soyate by pressurized-differential scanning calorimetry. *Trans ASAE*. 43, 1203–1208.

Dunn, R. O. (2002) Effect of oxidation under accelerated conditions on fuel properties of methyl soyate (biodiesel). *J Am Oil Chem Soc*. 79, 915–920.

Dunn, R. O. (2005) Effect of antioxidants on the oxidative stability of methyl soyate (biodiesel) *Fuel Processing Technology* 86, 1071– 1085

Dunn, R. O. (2008) Antioxidants for improving storage stability of biodiesel, *Biofuels, Bioprod. Bioref.* 2:304–318 DOI: 10.1002/bbb.83

Dunn, R.O. (2005) Oxidative stability of soybean oil fatty acid methyl esters by oil stability index (OSI). *J Amer Oil Chem Soc* 82, 381–387 <https://doi.org/10.1007/s11746-005-1081-6>

Elaine, C. R. M., Dionísio, B., Ivanira, M, et al. (2011), Study of the biodiesel B100 oxidative stability in mixture with antioxidants, *Fuel Processing Technology* 92, 1750–1755

Elias, R. C., Senra, M. Soh, L. (2016) Cold Flow Properties of Fatty Acid Methyl Ester Blends with and without Triacetin, *Energy Fuels*, 30, 9, 7400-7409

Endres, H., Spei, B., Breuer, W., et al. (1991), Patent on Sorption valuable process in the treatment of effluent and sewage using hydrotalcite layer cpd. as sorption agent for removing weakly polar and non-polar organic substances from polar medium DE 4140746 A1

Eskiner, M., (2020) Konzept zur Bestimmung der Kraftstoffqualität für den Betrieb in Plug-in Hybridfahrzeugen. Dissertation; Leuphana Universität Lüneburg

Eskiner, M., Bär, F., Rossner, M., et al. (2015), Determining the aging degree of domestic heating oil blended with biodiesel by means of dielectric spectroscopy, *Fuel* 143, 327–333

EU (2012) Regulation CO₂ emissions from new passenger cars as of 2020 cep Policy Brief No.2012-46 of 12 November 2012 <http://www.cep.eu/en/analyses-of-eu-policy/climate-protection/low-carbon-economy> (assessed 13/2/17)

Fang, H.L., Alleman, T. L., McCormick, R. L. (2006), “Quantification of Biodiesel Content in Fuels and Lubricants by FTIR and NMR Spectroscopy,” Document Number 2006-01-3301

Fang, H, McCormick, R.L. (2006) Spectroscopic study of biodiesel degradation pathways. SAE Technical Paper No. 2006–01-3300

Fang, H.L., Shawn, D.W., Yamaguchi, S., et al. (2007), Biodiesel Impact on Wear Protection of Engine Oils”, *Powertrain & Fluid Systems Conf.*, Chicago, IL, Oct. 2007, 2007-01-4141.

Farajzadeh, M. A., EbrahimMortaza, I., Ranji, A., et al. (2006), HPLC and GC Methods for Determination of Lubricants and Their Evaluation in Analysis of Real Samples of Polyethylene; *Microchim Acta* 153, 73–78 DOI 10.1007/s00604-005-0429-1

Fattah, I.M., Rizwanul, M. H.H. I, Kalam, M.A., et al. (2014), Effect of antioxidants on oxidation stability of biodiesel derived from vegetable and animal-based feedstocks, *Renewable and Sustainable Energy Reviews* 30, 356–370

Fereidoon, S., Ying, Z. (2015) Measurement of antioxidant activity, *Journal of functional foods* 18, 757–781

Fetterman, P. (2007), Biodiesel Effects on Crankcase Lubricants, International Lubricants and Waxes Meeting

Flitsch, S., Neu P. M., Schober, S. et al. (2014), Quantitation of Aging Products Formed in Biodiesel during the Rancimat Accelerated Oxidation Test; *Energy & Fuels*, 28, 5849–5856;

Frankel, E.N. (1985). Chemistry of autoxidation: mechanism, products and flavor significance. In: Min DB, Smouse T, editors. Flavor chemistry of fats and oils. Champaign, Ill.: American oil Chemists' Society. Pg 1–37;

Frankel, E.N. (2005), Lipid oxidation. Bridgwater, England: The Oily Press LTD. P. 486

Frauscher, M., Besser, C., Allmaier, G., et al. (2017) Oxidation Products of Ester-Based Oils with and without Antioxidants Identified by Stable Isotope Labelling and Mass Spectrometry. *Appl. Sci.* 7, 396; doi:10.3390/app7040396

Freja from Østerstrøm, Anderson, J. E., Mueller, S. A., et al. (2016), Oxidation Stability of Rapeseed Biodiesel/Petroleum Diesel Blends, *Energy Fuels*, 30, 1, 344-351

Fujita, E. M., Campbell, D. E. and Zielinska, B. (2006), FINAL TECHNICAL REPORT Chemical Analysis of Lubrication Oil Samples from a Study to Characterize Exhaust Emissions from Light-Duty Gasoline Vehicles in the Kansas City Metropolitan Area NREL Subcontract Number ACI-5-55528-01 and CRC E-69A December 21, 2006;

Fulmer, G. R., Miller, A. J. M., Sherden, N. H., et al. (2010), NMR Chemical Shifts of Trace Impurities: Common Laboratory Solvents, Organics, and Gases in Deuterated Solvents Relevant to the Organometallic Chemist, *Organometallics*, 29, 2176–2179 DOI: 10.1021/om100106e

Gaurav D., Sharma, M.P. (2014), Impact of Antioxidant and Metals on Biodiesel Stability- A Review, *J. Mater. Environ. Sci.* 5 (5) 1412-1425

Germany 2020 Energy Policy Review

Geyer, S. M., Jacobus, M. J., Lestz, S. S., (2013), Comparison of Diesel Engine Performance and Emissions from Neat and Transesterified Vegetable Oils, *Transactions of the ASAE* Vol. 27 (2): 0375-0381 (Doi: 10.13031/2013.32795),

Ghosh, S., Dutta, D., (2012) A Comparative Study of the Performance & Emission Characteristics of a Diesel Engine Operated on Soybean Oil Methyl Ester (SOME), Pongamia Pinata Methyl Ester (PME) and Diesel, International Refereed Journal of Engineering and Science (IRJES) 2319-1821 Vol 1 (4), PP.22-27

Gili, F., Igartua, A., Luther, R. et al. (2011), The impact of biofuels on engine oil performance, Lubrication Science; 23: 313–330 DOI: 10.1002/lis.158

Goodrum, J.W. (2002) Volatility and boiling points of biodiesel from vegetable oils and tallow, Biomass and Bioenergy 22, 205 – 211

Graboski, M.S., and McCormic, R.L. (1998), Combustion of Fat and Vegetable Oil Derived Fuels in Diesel Engines. Prog. Energy Combust. Sci. Vol 24, pp 125-164

Guan, L., Feng, X.L., Xiong G., et al. (2011) Application of dielectric spectroscopy for engine lubricating oil degradation monitoring. Sensors and Actuators A 168, 22–29

Guillen, M.D. and Ruiz, A. (2005) Study by proton nuclear magnetic resonance of the thermal oxidation of oils rich in oleic acyl groups. J. Am. Oil Chem. Soc., 82: 349-355.

Gulzar, M., Masjuki, H.H., Varman, M., et al. (2016) “Effects of biodiesel blends on lubricating oil degradation and piston assembly energy losses,” Energy 111, 713e721

Gunstone, F.D., Harwood, J.L., and Dijkstra, A.J. (2010), The Lipid Handbook with CD-ROM. CRC Press

Gurumurthy, B. R., Dinesh B., Ramesh, K.P. (2017), Structural Analysis of Merino Wool, Pashmina and Angora Fibers Using Analytical Instruments Like Scanning Electron Microscope and Infra-Red Spectroscopy, 4 (8) ISSN 2394 – 3386

Hamberg, M., Gotthammer, B. A New Reaction of Unsaturated Fatty Acid

He, X., Williams, A., Christensen, E. et al. (2011) Biodiesel Impact on Engine Lubricant Dilution During Active Regeneration of Aftertreatment Systems, SAE International, doi:10.4271/2011-01-2396

Hilligoss, D., (2012) Analysis of Wear Metals and Additive Package Elements in New and Used Oil Using the Optima 8300 ICP-OES with Flat Plate Plasma Technology, PerkinElmer, Inc. Shelton, CT USA;

<http://www.biodieselmagazine.com/articles/1443/improving-biodiesel-stability-with-fuel-additives>

<https://blog.amsoil.com/what-is-fuel-dilution-and-why-is-it-bad>

https://dieselnet.com/tech/fuel_biodiesel_std.php5-05-2020

<https://en.oelcheck.com/wiki/Viscosity> (accessed on 04/07/2019)

<https://www.agqm-biodiesel.de/application/files/2515/4840/9678/Analytics.pdf>

<https://www.astm.org/Standards/D2270.htm>

https://www.bmwi.de/Redaktion/DE/Downloads/G/germany-2020-energy-policy-review.pdf?__blob=publicationFile&v=4

<https://www.fuels-jrg.de/deutsch/verrichtungenen/2014-band-04-10/>

https://www.iea-amf.org/content/fuel_information/fatty_acid_esters/properties

https://www.isi.fraunhofer.de/content/dam/isi/dokumente/ccx/2019/The_State_of_RES_in_Europe-2018-GB.pdf

<https://www.lubricants.total.com/news-press-releases/fuel-dilution-engine-oil-causes-and-effects>

<https://www.machinerylubrication.com/magazine/issue/practicing%20oil%20analysis/5/2007>

https://www.syntheticoils.us/Files/News/2009/2009_sept_fuel_dilution_diesels.pdf

https://www.ufop.de/files/7515/7797/1943/WEB_UFOP_Global_Supply_Report_A5_EN_19_20.pdf, assessed on 8/5/2020

Hu, T., Teng, H., Luo, X., et al. (2015), Impact of Fuel Injection on Dilution of Engine Crankcase Oil for Turbocharged Gasoline Direct-Injection Engines, SAE Int. J. Engines 8(3):1107-1116, <https://doi.org/10.4271/2015-01-0967>.

Hussein, I. K., Mohammed, J. M. H., and Omer, A. H. (2012), Separation & Identification of Organic Compounds in Lubricating Oil Additives Using TLC & GC-MS; Journal of Al-Nahrain University Vol.15 (3), pp.62-68

Infineum Insight, Higher Tolerance, June 2007, p.1

Jain, S., and Sharma, M. P. (2011) Thermal stability of biodiesel and its blends: a review. *Renew. Sust. Energy Rev.* 15, 438–448. DOI: 10.1016/j.rser.2010.08.022

Jain, S., and Sharma, M. P., (2012) Correlation development between the oxidation and thermal stability of biodiesel, *Fuel*, 102, Pages 354-358

Jamieson, G. S, *Vegetable Fats and Oils*, Reinhold Publishing Corporation, New York 1943.

Jankowski, A. and Baczewski, K. (2010), Aging Processes of Biodiesel and Biodiesel/Diesel Fuel Blends, *Journal of KONES Powertrain and Transport*, Vol. 17, No. 2

Jiang, Y., Zhang, Y. (2016), Supply chain optimization of biodiesel produced from waste cooking oil, *The 9th International Conference on City Logistics, Tenerife, Canary Islands (Spain)*, 17-19 June 2015, *Transportation Research Procedia* 12, 938 – 949, 2352-1465

Jiayu, X., Imahara, H., Saka, S. (2009), Kinetics on the oxidation of biodiesel stabilized with antioxidant. *Fuel*;88(2):282–6.

Kamal-Eldin, A., Min, D.B. (2010), *Lipid oxidation pathways*. Vol. 2. Champaign, Ill.: AOCS Publishing. Pg 324

Kans, O. (2011) <https://www.mcchemical.com/?id=57:crankcase-oil-dilution-additive-solution>) (Assessed on 08-11-2019)]

Kapilan, N., Reddy, R.P. (2008) Evaluation of methyl esters of mahua oil (*Madhuca Indica*) as Diesel Fuel. *J American Oil Chemists' Society*, 85(2), 185-188.

Karavalakis, G., Hilari, D., Givalou, L., et al. (2011) Storage stability and aging effect of biodiesel blends treated with different Antioxidants, *Energy* 36. 369-374

Karavalakis, G., Stournas, S., Dimitrios, K. (2010) Evaluation of the oxidation stability of diesel/biodiesel blends, *Fuel* 89, 2483–2489

Kenreck, G. (2007) <http://www.biodieselmagazine.com/articles/1443/improving-biodiesel-stability-with-fuel-additives>

Kerkering, S. and Andersson, J. T. (2015), Chemical Changes in Fossil and Biogenic Heating Oils on Long-Term Storage, *Energy Fuels*, 29, 849–857, DOI: 10.1021/ef502344d

Khalid, A., Tamaldin, N., Jaat, M., et al. (2013) Impacts of Biodiesel Storage Duration on Fuel Properties and Emissions, *Procedia Engineering* 68, 225 – 230

Khuong, L. S., Zulkifli, N. W. M., Masjuki, H. H., et al. (2016), A review on the effect of bioethanol dilution on the properties and performance of automotive lubricants in gasoline engines; *RSC Adv.*, 6, 66847

Kim, J.K., Jeon, C.H., Lee, H.W., et al. (2018), Effect of Accelerated High Temperature on Oxidation and Polymerization of Biodiesel from Vegetable Oils, *Energies*, 11, 3514; Doi:10.3390/en11123514

Kittirattanapiboon, K. and Krisnangkura, K., (2008) Separation of acylglycerols, FAME and FFA in biodiesel by size exclusion chromatography, *European Journal Of Lipid Science and Technology*, 110, 5, Pages 422-427

Kivevele, T. T., Mbarawa, M. M., Bereczky, A., et al. (2011). Impact of antioxidant additives on the oxidation stability of biodiesel produced from Croton Megalocarpus oil. *J.Fuel Process. Technol.* 92, 1244–1248. DOI: 10.1016/j.fuproc.2011.02.009

Kivevele, T., Zhongjie, H. (2015), Review of the stability of biodiesel produced from less common vegetable oils of African origin. *S Afr. J Sci.* 111(9/10), Art. #2014-0434, 7 <http://dx.doi.org/10.17159/sajs.2015/20140434>

Knorr, M., Singer, A., and Krahl, J. (2016) Base Oil Aging with Contemporary Biofuels DOI: 10.1007/s40111-015-0513-4)

Knothe, G. (2001) Determining the blend level of mixtures of biodiesel with conventional diesel fuel by fiber-optic near-infrared spectroscopy and ¹H nuclear magnetic resonance spectroscopy. *J Amer Oil Chem Soc* 78, 1025–1028. <https://doi.org/10.1007/s11746-001-0382-0>

Knothe, G. (2006), Analysis of oxidized biodiesel by 1H-NMR and effect of contact area with air, *Eur. J. Lipid Sci. Technol.* 108,493–500 DOI 10.1002/ejlt.200500345

Knothe, G. (2007), Review: Some aspects of biodiesel oxidative stability, *Fuel Processing Technology* 88, 669–677

Knothe, G. and Dunn, R. O. (2003) Dependence of Oil Stability Index of Fatty Compounds on Their Structure and Concentration and Presence of Metals, Paper no. J10500 in *JAOCS* 80, 1021–1026

Knothe, G., & Razon, L. F. (2017), Biodiesel fuels. *Progress in Energy and Combustion Science*, 58, 36-59. Doi: 10.1016/j.pecs.2016.08.001

Koch, M. (2009), Entwicklung einer Methode zur Motorölalterungsuntersuchungen bei Diesel-PKW; Dissertation; Leuphana Universität Lüneburg

Köstner, T., Staufenbiel, J., Scheler, M., et al. (2019) Fuel Sensor for Detection of Fuel Condition. Projektbericht 1204, Coburg.

Krahl, J., Zimon, A., Schröder, O., et al. (2012) Diesel regenerativ, *Fuels Joint Research Group Band 2*, Cuvillier Verlag Göttingen, ISBN 978-3-95404-174-9 Herausgeber: Jürgen Krahl, Axel Munack, Peter Eilts, Jürgen Büniger, pg 15 (2012).

Kumar, B.R., Saravanan, S., (2016) “Use of higher alcohol biofuels in diesel engines: A review,” *Renewable and Sustainable Energy Reviews* 60, 84–115

Kumar, N. (2017), Oxidative stability of biodiesel: Causes, effects, and prevention *Fuel* 190, 328–350

Lacoste, F., Lagardere, L., (2003) Quality parameters evolution during biodiesel oxidation using Rancimat test, *Eur. J. Lipid Sci. Technol.* 105, 149–155

Laguerre, M., Lecomte, J., and Villeneuve, P. (2007), Evaluation of the ability of antioxidants to counteract lipid oxidation: existing methods, new trends and challenges. *Prog Lipid Res* 46:244–82;

Larsson, M. A.C., (2007), Combustion of Fischer-Tropsch, RME and Conventional Fuels in a Heavy-Duty Diesel Engine”, Document Number: 2007-01-4009, Powertrain & Fluid Systems Conference and Exhibition, October 2007, Chicago, IL, USA

Le Seigneur, V. J. (2018), *The State of Renewable Energies in Europe*, 18th Edition Euroobserver Report

Leung, D.Y.C., Koo, B.C.P. & Guo, Y. (2006) Degradation of biodiesel under different storage conditions. *Bioresource Technology*, Vol. 97, pp. 250–256, ISSN 0960-8524

Liang, Y. C., May, C. Y., Foon, C. S., et al. (2006), The effect of natural and synthetic antioxidants on the oxidative stability of palm diesel, *Fuel* 85, 867–870

Lin, C.Y., Chiu, C.-C. (2010) Burning characteristics of palm-oil biodiesel under long-term storage conditions, *Energy Conversion and Management*, 51, 7, Pages 1464-1467

Ljubas, D., Krpan, H., Matanoviæ, I., (2010) Influence of engine oils dilution by fuels on their viscosity, flash point, and fire point; *NAFTA* 61 (2) 73-79

Macian, M. V., Tormos, B., Gomez, E., et al. (2012). Proposal of an FTIR Methodology to Monitor Oxidation Level in Used Engine Oils: Effects of Thermal Degradation and Fuel Dilution. *Tribology Transactions*. 55:872-882. doi:10.1080/10402004.2012.721921.

Mannekote, J. K., Kailas, S.V. (2012), The Effect of Oxidation on the Tribological Performance of Few Vegetable Oils. *Journal of Materials Research and Technology* 1(2):91-95

Mantovani, A.C.G., Chendynski, L.T., Galvan, D., et al. (2020) Evaluation of the Oxidation Degradation Process of Biodiesel via ¹H NMR Spectroscopy, *J. Braz. Chem. Soc.*, Vol. 00, No. 00, 1-7,

Manual 873 Biodiesel Rancimat 2009

Markova, L. V., Myshkin, N.K., Ossia, C.V., et al. (2007) Fluorescence Sensor for Characterization of Hydraulic Oil Degradation, *Tribology in industry*, Volume 29, No. 1&2.

Marsh, S., Corradi, M. (2007), The Effect of Biodiesel on Engine Lubricants; *Lubes and Greases*, June 2007, p.1

McCormick and Westbrook (2007) Empirical Study of the Stability of Biodiesel and Biodiesel Blends. Milestone Report. NREL/TP-540-41619 May 2007

McCormick, R. L., and Westbrook, S. R. (2010). Storage Stability of Biodiesel and Biodiesel Blends. *Energy & Fuels*, 24, 690–698: DOI:10.1021/ef900878u

McCormick, R.L., Ratcliff, M., Moens, L., et al. (2007) Several factors affecting the stability of biodiesel in standard accelerated tests, *Fuel Processing Technology*, 88, 7, Pages 651-657

McTavish, S., (2008) Biodiesel Effects on Crankcase Lubricant Performance”, 7th International ATA Conference on Engines, October 2008

Meher, L. C., Sagar. D. V. and Naik, S. N. (2006) 2004 Technical aspects of biodiesel production by transesterification-a review *Renewable and Sustainable Energy Reviews*, Volume 10, Issue 3, June, Pages 248-268

Mendiara, S. N., Coronel, M. E. J. (2006), Evidence for the Development of Persistent Carbon-Centered Radicals from a Benzyl Phenolic Antioxidant: an Electron Paramagnetic Resonance Study. *Appl. Magn. Reson.* 30, 103-120

Mittelbach, M. and Gangl, S., (2001), Long Storage Stability of Biodiesel Made from Rapeseed and Used Frying Oil, *JAOCS*, Vol. 78, no. 6

Mittelbach, M., Schober, S., (2003) The Influence of Antioxidants on the Oxidation Stability of Biodiesel, *J Am Oil Chem Soc* 80, 8, Pages 817-823, <https://doi.org/10.1007/s11746-003-0778-x>

Mohamad, Y. A., Zulkurnain, S., Munzilah, M. R., et al. (2014) Effects of Aging on the Physical and Rheological Properties of Asphalt Binder Incorporating Rediset *Jurnal Teknologi (Sciences & Engineering)* 70:7, 111–116

Molina, G. J. M., Soloiu, V., Mosfequr, R., et al. (2014), Wear Effects of Mineral Oil Lubricant Dilution with Biofuels. 2014 STLE Annual Meeting & Exhibition. May 18-22, 2014 Disney's Contemporary Resort Lake Buena Vista, Florida, USA

Monyem, A., Canakci, M., Van Gerpen, J.H. (2000) Investigation of biodiesel thermal stability under simulated in-use conditions. *Appl Eng Agric*; 16:373.

Monyem, A., (1998), The effect of biodiesel oxidation on engine performance and emissions. *Retrospective Theses and Dissertations.* 11950. <https://lib.dr.iastate.edu/rtd/11950>

Monyem, A., Van Gerpen, J.H. (2001). The effect of biodiesel oxidation on engine performance and emissions. *Biomass Bioenergy* 20, 317–325. [http://dx.doi.org/10.1016/S0961-9534\(00\)00095-7](http://dx.doi.org/10.1016/S0961-9534(00)00095-7).

Moraes, R. and Bahia, H. U. (2015): Effect of mineral filler on changes in the molecular size distribution of asphalts during oxidative aging, *Road Materials and Pavement Design*, DOI: 10.1080/14680629.2015.1076998

Morita, M., Tokita, M. (2006), The real radical generator other than the main product hydroperoxide in lipid autoxidation. *Lipids*; 41:91.

Moritani, H., Nozawa, Y. (2004), Oil Degradation in Second-Land Region of Gasoline Engine Pistons. *R&D Review of Toyota CRDL*, 38(3), 36-43

Mortier, R. M., Fox, M. F. and Orszulik, S. T. (Editors) (2010) *Chemistry and Technology of Lubricants*, Third Edition. Springer Dordrecht Heidelberg London New York, ISBN 978-1-4020-8661-8 e-ISBN 978-1-4020-8662-5. DOI 10.1023/b105569;

Moser, B.R., (2012). Efficacy of gossypol as an antioxidant additive in biodiesel. *J. Renew. Energ.*, 40(1): 65-70.

Moser, D, Eckerstorfer, M., Pascher, K., et al. (2013) Potential of genetically modified oilseed rape for biofuels in Austria: Land use patterns and coexistence constraints could decrease domestic feedstock production. *Biomass Bioenergy*; 50:35–44.

Mozammil Hasnain, S.M. and Sharma, R.P. (2019) Evaluation of the performance and emission and spectroscopic analysis of an improved soy methyl ester, *RSC Adv.*, 9, 26880

Munari, F., Cavagnino, D., Cadoppi, A., Determination of Total FAME and Linolenic Acid Methyl Ester in Pure Biodiesel (B100) by GC in Compliance with EN 14103, Thermo Fisher Scientific, Milan, Italy
https://www.analiticaweb.com.br/newsletter/01/biodiesel_an10212.pdf

Muniyappa, P. R., Brammer, S. C., and Nouredini, H., (1996), Improved conversion of plant oils and animal fats into biodiesel and co-product, *Papers in Biomaterials*. 20.

Naidu, S. K., Klaus, E. E., Duda, J. L. (1984). Evaluation of Liquid Phase Oxidation Products of Ester and Mineral Oil Lubricants Industrial & Engineering Chemistry Product Research and Development 1984 23 (4), 613-619

Negrea A., Mihailescu M., Mosoarca G., et al. (2020) Estimation on Fixed-Bed Column Parameters of Breakthrough Behaviors for Gold Recovery by Adsorption onto Modified/Functionalized Amberlite XAD7, Int. J. Environ. Res. Public Health 2020, 17, 6868; doi:10.3390/ijerph17186868

Niculescu, R., Nastase, M., Clenci, A., et al. (2019), Issues Concerning the Determination of the Correspondence Between Low Pressure Distillation and Gas Chromatography Analysis of Biodiesel. Preliminary Results. In: Burnete N., Varga B. (eds) Proceedings of the 4th International Congress of Automotive and Transport Engineering (AMMA 2018). AMMA2018. Proceedings in Automotive Engineering. Springer, Cham

Nogales-Delgado, S., Encinar, J.M. and González, J.F. (2019) Safflower Biodiesel: Improvement of its Oxidative Stability by Using BHA and TBHQ, Energies 12, 1940; doi:10.3390/en12101940

NREAP, (2019) (<https://www.epure.org/media/1758/180903-def-rep-overview-of-biofuel-policies-and-markets-across-the-eu-28.pdf>)

Obadiah, A., Kannan, R., Ramasubbu, A., et al. (2012), Studies on the effect of antioxidants on the long-term storage and oxidation stability of Pongamia pinnata (L.) Pierre biodiesel, Fuel Processing Technology 99, 56–63

Obiols, J., (2003) Lubricant Oxidation Monitoring Using FTIR Analysis - Application to the Development of a Laboratory Bulk Oxidation Test and to In-Service Oil Evaluation, SAE Technical Paper 2003-01-1996, <https://doi.org/10.4271/2003-01-1996>.

Ogawa, T., Kajiya, S., Kosaka, S., et al. (2009). Analysis of Oxidative Deterioration of Biodiesel Fuel. SAE International Journal of Fuels and Lubricants, 1(1), 1571-1583. Retrieved May 7, 2020, from www.jstor.org/stable/26272118

Osawa, W.O., Sahoo, P.K., Onyari, J.M. *et al.* (2016) Effects of antioxidants on oxidation and storage stability of Croton megalocarpus biodiesel. Int J Energy Environ Eng 7, 85–91 <https://doi.org/10.1007/s40095-015-0191-z>

Pattamaprom, W. P., and Ngamjaroen, S. (2012), Storage Degradation of Palm-Derived Biodiesels: Its Effects on Chemical Properties and Engine Performance, *Renewable Energy*, vol. 37, no. 1, pp. 412–418,

Pereira, G.G., Morales, A., Marmesat, S., et al. (2015). Effect of temperature on the oxidation of soybean biodiesel. *Grasas Aceites* 66 (2): e072. DOI: <http://dx.doi.org/10.3989/gya.083514>

Pereira, GG, Marmesat, S, Barrera-Arellano, D., et al. (2013), Evolution of oxidation in soybean oil and its biodiesel under the conditions of the oxidation stability test. *Grasas Aceites* 64, 482–488. <http://dx.doi.org/10.3989/gya.036913>.

Pérez, A.T., and Hadfield, M. (2011) Low-Cost Oil Quality Sensor Based on Changes in Complex Permittivity. *Sensors*, 11, 10675–10690.

Perez, J. M. (2000), Oxidative properties of lubricants using thermal analysis, *Thermochimica Acta* 357-358, 47-56

Perkinelmer (2011) Human Health and Environment, lubricants analysis, complete solutions for your lab. www.perkinelmer.com/lubricants

Pinzi, S., Garcia, I. L., Lopez-Gimenez, F. J., et al. (2009), The Ideal Vegetable Oil-based Biodiesel Composition: A Review of Social, Economical and Technical Implications, *Energy Fuels*, 235, 2325-2341,

Pischinger, G.H., Siekmann, R.W., Falcon, A.M., et al. (1982), Methyl esters of plant oils as diesel fuels, either straight or in blends. United States: N.

Prajapati, K. V P., Nandlal, M. (2015), A Review of Palm Oil Biodiesel under Long-Term Storage Conditions, *International Journal on Recent and Innovation Trends in Computing and Communication (IJRITCC)*, (3)(1), ISSN: 2321-8169, PP: 313 - 317,

PubChem Database. National Center for Biotechnology Information. CID=74370, <https://pubchem.ncbi.nlm.nih.gov/compound/Antioxidant-330> (accessed on May 27, 2020)

Pullen, J., Saeed, K., (2012) An overview of biodiesel oxidation stability, *Renewable and Sustainable Energy Reviews* 16, 5924–5950

Raposo H., Farinha J. T., Fonseca I. et al. (2019) Condition Monitoring with Prediction Based on Diesel Engine Oil Analysis: A Case Study for Urban Buses, *Actuators*, 8, 14; doi:10.3390/act8010014

Rasberger, M. (1992) Oxidative degradation and stabilization of mineral oil-based lubricants. In: Mortier, R.M., Orszulik, S.T. (eds) *Chemistry and Technology of Lubricants*. Springer, Boston, MA

Refaat, A.A. (2009) Correlation between the chemical structure of biodiesel and its physical properties. *Int. J. Environ. Sci. Tech.*, 6 (4), 677-694

Rhet de Guzman, Haiying, T., Salley, S. et al. (2009), Synergistic Effects of Antioxidants on the Oxidative Stability of Soybean Oil- and Poultry Fat-Based Biodiesel *Am Oil Chem Soc.* 86:459–467

Rodriguez-Fernández, J., Lapuerta, M., Sánchez-Valdepeñas, J. (2016), Regeneration of diesel particulate filters: effect of renewable fuels, *Renewable Energy* doi: 10.1016/j.renene.2016.11.059

Ross, J.R. Gebhart, A.I., Gerecht, J.F. (1949) The Autoxidation of Methyl Oleate, *J. Am. Chem. Soc.*, 71, 282-286.

Sadeghinezhad, E., Kazi, S.N., Badarudin, A., et al. (2013), A comprehensive review of biodiesel as alternative fuel for compression ignition engines, *Renewable and Sustainable Energy Reviews* 28, 410–424

Saifuddin, N., and Refal, H., (2014) Spectroscopic Analysis of Structural Transformation in Biodiesel Degradation. *Research Journal of Applied Sciences, Engineering and Technology* 8(9): 1149-1159, DOI:10.19026/rjaset.8.1079

Saltas, E., Bouilly, J., Geivanidis, S. (2017) Investigation of the effects of biodiesel aging on the degradation of standard rail fuel injection systems *Fuel* Volume 200, 15 July 2017, Pages 357-370

Sappok, A. G. and Wong, V. W., (2007) Impact of Biodiesel on Ash Emissions and Lubricant Properties Affecting Fuel Economy and Engine Wear”, *Diesel Engine Efficiency and Emissions Research Conference*, Detroit, 2007

Sappok, A. G. and Wong, V.W. (2008), Impact of Biodiesel on Ash Emissions and Lubricant Properties Affecting Fuel Economy and Engine Wear: Comparison with Conventional Diesel Fuel, SAE 2008-01-1395.

Schaich, K. (2005), Lipid oxidation: Theoretical aspects. In: Shahidi F, editor. Bailey's industrial oil and fat products. 6th Ed. New York: John Wiley & Sons.

Schaich, KM, Shahidi, F, Zhong, Y, et al. (2013), Lipid oxidation. In: Eskin NAM, Shahidi F, editors. Biochemistry of foods. 3rd ed. London: Academic Press. p 419–78

Schmidt, L., Krahl, J., Schröder, O., et al. (2014) Interactions among fuel molecules from diesel fuel and biodiesel, International Conference „Tailor-Made Fuels from Biomass, “2013, Aachen, Germany

Schneider, C., Porter, N.A., Brash, A.R. (2008), Routes to 4-hydroxynonenal: fundamental issues in the mechanisms of lipid peroxidation. J Biol Chem; 283:15539.

Schneider, M. A., Aachen (DE); Yacoub, Yasser M. S., Koeln (DE), Waalre, M. B. (NL) (2013) Patent Application Publication Pub. No.: US 0013177 A1 A Z

Schober, S., & Mittelbach, M. (2004). The Impact of Antioxidants on Biodiesel Oxidation Stability. European Journal of Lipid Science and Technology. 106. 382 - 389. 10.1002/ejlt.200400954.

Schroder, O., Bünger, J., Munack, A., et al. (2017) Regenerative fuel concepts for plug-in hybrid vehicles/Regenerative kraftstoffkonzepte für Plug-In-Hybrid-Fahrzeuge. Landbauforschung, vol. 67, no. 1, p. 17+. Gale Academic OneFile, (Accessed 7 May 2020)

Schumacher, S. (2013), Untersuchungen zum Einfluss verschiedener Diesel- und Biodieselskomponenten auf den Mechanismus der Ölschlamm-Bildung im Motorenöl; Dissertation; Otto-von-Guericke-Universität Magdeburg

Sejkorová, M., Glos, J. (2017) Analysis of Degradation of Motor Oils Used in Zetor Tractors: Acta Universitatis Agriculturae Et Silviculturae Mendelianae Brunensis: Volume 65: Number 1, <https://doi.org/10.11118/actaun201765010179>

Sem, T. R. (2004) Effect of Various Lubricating Oils on Piston Deposits in Biodiesel Fueled Engines, SAE 2004-01-0098.

Serrano, M., Oliveros, R., Sánchez, M., et al. (2014), Influence of blending vegetable oil methyl esters on biodiesel fuel properties: Oxidative stability and cold flow properties. *Energy* 65, 109–115.

Shahabuddin, M., Kalam, M. A., Masjuki, H. H., et al. (2012), An Experimental Investigation into Biodiesel stability by Means of Oxidation and Property Determination, *Energy*, vol. 44, no. 1, pp. 616–622

Shanta, S. M. (2011) Investigations of the Tribological Effects of Engine Oil Dilution by Vegetable and Animal Fat Feedstock Biodiesel on Selected Surfaces Electronic Theses & Dissertations. 776. <http://digitalcommons.georgiasouthern.edu/etd/776>

Shanta, S. M., Molina, G. J., and Soloiu, V. (2011), Tribological Effects of Mineral-Oil Lubricant Contamination with Biofuels: A Pin-on-Disk Tribometry and Wear Study; *Advances in Tribology Volume 2011*, Article ID 820795, p 7 <http://dx.doi.org/10.1155/2011/820795>

Sharma, B. K., Suarez, P. AZ, Perez, J. M., et al. (2009) Oxidation and low-temperature properties of biofuels obtained from pyrolysis and alcoholysis of soybean oil and their blends with petroleum diesel. *Fuel Processing Technology*

Sharma, Y.C and Singh, B. (2009), Development of biodiesel: Current scenario, *Renewable and Sustainable Energy Reviews* (13), 6–7, Pages 1646-1651

Sharp, C.A., Howell, S.A., Jobe, J. (2000), The Effect of Biodiesel Fuels on Transient Emissions from Modern Diesel Engines, Part I Regulated Emissions and Performance,” *Society of Automotive Engineers Paper No. 2000-01-1967*, SAE, Warrendale, Penn.

Siddharth, J. and Sharma, M.P. (2010) Stability of biodiesel and its blends: A review, *Renewable and Sustainable Energy Reviews* 14, 667–678;

Sierra-Cantor, J.F. and Guerrero-Fajardob, C. A. (2017), Methods for improving the cold flow properties of biodiesel with high saturated fatty acids content: A review, *Renewable and Sustainable Energy Reviews* 72, 774–790;

Silitonga, A.S, Masjuki, H.H., Mahlia, T.M.I., et al. (2013) Overview properties of biodiesel diesel blends from the edible and non-edible feedstock. *Renew Sustain Energy Rev*; 22:346–60

Singer, A., Ruck, W., Krahl, J. (2014) Influence of Different Biogenic Fuels on Base Oil Aging, SAE-Technical Paper 2014-01-2788, 7 S.,

Singh, M., Singh, D., Gandhi, S., et al. (2019), Effect of Metal Contaminants and Antioxidants on the Oxidation Stability of *Argemone mexicana* Biodiesel: Experimental and Statistical Study. *Waste Biomass Valor.* <https://doi.org/10.1007/s12649-019-00886-5>

Soleimania, M., Sophocleous, M., Wang, L., et al. (2014) Base oil oxidation detection using novel chemical sensors and impedance spectroscopy measurements. *Sensors and Actuators B* 199, 247–258

Song B.H., Choi Y.H. (2008) Investigation of variations of lubricating oil diluted by post-injected fuel for the regeneration of CDPF and its effects on engine wear, *J. Mech. Sci. Technol.* 22, 2526–2533. Doi:10.1007/s12206-008-0903-x;

Speight, J. G., *Handbook of Petroleum Product Analysis*, A John Wiley & Sons, Inc., Publication. 2002, John Wiley & Sons, Inc., Hoboken, New Jersey. ISBN: 0-471-20346-7

Starck, L., Fortunato, A. M., Takuyu, T., et al. (2015), Oxidation stability of Diesel/Biodiesel Blends: Impact of Fuels Physio-Chemical Properties Over Ageing Duration Storage and Accelerated Oxidation. SAE 2015-01-1930

STM D 5554: Standard Test Method for Determination of the Iodine Value of Fats and Oils; ASTM International: West Conshohocken, PA, USA, 2006.

Thornton, M. J., Alleman, T. L., Luecke, J., et al. (2009), Impacts of Biodiesel Fuel Blends Oil Dilution on Light-Duty Diesel Engine Operation, presented at the 2009 SAE International Powertrains, Fuels, and Lubricants Meeting, Florence, Italy, June 15–17, Fang HL, Whitacre SD, SAE Technical Paper. 2009.

Tič, V. and Lovrec, D., (2011) Detecting and Analysing Condition of Hydraulic Oils with on-line Sensors. UDC 676.085, Series: Mechanical Engineering Vol. 9, No 1, pp. 71 – 78

Tischinger-Wagner, H., Endres, W., Rupprecht, H., et al. (1987) Oxidative degradation of linoleic acid methyl ester in suspensions of inorganic excipients. *Pharmazie*. 42(5):320-324.

Tschöke, H, Braungarten, G, Patze, U. (2009) Oil dilution of a Passenger Diesel Engine in Operation with blended Diesel Fuel B10; Final Report Abstract, 22010007(07NR100) IMS-Otto-Von Guericke University Magdeburg, June 4,

Van Gerpen, J., He, B.B., Duff, K., (2011) Measurement and Control Strategies for Sterol Glucosides to Improve Biodiesel Quality – Year 2 Final Report Klk759 N11-01, National Institute for Advanced Transportation Technology University of Idaho

Van Lierop B., Castle, L., Feigenbaum, A., et al. (1998), 1,3,5-Trimethyl-2,4,6-tris(3,5-di-tert-butyl-4-hydroxybenzyl) benzene. In: *Spectra for the Identification of Additives in Food Packaging*. Springer, Dordrecht

Varatharajan, K., Pushparani, D. S. (2017) Screening of antioxidant additives for biodiesel fuels. *Renewable and Sustainable Energy Reviews*.

Wakiru, J M, Pintelon, L, Karanović, V .V., et al. (2018) Analysis of lubrication oil towards maintenance grouping for multiple equipment using fuzzy cluster analysis, *IOP Conf. Series: Materials Science and Engineering* 393, 012011 doi:10.1088/1757-899X/393/1/012011

Wakiru, J., Pintelon, L., Chemweno, P., et al. (2017), Analysis of lubrication oil contamination by fuel dilution with application of cluster analysis, XVII International Scientific Conference on Industrial Systems (IS'17) Novi Sad, Serbia, October 4. – 6.

Wang, H., Tang, H., Wilson, J., et al. (2008) Total Acid Number Determination of Biodiesel and Biodiesel Blends, *J Am Oil Chem Soc* 85:1083–1086

Wang, S.S., (2001) Road tests of oil condition sensor and sensing technique, *Sensors and Actuators B* 73, 106-111

Wang, Y., Zhao, M., Tang, S. et al. (2010) Evaluation of the Oxidative Stability of Diacylglycerol-Enriched Soybean Oil and Palm Olein Under Rancimat-Accelerated

Oxidation Conditions. *J Am Oil Chem Soc* 87, 483–491. <https://doi.org/10.1007/s11746-009-1521-1>

Watson, S. A.G. and Wong, V. W. (2008), The Effects of Fuel Dilution with Biodiesel on Lubricant Acidity, Oxidation and Corrosion – a Study with CJ-4 and CI-4 PLUS Lubricants, 2008 Diesel Engine-Efficiency and Emissions Research (DEER) Conference August 7th, 2008

Watson, S.A., Wong, V.W. (2008) The Effects of Fuel Dilution with Biodiesel and Low Sulfur Diesel on Lubricant Acidity, Oxidation and Corrosion A Bench Scale Study with CJ 4 and CI 4+ Lubricants”, ASME/STLE IJTC2008 71221, Miami, FL, Oct. 2008.

Waynick, J.A., (2005) Characterization of Biodiesel Oxidation and Oxidation Products Crc Project No. Avfl-2b, Swri® Project No. 08-10721, Nrel/Tp-540-39096 November 2005

Westberg, E. (2012), Qualitative and Quantitative Analysis of Biodiesel Deposits Formed on a Hot Metal Surface, Master’s Thesis conducted at Exova AB Linköping, 2012-06-20

Westbrook, S. R. (2005) An Evaluation and Comparison of Test Methods to Measure the Oxidation Stability of Neat Biodiesel, NREL/SR-540-38983; National Renewable Energy Laboratory: Golden, Colorado, USA, 2005.

Wolak, A. (2018) Changes in Lubricant Properties of Used Synthetic Oils Based on the Total Acid Number, Measurement and Control 1–8 DOI: 10.1177/0020294018770916

Wooton, D. L., Lawrance, B. J., Damrath, J. G. (1984) SAE Paper No. 841372, SP-589, 71.

Woydt, M., Luther, R., Gili, F., et al. (2009), When alternative lubes meet alternative fuels. 2nd European Conference on Tribology (ECOTRIB), Pisa, 9 June 2009.

Woydt, M., Spaltmann, D., Igartua, A., et al. (2008) Perspectives of non-hydrocarbon-based engine oils and triboactive materials. LUBMAT08 Conference Proceedings, San Sebastián: 105

Xin, J., Imahara, H., Saka, S., (2009) Kinetics on the oxidation of biodiesel stabilized with antioxidant, *Fuel* 88, 282–286

Yaakob, Z., Narayanan, B. N., Silija, P., et al. (2014), A review on the oxidation stability of biodiesel, *Renewable and Sustainable Energy Reviews* 35,136–153

Yahagi, S. S., Roveda, A. C., Sobral, A. T., et al. (2019). An Analytical Evaluation of the Synergistic Effect on Biodiesel Oxidation Stability Promoted by Binary and Ternary Blends Containing Multifunctional Additives. *International journal of analytical chemistry*, 2019, 6467183. <https://doi.org/10.1155/2019/6467183>

Youk-Meng, C., and Hsiu-Jung, (2001) Gas Chromatographic Determination of Synthetic Antioxidants in Edible Fats and Oils –A Simple Methylation Method, *Journal of Food and Drug Analysis*, Vol. 9, No. 1, Pages 20-26

Yuegang, Z. (2016) *Oil Analysis Handbook for Predictive Equipment Maintenance*, Third Edition. Spectro Scientific; Technical Committee of Petroleum Additive Manufacturers in Europe, *Lubricant Additives: Use and Benefits*, AUGUST 2016 / ATC DOCUMENT 118

Yüksek L., Hakan, K., Orkun, Ö., et al. (2009), The Effect and Comparison of Biodiesel-Diesel Fuel on Crankcase Oil, Diesel Engine Performance and Emissions, *FME Transactions*, 37, 91-97

Zdrodowski, R, Gangopadhyay, A, Anderson, J.E, et al. (2010) Effect of biodiesel (B20) on vehicle-aged engine oil properties. *SAE International Journal of Fuels and Lubricants* Vol. 3, No. 2 pp. 579-597

Zhou, J., Yun, X., Xiao, L. (2017), Evaluation of the oxidation stability of biodiesel stabilized with antioxidants using the Rancimat and PDSC methods, *Fuel* 188, 61–68

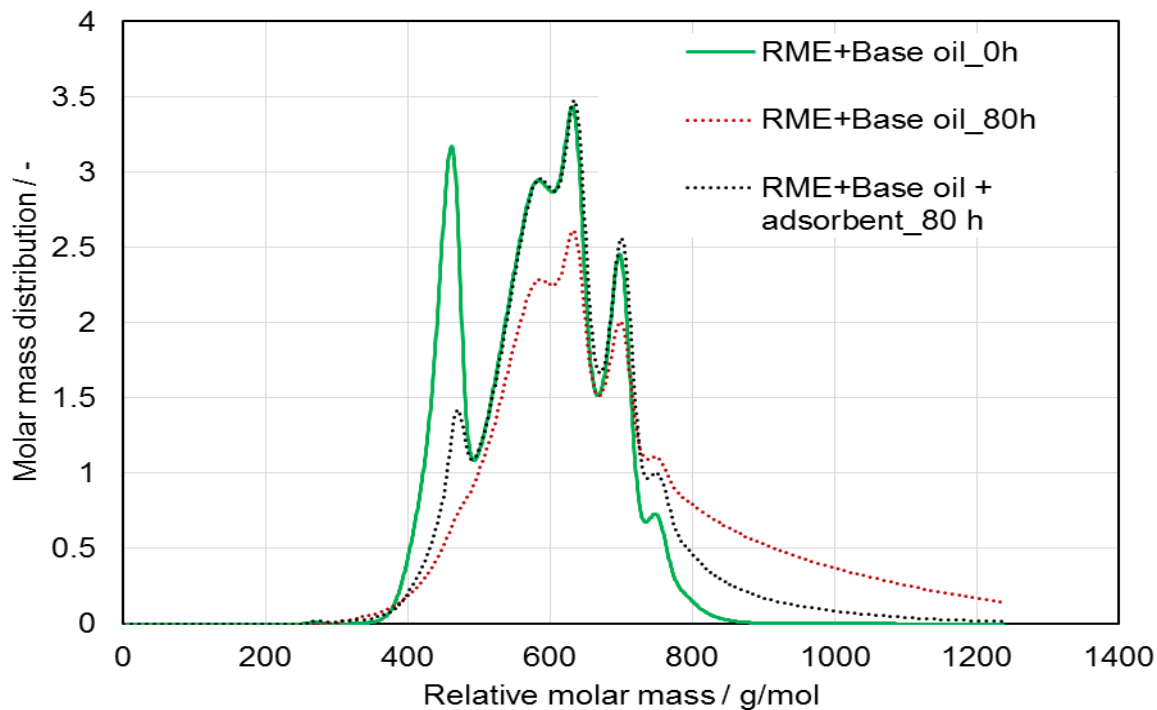
Ziejewski, M. and Kaufman, K. (1983), Vegetable Oils as a Potential Alternate Fuel in Direct Injection Diesel Engines, *SAE Technical Paper* 831359, <https://doi.org/10.4271/831359>

Zuleta, E.C., Rios, L.A., Benjumea, P.N. (2012), Oxidative stability and cold flow behavior of palm, sacha-inchi, jatropha, and castor oil biodiesel blends. *Fuel Process Technol*; 102:96–101

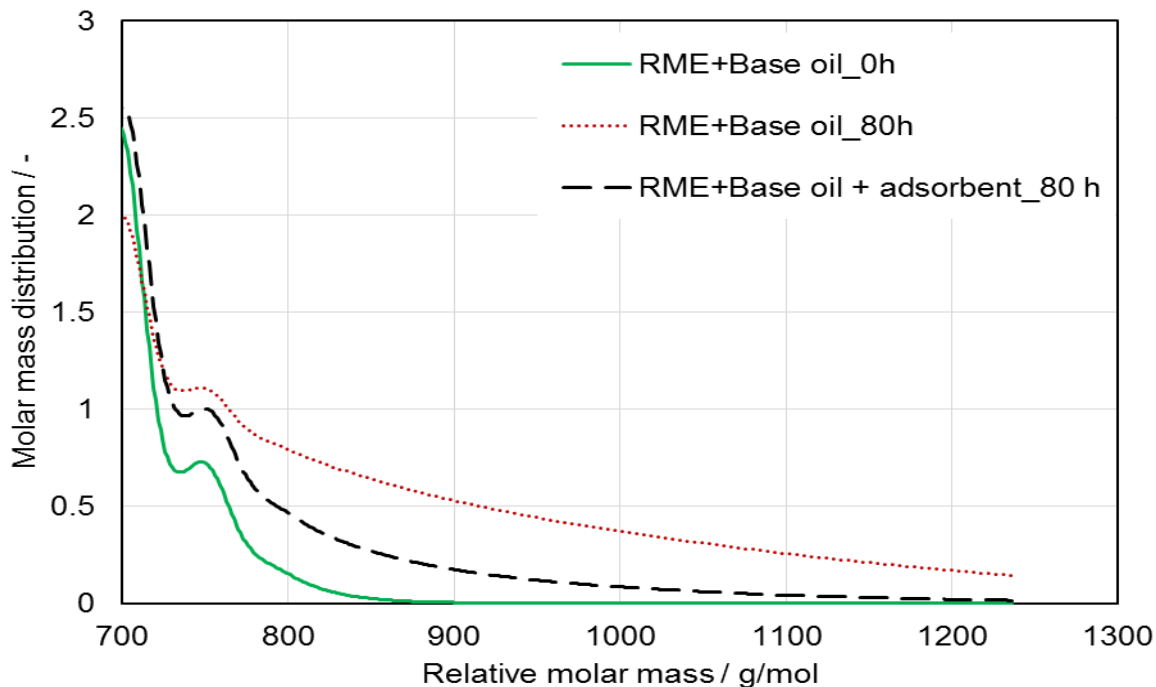
Zuleta, E.C, Baenall, L., Riosl, L.A., et al. (2012), The oxidative stability of biodiesel and its impact on the deterioration of metallic and polymeric materials: a review, J. Braz. Chem. Soc. vol.23 no.12

10 Appendix

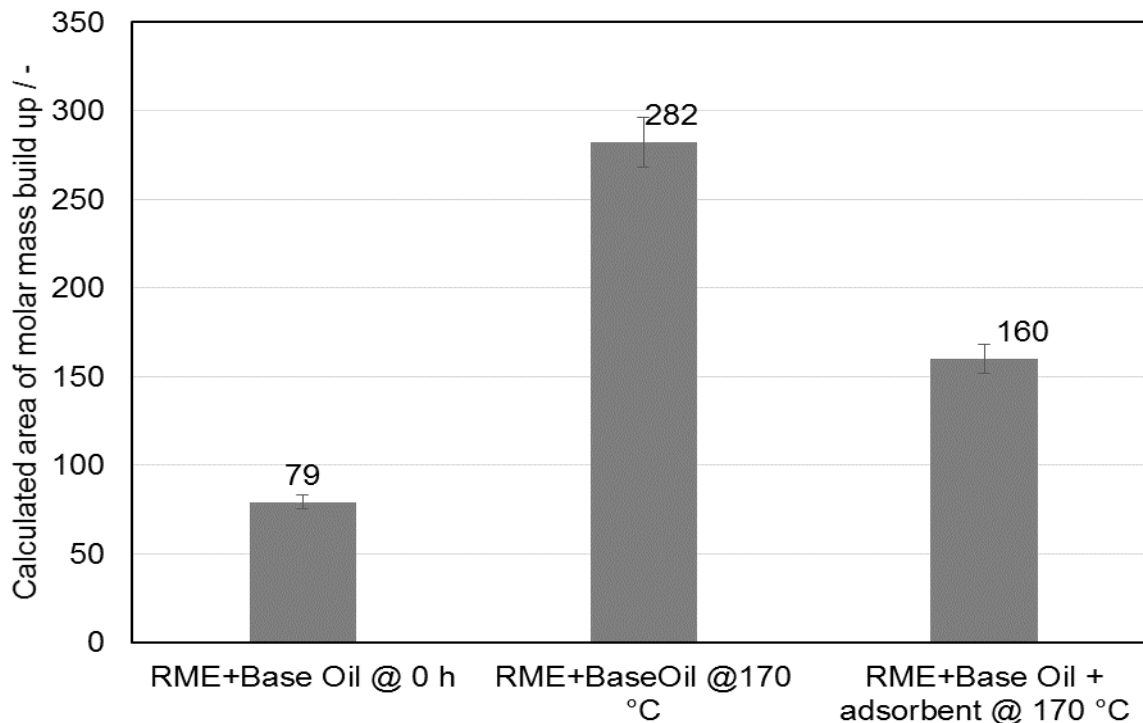
200 mL volume of RME and base oil mixture treated with 1.5 g adsorbent and aged at 170 °C for 80 h duration in locally assembled aging apparatus



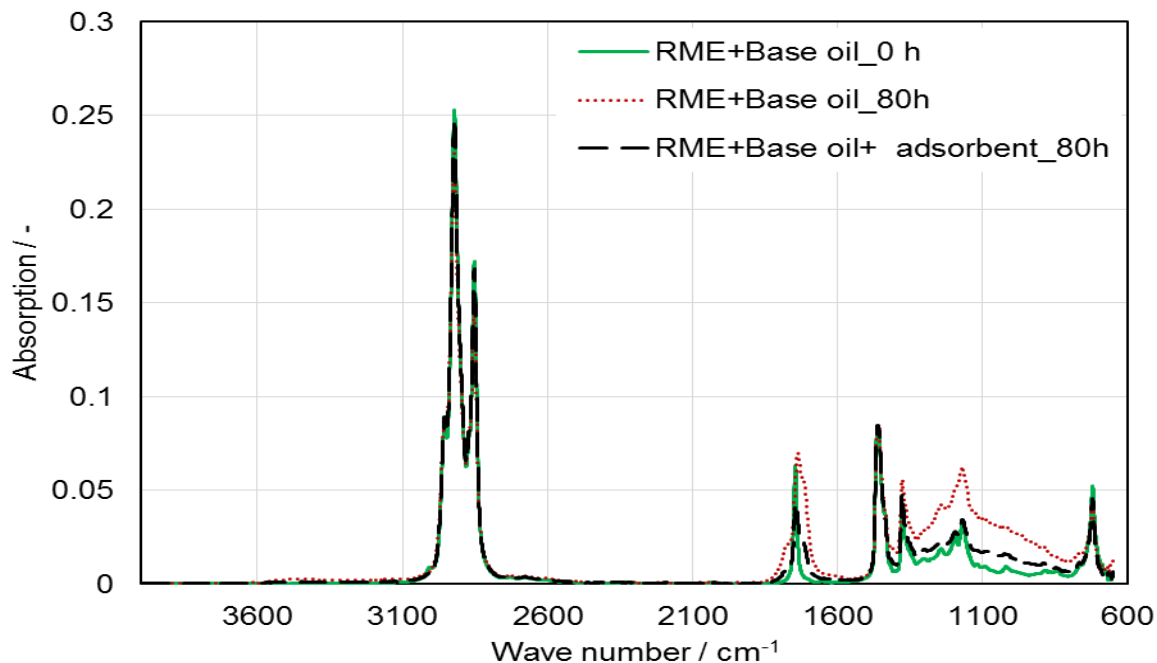
Figure_Apx 1: SEC of 200 mL of 80 % base oil blended with 20 % RME and treated with and without combined 1.5 g adsorbents of magnesium-aluminum hydrotalcite and 1,3,5-trimethyl-2,4,6-tris(3,5-di-tert-butyl-4-hydroxybenzyl) benzene in a ratio of 1:2 respectively and aged at 170 °C with air flow of 300 mL/h for 8 h per day for total of 80 h with local laboratory assembled aging apparatus



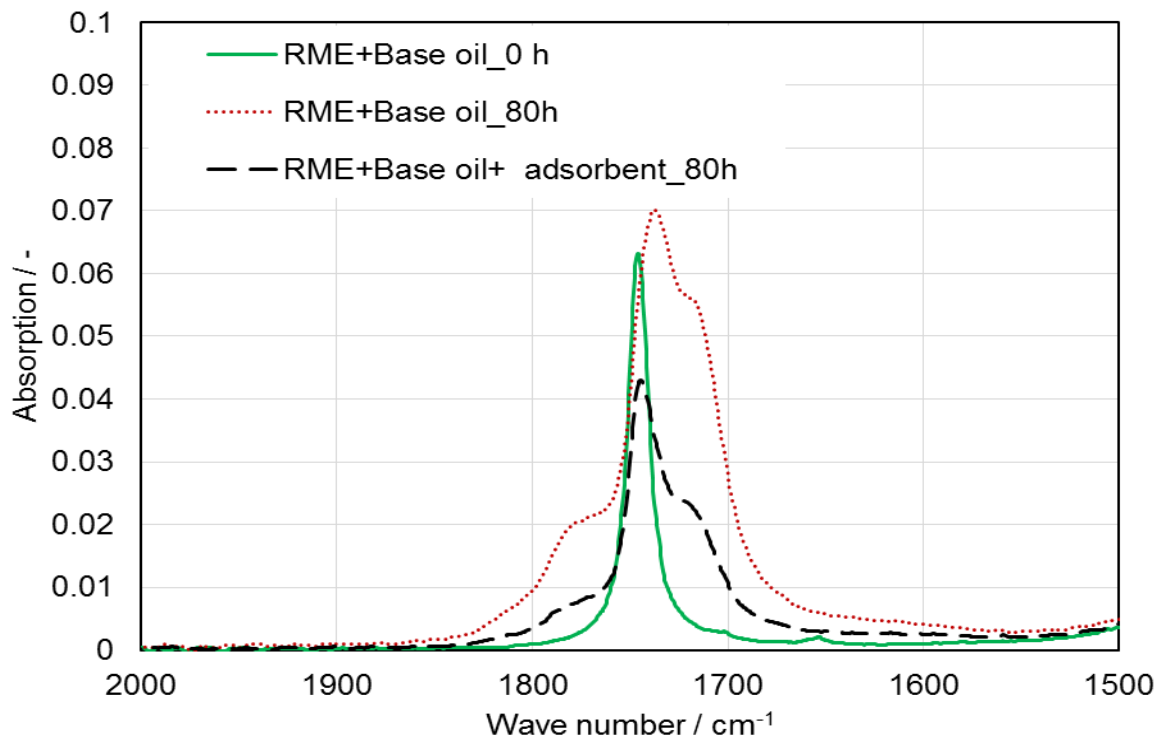
Figure_Apx 2: zoom in on the region of higher molecular masses of 200 mL of 80 % base oil blended with 20 % RME and treated with and without combined 1.5 g adsorbents of magnesium-aluminum hydrotalcite and 1,3,5-trimethyl-2,4,6-tris(3,5-di-tert-butyl-4-hydroxybenzyl) benzene in a ratio of 1:2 respectively and aged at 170 °C with air flow of 300 mL/h for 8 h per day for total of 80 h with local laboratory assembled aging apparatus



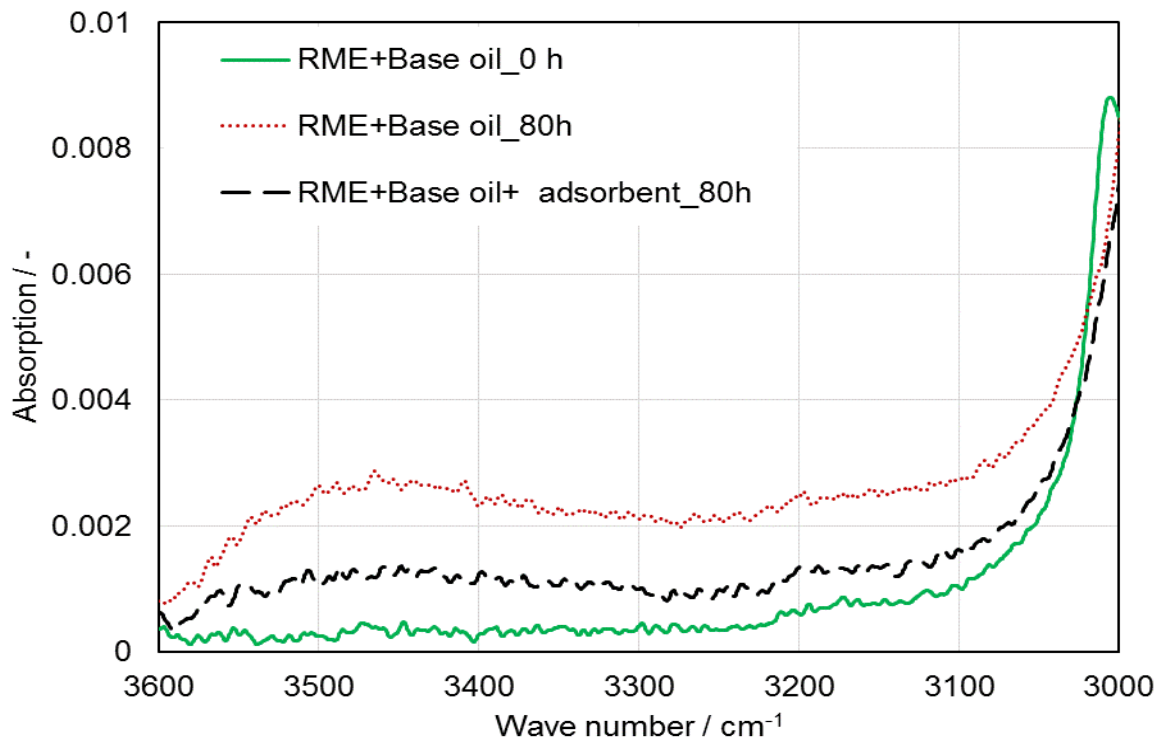
Figure_Apx 3: calculated area of SEC of 200 mL of 80 % base oil blended with 20 % RME and treated with and without combined 1.5 g adsorbents of magnesium-aluminum hydrotalcite and 1,3,5-trimethyl-2,4,6-tris(3,5-di-tert-butyl-4-hydroxybenzyl) benzene in a ratio of 1:2 respectively and aged at 170 °C with air flow of 300 mL/h for 8 h per day for total of 80 h with local laboratory assembled aging apparatus



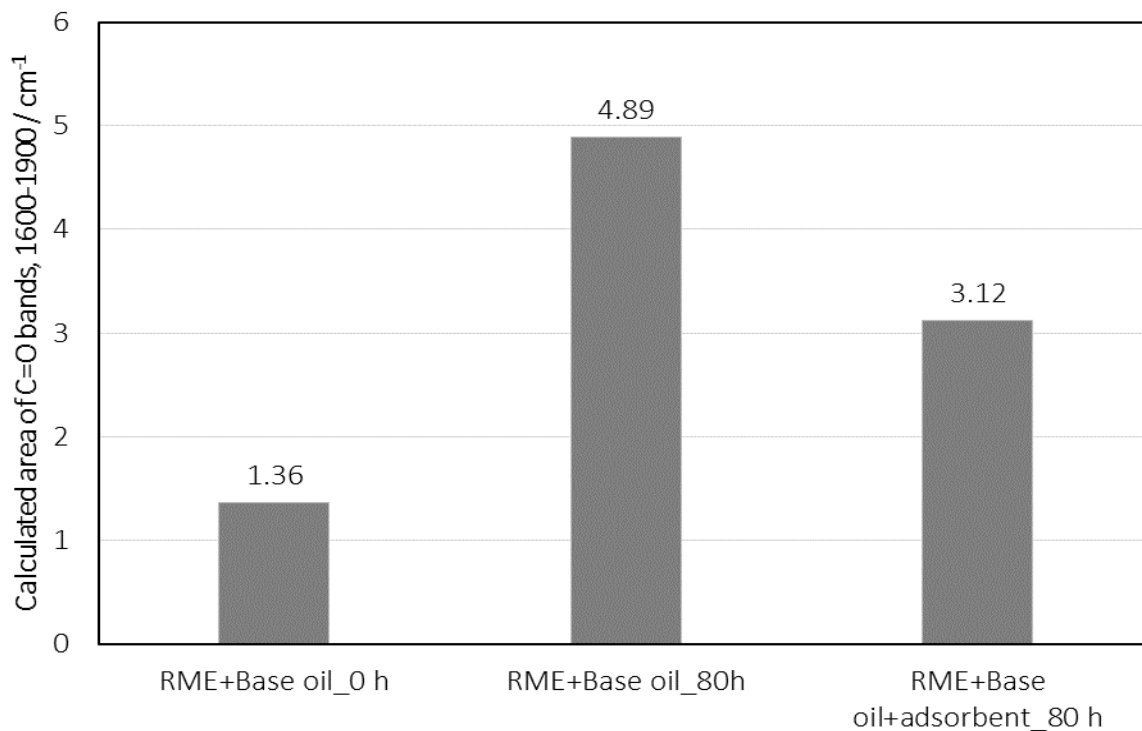
Figure_Apx 4: FTIR spectra of 200 mL of 80 % base oil blended with 20 % RME and treated with and without combined 1.5 g adsorbents of magnesium-aluminum hydrotalcite and 1,3,5-trimethyl-2,4,6-tris(3,5-di-tert-butyl-4-hydroxybenzyl) benzene in a ratio of 1:2 respectively and aged at 170 °C with air flow of 300 mL/h for 8 h per day for total of 80 h with local laboratory assembled aging apparatus



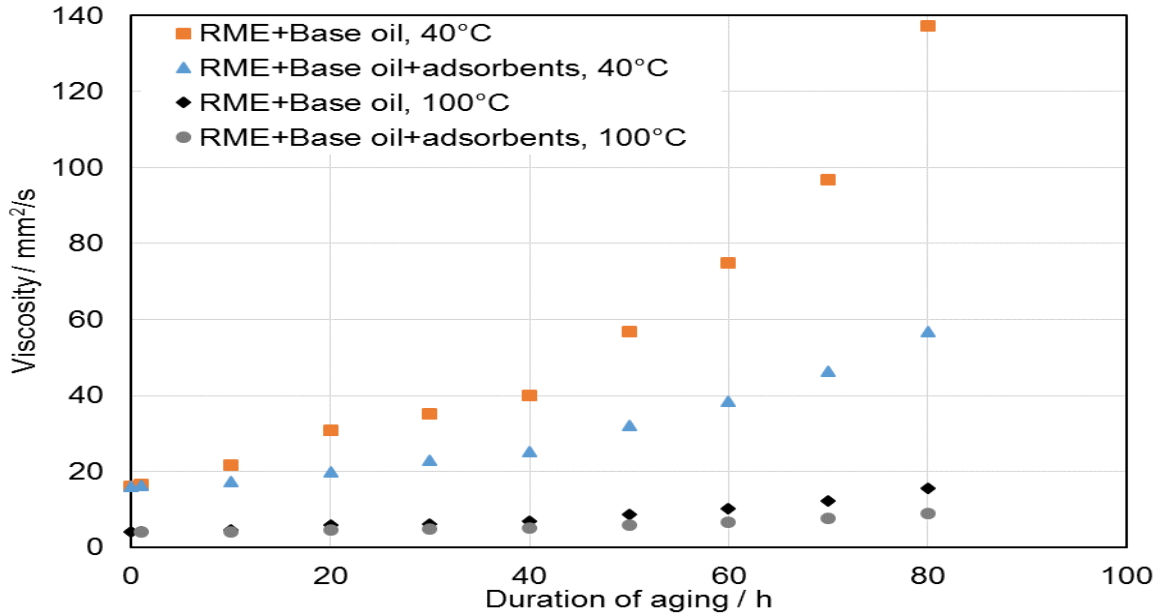
Figure_Apx 5: Zoom in on the carbonyl region of the FTIR spectra of 200 mL of 80 % base oil blended with 20 % RME and treated with and without combined 1.5 g adsorbents of magnesium-aluminum hydrotalcite and 1,3,5-trimethyl-2,4,6-tris(3,5-di-tert-butyl-4-hydroxybenzyl) benzene in a ratio of 1:2 respectively and aged at 170 °C with air flow of 300 mL/h for 8 h per day for total of 80 h with local laboratory assembled aging apparatus



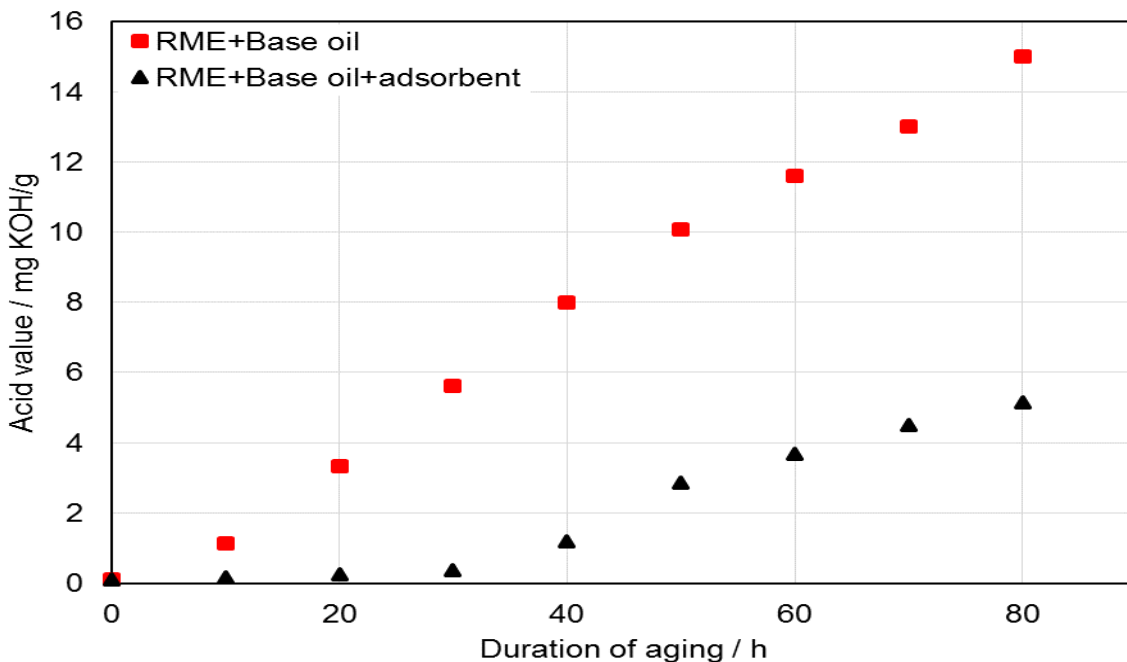
Figure_Apx 6: Zoom in on the hydroxyl region of the FTIR spectra of 200 mL of 80 % base oil blended with 20 % RME and treated with and without combined 1.5 g adsorbents of magnesium-aluminum hydrotalcite and 1,3,5-trimethyl-2,4,6-tris(3,5-di-tert-butyl-4-hydroxybenzyl) benzene in a ratio of 1:2 respectively and aged at 170 °C with air flow of 300 mL/h for 8 h per day for total of 80 h with local laboratory assembled aging apparatus



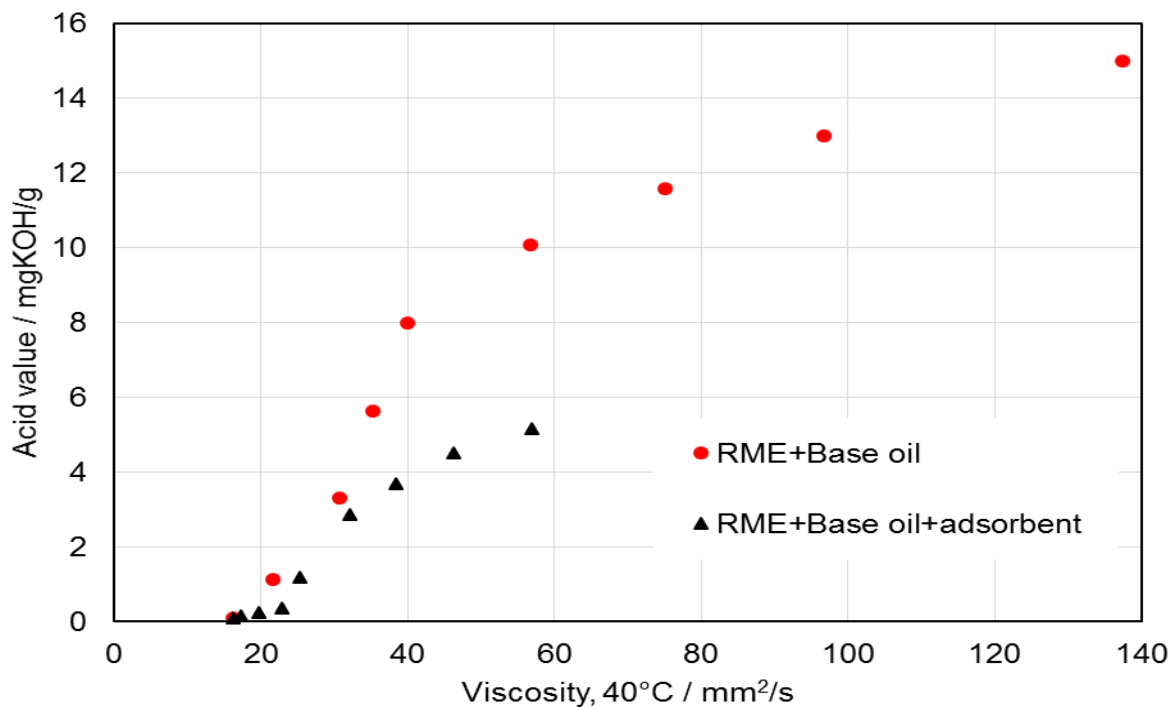
Figure_Apx 7: Calculated C=O band areas of the FTIR spectra of 200 mL of 80 % base oil blended with 20 % RME and treated with and without combined 1.5 g adsorbents of magnesium-aluminum hydrotalcite and 1,3,5-trimethyl-2,4,6-tris(3,5-di-tert-butyl-4-hydroxybenzyl) benzene in a ratio of 1:2 respectively and aged at 170 °C with air flow of 300 mL/h for 8 h per day for total of 80 h with local laboratory assembled aging apparatus



Figure_Apx 8: Viscosity of 200 mL of 80 % base oil blended with 20 % RME and treated with and without combined 1.5 g adsorbents of magnesium-aluminum hydrotalcite and 1,3,5-trimethyl-2,4,6-tris(3,5-di-tert-butyl-4-hydroxybenzyl) benzene in a ratio of 1:2 respectively and aged at 170 °C with air flow of 300 mL/h for 8 h per day for total of 80 h with local laboratory assembled aging apparatus



Figure_Apx 9: Acid value of 200 mL of 80 % base oil blended with 20 % RME and treated with and without combined 1.5 g adsorbents of magnesium-aluminum hydrotalcite and 1,3,5-trimethyl-2,4,6-tris(3,5-di-tert-butyl-4-hydroxybenzyl) benzene in a ratio of 1:2 respectively and aged at 170 °C with air flow of 300 mL/h for 8 h per day for total of 80 h with local laboratory assembled aging apparatus



Figure_Apx 10: Viscosity at 40 °C versus the acid value of 200 mL of 80 % base oil blended with 20 % RME and treated with and without combined 1.5 g adsorbents of magnesium-aluminum hydrotalcite and 1,3,5-trimethyl-2,4,6-tris(3,5-di-tert-butyl-4-hydroxybenzyl) benzene in a ratio of 1:2 respectively and aged at 170 °C with air flow of 300 mL/h for 8 h per day for total of 80 h with local laboratory assembled aging apparatus

11 Glossary

AO	Antioxidant
B.D.E.	Bond Dissociation Energy
Bx	Biodiesel blend ratio (where x is the weight percentage of biodiesel)
B20	Diesel blend consisting of 20 % biodiesel
DPF	Diesel Particulate Filter
EU	European Union
FAME	Fatty Acid Methyl Ester
FID	Flame Ionization Detector
GC	Gas Chromatography
MS	Mass Spectrometry
RME	Rapeseed Methyl Ester
VOCs	Volatile Organic Compounds
SEC	Size Exclusion Chromatography
FTIR	Fourier Transform Infrared Spectroscopy
TAN	Total Acid Number
AdOH	Adsorbents
PEG	Polyethylene Glycol
THF	Tetrahydrofuran
GPC	Gel Permeation Chromatography
NMR	Nuclear Magnetic Resonance